NUTRIENT FLUXES AND REMOVAL MECHANISMS IN A CONTROLLED DRAINAGE AND A POND-WETLAND SYSTEM TREATING CROPPING SYSTEM DRAINAGE IN EASTERN ONTARIO, CANADA

Shruti Sharad Tanga

Thesis submitted to the University of Ottawa
in partial Fulfillment of the requirements for the degree of
Ph.D. in Environmental Engineering

Ottawa-Carleton Institute for Environmental Engineering
Department of Civil Engineering
Faculty of Engineering
University of Ottawa

Abstract

Tile drainage, a necessity in humid continental cropping systems, acts as a direct conduit for nutrient- and sediment- rich water to surface water bodies. With increasing agricultural intensification, this pathway has become a significant non-point source (NPS) of pollution, contributing to anthropogenic eutrophication and downstream hypoxia. Environmental directives targeting agricultural NPS pollution, such as the Canada-Ontario Lake Erie Action Plan and Ontario's Domestic Action Plan, emphasize targeted, on-farm Beneficial Management Practises (BMPs) that deliver multi-pollutant mitigation and are supported by practical, evidence-based knowledge sharing across jurisdictions. The central objective of this multi-year, full-scale research study was to evaluate two BMP technologies - controlled drainage (CD) and pond-wetland systems - for treating cropping system drainage during non-frozen periods (April to November) in cold-climate regions, such as Eastern Ontario, while addressing technology-specific knowledge gaps related to their performance and removal mechanisms.

While CD studies in these regions often focus on the growing season, the fate of retained water and nutrients after stoplog removal (flush) and potential CD residual effects during post-harvest period remain unclear. In this study, CD optimally maintained at 0.38–0.44 m below the soil surface during the Growing Period (GP) reduced flow and nutrient loads by 51- 76% compared with free drainage (FD). Stoplog damming significantly reduced solids (TSS) and particulate phosphorus (PP) export, created conducive environment for nitrate (NO_3^--N) reduction during dry GP periods, and potentially enhanced sorption of soluble reactive phosphorus (SRP) - increasing water and nutrient availability during crop-stress periods. During the Flush Period, flow and nutrient losses increased at CD before returning to background levels. Evidence of denitrification was indicated by NO_3^--N gradients in the dammed soil profile during flush and a 35% higher relative abundance of NO_3^--N-reducing bacteria under CD compared with FD. No residual GP effects were observed in post-harvest period, except for SRP. Overall, CD implemented in GP effectively offset the hydrological and nutrient exports of the Flush and Post-Harvest Periods, reducing total flow (37%), NO_3^--N (21%), and SRP (57%) load from planting to freeze-up.

Although warmer-climate pond and constructed wetland systems report high nutrient removal, their long-term effectiveness in cold-climate, treating cropping systems remains

uncertain, as attenuation of NO_3^--N-rich, low-carbon drainage can become temperature-limited. In this 5-year study, 0.4 ha pond-wetland system (system-to-catchment area ratio = 0.93%) and varying mean depths of 0.1 to 1.3 m, exhibited strong seasonal and annual variations driven by flow and internal processes. Overall, inlet-outlet concentration monitoring, revealed that the system was most effective in retaining TSS (49%), followed by NO_3^--N (30%), PP (22%), and SRP (14%), suggesting system functioned as a net sink for all parameters. However, seasonal patterns showed high variability, from intermittent to negative removals in colder, high-flow periods (Late Spring, Fall and Spring-melt) to consistent highest removals in warmer, low-flow Summer on both concentration and mass basis. However, high relative removal during low-flow periods did not necessarily translate into substantial reductions in annual exports. Internal monitoring revealed pronounced pond-to-pond gradients, uniquely providing insights relative to different depths. The deepest, unvegetated pond (mean depth = 1.3 m) achieved the highest retention of TSS and PP via sedimentation. In contrast, the shallow inlet pond (0.1 m) consistently promoted resuspension and algal growth, acting as sources of solids and PP, especially during Summer and Fall. The terminal, wetland-like outlet pond (0.3 m) provided no additional treatment benefits across all parameters under the observed hydraulic and loading conditions. SRP dynamics was highly variable, showing no consistent system physical controls, indicating internal biological and geochemical processes can exceed net retention in this low P loading system.

Denitrification kinetics were best described by a cascading pond-to-pond areal-based first order P-k-C* model ($k = 0.14$ m/d; $\theta = 1.19$), outperforming traditional inlet-outlet and volumetric (HRT-based) formulations, indicating NO_3^--N removal scaled more strongly with benthic surface area than with water-column volume. Consistent with this, kinetic analyses also showed ponds of ~0.6-0.7 m were sufficient for NO_3^--N removal, while deeper pond (1.3 m) provided no additional benefit. Long-term total N mass balance revealed 87% of retained TN was attributable to atmospheric N loss, indicating that effective microbial denitrification can develop in cold-region pond-wetland systems, even prior to extensive vegetation establishment or long-term soil accretion. Field-based microbiome community analyses and controlled, anoxic, batch-scale denitrification trails revealed sediments as the dominant habitat of NO_3^--N removal compared to stem-associated biofilms (x2.8 relative abundance of denitrifying taxa and x3 to x9 rate constant normalised to habitat-surface area). The bench-scale results also found denitrification was strongly

constrained by temperature at 4°C across all habitats, whereas organic carbon availability became the dominant limiting factor at 20°C. Overall, this comprehensive study shows that minimally invasive CD and a small footprint pond-wetland system (<1% of farmland) are effective, targeted, implementable engineering BMPs for TSS and N, that provide strong environmental benefits and support broader adoption in cold-climate grain-farming regions.

Preface

This dissertation is an original work performed by Shruti Tanga, under the supervision of Dr. Christopher Kinsley, and includes four manuscripts. The manuscripts herein have either been published or will be submitted for publication in peer reviewed journal. Author contributions are described below using the CRediT (Contributor Roles Taxonomy).

Chapter 3: Tanga, S., Lebeau, B., Crolla, A., Tsitouras, A., Garduño-Ibarra, I. R., & Kinsley, C. (2025). Controlled drainage – Effects on nutrient attenuation and water quality – A field study in Eastern Ontario, Canada. *Agricultural Water Management*, *319*, 109764.

Shruti Tanga: Methodology; Investigation; Formal analysis; Data curation.; Visualization; Software; Writing – original draft.
Benoit Lebeau: Conceptualization; Methodology; Writing – review & editing.
Anna Crolla: Conceptualization; Methodology; Writing – review & editing.
Alexandra Tsitouras: Software; Formal analysis; Writing – review & editing.
I. Rafael Garduño-Ibarra: Writing – review & editing.
Christopher Kinsley: Conceptualization; Supervision; Methodology; Validation; Funding acquisition; Resources; Writing – review & editing.

Chapter 4: Tanga, S., Mathew, K., Lebeau, B., Crolla, A., Delatolla, R., Kinsley, C. Constructed pond-wetland systems for treating cropping tile drainage in Eastern Canada: insights into solids and phosphorus retention.

Shruti Tanga: Methodology; Investigation; Formal analysis; Data curation.; Visualization; Software; Writing – original draft.
Krupa Rochelle Mathew: Methodology; Investigation; Formal analysis; Data curation; Writing – review & editing
Benoit Lebeau: Conceptualization; Methodology; Writing – review & editing.
Anna Crolla: Conceptualization; Methodology; Writing – review & editing.
Robert Delatolla: Supervision; Writing – review & editing.
Christopher Kinsley: Conceptualization; Supervision; Methodology; Validation; Funding acquisition; Resources; Writing – review & editing.

Chapter 5: Tanga, S., Mathew, K., Lebeau, B., Crolla, A., Delatolla, R., & Kinsley, C. Nitrogen dynamics and removal in a constructed pond-wetland treating tile drainage from a cold climate cropping system.

Shruti Tanga: Methodology; Investigation; Formal analysis; Data curation.; Visualization; Software; Writing – original draft.
Krupa Rochelle Mathew: Methodology; Investigation; Formal analysis; Data curation; Writing – review & editing
Benoit Lebeau: Conceptualization; Methodology; Writing – review & editing.
Anna Crolla: Conceptualization; Methodology; Writing – review & editing.
Robert Delatolla: Supervision; Writing – review & editing.
Christopher Kinsley: Conceptualization; Supervision; Methodology; Validation; Funding acquisition; Resources; Writing – review & editing.

Chapter 6: Tanga, S., Tsitouras, A., Garduño-Ibarra, I. R., & Kinsley, C. Relative impact of sediments versus stem-associated biofilms on nitrate removal in cold-climate pond-wetland system: Role of microbial potential and environmental constraints.

Shruti Tanga: Methodology; Investigation; Formal analysis; Data curation.; Visualization; Software; Writing – original draft.
Alexandra Tsitouras: Software; Formal analysis.
I. Rafael Garduño-Ibarra: Writing – review & editing.
Christopher Kinsley: Conceptualization; Supervision; Methodology; Validation; Funding acquisition; Writing – review & editing.

I am aware of the University of Ottawa Academic Regulations; I certify that the above material describes work completed during my full-time registration as a graduate student at the University of Ottawa.

Acknowledgements

First and foremost, I extend my deepest gratitude to my supervisor, Dr. Chris Kinsley. Your guidance, knowledge, and unwavering support throughout these years have shaped every part of this journey. Your insights, encouragement, and the opportunities you opened for me have profoundly influenced both my research and my personal growth. I am especially grateful for your kindness, and for the trust you placed in me. I truly could not have asked for a better mentor – this work would not have been possible without you.

To Benoit Lebeau and Dr. Anna Crolla, thank you for your direction, thoughtful guidance, and professional expertise throughout this research. Your encouragement, kindness, and the opportunities you provided while working with you and the Ontario Ministry of Agriculture, Food, and Agribusiness (OMAFA) team have been transformative. A special thank you to Anna – your support and friendship have meant more to me than words can express, and your confidence in me has been a constant source of motivation.

I am sincerely grateful to Marc Bercier and his family for granting unrestricted access to their farm and for their assistance when needed. I also acknowledge OMAFA, Natural Sciences and Engineering Research (NSERC), South Nation Conservation Authority (SNCA), Alternative Land Use Services (ALUS) Canada, and Ducks Unlimited for providing equipment and financial support.

During my time at uOttawa, I was fortunate to collaborate with talented individuals whose support has been invaluable. Dr. Alexandra Tsitouras, Dr. James Butcher, thank you for knowledge and collaboration on the microbiome analysis – this component of the research would not have been possible without you. I am grateful to Rochelle Mathew, Rukmini Bista, and Olatian Edu for providing data from your Master's thesis/project, and to Regan, Pierre, and Meet for their assistance with field and lab work. I am also thankful to my colleagues who have become friends - Dr. Alexandra Tsitouras, Dr. Rafael Garduño-Ibarra, Dr. Juliet Ikem - for the knowledge, support and camaraderie. To my incredible friends outside of University – Harishyam, Prathiksha, Anoopa, Purushoth, Priyanka, and Garry – thank you for grounding me, cheering me on, and being there when I needed you the most. A special thank you to Dr. Rima Kinsley for your thoughtful

perception, support, and friendship over the years, and to the rest of the Kinsley family for their warmth and kindness.

Finally, to my parents, Dr. Sharad, and Dr. Sneha and to my sister, Shradha – words cannot express how grateful I am for your unwavering support, understanding, and patience throughout this journey. Everything I am today reflects your love, guidance, and the values you have instilled in me. Thank you, family. This accomplishment is as much yours as it is mine.

Table of Contents

List of Tables

List of Figures

List of Abbreviations

ANOSIM	Analysis of Similarities
ANOVA	Analysis of Variance
AOB	Ammonia-Oxidizing Bacteria
BMP	Beneficial Management Practice
CD	Controlled Drainage
COD	Chemical Oxygen Demand
CW	Constructed Wetland

DNRA	Dissimilatory Nitrate Reduction to Ammonium
DO	Dissolved Oxygen
DOC	Dissolved Organic Carbon
DON	Dissolved Organic Nitrogen
DP	Dissolved Phosphorus
ET	Evapotranspiration
FD	Free Drainage
FP	Flush Period
FWS	Free-Surface Wetland
GHG	Greenhouse Gas
GLWQA	Great Lakes Water Quality Agreement
GP	Growing Period
HAB	Harmful Algal Blooms
HLR	Hydraulic Loading Rate
HRT	Hydraulic Residence Time
N	Nitrogen
NMA	Nutrient Management Act
NOB	Nitrite-Oxidizing Bacteria
NPS	Non-Point Source
OTU	Operational Taxonomic Unit
P	Phosphorus
PCoA	Principal Coordinates Analysis
PCR	Polymerase Chain Reaction
PHP	Post-Harvest Period
PP	Particulate Phosphorus
RMSE	Root Mean Square of Errors
RNA	Ribonucleic Acid
rRNA	ribosomal Ribonucleic Acid
sCOD	soluble Chemical Oxygen Demand
SP	Soluble Phosphorus
SRP	Soluble Reactive Phosphorus

SWE	Snow Water Equivalent
TCOD	Total Chemical Oxygen Demand
TIS	Tanks In Series
TN	Total Nitrogen
TOC	Total Organic Carbon
TP	Total Phosphorus
TS	Total Solids
TSS	Total Suspended Solids
VS	Volatile Solids

Chapter 1 - Introduction

1.1. Background

Agricultural intensification has increased markedly in Canada over the past three decades, with land under cropping systems expanding by approximately 40% (AAFC, 2025). In Eastern Canada, much of this cropland is established on fine-textured, poorly draining soils (Brevé & Skaggs, 1994), necessitating widespread installation of subsurface tile drainage to reduce waterlogging, and improve yield stability. Approximately 14% of Canada's croplands are tile drained, increasing to nearly 48% (~1.75 million hectares) in Ontario (Smith, 2015; Sunohara et al., 2015), making tile drainage a defining feature of regional agroecosystems.

The expansion of tile drainage, together with increased reliance on inorganic nitrogen (N) and phosphorus (P) fertilizers and climate-driven shifts in precipitation and temperature regimes, has accelerated nutrient export, establishing agriculture as a dominant source of non-point source pollution (Fortier, 2022; Statista, 2024; Watson et al., 2016). By enhancing field-to-stream connectivity, tile drainage facilitates the transport of dissolved nutrients, including nitrate (NO_3^--N) and soluble reactive phosphorus (SRP), as well as sediments, and solid-bound nutrients to surface waters. These fluxes contribute to harmful algal blooms, and hypoxic conditions, as observed in Lake Erie (OMECP, 2024) and to excessive NO_3^--N accumulation as seen in the Laurentian Great Lakes (Cooper, 2016) and St. Lawrence river basin (Working Group on the State of the St. Lawrence Monitoring, 2024).

To address these concerns, federal, provincial, and local initiatives have promoted beneficial management practises (BMPs) tailored to local soils, topography, and farming systems, with the aim of mitigating multiple water-quality parameters simultaneously (ECCC & OMECP, 2018; OMAFA, 2002; SNCA, 2025). Among these, controlled drainage (CD), and constructed wetlands (CWs), including free-water surface (FWS) systems, have been promoted by Agriculture and Agri-Food Canada (AAFC, 2010, 2023), while treatment ponds (retention ponds) are recommended under the St. Lawrence Action Plan (2021).

CD is a feasible upgrade to existing tile drainage systems that involves installing adjustable physical flow barriers (i.e., stoplogs) within drainage structures to artificially set a desired water

level and thereby regulate outflow (Drury et al., 2014; Nash et al., 2015; Saadat et al., 2018a). CD has been recognized as an edge-of-field practice that seeks to balance conservation goals and crop production by managing the timing and quantity of water discharged from cropping fields, thereby reducing nutrient loads in tile drainage.

Several studies report reductions in NO_3^--N and SRP loads under CD, largely attributed to decreased drainage volumes, although some studies suggest that changes in nutrient concentrations also contribute to these reductions (Cordeiro et al., 2014; King et al., 2022; Sunohara et al., 2016; Williams et al., 2015). Enhanced microbial denitrification under CD is theoretically plausible due to elevated water tables and reduced soil oxygen availability, which promote anaerobic conditions within soil pores. However, limited studies have directly identified this mechanism (Liu et al., 2019), and most existing evidence remains indirect, inferred from observed reductions or changes in NO_3^--N concentration or shifts in redox conditions (Adeuya et al., 2012; Drury et al., 2014; Fausey, 2005; Lavaire et al., 2017; Woli et al., 2010). A clearer understanding of denitrification under CD therefore requires characterization of soil denitrifying communities in terms of relative abundance, which remains largely unexplored in the existing studies.

In contrast, research findings on the effect of CD on SRP concentrations are limited and inconsistent, with several studies reporting significant increases in SRP under CD (Saadat et al., 2018b; Sanchez Valero et al., 2007; Satchithanantham et al., 2014). Similarly, research examining the impacts of CD on total suspended solids (TSS), total phosphorus (TP) and particulate phosphorus (PP) remains scarce. Although reported reductions in TP (18 -54%) and PP (33-37%) loads are generally attributed to flow control (Saadat et al., 2018b; Sanchez Valero et al., 2007; Satchithanantham et al., 2014), farm-scale investigations that explicitly quantify TSS responses to CD are lacking. It is hypothesized that damming effect of CD may reduce macropore development and thereby, limit solids mobilization.

In cold-climate regions such as Eastern Ontario, previous CD studies have primarily focused on the growing season in accordance with operational recommendations (Sunohara et al., 2016). However, the potential effects of the hydraulic flush following stoplog removal on flows, solids, and nutrient fluxes remain unquantified. In addition, the antecedent effect of CD on drainage or leaching during the post-harvest period are poorly understood. As a result, it remains

uncertain whether water quality improvements achieved under CD during growing period are offset by increased nutrient and solid losses during the flush and post-harvest periods, warranting multi-year evaluations spanning from planting to system freeze-up.

Treatment ponds have traditionally been employed for stormwater management, more recently, for agricultural surface runoff management. These engineered systems consist of a permanent pool of water with mean depths ranging from 1.0 to 2.5 m, whereas nutrient transformations primarily occur within the permanent water volume and associated sediments rather than within the littoral zone, where biological uptake may be limited (Gold et al., 2017; Nietch et al., 2001). Owing to their depth, agricultural ponds can remove > 50% of TSS and associated PP through sedimentation (Chrétien et al., 2016; Fiener et al., 2005; Robotham et al., 2021; Rushton & Bahk, 2001). However, little is known about their effectiveness in removing dissolved nutrients such as NO_3^--N and SRP, or about their performance in treating cropping-system tile drainage, as long-term monitoring remains limited.

CW have long been used to treat municipal and industrial wastewaters, urban stormwater, agricultural runoff and more recently, cropping drainage (Kadlec & Wallace, 2008; Mitsch & Gosselink, 2015). FWS CWs are shallow systems (0.2 to 0.4 m deep) that convey water above the hydric soils through dense vegetation. Functionally, CWs operate as complex integrated sediment-plant-microbe systems in which vegetation structure and redox gradients promote multiple, sequential pathways for TSS, N and P retention and removal (Mitsch & Gosselink, 2015; Reddy & DeLaune, 2008). However, among the limited studies evaluating FWS CWs for treating cropping system tile drainage or runoff, large variability in treatment efficiencies have been reported, reflecting sensitivity to hydrologic loading, seasonal conditions, system-scale, and geographic location. Uusheimo et al. (2018), Steidl et al. (2019), and Kadlec & Reddy (2001) emphasize that FWS CWs in northern, colder-climatic regions often exhibit strong seasonal variation in nutrient retention efficiency, as temperature-dependent N (particularly NO_3^--N) and P removal mechanisms are negatively affected. These findings highlight the need for full-scale, process-resolved studies in cold regions.

Constructed pond-wetland systems represent a potentially multifunctional BMP that combines the sedimentation capacity of treatment ponds with biogeochemical processing and

macrophyte uptake in free-water surface CWs. This hybrid configuration, characterized by varying water depths, can generate gradients in sediment redox conditions, hydrodynamics, organic carbon availability, temperature, and ecological diversity (e.g. vegetation, algae), making TSS, N and P removals within pond-wetland systems inherently spatially heterogeneous. Multiple, spatial sampling within such systems, rather than conventional inlet-outlet comparisons, can provide insights into internal processes and inform nutrient-specific design optimization. However, the application of such pond-wetland systems to treat low carbon, high NO_3^--N, and low P, cropping system tile drainage remains underexplored, particularly in temperate cold climate regions with winter freeze-up.

In addition to their environmental benefits, CD, and pond-wetland systems, when strategically positioned along discharge pathways, can intercept tile drainage without disrupting agricultural operations. These systems typically have long operational lifetimes (> 20 years), require minimal maintenance, and can provide cost-effective nutrient mitigation (Frankenberger et al., 2024; Kovacic et al., 2006). Accordingly, this thesis presents a multi-year, full-scale evaluation of CD and pond-wetland BMP technologies for treating cropping system drainage during non-frozen periods (April to November) in cold-climate regions, such as Eastern Ontario. By addressing technology-specific knowledge gaps related to performance and removal mechanisms, this work aims to support the adoption and optimization of these BMPs among grain producers in Eastern Ontario and comparable climatic zones.

1.2. Research objectives, and contributions

The central objective of this full-scale, multi-year research is to evaluate the effectiveness of controlled drainage and pond-wetland BMPs to attenuate water and nutrient fluxes from cropping system tile drainage and improve understanding of the underlying removal mechanisms in cold-climate conditions.

Controlled Drainage

Objective 1 (addressed in Chapter 3)- Evaluate the performance of the CD system from planting to freeze-up and compare it to free drainage in terms of effects on the water table, tile flow, and nutrient losses (mass and concentration basis).

Specifically:

i. Determine the impact of Flush Period (FP; after stoplog removal until CD flows, now freely flowing, were similar to free drainage) and the Post-Harvest Period (PHP; from the end of FP until freeze-up of drainage structures) on overall nutrient loads.
ii. Determine if denitrification is a significant mechanism for nitrate reduction at CD by examining nitrate concentration trends during the Growing Period (GP), FP, and analyses of microbial community.
iii. Evaluate whether CD implementation affects SRP removal.
iv. Assess the physical damming effect of CD on solids (TSS) and associated PP.

Pond-Wetland System

Objective 2 (addressed in Chapter 4) – Assess the performance and patterns of solids and phosphorus dynamics within the pond-wetland system, with implications for design and long-term retention.

Specifically:

i. Characterize spatial and seasonal variability of TSS, PP, and SRP concentrations and loads across ponds.
ii. Assess cumulative system-scale retention of TSS, PP and SRP, and their distribution among sediments, macrophytes, and soil.
iii. Evaluate the influence of system design factors (depth, area, and vegetation cover) on TSS, PP, and SRP retention under varying flow and seasonal conditions.

Objective 3 (addressed in Chapter 5) - Evaluate the efficacy of a pond-wetland system in treating high NO_3^--N, low carbon, tile drainage from cropping systems in cold, temperate region.

Specifically:

i. Characterize hydrological and seasonal controls on TN and NO_3^--N reduction from spring snowmelt to system freeze-up.
ii. Quantify internal, pond-scale N processing using spatially distributed concentration and mass-load analyses on an overall and seasonal basis.
iii. Evaluate denitrification kinetics within a cascading pond framework by comparing areal- and volumetric-based first-order models and assess implications for pond-wetland design (depth) in cold climates.

iv. Conduct a system-scale TN mass balance to partition removed N among temporary storage pools and permanent removal pathways.

Objective 4 (addressed in Chapter 6) - Investigate spatial patterns and environmental controls on the theoretical microbial NO_3^--N reduction potential within the pond-wetland using microbial community analysis and controlled, anoxic batch-scale denitrification trials.

Specifically:

i. Assess variations in microbial community composition, with emphasis on denitrifying taxa, between stem-associated biofilm and sediment habitats across depth gradients.
ii. Investigate the influence on temperature, stem depth relative to surface water, organic carbon availability, and sediment depth on the magnitude of denitrification potential and associated kinetic rate constants.
iii. Quantify and compare the relative impact of sediments and stem-associated biofilm habitats to denitrification potential based on habitat-specific surface area.

1.3. Novelty and contributions

Controlled Drainage

- Evaluates performance from planting to freeze-up, including the flush and post-harvest periods, providing a more complete assessment than previous research that focused only on growing season in similar climatic regions.
- Determines the significance of denitrification through microbiome analysis and concentration effects, which is a novel approach in CD research.
- Assesses CD effects on TSS, which has not been reported.

Pond-Wetland System

- Evaluates the multi-year performance of an integrated pond-wetland system for low carbon, high NO_3^--N, low P cropping system tile drainage in a cold-climate region, with winter freeze-up.
- Develops a best-fit areal pond-cascading kinetic framework for NO_3^--N , including kinetic co-efficients (rate constant, k, and temperature co-efficient, θ), providing practical design guidance.

- Provides evidence-based design recommendations for pond depth, area, and vegetation coverage to optimize retention and minimize internal resuspension and nutrient export.

1.4. Thesis organization

This dissertation is structured as a manuscript-based thesis as specified by the school of Graduate and Postdoctoral Studies at the University of Ottawa. The thesis is organized by articles as follows:

Chapter 2 provides a comprehensive literature overview of agricultural contributions to eutrophication, focusing on tile drainage from cropping systems and its effects on hydrology and nutrient export. The chapter also examines exiting regulatory framework for agricultural drainage and evaluates previous research on BMPs - controlled drainage, treatment ponds, and constructed wetlands - focusing on their effects on flow, solids, nitrogen, and phosphorus and the underlying mechanisms involved.

Chapter 3 is a published manuscript titled "Controlled drainage – Effects on nutrient attenuation and water quality – A field study in Eastern Ontario, Canada" and addresses Objective 1.

Chapter 4 encompasses a research manuscript entitled "Constructed pond-wetland systems for treating cropping tile drainage in Eastern Canada: insights into solids and phosphorus retention" and addresses Objective 2.

Chapter 5 is a research manuscript titled "Nitrogen dynamics and removal in a constructed pond-wetland treating tile drainage from a cold climate cropping system" and addresses Objective 3.

Chapter 6 entails a research manuscript titled "Relative impact of sediments versus stem-associated biofilms on nitrate removal in cold-climate pond-wetland system: Role of microbial potential and environmental constraints" and addresses Objective 4.

Chapter 7 presents the overall conclusions and recommendations based on research findings.

References

AAFC. (2010). *Controlled Tile Drainage : Increasing yields and helping the environment*. Agriculture and Agri-Food Canada.

AAFC. (2023). *Constructed Wetlands*. Agriculture and Agri-Food Canada = Agriculture et agroalimentaire Canada.

AAFC. (2025). *Agricultural land use*. https://agriculture.canada.ca/en/environment/resource-management/indicators/agricultural-land-use

Adeuya, R., Utt, N., Frankenberger, J., Bowling, L., Kladivko, E., Brouder, S., & Carter, B. (2012). Impacts of drainage water management on subsurface drain flow, nitrate concentration, and nitrate

loads in Indiana. *Journal of Soil and Water Conservation*, *67*(6), 474 LP – 484. https://doi.org/10.2489/jswc.67.6.474

Brevé, M. A., & Skaggs, R. W. (1994). Hydrologic and Water Quality Impacts of Agricultural Drainage. *Critical Reviews in Environmental Science and Technology*, *24*(1), 1–32. https://doi.org/10.1080/10643389409388459

Chrétien, F., Gagnon, P., Thériault, G., & Guillou, M. (2016). Performance Analysis of a Wet-Retention Pond in a Small Agricultural Catchment. *Journal of Environmental Engineering*, *142*(4), 04016005. https://doi.org/10.1061/(asce)ee.1943-7870.0001081

Cooper, M. J. (2016, March 1). Nitrogen limitation of algal biofilms in coastal wetlands of Lakes Michigan and Huron. *Great Lakes Connection, International Joint Commission*, *35*(1). https://doi.org/10.1086/684646

Cordeiro, M. R. C., Ranjan, R. S., Ferguson, I. J., & Cicek, N. (2014). Nitrate, phosphorus, and salt export through subsurface drainage from corn fields in the canadian prairies. *Transactions of the ASABE*, *57*(1), 43–50. https://doi.org/10.13031/trans.56.10370

Drury, C. F., Tan, C. S., Welacky, T. W., Reynolds, W. D., Zhang, T. Q., Oloya, T. O., McLaughlin, N. B., & Gaynor, J. D. (2014). Reducing Nitrate Loss in Tile Drainage Water with Cover Crops and Water-Table Management Systems. *Journal of Environmental Quality*, *43*(2), 587–598. https://doi.org/10.2134/jeq2012.0495

ECCC, & OMECP. (2018). *Canada-Ontario Lake Erie action plan : Partnering on achieving phosphorous loading reductions to Lake Erie from Canadian sources* (Number February).

Fausey, N. R. (2005). Drainage management for humid regions. *International Agricultural Engineering Journal*, *14*(4), 209–214. https://blancharddemofarms.org/wp-content/uploads/2021/06/DrainageWater-6.pdf

Fiener, P., Auerswald, K., & Weigand, S. (2005). Managing erosion and water quality in agricultural watersheds by small detention ponds. *Agriculture, Ecosystems and Environment*, *110*(3–4), 132–142. https://doi.org/10.1016/j.agee.2005.03.012

Fortier, R. (2022). *Seasonal trends in phosphorus export from three major Canadian Lake Erie tributaries* [McMaster Univeristy]. http://hdl.handle.net/11375/28275

Frankenberger, J., McMillan, S. K. W., Williams, M. R., Mazer, K., Ross, J., & Sohngen, B. (2024). Drainage Water Management: A review of nutrient load reductions and cost effectiveness. *Journal of the ASABE*, *67*(4), 1077–1092. https://doi.org/10.13031/ja.15549

Gold, A. C., Thompson, S. P., & Piehler, M. F. (2017). Water quality before and after watershed-scale implementation of stormwater wet ponds in the coastal plain. *Ecological Engineering*, *105*, 240–251. https://doi.org/10.1016/J.ECOLENG.2017.05.003

Kadlec, R. H., & Reddy, K. R. (2001). Temperature Effects in Treatment Wetlands. *Water Environment Research*, *73*(5), 543–557. https://doi.org/10.2175/106143001x139614

Kadlec, R. H., & Wallace, S. D. (2008). *Treatment Wetlands* (Second). Taylor & Francis Group, LLC.

King, K. W., Hanrahan, B. R., Stinner, J., & Shedekar, V. S. (2022). Field scale discharge and water quality response, to drainage water management. *Agricultural Water Management*, *264*(January), 107421. https://doi.org/10.1016/j.agwat.2021.107421

Kovacic, D. A., Twait, R. M., Wallace, M. P., & Bowling, J. M. (2006). Use of created wetlands to improve water quality in the Midwest—Lake Bloomington case study. *Ecological Engineering*, *28*(3), 258–270. https://doi.org/https://doi.org/10.1016/j.ecoleng.2006.08.002

Lavaire, T., Gentry, L. E., David, M. B., & Cooke, R. A. (2017). Fate of water and nitrate using drainage water management on tile systems in east-central Illinois. *Agricultural Water Management*, *191*, 218–228. https://doi.org/10.1016/j.agwat.2017.06.004

Liu, Y., Youssef, M. A., Chescheir, G. M., Appelboom, T. W., Poole, C. A., Arellano, C., & Skaggs, R. W. (2019). Effect of controlled drainage on nitrogen fate and transport for a subsurface drained grass field receiving liquid swine lagoon effluent. *Agricultural Water Management*, *217*, 440–451. https://doi.org/10.1016/J.AGWAT.2019.02.018

Mitsch, W., & Gosselink, J. (2015). Wetlands, 5th Edition. In *Wi Ley* (Vol. 91, Number 5). https://www.researchgate.net/publication/271643179_Wetlands_5th_edition

Nash, P. R., Nelson, K. A., Motavalli, P. P., Nathan, M., & Dudenhoeffer, C. (2015). Reducing Phosphorus Loss in Tile Water with Managed Drainage in a Claypan Soil. *Journal of Environmental Quality*, *44*(2), 585–593. https://doi.org/10.2134/jeq2014.04.0146

Nietch, C. T., Borst, M., & O'Shea, M. L. (2001). Stormwater treatment: Ponds vs. constructed wetlands. *Proceedings of the Engineering Foundation Conference*, *263*(Ms 104), 524–528. https://doi.org/10.1061/40602(263)39

OMAFA. (2002). *Nutrient Management Act, 2002, S.O. 2002, c. 4 | ontario.ca*. OMAFA. OMAFA. https://www.ontario.ca/laws/statute/02n04

OMECP. (2024). *Canada-Ontario Lake Erie Action Plan: 2024 Evaluation and Update Report*.

Reddy, K. R., & DeLaune, R. D. (2008). Biogeochemistry of Wetlands : Science and Applications. *Biogeochemistry of Wetlands*. https://doi.org/10.1201/9780203491454

Robotham, J., Old, G., Rameshwaran, P., Sear, D., Gasca-Tucker, D., Bishop, J., Old, J., & McKnight, D. (2021). Sediment and Nutrient Retention in Ponds on an Agricultural Stream: Evaluating Effectiveness for Diffuse Pollution Mitigation. *Water 2021, Vol. 13, Page 1640*, *13*(12), 1640. https://doi.org/10.3390/W13121640

Rushton, B. T., & Bahk, B. M. (2001). Treatment of stormwater runoff from row crop farming in Ruskin, Florida. *Water Science and Technology*, *44*(11–12), 531–538. https://doi.org/10.2166/wst.2001.0876

Saadat, S., Bowling, L., Frankenberger, J., & Kladivko, E. (2018a). Estimating drain flow from measured water table depth in layered soils under free and controlled drainage. *Journal of Hydrology*, *556*, 339–348. https://doi.org/10.1016/j.jhydrol.2017.11.001

Saadat, S., Bowling, L., Frankenberger, J., & Kladivko, E. (2018b). Nitrate and phosphorus transport through subsurface drains under free and controlled drainage. *Water Research*, *142*, 196–207. https://doi.org/10.1016/j.watres.2018.05.040

Sanchez Valero, C., Madramootoo, C. A., & Stämpfli, N. (2007). Water table management impacts on phosphorus loads in tile drainage. *Agricultural Water Management*, *89*(1–2), 71–80. https://doi.org/10.1016/j.agwat.2006.12.007

Satchithanantham, S., Sri Ranjan, R., & Bullock, P. (2014). Protecting water quality using controlled drainage as an agricultural bmp for potato production. *Transactions of the ASABE*, *57*(3), 815–826. https://doi.org/10.13031/trans.57.10385

Smith, P. (2015). Long-Term Temporal Trends in Agri-Environment and Agricultural Land Use in Ontario, Canada: Transformation, Transition and Significance. *Journal of Geography and Geology*, *7*(2). https://doi.org/10.5539/jgg.v7n2p32

SNCA. (2025). *Clean Water Program*. www.nation.on.ca/fr/programme-dassainissement-de-leau

St. Lawrence Action Plan. (2021). *Nonpoint source pollution - Projects 2021 -2026*. EECE. https://www.planstlaurent.qc.ca/en/developping-knowledge/water-quality/nonpoint-source-pollution

Statista. (2024, December 2). *Canada: fertilizer consumption by nutrient* . Statists Research Department. https://www.statista.com/statistics/1330033/canada-fertilizer-consumption-by-nutrient/

Steidl, J., Kalettka, T., & Bauwe, A. (2019). Nitrogen retention efficiency of a surface-flow constructed wetland receiving tile drainage water: A case study from north-eastern Germany. *Agriculture, Ecosystems and Environment*, *283*. https://doi.org/10.1016/j.agee.2019.106577

Sunohara, M. D., Gottschall, N., Craiovan, E., Wilkes, G., Topp, E., Frey, S. K., & Lapen, D. R. (2016). Controlling tile drainage during the growing season in Eastern Canada to reduce nitrogen, phosphorus, and bacteria loading to surface water. *Agricultural Water Management*, *178*(3), 159–170. https://doi.org/10.1016/j.agwat.2016.08.030

Sunohara, M. D., Gottschall, N., Wilkes, G., Craiovan, E., Topp, E., Que, Z., Seidou, O., Frey, S. K., & Lapen, D. R. (2015). Long-Term Observations of Nitrogen and Phosphorus Export in Paired-Agricultural Watersheds under Controlled and Conventional Tile Drainage. *Journal of Environmental Quality*, *44*(5), 1589–1604. https://doi.org/10.2134/jeq2015.01.0008

Uusheimo, S., Tulonen, T., Aalto, S. L., & Arvola, L. (2018). Mitigating agricultural nitrogen load with constructed ponds in northern latitudes: A field study on sedimental denitrification rates. *Agriculture, Ecosystems and Environment*, *261*, 71–79. https://doi.org/10.1016/j.agee.2018.04.002

Watson, S. B., Miller, C., Arhonditsis, G., Boyer, G. L., Carmichael, W., Charlton, M. N., Confesor, R., Depew, D. C., Höök, T. O., Ludsin, S. A., Matisoff, G., McElmurry, S. P., Murray, M. W., Peter Richards, R., Rao, Y. R., Steffen, M. M., & Wilhelm, S. W. (2016). The re-eutrophication of Lake Erie: Harmful algal blooms and hypoxia. *Harmful Algae*, *56*, 44–66. https://doi.org/10.1016/J.HAL.2016.04.010

Williams, M. R., King, K. W., & Fausey, N. R. (2015). Contribution of tile drains to basin discharge and nitrogen export in a headwater agricultural watershed. *Agricultural Water Management*, *158*(3), 42–50. https://doi.org/10.1016/j.agwat.2015.04.009

Woli, K. P., David, M. B., Cooke, R. A., McIsaac, G. F., & Mitchell, C. A. (2010). Nitrogen balance in and export from agricultural fields associated with controlled drainage systems and denitrifying bioreactors. *Ecological Engineering*, *36*(11), 1558–1566. https://doi.org/10.1016/j.ecoleng.2010.04.024

Working Group on the State of the St. Lawrence Monitoring. (2024). *Overview of the State of the St. Lawrence 2024*.

Chapter 2 - Literature Review

2.1. Background – Impacts of agriculture on eutrophication

Agricultural practises have evolved in response to growing population and increased food demand through the process of agricultural intensification. This approach enhances nutrient and water use efficiency to achieve higher quality and quantity of diverse crops per acreage of land. However, such intensification has led to excessive application of both commercial inorganic and organic fertilizers to attain desire crop yields. In the era of climate change, agricultural farms face heightened vulnerability to unpredictable and uncontrollable losses due to factors such as drought, frost, highly variable precipitation (in terms of amount and frequency), natural disasters, and invasive species. Fertilizer application is a controllable variable that positively influences crop growth, quality, and yield. To tailor fertilizer, use to the specific needs of a crop, extensive background testing such as soil analyses are necessary, and these preliminary processes can be labour intensive, expensive, and often time consuming. Consequently, due to the relative affordability of fertilizers, they are frequently applied in excess of the actual nutrient requirement.

From a global perspective, from 2000 to 2015, population growth was 20%, while the total fertilizer (including nitrogenous, potash and phosphate fertilizers) used per area increased by 34% (from 85.9 kg/ha to 115.1 kg/ha) (FAO, 2022). In Europe, over 10 years (2001 to 2011) the quantity of reactive nitrogen resulting from fertilizer application had tripled, with 40 to 70% being lost to the environment (Sutton et al., 2011). In Canada, since 2010, the application of agricultural fertilizers has risen by approximately 60%, with nitrogen-based fertilizer accounting for the largest share, amounting to 2.9 million tonnes out of a total 4.6 million tonnes in 2022 (Statista, 2024). However, Canada's nitrogen (N) use efficiency of applied fertilizers averaged 64% from 2020 to 2022 (FAOSTAT, 2025), indicating that 36% of N was not absorbed by crops. This suggests an overapplication of fertilizer, leading to surplus nutrient losses to leaching and runoff. Excess fertilizer, along with sediments, pathogens and pesticides can migrate to surface water via subsurface tile drainage systems - a necessity in humid agricultural landscapes like Canada - or through overland flow from fields, thereby contributing to anthropogenic eutrophication, hypoxia (< 2 mg/L dissolved oxygen) and eventually the formation of 'dead zones' (Watson et al., 2016).

Harmful algal bloom (HAB) induced eutrophication associated to non-point sources (NPS), particularly from agricultural sources, have been reported globally. It is estimated that there are at least 500 hypoxic near coastal sites worldwide, a number that has quadrupled since 1950s (Breitburg et al., 2018). The Gulf of Mexico hypoxic zone is the second largest dead zone in the world, covering approximately 17,366 km^2 in 2024, according to an annual dead zone survey (NOAA, 2024) and it can expand to 23,000 km^2 during peak HABs growth (Rabalais et al., 2002). It is estimated that the 25% of total nitrogen (TN) and 38% of total phosphorus (TP) loads in the Mississippi River basin, which contributes to this hypoxia, can be traced back to fertilizers in agricultural drainage (Robertson & Saad, 2021). In Europe, similar eutrophication issues due to excess agricultural N have been reported, such as in the coastal region of Southern Sweden (Larsson et al., 1985; Stålnacke et al., 1999), Denmark (Aslyng, 1980), the Nemunas River in Lithuania (Sileika et al., 2006), Venice Lagoon and the coastal waters of Adriatic in Italy (Borin et al., 2001). A report published by European Environmental Agency (EAA) in 2024 indicated that pressures from agricultural diffused pollution affect 32% of groundwaters and 29% of surface water, continuing to be the most significant pressure on water quality (EEA, 2024).

Over the last five decades, the Laurentian Great Lakes have experienced significant nutrient loading from both point sources, including wastewater treatment plants, stormwater discharges and industrial activities, and non-point sources including agricultural drainage and runoff and decentralized wastewater discharges (Figure 2-1). This has resulted in serious eutrophication (manifested through toxic HABs), with over 20 hypoxic zones in the Great Lakes, particularly Lake Erie's zone covering 1.2 million ha (Michalak et al., 2013; Tellier et al., 2022). The direct and indirect effects of these zones on humans, wildlife and livestock health are well documented. The economic repercussions have been substantial; for instance, the 2014 HAB in western Lake Erie necessitated a multi-day drinking water advisory in Toledo, United States (U.S.), and subsequent upgrades to the treatment plant, incurring costs of US $65 million (CAD $87 million) in expenditure (Alliance for the Great Lakes, 2022; Bingham et al., 2015). Projections indicate that Lake Erie HABs could impose a financial burden of up to CAD $5.3 billion (approximately US $4 billion) on Canadians over the next 30 years (GLSAB & GLWQB, 2023), whereas mitigation efforts to control these blooms are estimated to cost CAD $2.8 billion.

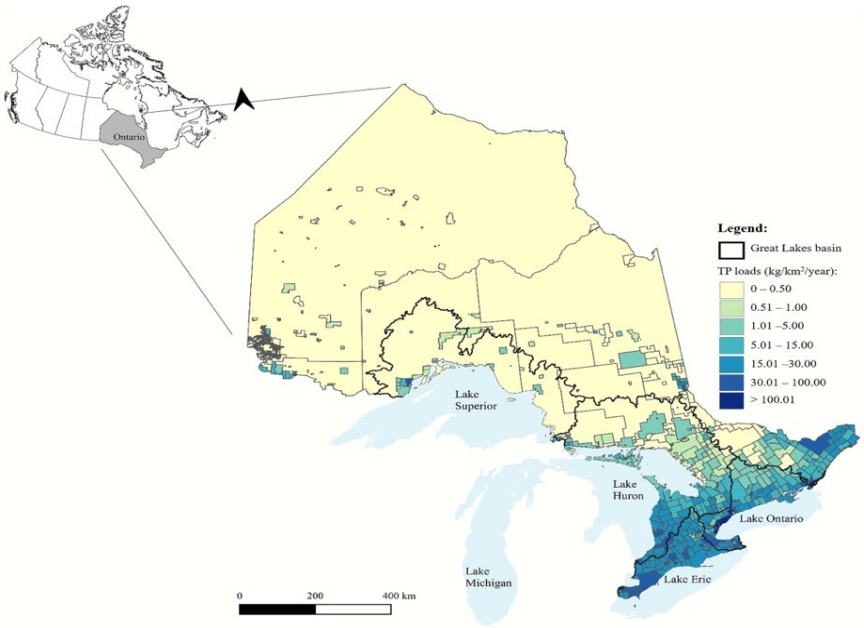

Figure 2-1. Total Phosphorous loadings to surface waters in 2016 (kg/km^2/year) from point and non-point sources in Ontario at subdivision level. Source: Garcia-Hernandez et al. (2022). Note: Ottawa region falls under >100.01 kg/km^2/year.

2.2. Tile drainage – The growing problem

Drainage, a key component of the water cycle, is a natural process that occurs in any landscape. In agricultural/cropping systems, this process is crucial because it reduces waterlogging, increases crop yields, and reduces yield variability. However, natural drainage is insufficient in farms with low soil hydraulic conductivity, increasing the vulnerability to waterlogged conditions. Consequently, approximately 11% of the world's agricultural cropland is artificially drained (Kokulan, 2019). Furthermore, 13.5% of croplands in developed countries, 9% in emerging/developing countries, and 0.9% in the least developed countries are artificially drained (ICID, 2018). In Canada, 14% of agricultural land are tile-drained and whereas, percentage is much higher in the U.S. (27%) (ICID, 2018; Sunohara et al., 2015).

Agricultural drainage includes i) surface drainage, which occurs via on-farm swales and ditches to reroute or store water, and/or ii) artificial subsurface (tile) drainage systems of perforated subsurface pipe systems that allow excess water from subsurface soil for discharge into a receiving water body. In Eastern Canada, cropping systems have been predominantly developed on drained wetlands, formed due to fine, poorly draining, glacially derived soils (Brevé & Skaggs, 1994) with the help of surface ditches and subsurface drainage. In North America, in the late 1800s, the

original tile drains installed in the midwestern United States consisted of pipes with clay, concrete, and wood sections (King, et al., 2015; Kokulan, 2019). Extensive tile drainage systems have been installed since their initial introduction, with plastic pipes substituting for concrete and clay in the tile. In the 1970s, random wet spot drainage was replaced with systematic placements across all fields, with reduced inter-drain spacing owing to the addition of new drains between existing drains (King, et al., 2015).

The tiles are perforated pipes installed in the vadose zone (the unsaturated soil zone between ground surface and regional groundwater table), at depths from 0.6 m to 1.2 m and spacing from 10 to 100 m apart, depending on type of the soils and crop cultivated at the farmland (Moore, 2016). Subsurface drainage systems discharge water primarily through open tile heads or outlets into open ditches or streams (Figure 2-2). The tile drainage system provides an accessible pathway for water in the soil to drain, lowering the water table, improving soil aeration in the upper layers, facilitating deeper root growth, and decreasing crop damage from saturated soil and stagnant water, leading to an increase in crop yields during the growing season (Skaggs et al., 2012; Strock et al., 2010). This system also decreases consecutive year crop yield variability, ensuring stable production under climate change (Blann et al., 2009). Additionally, drainage systems improve accessibility for agricultural operations, allow for earlier and timely sowing and harvesting, and provide a wider choice of crop varieties. However, this subsurface system acts as direct conduit for high flow and nutrient rich water to surface waters. Its influence on hydrology, N and P loading at field and watershed scale is discussed below.

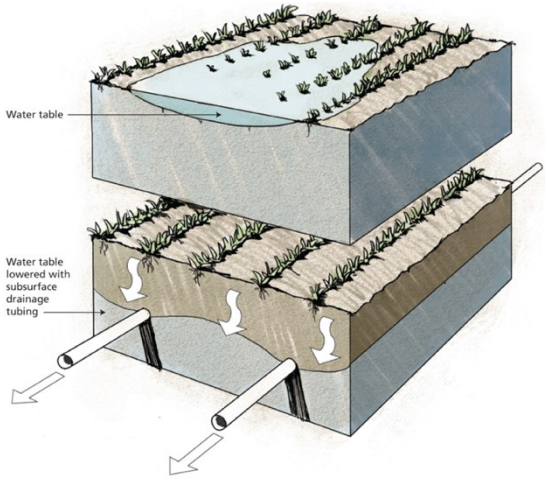

Figure 2-2. Illustration comparing farmland without (Top) and with (Bottom) with subsurface tile system (ASN-OSU, 2017)**.**

2.2.1. Effects of tile drainage on field hydrology

The installation of tile drains to formerly undrained land effectively modifies the vadose zone properties of the field, in turn altering field hydrology and bio-geochemical processes. Tile drainage often increases the annual quantity of precipitation discharged at the expense of groundwater storage and evapotranspiration losses, leading to a 10 to 25% increase in drainage water yields from farmlands (King, et al., 2015). A North American review of nearly 400 tile drainage studies carried out by Christianson and Harmel (2015) reported that from 1961 – 2012, 1279 sites demonstrated tile drainage outflow accounted for a mean of 25% (range 6–49%) of annual precipitation received. Similar ranges were reported in studies carried out in Lithuania (Bučienė et al., 2007) and New Zealand (Tanner & Sukias, 2011). Several studies observed higher a range of 47 to 97% of annual tile outflow as a percentage of total field water output (King et al., 2014; Tan & Zhang, 2011; Van Esbroeck, 2015). Variety of factors influence the hydrologic behaviour of tile drained fields (Moore, 2016), some positively or variably, such as precipitation amount and intensity (positive), antecedent soil moisture content (positive), soil texture (variable), cropping and tillage (variable) and system design (variable).

Although tile drainage increases the total water yield, research studies have shown that surface runoff is rarely observed in tile-drained farms, along with a significant decrease in sediment yield (Brevé & Skaggs, 1994; Dolezal et al., 2001; Van Esbroeck et al., 2016). This response is due to the increased infiltration capacity of tile-drained soils. The soil absorbs precipitation and decreases peak and surface runoff volumes. Surface runoff is only observed during excessively wet conditions, when the water quantity in fields exceeds the tile drainage capacity or when precipitation occurs at a greater rate than the soil infiltration capacity (Dolezal et al., 2001; King, et al., 2015; Macrae et al., 2007). Tile drainage reduces surface runoff, erosion, and related soil nutrient losses from eroded soil particles high in nutrient content.

2.2.2. Effect of tile drainage on N concentrations and loads

2.2.2.1. Forms of N

Nitrogen, the most abundant element in the atmosphere, exists in both organic and inorganic forms within agricultural systems. Figure 2-3 illustrates the major forms and transformation pathways of N takes as it cycles through an agricultural production system. Cropping systems receive N via fertilizers or through N fixing legumes to enhance crop yields. Following application, inorganic N

enters the soil primarily as ammonium (NH_4^+) or is rapidly hydrolyzed to NH_4^+ (e.g., urea-based fertilizers). NH_4^+ maybe be taken up by plants, temporarily retained on soil exchange sites, or incorporated into microbial biomass through immobilization.

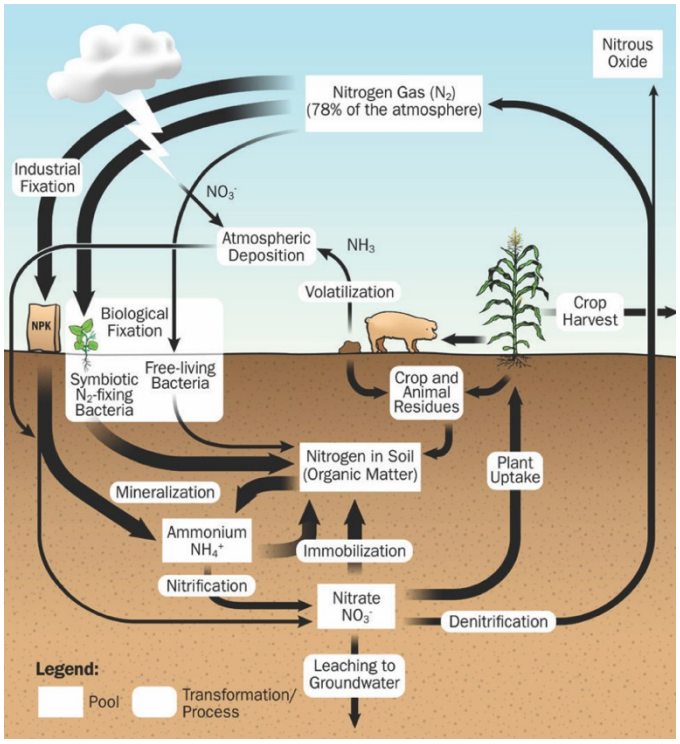

Figure 2-3. Conceptual representation of the nitrogen (N) cycle in agricultural systems, illustrating major N inputs, transformations, and loss pathways (OMAFA, 2025).

NH_4^+ may subsequently be oxidised to nitrate (NO_3^-) via nitrification under oxic conditions. Within the rooting zone, NO_3^- may be reduced to nitrogen (N_2) through bio-mediated denitrification under low oxygen conditions in the presence of labile organic carbon. Such conditions are favoured in soils with slow internal drainage, fine-textured soils, and during periods of saturation. N can move from agricultural soils to surface waters and groundwater in both soluble and particulate forms. Soluble N losses occur predominantly as NO_3^- ions with smaller contributions from dissolved organic N (DON) and NH_4^+ (Rasouli, 2013). The negatively charged NO_3^- is highly mobile and susceptible to leaching through soil matrix into tile drainage water when compared to positively charged NH_4^+ ions. Typically, NH_4^+ binds with negatively charged clay or organic matter in soil which are then stored in plant-available form, reducing its mobility. Hence, the greatest losses of N from tile drains occur as NO_3^- ions and are often reported as NO_3^- - N for

tile drainage water N concentrations (Dinnes et al., 2002; Kladivko et al., 1991). The other forms of N such as TN or NH_4^+ are rarely reported in previous studies.

2.2.2.2. N in tile drainage

Tile drainage often contributes to a significant N loss from agricultural fields (Table 2-1). Randall & Goss (2008), in a review of 26 studies across Europe and North America, reported that tile drain NO_3^- loads ranged from <1 to 100 kg/ha, with mean loads around 25 kg/ha. Quantitatively, on average, tile drains contribute 54% of the annual watershed NO_3^- loads (Schilling & Zhang, 2004; Williams et al., 2015a). The variation in NO_3^- concentrations in tile drainage water is influenced by uncontrollable factors such as precipitation, temperature and soil organic matter mineralization (could be manipulated to a degree by tillage) or by controllable factors such as N fertilizer application rates and timing, the form of N used, tile flow rate, tile spacing and depth, tillage system, cropping systems, improper crediting of N from organic sources, and addition of nitrification inhibitors (Brouder et al., 2005; Dinnes et al., 2002).

Table 2-1. Range and mean of nitrate concentrations in tile drainage as reported in literature.

Location	Climatic Zone^	Crops Grown	Soil type	Concentration (mg N/L) Range (Mean)	Reference
USA	*Cfa*	Corn	Silt loam	(18.6 to 25,16.9 to 31, 28.3 to 34.6)	Kladivko et al. (1999)
Italy	*Cfa*	Corn, sugar beets	Sandy Loam	M: 33	Borin et al. (2001)
Canada	*Dfb*	Corn-soybean	Clay loam	(7.3 to11.4)	Drury et al. (2001)
USA	*Dfa*	Corn-Soybean	Fine loamy	5 to 45 (6 to 28)	Jaynes et al. (2001)
Canada	*Dfa*	Corn	Sandy loam	5.8 to 40.9 (19.2*)	Ng et al. (2002)
USA		Corn-Soybean	Silty clay loam	10.2 to 20.4*	Sands et al. (2008)
USA	*Dfa*	Corn-Soybean	Clay loam	(3.9 to 28.7*)	Lawlor et al. (2008)
Canada	*Dfa*	Corn-Soybean	Clay loam	(10.7 to 11.9[a]) (5.59-5.66[b])	Drury et al. (2009)
Lithuania	*Dfb*	Winter wheat	Loam Sandy	5 to 23	Ramoska et al. (2011)
Sweden	*Dfb*	Potato, sugar beet, cereals	Sandy Loam	0.4 to 5.1	Wesström et al. (2014)
USA	*Cfa*	Corn-Soybean	Silt loam – Clay loam	0.1 to 70.5 (7.4 to 10.8)	Williams et al. (2015b)
USA	*Dfa*	Corn-Soybean	Fine loamy	(M: 10.5 to 17.8)	Ghane et al. (2016)
Netherlands	*Cfb*		Clay	0.5 to 15.1	Rozemeijer et al. (2016)

Location	Climatic Zone^	Crops Grown	Soil type	Concentration (mg N/L) Range (Mean)	Reference
USA	*Dfa*	Corn-Soybean	Silt clay loam, Silt loam	0.9 to 14.4	Lavaire et al. (2017)
Denmark	*Cfb*	Winter wheat	Silty loam	6.8 to 8.2	Carstensen et al. (2019)

^Köppen−Geiger climate classification (Kottek et al., 2006)
*Flow weighted concentration
[a]Growing season
[b]Non-growing season
M represents median of N concentrations

2.2.3. Effect of tile drainage on P concentrations and loads

2.2.3.1. Forms of P

Phosphorus in agricultural systems occurs un both organic and inorganic forms and cycles primarily within the soil-plant-microbe continuum. Figure 2-4 illustrates the major forms and transformation pathways of P in agricultural soils. Cropping systems receive P mainly through mineral fertilizers and organic amendments applied to support crop growth. Following application, P attaches to soil particles and metal oxides such as iron, aluminum, calcium, manganese, and magnesium, which strongly regulate its. Mobility and bioavailability in soils (Sims et al., 1998). The sorption-desorption behavior of P in soil is influenced by soil pH and under saturated or reduced conditions, by redox processes that affect the solubility of iron- and manganese-associated P compounds (Scalenghe et al., 2002). As a result, soil P is partitioned among soluble and particulate pools and between inorganic and organic forms that may be interconverted through biological mineralization, immobilization, and geochemical reactions. While soluble inorganic P is directly available for plant uptake, much of the soil P pool remains strongly bound and is only slowly released over time (Karsten & Vanek, 2021).

P can be transported from agricultural soils primarily through erosion and runoff as particulate P (PP), or through leaching as dissolved P (DP). Dissolved P losses are generally lower than NO_3^- loses due to strong soil retention but may increase in soils with low P sorption capacity or following saturation events or conditions (King, et al., 2015). In agricultural studies, soil and drainage P are commonly characterized using operationally defined fractions, including TP, PP and DP. Studies also report soluble reactive phosphorus (SRP), which is synonymous with dissolved reactive phosphorus, a measure of orthophosphate that is bioavailable for uptake by microorganisms, including bacteria, algae, and plants (APHA, 2017).

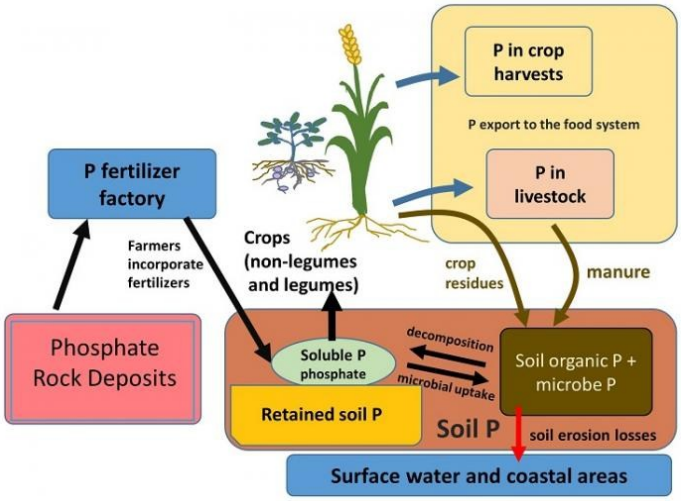

Figure 2-4. Conceptual phosphorus (P) cycle in agricultural systems, showing major inputs, soil transformations, and loss pathways (Karsten & Vanek, 2021)

2.2.3.2. P in tile drainage

Under general baseflow conditions, DP has been found to be a significant form of P in tile drainage (Heathwaite & Dils, 2000; King et al., 2016). However, under specific conditions, such as high flow, immediately after storm events following periods of low rainfall, during spring snowmelt, or after fertilizer application, PP was found to be the dominant component of TP, ranging from 47 to 92% (Carefoot & Whalen, 2003; Simard, 2005; Tan & Zhang, 2011). The DP and PP loads in tile drains are mostly controlled by preferential macropore flow, which connects the soil surface to the drains. DP loss is favored when mineral fertilizers or manure are used, along with post-application precipitation or snowmelt events. Such circumstances cause P to desorb and leach (Heckrath et al., 1995) due to soil waterlogging and ideal reducing conditions (Scalenghe et al., 2002). However, PP loss correlates with the loss of particles and associated P that occurs during peak flow events (Gentry et al., 2007; Ulén, 2004) and is more frequent in fine-textured soils (Eastman et al., 2010; Uusitalo et al., 2001).

Table 2-2. Range and mean P Concentrations in Tile drainage reported in literature.

Location	Climatic Zone^	Crops grown	Soil type	TP (mg P/L) Range (Mean)	DP (mg P/L) Range (Mean)	Reference
Finland	*Dfb*	Barley-wheat	Clay	0.46 to 1.42	0.03 to 0.078	Uusitalo et al. (2001)
Canada	*Dfb*	Corn-soybeans	Loam-sandy loam	0.04 to 0.13 (0.01) 0.02 to 0.04 (0.13)	0.01 to 0.03 (0.03) <0.01 – 0.01 (0.01)	Beauchemin et al. (2003)

Location	Climatic Zone^	Crops grown	Soil type	TP (mg P/L) Range (Mean)	DP (mg P/L) Range (Mean)	Reference
Canada	*Dfb*	Corn, soybeans, barley	Clay loam	M:0.167 to 0.198 M: 0.013 to 0.053	M: 0.069 to 0.082 M: 0.002 to 0.024	Simard (2005)
Spain	*Csa*	Cotton, sugar beets	Clay	0.072 to 0.152	0.039 to 0.073	Delgado et al. (2006)
Canada	*Dfb*	Corn, soybeans, wheat	Loam, silt loam	0.005 to 8.275 (0.044 - 1.5)	0.001 to 2.85 (0.009 - 0.549)	Macrae et al. (2007)
Sweden	*Dfb*	Potato, small grains	Loamy sand	(0.022)	(0.006)	Wesström & Messing (2007)
Canada	*Dfb*	Corn-soybeans	Clay	(0.480*[a])	(0.034*[a])	Tan & Zhang (2011)
Canada	*Dfb*	Wheat, corn-soybeans	Silt loam, clay loam	(0.01 to 0.02)	(0.001 to 0.002)	Van Esbroeck (2015)
Sweden	*Cfb*	Wheat, small grains	Clay	0.72	0.19	Ulén et al. (2016)

M represents median of Phosphorus concentrations
[a]Mean of 5-years of study
*Flow weighted mean concentration

Extensive research studies have documented that significant P concentrations are transported by tile drainage systems. This is generally attributed to the increased infiltration capacity (i.e., increased vertical movement) owing to tile drainage, which provides P, a direct connection from a field to nearby water bodies. Thus, nutrients that reach the tile drain can be carried from a larger area than would otherwise be possible runoff (Heathwaite & Dils, 2000). In fact, in the Lake Champlain Basin (covering New York, Vermont and Quebec), it is estimated that 7.3% of the total 13% of the annual TP load to surface water could be attributed to tile drainage (Moore, 2016). From Table 2-2, ranges vary largely because of soil characteristics, drainage intensity (depth and spacing), management practices (tillage, cropping system, soil test P, P source, P application (rate and timing)), hydrology (base flow, event flow), and season.

2.3. Regulatory framework concerning water quality from agricultural drainage

The Canadian federal regulatory framework takes a guideline approach (science-based benchmark) while the Province of Ontario takes an objectives approach (minimum acceptable water quality level) to address the levels of contaminants in surface waters (MOE, 1979) and protection of aquatic life (CCME, 2025). The existing limits and guidelines are as follows –

Table 2-3. List of Existing Federal and Provincial Guidelines/ Objectives/ Standards for Water Quality

Parameter	Level of Government	Guideline/Objective/ Standard	Concentration Description	Reference
Nitrate as N	Federal	Guideline for protection of aquatic life in freshwater	3 mg NO_3^--N/L for long term exposure and 124 mg NO_3^--N/L for short-term exposure	CCME (2012)
Ammonia (unionised)	Federal	Guideline for protection of aquatic life in freshwater	0.019 mg NH_3-N/L	CCME (2010)
	Provincial[O]	Objective for water quality	0.020 mg NH_3-N/L	MOEE (1994)
Phosphorus (Total)*	Federal	Guideline for protection of aquatic life in freshwater	Tiered approach, concentrations should not exceed 'trigger ranges' and should not increase more than 50% over the reference (baseline). Ranges are: ultra-oligotrophic (<4 µg/L) oligotrophic (4-10 µg/L) mesotrophic (10-20 µg/L) meso-eutrophic (20-35 µg/L) eutrophic (35-100 µg/L) and hyper-eutrophic (>100 µg/L)	CCME (2004)
	Provincial[O]	Guideline (Interim) for water quality	Ice-free period – should not exceed 20 µg/L, a high-level protection against aesthetic deterioration will be provided at 10 µg/L or less excessive plant growth in rivers and streams should be protected below 30 µg/L	MOEE (1994)
Solids	Federal	Guideline for protection of aquatic life in freshwater	From background levels, Clear flow, short term exposure (less than or equal to 24 hours) - maximum increase of 25 mg TSS/L Clear flow, longer term exposures (1 to 30 days) - maximum average increase of 5 mg/L. High flow - same applied for background concentrations between 25-250 mg TSS/L, however, should not increase more than 10% for background levels greater than 250 mg TSS/L.	CCME (1999)

*There is no regulated criterion or guideline under the CCME or PWQO for SRP, however, the CCME guideline for trophic levels of freshwater systems and the provincial interim guideline for TP is considered to apply for SRP as well (CCME, 2004; MOEE, 1994).
[O]Province of Ontario

Point sources have been subject to stringent regulation for many years through federal mandates such as Wastewater Systems Effluent Regulations (WSER) under the Fishers Act, which governs that regulates point source discharges from municipal treated wastewater into fish-bearing surface waters (ECCC, 2012). Under WSER, effluent quality standards are set at ≤ 25 mg/L for

Carbonaceous Biological Oxygen Demand (cBOD) and TSS. Provincial regulations under the Ontario Environmental Protection Act (OEPA) (OMECP, 1990a) and the Ontario Water Resources Act (OWRA) prohibit the discharge of pollutants into surface or groundwater without approval, addressing both municipal and industrial discharges (OMECP, 1990b).

In contrast, the identification and mitigation of NPS pollution is challenging due to its variable interactions with precipitation, geography, and soil stratigraphy (US EPA, 2014). This issue is critical, as nutrient load from NPS, largely associated with agricultural activities, is now reported as the main contributor to HAB in Gulf of Mexico, Lake Erie (GLSAB & GLWQB, 2023). In fact, agricultural NPS pollution is estimated to negatively affect 50% of river miles in the US (US EPA, 2007), and over 75% of TP loading to Lake Erie originates from NPSs, with agriculture constituting a major pathway for P (OMECP, 2024). However, loadings from non-point sources (NPS), specifically, agricultural NPSs are not regulated by federal regulations and at provisional level, are indirectly regulated through Nutrient Management Act (NMA) via management planning, application rates and BMPs, rather than strict numeric discharge standards as in point source regulations (OMAFA, 2002). The NMA, through a nutrient management strategy (NMS), nutrient management plan (NMP) or non-agricultural source material plan (NASM plan), aims to provide environmental protection and a sustainable future for agricultural operations and rural development by helping producers manage land application of nutrients under their control. Under regulation O. Reg. 267/03, NMPs must balance N inputs with crop needs, establish setbacks from wells and watercourses, prohibit land application of manure, commercial fertilizers on snow covered soils and specifies manure storage standards (OMAFA, 2002). For phosphorus, NMP must limit P application limit to crop removal rates, include soil P test every 5 years, restrict P application on high-testing soils (Between $\geq$ 60 ppm and $<$ 120 ppm, P can only be applied or at crop removal) and establish setbacks and no-spread zones from watercourses if risk factors such as slopes, high P soil exist (OMAFA, 2002).

In the US, national and regional hypoxia task forces have been established to address localised eutrophication issues. The Gulf of Mexico Action Plan, initially formulated in 2001 and subsequently updated in 2008 and 2015, aims to reduce the five-year running average area of the hypoxic zone to less than 5,000 km^2 by 2035. This plan includes a significant commitment to achieving a 20% reduction of influent N and P loading by 2025 (US EPA, 2015). The Bipartisan

Infrastructure Law (US EPA, 2022) allocates funding for workplans developed by 12 states to support the commitments of the action plan. These plans involve conducting high-frequency surface and groundwater quality monitoring, identifying, and implementing agricultural BMPs and conservation strategies at both farm and watershed levels (trial programs) and creating community outreach programs.

Regulatory agreements, directives, and initiatives have been implemented by Canada and the U.S. to tackle the hypoxia in the Laurentian Great Lakes. Notably, the 1972 Great Lakes Water Quality Agreement (GLWQA) between Canadian and US governments (last amended in 2012) and the Canada-Ontario Lake Erie Action Plan (LEAP) (ECCC, 2018a) aim to reduce TP loadings to Lake Erie by 40% by 2025 (from 2008 spring levels). Various domestic action plans (DAPs) have been developed, which are site- and agricultural sector- specific. These include the Great Lakes Protection Initiative (GLPI) (ECCC, 2018b) and Ontario province specific plans such as the Lake Erie Agriculture Demonstrating Sustainability (LEADS) program (OSCIA, 2023) and On-Farm Applied Research program (OMAFA & OSCIA, 2019). Situated in the Lake Erie region, Ontario accounted for 26% of total farms and 8% (11.8 million acres) of total farmland in Canada, leading all provinces in corn (60%) and soybean (54%) grain acreage in 2021 (Statistics Canada, 2022). Of this, an estimated 1.75 million hectares or approximately 48% of cropland in Ontario is tile drained. However, it is believed that the modern records of tile drainage are incomplete, and the true extent is likely much larger (Eimers et al., 2020; Lockett et al., 2024). Moreover, the concentrations of nutrients in drainage and runoff from cropland is relative to various, interrelated factors, such as – land management practises, soil type and characteristics, topography, climatic conditions, etc. As shown in Table 2-1 and 2-2, the NO_3^- and P concentrations vary among different sites; however, they are still high, surpassing federal and provincial guidelines, objectives and standards for these parameters listed in Table 2-3. Therefore, Ontario DAP programs emphasize the on-farm implementation and evaluation of agricultural Beneficial Management Practises (BMPs) and aim to establish comprehensive long-term research data to validate performance of BMPs across various jurisdictions.

A variety of practises – In-field and Edge-of-field, have been identified to manage tile drainage in agricultural production systems. In-field methods include agronomic management like the 4R principle (**R**ight fertilizer source, **R**ight rate, **R**ight time and **R**ight place) (Dinnes et al.,

2002; King, 2015), reduced tillage and no-till cultivation practices, crop rotation & cover crops (Drury et al., 2014a; Zhang et al., 2017) and unconventional methods such as using nitrification inhibitors (popular in U.S. upper Midwest) (Dinnes et al., 2002). Conversely, edge-of-field methods provide producers a way to reduce drawbacks associated with tile drainage without having to comprise on productivity or change their farming practices, such as – drainage ditch management, constructed wetlands (CW), controlled drainage (CD), treatment ponds, buffers and vegetative filter strips, woodchip bioreactors, side – inlet controls and reactive barriers.

2.4. Controlled Drainage

Controlled drainage, interchangeably synonymous with drainage water management, controlled tile drainage or conservation drainage, is a BMP and conservation engineering practice aimed at managing water discharges from subsurface agricultural drainage systems (BRDFN, 2018). CD has been recognized as an edge-of-field practice that balances crop production and conservation goals by managing the timing and quantity of water discharged from farmlands, thereby reducing N and P loads in tile drainage. This type of drainage system involves retrofitting existing tile drainage systems with one or more flow-restricting devices such as stop logs, risers, gates, or valves (Figure 2-5). CD holds water in the soil column while deployed, increasing plant moisture availability during dry periods and reducing tile discharge, while permitting drainage when there is excess soil moisture.

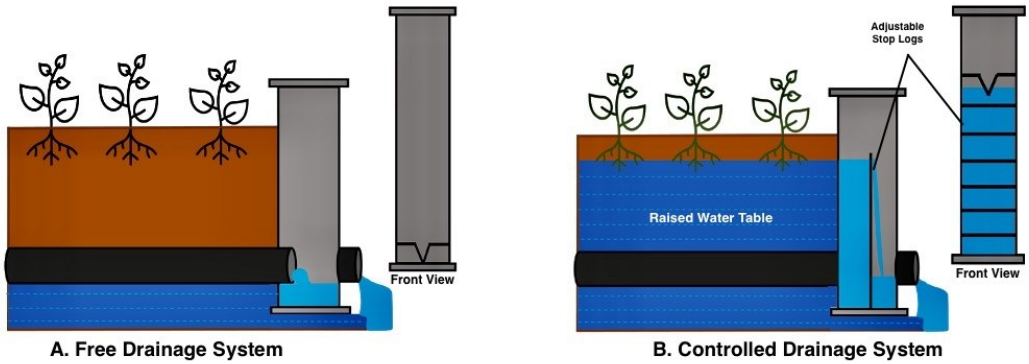

Figure 2-5. Free flowing drainage (A) and controlled drainage (B) systems. The front views show the placement of V-Notch weir and adjustable stop logs in the two systems.

Currently, three types of CD technologies exist (OSCIA 2018) – 1. manually controlled structures, where the water level is maintained through manual addition or removal of physical flow barriers (such as stoplogs) during physical visits by farmers; 2. basic automatic which

involves placing two valves inside the structure and running a program set by the farm operator during an annual visit; and 3. remote controlled automatic systems which are like basic automatic systems but can be operated remotely; that is, no visits are required. The CD is suitable for fields where a pattern drainage system is installed or feasible, as opposed to a random system. To be effective, CD requires flat fields (<1%) with a narrower drain spacing (preferred). Crop lands are divided into "drainage management zones," where one control structure manages each zone and can typically control at up to 40,000 m^2 or 80,000 m^2 of land (Frankenberger et al., 2006). The life expectancy of a CD system is expected to be as long as that of a conventional tile drainage system, typically >50 years (PAMI, 2018).

The outlet depth (i.e., the height of the physical barriers placed) is crucial in drainage water management practices and is determined based on factors such as the season, field operation, precipitation, and crop growth stage (Frankenberger et al., 2006). For instance, during heavy precipitation, excess water is drained, preventing waterlogging of crop roots, whereas during dry periods, barriers are maintained. Once physical barriers are installed, the water table must rise to the outlet depth for flow to occur, as shown in Figure 2-5 B. In warmer climates, outlet depths are changed four times a year: lowered before planting (to allow field operations), raised again after planting (water storage during mid-summer for crops), lowered again before harvesting (to allow field operations) and raised after harvest (reduced drainage outflow during the off-season) (Frankenberger et al., 2006; Skaggs et al., 2012). However, in colder climates such as Eastern Ontario, CD is not recommended in winter due to ice buildup inside control structures and drainage ditches (Frankenberger et al., 2006; Sunohara et al., 2016), possible increases in phosphorus (P) mobilization from soil saturation (Ball Coelho et al., 2012; King, et al., 2015), and chances of ice sheeting and shallower, longer-lasting soil frost, leading to longer spring warming periods (OMAFRA, 1991). Although the optimum outlet height during the growing season is yet to be determined, researchers suggest an outlet depth of 2 feet or 0.6 m below the field surface (Frankenberger et al., 2006). This ensures that sufficient drainage is provided for good aeration and root development, along with the capture of water that would otherwise be drained freely, thereby minimizing surface water ponding.

2.4.1. Effect on water table

In free drainage (FD) systems, drain flow is continuous, and the water table fluctuates in response

to meteorological conditions and crop water use. Beeper drain placement limits capillary rise to the root zone and promotes deep percolation, increasing drainage losses (Ayars et al., 2006). In contrast, CD maintains a shallower water table by reducing hydraulic gradients, thereby limiting deep percolation below root zone, and enhancing upward capillary flow. As a result, tile outflow is reduced and soil water availability for crops is increased. Field studies generally report higher soil moisture contents and shallower water tables under CD compared with FD. Ng et al. (2002) observed a mean FD-to-CD soil water content ratio of 0.82 and a water table depth ratio of 1.59, indicating substantially greater moisture availability in CD plots. Similar improvements in soil moisture under CD have been reported during critical crop growth periods by Mejia et al. (2000). However, not all studies show this response; in an Illinois study, Woli et al. (2010) reported lower soil moisture at the surface and at 20 cm depth under CD, attributing this to the failure of tile water to reach the outlet control depth, highlighting the importance of appropriate drainage outlet depth.

Seasonal and event-based variations in water table depth have been reported under CD. During their 4 years of study, Helmers et al. (2012) documented consistently higher water tables under CD than FD in spring and fall, with an average difference of approximately 20 cm and rapid water level increases following rainfall events that typically subsided within two days. Other studies have similarly shown that although CD and FD may respond comparably to precipitation, water tables under CD remain elevated for longer periods and decline more slowly, potentailly refelcting increases soil water retention (Sanchez Valero et al., 2007; Sunohara et al., 2014). Jaynes (2012) reported that target control depths were rarely achieved during winter but were often reached in early spring following soil thaw and the resumption of infiltration. During growing season, water tables commonly declined below control level due to increases evapotranspiration and reduced precipitation, despite the presence of outlet controls. Similar observations were reported for growing season by few studies in the U.S. Sanchez Valero et al. (2007) and Stampfli, (2003) in combination with observed lateral water movement. Overall, while CD systems consistently maintain higher water tables than FD systems, the magnitude and persistence of this effect vary with climate, soil properties, outlet management, and crop water use. These factors should be carefully considered when comparing results across studies and assessing the hydrological benefits of CD.

2.4.2. Effect on tile outflows

A characteristic outcome of CD implementation is its influence on total tile outflows. CD has been widely adopted in the U.S. for more than three decades (Frankenberger et al., 2024; Ross et al., 2016a; Skaggs et al., 2012), where it is often operated year-round due to favourable climatic conditions. Across these studies (Table 2-4), CD generally reduces tile drainage relative to FD, with reported reductions ranging from 8% and 100% reduction and an average of 44%. Water retained by outlet controls increases evapotranspiration, plant water use, and infiltration, thereby limiting drainage outflow. However, the magnitude of flow reduction varies considerably and is strongly influenced by outlet control height, site characteristics, and precipitation amount and timing.

Outlet height in a key determinant of CD effectiveness. Although an optimum outlet height has not been definitely established, researchers suggest maintaining height at 0.6 m below the soil surface (Frankenberger et al., 2006). Williams et al. (2015b), however, reported annual flow reductions (8-34%) when outlet control was set at 0.45 m below the soil surface, compared with studies employing 0.6 m outlet elevations. The authors conclude that greater flow reductions are generally achieved as outlet control levels approaches the soil surface. Seasonal adjustment of outlet heights has also been shown to enhance drainage control efficiency, particularly when aligned with crop growth stages and field operations (Adeuya et al., 2012; Skaggs et al., 2012).

Topography imposes an additional constraint on CD performance by limiting the proportion of a field influenced by outlet control. Jayne (2012) observed a 21% reduction in flow under CD on a moderately sloped field (0.8%), where drainage control effects were spatially restricted. In general, CD is most effective on flatter landscapes, typically with slopes below 1% and optimally between 0 to 0.5%. Ross et al. (2016) showed that, for the 25 sites reviewed, CD reduced growing season outflow by 43.8% (p-value <0.001), with greater reductions occurring at sites with deeper and/or narrower drain spacing that increased water storage within the controlled zone.

Precipitation patterns exert a dominant control on CD performance. Most studies indicate that the annual tile outflow from CD systems closely follows precipitation trends, such that during very dry conditions, CD may eliminate drainage entirely, whereas during very wet years differences between CD and FD may be minimal (Evans et al., 1995). In studies where CD was

operated year-around, flow reductions were generally more pronounced during the growing season due to increased evapotranspiration, while a larger proportion of drainage occurred during the non-growing season (Helmers et al., 2012; P. Nash et al., 2015; Riley et al., 2009). Poole et al. (2018) further demonstrated that CD is most effective when periods of excess rainfall are followed by dry periods (69% reduction), but substantially less effective when rainfall is evenly distributed and meets or exceeds evapotranspiration demand (only 19% reduction). Beyond cumulative flow volumes, CD can also modify peak drainage behaviour. Reduced magnitude and frequency of peak discharge events have been reported under CD when antecedent water levels are below the outlet control height, allowing precipitation to recharge soil storage before drainage occurs (Gunn et al., 2015). Under such conditions, CD can attenuate peak flows by delaying or limiting drainage responses. However, this effect is likely diminished or absent in years with evenly distributed precipitation or when antecedent water levels are already at or near the outlet control height.

In contrast to U.S. studies, CD research in Canada is limited to the growing season, from planting to pre – harvest, due to climatic constraints. Studies conducted in Ontario, Quebec, and Nova Scotia, report average tile flow reduction of 31%, with values ranging from 9% and 64% when CD is compared with FD (Table 2-4). When CD is employed from May to mid-October, substantial reductions have been observed; for example, Sunohara et al. (2016) reported a 60% reduction (p-value < 0.05) in total drainage flows over nine growing seasons, with significantly muted to absent drainage responses under CD relative to FD. Conversely, under wetter-than-normal conditions, CD effectiveness has been shown to decline, with relatively small reductions (< 12%) in total drainage volume (Smith & Kellman, 2011). Other studies have reported little to no effect due to dry weather (Madramootoo et al., 2001) or increased drainage flows from high rainfall (Stampfli, 2003).

Taken together, North American evidence indicates that CD can substantially reduce tile outflow, particularly during the growing season. However, existing studies have focused primarily on cumulative drainage volumes only when CD is employed. The short-term drainage behaviour immediately following stoplog removal and its contribution to cumulative drainage losses and overall water retention has not been explicitly quantified. This potential drainage flush during transitions in CD management represents a critical but overlooked component of CD performance.

Table 2-4. Summary of Effects of Controlled Drainage on Drainage Outflow as reported in the literature.

Location (Province/State, Country)	Soil	Climate Type[C]	Years	Area (ha)	Drain Spacing (m)	Drain Depth (m)	Control depth (m)	Reduction in drainage (%)	Reference
Quebec, Canada	Sandy Loam	*Dfb*	2[G]	4.2 (6)		1.4	0.6	0 & 20[¶]	Madramootoo et al. (2001)
Ontario, Canada	Clay loam	*Dfb*	2[G]	0.1	7.5	0.6	0.3	16 [P]	Gaynor et al. (2002)
Ontario, Canada	Sandy Loam	*Dfb*	1[G]	3.8 (2)	6.1		0.6	8[¶]	Ng et al. (2002)
Ohio, U.S.A.	Silt Clay	*Dfa*	5	0.72 (12)	6	0.8	0.3	40	Fausey (2005)
Quebec, Canada	Fine Sandy Loam	*Dfb*	1[G]	4.2		1	0.6	27[¶, P]	Sanchez Valero et al. (2007)
Ontario, Canada	Clay loam	*Dfb*	4[G]	1.51 (15)	7.5	0.6	0.3	38-49[¶, P]	Drury et al. (2009)
Illinois, U.S.A.	Silty Clay Loam	*Cfa*	2[G]	11 & 13	34.5		0.15*	74 [P]	Woli et al. (2010)
Ontario, Canada	Clay	*Dfb*	5	0.66 (2)	4.6	0.6	0.6 to 0.4	32.5 [P]	Tan & Zhang (2011)
Nova Scotia, Canada	Sandy Loam	*Dfb*	1[G]	3.5	12	0.8	0.8 to 0.6, 0.2	12.7	Smith & Kellman (2011)
Indiana, U.S.A.	Fine Loam	*Cfa*	2	3	21	1	0.15 to 0.6*	19	Adeuya et al. (2012)
Iowa, U.S.A.	Clay Loam	*Dfa*	2	22 (6)	27.4 & 36.5	1.42	0.61 to 1.22*	17.2	Fang et al. (2012)
Iowa, U.S.A.	Clay Loam	*Dfa*	4	22 (5)	36.5	1.22	1.2 to 0.61 to 0.15	21 [P]	Jaynes (2012)
Iowa, U.S.A.	Silty Clay Loam	*Dfa*	4	17 (8)	18	1.2	0.76 to 0.3*	37	Helmers et al. (2012)
Illinois, U.S.A.	Silt clay loam Silt clay loam, Silt loam Silt loam Silt clay loam	*Cfa*	2 2 2 2	15 8.1 5.7 16.2	30 15 18 to 21 12	1.15 1.15 1.15 0.85	0.15 0.15 0.15 0.15	44 44 89 38	Verma & Cooke (2012)
Ontario, Canada	Clay Loam	*Dfb*	6	16	7.5	0.6 – 0.7	0.3	9 to 28[¶]	Drury et al. (2014b)
Ontario, Canada	Silt Loam	*Dfb*	4[G]	2 to 7 (8)	17	1	0.6	50 to 64	Sunohara et al. (2014)
Ohio, U.S.A.	Silty Clay Silty Clay Loam Clay Silty Clay	*Dfa*	5	7.2/7.3 20.2/8.1 15/14.2 8.1/7.7 7.7/11.7	12 12 10 12 15	0.8 - 1.2	0.45 or 0.5 to 0.3*	60.3 73.1 74.3 86.2 100	Gunn et al. (2015)
Missouri, U.S.A.	Silt Loam	*Dfa*	4	0.06, 0.08	6.1		0.6	63	Nash et al. (2015)

Location (Province/State, Country)	Soil	Climate Type[C]	Years	Area (ha)	Drain Spacing (m)	Drain Depth (m)	Control depth (m)	Reduction in drainage (%)	Reference
Ontario, Canada	Silt Loam	*Dfb*	7[G]	250, 467	12 to 17	1	0.6	20 to 22 [P]	Sunohara et al. (2015)
Ohio, U.S.A.	Silt loam, Clay Loam	*Dfa*	7	389	15	1	0.45	8 to 34	Williams et al. (2015b)
Ontario, Canada	Silt Loam	*Dfb*	9[G]	2 to 10 (14)	15 to 17	1	0.6	60 [P]	Sunohara et al. (2016)
Illinois, U.S.A.	Silty clay loam, Silt Loam	*Cfa*	2	10.9, 23.1	15.1	0.76	0.32 to 1.06*	10 to 27	Lavaire et al. (2017)
Iowa, U.S.A.	Silty Clay Loam	*Dfa*	4	17 (8)	18	1.2	0.3	60	Schott et al. (2017)
North Carolina, U.S.A.	Sandy Loam	*Cfa*	9	13.8 (8)	22.9	0.9 – 1.15	0.3 0.45 or 0.5	33	Poole et al. (2018)
Indiana, U.S.A.	Silty clay loam Silty Loam Clay loam Silt Loam	*Cfa*	10	3.5 to 3.7 (4)	14	1	0.4 to 0.1	25 to 39[P]	Saadat et al. (2018a)
Nova Scotia, Canada	Sandy Loam	*Dfb*	3[G]	3.5 (9)	12	0.8	0.8 to 0.6, 0.2	24 to 37	Smith et al. (2019)
Ohio, U.S.A.	Silt loam, Clay loam	*Dfa*	10	14.9, 13.8			0.45	8 to 23	Shedekar et al. (2021)

[C] Köppen climate classification used to identify climate type.
[P] indicates significant difference (p-value ≤ 0.05)
* Higher control depth was maintained in the growing period and lowered during rest of the year.
¶ CD with sub-irrigation or bioreactor
(Number) No. of plots used in the study.
[G] indicates CD was employed in growing or cropping season only

2.4.3. Effect on nitrogen concentration and load

Nitrogen losses from tile drainage occur predominantly as NO_3^--N; therefore, the effect of CD on NO_3^--N concentration and load has been extensively investigated. Field studies in North America summarized in Table 2-5 consistently demonstrate that CD reduces NO_3^--N export relative to FD, although the magnitude of reduction and the dominant controlling mechanisms vary across sites and management conditions. Three primary mechanisms have been proposed to explain NO_3^--N reductions under CD (Dinnes et al., 2002): (i) reduced drainage flow, (ii) microbial denitrification under elevated and sustained water tables, and (iii) increased plant N uptake. Among these, reduced drainage flow is the most consistently observed mechanism, while the contribution of biogeochemical and plant-mediated processes depends on control depth, soil type, and seasonal conditions.

Across nearly all studies, NO_3^--N load reduction was strongly associated with reduced drain discharge, indicating that CD primarily functions as a hydrologic control practice. Long-term and multi-site studies conducted in Ontario, the U.S. Midwest, and Atlantic Canada reported NO_3^--N load reductions typically ranging from 8 to 51%, even when flow-weighted or average NO_3^--N concentrations showed little or no change (Drury et al., 2009; Helmers et al., 2012; Jaynes, 2012; Shedekar et al., 2021; Sunohara et al., 2016; Williams et al., 2015b). The magnitude of flow reduction (8 to 60%) was generally comparable to NO_3^--N load reduction, indicating flow dominance over concentration changes and suggesting that reductions in NO_3^--N export can occur without permanent removal of NO_3^--N from the soil system.

The effectiveness of CD is further influenced by site-specific factors, such as soil type and season. Fine-textured soils occasionally exhibited both NO_3^--N load and concentration reductions, whereas coarse-textured sandy soils generally showed load reductions driven almost exclusively by reduced drainage flow (Madramootoo et al., 2001; Satchithanantham et al., 2014; Smith & Kellman, 2011). A recent synthesis by Frankenberger et al. (2024) reported lower NO_3^--N load reductions in poorly drained soils, however, higher reductions observed in less poorly drained soils may partly reflect seepage losses rather than CD effectiveness. Seasonally, NO_3^--N load reductions were typically greatest during the growing season, while elevated concentrations and episodic exports were reported during non-growing periods and spring snowmelt due to increased mineralization, high drainage volumes, and limited plant uptake (Satchithanantham et al., 2014;

Wesström & Messing, 2007).

While hydrologic control dominates NO_3^--N load reduction, several studies suggest that plant uptake and denitrification may contribute to NO_3^--N concentration reduction under favourable conditions. Increased plant N uptake under CD has been attributed to enhanced soil water availability and evapotranspiration, leading to improved N use efficiency and decreased NO_3^--N leaching (Borin et al., 2001; Skaggs et al., 2012; Williams et al., 2015b). Sunohara et al. (2014) credited a significant 59% reduction in N to 3 - 4% higher N in corn-soybean biomass obtained from CD plots, particularly in wetter growing seasons. Similar result was observed by Poole et al. (2018), where 30% reduction (average reduction of 6.3 kg/ha/year) in NO_3^--N export was equal to increase in N removed by harvested grain.

Microbial denitrification is theoretically plausible under CD due to elevated water tables and reduced soil oxygen availability, creating an anaerobic environment within soil pores. However, evidence is largely indirect and inferred from changes in NO_3^--N concentration or redox conditions (Adeuya et al., 2012; Drury et al., 2014b; Elmi et al., 2000; Fausey, 2005; Lavaire et al., 2017; Madramootoo et al., 2001; Woli et al., 2010). Only a limited number of studies have attempted to explicitly identify or justify denitrification within CD. Liu et al. (2019) estimated that approximately 67% of N loss under CD could be attributed to denitrification using a N mass balance approach, though such methods cannot directly confirm microbial pathways. A small number of isotope-based studies have yielded mixed conclusions: Carstensen et al. (2019) reported a 23% reduction in NO_3^--N load with only an 11% reduction in flow, and inferred possible denitrification based on isotope analysis and changes in SO_4^{2-} and NH_4^- concentrations whereas Smith & Kellman (2011) found no isotopic evidence of denitrification and attributed NO_3^--N load reduction primarily to reduced drainage flow.

Overall, the literature indicates that CD consistently reduces NO_3^--N loads primarily through flow control, while reductions in NO_3^--N concentrations and permanent removal via denitrification occur inconsistently and under site-specific conditions. To date, denitrification under CD has not been conclusively demonstrated using soil microbiome-based analyses, leaving uncertainty regarding whether NO_3^--N retained by CD is permanently removed or temporarily stored and later mobilized following stoplog removal and during the post-harvest period.

Table 2-5. Summary of Controlled Drainage on nitrate as N Loads as reported in previous studies.

Location	Soil Type	No. of years	NO_3-N Conc (mg N/L)	Reduction NO_3-N loads (kg/ha)	Mechanism			Reference
			%reduction (conc)	%reduction (load)	Drain flow	Denitrification	Plant uptake	
Ontario, Canada	Clay Loam	3.5 G 4 G	38.5 (FWMC – 11.4 vs 7) 41.7 (FWMC – 7.3 vs 4)	55 (77.2 vs 34.9) 66 (57.6 vs 19.7)	Yes	-	-	Drury et al. (2001)
Quebec, Canada	Sandy Loam	2 G	74 to 80.3[P]	58.3 to 80.4 (A – 7.2, 3 vs 1.41, 1.2)	Yes (only 1st yr)	Yes*	-	Madramootoo et al. (2001)
Ontario, Canada	Sandy loam	1	41 (FWMC – 19.2 vs 11.3)	36 (36.6 vs 57.9)	-	-	Yes*	Ng et al. (2002)
Ohio, U.S.A.	Silty clay	5	0.4 [P] (A – 15.9 vs 15.5) 12.1 (A – 16.4 vs 14.4)	45.4 (A - 26.4 vs 14.1) 26.7 (A – 24 vs 17.6)	Yes	Yes*	-	Fausey (2005)
Ontario, Canada	Clay loam	4	28.1 (FWMC -7.31 vs 5.25) -7.5 (FWMC - 7.56 vs 8.13)	44.7 (14.4 vs 7.96) 31.4 (19.1 vs 13.1)	Yes Yes	Yes* -	Yes* -	Drury et al. (2009)
Illinois, U.S.A.	Silty Clay Loam	2 G	-9.6 (FWMC – 14.1 vs 15.6)	70 (A: 57.2 vs 17)	Yes	No	-	Woli et al. (2010)
Nova Scotia, Canada	Sandy Loam	1	-12.1 (A - 6.6 vs 7.4)	14.3 (A – 39.1 vs 33.5)	Yes	No	-	Smith & Kellman (2011)
Indiana, U.S.A.	Fine Loam	2		18-23	Yes	Yes	-	Adeuya et al. (2012)
Illinois, U.S.A.	Silt clay loam Silt loam Silt clay loam	2		52 79 37	Yes	-	-	Verma & Cooke (2012)
Iowa, U.S.A.	Slit clay loam	4	10 (A: 10 vs 9)	36 [P] (A: 35 vs 21)	Yes	-	-	Helmers et al. (2012)
Iowa, U.S.A.	Clay Loam	4	7.2 to 14.5 (6.9 to 13.1 vs 6.4 vs 11.2)	29 [P] (A: 34.9 vs 23.9)	Yes[a]	-	-	Jaynes (2012)
Manitoba, Canada	Loam	2 G	48.3 (FWMC – 41.2 vs 21.3) 98.2 [P] (FWMC- 98.9 vs 1.7)	72.2 (A – 36 vs 10) 100 [P] (A – 138 vs 0.07)	Yes	-	-	Cordeiro et al. (2014)
Ontario, Canada	Clay loam	6	15.1 (FWMC – 9.45 vs 8.02)	37.5 (A – 102 vs 63.7)	Yes	Yes*	-	Drury et al. (2014b)
Manitoba, Canada	Sandy Loam	2	21 (FWMC – 66.8 vs 52.9)	82 (A- 16.7 vs 3.1)	Yes	-	-	Satchithanantham et al. (2014)
Ontario, Canada	Silt Loam	4 G	-	59 (A: 3.2 vs 1.7) 44 (A: 2.5 vs 0.8)	Yes	Yes*	Yes	Sunohara et al. (2014)
Ontario, Canada	Silt Loam	7 G	-	25 to 34 (A – 173 to 196 vs 129)	Yes	-	-	Sunohara et al. (2015)

Location	Soil Type	No. of years	NO_3-N Conc (mg N/L)	Reduction NO_3-N loads (kg/ha)	Mechanism			Reference
			%reduction (conc)	%reduction (load)	Drain flow	Denitrification	Plant uptake	
Ohio, U.S.A.	Slit loam, clay loam	7	-	-8 vs 44 [P]	Yes	-	-	Williams et al. (2015b)
Ontario, Canada	Silt loam	9	0.004 (A – 6.33 vs 6.3)	51 (A - 0.0364 vs 0.0179)	Yes	-	-	Sunohara et al. (2016)
Illinois, U.S.A.	Silt clay loam, silt loam	3	-7.1 to 2.8 (9.8,10.1 vs 10.5,10.4)	8.3 to 70.1 (34.8, 25.8 vs 31.9, 7.6)	Yes	No	-	Lavaire et al. (2017)
North Carolina, U.S.A.	Sandy Loam	9	-16.4 (FWMC- 5.5 vs 6.4)	30.3 (A – 20.7 vs 14.5)	Yes	-	Yes*	Poole et al. (2018)
Indiana, U.S.A.		10	-1.2 (A: 8.4 vs 8.5)	36.7 [P] (A – 30 vs 19)	Yes	No*	-	Saadat et al. (2018b)
Nova Scotia, Canada	Sandy Loam	3 G	24 to 36 (A – 15.6 vs 11.75)	42.3 to 58.2 (A – 6.53 vs 3.6)	Yes	-	Yes*	Smith et al. (2019)
Ohio, U.S.A.	Silt Loam, Clay Loam	10	-50.6 to 2.5 (A – 7.7,11.9 vs 11.6,11.6)	22.5 to 25.3 (37.4, 40.7 vs 29,30.4)	Yes	-	-	Shedekar et al. (2021)

[a] No significant decrease in nitrate N concentration was observed.
[b] Significant decrease in nitrate N concentration was observed.
G indicates study conducted only in growing season
(A) Average concentration or loads
(FWMC) Flow weighted mean concentration.
* Potential denitrification or plant uptake may be taking place due to saturated zones formed and/or enhanced evapotranspiration respectively.
[P] Indicates significant difference (p-value ≤ 0.05)

2.4.4. Effect on phosphorus concentrations and loads

Compared to NO_3^--N, fewer studies have evaluated the effectiveness of CD in reducing P losses via tile drainage, with most studies focusing on DP, more specifically, SRP, rather than PP or TP. This reflects the nature of tile drainage systems, which operate under low-energy flow conditions and through a soil matrix that effectively filters suspended material, resulting in tile effluent dominated by dissolved nutrient species (King, et al., 2015; Moore, 2016). Existing studies nonetheless indicate that CD can reduce P load primarily through reductions in drainage outflow, while effects on P concentrations are less consistent.

Most North American studies report reductions in P loads under CD that closely mirror reductions in tile drainage outflow, with reported decreases ranging from -40 to 96% for DP and 11 to 66% for TP (Table 2-6). In contrast, CD has frequently been shown to have little to no influence on P concentrations. At a watershed scale, Sunohara et al. (2015) observed reductions in TP and SRP loads under CD (11% and 18% respectively over 4 years) relative to FD, while flow-weighted mean concentration responses were mixed and inconclusive, indicating that reduced drainage flow was the dominant control on P exports during the growing season. Similar observations were made by Cordeiro et al. (2014) and Williams et al. (2015b). However, in some cases, increased DP concentrations have been observed under CD. Elevated water tables and prolonged soil saturation may alter redox conditions, promote the reduction of iron-bound P, and increase DP mobility, particularly in soils with high legacy P content (Jouni et al., 2018; King, et al., 2015). Observations of higher DP under CD have been reported in both growing and non-growing seasonal averages (Sanchez Valero et al., 2007; Stampfli, 2003), though responses remain highly site-specific and inconsistent across studies.

Crop uptake represents a secondary control on P dynamics under CD during the growing season. Nash et al. (2015) reported significantly lower flow-weighted SRP concentration with CD (0.09 mg P/L) compared to that of FD (0.15 mg P/L), hypothesizing that during summer, CD conserved water, increased uptake of water and P by crops, thereby reducing amount of P available for loss through leaching. Tan & Zhang (2011) also credited crop uptake induced concentration reduction (hence loads) in their study. Because only a portion of crop P uptake is removed at harvest, this mechanism primarily represents short-term retention, with retained P remaining susceptible to mobilization during the non-growing season or following stoplog removal.

Although PP is generally considered a minor component of tile drainage under typical flow conditions, it may become relevant during short-duration, high-flow events when preferential flow paths are activated or previously retained material is mobilized. Under such conditions, rapid transport of sediment-associated P may bypass the buffering capacity of the soil matrix (Gentry et al., 2007; Heathwaite & Dils, 2000; King, et al., 2015; Macrae et al., 2007). Accordingly, FD may exhibit sharper event driven PP/TP export peaks, whereas CD could potentially attenuate these peaks by physically trapping PP/TP and associated solids in addition to reducing and delaying drainage outflow. Evidence from CD studies remains limited and mixed for concentration responses: some report minimal to no change in PP and TP concentrations (Tan & Zhang, 2011; Zhang et al., 2015), while other report significantly higher TP concentrations under CD (Saadat et al., 2018b; Sanchez Valero et al., 2007; Sunohara et al., 2016). Nevertheless, these studies consistently report reductions in PP and TP loads under CD compared to free drainage (FD) (33 to 37% and 18 to 54%, respectively) due to reduction in flow.

Seasonal variability further governs the timing and magnitude of P export under both CD and FD systems. Periods such as spring snowmelt and late fall precipitation are characterized by limited plant uptake, elevated soil moisture, and high drainage responsiveness, increasing the susceptibility of stored P to mobilization (Satchithanantham et al., 2014; Wesström & Messing, 2007). During these periods, short duration hydrologic pulses can dominate P export irrespective of average seasonal concentrations. While seasonal hydrologic conditions influence when phosphorus is most susceptible to mobilization, stoplog removal at the end of CD employment may represent a distinct and underexamined trigger for P export, with such transitions potentially offsetting some of the benefits achieved during the growing season.

Table 2-6. Summary of Effects of Controlled Drainage on P loads as reported in previous studies.

Location	Soil Type	No. of years	P Conc (mg P/L) reduction % (conc, FD vs CD)	P loads (kg P/ha) reduction % (load, FD vs CD)	Mechanism			Reference
Quebec, Canada	Fine Sandy Loam	1 G	TP: -131 (A: 0.03 vs 0.07) SRP: -178 (A: 0.02 vs 0.05)	-	Yes	No[a]	-	Sanchez Valero et al. (2007)
Ontario, Canada	Clay	5	SRP: 26.5 (FWMC: 0.04 vs 0.03) PP: 5.9 (FWMC: 0.39 vs 0.37) TP: 4.8 (FWMC: 0.48 vs 0.46)	SRP: 13.2 (0.38 vs 0.33) PP: 37.1 (4.45 vs 2.8) TP: 35.4 (5.4 vs 3.5)	Yes	Yes	Yes*	Tan & Zhang (2011)
Manitoba, Canada	Loam	2	OPO_4: 25 to 40.6[P] (0.4, 0.32 vs 0.3,0.19)	OPO_4^-: 70.4 [P] to 86.7 [P] (0.60,0.27 vs 0.08,0.08)	Yes	-	-	Cordeiro et al. (2014)
Manitoba, Canada	Sandy Loam	2	OPO_4: -37.5, -92.9 (FWMC: 0.56,0.14 vs 0.77, 0.27)	OPO_4: 96.1, -53.3 (1.28,0.15 vs 0.05, 0.23)	Yes	No[a]	-	Satchithanantham et al. (2014)
Missouri, U.S.A.	Claypan	4	OPO_4-P: 40 [P] (0.15 vs 0.09)	OPO_4-80 (A: 0.18 vs 0.036)	Yes	Yes	Yes*	Nash et al. (2015)
Ontario, Canada	Silt loam	7 G	-	TP: -11 to 18 [P] (0.052, 0.07 vs 0.057) SRP: -18 to -61 (0.01 to .013 vs 0.02)	Yes	No[a]	-	Sunohara et al. (2015)
Ohio, U.S.A.	Silt loam, clay loam	7	SRP: 18.1 (A: 0.11 vs 0.09)	SRP – 40 to 68 (0.51 vs 0.04)	Yes	-	-	Williams et al. (2015b)
Ontario, Canada	Clay Loam	4	SRP: 20 (A: 0.2 vs 0.16) PP: - (A: 0.4 vs 0.4) TP: 3 (A: 0.66 vs 0.64)	SRP: 44 (0.34 vs 0.19) PP: 33 (0.69 vs 0.46) TP: 36 (1.14 vs 0.73)	Yes	-	-	Zhang et al. (2015)
Ontario, Canada	Silt loam	9 G	SRP: 18.5 (A: 9.18 x 10^{-3} vs 7.48 x 10^{-3}) TP: - (A: 0.04 vs 0.04)	SRP: 66 (A: 3.27 x 10^{-5} vs 1.12 x 10^{-5}) TP: 66 (2.13 x 10^{-4} vs 7.27 x 10^{-5})	Yes	-	-	Sunohara et al. (2016)

SRP = Soluble reactive P; PP = Particulate P; TP = Total P; FWMC = flow-weighted mean concentration, OPO_4^-: orthophosphate ion
[P] Indicates significant difference (p-value ≤ 0.05)
(A) denotes average concentration reported
[a] Increased P concentration due to CDS = negative P load reduction
* Uptake by plants speculated

2.5. Treatment Ponds

Treatment ponds (also referred to as sedimentation ponds, farm ponds, attenuation ponds, or retention ponds) are edge-of-field technologies primarily employed for stormwater management or irrigation in agricultural contexts. These engineered ponds function as designed reactors, comprising a permanent pool created by utilizing a natural depression, excavating a new depression, or constructing embankments (NWRM Project, 2013; Robotham et al., 2021). In municipal areas, stormwater ponds are commonly used to temporarily store water and reduce contaminant levels in downstream water bodies (Mallin et al., 2002) and are regarded as fundamental components of stormwater management policies in North America. Within agricultural settings, treatment ponds are strategically positioned along water discharge pathways to intercept drainage water and/or any overland flow without disrupting farming activities. In Canada, farm ponds are typically constructed in clay soils, about 3 m deep and are completely covered with ice from November to March (AAFC, 2024), a characteristic feature of cold regions.

Treatment ponds operate analogously to natural lake systems. These ponds remove nutrients, pathogens, and particulates through various hydrogeochemical pathways, with effectiveness varying by season and operating conditions (Beckingham et al., 2019; Shilton, 2005). Nutrient transformations mainly occur within the permanent volume of water and associated sediments, rather than the littoral zone, where biological uptake is often limited in engineered pond designs (Gold et al., 2017; Harper & Herr, 1993; Nietch et al., 2001). The permanent pool typically has a mean depth of 1-2 m, with a maximum depth of 3 m to avoid re-suspension of solids and prevent prolonged anoxic conditions (OMECP, 2020). While treatment ponds for stormwater management have been extensively researched over the past four decades, a very few studies have focused on their efficiency in agricultural systems (Chrétien et al., 2016; Marques & Mandrak, 2024). A comprehensive review on agricultural BMPs by Clary et al. (2012) identified only ten publications reporting treatment efficiency by retention structures (including dams), of which three examined ponds in agricultural settings. Accordingly, this review draws on findings from both stormwater and agricultural pond studies.

2.5.1. Effect on flow events

Stormwater ponds are engineered to mitigate peak flow and volume during storm events (Vogel

& Moore, 2016) by decreasing flow velocity and gradually releasing stored water over a period of time. North American urban stormwater ponds have been shown to reduce runoff volume by an average of 20% and attenuate peak flows by 60% (Harper & Baker, 2007; Lawrence et al., 1996; Nietch et al., 2001). In a five-year study in Quebec, Canada, Chrétien et al. (2016) monitored three constructed ponds receiving storm runoff from a 96.8 ha cropping system and reported average peak flow reductions of 38%, with negative correlations to precipitation and runoff depths. Significant peak flow reductions were also observed in German study, where peak runoff was reduced by a factor of three by four ponds in adjacent agricultural watersheds (Fiener et al., 2005). Additionally, a Soil Water Assessment Tool (SWAT) model study in Southern Sweden demonstrated a 11% reduction in streamflow and volume by ponds receiving agricultural runoff (Oduor et al., 2023).

2.5.2. Effect on solids

Total suspended solids (TSS) and other particulates are primarily removed through sedimentation and, where present, filtration by vegetation. Solids retention is a key characteristic of treatment ponds due to their design depth, as reflected in reported high TSS and particulate removal efficiencies in previous studies. These studies have documented removal efficiencies ranging from 50 to 94% in urban stormwater ponds (Harper & Baker, 2007; Jones et al., 2012; Lawrence et al., 1996; SC DHEC, 2005; Schueler & Holland, 2000) and from 54 to 98% in agricultural ponds (Fiener et al., 2005; Rushton & Bahk, 2001). Research conducted in cold climates (Brunet et al., 2021; Chrétien et al., 2016) have also observed TSS removal efficiencies exceeding 50%, with negative correlations with precipitation, leading to a 'washout' of solids during peak flow events. A study of three interconnected agricultural ponds in the United Kingdom (Robotham et al., 2021), situated in humid temperate oceanic climate, reported similar trends in TSS retention, with greatest retention during baseflow, reduced peak concentrations during small to moderate storm events, and a resuspension with net export of deposited sediment during high storm events.

2.5.3. Effect on nitrogen

The mechanisms for N removal vary according to N species involved. NO_3^- are removed through denitrification and plant uptake, particulate or organic N by sedimentation and mineralization, and ammonia through volatilisation or transformed through nitrification (Figure 2-6 Left).

Urban stormwater ponds have demonstrated the capability to reduce TN concentrations

(Table 2-7) by an average 4 to 63% of TN (Harper & Baker, 2007; SC DHEC, 2005), NO_3^- by negative to 32% (Gold et al., 2017; Ivanovsky et al., 2018; Koch et al., 2014) and ammonia by 29% (Koch et al., 2014). On the other hand, agricultural ponds report that TN is reduced by 26% (Clary et al., 2020), NO_3^- varied from 5 to 82% and ammonia from 28 to 76% (Robotham et al., 2021; Rushton & Bahk, 2001).

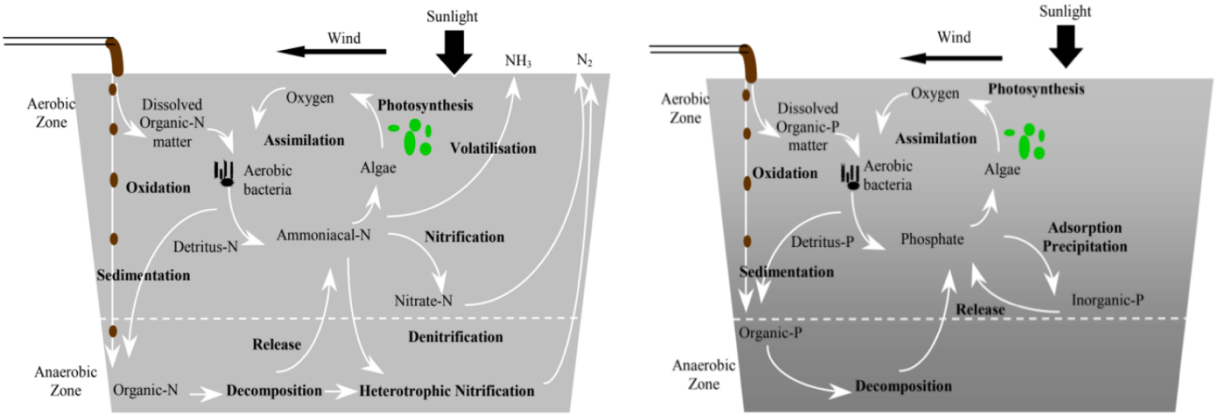

Figure 2-6. Overview of hydrological, physical, and biogeochemical processes that occur in a typical treatment pond with respect to nitrogen (Left) and phosphorus (Right) (Shilton, 2005)

Agricultural drainage and runoff are typically rich in NO_3^- compared to other dissolved forms of N. This was observed in a farm pond in Iowa (pond-to-catchment ratio = 1.8%, mean depth = 1.8 m and maximum depth = 4 m), where NO_3^- dominated influent TN and total dissolved nitrogen load, while particulate N dominated during high-discharge events (Brunet et al., 2021). Although significant NO_3^--N load removal (64% of 19.8 kg/ha inflow) was achieved, overall TN load reduction was substantially lower at 36% than NO_3^--N. The authors speculate that this difference was likely due to the incomplete setting and export of particulate N (up to 45% of TN on occasions) and other dissolved N during high discharge events and, thereby skewing the overall effectiveness of this BMP. The study further suggested that dissimilatory NO_3^- reduction to ammonia (DNRA) mechanism could be a significant pathway for NO_3^- in the pond's sediment layer from April to June, based of elevated ammonia concentration in the anoxic bottom waters, and reduced TN removal. Similar observation was made by Beutel et al. (2009), where sedimentation pond tended to be a source of organic N, even though NO_3^- concentrations were reduced in the range of 20-30%. Studies conducted in colder temperate sedimentation ponds in Finland reported insignificant to highly variable N reductions, speculating the poor results could be either due to low retention time or decreased N microbial transformations under cold climate conditions (Uusheimo et al., 2018).

2.5.4. Effect on phosphorus

Phosphorus in influent water is partitioned either as PP or DP. Sedimentation and filtration dominate PP removal (a function of particle size, density distribution) whereas DP (also referred to as orthophosphates or reactive P) can be removed through sorption, precipitation, or assimilation by microorganisms or plants when present (Figure 2-6 Right).

As discussed in section 2.5.3., most prior studies have documented substantial solids retention. Consequently, PP and its fraction of TP, tend to settle within pond systems. As a result, urban and agricultural ponds have demonstrated significant reductions in TP and PP concentrations (Table 2-8), ranging from 48 to 89% (Chrétien et al., 2016; Clary et al., 2012, 2020; Harper & Baker, 2007; Oduor et al., 2023; Rushton & Bahk, 2001). In all of these studies, PP constituted the dominant component of TP, and the trend in TP mirrored TSS removals/exports within the system during peak storm events (R^2>0.9). However, Brunet et al. (2021) observed a shift in the dominant P form within TP based at flow conditions, with DP export prevailing during low flow events and PP export during high flow conditions.

The few studies that reported DP concentrations found removal efficiencies ranging from 29 to 35% (Clary et al., 2012; Robotham et al., 2021; Rushton & Bahk, 2001). The mechanisms potentially involved in DP removal, such as sorption/precipitation or uptake are functions of hydraulic retention time (HRT) (Fiener et al., 2005; Walker, 1998). Shorter HRTs can hinder sorption of DP to cations of iron (typically dominant), aluminium, and calcium (Peng et al., 2007). The accreted sediment (deposited dead plant matter or soil with high clay content) within a system, particularly in newly established systems, is considered as a sink of P with numerous sorption sites (Beckingham et al., 2019). In addition to retention time, soil and sediment cation exchange capacity and background P are key factors for P sorption. As the system matures, the removal efficiency of both PP and DP is suspected to diminish due to reductions in cation exchange capacity, pond depth, and pond volume, rendering key removal mechanisms ineffective. Therefore, it is recommended that these ponds undergo regular maintenance, including dredging of settled material (Beckingham et al., 2019).

Older ponds may become a source of accumulated “legacy” P, where cation-bound sediment P is released as DP due to dissimilatory iron reduction under eutrophic conditions or changes in environmental conditions (e.g., redox, pH, sulfate, metals concentrations) and poses a

challenge in lake systems as well (Cravotta et al., 2024; Muenich et al., 2016; Randall et al., 2019; Stackpoole et al., 2019). This potential release undermines the BMP's effectiveness, even if P inputs are reduced through other BMPs. Studies by Brunet et al. (2021) and Robotham et al. (2021) reported poor (negative to 8%) TP removal within the hypereutrophic agricultural ponds, attributing to seasonal internal loading and legacy sediment P release causing increased phytoplankton blooms and export of organic matter containing P.

Despite the widespread application of treatment ponds in urban stormwater management, field-scale evaluations of their performance in agricultural cropping systems remain limited, particularly for systems receiving tile drainage. Existing agricultural pond studies report highly variable nutrient removal efficiencies, reflecting strong controls by HRT, event-driven hydrology, and seasonal processes. These uncertainties are further amplified in cold-climate regions, where prolonged ice-cover, reduced microbial activity, and freeze-thaw cycles may constrain nutrient transformations and promote episodic export. Collectively, these gaps highlight the need for targeted, field-based assessment of treatment pond performance in cold-climate cropping systems.

Table 2-7 Summary of N Removal Efficiencies of Treatment Ponds and FWS treating effluent (Stormwater, Agricultural Drainage or Runoff) as reported in previous studies

Location (Country)	Climatic Zone^	Source	Depth (m)	Area (ha) (Area: Catchment Ratio%)	Study Time (year)	Influent Concentration (mg N/L), Range (Mean)	Average N Retention % Concentration (% Loading)	Possible Mechanism	Reference
TREATMENT POND									
USA	*Cfa*	Stormwater runoff from row crop farm	0.6 to 0.76		2	NO_3—N+NO_2: (0.43, 0.13) NH_4-N: (0.1,0.053) Org-N: (1.1,0.9)	NO_3—N+NO_2: 66, 95(81.5) NH_4-N: 34, 28 (76) Org-N: 25, -25(40)		Rushton & Bahk (2001)
USA	*Cfa*	Municipal Stormwater runoff*		3.4	7		NH_4-N[a]: 21 NO_3—N: -20	NH_4-N – plant and phytoplankton uptake or nitrification	Gold et al. (2017)
France	*Cfb*	Municipal Stormwater runoff*	1.5 to 2.5	3	1	NO_3—N: 0.1 to 4.6 (0.71) NH_4-N[a]: 0.02 to 5.2 (1.6)	NO_3—N: 24 NH_4-N[a]: 93	Sedimentation Uptake by macrophytes and Phytoplankton	Ivanovsky et al. (2018)
USA		Municipal Stormwater			0.6 2	TN: 1.24[a] TN: 1.63[a]	TN: (16.6) TN: (26.6)	Denitrification	Clary et al. (2020)
USA	*Dfa*	Runoff*	Mean – 1.8 Max - 4	1.8	0.5	TN: 0.6 to 15.9 (5.6)	TN: (36) NO_3^-+NO_2-N: (64)	Denitrification Plant uptake Phytoplankton uptake + particle settling DNRA	Brunet et al. (2021)
UK	*Cfb*	Agricultural runoff*		0.2	1	NO_3^-: (36.56) NH_4^+: (0.023)	NO_3^-: 5 NH_4^+: -61	Denitrification (min to none)	Robotham et al. (2021)
FWS CONSTRUCTED WETLAND									
USA	*Cfa*	Cropping drainage	0.9 0.4 0.7	0.6 (4) 0.3 (6) 0.8 (3)	4 6 3	NO_3^--N[a]: (13) NO_3^--N[a]: (10.3) NO_3^--N[a]: (8.5)	TN: (39) NO_3^--N: 13.8 (40.7) TN: (43) NO_3^--N: 28.2 (43.7) TN: (31.3) NO_3^--N: 30.6 (34.3)	Denitrification (90%), plant uptake (10%)	Kovacic et al. (2000)
Norway	*Dfc*	Runoff*		0.09 (0.06) 0.03 (0.07) 0.09 (0.08) 0.05 (0.21) 0.08 (0.38)	7 7 4 3 3	TN: (3.2), NO_3^--N[a]: (2.3) TN: (3.5), NO_3^--N[a]: (2.2) TN: (1.6), NO_3^--N[a]: (0.8) TN: (5.1), NO_3^--N[a]: (2.8) TN: (5.1), NO_3^--N[a]: (2.8)	TN: 3, NO_3^--N: 0, Org-N: 16 TN: 4, NO_3^--N: -1, Org-N: 18 TN: 6, NO_3^--N: 3, Org-N: 11 TN: 14, NO_3^--N: 9, Org-N: 27 TN: 15, NO_3^--N: 7, Org-N: 32	Sedimentation in organic particles (under high hydraulic load) Denitrification (under low hydraulic load) Plant uptake (2 to 21%)	Braskerud (2002a)

Location (Country)	Climatic Zone^	Source	Depth (m)	Area (ha) (Area: Catchment Ratio%)	Study Time (year)	Influent Concentration (mg N/L), Range (Mean)	Average N Retention % Concentration (% Loading)	Possible Mechanism	Reference
Finland	*Dfb*	Cropping drainage Runoff*	2 1.5 -	0.6 (5) 0.48 (0.5) 60 (3)	1.3-2.2	TN: (9.8), NO_3^--N[a]: (7.9) TN: (8.4), NO_3^--N[a]: (6.8) TN: (3.1), NO_3^--N[a]: (2.4)	TN: (36), NO_3^--N: (35) TN: (-256) NO_3^--N: (-254) TN: (42), NO_3^--N: (10)	Denitrification Sedimentation of organic N Plant uptake (min to none)	Koskiaho et al. (2003)
New Zealand	*Cfb*	Grazed diary pasture drainage	0.3	0.03 (1)	2	NO_3^--N[a,b]: 9 to 12 Org N[a,b]: 14 -15	TN: (50), NO_3^--N: (30) Org-N: (95.3), NH_4-N: -64.5	Denitrification Mineralization	Tanner et al. (2005)
USA	*Dfa*	Runoff and drainage*	0.48 0.52	0.16 (7) 0.4 (3)	1.67	TN: (15.6), NO_3^--N[a]: (15.5), Org N: (0.1), NH_4-N: (0.05) TN: (18.4), NO_3^--N[a]: (18.3), Org N: (0.14), NH_4-N: (0.02)	TN: (32.5), NO_3^--N: 42 (28), Org N: (72.5), NH_4-N: (-15) TN: (38), NO_3^--N: 31 (37), Org N: (48.5), NH_4-N: (-38.5)	Denitrification Sedimentation of organic N	Kovacic et al. (2006)
New Zealand	*Cfb*	Dairy		0.1(1)	3	TN[b]: (1.9), NO_3^--N[b]: (0.01), NH_4-N[b]: (0.034), PN [a,b] : (0.97)	TN[b]: (46), NO_3^--N[b]: (-23), NH_4-N[b]: (14), PN [a,b] : (94)	Sedimentation of particulate forms Nitrification	Wilcock et al. (2012)
Germany	*Cfb*	Cropping drainage	0.7 to 1.8	0.5 (0.5)	4	TN[b]: 2 to 21.4 (7.2 to 14.2), NO_3—N [a,b]: 7.1 to 18 (7.3 to 12.3), Org N[b]: 0 to 8 (0.6 to 1.2)	TN: (2.9)	Denitrification Plant uptake Sedimentation	Steidl et al. (2019)
Sweden	*Cfb*	Runoff +Drainage*	0.5 to 2.2	0.018 to 0.26 (9 wetlands)	1.5 to 3	N: 2.2 to 13	N: (-28 to 8)	Denitrification Plant uptake	(Nilsson et al., 2023)
Denmark	*Cfb*	Agricultural drainage	0.3 to 1	0.28 (0.6)	3.5	TN: 0 to 18.6	TN: (39.5)	Denitrification Sedimentation of particulate	Pugliese et al. (2023)

Note: Negative values (-) for average N retention indicate an export of N by the system.
^Köppen−Geiger climate classification (Kottek et al., 2006)
*Watershed scale – only studies with >80% watershed area with agricultural/cropping systems.
[a]Dominant fraction of TN
[b]median value
DNRA = Dissimilatory nitrate reduction to ammonia

Table 2-8. Summary of P Removal Efficiencies of Treatment Ponds and FWS treating effluent (Stormwater, Agricultural Drainage or Runoff) as reported in previous studies

Location (Country)	Climatic Zone^	Source	Depth (m)	Area (ha) (Area: Catchment Ratio%)	Monitoring Time (year)	Influent Concentration (mg P/L), Range (Mean)	Average P Retention % Concentration (% Loading)	Possible Mechanism	Reference
TREATMENT POND									
USA	*Cfa*	Stormwater runoff from row crop farm	0.6 to 0.76		2	TP: (0.96, 1.8) Ortho – P: (0.8, 0.9)	TP: (70,80) Ortho-P: (50, 82)	Sedimentation	Rushton & Bahk (2001)
Canada	*Dfb*	Agricultural runoff	0.8		5	TP: (0.2)	TP: 48 (59)	Sedimentation	Chrétien et al. (2016)
France	*Cfb*	Municipal Stormwater runoff*	1.5 to 2.5	3	1	Ortho – P: 0.07 to 0.78 (0.42)	Ortho – P: 28	Sedimentation Sorption Uptake	
USA		Municipal Stormwater			1.5 3	TP: 0.25[c] TP: 0.25[c]	TP: 25.6[c] TP: 52.5[c]	Sedimentation Sorption	Clary et al. (2020)
USA	*Dfa*	Runoff*	Mean – 1.8 Max - 4	1.8	0.5	TP: 0.06 to 1.5 (0.23) TDP: 0.04 to 0.84 (0.15)	TP: (8)	Sedimentation	Brunet et al. (2021)
UK	*Cfb*	Agricultural runoff*		0.2	1	TP: (0.081), SRP: (0.008), PP: (0.04)	TP: -34, SRP: 29, PP: -237	Sedimentation Sorption	Robotham et al. (2021)
Sweden	*Dfb*	Runoff/drainage*,M			15		TP: (50) DP: (36)	Sedimentation	Oduor et al. (2023)
FWS CONSTRUCTED WETLAND									
USA	*Dfa*	Cropping drainage	0.9 0.4 0.7	0.6 (4) 0.3 (6) 0.8 (3)	4 6 3	Ortho P: (0.21) Ortho P: (0.12) Ortho P: (0.11)	TP: (20.7) Ortho P: -23.8 (28) TP: (35) Ortho P: -16.6 (56.7) TP: (-18.1) Ortho P: -9.1 (29)	Sedimentation	Kovacic et al. (2000)
Norway	*Dfc*	Runoff*		0.09 (0.06) 0.03 (0.07) 0.09 (0.08) 0.05 (0.21) 0.08 (0.38)	7 7 4 3 3	TP: 0.17 TP: 0.25 TP: 0.22 TP: 0.43 TP: 0.43	TP: 41 TP: 32 TP: 21 TP: 37 TP: 44	Sedimentation	Braskerud (2002b)
Finland	*Dfb*	Cropping drainage + Runoff*	2[a] 1.5[a] -	0.6 (5) 0.48 (0.5) 60 (3)	1.3 to 2.2	TP: (0.51), DRP: (0.038) TP: (0.12), DRP: (0.026)	TP: (62), DRP: (27) TP: (-6 to 19), DRP: (-6 to -33) TP: (14 to 15), DRP: (0 to 15)	Sedimentation Sorption Plant uptake (low)	Koskiaho et al. (2003)

Location (Country)	Climatic Zone^	Source	Depth (m)	Area (ha) (Area: Catchment Ratio%)	Monitoring Time (year)	Influent Concentration (mg P/L), Range (Mean)	Average P Retention % Concentration (% Loading)	Possible Mechanism	Reference
						TP: (0.07), DRP: (0.009)			
Switzerland	*Cfb*	Grassland drainage	0.6	0.24 (0.012)	2		TP: (23), DRP: (55), PP: (-26)	Sedimentation(solids, phytoplankton, macroalgae) Plant uptake (low)	Reinhardt et al. (2005)
New Zealand	*Cfb*	Grazed diary pasture drainage	0.3	0.03 (1.0)	2	TP: 0.18- 0.2 DRP: 0.02-0.04	TP: (-44.5) DRP: (-23)	Export – release of soil bound P	Tanner et al. (2005)
USA	*Dfa*	Runoff and drainage*	0.48 0.52	0.16 (7.3) 0.4 (3.3)	1.67	TP: (0.1), Ortho: (0.04), OP: (0.07) TP: (0.13), Ortho: (0.04), OP: (0.07)	TP: 58(68), Ortho: 72 (78.5), OP: 61 (68) TP: 50 (44), Ortho: 53 (42.5), OP: 50 (45.5)	Sedimentation	Kovacic et al. (2006)
New Zealand	*Cfb*	Tile drainage from pasture sites	0.3 – 0.8 0.3 0.3	0.09 (2.0) 0.03 (1.0) 0.01 (0.7)	3 5 4	TP: (0.26), DRP: (0.05) TP: (0.07), DRP: (0.06) TP: (0.3), DRP: (0.14)	TP: -24.3, DRP:-263 TP: -101.2, DRP:-82.6 TP: -58.3, DRP:-6.5	Export – release of Fe bound P/ vegetation decay	Tanner & Sukias (2011)
New Zealand	*Cfb*	Dairy		0.1(1)	3	TP: 0.012 – 58.2 DRP: 0.001-0.02	TP: 93% (89%) SRP: -53% (-20%)	Sedimentation Co-precipitation	Wilcock et al. (2012)
Sweden	*Dfb*	Cropping tile drainage	0.3 to 1	0.08 (0.3)	2	TP: (0.3) DRP: (0.1)	TP: 40 (36) DRP: 40 (9) PP: (36)	Sedimentation	Kynkäänniemi et al. (2013)
Sweden	*Cfb*	Agricultural drainage/runoff	0.5 to 1 [b]	0.22 to 2.1[b] (0.06 to 2.2)	2 to 9	TP: 0 - 2.1 (0.02 to 0.26)	-	-	Johannesson et al. (2017)
Denmark	*Cfb*	Cropping drainage	0.3 to 1	0.9 (1.1) 2.2 (0.9) 0.8 (1.1)	3	TP: (0.18)[c] TP: (0.21) [c] TP: (0.22) [c]	TP: 29-48 TP: 31-51 TP: 14-48	Sedimentation Sorption	Mendes et al. (2018)
Italy	*Cfa*	Cropping drainage	0.4	0.4 (3.0)	2	TP: (0.05)	TP: 60 (-27)	Event driven export of P, vegetation decay	Lavrnić et al. (2020)

^Köppen−Geiger climate classification (Kottek et al., 2006)
* Watershed scale – only studies with >80% watershed area with agricultural/cropping systems
[a]Maximum water depth
[b]consists of 7 wetlands
[c]median concentrations
[M]Modelling study

2.6. Constructed Wetland System

Constructed wetlands have long been employed to treat municipal and industrial wastewaters to more recently urban stormwater and agricultural runoff and drainage (Kadlec & Wallace, 2008; Mitsch & Gosselink, 2015). Wetlands are commonly defined as areas that are saturated for part or all of the year and function as transitional zones between upland terrestrial systems and aquatic or flooded systems (Kadlec & Wallace, 2008). These systems are unique, biologically active ecosystems characterised by hydric soil and plant species adapted to prolonged saturation. Functionally, wetlands operate as complex bioreactors that act simultaneously as filters (particulate removal), sinks (nutrient accumulation) and transformers (nutrient conversion to various forms), driven by interacting physical, chemical, and biological processes (Kadlec & Wallace, 2008; Vymazal, 2017a).

CWs also referred to as artificial or engineered or treatment wetlands, are designed to simulate and enhance the workings of a natural wetlands under controlled hydraulic and ecological conditions. A noteworthy advantage of CWs is that they can be built on any land and are more effective when placed at critical downstream location of wastewater source thereby acting as impact buffer on receiving waters (Crumpton et al., 2020; Kovacic et al., 2000; Mitsch et al., 2001). CWs are cost-effective, easy to maintain and are resilient to variable types of wastewater inputs, be it surface runoff or subsurface tile drainage, although they are land intensive (Masi et al., 2018; Strock et al., 2010). CWs are broadly classified into two hydrologic types (Kadlec & Wallace, 2008):

i. Surface flow wetlands or also known as free water surface flow wetlands (FWS), which convey water above the soil surface through emergent, submerged, or floating vegetation.
ii. Subsurface flow wetlands, in which water flows through a porous media either horizontally or vertically below the surface.

This review focuses exclusively on FWS wetlands, as these systems most closely resemble natural wetlands and commonly integrated with treatment ponds in pond-wetland configurations. FWS wetlands are well suited to treating agricultural drainage due to their ability to accommodate variable inflows, pulsed hydrology, and fluctuating water levels. When designed as single or multi-cell systems in series or parallel, FWS wetlands have been widely reported as sinks for both P

(Braskerud, 2002b; Geranmayeh (Kynkäänniemi) et al., 2013; Johannesson et al., 2011) and N (Kovacic et al., 2000; Mitsch et al., 2012). In addition to nutrient attenuation, FWS wetlands offer ancillary benefits including biomass production, habitat provision, biodiversity enhancement, and recreational or aesthetic value (Knight, 1992). Their long operational lifespan and minimal mechanical requirements make them attractive components of integrated agricultural BMPs, particularly when paired with treatment ponds. Accordingly, the following review emphasizes process-level understanding of nutrient retention and removal within FWS CWs, with particular attention to cold-climate constraints relevant to pond-wetland systems treating tile drainage.

2.6.1. Effect on total suspended solids

TSS entering FWS CW are removed primarily through sedimentation, flocculation, filtration and interception by vegetation (Kadlec & Wallace, 2008). At the same time, CWs can internally generate TSS through processes such as death of biomass (algae or invertebrates), litterfall, litter attrition, and chemical precipitation. Both retained and internally generated solids accumulate over time as either unconsolidated sediments or consolidated wetland soils, a process that plays a central role in nutrient attenuation by trapping particle-bound P and N (Kadlec & Wallace, 2008). Despite their retention capacity, accumulated solids are susceptible to resuspension driven by high inflow velocities, wind-induced turbulence, and bioturbation, which can reduce TSS removal efficiency and lead to episodic export. Consequently, TSS dynamics in wetlands reflect a balance between deposition and resuspension processes rather than unidirectional removal.

The effectiveness of TSS retention in FWS wetlands is governed by several interacting factors, including influent TSS load (which is strongly dependent on temperature, precipitation, crop management, etc.), drainage characteristics (flowrate), HRT, wetland-to-catchment ratio, particle size distribution or wetland age and vegetation structure (Braskerud et al., 2005; Krzeminska et al., 2023). For agricultural influent, reported TSS removal efficiencies in FWS wetlands typically range from 28 to 91%, with strong seasonal variability (Johannesson et al., 2011; Lavrnić et al., 2020; Maynard et al., 2009; Newman & Clausen, 1997). Seasonal patterns consistently show highest TSS retention during summer, when influent loads and flow velocities are low, HRT is high, and vegetation is fully established. Retention generally declines in spring and fall, and is lowest in winter, when high inflows, reduced vegetation cover, litterfall, and shortened HRT promote TSS export. Event-driven resuspension during high-flow conditions can

result in net TSS export, particularly during storm runoff or snowmelt periods (Braskerud et al., 2005; Díaz et al., 2012). Particle characteristics also influence retention, with clay-sized particles more prone to export than sand- or slit-sized fractions due to slower settling velocities (Maynard et al., 2009).

In cold-climate regions, TSS dynamics are strongly influenced by snowmelt and freeze-thaw processes, which often contribute to a large fraction of annual TSS loading over short periods. Studies from northern Europe, Mid-West U.S., have reported that spring snowmelt accounts for the majority of TSS inflow and is frequently associated with substantial TSS export from wetlands (Koskiaho et al., 2003; Krzeminska et al., 2023; Kynkäänniemi et al., 2013; Ulén et al., 2019). Although ice cover can suppress wind-driven resuspension and promote settling during winter, a pronounced flush of accumulated solids often occurs during thaw and early spring runoff. Wetland vegetation influences TSS retention by reducing near-bed flow velocities, promoting particle settling, and trapping solids within plant detritus (Brix, 1997). However, in cold climate systems, the stabilizing effect of vegetation is largely confined to the growing season, when agricultural drainage volumes are typically lowest. During non-growing seasons, reduced plant cover and increased hydrologic forcing limit the capacity of CWs to retain TSS.

Overall, FWS CWs can function as effective sinks for TSS under stable hydraulic conditions, but their performance is highly variable and sensitive to seasonality, hydraulic loading, and particle characteristics. In pond-wetland systems, treatment ponds may therefore play a critical role in dampening TSS inputs, reducing resuspension risk within CW sections, and enhancing the long-term stability of particulate-associated nutrient retention.

2.6.2. Effect on phosphorus - Forms, mechanisms, and effect of CW

Phosphorus is a limiting nutrient in most freshwater systems, and excessive P inputs can disrupt the ecosystem structure and function by altering the canonical Redfield ratio, C:N:P = 106:16:1 (Hillebrand & Sommer, 1999; Redfield, 1958). CWs can retain P over both short- and long-term scales through a combination of physical, chemical, and biological processes, although retention efficiency varies widely with influent P form, hydraulic conditions, and wetland characteristics.

P entering FWS CWs occurs primarily as PP and DP, the latter consisting of dissolved inorganic P (commonly orthophosphate) and dissolved organic P. Orthophosphate species (HPO_4^{2-}

and $H_2PO_4^-$) dominate within the pH range typical of agricultural waters (4<pH<9) and represent the most bioavailable fraction of P (Morel & Hering, 1993). The relative proportion of PP and DP strongly governs retention mechanisms and overall wetland performance.

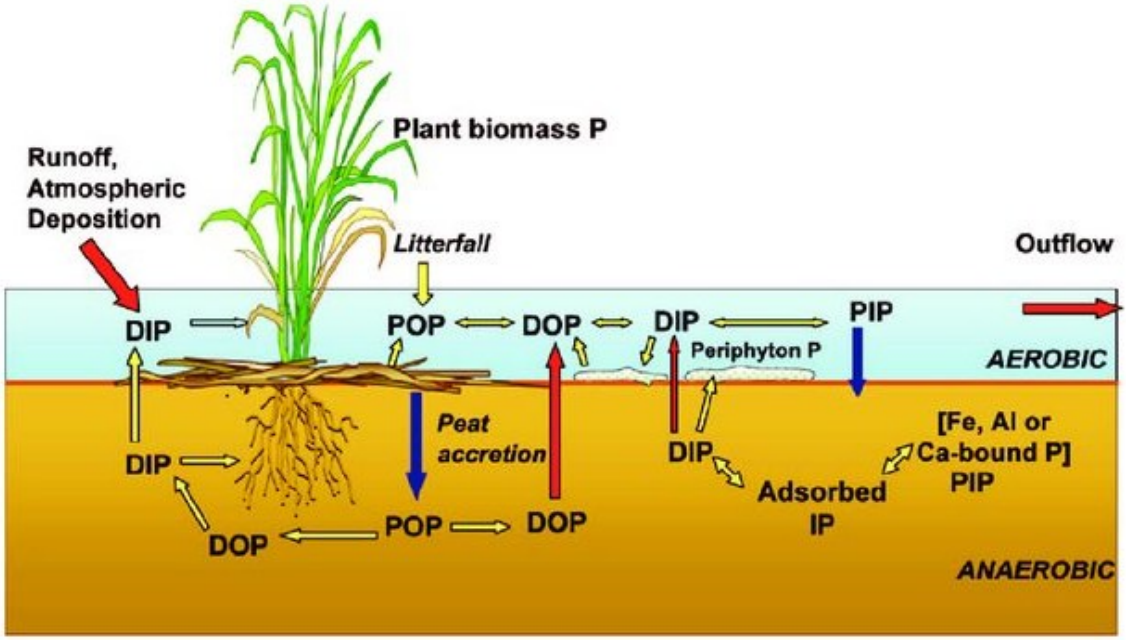

Figure 2-7. Phosphorus (P) cycle in wetlands. Adapted from (Reddy & DeLaune, 2008). Note: POP = particulate organic P; PIP = particulate inorganic P; DIP = dissolved inorganic P; DOP = dissolved organic P; IP = inorganic P; Al = Aluminium; Fe = Iron; Ca = Calcium.

P retention in wetlands occurs through interaction among multiple P pools, including water, sediment, soil, biomass, and microbial communities (Figure 2-7). Dominant retention mechanisms include sedimentation and accretion of PP, sorption of DP to sediments and soils, and temporary storage in plant and microbial biomass (Kadlec & Wallace, 2008). Sedimentation and accretion represent the most durable P retention pathways. PP associated with suspended solids settles under reduced flow velocities and becomes incorporated into wetland sediments, where long-term burial can occur. This accretion process is considered primary mechanism for permanent P removal in FWS CWs, although accumulated sediments remain vulnerable to resuspension during high-flow events. PP maybe also be transformed to other dissolved forms through biogeochemical cycles (James et al., 2002; Uusitalo et al., 2003). Sorption of DP occurs predominantly through interactions with metal oxides and hydroxides, particularly iron (Fe), aluminum (Al), and calcium (Ca), with Fe-mediated sorption often dominant under aerobic conditions (Reddy et al., 1999). Sorption capacity is influenced by sediment mineralogy, clay content, and available sorption sites, and is therefore finite and saturable (Vymazal, 2007). Under reducing conditions, particularly

when iron (Fe) (III) is reduced to Fe (II), previously sorbed P may be released back into the water column.

Plant-mediated P uptake represents a transient retention pathway, involving assimilation of P into above- and below-ground biomass during the growing season, followed by partial release during senescence and decomposition or mineralization (Vymazal, 1995). Vegetation also indirectly enhances P retention by reducing flow velocities (thereby reducing turbulence), promoting sedimentation, and contributing organic matter (residual P) that facilitates sediment accretion. Although plant uptake typically accounts for a small fraction of total P retention (Hoagland et al., 2001; Koskiaho et al., 2003), it can be locally significant under low P loading conditions and in well-vegetated systems (Brix, 1997; Gottschall et al., 2007; Gu & Dreschel, 2008; Kill et al., 2022).

FWS CWs can function as sinks for P (Braskerud, 2002b; Geranmayeh (Kynkäänniemi) et al., 2013; Johannesson et al., 2011; Tolomio et al., 2019); however, they may also act as sources of P (Kovacic et al., 2000; Reinhardt et al., 2005; Tanner et al., 2005; Tanner & Sukias, 2011) (Table 2-8) particularly when receiving event-driven drainage. The efficiency of CWs is contingent upon factors such as P load, the predominant form of P, and wetland design, which collectively influence HRT and hydraulic efficiency of the CW. A significant variability in P retention is seen as these parameters vary seasonally and annually.

HRT and hydraulic loading rate (HLR) exert strong control over P retention by regulating settling, sorption, and diffusion processes. PP retention generally requires shorter (yet sufficient) HRTs than DP retention, as particle settling occurs rapidly once flow velocities decrease at the wetland inlet. Studies have shown that CWs receiving predominantly PP loads can maintain high TP retention under relatively short HRTs (Braskerud, 2002b; Johannesson et al., 2011; Mendes et al., 2018). In contrast, DP retention and release is diffusion-controlled and highly sensitive to HRT, redox conditions, and geochemical gradients across the sediment-water interface (Dunne et al., 2005; Reddy et al., 1999). Reinhardt et al. (2005) reported that DP retention exceeding 50% required HRTs greater than seven days in a Swiss FWS wetland. Furthermore, Tanner & Sukias (2011) reported that FWS CWs in their study received larger fractions of DP (15 to 93%) in their TP load, resulting in overall negative TP retention. The CWs exhibited >75% net P generation

which was correlated with the potential release of soil P under high flow conditions and P export under short HRT. Increased HLR promotes preferential flow paths and reduces effective treatment volume, thereby diminishing P retention efficiency (Mendes, 2020). HLR also influences P speciation: under low HLR and P-limited conditions, microbial enzymes can convert DOP to bioavailable DIP for plant growth, whereas high HLR suppresses these transformations (Gu & Dreschel, 2008). Inlet P concentration, in combination with HLR, has therefore been identified as a key predictor of TP retention across wetland systems (Dunne et al., 2012; Land & Lu, 2016; Mendes et al., 2018).

Wetland geometry and wetland-to-catchment ratio strongly influence hydraulic efficiency and retention potential. Ratios of 0.5 to 2% are commonly recommended to achieve sufficient HRT and stable flow velocities for P retention (Wilcock et al., 2012), although under low P loading conditions vegetation cover may exert greater control than area alone (Kill et al., 2022). Vegetation density enhances P retention by increasing hydraulic roughness, facilitating particle trapping, and contributing to sediment accretion. Kill et al. (2022) reported that wetlands with >20% vegetation cover exhibited approximately double the annual TP retention rate compared to sparsely vegetated systems, with retention increasing as wetlands matured. However, accumulated plant material also contributes to internal P cycling and potential DP release during decomposition.

Temperature and seasonality strongly regulate P retention processes in cold-climate wetlands. PP retention is primarily governed by hydrologic conditions and particle residence time, with highest retention typically observed during summer, followed by spring and fall, and lowest retention during winter in temperate studies (Kovacic et al., 2000; Krzeminska et al., 2023; Ulén et al., 2019). Under ice cover, settling highest PP retention may occur, but accumulated material is often mobilized during spring thaw and high-flow events. DP retention is affected by low temperature, which reduce sorption capacity by sediment (more apparent in CWs with low vegetation cover), microbial activity, and plant uptake. Consequently, TP retentions in cold climates are highly variable and strongly dependent on the dominant form of present in the influent.

Within pond-wetland systems, treatment ponds can reduce PP and solids loading, thereby limiting sediment accumulation and resuspension within wetland sections. This hydraulic and particulate treatment may enhance the stability of P retention within the system and reduce the risk

of internal P loading. However, DP retention remains constrained by HRT, geochemical conditions, and seasonal limitations, underscoring the importance of system-scale design and long-term mass balance evaluation in cold-climate applications.

2.6.3. Effect on nitrogen – forms and mechanisms

In CWs, N occurs in multiple inorganic and organic forms, primarily as NO_3^-, ammonium (NH_4^+), and Organic N (Org N) (Kadlec & Wallace, 2008). As with P, the relative proportion of influent N forms strongly governs CW performance and determines whether CWs function as net N sinks or sources (Vymazal, 2017b). N retention and transformations in FWS CWs occur through interactions among the water column, sediments, vegetation, and microbial communities, encompassing multiple N pools and transformation pathways (Figure 2-8) (Reddy & DeLaune, 2008). While these mechanisms are not strictly sequential, they can be described as a typical progression with branching and feedbacks, reflecting the concurrent and spatially heterogenous nature of N cycling in CWs.

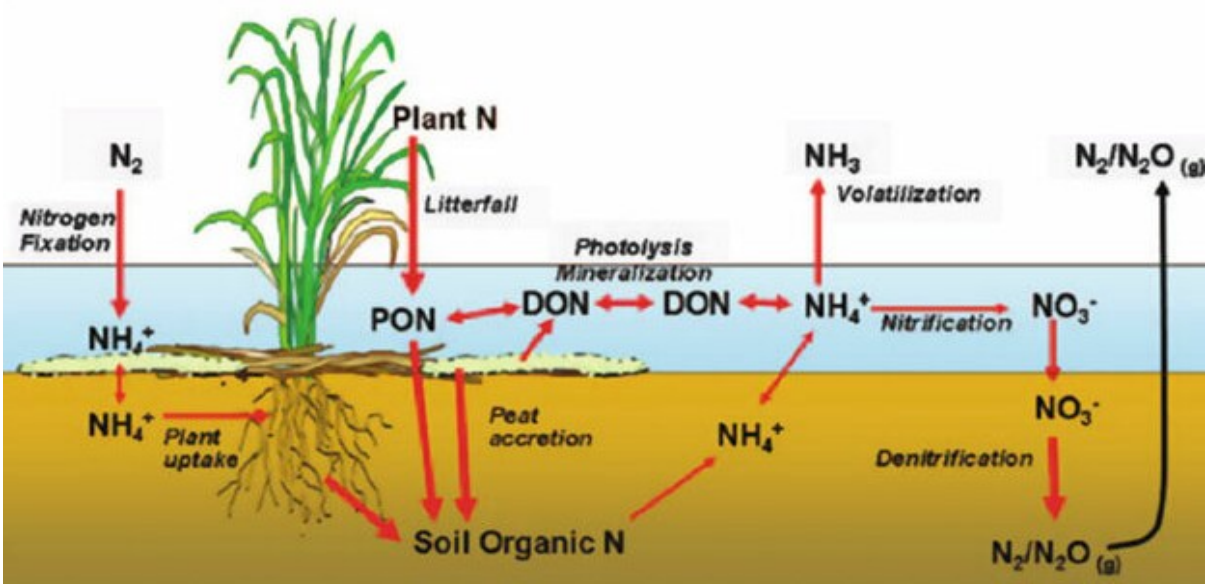

Figure 2-8. Nitrogen (N) cycle in wetland. Adapted from (Reddy & DeLaune, 2008). Note: PON = particulate organic N; DON = dissolved organic N; NH_4^+ = ammonium ion; NH_3 = ammonia; NO_3^- = nitrate ion; N_2O = nitrous oxide; N_2 = nitrogen gas.

N enters CWs as a mixture of dissolved forms (NO_3^-, NH_4^+, org N) and particulate org N (PON). Physical N processes regulate the initial distribution and residence time of these forms and include sedimentation and accretion of PON, resuspension under high-flow conditions, and diffusion-driven exchange of dissolved N species across the sediment-water interface (Kadlec & Wallace, 2008). Sedimentation of PON can result in temporary N storage in sediments, particularly

near wetland inlets; however, this storage remains vulnerable to resuspension during flow/wind-driven turbulences (Groh et al., 2015; Kovacic et al., 2006). As a result, physical retention primarily delays downstream N transport rather than constituting a durable removal pathway.

Once retained or deposited within the wetland, Org N undergoes continuous internal cycling through litterfall, incorporation into soil Org N pools, and microbial transformation (Reddy & DeLaune, 2008). Microbial mineralization, also referred as ammonification, involves conversion of Org N from plant detritus, DON, and sediments into NH_4^+ (Kadlec & Wallace, 2008; Lee et al., 2009a). This process occurs at the fastest rate in aerobic zones, decreasing as conditions switch to facultative anaerobic, and strictly anaerobic conditions, linking relatively immobile Org N pools to more reactive inorganic forms (Reddy & Patrick, 1984; Vymazal, 2007). Importantly, mineralization regulates N availability rather than providing a removal pathway, as its contribution is very limited compared to redox transformations (White & Reddy, 2009).

NH_4^+ produced through mineralization occupies a central position in CW N cycling and can follow multiple pathways depending on environmental conditions. NH_4^+ may (i) solubilize and accumulate in sediment or the water column, (ii) be assimilated by plants and microorganisms, (iii) adsorb weakly to sediments and organic matter, (iv) volatize as ammonia (NH_3), or (v) be oxidized to NO_3^- via nitrification. NH_4^+ volatilization becomes relevant in NH_4^+ rich waters, when the equilibrium of NH_4^+ and NH_3 shifts to a higher share of NH_3 as pH (> 9.3) and temperature increases (Vymazal, 2007). NH_4^+ may be adsorbed/desorbed as an exchangeable ion through a cation exchange reaction with plant detritus, inorganic sediments or soils (especially clay and humic substances), however, the mass of sorbed NH_4^+ is negligible (Kadlec & Wallace, 2008). Adsorption and volatilization represent reversible or condition-dependent pathways, contributing to short-term redistribution rather than permanent N retention.

Biological assimilation of NH_4^+ and NO_3^-, i.e., converted to organic compounds by macrophytes, microorganisms and algae, represents a transient N retention pathway in CWs. Although NH_4^+ is the preferred source of assimilation, NO_3^- may serve as a major source in NO_3^--rich waters (Vymazal, 2007). Assimilated N is incorporated into plant tissues and microbial biomass during periods of active growth, particularly in the growing season, and is subsequently released back into the system during senescence, decomposition, and mineralization (Vymazal,

2007; White & Reddy, 2003). While a small fraction of assimilated N may become permanently buried in accreting sediments, most plant-mediated N uptake functions as seasonal storage rather than long-term removal. The role of vegetation in net N removal remains variable and context-dependent. Breen (1990) suggested that routine harvesting of plants can optimize nutrient removal potential. However, Kadlec & Knight (1996) critically pointed out this would be an expensive task in full-scale application. In a study carried out by Thorén et al. (2004), an 18-ha constructed wetland in southeast Sweden was exporting N due to wetland plant decomposition with correlation between the release of N and submerged plant decay.

Nitrification and denitrification represent sequential microbially mediated redox transformations linking reduced and oxidized N species (Reddy & DeLaune, 2008). Nitrification is a two-step aerobic, oxidation of NH_4^+ to nitrite (NO_2^-) and subsequently to NO_3^-. The first step is carried out by strictly chemolithotrophic ammonia-oxidizing bacteria (AOB), commonly represented by genera such as *Nitrosomonas, Nitrosospira*, and *Nitrosococcus*, while the second step is mediated by facultative chemolithotrophic nitrite-oxidizing bacteria (NOB), including *Nitrobacter* and *Nitrospira* (Reddy & Patrick, 1984; Schmidt et al., 2003). These microorganisms use NH_4^+ or NO_2^- as electron donor, O_2 as electron acceptor and carbon dioxide as carbon source. The overall mechanism can be expressed by the following equations (Reddy & Patrick, 1984):

$$NH_4^+ + 1.5O_2 \rightarrow NO_2^- + H_2O + 2H^+ \text{ (Equation 2-1)}$$

$$NO_2^- + 0.5O_2 \rightarrow NO_3^- \text{ (Equation 2-2)}$$

Because complete nitrification requires high O_2 (4.20 - 4.57 g-O_2/g- NH_4^+) and generally proceeds more slowly than mineralization, its expression is often spatially limited and sensitive to temperature, O_2 supply, pH (6.5 to 8.0), alkalinity, and hydraulic conditions (Lee et al., 2009a; Metcalf & Eddy, 2014; Vymazal, 2007). Apart from autotrophic nitrification, heterotrophic nitrifiers belonging to genus such as *Actinomycetes, Arthrobacter, Aerobacter*, and *Thiospaera* can also support nitrification, however their rates are substantially lower when compared to *Nitrosomonas* and *Nitrobacter* groups (Saeed & Sun, 2012; Vymazal, 2007). Although nitrification does not remove N from the system, it regulates NO_3^- availability and therefore, governs the potential for subsequent denitrification. NO_3^- is biologically reduced to gaseous form (N_2) via denitrification mechanism under anoxic conditions. Within CW system, these processes

occur across oxic-anoxic interfaces of sediments, biofilms, and plant-associated microenvironments (Kadlec & Wallace, 2008). Denitrification, a pathway for permanent N removal is examined in detail in the following section.

Nitrogen concentration and loading comparisons are difficult to extrapolate among CWs in agricultural settings across the globe as flow and nitrogen load vary across a wide range of temporal scales along with differences in wetland characteristics (Table 2-7). As N transformations are microbial dependent mechanisms, the removal efficiency of N varies with temperature and season. In a study conducted by Beutel et al. (2009) concentration removal efficiency of over 90% for NO_3^- were reported. The overall seasonal NO_3^- removal significantly correlates with temperature, with 2 to 3 times higher removal rates observed in summer vs cooler months, with lowest rates observed in the Spring. This was attributed to efficient removal via bacterial activity at 20 to 25°C (Spieles & Mitsch, 1999).

N removal efficiency is critically linked to water loading and as such, flood events can cause temporal export of N. An interesting observation was made by Phipps & Crumpton (1994), who correlated N removal efficiency with influent NO_3^- concentrations and season in CWs receiving agricultural waters. N removal efficiency was highest with up to 93% in fall season, when NO_3^- constituted most of the TN input load. In contrast, in summer N removal was as low as 8%, when organic N was dominant part of TN load, thus turning CW into a N source. In a survey of 41 CWs, Vymazal (2017b) reported a moderate relationship ($R^2 = 0.61$) between inflow and removal nitrogen loads, but a much higher correlation ($R^2 = 0.82$, p-value <0.001) was observed by Saunders & Kalff (2001) in their review for the same.

Another factor critical to the net removal of nitrogen is the residence time. Koskiaho et al. (2003) studied two wetlands of areas 0.48 and 0.6 ha, with HRT of 0.25-1.6 days respectively. The author reported no removal for HRT of 0.25 days and N removal increased with increase in HRT and suggested HRT should be longer than at least one day. Sometimes, a short residence time can cause resuspension of nitrogen instead of removal. On the contrary, long HRT can allow organic N release, decreasing NO_3^- removal (Díaz et al., 2012). However, determining HRT for highly variable agricultural drainage can be difficult (Vymazal, 2017b).

2.6.3.1. Denitrification

Denitrification is widely recognized as the dominant pathway for the permanent N removal in FWS CWs and treatment pond systems (Beutel et al., 2009; Karpuzcu & Stringfellow, 2012; Vymazal, 2007; Xue et al., 2009). This microbially mediated anaerobic respiratory process reduces oxidized inorganic N species to gaseous end products, thereby permanently removing reactive N from the system (Kadlec & Wallace, 2008). Under oxygen-limited conditions, taxonomically diverse facultative anaerobic microorganisms utilize NO_3^- and NO_2^- as terminal electron acceptors, coupling their reduction to the oxidation of organic carbon.

Heterotrophic denitrification proceeds via a conserved sequence of enzyme-catalyzed redox reactions in which NO_3^- is reduced stepwise to dinitrogen gas (Equation 2-3) These transformations are mediated by functionally distinct enzymes - nitrate reductase (Nar or Nap), nitrite reductase (NirS or NirK), nitric oxide reductase (Nor), and nitrous oxide reductase (NosZ) - whose expression and activity collectively regulate reaction completeness and intermediate accumulation. The reduction of NO_3^- is stoichiometrically coupled to organic carbon oxidation (Equation 2-4), yielding the overall reaction shown in Equation 2-5 (Kadlec & Wallace, 2008; Vymazal, 2007).

$$\text{Nitrate} \rightarrow \text{Nitrite} \rightarrow \text{Nitric oxide} \rightarrow \text{Nitrous oxide} \rightarrow \text{dinitrogen gas}$$

$$2NO_3^- \rightarrow 2NO_2^- \rightarrow 2NO \rightarrow N_2O \rightarrow N_2 \text{ (Equation 2-3)}$$

$$CH_2O + H_2O \rightarrow CO_2 + 4H^+ + 4e^- \text{ (Equation 2-4)}$$

$$4NO_3^- + 5CH_2O + 4H^+ \rightarrow 2N_2 + 5CO_2 + 7H_2O \text{ (Equation 2-5)}$$

Denitrification is carried out by a phylogenetically diverse group of microorganisms, including organotrophs, chemolithotrophs, diazotrophs, and archaea, collectively referred to as denitrifiers. These organisms span multiple bacterial phyla, most prominently Proteobacteria, Bacteroidetes, Firmicutes, and Actinobacteria (Lee et al., 2009b; Mellado & Vera, 2021; Wang et al., 2022). At the genus-level, denitrifying taxa commonly reported in aquatic treatment systems include *Pseudomonas, Rhodoferax, Pseudoxanthomonas, Rhodobacter, Dechloromonas*, *Devosia, Sulfurospirillum, Magnetospirillum, Methylobacterium-Methylorubrum,* and *midas_g_2171* (Dueholm et al., 2022; Goris & Diekert, 2016; Lee et al., 2009b; Liu et al., 2025; Smriga et al.,

2021). This broad taxonomic distribution underscores that denitrification potential is widespread across microbial communities, while the realized expression of denitrification may be governed by environmental constraints and habitat-specific conditions.

Denitrification is spatially constrained within pond-wetland systems, occurring predominantly in microbial communities associated with sediments and other submerged surfaces, such as macrophytes, algae, litter, and wood (Bastviken et al., 2005; Pang et al., 2016; S. Zhang et al., 2016). These habitats provide diffusion-limited microenvironments where O_2 depletion, NO_3^- availability, and carbon supply intersect, creating favorable conditions for NO_3^- reduction. Denitrification in the bulk water column is generally limited, occurring only under sufficiently reducing conditions and typically contributing less to whole-system N removal (Bachand & Horne, 2005; Bastviken et al., 2004; Kadlec & Wallace, 2008). Sediments are widely regarded as the dominant site of denitrification due to persistent anoxia and relatively stable access to organic carbon (Kjellin et al., 2007; Whitmire & Hamilton, 2005). O_2 penetration into sediments is typically restricted to the upper millimeters, below which steep redox gradients develop, transitioning rapidly from oxic (often <1 to 5 mm thick), to suboxic and anoxic conditions. Denitrification is therefore concentrated just beneath the oxic-anoxic interface, where downward-diffusing NO_3^- overlaps with abundant organic carbon. At greater sediment depths, NO_3^- limitation constraints denitrification as electron acceptors are rapidly consumed in the upper layers (Kadlec & Wallace, 2008).

Macrophyte presence introduces additional spatial complexity by generating structurally and biogeochemically distinct biofilm habitats. Vegetation influences denitrification by (i) providing extensive surface area for biofilm colonization (Soana et al., 2018, 2025), (ii) supplying fresh, labile organic matter (carbon) through root exudation and decaying detritus (Bastviken et al., 2005; Sun et al., 2024), and (iii) locally modifying redox conditions via root radial oxygen loss, which is crucial for nitrification - denitrification at plant-soil-water interface (Mei et al., 2014; Sun et al., 2024). Biofilms constitute heterogeneous microbial matrices in which steep O_2 gradients develop over millimetre scales, enabling the coexistence of aerobic and anaerobic processes (Battin et al., 2016; Soana et al., 2018; Stewart, 2003). Rhizospheric biofilms form within the sediment-root interface, where tightly coupled oxic and anoxic microsites facilitate internal nitrification-denitrification coupling: NO_3^- produced near oxygenated root surfaces diffuses into

adjacent anoxic zones where denitrification proceeds (Alldred & Baines, 2016; Mei et al., 2014; Sun et al., 2024). In contrast, epiphytic (stem-associated) biofilms are embedded within oxygenated water columns (Eriksson & Weisner, 1997; Toet et al., 2003). As such, these biofilms exhibit steep vertical O_2 gradients, with oxic conditions at the biofilm-water interface and suboxic or anoxic micro-zones developing in the deeper layers (Battin et al., 2016). Therefore, stem-associated biofilms are carbon-limited, relying on NO_3^- availability from external supply (water column) or from nitrification occurring in the oxic layer within the same biofilm. Macrophyte-associated biofilms, although highly variable across plant species and areal coverage, can sustain denitrification rates comparable to or exceeding those observed in sediments locally or under favourable conditions (Bastviken et al., 2004, 2005; Eriksson & Weisner, 1997; Soana et al., 2025). However, these rates are typically localized and subject to strong spatial and temporal variability due to fluctuating oxygen conditions and limited carbon availability within biofilm microenvironments. Consequently, while biofilm-associated denitrification has been documented, its relative contribution to whole-system NO_3^- removal, particularly in comparison with sediment-based processes across pond- and wetland- like sections, remains uncertain.

In treatment ponds and CWs, denitrification efficiency is primarily regulated by interacting environmental factors rather than any single controlling factor, including redox potential (Eh = +350 to +100 mV), dissolved oxygen content (DO), NO_3^- supply, pH (6 to 8), organic carbon bioavailability, temperature, macrophyte coverage, and overlying water depth (Bastviken et al., 2004; Poe et al., 2003a; Vymazal, 2007). Organic carbon serves as both an energy source and a substrate for microbial growth, making it a key constraint on denitrification potential (Knowles, 1982). Carbon limitation is commonly expressed as a carbon-to-nitrogen (C/N) ratio, reflecting the balance between electron donor supply and NO_3^- reduction demand. Although stoichiometric requirements for heterotrophic denitrification suggest relatively low C/N ratio (~ 2.47:1), higher values (~ 3.02:1) are typically required in wetlands due to concurrent aerobic carbon oxidation under partially oxygenated conditions (Kadlec & Wallace, 2008; Vymazal, 2007). Empirical studies demonstrate that increasing carbon availability can substantially enhance NO_3^- removal up to thresholds (e.g. ~ 20:1), beyond which additional carbon yields diminishing returns (Grebliunas & Perry, 2016; Lu et al., 2009). In natural and treatment wetlands, carbon sources derive primarily from sediment organic matter, plant root exudates, and influent water, resulting in strong spatial variability in carbon availability and, consequently, denitrification expression.

NO_3^- availability can stimulate denitrification under N-limited conditions, with several studies reporting substantial increases in rates following NO_3^- loading events: Poe et al. (2003b) reported denitrification rates increased by 100 to 400% post rainfall, following high dissolved inorganic N loading, and Grebliunas & Perry (2016) observed denitrification rates in wetland sediments doubled when NO_3^- concentration was increased ten-fold. However, other studies report weak or an absence of NO_3^- limitation, indicating that NO_3^- effects are strongly context-dependent and mediated by habitat-specific transport and redox constraints (Beutel et al., 2009; Braskerud, 2002a).

Temperature exerts a dominant control on denitrification by regulating enzymatic activity and diffusive transport across sediment-water and biofilm interfaces (Phipps & Crumpton, 1994; Stewart, 2003; Wang et al., 2022). Denitrification rates typically increase exponentially with temperature (Vymazal, 2007), with reported optima near 20 to 25°C (Lee et al., 2009b). Sirivedhin & Gray (2006) observed a two-order-of-magnitude increase in wetland sediment denitrification rates as temperature rose from 4°C to 25°C, while Ng & Gunaratne (2011) reported that rates doubled with each 10°C increase in temperature. Although denitrification is often considered negligible below 5°C (Yan & Xu, 2013), measurable activity has been reported at 4°C or lower, albeit at lower rates (Richardson et al., 2011). As an anoxic process, denitrification is considered to be inhibited when DO concentrations in the soil water exceed 0.2 mg/L (Beauchamp et al., 1989; Tate, 2020). However, denitrification is still observed in wetlands with DO presence in its surface water, attributing this anomaly to complex microscopic spatial zoning within the system (Kadlec & Wallace, 2008). This was confirmed by Bachand & Horne (1999), who found no correlation between surface DO concentrations and NO_3^- removal rates in mesocosm studies.

Although denitrification is well established as a dominant N removal pathway in treatment pond and CW systems, uncertainty remains regarding how habitat structure, microbial community composition, and environmental constraints interact to regulate realized NO_3^- reduction rates in a combined pond-wetland system. Few studies infer denitrification potential from microbiome analyses or gene presence, while others quantify bulk NO_3^- removal without resolving habitat-specific mechanisms. This disconnect limits mechanistic understanding of how spatial variability translates into system-scale performance, particularly on cold-climate treatment systems receiving low carbon, high NO_3^- tile drainage inputs.

2.6.3.2. Kinetic model

The design and evaluation of FWS CW for nutrient removal have traditionally relied on first-order kinetic models, originally developed for municipal wastewater treatment wetlands (Kadlec & Wallace, 2008). These models provide a simplified framework for describing bulk N attenuation by relating influent and effluent concentrations to HRT and system geometry. Although widely applied, their suitability for cropping draining systems, particularly cold-climate pond-wetland configurations, remains uncertain due to differences in hydrologic regimes, influent concentrations, and dominant removal pathways.

In FWS CWs, nutrient concentration profiles typically decline exponentially along the flow path, supporting the application of first-order decay kinetics (Knight et al., 2000). Reed et al. (1995) proposed a volumetric first-order plug-flow model (Equation 2-6), expressed as:

$$\ln\left(\frac{C_i}{C_e}\right) = k\frac{V.n}{Q} \quad \text{(Equation 2-6)}$$

where, C_i and C_e are influent and effluent constituent concentrations, respectively (mg/L), k is volumetric first-order kinetic rate constant (d^{-1}), V is treatment volume of the wetland (m^3), n is porosity of the soil and Q is the average flow rate through the wetland (m^3/d). This model assumes plug-flow conditions and uniform treatment throughout the wetland volume.

Knight et al. (2000) noted that although flow in a CW typically lies between plug flow and completely mixed, first-order models with plug-flow assumptions provides conservative design estimates. To better represent internal nutrient generation, Kadlec & Knight (1996) introduced an areal-based first order model, commonly referred to as the k-C* model (Equation 2-7), which incorporates a background concentration (C*) representing internally generated or non-removable constituents:

$$\ln\left(\frac{C_{out} - C^*}{C_{in} - C^*}\right) = -\frac{K_T}{q} \quad \text{(Equation 2-7)}$$

where, C^* is the background concentration (mg/L), K_T is the rate constant adjusted for temperature (m/day) and q is the hydraulic loading rate (m/day). Values of C* may be selected based on typical regional surface-water concentrations (Jamieson et al., 2007), assumed to be zero based on influent constituent concentration (Knight et al., 2000), or statistically generated based on influent and

effluent concentrations (Rozema et al., 2016; Stone et al., 2004). Merriman et al. (2017) further refined estimates of C* values using complied data from CW studies.

Because biological and physiochemical processes governing N removal are temperature dependent, rate constants are commonly adjusted using the Arrhenius equation (Equation 2-8) and is often used for model calibrations. $\theta = 1$ denotes temperature independence, while θ lesser than or greater than 1 signifies a negative or positive effect on treatment, respectively (Kadlec & Wallace, 2008)

$$k_T = k_{20}\theta^{T-20} \text{ (Equation 2-8)}$$

where, k_T rate constant adjusted for temperature (m/day), k_{20} is the rate constant adjusted for temperature (m/day) at 20°C, T is the target temperature and θ is the Arrhenius temperature coefficient. This adjustment is particularly important in cold-climate wetlands, where seasonal temperature variation strongly influences microbial activity and diffusion processes.

A limitation of conventional k-C* models is the assumption of equal inflow and outflow, which may not hold under field conditions due to precipitation, evapotranspiration, seepage, and storage effects. To address this, Jamieson et al. (2007) proposed a flow-adjusted areal rate constant, incorporating the ratio of outflow to inflow:

$$k_{aT} = -q \ln\left[\frac{C_{out}\left(\frac{Q_{out}}{Q_{in}}\right) - C^*}{C_{in} - C^*}\right] \text{ (Equation 2-9)}$$

where, k_a is the modified areal rate constant adjusted for temperature (m/d), $\frac{Q_{out}}{Q_{in}}$ is the ratio of outflow to inflow (dimensionless). This model improves representation of concentration dilution or enrichment driven from hydrologic imbalance.

To better represent non-ideal hydraulics and spatial heterogeneity, Kadlec & Wallace (2008) further proposed a relaxed tanks-in-series (P-k-C*) model (Equation 2-10), which integrates first-order decay with continuously stirred tank reactor behavior:

$$\left(\frac{C_{out} - C^*}{C_{in} - C^*}\right) = \left(1 + \frac{k}{Pq}\right)^{-P} = \left(1 + \frac{k_v \tau}{P}\right)^{-P} \text{ (Equation 2-10)}$$

where, k is first-order areal rate constant (m/d), k_v is first order volumetric rate constant (d^{-1}) and P is apparent number of tanks in series (TIS). This model accommodates a range of hydraulic conditions and has been shown to better describe nutrient attenuation in wetlands with complex flow dynamics (Merriman et al., 2017). The rate constants are adjusted to ambient temperature by using Equation 2-8.

In pond-wetland systems, NO_3^- processing may occur sequentially along the flow path, across interconnected ponds and wetlands with contrasting depths, HRT, and biogeochemical conditions. Conventional first-order approaches assume uniform treatment within a single control volume and therefore cannot resolve spatial variability in process rates. These limitations are particularly relevant in systems where NO_3^- attenuation may be partitioned among multiple treatment units (Shilton, 2005). Moreover, while denitrification in FWS CWs is commonly conceptualised as an areal process governed by sediment-water interface area (Vymazal, 2007), treatment ponds concentrate activity within the permanent water column and associated sediments, where depth, volume and HRT exert stronger controls on NO_3^- transformations (Harper & Herr, 1993). Consequently, the applicability of areal- versus volumetric-based P-k-C* models for describing NO_3^- removal in integrated pond-wetland systems remains unresolved, particularly in cold-climate environments.

Together, these findings support the conceptual basis for integrated pond-wetland systems as multifunctional BMPs capable of addressing both hydraulic and biogeochemical limitations of individual practices. However, long-term, full-scale, cold-climate evaluations of such systems treating cropping-system tile drainage remain scarce, providing the motivation for the present study.

References

AAFC. (2024). *Farm surface water management* . Agriculture and Agri-Food Canada (AAFC). https://agriculture.canada.ca/en/agricultural-production/water/ponds-and-dugouts/farm-surface-water-management

Adeuya, R., Utt, N., Frankenberger, J., Bowling, L., Kladivko, E., Brouder, S., & Carter, B. (2012). Impacts of drainage water management on subsurface drain flow, nitrate concentration, and nitrate loads in Indiana. *Journal of Soil and Water Conservation*, *67*(6), 474 LP – 484. https://doi.org/10.2489/jswc.67.6.474

Alldred, M., & Baines, S. (2016). Effects of wetland plants on denitrification rates: a meta-analysis. In *Source: Ecological Applications* (Vol. 26, Number 3).

Alliance for the Great Lakes. (2022). *Western Lake Erie Basin Drinking Water Systems: Harmful Algal Bloom Cost of Intervention May 2022 Alliance for the Great Lakes*. www.greatlakes.org

APHA. (2017). *Standard Methods for the Examination of Water and Wastewater* (23rd ed.). American Public Health Association.

ASN-OSU. (2017). *Tile and Drainage | Agronomic Crops Network*. Agronomic Crops Network - Ohio State University . https://agcrops.osu.edu/specialization-areas/tile-and-drainage

Ayars, J. E., Christen, E. W., & Hornbuckle, J. W. (2006). Controlled drainage for improved water management in arid regions irrigated agriculture. *Agricultural Water Management*, *86*(1–2), 128–139. https://doi.org/10.1016/j.agwat.2006.07.004

Bachand, P. A. M., & Horne, A. J. (1999). Denitrification in constructed free-water surface wetlands: I. Very high nitrate removal rates in a macrocosm study. *Ecological Engineering*, *14*(1), 9–15. https://doi.org/https://doi.org/10.1016/S0925-8574(99)00016-6

Bachand, P. A. M., & Horne, A. J. (2005). Denitrification in Constructed free-water surface wetlands: II. Effects of vegetation and temperature. *Ecological Engineering*, *14*(1), 17–32. https://doi.org/10.1556/Pollack.10.2015.1.8

Ball Coelho, B., Murray, R., Lapen, D., Topp, E., & Bruin, A. (2012). Phosphorus and sediment loading to surface waters from liquid swine manure application under different drainage and tillage practices. *Agricultural Water Management*, *104*, 51–61. https://doi.org/10.1016/j.agwat.2011.10.020

Bastviken, S. K., Eriksson, P. G., Martins, I., Neto, J. M., Leonardson, L., & Tonderski, K. (2004). Potential Nitrification and Denitrification on Different Surfaces in a Constructed Treatment Wetland. *Journal of Environmental Quality*, *33*(1), 411–411. https://doi.org/10.2134/jeq2004.4110

Bastviken, S. K., Eriksson, P. G., Premrov, A., & Tonderski, K. (2005). Potential denitrification in wetland sediments with different plant species detritus. *Ecological Engineering*, *25*(2), 183–190. https://doi.org/10.1016/J.ECOLENG.2005.04.013

Battin, T. J., Besemer, K., Bengtsson, M. M., Romani, A. M., & Packmann, A. I. (2016). The ecology and biogeochemistry of stream biofilms. *Nature Reviews Microbiology*, *14*(4), 251–263. https://doi.org/10.1038/NRMICRO.2016.15;SUBJMETA

Beauchamp, E. G., Trevors, J. T., & Paul, J. W. (1989). *Carbon Sources for Bacterial Denitrification BT - Advances in Soil Science: Volume 10* (B. A. Stewart, Ed.; pp. 113–142). Springer New York. https://doi.org/10.1007/978-1-4613-8847-0_3

Beauchemin, S., Simard, R., Bolinder, M., Nolin, M. C., & Cluis, D. (2003). Prediction of phosphorus concentration in tile-drainage water from the Montreal Lowlands soils. *Canadian Journal of Soil Science*, *83*(1), 73–87. https://doi.org/10.4141/S02-029

Beckingham, B., Callahan, T., & Vulava, V. (2019). Stormwater Ponds in the Southeastern U.S. Coastal Plain: Hydrogeology, Contaminant Fate, and the Need for a Social-Ecological Framework. *Frontiers in Environmental Science*, *7*(July), 1–14. https://doi.org/10.3389/fenvs.2019.00117

Beutel, M. W., Newton, C. D., Brouillard, E. S., & Watts, R. J. (2009). Nitrate removal in surface-flow constructed wetlands treating dilute agricultural runoff in the lower Yakima Basin, Washington. *Ecological Engineering*, *35*(10), 1538–1546. https://doi.org/https://doi.org/10.1016/j.ecoleng.2009.07.005

Bingham, M., Sinha, S. K., & Lupi, F. (2015). *Economic Benefits of Reducing Harmful Algal Blooms in Lake Erie*. https://legacyfiles.ijc.org/tinymce/uploaded/Publications/Economic-Benefits-Due-to-Reduction-in-HABs-October-2015.pdf

Blann, K., Anderson, J., Sands, G., & Vondracek, B. (2009). Effects of Agricultural Drainage on Aquatic Ecosystems: A Review. *Critical Reviews in Environmental Science and Technology - CRIT REV ENVIRON SCI TECHNOL*, *39*, 909–1001. https://doi.org/10.1080/10643380801977966

Borin, M., Bonaiti, G., & Giardini, L. (2001). Controlled Drainage and Wetlands to Reduce Agricultural Pollution: A Lysimetric Study. *Journal of Environmental Quality*, *30*(4), 1330–1340. https://doi.org/10.2134/jeq2001.3041330x

Braskerud, B. C. (2002a). Factors affecting nitrogen retention in small constructed wetlands treating agricultural non-point source pollution. *Ecological Engineering*, *18*(3), 351–370. https://doi.org/10.1016/S0925-8574(01)00099-4

Braskerud, B. C. (2002b). Factors affecting phosphorus retention in small constructed wetlands treating agricultural non-point source pollution. *Ecological Engineering*, *19*(1), 41–61. https://doi.org/10.1016/S0925-8574(02)00014-9

Braskerud, B. C., Tonderski, K. S., Wedding, B., Bakke, R., Blankenberg, A. -G. B., Ulén, B., & Koskiaho, J. (2005). Can constructed wetlands reduce the diffuse phosphorus loads to eutrophic water in cold temperate regions? *Journal of Environmental Quality*, *34*(6), 2145–2155. https://doi.org/10.2134/JEQ2004.0466

BRDFN. (2018). *Drainage Water Management*. Blanchard River Demonstration Farms Network. https://blancharddemofarms.org/practices/drainage-water-management-structures

Breen, P. F. (1990). A mass balance method for assessing the potential of artificial wetlands for wastewater treatment. *Water Research*, *24*(6), 689–697. https://doi.org/https://doi.org/10.1016/0043-1354(90)90024-Z

Breitburg, D., Levin, L. A., Oschlies, A., Grégoire, M., Chavez, F. P., Conley, D. J., Garçon, V., Gilbert, D., Gutiérrez, D., Isensee, K., Jacinto, G. S., Limburg, K. E., Montes, I., Naqvi, S. W. A., Pitcher, G. C., Rabalais, N. N., Roman, M. R., Rose, K. A., Seibel, B. A., … Zhang, J. (2018). Declining oxygen in the global ocean and coastal waters. *Science*, *359*(6371). https://doi.org/10.1126/SCIENCE.AAM7240/ASSET/5ABDCCC4-FCCB-4103-A62B-F643E8891DDE/ASSETS/GRAPHIC/359_AAM7240_FA.JPEG

Brevé, M. A., & Skaggs, R. W. (1994). Hydrologic and Water Quality Impacts of Agricultural Drainage. *Critical Reviews in Environmental Science and Technology*, *24*(1), 1–32. https://doi.org/10.1080/10643389409388459

Brix, H. (1997). Do macrophytes play a role in constructed treatment wetlands? *Water Science and Technology*, *35*(5), 11–17. https://doi.org/10.1016/S0273-1223(97)00047-4

Brouder, S., Hofmann, B., Kladivko, E., Turco, R., & Bongen, A. (2005). *Interpreting Nitrate Concentration in Tile Drainage Water*. https://www.extension.purdue.edu/extmedia/AY/AY-318-W.pdf

Brunet, C. E., Gemrich, E. R. C., Biedermann, S., Jacobson, P. J., Schilling, K. E., Jones, C. S., & Graham, A. M. (2021). Nutrient capture in an Iowa farm pond: Insights from high-frequency observations. *Journal of Environmental Management*, *299*. https://doi.org/10.1016/j.jenvman.2021.113647

Bučienė, A., Šarūnas, A., Audronė, M., & and Šimanskaitė, D. (2007). Nitrogen and Phosphorus Losses with Drainage Runoff and Field Balance as a Result of Crop Management. *Communications in Soil Science and Plant Analysis*, *38*(15–16), 2177–2195. https://doi.org/10.1080/00103620701549124

Carefoot, J., & Whalen, J. (2003). Phosphorus concentration in subsurface water as influenced by cropping systems and fertilizer sources. *Canadian Journal of Soil Science*, *83*, 203–212. https://doi.org/10.4141/S02-027

Carstensen, M. V., Børgesen, C. D., Ovesen, N. B., Poulsen, J. R., Hvid, S. K., & Kronvang, B. (2019). Controlled Drainage as a Targeted Mitigation Measure for Nitrogen and Phosphorus. *Journal of Environmental Quality*, *48*(3), 677–685. https://doi.org/10.2134/jeq2018.11.0393

CCME. (1999). *Canadian Environmental Quality Guidelines - Suspended sediments* (pp. 1–2). CCME.

CCME. (2004). Phosphorus: Canadian Guidance Framework for the Management of Freshwater Systems. In *Canadian Water Quality Guidelines for the Protection of Aquatic Life*.

CCME. (2010). Canadian Water Quality Guidelines for the Protection of Aquatic Life: AMMONIA. In *CCME*.

CCME. (2012). Canadian Water Quality Guidelines for the Protection of Aquatic Life NITRATE ION. In *CCME* (Number 3). https://ccme.ca/en/res/nitrate-ion-en-canadian-water-quality-guidelines-for-the-protection-of-aquatic-life.pdf

CCME. (2025). *Canadian Environmental Quality Guidelines (CEQRs)*. Canadian Council of Ministers of the Environment | Le Conseil Canadien Des Ministres de l'environment. https://ccme.ca/en/current-activities/canadian-environmental-quality-guidelines

Chrétien, F., Gagnon, P., Thériault, G., & Guillou, M. (2016). Performance Analysis of a Wet-Retention Pond in a Small Agricultural Catchment. *Journal of Environmental Engineering*, *142*(4), 04016005. https://doi.org/10.1061/(asce)ee.1943-7870.0001081

Christianson, L. E., & Harmel, R. D. (2015). The MANAGE Drain Load database: Review and compilation of more than fifty years of North American drainage nutrient studies. *Agricultural Water Management*, *159*, 277–289. https://doi.org/https://doi.org/10.1016/j.agwat.2015.06.021

Clary, J., Leisenring, M., & Strecker, E. (2020). *International Stormwater BMP Database: 2020 Summary Statistics*. www.waterrf.org

Clary, J., Wildfire, L., & Lord, B. (2012). *Agricultural Best Management Practices (BMP) Database Phase 1 Literature Review*. https://static1.squarespace.com/static/5f8dbde10268ab224c895ad7/t/5fbd569ae2e3e53d256f2a81/1606243997348/2012_Phase1AgriculturalBMPDatabaseLiteratureReview.pdf

Cordeiro, M. R. C., Ranjan, R. S., Ferguson, I. J., & Cicek, N. (2014). Nitrate, phosphorus, and salt export through subsurface drainage from corn fields in the canadian prairies. *Transactions of the ASABE*, *57*(1), 43–50. https://doi.org/10.13031/trans.56.10370

Cravotta, C. A., Tasker, T. L., Smyntek, P. M., Blomquist, J. D., Clune, J. W., Zhang, Q., Schmadel, N. M., & Schmer, N. K. (2024). Legacy sediment as a potential source of orthophosphate: Preliminary conceptual and geochemical models for the Susquehanna River, Chesapeake Bay watershed, USA. *Science of The Total Environment*, *912*, 169361. https://doi.org/10.1016/J.SCITOTENV.2023.169361

Crumpton, W. G., Stenback, G. A., Fisher, S. W., Stenback, J. Z., & Green, D. I. S. (2020). Water quality performance of wetlands receiving nonpoint-source nitrogen loads: Nitrate and total nitrogen removal efficiency and controlling factors. *Journal of Environmental Quality*, *49*(3), 735–744. https://doi.org/10.1002/jeq2.20061

Delgado, A., Hurtado, M. D., & Andreu, L. (2006). Phosphorus Loss in Tile Drains from a Reclaimed Marsh Soil Amended with Manure and Phosphogypsum. *Nutrient Cycling in Agroecosystems*, *74*(2), 191–202. https://doi.org/10.1007/s10705-005-6240-x

Díaz, F. J., Ogeen, A. T., & Dahlgren, R. A. (2012). Agricultural pollutant removal by constructed wetlands: Implications for water management and design. *Agricultural Water Management*, *104*, 171–183. https://doi.org/10.1016/j.agwat.2011.12.012

Dinnes, D. L., Karlen, D. L., Jaynes, D. B., Kaspar, T. C., Hatfield, J. L., Colvin, T. S., & Cambardella, C. A. (2002). Nitrogen management strategies to reduce nitrate leaching in tile-drained midwestern soils. *Agronomy Journal*, *94*(1), 153–171. https://doi.org/10.2134/agronj2002.0153

Dolezal, F., Kulhavy, Z., Soukup, M., & Kodesova, R. (2001). Hydrology of tile drainage runoff. *Physics and Chemistry of the Earth, Part B: Hydrology, Oceans and Atmosphere*, *26*(7), 623–627. https://doi.org/https://doi.org/10.1016/S1464-1909(01)00059-4

Drury, C. F., Tan, C. S., Gaynor, J. D., Reynolds, W. D., Welacky, T. W., & Oloya, T. O. (2001). Tile Nitrate Loss in Continuous Corn and in a Soybean-Corn Rotation. *The Scientific World*, *1*, 163–169. https://doi.org/10.1100/tsw.2001.268

Drury, C. F., Tan, C. S., Reynolds, W. D., Welacky, T. W., Oloya, T. O., & Gaynor, J. D. (2009). Managing Tile Drainage, Subirrigation, and Nitrogen Fertilization to Enhance Crop Yields and Reduce Nitrate Loss. *Journal of Environmental Quality*, *38*(3), 1193–1204. https://doi.org/10.2134/jeq2008.0036

Drury, C. F., Tan, C. S., Welacky, T. W., Reynolds, W. D., Zhang, T. Q., Oloya, T. O., McLaughlin, N. B., & Gaynor, J. D. (2014a). Reducing Nitrate Loss in Tile Drainage Water with Cover Crops and Water-Table Management Systems. *Journal of Environmental Quality*, *43*(2), 587–598. https://doi.org/10.2134/jeq2012.0495

Drury, C. F., Tan, C. S., Welacky, T. W., Reynolds, W. D., Zhang, T. Q., Oloya, T. O., McLaughlin, N. B., & Gaynor, J. D. (2014b). Reducing Nitrate Loss in Tile Drainage Water with Cover Crops and Water-Table Management Systems. *Journal of Environmental Quality*, *43*(2), 587–598. https://doi.org/10.2134/jeq2012.0495

Dueholm, M. K. D., Nierychlo, M., Andersen, K. S., Rudkjøbing, V., Knutsson, S., MiDAS Global Consortium, Albertsen, M., & Nielsen, P. H. (2022). MiDAS 4: A global catalogue of full-length 16S rRNA gene sequences and taxonomy for studies of bacterial communities in wastewater treatment plants. *Nature Communications 2022 13:1*, *13*(1), 1–15. https://doi.org/10.1038/s41467-022-29438-7

Dunne, E. J., Coveney, M. F., Marzolf, E. R., Hoge, V. R., Conrow, R., Naleway, R., Lowe, E. F., & Battoe, L. E. (2012). Efficacy of a large-scale constructed wetland to remove phosphorus and suspended solids from Lake Apopka, Florida. *Ecological Engineering*, *42*, 90–100. https://doi.org/10.1016/J.ECOLENG.2012.01.019

Dunne, E. J., Culleton, N., O'Donovan, G., Harrington, R., & Daly, K. (2005). Phosphorus retention and sorption by constructed wetland soils in Southeast Ireland. *Water Research*, *39*(18), 4355–4362. https://doi.org/https://doi.org/10.1016/j.watres.2005.09.007

Eastman, M., Gollamudi, A., Stämpfli, N., Madramootoo, C. A., & Sarangi, A. (2010). Comparative evaluation of phosphorus losses from subsurface and naturally drained agricultural fields in the Pike River watershed of Quebec, Canada. *Agricultural Water Management*, *97*(5), 596–604. https://doi.org/https://doi.org/10.1016/j.agwat.2009.11.010

ECCC. (2012). *Wastewater Systems Effluent Regulations (SOR/2012-139)*. Https://Laws-Lois.Justice.Gc.ca/Eng/Regulations/Sor-2012-139/Fulltext.Html.

ECCC. (2018a). *Canada-Ontario Lake Erie action plan - Partnering on Achieving Phosphorus Loading Reductions to Lake Erie from Canadian Sources* (Number February). https://www.canada.ca/en/environment-climate-change/services/great-lakes-protection/action-plan-reduce-phosphorus-lake-erie.html#toc0

ECCC. (2018b). Great Lakes Freshwater Ecosystem Initiative. In *ECCC*. https://www.canada.ca/en/canada-water-agency/freshwater-ecosystem-initiatives/great-lakes/great-lakes-protection.html

EEA. (2024). *Europe's state of water 2024 : the need for improved water resilience*. Publications Office of the European Union. https://www.eea.europa.eu/en/analysis/publications/europes-state-of-water-2024

Eimers, M. C., Liu, F., & Bontje, J. (2020). Land Use, Land Cover, and Climate Change in Southern Ontario: Implications for Nutrient Delivery to the Lower Great Lakes. *Handbook of Environmental Chemistry*, *101*, 235–249. https://doi.org/10.1007/698_2020_519

Elmi, A. A., Madramootoo, C., & Hamel, C. (2000). Influence of water table and nitrogen management on residual soil NO3- and denitrification rate under corn production in sandy loam soil in Quebec. *Agriculture, Ecosystems and Environment*, *79*(2–3), 187–197. https://doi.org/10.1016/S0167-8809(99)00157-7

Eriksson, P. G., & Weisner, S. E. B. (1997). Nitrogen Removal in a Wastewater Reservoir: The Importance of Denitrification by Epiphytic Biofilms on Submersed Vegetation. *Journal of Environmental Quality*, *26*(3), 905–910. https://doi.org/10.2134/JEQ1997.00472425002600030043X;PAGE:STRING:ARTICLE/CHAPTER

Evans, R. O., Skaggs, R. W., & Gilliam, J. W. (1995). Controlled versus conventional drainage effects on water quality. *Journal of Irrigation and Drainage Engineering*, *121*(4), 271,276.

Fang, Q. X., Malone, R. W., Ma, L., Jaynes, D. B., Thorp, K. R., Green, T. R., & Ahuja, L. R. (2012). Modeling the effects of controlled drainage, N rate and weather on nitrate loss to subsurface drainage. *Agricultural Water Management*, *103*, 150–161. https://doi.org/10.1016/j.agwat.2011.11.006

FAO. (2022). *Land, Inputs and Sustainability: Fertilizers by Nutrient*.

FAOSTAT. (2025). *Cropland Nutrient Balance*. Food and Agriculture Organization of the United Nations (FAO). https://www.fao.org/faostat/en/#data/ESB/visualize

Fausey, N. R. (2005). Drainage management for humid regions. *International Agricultural Engineering Journal*, *14*(4), 209–214. https://blancharddemofarms.org/wp-content/uploads/2021/06/DrainageWater-6.pdf

Fiener, P., Auerswald, K., & Weigand, S. (2005). Managing erosion and water quality in agricultural watersheds by small detention ponds. *Agriculture, Ecosystems and Environment*, *110*(3–4), 132–142. https://doi.org/10.1016/j.agee.2005.03.012

Frankenberger, J., Kladivko, E., Sands, G., Jaynes, D., Fausey, N., Helmers, M., Cooke, R., Strock, J., Nelson, K., & Brown, L. (2006). *Questions and answers about drainage water management for the Midwest*. https://www.extension.purdue.edu/extmedia/wq/wq-44.pdf

Frankenberger, J., McMillan, S. K. W., Williams, M. R., Mazer, K., Ross, J., & Sohngen, B. (2024). Drainage Water Management: A review of nutrient load reductions and cost effectiveness. *Journal of the ASABE*, *67*(4), 1077–1092. https://doi.org/10.13031/ja.15549

Garcia-Hernandez, J. A., Brouwer, R., & Pinto, R. (2022). Estimating the Total Economic Costs of Nutrient Emission Reduction Policies to Halt Eutrophication in the Great Lakes. *Water Resources Research*, *58*. https://doi.org/10.1029/2021WR030772

Gaynor, J. D., Tan, C., Drury, C., Welacky, T. W., Ng, H. Y. F., & Reynolds, D. (2002). Runoff and Drainage Losses of Atrazine, Metribuzin, and Metolachlor in Three Water Management Systems. *Journal of Environmental Quality*, *31*, 300–308. https://doi.org/10.2134/jeq2002.0300

Gentry, L., David, M., Royer, T., Mitchell, C. A., & Starks, K. (2007). Phosphorus Transport Pathways to Streams in Tile-Drained Agricultural Watersheds. *Journal of Environmental Quality*, *36*, 408–415. https://doi.org/10.2134/jeq2006.0098

Geranmayeh (Kynkäänniemi), P., Ulén, B., Torstensson, G., & Tonderski, K. (2013). Phosphorus Retention in a Newly Constructed Wetland Receiving Agricultural Tile Drainage Water. *Journal of Environmental Quality*, *42*, 596–605. https://doi.org/10.2134/jeq2012.0266

Ghane, E., Ranaivoson, A. Z., Feyereisen, G. W., Rosen, C. J., & Moncrief, J. F. (2016). Comparison of contaminant transport in agricultural drainage water and urban stormwater runoff. *PLoS ONE*, *11*(12), 1–23. https://doi.org/10.1371/journal.pone.0167834

GLSAB, & GLWQB. (2023). *Nutrients in Lake Erie and Lake Ontario: Synthesis of International Joint Commission Recommendations and Assessment of Domestic Action Plans*. https://www.ijc.org/sites/default/files/SAB_WQB_NutrientSynthesisReport_2023.pdf

Gold, A. C., Thompson, S. P., & Piehler, M. F. (2017). Water quality before and after watershed-scale implementation of stormwater wet ponds in the coastal plain. *Ecological Engineering*, *105*, 240–251. https://doi.org/10.1016/J.ECOLENG.2017.05.003

Goris, T., & Diekert, G. (2016). The Genus Sulfurospirillum. *Organohalide-Respiring Bacteria*, 209–234. https://doi.org/10.1007/978-3-662-49875-0_10

Gottschall, N., Boutin, C., Crolla, A., Kinsley, C., & Champagne, P. (2007). The role of plants in the removal of nutrients at a constructed wetland treating agricultural (dairy) wastewater, Ontario, Canada. *Ecological Engineering*, *29*(2), 154–163. https://doi.org/10.1016/j.ecoleng.2006.06.004

Grebliunas, B. D., & Perry, W. L. (2016). The role of C:N:P stoichiometry in affecting denitrification in sediments from agricultural surface and tile-water wetlands. *SpringerPlus*, *5*(1). https://doi.org/10.1186/s40064-016-1820-6

Groh, T. A., Gentry, L. E., & David, M. B. (2015). Nitrogen Removal and Greenhouse Gas Emissions from Constructed Wetlands Receiving Tile Drainage Water. *Journal of Environmental Quality*, *44*(3), 1001–1010. https://doi.org/10.2134/JEQ2014.10.0415

Gu, B., & Dreschel, T. (2008). Effects of plant community and phosphorus loading rate on constructed wetland performance in Florida, USA. *Wetlands*, *28*(1), 81–91. https://doi.org/10.1672/07-24.1/METRICS

Gunn, K. M., Fausey, N. R., Shang, Y., Shedekar, V. S., Ghane, E., Wahl, M. D., & Brown, L. C. (2015). Subsurface drainage volume reduction with drainage water management: Case studies in Ohio, USA. *Agricultural Water Management*, *149*, 131–142. https://doi.org/https://doi.org/10.1016/j.agwat.2014.10.014

Harper, H. H., & Baker, D. M. (2007). *Evaluation of Current Stormwater Design Criteria within the State of Florida: Final Report*.

Harper, H. H., & Herr, J. L. (1993). *Treatment Efficiencies of Detention with Filtration Systems* (Number August).

Heathwaite, A. L., & Dils, R. M. (2000). Characterising phosphorus loss in surface and subsurface hydrological pathways. *Science of The Total Environment*, *251–252*, 523–538. https://doi.org/https://doi.org/10.1016/S0048-9697(00)00393-4

Heckrath, G., Brookes, P. C., Poulton, P. R., & Goulding, K. W. T. (1995). Phosphorus Leaching from Soils Containing Different Phosphorus Concentrations in the Broadbalk Experiment. *Journal of Environmental Quality*, *24*(5), 904–910. https://doi.org/https://doi.org/10.2134/jeq1995.00472425002400050018x

Helmers, M., Christianson, R., Brenneman, G., Lockett, D., & Pederson, C. (2012). Water table, drainage, and yield response to drainage water management in southeast Iowa. *Journal of Soil and Water Conservation*, *67*(6), 495 LP – 501. https://doi.org/10.2489/jswc.67.6.495

Hillebrand, H., & Sommer, U. (1999). The nutrient stoichiometry of benthic microalgal growth: Redfield proportions are optimal. *Limnology and Oceanography*, *44*(2), 440–446. https://doi.org/https://doi.org/10.4319/lo.1999.44.2.0440

Hoagland, C. R., Gentry, L. E., David, M. B., Kovacic, D. A., Hoaglanda, C. R., Gentryb, L. E., & Davidc, M. B. (2001). Plant Nutrient Uptake and Biomass Accumulation in a Constructed Wetland. *Journal of Freshwater Ecology*, *16*(4), 527–540. https://doi.org/10.1080/02705060.2001.9663844

ICID. (2018). *World Drained Area -2018*. https://www.icid.org/world-drained-area.pdf

Ivanovsky, A., Belles, A., Criquet, J., Dumoulin, D., Noble, P., Alary, C., & Billon, G. (2018). Assessment of the treatment efficiency of an urban stormwater pond and its impact on the natural downstream watercourse. *Journal of Environmental Management*, *226*, 120–130. https://doi.org/10.1016/J.JENVMAN.2018.08.015

James, W. F., Barko, J. W., Eakin, H. L., Jamesa, W. F., Barkoaeb, J. W., & Eakina, H. L. (2002). Labile and refractory forms of phosphorus in runoff of the redwood river basin, minnesota. *Journal of Freshwater Ecology*, *17*(2), 297–304. https://doi.org/10.1080/02705060.2002.9663898

Jamieson, R., Gordon, R., Wheeler, N., Smith, E., Stratton, G., & Madani, A. (2007). Determination of first order rate constants for wetlands treating livestock wastewater in cold climates. *Journal of Environmental Engineering and Science*, *6*(1), 65–72. https://doi.org/10.1139/S06-028

Jaynes, D. B. (2012). Changes in yield and nitrate losses from using drainage water management in central Iowa, United States. *Journal of Soil and Water Conservation*, *67*(6), 485 LP – 494. https://doi.org/10.2489/jswc.67.6.485

Jaynes, D. B., Colvin, T. S., Karlen, D. L., Cambardella, C. A., & Meek, D. W. (2001). Nitrate Losss in Subsurface Drainage as Affected by Nitrogen Fertilization Rate. *Journal of Environmental Quality*, *30*, 1305–1314. https://doi.org/10.1515/9781400862771

Johannesson, K. M., Andersson, J. L., & Tonderski, K. S. (2011). Efficiency of a constructed wetland for retention of sediment-associated phosphorus. *Hydrobiologia*, *674*(1), 179–190. https://doi.org/10.1007/s10750-011-0728-y

Johannesson, K. M., Tonderski, K. S., Ehde, P. M., & Weisner, S. E. B. (2017). Temporal phosphorus dynamics affecting retention estimates in agricultural constructed wetlands. *Ecological Engineering*, *103*, 436–445. https://doi.org/10.1016/j.ecoleng.2015.11.050

Jones, J., Clary, J., Strecker, E., Quigley. M., & Moeller, J. (2012, March 1). *BMP Effectiveness for Nutrients, Bacteria, Solids, Metals, and Runoff Volume | Stormwater Solutions*. Stormwater Solutions. https://www.stormwater.com/bmps/article/13006936/bmp-effectiveness-for-nutrients-bacteria-solids-metals-and-runoff-volume

Jouni, H. J., Liaghat, A., Hassanoghli, A., & Henk, R. (2018). Managing controlled drainage in irrigated farmers' fields: A case study in the Moghan plain, Iran. *Agricultural Water Management*, *208*(July), 393–405. https://doi.org/10.1016/j.agwat.2018.06.037

Kadlec, R. H., & Knight, R. L. (1996). *Treatment Wetland*. Lewis Publishers Inc.

Kadlec, R. H., & Wallace, S. D. (2008). *Treatment Wetlands* (Second). Taylor & Francis Group, LLC.

Karpuzcu, M. E., & Stringfellow, W. T. (2012). Kinetics of nitrate removal in wetlands receiving agricultural drainage. *Ecological Engineering*, *42*, 295–303. https://doi.org/10.1016/j.ecoleng.2012.02.015

Karsten, H., & Vanek, S. (2021). *6.2.5: The Phosphorus Cycle and Human Management of Soils - Engineering LibreTexts*. LibreTexts Engineering.

Kill, K., Grinberga, L., Koskiaho, J., Mander, Ü., Wahlroos, O., Lauva, D., Pärn, J., & Kasak, K. (2022). Phosphorus removal efficiency by in-stream constructed wetlands treating agricultural runoff: Influence of vegetation and design. *Ecological Engineering*, *180*. https://doi.org/10.1016/j.ecoleng.2022.106664

King, K., Fausey, N., & Williams, M. (2014). Effect of subsurface drainage on streamflow in an agricultural headwater watershed. *Journal of Hydrology*, *519*, 438–445. https://doi.org/https://doi.org/10.1016/j.jhydrol.2014.07.035

King, K., Williams, M., & Fausey, N. (2015). Contributions of Systematic Tile Drainage to Watershed-Scale Phosphorus Transport. *Journal of Environmental Quality*, *44*(2), 486–494. https://doi.org/10.2134/jeq2014.04.0149

King, K., Williams, M., & Fausey, N. R. (2016). Effect of crop type and season on nutrient leaching to tile drainage under a corn-soybean rotation. *Journal of Soil and Water Conservation*, *71*, 56–68. https://doi.org/10.2489/jswc.71.1.56

King, K., Williams, W., Macrae, M. L., Fausey, N. R., Frankenberger, J., Smith, D. R., Kleinman, P. J. A., & Brown, L. C. (2015). Phosphorus Transport in Agricultural Subsurface Drainage: A Review. *Journal of Environmental Quality*, *44*(2), 467–485. https://doi.org/10.2134/jeq2014.04.0163

Kjellin, J., Hallin, S., & Wörman, A. (2007). Spatial variations in denitrification activity in wetland sediments explained by hydrology and denitrifying community structure. *Water Research*, *41*(20), 4710–4720. https://doi.org/10.1016/j.watres.2007.06.053

Kladivko, E. J., Grochulska, J., Turco, R. F., Van Scoyoc, G. E., & Eigel, J. D. (1999). Pesticide and Nitrate Transport into Subsurface Tile Drains of Different Spacings. *Journal of Environmental Quality*, *28*(3), 997–1004. https://doi.org/https://doi.org/10.2134/jeq1999.00472425002800030033x

Kladivko, E. J., Van Scoyoc, G. E., Monke, E. J., Oates, K. M., & Pask, W. (1991). Pesticide and Nutrient Movement into Subsurface Tile Drains on a Silt Loam Soil in Indiana. *Journal of Environmental Quality*, *20*(1), 264–270. https://doi.org/10.2134/jeq1991.00472425002000010043x

Knight, R. L. (1992). Ancillary benefits and potential problems with the use of wetlands for nonpoint source pollution control. *Ecological Engineering*, *1*(1), 97–113. https://doi.org/https://doi.org/10.1016/0925-8574(92)90027-Y

Knight, R. L., Payne Jr, V. W. E., Borer, R. E., Clarke, R. A., & Pries, J. H. (2000). Constructed Wetlands for livestock wastewater management. *Ecological Engineering*, *15*, 41–55.

Knowles, R. (1982). Denitrification. *Microbiol*, *46*(1), 43–70.

Koch, B. J., Febria, C. M., Gevrey, M., Wainger, L. A., & Palmer, M. A. (2014). Nitrogen Removal by Stormwater Management Structures: A Data Synthesis. *JAWRA Journal of the American Water Resources Association*, *50*(6), 1594–1607. https://doi.org/10.1111/JAWR.12223

Kokulan, V. (2019). *Environmental and Economic Consequences of Tile Drainage Systems in Canada* (Number June). https://capi-icpa.ca/wp-content/uploads/2019/06/2019-06-14-CAPI-Vivekananthan-Kokulan-Paper-WEB.pdf

Koskiaho, J., Ekholm, P., Räty, M., Riihimäki, J., & Puustinen, M. (2003). Retaining agricultural nutrients in constructed wetlands—experiences under boreal conditions. *Ecological Engineering*, *20*(1), 89–103. https://doi.org/https://doi.org/10.1016/S0925-8574(03)00006-5

Kottek, M., Grieser, J., Beck, C., Rudolf, B., & Rubel, F. (2006). World map of the Köppen-Geiger climate classification updated. *Meteorologische Zeitschrift*, *15*(3), 259–263. https://doi.org/10.1127/0941-2948/2006/0130

Kovacic, D. A., David, M. B., Gentry, L. E., Starks, K. M., & Cooke, R. A. (2000). Effectiveness of Constructed Wetlands in Reducing Nitrogen and Phosphorus Export from Agricultural Tile Drainage. *Journal of Environmental Quality*, *29*(4), 1262–1274. https://doi.org/10.2134/jeq2000.00472425002900040033x

Kovacic, D. A., Twait, R. M., Wallace, M. P., & Bowling, J. M. (2006). Use of created wetlands to improve water quality in the Midwest—Lake Bloomington case study. *Ecological Engineering*, *28*(3), 258–270. https://doi.org/https://doi.org/10.1016/j.ecoleng.2006.08.002

Krzeminska, D., Blankenberg, A.-G. B., Bechmann, M., & Deelstra, J. (2023). The effectiveness of sediment and phosphorus removal by a small constructed wetland in Norway: 18 years of monitoring and perspectives for the future. *Catena*, *223*, 106962. https://doi.org/10.1016/j.catena.2023.106962

Kynkäänniemi, P., Ulén, B., Torstensson, G., & Tonderski, K. S. (2013). Phosphorus retention in a newly constructed wetland receiving agricultural tile drainage water. *Journal of Environmental Quality*, *42*(2), 596–605. https://doi.org/10.2134/jeq2012.0266

Land, M. R., & Lu, L. (2016). An Upper Bound on the Burning Number of Graphs. *Lecture Notes in Computer Science (Including Subseries Lecture Notes in Artificial Intelligence and Lecture Notes in Bioinformatics)*, *10088 LNCS*, 1–8. https://doi.org/10.1007/978-3-319-49787-7_1

Larsson, U., Elmgren, R. (Stockholm Univ. (Sweden). Z. Inst.), & Wulff, F. (1985). Eutrophication and the Baltic Sea: causes and consequences. *Ambio*, *14*(1), 9–14.

Lavaire, T., Gentry, L. E., David, M. B., & Cooke, R. A. (2017). Fate of water and nitrate using drainage water management on tile systems in east-central Illinois. *Agricultural Water Management*, *191*, 218–228. https://doi.org/10.1016/j.agwat.2017.06.004

Lavrnić, S., Nan, X., Blasioli, S., Braschi, I., Anconelli, S., & Toscano, A. (2020). Performance of a full scale constructed wetland as ecological practice for agricultural drainage water treatment in Northern Italy. *Ecological Engineering*, *154*. https://doi.org/10.1016/j.ecoleng.2020.105927

Lawlor, P. A., Helmers, M. J., Baker, J. L., Melvin, S. W., & Lemke, D. W. (2008). Nitrogen application rate effect on nitrate-nitrogen concentration and loss in subsurface drainage for a corn-soybean rotation. *Agricultural and Biosystems Engineering*, *51*(1), 83–94.

Lawrence, A. I., Marsalek, J., Ellis, J. B., & Urbonas, B. (1996). Stormwater detention & BMPs. *Journal of Hydraulic Research*, *34*(6), 799–813. https://doi.org/10.1080/00221689609498452

Lee, C. G., Fletcher, T. D., & Sun, G. (2009a). Nitrogen removal in constructed wetland systems. In *Engineering in Life Sciences* (Vol. 9, Number 1, pp. 11–22). https://doi.org/10.1002/elsc.200800049

Lee, C. G., Fletcher, T. D., & Sun, G. (2009b). Nitrogen removal in constructed wetland systems. *Engineering in Life Sciences*, *9*(1), 11–22. https://doi.org/10.1002/ELSC.200800049;JOURNAL:JOURNAL:15213846;WGROUP:STRING:PUBLICATION

Liu, Y., Gao, H., Wang, Z., Xue, P., Chen, X., Wang, B., & Wen, G. (2025). Nitrogen cycling blocked in constructed wetlands: Mechanisms, developments, and challenges—A review. *Water Research X*, *29*, 100401. https://doi.org/10.1016/J.WROA.2025.100401

Liu, Y., Youssef, M. A., Chescheir, G. M., Appelboom, T. W., Poole, C. A., Arellano, C., & Skaggs, R. W. (2019). Effect of controlled drainage on nitrogen fate and transport for a subsurface drained

grass field receiving liquid swine lagoon effluent. *Agricultural Water Management*, *217*, 440–451. https://doi.org/10.1016/J.AGWAT.2019.02.018

Lockett, B. R., Buttle, J. M., Leach, J. A., Liu, F., Sorichetti, R. J., & Eimers, M. C. (2024). Agricultural intensification and urban expansion affect the seasonal flow regime in southern Ontario watersheds. *Hydrological Processes*, *38*(6), e15175. https://doi.org/10.1002/HYP.15175

Lu, S., Hu, H., Sun, Y., & Yang, J. (2009). Effect of carbon source on the denitrification in constructed wetlands. *Journal of Environmental Sciences*, *21*(8), 1036–1043. https://doi.org/10.1016/S1001-0742(08)62379-7

Macrae, M., English, M., Schiff, S., & Stone, M. (2007). Intra-annual variability in the contribution of tile drains to basin discharge and phosphorus export in a first-order agricultural catchment. *Agricultural Water Management*, *92*, 171–182. https://doi.org/10.1016/j.agwat.2007.05.015

Madramootoo, C. A., Helwig, T. G., & Dodds, G. T. (2001). Managing Water Tables to improve Drainage Water Quality in Quebec, Canada. *American Society of Agricultural Engineers*, *44*(6), 1511–1519.

Mallin, M. A., Ensign, S. H., Wheeler, T. L., & Mayes, D. B. (2002). Pollutant Removal Efficacy of Three Wet Detention Ponds. *Journal of Environmental Quality*, *31*(2), 654–660. https://doi.org/https://doi.org/10.2134/jeq2002.6540

Marques, P., & Mandrak, N. E. (2024). Ecosystem Functions in Urban Stormwater Management Ponds: A Scoping Review. *Sustainability*, *16*(17), 7766. https://doi.org/10.3390/SU16177766/S1

Masi, F., Rizzo, A., & Regelsberger, M. (2018). The role of constructed wetlands in a new circular economy, resource oriented, and ecosystem services paradigm. *Journal of Environmental Management*, *216*, 275–284. https://doi.org/https://doi.org/10.1016/j.jenvman.2017.11.086

Maynard, J. J., O'Geen, A. T., & Dahlgren, R. A. (2009). Bioavailability and fate of phosphorus in constructed wetlands receiving agricultural runoff in the San Joaquin Valley, California. *Journal of Environmental Quality*, *38*(1), 360–372. https://doi.org/10.2134/JEQ2008.0088

Mei, X. Q., Yang, Y., Tam, N. F. Y., Wang, Y. W., & Li, L. (2014). Roles of root porosity, radial oxygen loss, Fe plaque formation on nutrient removal and tolerance of wetland plants to domestic wastewater. *Water Research*, *50*, 147–159. https://doi.org/10.1016/J.WATRES.2013.12.004

Mejia, M. N., Madramootoo, C. A., & Broughton, R. S. (2000). Influence of water table management on corn and soybean yields. *Agricultural Water Management*, *46*, 73–89.

Mellado, M., & Vera, J. (2021). Microorganisms that participate in biochemical cycles in wetlands. In *Canadian Journal of Microbiology* (Vol. 67, Number 11, pp. 771–788). Canadian Science Publishing. https://doi.org/10.1139/cjm-2020-0336

Mendes, L. R. D. (2020). Edge-of-Field technologies for phosphorus retention from agricultural drainage discharge. *Applied Sciences (Switzerland)*, *10*(2). https://doi.org/10.3390/app10020634

Mendes, L. R. D., Tonderski, K., Iversen, B. V., & Kjaergaard, C. (2018). Phosphorus retention in surface-flow constructed wetlands targeting agricultural drainage water. *Ecological Engineering*, *120*, 94–103. https://doi.org/10.1016/j.ecoleng.2018.05.022

Merriman, L. S., Hathaway, J. M., Burchell, M. R., & Hunt, W. F. (2017). Adapting the relaxed tanks-in-series model for stormwaterwetland water quality performance. *Water (Switzerland)*, *9*(9). https://doi.org/10.3390/w9090691

Metcalf, & Eddy. (2014). *Wastewater Engineering: Treatment and Resource Recovery* (5th ed.).

Michalak, A. M., Anderson, E. J., Beletsky, D., Boland, S., Bosch, N. S., Bridgeman, T. B., Chaffin, J. D., Cho, K., Confesor, R., Daloglu, I., DePinto, J. V., Evans, M. A., Fahnenstiel, G. L., He, L., Ho, J. C., Jenkins, L., Johengen, T. H., Kuo, K. C., LaPorte, E., … Zagorski, M. A. (2013). Record-setting algal bloom in Lake Erie caused by agricultural and meteorological trends consistent with

expected future conditions. *Proceedings of the National Academy of Sciences of the United States of America*, *110*(16), 6448–6452. https://doi.org/10.1073/PNAS.1216006110/SUPPL_FILE/PNAS.201216006SI.PDF

Mitsch, W., Day, J., Gilliam, W., Groffman, P., Hey, D., RANDALL, G., & Wang, N. (2001). Reducing Nitrogen Loading to the Gulf of Mexico from the Mississippi River Basin: Strategies to Counter a Persistent Ecological Problem. *Bioscience*, *51*. https://doi.org/10.1641/0006-3568(2001)051[0373:RNLTTG]2.0.CO;2

Mitsch, W., & Gosselink, J. (2015). Wetlands, 5th Edition. In *Wi Ley* (Vol. 91, Number 5). https://www.researchgate.net/publication/271643179_Wetlands_5th_edition

Mitsch, W. J., Zhang, L., Stefanik, K. C., Nahlik, A. M., Anderson, C. J., Bernal, B., Hernandez, M., & Song, K. (2012). Creating Wetlands: Primary Succession, Water Quality Changes, and Self-Design over 15 Years. *BioScience*, *62*(3), 237–250. https://doi.org/10.1525/bio.2012.62.3.5

MOE. (1979). *Rationale for the Establishment of Ontario's Water Quality Objectives*. Ontario Ministry of Environment. https://www.ontario.ca/page/water-management-policies-guidelines-provincial-water-quality-objectives#fn121

MOEE. (1994). *Water management: policies, guidelines, provincial water quality objectives | Ontario.ca*. https://www.ontario.ca/page/water-management-policies-guidelines-provincial-water-quality-objectives#section-13

Moore, J. (2016). Tile Drainage and Phosphorus Losses from Agricultural Land. In *Lake Champlain Basin Program*. http://www.lcbp.org/media-center/publications-library/publication-database/

Morel, F. M. M., & Hering, J. G. (1993). *Principles and Applications of Aquatic Chemistry*. Wiley. https://books.google.ca/books?id=Rs31PfkeBaIC

Muenich, R. L., Kalcic, M., & Scavia, D. (2016). Evaluating the Impact of Legacy P and Agricultural Conservation Practices on Nutrient Loads from the Maumee River Watershed. *Environmental Science and Technology*, *50*(15), 8146–8154. https://doi.org/10.1021/ACS.EST.6B01421/SUPPL_FILE/ES6B01421_SI_001.PDF

Nash, P., Nelson, K., & Motavalli, P. (2015). Reducing Nitrogen Loss with Managed Drainage and Polymer-Coated Urea. *Journal of Environmental Quality*, *44*(1), 256–264. https://doi.org/10.2134/JEQ2014.05.0238

Nash, P. R., Nelson, K. A., Motavalli, P. P., Nathan, M., & Dudenhoeffer, C. (2015). Reducing Phosphorus Loss in Tile Water with Managed Drainage in a Claypan Soil. *Journal of Environmental Quality*, *44*(2), 585–593. https://doi.org/10.2134/jeq2014.04.0146

Newman, J. M., & Clausen, J. C. (1997). Seasonal effectiveness of a constructed wetland for processing milkhouse wastewater. *Wetlands*, *17*(3), 375–382. https://doi.org/10.1007/BF03161427/METRICS

Ng, H. Y. F., Tan, C. S., Drury, C. F., & Gaynor, J. D. (2002). Controlled drainage and subirrigation influences tile nitrate loss and corn yields in a sandy loam soil in Southwestern Ontario. *Agriculture, Ecosystems & Environment*, *90*(1), 81–88. https://doi.org/https://doi.org/10.1016/S0167-8809(01)00172-4

Ng, W. J., & Gunaratne, G. (2011). Design of tropical constructed wetlands. *Wetlands for Tropical Applications: Wastewater Treatment by Constructed Wetlands*, 69–93. https://doi.org/10.1142/9781848162983_0005

Nietch, C. T., Borst, M., & O'Shea, M. L. (2001). Stormwater treatment: Ponds vs. constructed wetlands. *Proceedings of the Engineering Foundation Conference*, *263*(Ms 104), 524–528. https://doi.org/10.1061/40602(263)39

Nilsson, J. E., Weisner, S. E. B., & Liess, A. (2023). Wetland nitrogen removal from agricultural runoff in a changing climate. *Science of the Total Environment*, *892*(2023). https://doi.org/10.1016/j.scitotenv.2023.164336

NOAA. (2024, August 1). *Gulf of Mexico 'dead zone' larger than average, scientists find | National Oceanic and Atmospheric Administration*. National Oceanic and Atmospheric Administration. https://www.noaa.gov/news-release/gulf-of-mexico-dead-zone-larger-than-average-scientists-find

NWRM Project. (2013). Retention Ponds. In *NWRM*.

Oduor, B. O., Campo-Bescós, M. Á., Lana-Renault, N., Kyllmar, K., Mårtensson, K., & Casalí, J. (2023). Quantification of agricultural best management practices impacts on sediment and phosphorous export in a small catchment in southeastern Sweden. *Agricultural Water Management*, *290*, 108595. https://doi.org/10.1016/J.AGWAT.2023.108595

OMAFA. (2002). *Nutrient Management Act, 2002, S.O. 2002, c. 4 | ontario.ca*. OMAFA. OMAFA. https://www.ontario.ca/laws/statute/02n04

OMAFA. (2025). *Environmental Impacts of Nitrogen Use in Agriculture (Factsheet: 25-013)*.

OMAFA, & OSCIA. (2019). *ONFARM applied research and monitoring*. OSCIA. https://www.ontariosoilcrop.org/onfarm/

OMAFRA. (1991). *Risk Of Alfalfa Winterkill*. http://www.omafra.gov.on.ca/english/crops/facts/91-072.htm#RISKO

OMECP. (1990a). *Environmental Protection Act, R.S.O. 1990, c. E.19*. Https://Www.Ontario.ca/Laws/Statute/90e19.

OMECP. (1990b). *Ontario Water Resources Act, R.S.O. 1990, c. O.40*. Https://Www.Ontario.ca/Laws/Statute/90o40#BK0.

OMECP. (2020). *Stormwater Management Planning and Design Manual: Stormwater management plan and SWMP design | Ontario.ca*. Ontario Ministry of Environment, Conservation and Parks. https://www.ontario.ca/document/stormwater-management-planning-and-design-manual/stormwater-management-plan-and-swmp-design

OMECP. (2024). *Canada-Ontario Lake Erie Action Plan: 2024 Evaluation and Update Report*.

OSCIA. (2018). *Controlled Tile Drainage | OSCIA*. Ontario Soil and Crop Improvement Association. https://www.ontariosoilcrop.org/research-resources/research-projects/controlled-tile-drainage/

OSCIA. (2023). *Lake Erie Agriculture Demonstrating Sustainability* . OSCIA. https://www.ontariosoilcrop.org/lake-erie-agriculture-demonstrating-sustainability/

PAMI. (2018). *Beneficial Management Practises for Agricultural Tile Drainage in Manitoba - Controlled Tile Drainage, IF-04*.

Pang, S., Zhang, S., Lv, X. Y., Han, B., Liu, K., Qiu, C., Wang, C., Wang, P., Toland, H., & He, Z. (2016). Characterization of bacterial community in biofilm and sediments of wetlands dominated by aquatic macrophytes. *Ecological Engineering*, *97*, 242–250. https://doi.org/10.1016/J.ECOLENG.2016.10.011

Peng, J. feng, Wang, B. zhen, Song, Y. hui, Yuan, P., & Liu, Z. (2007). Adsorption and release of phosphorus in the surface sediment of a wastewater stabilization pond. *Ecological Engineering*, *31*(2), 92–97. https://doi.org/10.1016/J.ECOLENG.2007.06.005

Phipps, R. G., & Crumpton, W. G. (1994). Factors affecting nitrogen loss in experimental wetlands with different hydrologic loads. *Ecological Engineering*, *3*(4), 399–408. https://doi.org/https://doi.org/10.1016/0925-8574(94)00009-3

Poe, A. C., Piehler, M. F., Thompson, S. P., & Paerl, H. W. (2003a). Denitrification in a constructed wetland receiving agricultural runoff. *Wetlands*, *23*(4), 817–826. https://doi.org/10.1672/0277-5212(2003)023[0817:DIACWR]2.0.CO;2

Poe, A. C., Piehler, M. F., Thompson, S. P., & Paerl, H. W. (2003b). Denitrification in a constructed wetland receiving agricultural runoff. *Wetlands*, *23*(4), 817–826. https://doi.org/10.1672/0277-5212(2003)023[0817:DIACWR]2.0.CO;2

Poole, C. A., Skaggs, R. W., Youssef, M. A., Chescheir, G. M., Crozier, C. R., & Schilfgaarde, V. (2018). Effect of Drainage Water Management on Nitrate Nitrogen Loss to Tile Drains in North Carolina. *Transactions of the ASABE*, *61*(3), 233–244. https://doi.org/10.13031/trans.12296

Pugliese, L., Heckrath, G. J., Iversen, B. V., & Straface, S. (2023). Treatment Systems for Agricultural Drainage Water and Farmyard Runoff in Denmark: Case Studies. In *Handbook of Environmental Chemistry* (Vol. 117). https://doi.org/10.1007/698_2021_784

Rabalais, N. N., Turner, R. E., & Wiseman, W. J. (2002). Gulf of Mexico Hypoxia, A.K.A. "The Dead Zone." *Annual Review of Ecology and Systematics*, *33*(1), 235–263. https://doi.org/10.1146/annurev.ecolsys.33.010802.150513

Ramoska, E., Bastiene, N., & Saulys, V. (2011). Evaluation of controlled drainage efficiency in Lithuania. *Irrigation and Drainage*, *60*(2), 196–206. https://doi.org/10.1002/ird.548

Randall, G. W., & Goss, M. J. (2008). Nitrate Losses to Surface Water Through Subsurface, Tile Drainage. In J. L. Hatfield & R. F. Follett (Eds.), *Nitrogen in the Environment: Sources, Problems, and Management* (2nd ed., pp. 145–175). Elsevier Science & Technology.

Randall, M. C., Carling, G. T., Dastrup, D. B., Miller, T., Nelson, S. T., Rey, K. A., Hansen, N. C., Bickmore, B. R., & Aanderud, Z. T. (2019). Sediment potentially controls in-lake phosphorus cycling and harmful cyanobacteria in shallow, eutrophic Utah Lake. *PLOS ONE*, *14*(2), e0212238. https://doi.org/10.1371/JOURNAL.PONE.0212238

Rasouli, S. (2013). *Soluble and particulate nitrogen losses from tile drained agricultural fields in southern Quebec, Canada*. McGill Univeristy, Montreal.

Reddy, K. R., & DeLaune, R. D. (2008). Biogeochemistry of Wetlands : Science and Applications. *Biogeochemistry of Wetlands*. https://doi.org/10.1201/9780203491454

Reddy, K. R., Kadlec, R. H., Flaig, E., & Gale, P. M. (1999). Streams and Wetlands: A Review. *Critical Reviews in Environmental Science and Technology*, *29*(1), 83–146.

Reddy, K. R., & Patrick, W. H. (1984). Nitrogen transformations and loss in flooded soils and sediments. *Critical Reviews in Environmental Science and Technology*, *13*(4), 273–309. https://doi.org/10.1080/10643388409381709

Redfield, A. C. (1958). THE BIOLOGICAL CONTROL OF CHEMICAL FACTORS IN THE ENVIRONMENT. *American Scientist*, *46*(3), 230A – 221. http://www.jstor.org/stable/27827150

Reed, S. C., Crites, R. W., & Middlebrooks, E. J. (1995). *Natural Systemd for Waste Management and Treatment - Second Edition*. McGraw Hill Co.

Reinhardt, M., Gächter, R., Wehrli, B., & Müller, B. (2005). Phosphorus retention in small constructed wetlands treating agricultural drainage water. *Journal of Environmental Quality*, *34*(4), 1251–1259. https://doi.org/10.2134/jeq2004.0325

Richardson, W. B., Strauss, E. A., Bartsch, L. A., Monroe, E. M., Cavanaugh, J. C., Vingum, L., & Soballe, D. M. (2011). Denitrification in the Upper Mississippi River: rates, controls, and contribution to nitrate flux. *Https://Doi.Org/10.1139/F04-062*, *61*(7), 1102–1112. https://doi.org/10.1139/F04-062

Riley, K. D., Helmers, M. J., Lawlor, P. A., & Singh, R. (2009). Water Balance Investigation of Drainage Water Management in Non-Weighing Lysimeters. *Applied Engineering in Agriculture*, *25*(4), 507–514. https://doi.org/10.13031/2013.27470

Robertson, D. M., & Saad, D. A. (2021). Nitrogen and Phosphorus Sources and Delivery from the Mississippi/Atchafalaya River Basin: An Update Using 2012 SPARROW Models. *JAWRA Journal of the American Water Resources Association*, *57*(3), 406–429. https://doi.org/10.1111/1752-1688.12905

Robotham, J., Old, G., Rameshwaran, P., Sear, D., Gasca-Tucker, D., Bishop, J., Old, J., & McKnight, D. (2021). Sediment and Nutrient Retention in Ponds on an Agricultural Stream: Evaluating Effectiveness for Diffuse Pollution Mitigation. *Water 2021, Vol. 13, Page 1640*, *13*(12), 1640. https://doi.org/10.3390/W13121640

Ross, J. A., Herbert, M. E., Sowa, S. P., Frankenberger, J. R., King, K. W., Christopher, S. F., Tank, J. L., Arnold, J. G., White, M. J., & Yen, H. (2016a). A synthesis and comparative evaluation of factors influencing the effectiveness of drainage water management. *Agricultural Water Management*, *178*, 366–376. https://doi.org/10.1016/j.agwat.2016.10.011

Ross, J. A., Herbert, M. E., Sowa, S. P., Frankenberger, J. R., King, K. W., Christopher, S. F., Tank, J. L., Arnold, J. G., White, M. J., & Yen, H. (2016b). A synthesis and comparative evaluation of factors influencing the effectiveness of drainage water management. *Agricultural Water Management*, *178*, 366–376. https://doi.org/10.1016/j.agwat.2016.10.011

Rozema, E. R., VanderZaag, A. C., Wood, J. D., Drizo, A., Zheng, Y., Madani, A., & Gordon, R. J. (2016). Constructed wetlands for agricultural wastewater treatment in northeastern North America: A review. In *Water (Switzerland)* (Vol. 8, Number 5, pp. 1–14). https://doi.org/10.3390/w8050173

Rozemeijer, J. C., Visser, A., Borren, W., Winegram, M., Van Der Velde, Y., Klein, J., & Broers, H. P. (2016). High-frequency monitoring of water fluxes and nutrient loads to assess the effects of controlled drainage on water storage and nutrient transport. *Hydrology and Earth System Sciences*, *20*(1), 347–358. https://doi.org/10.5194/hess-20-347-2016

Rushton, B. T., & Bahk, B. M. (2001). Treatment of stormwater runoff from row crop farming in Ruskin, Florida. *Water Science and Technology*, *44*(11–12), 531–538. https://doi.org/10.2166/wst.2001.0876

Saadat, S., Bowling, L., Frankenberger, J., & Kladivko, E. (2018a). Estimating drain flow from measured water table depth in layered soils under free and controlled drainage. *Journal of Hydrology*, *556*, 339–348. https://doi.org/10.1016/j.jhydrol.2017.11.001

Saadat, S., Bowling, L., Frankenberger, J., & Kladivko, E. (2018b). Nitrate and phosphorus transport through subsurface drains under free and controlled drainage. *Water Research*, *142*, 196–207. https://doi.org/10.1016/j.watres.2018.05.040

Saeed, T., & Sun, G. (2012). A review on nitrogen and organics removal mechanisms in subsurface flow constructed wetlands: Dependency on environmental parameters, operating conditions and supporting media. *Journal of Environmental Management*, *112*, 429–448. https://doi.org/10.1016/J.JENVMAN.2012.08.011

Sanchez Valero, C., Madramootoo, C. A., & Stämpfli, N. (2007). Water table management impacts on phosphorus loads in tile drainage. *Agricultural Water Management*, *89*(1–2), 71–80. https://doi.org/10.1016/j.agwat.2006.12.007

Sands, G. R., Song, I., Busman, L. M., & Hansen, B. J. (2008). The Effects of Subsurface Drainage Depth and intensity of Nitrate Loads in the Northern Cornbelt. *Transactions of the ASABe*, *51*(3), 937–946. https://doi.org/10.13031/2013.24532

Satchithanantham, S., Sri Ranjan, R., & Bullock, P. (2014). Protecting water quality using controlled drainage as an agricultural bmp for potato production. *Transactions of the ASABE*, *57*(3), 815–826. https://doi.org/10.13031/trans.57.10385

Saunders, D. L., & Kalff, J. (2001). Nitrogen retention in wetlands, lakes and rivers. *Hydrobiologia*, *443*(1), 205–212. https://doi.org/10.1023/A:1017506914063

SC DHEC. (2005). *South Carolina Storm Water Management BMP Handbook*. https://scdhec.gov/Environment/WaterQuality/Stormwater/BMPHandbook/

Scalenghe, R., Edwards, A. C., Ajmone Marsan, F., & Barberis, E. (2002). The effect of reducing conditions on the solubility of phosphorus in a diverse range of European agricultural soils. *European Journal of Soil Science*, *53*(3), 439–447. https://doi.org/https://doi.org/10.1046/j.1365-2389.2002.00462.x

Schilling, K., & Zhang, Y.-K. (2004). Baseflow contribution to nitrate-nitrogen export from a large, agricultural watershed, USA. *Journal of Hydrology*, (295), 305–316. https://doi.org/10.1016/j.jhydrol.2004.03.010

Schmidt, I., Sliekers, O., Schmid, M., Bock, E., Fuerst, J., Kuenen, J. G., Jetten, M. S. M., & Strous, M. (2003). New concepts of microbial treatment processes for the nitrogen removal in wastewater. *FEMS Microbiology Reviews*, *27*(4), 481–492. https://doi.org/10.1016/S0168-6445(03)00039-1

Schott, L., Lagzdins, A., Daigh, A. L. M., Pederson, C., Brenneman, G., & Helmers, M. J. (2017). Drainage water management effect on corn planting date in southeast Iowa. *Journal of Soil and Water Conservation*, *72*(6), 564–574. https://doi.org/10.2489/jswc.72.6.564

Schueler, T., & Holland, H. (2000). *Article 65: Irreducible Pollutant Concentrations Discharged From Stormwater Practices*. https://owl.cwp.org/mdocs-posts/elc_pwp65/

Shedekar, V. S., King, K. W., Fausey, N. R., Islam, K. R., Alfred, B., Soboyejo, O., Kalcic, M. M., & Brown, L. C. (2021). Exploring the effectiveness of drainage water management on water budgets and nitrate loss using three evaluation approaches. *Agricultural Water Management*, *243*(August 2020), 106501. https://doi.org/10.1016/j.agwat.2020.106501

Shilton, A. N. (Andy N.). (2005). *Pond Treatment Technology*. IWA.

Simard, G. (2005). *Monitoring and Simulation of Nutrient Transport from Agricultural Fields*. Macdonald Campus, McGill Univeristy, Montreal, Quebec.

Sims, J. T., Simard, R. R., & Joern, B. C. (1998). Phosphorus Loss in Agricultural Drainage: Historical Perspective and Current Research. *Journal of Environmental Quality*, *27*(2), 277–293. https://doi.org/https://doi.org/10.2134/jeq1998.00472425002700020006x

Sirivedhin, T., & Gray, K. A. (2006). Factors affecting denitrification rates in experimental wetlands: Field and laboratory studies. *Ecological Engineering*, *26*(2), 167–181. https://doi.org/https://doi.org/10.1016/j.ecoleng.2005.09.001

Skaggs, R. W., Fausey, N. R., & Evans, R. O. (2012). Drainage water management. *Journal of Soil and Water Conservation*, *67*(6), 167–172. https://doi.org/10.2489/jswc.67.6.167A

Smith, E. L., & Kellman, L. M. (2011). Nitrate Loading and Isotopic Signatures in Subsurface Agricultural Drainage Systems. *Journal of Environmental Quality*, *40*(4), 1257–1265. https://doi.org/https://doi.org/10.2134/jeq2010.0489

Smith, E. L., Vosman, A., Kellman, L., & Rodd, V. (2019). Impact of drainage type on simultaneous nitrogen losses in Atlantic Canada. *Canadian Journal of Soil Science*, *99*(1), 70–79. https://doi.org/10.1139/cjss-2018-0115

Smriga, S., Ciccarese, D., & Babbin, A. R. (2021). Denitrifying bacteria respond to and shape microscale gradients within particulate matrices. *Communications Biology 2021 4:1*, *4*(1), 570-. https://doi.org/10.1038/s42003-021-02102-4

Soana, E., Gavioli, A., Tamburini, E., Fano, E. A., & Castaldelli, G. (2018). To mow or not to mow: reed biofilms as denitrification hotspots in drainage canals. *Ecological Engineering*, *113*, 1–10. https://doi.org/10.1016/j.ecoleng.2017.12.029

Soana, E., Vincenzi, F., Gavioli, A., & Castaldelli, G. (2025). Different Denitrification Capacity in Phragmites australis and Typha latifolia Sediments: Does the Availability of Surface Area for Biofilm Colonization Matter? *Water 2025, Vol. 17, Page 560*, *17*(4), 560. https://doi.org/10.3390/W17040560

Spieles, D. J., & Mitsch, W. J. (1999). The effects of season and hydrologic and chemical loading on nitrate retention in constructed wetlands: a comparison of low- and high-nutrient riverine systems. *Ecological Engineering*, *14*(1), 77–91. https://doi.org/https://doi.org/10.1016/S0925-8574(99)00021-X

Stackpoole, S. M., Stets, E. G., & Sprague, L. A. (2019). Variable impacts of contemporary versus legacy agricultural phosphorus on US river water quality. *Proceedings of the National Academy of Sciences of the United States of America*, *116*(41), 20562–20567. https://doi.org/10.1073/PNAS.1903226116/SUPPL_FILE/PNAS.1903226116.SAPP.PDF

Stålnacke, P., Grimvall, A., Sundblad-Tonderski, K., & Tonderski, A. (1999). Estimation of the riverine loads of nitrogen and phosphorus to the Baltic Sea. *Environmental Monitoring and Assessment*, *58*, 173.

Stampfli, N. (2003). *The effect of water table management on the migration of phosphorus and on grain corn yields* [McGill Univeristy]. https://escholarship.mcgill.ca/concern/theses/9p290c71c

Statista. (2024, December 2). *Canada: fertilizer consumption by nutrient* . Statists Research Department. https://www.statista.com/statistics/1330033/canada-fertilizer-consumption-by-nutrient/

Statistics Canada. (2022, June 15). *Ontario is an agricultural powerhouse that leads in many farming categories*. Statistics Canada. https://www150.statcan.gc.ca/n1/pub/96-325-x/2021001/article/00006-eng.htm

Steidl, J., Kalettka, T., & Bauwe, A. (2019). Nitrogen retention efficiency of a surface-flow constructed wetland receiving tile drainage water: A case study from north-eastern Germany. *Agriculture, Ecosystems and Environment*, *283*. https://doi.org/10.1016/j.agee.2019.106577

Stewart, P. S. (2003). Diffusion in biofilms. *Journal of Bacteriology*, *185*(5), 1485–1491. https://doi.org/10.1128/JB.185.5.1485-1491.2003;WEBSITE:WEBSITE:ASMJ;REQUESTEDJOURNAL:JOURNAL:JB;JOURNAL:JOURNAL:JB;ISSUE:ISSUE:DOI

Stone, K. C., Poach, M. E., Hunt, P. G., & Reddy, G. B. (2004). Marsh-pond-marsh constructed wetland design analysis for swine lagoon wastewater treatment. *Ecological Engineering*, *23*(2), 127–133. https://doi.org/10.1016/j.ecoleng.2004.07.008

Strock, J. S., Kleinman, P. J. A., King, K. W., & Delgado, J. A. (2010). Drainage water management for water quality protection. *Journal of Soil and Water Conservation*, *65*(6). https://doi.org/10.2489/jswc.65.6.131A

Sun, H., Zhou, Y., & Jiang, C. (2024). Regulating Denitrification in Constructed Wetlands: The Synergistic Role of Radial Oxygen Loss and Root Exudates. *Water 2024, Vol. 16, Page 3706*, *16*(24), 3706. https://doi.org/10.3390/W16243706

Sunohara, M. D., Craiovan, E., Topp, E., Gottschall, N., Drury, C. F., & Lapen, D. R. (2014). Comprehensive Nitrogen Budgets for Controlled Tile Drainage Fields in Eastern Ontario, Canada. *Journal of Environmental Quality*, *43*(2), 617–630. https://doi.org/10.2134/jeq2013.04.0117

Sunohara, M. D., Gottschall, N., Craiovan, E., Wilkes, G., Topp, E., Frey, S. K., & Lapen, D. R. (2016). Controlling tile drainage during the growing season in Eastern Canada to reduce nitrogen, phosphorus, and bacteria loading to surface water. *Agricultural Water Management*, *178*(3), 159–170. https://doi.org/10.1016/j.agwat.2016.08.030

Sunohara, M. D., Gottschall, N., Wilkes, G., Craiovan, E., Topp, E., Que, Z., Seidou, O., Frey, S. K., & Lapen, D. R. (2015). Long-Term Observations of Nitrogen and Phosphorus Export in Paired-Agricultural Watersheds under Controlled and Conventional Tile Drainage. *Journal of Environmental Quality*, *44*(5), 1589–1604. https://doi.org/10.2134/jeq2015.01.0008

Sutton, M. A., Howard, C. M., Erisman, J., Billen, G., Bleeker, A., Grennfelt, P., Grinsven, H., & Grizzetti, B. (2011). *European Nitrogen Assessment (ENA) | Nitrogen in Europe* (1st ed.). Cambridge University Press. http://www.nine-esf.org/node/360/ENA-Book

Tan, C. S., & Zhang, T. Q. (2011). Surface Runoff and Sub-surface Drainage Phosphorus Losses under Regular Free Drainage and Controlled Drainage with Sub-irrigation Systems in Southern Ontario. *Canadian Journal of Soil Science*, *91*(3), 349–359. https://doi.org/10.4141/CJSS09086

Tanner, C. C., Nguyen, M. L., & Sukias, J. P. S. (2005). Nutrient removal by a constructed wetland treating subsurface drainage from grazed dairy pasture. *Agriculture, Ecosystems and Environment*, *105*(1–2), 145–162. https://doi.org/10.1016/j.agee.2004.05.008

Tanner, C. C., & Sukias, J. P. S. (2011). Multiyear Nutrient Removal Performance of Three Constructed Wetlands Intercepting Tile Drain Flows from Grazed Pastures. *Journal of Environmental Quality*, *40*(2), 620–633. https://doi.org/10.2134/jeq2009.0470

Tate, R. L. (2020). Denitrification. In *Soil Microbiology* (pp. 447–476). https://doi.org/https://doi.org/10.1002/9781119114314.ch14

Tellier, J. M., Kalejs, N. I., Leonhardt, B. S., Cannon, D., Höök, T. O., & Collingsworth, P. D. (2022). Widespread prevalence of hypoxia and the classification of hypoxic conditions in the Laurentian Great Lakes. *Journal of Great Lakes Research*, *48*(1), 13–23. https://doi.org/10.1016/J.JGLR.2021.11.004

Thorén, A. K., Legrand, C., & Tonderski, K. S. (2004). Temporal export of nitrogen from a constructed wetland: Influence of hydrology and senescing submerged plants. *Ecological Engineering*, *23*(4–5), 233–249. https://doi.org/10.1016/j.ecoleng.2004.09.007

Toet, S., Huibers, L. H. F. A., Van Logtestijn, R. S. P., & Verhoeven, J. T. A. (2003). Denitrification in the periphyton associated with plant shoots and in the sediment of a wetland system supplied with sewage treatment plant effluent. *Hydrobiologia*, *501*(1), 29–44. https://doi.org/10.1023/A:1026299017464/METRICS

Tolomio, M., Ferro, N. D., & Borin, M. (2019). Multi-year N and P removal of a 10-year-old surface flow constructed wetland treating agricultural drainage waters. *Agronomy*, *9*(4). https://doi.org/10.3390/agronomy9040170

Ulén, B. (2004). Size and Settling Velocities of Phosphorus-Containing Particles in Water from Agricultural Drains. *Water, Air, and Soil Pollution*, *157*(1), 331–343. https://doi.org/10.1023/B:WATE.0000038906.18517.e2

Ulén, B., Geranmayeh, P., Blomberg, M., & Bieroza, M. (2019). Seasonal variation in nutrient retention in a free water surface constructed wetland monitored with flow-proportional sampling and optical sensors. *Ecological Engineering*, *139*. https://doi.org/10.1016/j.ecoleng.2019.105588

Ulén, B., Stenberg, M., & Wesström, I. (2016). Use of a flashiness index to predict phosphorus losses from subsurface drains on a Swedish farm with clay soils. *Journal of Hydrology*, *533*, 581–590. https://doi.org/10.1016/j.jhydrol.2015.12.044

US EPA. (2007). *National Water Quality Inventory: Report to Congress, 2002 Reporting Cycle*. http://www.epa.gov/305b

US EPA. (2014). *Non-Point Source Pollution: The Nation's Largest Water Quality Problem*.

US EPA. (2015). *Hypoxia Task Force Action Plans and Goal Framework | US EPA*. United States Environmental Protection Agency. https://www.epa.gov/ms-htf/hypoxia-task-force-action-plans-and-goal-framework

US EPA. (2022). *Bipartisan Infrastructure Law: Gulf Hypoxia Program State Workplan Summaries*. https://www.epa.gov/system/files/documents/2023-03/GHP%20HTF%20State%20Workplan%20Summaries%20March%202023_508.pdf

Uusheimo, S., Tulonen, T., Aalto, S. L., & Arvola, L. (2018). Mitigating agricultural nitrogen load with constructed ponds in northern latitudes: A field study on sedimental denitrification rates. *Agriculture, Ecosystems and Environment*, *261*, 71–79. https://doi.org/10.1016/j.agee.2018.04.002

Uusitalo, R., Turtola, E., Kauppila, T., & Lilja, T. (2001). Particulate Phosphorus and Sediment in Surface Runoff and Drainflow from Clayey Soils. *Journal of Environmental Quality*, *30*, 589–595. https://doi.org/10.2134/jeq2001.302589x

Uusitalo, R., Turtola, E., Puustinen, M., Paasonen-Kivekäs, M., & Uusi-Kämppä, J. (2003). Contribution of Particulate Phosphorus to Runoff Phosphorus Bioavailability. *Journal of Environmental Quality*, *32*(6), 2007–2016. https://doi.org/10.2134/JEQ2003.2007

Van Esbroeck, C. J. G. (2015). *Edge of Field Phosphorus Export via Tile Drainage and Overland Flow from Reduced Tillage Systems in Ontario*. http://hdl.handle.net/10012/9175

Van Esbroeck, C. J., Macrae, M. L., Brunke, R. I., & McKague, K. (2016). Annual and seasonal phosphorus export in surface runoff and tile drainage from agricultural fields with cold temperate climates. *Journal of Great Lakes Research*, *42*(6), 1271–1280. https://doi.org/https://doi.org/10.1016/j.jglr.2015.12.014

Verma, S., & Cooke, R. (2012). Performance of drainage water management systems in Illinois, United States. *Journal of Soil and Water Conservation*, *67*, 453–464. https://doi.org/10.2489/jswc.67.6.453

Vogel, J., & Moore, T. (2016). Urban Stormwater Characterization, Control, and Treatment. *Water Environment Research*, *88*, 1918–1950. https://doi.org/10.2175/106143016X14696400495938

Vymazal, J. (1995). *Algae and element cycling in wetlands.* Lewis Publishers Inc.

Vymazal, J. (2007). Removal of nutrients in various types of constructed wetlands. *Science of The Total Environment*, *380*(1), 48–65. https://doi.org/https://doi.org/10.1016/j.scitotenv.2006.09.014

Vymazal, J. (2017a). The Use of Constructed Wetlands for Nitrogen Removal from Agricultural Drainage: A Review. *Scientia Agriculturae Bohemica*, *48*(2), 82–91. https://doi.org/10.1515/sab-2017-0009

Vymazal, J. (2017b). The Use of Constructed Wetlands for Nitrogen Removal from Agricultural Drainage: A Review. *Scientia Agriculturae Bohemica*, *48*(2), 82–91. https://doi.org/10.1515/sab-2017-0009

Walker, D. J. (1998). Modelling residence time in stormwater ponds. *Ecological Engineering*, *10*(3), 247–262. https://doi.org/10.1016/S0925-8574(98)00016-0

Wang, J., Long, Y., Yu, G., Wang, G., Zhou, Z., Li, P., Zhang, Y., Yang, K., & Wang, S. (2022). A Review on Microorganisms in Constructed Wetlands for Typical Pollutant Removal: Species, Function, and Diversity. In *Frontiers in Microbiology* (Vol. 13). Frontiers Media S.A. https://doi.org/10.3389/fmicb.2022.845725

Watson, S. B., Miller, C., Arhonditsis, G., Boyer, G. L., Carmichael, W., Charlton, M. N., Confesor, R., Depew, D. C., Höök, T. O., Ludsin, S. A., Matisoff, G., McElmurry, S. P., Murray, M. W., Peter Richards, R., Rao, Y. R., Steffen, M. M., & Wilhelm, S. W. (2016). The re-eutrophication of Lake Erie: Harmful algal blooms and hypoxia. *Harmful Algae*, *56*, 44–66. https://doi.org/10.1016/J.HAL.2016.04.010

Wesström, I., Joel, A., & Messing, I. (2014). Controlled drainage and subirrigation - A water management option to reduce non-point source pollution from agricultural land. *Agriculture, Ecosystems and Environment*, *198*, 74–82. https://doi.org/10.1016/j.agee.2014.03.017

Wesström, I., & Messing, I. (2007). Effects of controlled drainage on N and P losses and N dynamics in a loamy sand with spring crops. *Agricultural Water Management*, *87*(3), 229–240. https://doi.org/10.1016/j.agwat.2006.07.005

White, J. R., & Reddy, K. R. (2003). Nitrification and Denitrification Rates of Everglades Wetland Soils along a Phosphorus-Impacted Gradient. *Journal of Environmental Quality*, *32*(6), 2436–2443. https://doi.org/https://doi.org/10.2134/jeq2003.2436

White, J. R., & Reddy, K. R. (2009). Biogeochemical Dynamics I: Nitrogen Cycling in Wetlands. In *The Wetlands Handbook* (pp. 213–227). https://doi.org/10.1002/9781444315813.ch9

Whitmire, S. L., & Hamilton, S. K. (2005). Rapid Removal of Nitrate and Sulfate in Freshwater Wetland Sediments. *Journal of Environmental Quality*, *34*(6), 2062–2071. https://doi.org/10.2134/JEQ2004.0483;PAGE:STRING:ARTICLE/CHAPTER

Wilcock, R. J., Müller, K., Van Assema, G. B., Bellingham, M. A., & Ovenden, R. (2012). Attenuation of nitrogen, phosphorus and E. coli inputs from pasture runoff to surface waters by a farm wetland: The importance of wetland shape and residence time. *Water, Air, and Soil Pollution*, *223*(2), 499–509. https://doi.org/10.1007/S11270-011-0876-8/METRICS

Williams, M. R., King, K. W., & Fausey, N. R. (2015a). Contribution of tile drains to basin discharge and nitrogen export in a headwater agricultural watershed. *Agricultural Water Management*, *158*(3), 42–50. https://doi.org/10.1016/j.agwat.2015.04.009

Williams, M. R., King, K. W., & Fausey, N. R. (2015b). Drainage water management effects on tile discharge and water quality. *Agricultural Water Management*, *148*, 43–51. https://doi.org/10.1016/j.agwat.2014.09.017

Woli, K. P., David, M. B., Cooke, R. A., McIsaac, G. F., & Mitchell, C. A. (2010). Nitrogen balance in and export from agricultural fields associated with controlled drainage systems and denitrifying bioreactors. *Ecological Engineering*, *36*(11), 1558–1566. https://doi.org/10.1016/j.ecoleng.2010.04.024

Xue, Y., Kovacic, D., David, M., Gentry, L., Mulvaney, R., & Lindau, C. (2009). In Situ Measurements of Denitrification in Constructed Wetlands. *Journal of Environmental Quality - J ENVIRON QUAL*, *28*. https://doi.org/10.2134/jeq1999.00472425002800010032x

Yan, Y., & Xu, J. (2013). Improving Winter Performance of Constructed Wetlands for Wastewater Treatment in Northern China: A Review. *Wetlands 2013 34:2*, *34*(2), 243–253. https://doi.org/10.1007/S13157-013-0444-7

Zhang, S., Pang, S., Wang, P., Wang, C., Guo, C., Addo, F. G., & Li, Y. (2016). Responses of bacterial community structure and denitrifying bacteria in biofilm to submerged macrophytes and nitrate. *Scientific Reports*, *6*. https://doi.org/10.1038/srep36178

Zhang, T. Q., Tan, C., Zheng, Z., Welacky, T., & Wang, Y. (2017). Drainage water management combined with cover crop enhances reduction of soil phosphorus loss. *Science of The Total Environment*, *586*. https://doi.org/10.1016/j.scitotenv.2017.02.025

Zhang, T., Tan, C. S., Zheng, Z. M., Welacky, T. W., & Reynolds, W. D. (2015). Impacts of Soil Conditioners and Water Table Management on Phosphorus Loss in Tile Drainage from a Clay Loam Soil. *Journal of Environmental Quality*, *44*(2), 572–584. https://doi.org/10.2134/jeq2014.04.0154

Chapter 3 - Controlled Drainage - Effects on nutrient attenuation and water quality – A field study in Eastern Ontario, Canada

(Published in Agricultural Water Management Journal)

Abstract

Controlled drainage (CD) is a promising practice for mitigating the adverse effects of tile drainage on downstream waterbodies by reducing pollutants while maintaining agro-economic benefits. In cold-climate regions, like Eastern Ontario, Canada, previous CD studies have typically focused on growing season based on operational recommendations. However, the fate of retained water and nutrients after stoplog removal (flush) and any CD residual effects during non-frozen, post-harvest period remain unclear. The central objective of this three-year study was to assess CD versus free drainage from planting to freeze-up (May to November) by analyzing Growing, Flush and Post-Harvest Periods (GP, FP, PHP). Greatest reductions in flow (68%) and nutrient loads (nitrate by 51%, soluble reactive phosphorus (SRP) by 76%) occurred in GP under CD. During FP, flow and nutrient losses at CD increased significantly before returning to background levels. CD plots showed 35% significantly greater relative abundance of nitrate-reducing bacteria in soil, suggesting enhanced denitrification. However, any positive effects of denitrification and crop uptake on nitrate reductions in dry GP subperiods were outweighed by increased leaching losses in the wet subperiods (19%). CD significantly reduced total suspended solids and total phosphorus migration in GP+FP likely due to stoplog damming reducing macropore flow. While SRP concentrations at CD were 35-85% significantly lower during GPs, they increased three to seven times during FP, indicating possible desorption under stagnant conditions. Overall, CD implemented in GP reduced total flow (37%), nitrate (21%), and SRP (57%) loads from planting to freeze-up, highlighting its potential for cold-climate cropping systems.

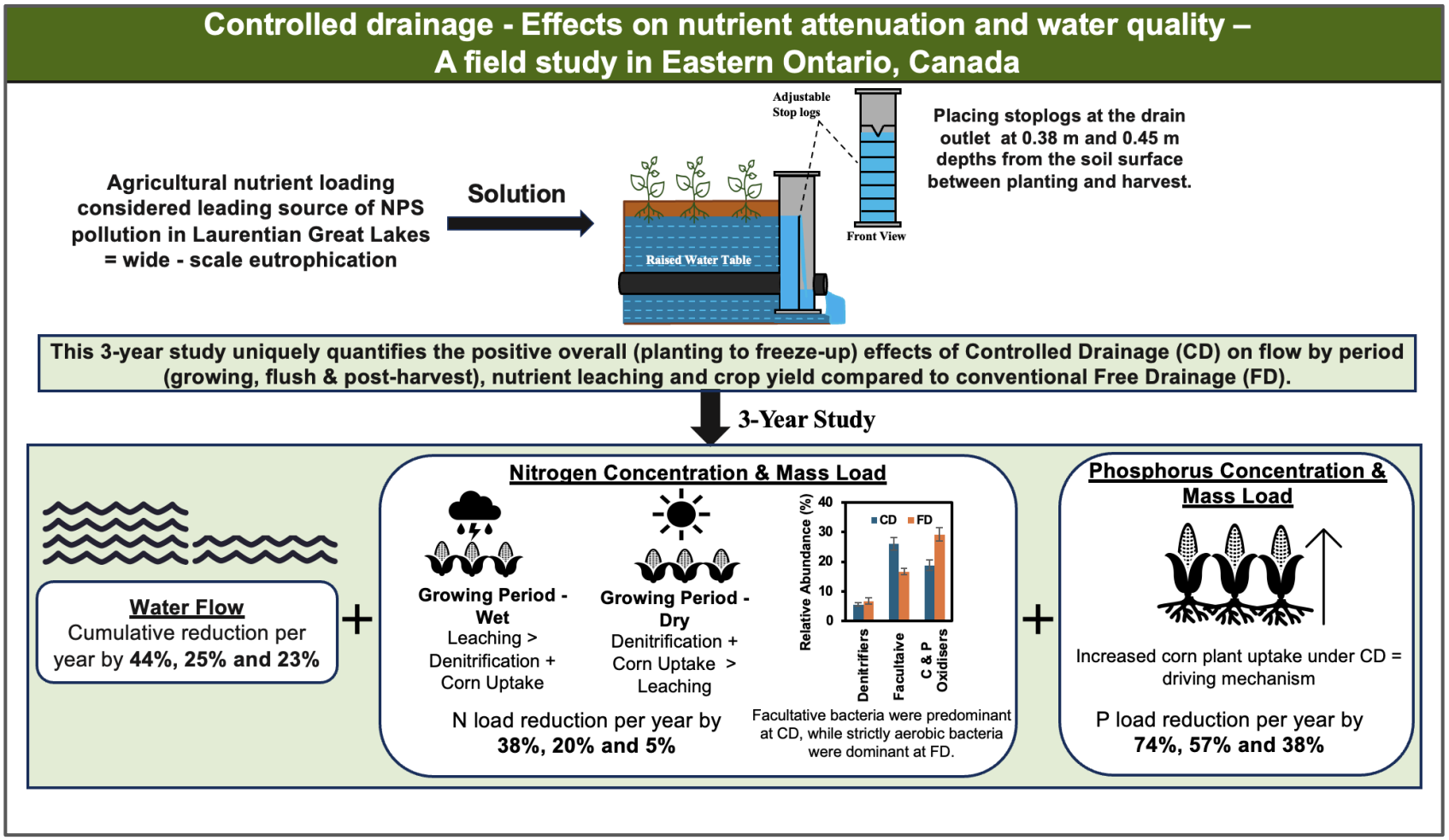

Figure 3-1. Graphical Abstract

3.1. Introduction

Drainage, a critical component of cropping systems, is often insufficient in low permeability croplands. Tile drainage is implemented to reduce waterlogging, increase crop yields, and reduce yield variability. Approximately 11% of the world's croplands are tile-drained (Kokulan, 2019), increasing to 14% in Canada and 27% in the United States (ICID, 2018; Sunohara et al., 2015). However, tile drainage can also contribute to the problem of agricultural non-point source (NPS) pollution by transporting limiting nutrients, sediments, pathogens, and pesticides from fields to surface water bodies. These exports can stimulate algal growth, eutrophication, and hypoxic conditions, as observed in Lake Erie (Watson et al., 2016) and the Gulf of Mexico (David et al., 2010; Rabalais et al., 2002). Agricultural NPS pollution is estimated to be the main cause of water quality impairment in the US, affecting 50% of river miles (US EPA, 2007). With environmental directives focusing on agricultural NPS in place, such as the Canada-Ontario Lake Erie Action Plan (ECCC, 2018), implementing tailored conservation practices is necessary to address multiple pollutants in areas impacting water quality (US EPA, 2023).

Controlled drainage (CD) is a feasible upgrade to existing tile drainage systems that involves installing physical flow barriers (i.e., stoplogs) within drainage structures to artificially set a desired water level. In warmer climates, outlet depths are changed four times a year: lowered before planting (to allow field operations), raised again after planting (water storage during mid-summer for crops), lowered again before harvesting (to allow field operations) and raised after harvest (reduced drainage outflow during the off-season) (Frankenberger et al., 2006; Skaggs et al., 2012). However, in colder climates such as Canada, CD is not recommended in winter due to ice buildup inside control structures and drainage ditches (Frankenberger et al., 2006; Sunohara et al., 2016), possible increases in phosphorus (P) mobilization from soil saturation (Ball Coelho et al., 2012; King et al., 2015), and chances of ice sheeting and shallower, longer-lasting soil frost, leading to longer spring warming periods (OMAFRA, 1991).

CD can be an agricultural beneficial management practice (BMP) that offers immediate environmental quality benefits, unlike passive technologies such as wetlands and vegetative buffers, which require a development period (Sunohara et al., 2016) and is an inexpensive, minimally invasive solution. North American studies during growing seasons show CD effectively controls the water table and reduces water flow by 8 to 100% (Drury et al., 2014; Nash et al., 2015;

Saadat et al., 2018a; Schott et al., 2017; Smith et al., 2019). However, some studies have reported either little to no effect (Madramootoo et al., 2001) due to dry weather or increased drainage flows (Stampfli, 2003) from high rainfall.

The use of CD has been demonstrated to be effective in reducing nitrate load, either by reducing drainage outflows (Cordeiro et al., 2014; Helmers et al., 2022; King et al., 2022; Shedekar et al., 2021; Sunohara et al., 2016; Verma & Cooke, 2012; Williams et al., 2015a) or through concentration reduction potentially attributable to denitrification (Adeuya et al., 2012; Drury et al., 2014; Fausey, 2005), increased crop uptake (Ng et al., 2002; Poole et al., 2018), or both (Drury et al., 2009; Sunohara et al., 2014). Limited studies, such as that of Liu et al. (2019) via nitrogen (N) mass balance across CD system, attributed 67% of N loss likely to denitrification. However, to the author's knowledge, evidential proof of denitrification as a significant mechanism in CD using soil microbiome analysis, has not been demonstrated.

Existing research findings on its impact on soluble phosphorus (SP) are conflicting and limited in scope. Among the few North American studies, the majority reported SP load reductions ranging from 11% to 85% due to decreased tile flows (Cordeiro et al., 2014; Saadat et al., 2018b; Sunohara et al., 2016; Zhang et al., 2015). Nash et al. (2015) and Tan & Zhang (2011) observed reduced SP loads as a function of concentration, plant uptake, and tile flow at CD sites with clay soils. However, other studies have reported increased SP concentrations (Saadat et al., 2018b; Sanchez Valero et al., 2007; Satchithanantham et al., 2014; Stampfli, 2003). SP and nitrate behave differently: nitrate is a highly mobile nutrient, whereas SP binds to particles and oxides in the subsoil. The effects of CD on SP loads cannot be extrapolated from data on nitrate reduction by CD and shows conflicting results from literature warranting further investigation.

Limited research has been conducted on the effects of CD on total suspended solids (TSS), total phosphorus (TP), and particulate phosphorus (PP) concentrations in drainage water. Some studies have reported minimal to no change in PP and TP concentrations (Tan & Zhang, 2011; Zhang et al., 2015), while other studies reported significantly higher TP concentrations in drainage water (Saadat et al., 2018b; Sanchez Valero et al., 2007; Sunohara et al., 2015) under CD compared to free drainage (FD). However, all the above studies have reported 33 to 37% PP and 18 to 54% TP load reductions at CD due to reduction in flow, which implies an effect of CD on TSS. To the

author's knowledge, no farm-scale studies have examined the effect of CD on TSS.

Despite the documented environmental and agronomic benefits, such as increased crop yields, associated with CD installation in North America, its adoption in Ontario, Canada has been relatively low (OSCIA, 2017). A survey conducted by Dring et al. (2016) in the Eastern Ontario region (~4000 km^2) revealed that only two producers had adopted CD (out of a total of 100). Within the ~ 4000 km^2 river basin, approximately half of the cropland in the region is suitable for CD implementation, which translates to a potential reduction of 55% in flow and nitrate load during the growing season (Que et al., 2015). Field-scale research projects are crucial as they provide data on agronomic and environmental benefits to producers, thereby supporting the regional adoption of CD BMPs. It is important to recognize that previous CD studies in cold-climate regions have been primarily conducted in the growing season with stoplogs typically operational from planting until a few days before harvest. However, the potential impact of the hydraulic flush immediately after the removal of stoplogs on flow, solid and nutrient fluxes as well as any antecedent effect of CD on drainage or leaching in the post-harvest season have not been evaluated.

The central purpose of this 3-year field study is to analyze the performance of the CD system from planting to freeze-up and compare it to free drainage in terms of its effects on the water table, tile flow and nutrient losses. More specifically, based on the data/knowledge gaps recognized is to identify denitrification as a mechanism of nitrate reduction from CD, evaluate CD impact on soluble reactive phosphorus (SRP) concentration, assess the impact of CD on TSS and PP flux, and estimate the impact of Flush Period (FP) - period after stoplog removal until flows at CDs (now freely flowing) were similar to those of FD and the Post-Harvest Period (PHP) - period between the end of FP until freeze-up of drainage structures), on overall nutrient load in a cold-climate application. The practical objective of this study is to demonstrate the advantages of CD at the farm-scale to support technology adoption in Ontario, Canada and other similar climatic regions.

3.2. Methods and materials

3.2.1. Site description and farm management practises

The study was conducted at Ferme Agriber, an 850-ha cash crop operation located in Eastern Ontario, Canada, approximately 80 km east of Ottawa (Figure 3-2) which typically produces soybean, corn, and wheat, rotated yearly. Thirty-year normal annual precipitation (1981-2010) in the area is 943 mm, of which the months from May to November account for 609 mm. During these months, mean daily 30-yr air temperature is 13.9°C (maximum of 19.1°C and minimum of 8.7°C) (ECCC, 2020).

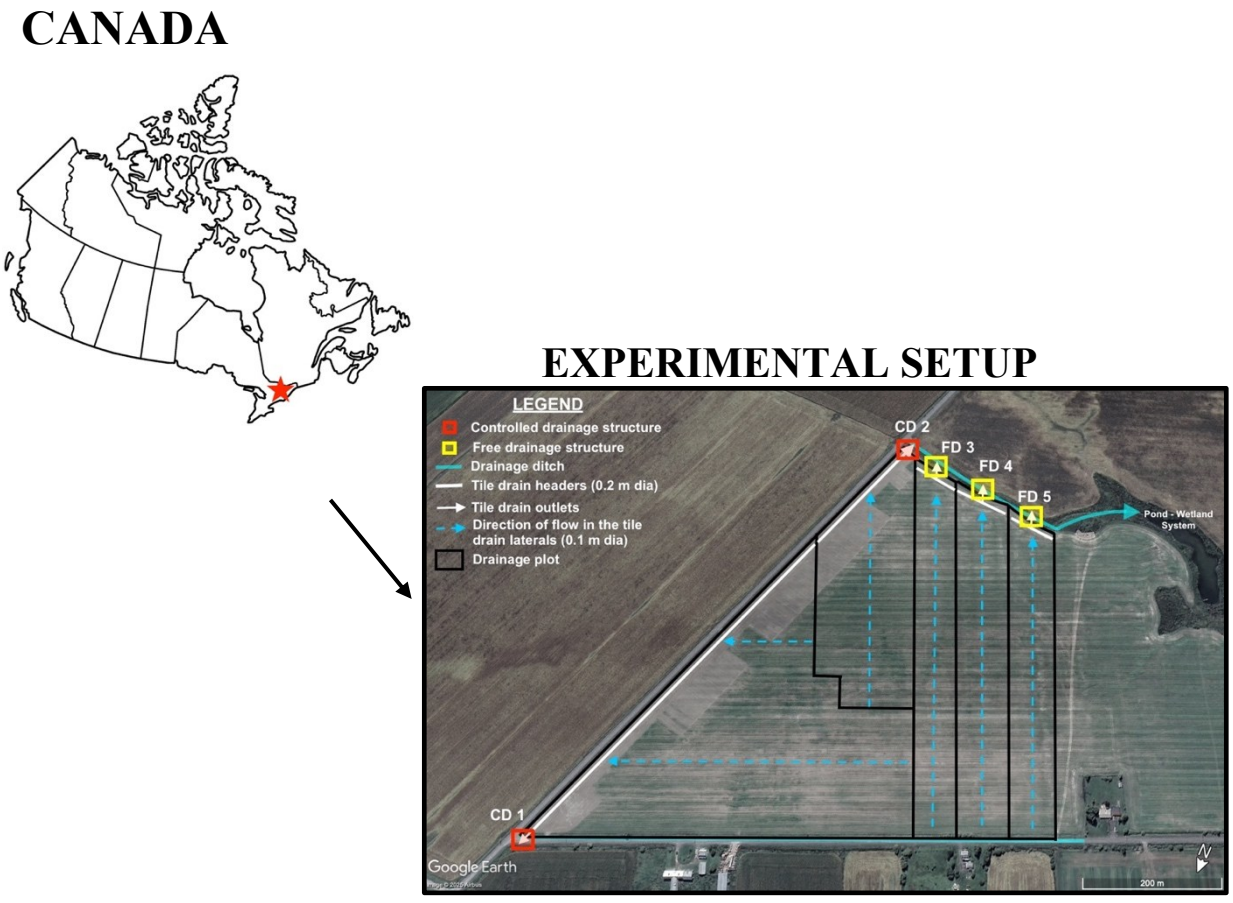

Figure 3-2. Location of field study: Top - Geographic location of the study site; Bottom - Aerial drainage layout of Ferme Agriber, the study area. Location of drainage structures with direction of flow in the tile drain laterals shown. These laterals, spaced at 12 m, converge at tile drain headers within each drainage plot, that ultimately outfalls into central drainage ditches. Google Earth Pro V 7.3.6.9796 imagery.

The topography of the fields is flat (slope < 1%). The existing tile drainage system has parallel subsurface drains at 0.91 m (3 ft) depth perpendicular to the drainage ditch fronts, with 10 cm (4-inch) diameter tiles spaced approximately 12 m (50 ft) part. Five in-line water level drainage

structures were installed at the tile outlets to manage and monitor the tile drain flow, creating five drainage plots (Figure 3-2). Flow and water table regulation was enforced using adjustable stoplog system in two of the five structures (CD 1 and CD 2) while three plots remained uncontrolled, i.e. FD system through their respective drainage structures (FD 3, 4, and 5). The outflow from CD 1 plot of (7.5 ha) drains into a ditch to the north of the property, while tile outflow from CD 2, FD 3, 4 and 5 (4, 4.8, 6.5 and 3.4 ha, respectively) plots drain into a central drainage ditch connecting to a pond-wetland system. The study was managed by the researchers and was conducted from planting to freeze-up in 2018, 2019, and 2021[1], from May to November/early December, after the stoplogs were placed at CD 1 and 2. As such, spring-melt was not captured in this study.

The soil on the farm is predominantly clay and clay loam, classified under hydrologic group C (Soil Classification Working Group, 1998), with approximately 30% clay and 25% sand. Soil nutrient analysis was conducted at the beginning (Spring 2018) and at the end of the study (Fall 2021) to determine background N and P concentrations. Average soil nitrate (NO_3 levels were 56.0±11.3 kg N/ha in Spring 2018 and were unchanged in Fall 2021 (57.5±6.3 kg N/ha), comparable to typical nitrate content in Ontario fine field soil levels of 55.4 to 59.3 kg/ha when soybean is cultivated in the prior year (McDonald & Janovicek, 2015; Sunohara et al., 2014). Average extractable P levels were 57.8±15.9 kg P/ha in Spring 2018 and 61.0±19.3 kg P/ha in Fall 2021, within typical Ontario clay soil range of 53.1 to 85 kg/ha (Labarge, 2022).

During the 3-year study, grain corn was grown in all the plots with minimum tillage and was planted between late April - early May and harvested in November. Crop sampling was carried out before harvest in 2018 and 2021 to understand potential crop uptake of N and P. Fertilization was carried out twice: dry broadcast application (N-P-K) before planting and N liquid side-dress application in June. Dry fertilizer was applied at following agronomic rates: in 2018 - 121.4 kg N/ha & 27.4 kg P_2O_5/ha (11.9 kg P/ha), in 2019 - 117.2 kg N/ha & 83.8 kg P_2O_5/ha (36.6 kg P/ha) and in 2021 – 120.6 kg N/ ha & 78.2 kg P_2O_5/ha (34.1 kg P/ha). Side-dress solution of 90.9, 118.5 and 98.8 kg N/ha fertilizer solution were applied in 2018, 2019 and 2021, respectively.

3.2.2. Edge-of-the field monitoring

Each drainage structure was fitted with one 22.5° V-notch weir stoplog for flow monitoring. At

[1] The system was not monitored in 2020 due to COVID -19 lockdown restrictions.

the start of 2018, stoplogs in CD 1 maintained an overflow depth of approximately 0.56 m below the soil surface relative to average field height. An additional 0.18 m stoplog was added on July 20, 2018, that raised the water table, decreasing CD 1 overflow depth to 0.38 m below the soil surface and was maintained thereafter. CD 2 overflow was set at 0.44 m from the soil surface across all three years These depths remained unadjusted until harvest for an average of 162 consecutive days yearly. For FD 3 and 5, V-notch weirs were set to 1.15 m from the field surface At FD 4, a 0.18 m stoplog under the V-notch weir log prevented backflow from the drainage ditch, decreasing the depth to 0.98 m. After removing CD 1 and CD 2 stoplogs in October 2018, a 0.18 m rectangular weir log was placed at the bottom of the structures and monitored as uncontrolled drainage. In 2019 and 2021, the method was modified by placing a 22.5° V-notch weir log at the bottom of the CD to structurally mimic FD. Detailed configurations can be found in Appendix C.

The data for each field season was divided into three periods: Growing Period (GP) – period between stoplog installation after planting until removal before harvest at CDs, FP - period after stoplog removal until flows at CDs (now freely flowing) were similar to those of FD and PHP - period between the end of FP until freeze-up of drainage structures. The stoplogs were removed in October, typically 10-14 days before harvest and the freeze-up of structures occurred towards the end of November or early December, to conclude that year's monitoring. Therefore, all drainage structures were not monitored during the winter. The division into three time periods allowed for the comparison of the flow and nutrient response of CD to that of FD in GP, the fate of the retained water in CD once the stoplogs were removed and the residual effect in PHP due to implementing CD in GP.

In this study, the potential for lateral seepage from CD to FD plots was determined to be insignificant. CD 1 is spatially isolated from all FDs, with flow directions diverging (Figure 3-2) and CD 2 is adjacent only to FD 3. Statistical analysis of daily flow across three GPs revealed no significant differences among FD 3, 4 and 5 (p-values ranging from 0.13 to 0.91, paired t-test), suggesting inconsequential seepage influence. In 2018, daily precipitation and ambient air temperature data were collected using a HOBO weather station (Onset Computer Corp.) operated by the farm. Weather data for 2019 and 2021 were obtained by combining data from Moose Creek station, positioned within 20 km of the farm site (ECCC, 2023) and St. Isidore Station, within 2 km of the farm (Agricrop, 2023).

3.2.3. Water quality sampling and analysis

ISCO 6712 full-size automatic portable samplers (Teledyne ISCO, Inc.) were used to collect tile water samples at each drainage structure with suction line affixed to a plastic pipe directly below the outlet V-notch elevation to only sample flowing water and to prevent sediment collection. Each sampler used a battery that was trickle-charged using a solar panel. Daily composite samples comprised 3 to 4 aliquots per day. At the start of FP at CD 1 and CD 2 in 2018 and 2021, water samples were collected every 5 min for the first 20 min, followed by hourly discrete sampling for 24 hours to capture the initial flush concentrations. In 2021, grab samples were also collected weekly to investigate nitrate trends in the dammed drainage waters. Samples were collected weekly from the ISCO samplers, transported to the laboratory in coolers with ice packs, and refrigerated until analysis. A total of 1150 samples were collected and analyzed during the entire study period.

100 mL samples were filtered through a 1.5 µm Whatman filter via a filtering apparatus connected to a Marathon Electric 110-115 ¼ HP vacuum pump (distributed by Thermo Fisher Scientific, Waltham, MA.). Nitrate (NO_3^--N, mg N/L) was measured using the ultraviolet light technique (Standard Methods 4500- NO_3^- B) (APHA, 2017). SRP was analyzed as phosphate (PO_4^{3-}) using a modified HACH Method 8048 (Phosphorus, Reactive (Orthophosphate) - low range - a kit version of Standard Methods 4500-P E. Ascorbic Acid Method), where the samples mixed with reagents were transferred from the vial to a 50 mm cuvette (Mathew, 2020) in 2018 and the Stannous Chloride method (Standard Methods 4500-P D) (APHA, 2017). In this study, SRP concentrations are reported as elemental phosphorus (mg P/L) to maintain consistency with other CD studies.

Initially all samples were analyzed for TP; however, TP concentrations were consistently equivalent to SRP, indicating negligible particulates in the tile drainage. Consequently, TSS and TP analyses were limited to samples that appeared turbid. TSS content was measured using Dried TSS at 103°-105°C Method 2540 D (APHA, 2017). TP was analyzed following a modified HACH Method 8190 where the samples with reagents were transferred from the vial to a 50 mm cuvette (Mathew, 2020) – low range (a kit version of Standard Methods 4500-P E Ascorbic acid method) in 2018 and by the Stannous Chloride method (Standard Methods 4500-P D) (APHA, 2017).

3.2.4. Determination of water heights and flow rates

Each drainage structure was installed with a HOBO water level data logger U20-001-04 (Onset Computer Corp.) to obtain the absolute pressure of water relative to the barometric pressure. Each data logger was placed flat at the bottom of the drainage structure upstream of the stoplogs to determine the water height flow rate. Water temperature (°C) and absolute pressure (kPa) were recorded every 15 min and manually downloaded using the HOBO Waterproof Shuttle during weekly visits. The data were transferred and processed using the HOBOware Pro software (Version 3.7.21, Onset Computer Corp). The resultant barometric pressure data underwent post-processing to compute the sensor depth below the water surface (Onset Computer Cooperation 2008). The equations[2] for calculating water height (h) are in in Appendix C. For the entire study season, 20,553 data points were analysed per drainage structure yearly. During the weekly visits, manual water height measurements were recorded using a dowel and measuring tape, which were deemed more accurate and used to verify and when necessary, recalibrate the heights calculated using equations in Appendix C. The instantaneous water flow for each time interval (15 min) was calculated using the empirical relationships between the calibrated effective water heights and discharge (Chun & Cooke, 2008; USBR, 2001). The modified empirical equations and constants for calculating water flows are in Appendix C. The flow rate (Q) was then converted to m^3/s for continuous time series and normalised to drainage area per sampling location.

3.2.5. Calculating water and nutrient loads

The volume of tile drainage water (m^3) for each time interval were calculated by multiplying the measured flow rate ((Q_i), m^3/s) by interval time (15 min). Daily water load (mm/day or m^3/ha/day) were obtained by summing the 15 min interval drainage water volumes and dividing them by the area of the drainage plot (m^2 or ha).

$$\text{Daily Water Load } \left(\frac{\text{mm}}{\text{day}} \text{ or } \frac{\text{m}^3}{\text{ha.day}}\right) = \frac{\sum Q_i \times 15 \times 60}{\text{Area}} \quad \text{(Equation 3-1)}$$

Daily tile drainage nutrient loads were calculated by multiplying the daily parameter concentrations (C_i) (mg P/L or mg N/L) by daily discharged water flux (m^3/day) (Q) and then dividing by area of drainage plot (ha) to get values in kg N or P/ha/day.

[2] Air temperature (°C) and absolute air pressure (kPa) required in these equations were obtained from a data logger set up at the farm. However, in 2021, due to malfunctioning of logger, data from moose creek weather station were used to re-calibrate values obtained from the logger.

$$\text{Daily Mass Nutrient Load } \left(\frac{\text{kg nutrient}}{\text{ha.day}}\right) = \frac{Q \times C_i}{\text{Area} \times 1000} \quad \text{(Equation 3-2)}$$

The percentage change in the mean loads between CD and FD was calculated as follows:

$$\text{Change (\%)} = \frac{(FD - CD)}{FD} \times 100 \quad \text{(Equation 3-3)}$$

3.2.6. Soil sampling and analysis

Soil samples were collected from four plots associated with two controlled drainage and two free drainage at 6-inch and 12-inch depths before fertilizer application in spring 2018 and after harvest in fall 2021. A standard push soil core sampler was used to collect soil at ten random spots within each plot, which were mixed thoroughly to form one homogeneous sample. They were sent to an external lab (Agriculture and Food Laboratory (AFL), Guelph), where the samples were analyzed for carbon (organic, inorganic, total carbon – only in 2021, combustion method), nitrogen (NH_4^+-N by KCl extractable NH_4, NO_3-N by KCl extractable NO_3-N, and total nitrogen by combustion method), and phosphorus (sodium bicarbonate extractable P). Additionally, in 2021, after stoplogs were removed at CD, soil samples were collected at a feet away from CD 2 and FD 5 structures, at depths of 15 cm, 31 cm, 46 cm, 61 cm, and 76 cm, which were analyzed for carbon (total, organic, and inorganic).

3.2.7. Crop sampling and analysis.

Aboveground corn biomass (stalk and kernel) was randomly hand-collected from the CD and FD plots before harvest in 2018 and 2021. In the laboratory, stalk sub-samples were broken down into approximately 5 cm pieces and mixed to form a homogenous sample. Kernels were separated from corn cobbs, mixed to form a full sample. These samples were sent for plant tissue TN and TP analyses to an external lab (AFL, Guelph). Using the dry weight of biomass at 15.5% (marketed standard moisture content for corn bushel at maturity), nutrient (N and P) concentrations and total plant nutrients (only above the soil) were calculated.

3.2.8. Sample collection and PCR sequencing

The effect of CD on the relative abundance of denitrifying bacteria in the soil was evaluated by Polymerase Chain Reaction (PCR) sequencing of the 16S rRNA gene. In 2021, post stoplog removal, soil samples were collected a foot way from CD 2 and FD 5 structures under sterile conditions. These samples were extracted and processed by an external lab (Microbiome Insights, Richmond), where a two-step PCR targeting the V4-region of the 16S gene was carried out

according to a previously described protocol (Kozich et al., 2013). The raw FASTQ files were quality-filtered with minor trimming to remove low-quality sequences (median 63% of reads passed per sample). The sequences were analyzed using the phyloseq package, in R, where rarefication was set to a sequencing depth of 3500. The reads were then transformed to relative abundances (%), operational taxonomic units (OTUs) were aggregated into taxonomic ranks. Genera were subsequently cross-referenced with established databases (e.g., MiDAS) and published literature to assign putative functional groupings. All functional interpretations presented in this study are therefore based on taxonomic affiliation and reported metabolic capabilities at the genus level.

3.2.9. Statistical analysis

The effect of controlled drainage on water flows and nutrient concentration was examined by using analysis of variance (ANOVA - one-way) and Paired t-test. A significance level (α) of 5% (p-value < 0.05) for water samples and soil microbiome and a of 10% (p-value < 0.1) for soil and corn were used to identify statistical differences between data sets. The arithmetic mean, standard deviation, confidence at 95%, and count were calculated for drainage flow, nutrient concentrations, and loads from the CD and FD plots. Lastly, analysis of similarities (ANOSIM) was performed in Prism 9.1.0 to test statistical significance between microbiome communities in soil samples, where a p-value < 0.05 was used.

3.3. Results and discussion

3.3.1. Meteorological conditions

Trends of monthly precipitation and average temperature at Ferme Agriber compared to 30-yr Normal (1981-2010) are shown in Figure 3-3. The study site received cumulative precipitation of 846 mm in 2018, 747 mm in 2019, and 793 mm in 2021, which is lower than the 30-yr normal average of 943 mm (ECCC, 2020). The precipitation levels for the 3-year study period were below the 30-year average by 3 to 12%, with 2019 being the driest year of the three. Considerable variations in the timing and amount of precipitation were observed throughout the study periods. Precipitation in August and September 2018, May and October 2019, and June, July, and October 2021 were >25% above normal. On the other hand, July, August, and November 2019, as well as May and November 2021, received >30% below normal precipitation. Average monthly temperatures during 2018 and 2019 were a degree higher than the norm, while 2021 was consistent

with the 30-yr normal (ECCC, 2020). In summary, the study period was characterised by very dry or very wet months with normal to slightly higher than normal temperatures. All three study years received less than typical precipitation.

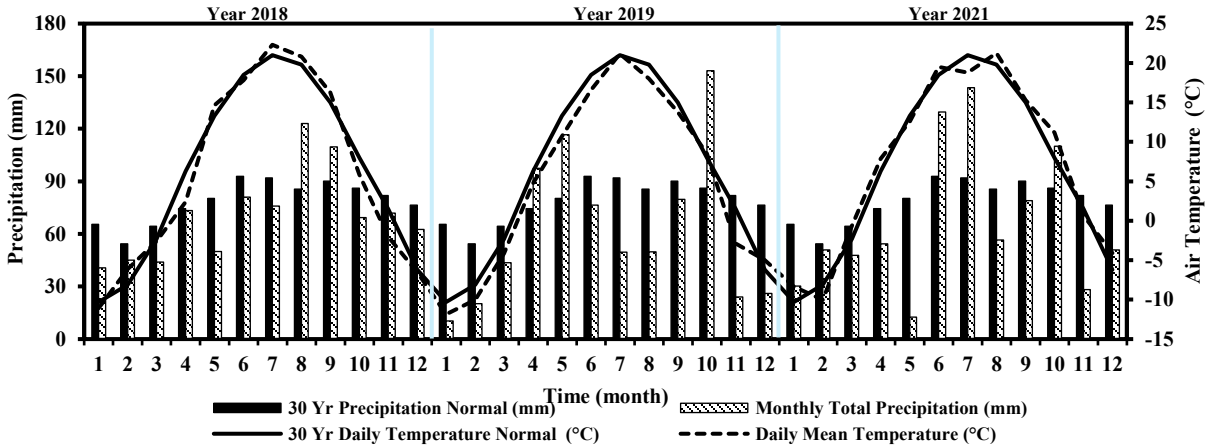

Figure 3-3. Trends of monthly precipitation (mm) and average temperature (°C) at Ferme Agriber - 3-yr study compared to the 30-yr Normal (1981-2010) (ECCC, 2020).

3.3.2. Flow rates and water table variations

The drainage flows varied widely based on precipitation, evapotranspiration (ET), and the application of CD during the three-year study The daily flow and precipitation trends at the drainage structures during the entire study is presented in Figure 3-4, with water table variations across the structures relative to field surface depth in Figure 3-5. At the beginning of GP, after the stoplogs placement, the water table rose and maintained higher levels at CD 1 and CD 2 in response to precipitation, due to low ET with corn crops absent or in emergence, VE stage (OMAFRA Field Crop Team, 2017), which is characterized by relatively low uptake of water (Licht et al., 2017). As the GP progressed, there was little to no flow at CD 1 and CD 2 as the water table dropped below the discharge depth with increased ET, rising periodically following precipitation events. FD water table levels showed little response to precipitation during the peak growing and reproductive stages of corn crops from July to August (Figure 4), characterized by high ET and water demand. Similar observations have been reported by (Nash et al., 2015; Riley et al., 2009; Williams et al., 2015a). In 2018, the water table at CDs were consistently higher than FDs (by an average of 56%) during the crop stress period (Appendix E), likely accounting for the 21% higher crop yield than FDs (Appendix E). While similar elevated water tables at CDs were observed in 2019 and 2021, plot-specific yields are unavailable for these years.

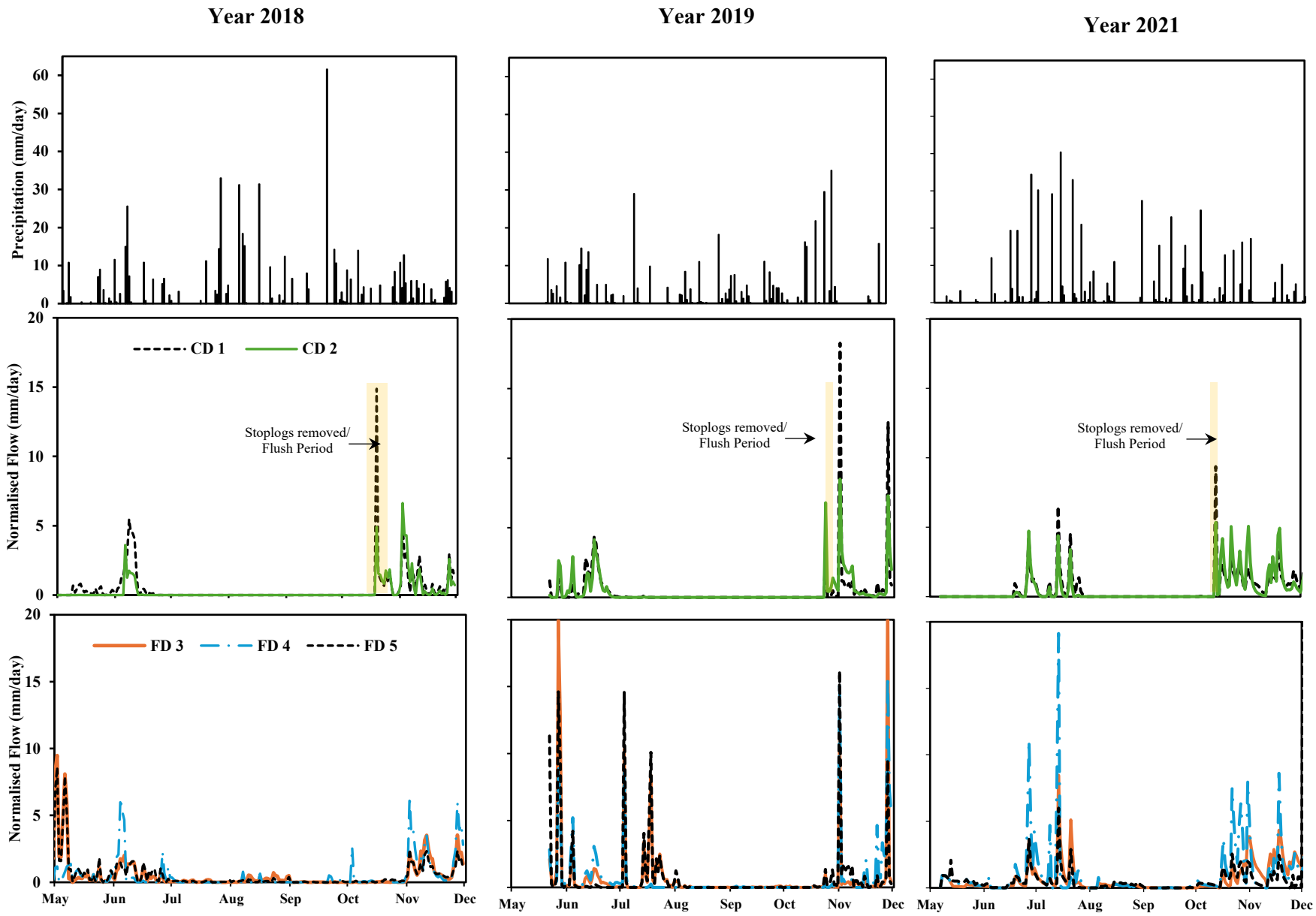

Figure 3-4. Normalised daily flow and precipitation Normalised daily flow and precipitation trend during the 3-year study. Top row - Precipitation (mm/day) during the study period; Center row - Normalised flow (mm/day) at controlled drainage structures (CD 1 and 2); Bottom row - Normalised flow (mm/day) at free drainage structures (FD 3, 4 and 5).

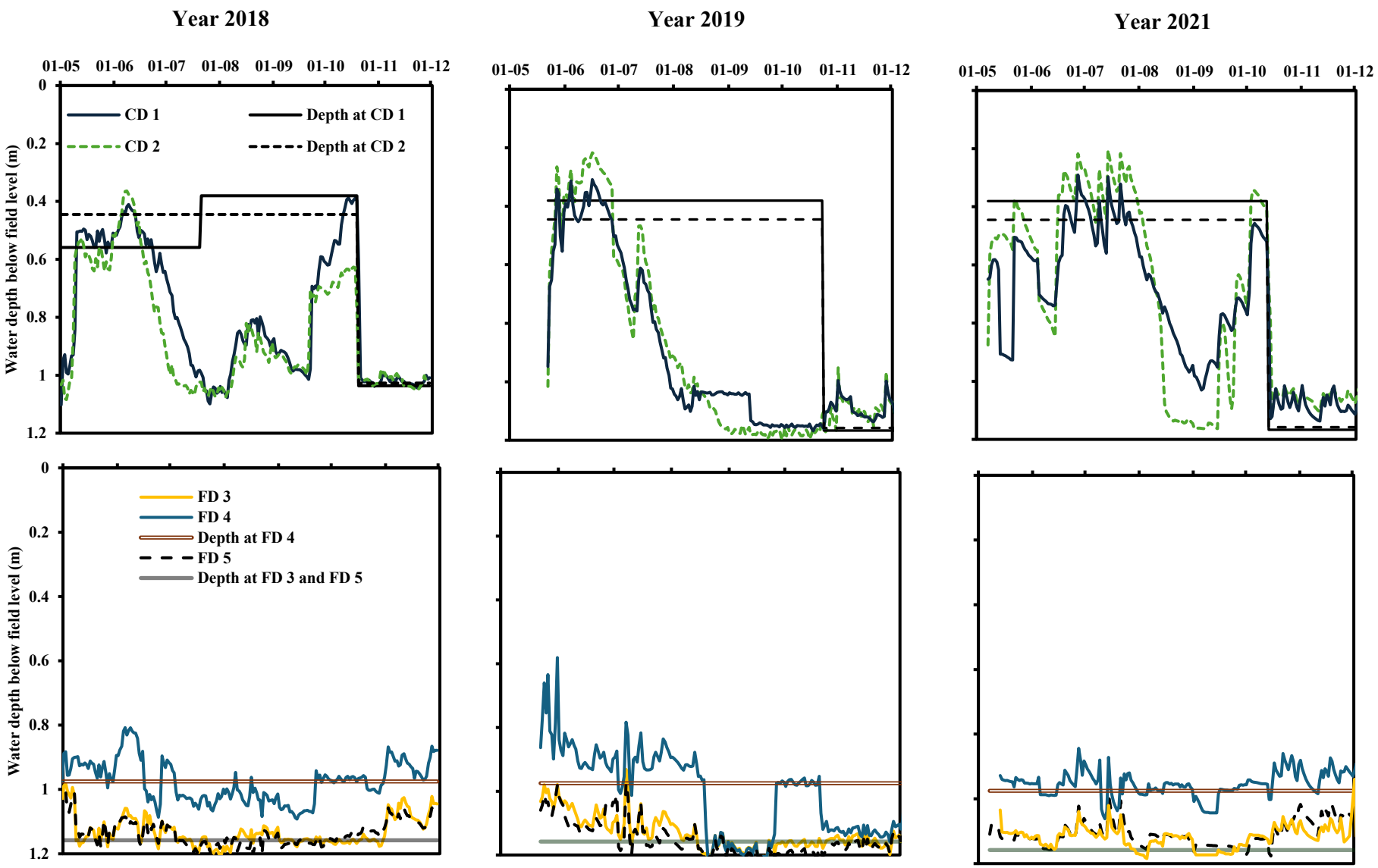

Figure 3-5. Water table variations and depth of stoplogs maintained below field level during the 3-year study. Top Row – Depth of water at Controlled Drainage structures (CD 1 and 2); Bottom row - Depth of water at Free Drainage structures (3, 4 and 5).

Towards the end of GP of 2018 and 2021, increased precipitation and reduced ET impacted the water table at CDs. This was not observed in 2019, as the water table in the fields was significantly lower than the drains. When the stoplogs were removed in October, water levels dropped rapidly through FP at CDs in 2018 and 2021, but not in 2019 due to drier summer conditions. After the initial flush, all drainage structures acted as FDs with water table fluctuating with precipitation. In the PHP, the water levels increased with low ET and increasing precipitation.

CD 1 and CD 2 flows were expected to be similar in GP, however, from April 30 to July 19, 2018, CD 1 behaved as a partially controlled drainage system, with flow trends comparable to FD 3-5 as illustrated in Figure 3-4. As such, an additional stoplog was placed at CD 1 on July 20, 2018, increasing the water table control from 0.56 m to 0.38 m from the field surface, reducing flow comparable to that of CD 2. CD 1 and CD 2 were maintained at 0.38 m and 0.44 m from the field surface, respectively, in the following study years, highlighting the importance of determining the optimum stoplog levels based on the depth of the CD outlet and field slope.

The CDs were maintained for 172, 155, and 157 d in 2018, 2019, and 2021, respectively. In GP, CD 1, and CD 2 experienced flow events for 37 and 8 days in 2018, 28 and 29 days in 2019, and 43 and 26 days in 2021, respectively. All flow events occurred during May-June of 2018 and 2019 and June -July in 2021 due to variable precipitation patterns. As expected, average CD flows were significantly lower than FD in the GP (p-values ranging from 2.7×10^{-8} to 9.9×10^{-3}, paired t-test) (Table 3-1). Detailed plot-by-plot comparisons are presented in Appendix F**.** When stoplogs were removed, significant water release caused a spike in CD 1 and 2 flows compared to FD flows (p-values ranging from 0.03 to 0.05, paired t-test). Draining of stored water to reach background FD flow levels took 2 to 9 days. The CDs drained 70%, 41% and 25%, on average, of the maximum potential volume of water stored behind the structures during the three FPs respectively. In the PHP all the drainage structures presented statistically similar mean flows (p-values ranging from 0.20 to 0.61, paired t-test) in all years (Table 3-1), suggesting that the implementation of CD did not have a longer-term impact on soil drainage properties.

The mean flows from planting to freeze-up were significantly lower at average CD versus average FD (p-values ranging from 0.004 to 0.02, paired t-test), except for 2021. On an average, CD successfully reduced mean flows by 44% in 2018, 39% in 2019 and 23% in 2021, when

compared to FD, despite varying precipitation A detailed analysis of 37 high precipitation events during the entire study (refer Appendix F) revealed that the beneficial effect of CD storage led to a 11% total volume and 14% peak attenuation (p-value = 0.34, 0.22, paired t-test), with no effect of CD (p-value = 0.39, 0.51, paired t-test) on water movement through the soil when the reservoir is full.

Table 3-1. Mean and standard deviation flows at drainage structures over the entire study season and subdivided time periods.

	Complete Study Period [a]			Growing Period [b]			Flush Period [c]			Post–Harvest Period [d]		
	2018	2019	2021	2018	2019	2021	2018	2019	2021	2018	2019	2021
Plot	**Mean Daily Flow (mm/day) across drainage structures**											
CD[e]	0.3±1.0$_P$	0.5±1.3$_P$	0.6±1.2$_P$	0.1±0.4$_P$	0.2±0.6$_P$	0.2±0.7$_P$	2.2±2.9$_P$	1.8±2.8$_P$	3.9±4.9$_P$	1.0±1.3	1.1±2.2	1.6±1.4
FD[f]	0.5±1.0	1.0±2.2	0.8±1.5	0.4±0.9	0.6±1.8	0.5±1.1	0.1±0.0	0.3±0.5	0.1±0.1	1.3±1.1	1.3±3.0	1.8±1.9

[a] Refers as period between April 30 to November 30 (2018), May 22 to December 19 (2019) and May 7 to December 14 (2021).
[b] Refers to growing season – April 30 to October 18 (2018), May 22 to October 23 (2019) and May 7 to October 12 (2021).
[c] Refers to flush period between October 19 to October 27 (2018), October 24 to October 26 (2019) and October 13 to October 14 (2021).
[d] Refers to post-harvest period – October 28 to November 30 (2018), October 27 to December 19 (2019) and October 15 to December 14 (2021).
[e] Controlled drainage system (CD) was calculated by averaging CD 1 and 2 daily flows. The system was controlled by placement of stoplogs in the drainage structures during the growing period and they drained freely in flush and post-harvest periods. Note – for the period of April 30 to July 19, 2018, CD 2 daily flows were used for CD 1 daily flows as it was deemed more representative.
[f] FD stands for Free drainage system and was calculated by averaging FD 3,4 and 5 daily flows.
$_P$ Significant difference (p-*value* < 0.05) observed when average CD paired with average FD using paired t-test.

The cumulative normalized seasonal flow and precipitation are presented in Figure 3-6 A and 5B. Cumulative flow represented 10–25% of the total precipitation for CDs and 19–38% for FDs. Precipitation during the GP represents the bulk of the total precipitation yearly, varying from 76 to 82%. During this period, CDs drained only 2 to 9% of the cumulative precipitation, whereas FDs drained 14 to 19%. This demonstrates the effect of CD during GP, attenuating water flows compared to FD by an average of 68% (57-83%) over the three years. These findings exceed both the average (27%) and range (16-44%) reported in *Dfb* Köppen−Geiger climatic zone studies with clay loam – clay soil at 0.3 to 0.6 m control depth from surface (Drury et al., 2001, 2009, 2014; Ng et al., 2002; Tan & Zhang, 2011; Zhang et al., 2015).

CD 1 and 2, positioned at 0.38 m and 0.45 m from surface respectively, effectively reduced cumulative flow in GP. These depths, while less than the recommended 0.6 m from surface (Frankenberger et al., 2006), fall within the typical mid-range for this region. CD at shallower depths could potentially reduce deep percolation of water below the root zone and increase capillary up flow of water, resulting in greater water retention behind the stoplogs and

consequently, more substantial reduction in flow. Furthermore, this approach emphasizes selecting site-specific depth levels based on field slope, drain slope, soil type, and climate.

As expected, CD 1 and 2 showed higher cumulative flows during FP compared to the three FDs, draining all water retained during GP. In 2018, 25% of the total cumulative flow of CDs was drained over nine days, whereas in 2019, 10% and in 2021, only 6% was drained in two and three days, respectively. The relative importance of FP drainage will vary yearly based on antecedent precipitation and ET but can contribute significantly to drainage flows, which has not to the author's knowledge been quantified in previous studies. The PHP received 91–138 mm of rainfall, accounting for 16–24% of the total study precipitation. The cumulative flows from CD (draining freely) and FD were similar in each PHP draining 42% to 63% of the total drainage.

The present study demonstrates that, despite FP contributing 63%, 15% and 20% on an average to growing season flow (GP+FP) and not impacting PHP cumulative flows, CD in GP consistently reduced total flow from planting to freeze-up compared to FD. This translated to a 44%, 25% and 23% reductions in average CD cumulative flows across three years. Though 2019 was driest and 2021 wettest, reductions in these two years were lower than 2018, indicating that CD performance relates to the seasonal precipitation patterns, with 2018 having a period of surplus moisture followed by deficit. In 2019, the dry conditions affected CD and FD equally (very little to muted flow), whereas 2021 had consistent flow events in both CD and FD.

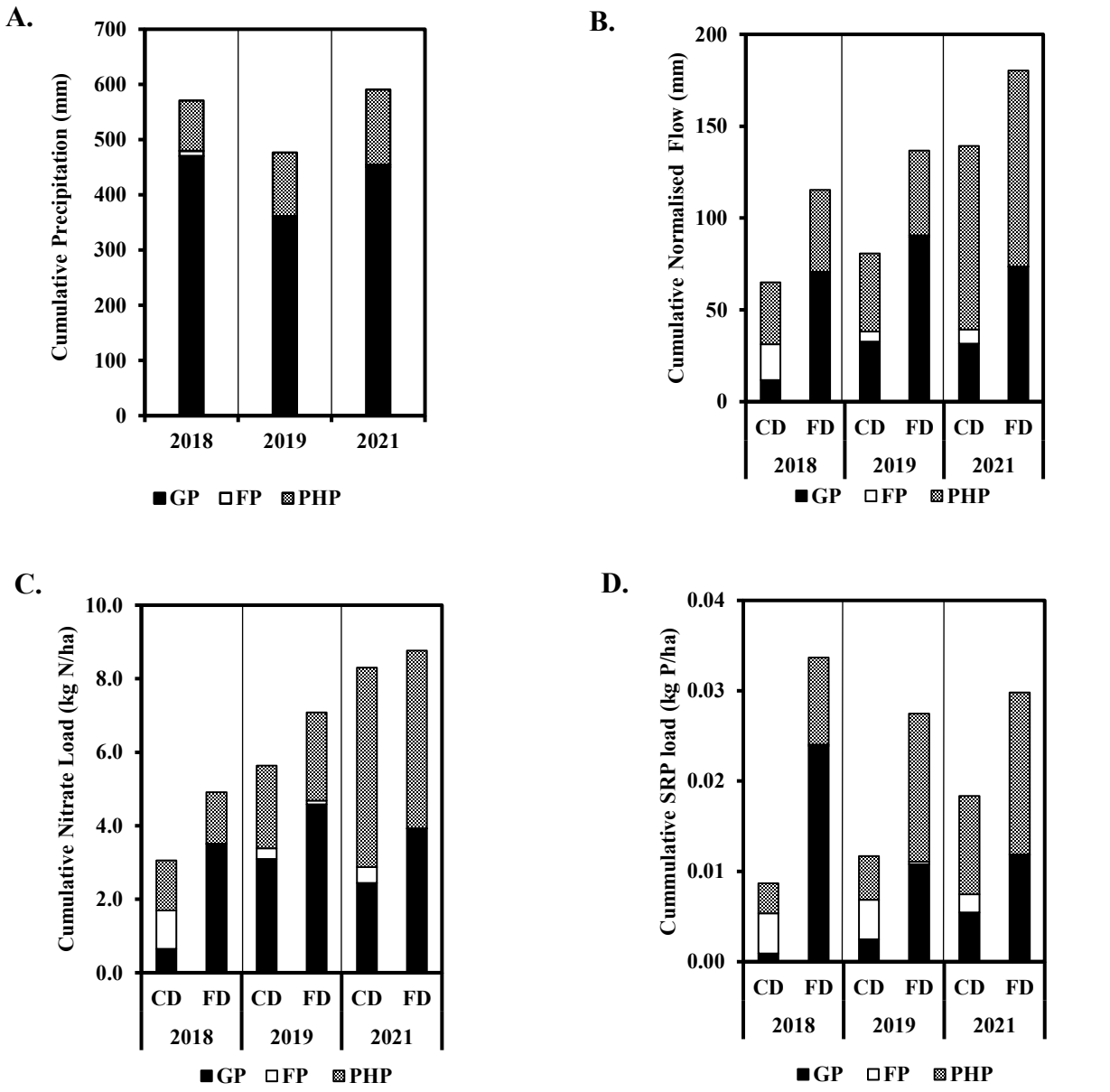

Figure 3-6. Cumulative trends during the 3-yr study – A. Precipitation (mm); B. Normalised Flow (mm), C. Nitrate Load (kg N/ha) and D. Soluble Reactive Phosphorous (SRP) Load (kg P/ha) with time period considerations across average controlled (CD) and free drainage (FD) structures. Note: GP stands for Growing Period (period between stoplog installation after planting until removal before harvest), FP for Flush Period (period after stoplog removal until flows at CDs (now freely flowing) were similar to those of FD), and PHP for Post-Harvest Period (period between the end of FP until freeze-up of drainage structures).

3.3.3. Nutrient concentration and mass loads

3.3.3.1. Nitrogen – concentration

Nitrate concentrations varied from 1.7 to 12.3 mg N/L across the CDs and from 2.8 to 14.1 mg N/L across FDs during the 3-year study period. The drainage water NO_3^--N concentration - time series at CDs and FDs is presented in Figure 3-7. NO_3^--N concentrations at all drainage structures

were elevated at the onset of each GP, declined during dry periods of GP 2018, but this decline was seen only at CDs in GP 2019 and GP 2021. Increases in concentrations at CDs occurred immediately after stoplog removal and the PHP concentrations returned to levels similar to those at the beginning of the GP in CDs and FDs.

For the entire study period, average NO_3^--N concentrations ranged from 6.1±2.3 to 8.9±2.0 mg N/L at CDs, higher than average FD in all years, with significant differences (*p*-values = $6.5x10^{-6}$, $1.2x10^{-3}$, ANOVA) observed in 2018 and 2019 (Table 3-1). This indicates no reduction in average NO_3^--N concentrations due to CD and suggests a possible plot effect at CD 1, skewing CDs averages. These concentrations are comparable to previous studies with the same soil type and crop growth (Drury et al., 2009; Helmers et al., 2012; Jaynes, 2012; Sunohara et al., 2016). Such comparison of overall averages is prevalent among earlier studies concluding that NO_3^--N concentration abatement is variable under the CD, with modest to no impact at all. However, this study further divided each study year into specific periods to further elucidate the impact of CD on seasonal concentration variations: GP-Wet (late spring to the day drains stopped flowing), GP-Dry (end of GP-Wet to the day stoplogs were removed), FP and PHP. The mean NO_3^--N concentrations were calculated for each period and compared, as shown in Table 3-2.

During GP-Wet, mean NO_3^- -N concentrations ranged from 6.5±1.4 to 10.1±1.3 mg N/L at average CDs and 5.7±0.6 to 7.7±0.9 mg N/L across average FDs, with CDs significantly higher than FDs (*p*-values ranging from $1.3x10^{-19}$ to $3.5x10^{-3}$, ANOVA). This suggests that CDs may enhance NO_3^--N leaching under wet conditions. It was also observed that spikes in NO_3^--N concentration at CDs were more pronounced than at FDs during high precipitation events, by as much as 2x (Figure 3-7), resulting in CD NO_3^--N standard deviations being twice as large as FD (Table 3-2). Wesström and Messing (2007) also observed NO_3^--N concentration peaks at CD sites during early growing period and suggested that mineralisation of organic N to NH_4^+-N and subsequently to NO_3^--N might be more prevalent at CD plots in wet conditions, leading to increased leaching following precipitation events.

Observations during GP - Dry provide good insight into the CD effect on NO_3^--N concentrations. In 2018, NO_3^--N concentrations decreased by an average of 4.2 mg N/L at both CDs and FDs compared to GP-Wet (Table 3-2). This indicates that plant uptake and possibly

denitrification were driving mechanisms during the GP-Dry. Previous studies by Mejia et al. (2000) and Skaggs et al.(2012) have suggested the possibility of denitrification with stagnant water in the drains, although the mechanism was not confirmed. Liu et al. (2019), via N mass balance across CD system, attributed 67% of N loss likely to denitrification. No flow was observed during 2019 GP-Dry while a clear difference between CDs and FDs was observed during 2021. Towards the end of 2021 GP-Wet, a distinct declining trend in NO_3^--N concentration was evident for CDs but not in the FDs, which remained similar to GP-Wet (Figure 3-7). During 2021, GP-Dry average CD NO_3^--N concentrations were significantly lower than FD (p-value = $2.5x10^{-12}$, ANOVA) despite CD NO_3^--N concentrations being higher than FDs during GP-Wet (Table 3-2). This difference was further corroborated by grab samples collected at CDs during the no-flow stage (Figure 3-7), wherein concentrations were as low as 50% of FD. The difference in concentrations can be attributed to either increased plant uptake or denitrification, or both, at CDs. The persistent stagnant water due to the physical abatement of flow at the CD has been attributed to the enhancement of anoxic conditions necessary for denitrification (Drury et al., 2014).

Table 3-2. Mean, standard deviation daily nitrate concentration at drainage structures over the entire study season and subdivided time periods.

	Complete Study Period [a]			**Growing Period (GP)** [b]						**Post-Harvest Period (PHP)** [c]		
				Wet Sub-period[c]			**Dry Sub-period**[d]					
	2018	**2019**	**2021**	**2018**	**2019**	**2021**	**2018**	**2019**	**2021**	**2018**	**2019**	**2021**
Plot	**Values across individual drainage structure**											
CD 1[f]	6.9±2.3	9.0±2.3	7.8±1.5	7.9±2.0	10.2±1.5	7.5±1.2	2.6±0.7	-	4.9±0.4	6.9±0.6	6.8±1.2	8.7±0.7
CD 2[f]	5.5±2.3	8.5±2.0	5.6±1.5	10.1±0.5	9.9±1.3	5.9±1.6	-	-	3.8±0.5	4.9±1.6	6.5±1.2	6.0±0.7
FD 3[g]	5.7±1.4[1]	8.1±2.7[1]	5.7±0.9[1]	6.6±0.4[1,2]	8.1±1.5[1,2]	5.4±0.5[1]	3.6±1.1[1]	-	7.0±0.8[1,2]	5.3±0.4[1]	5.1±0.9[1]	5.3±0.3[1,2]
FD 4[g]	5.2±2.2[1]	7.4±1.3[1,2]	5.9±0.8[1]	7.0±0.5[1,2]	7.5±1.0[1,2]	5.6±0.8[1]	2.7±0.7	-	6.5±0.8[1,2]	4.2±1.0[1]	6.3±1.3	5.8±0.5[1]
FD 5[g,h]	-	7.5±1.5[1,2]	6.4±0.8[1,2]	-	7.2±0.6[1,2]	6.4±0.8[1]	-	-	6.2±0.5[1,2]	-	6.8±1.8	6.5±1.1[1]
	Values across the systems											
Mean CD	6.1±2.3$_P$	8.9±2.0$_P$	6.3±1.6	7.9±2.0$_P$	10.1±1.3$_P$	6.5±1.4$_P$	2.6±0.7	-	4.0±0.7$_P$	6.0±0.9$_P$	6.6±1.0	7.1±1.1$_P$
Mean FD	5.2±1.8	7.9±2.0	6.0±0.8	6.8±0.3	7.7±0.9	5.7±0.6	3.1±1.1	-	6.8±0.7	4.8±0.9	6.3±1.3	5.8±0.5

[a] Refers as period between April 30 to November 30 (2018), May 22 to December 19 (2019) and May 7 to December 14 (2021).
[b] Refers to growing period – April 30 to October 18 (2018), May 22 to October 23 (2019) and May 7 to October 12 (2021).
[c] Refers to subperiod in GP from the day stoplogs are placed (start of study period) to the day the drains stop flowing in GP (typically in late July or early August - varies across each drainage structure every year).
[d] Refers to subperiod in GP from the day drains stop flowing in GP to the day stoplogs were taken out (end of GP and beginning of FP)
[c] Refers to post-harvest period – October 28 to November 30 (2018), October 27 to December 19 (2019) and October 15 to December 14 (2021).
[f] Controlled drainage structures (CD 1 and CD 2) were controlled by placement of stoplogs in the drainage structures during the growing period. However, they drained freely in FP and PHP.
[g] Free drainage structures (FD 3, 4 and 5) were left to drain freely.
[h] In 2018, ISCO sampler at FD 5 was removed in the month of June. Partial concentration has not been used to compare concentrations.
[1] Significant difference observed (p-*value* < 0.05) when compared to CD 1 using ANOVA single factor.
[2] Significant difference observed (p-*value* < 0.05) when compared to CD 2 using ANOVA single factor.
$_P$ Significant difference observed (p-*value* < 0.05) when compared to average FD using ANOVA single factor.

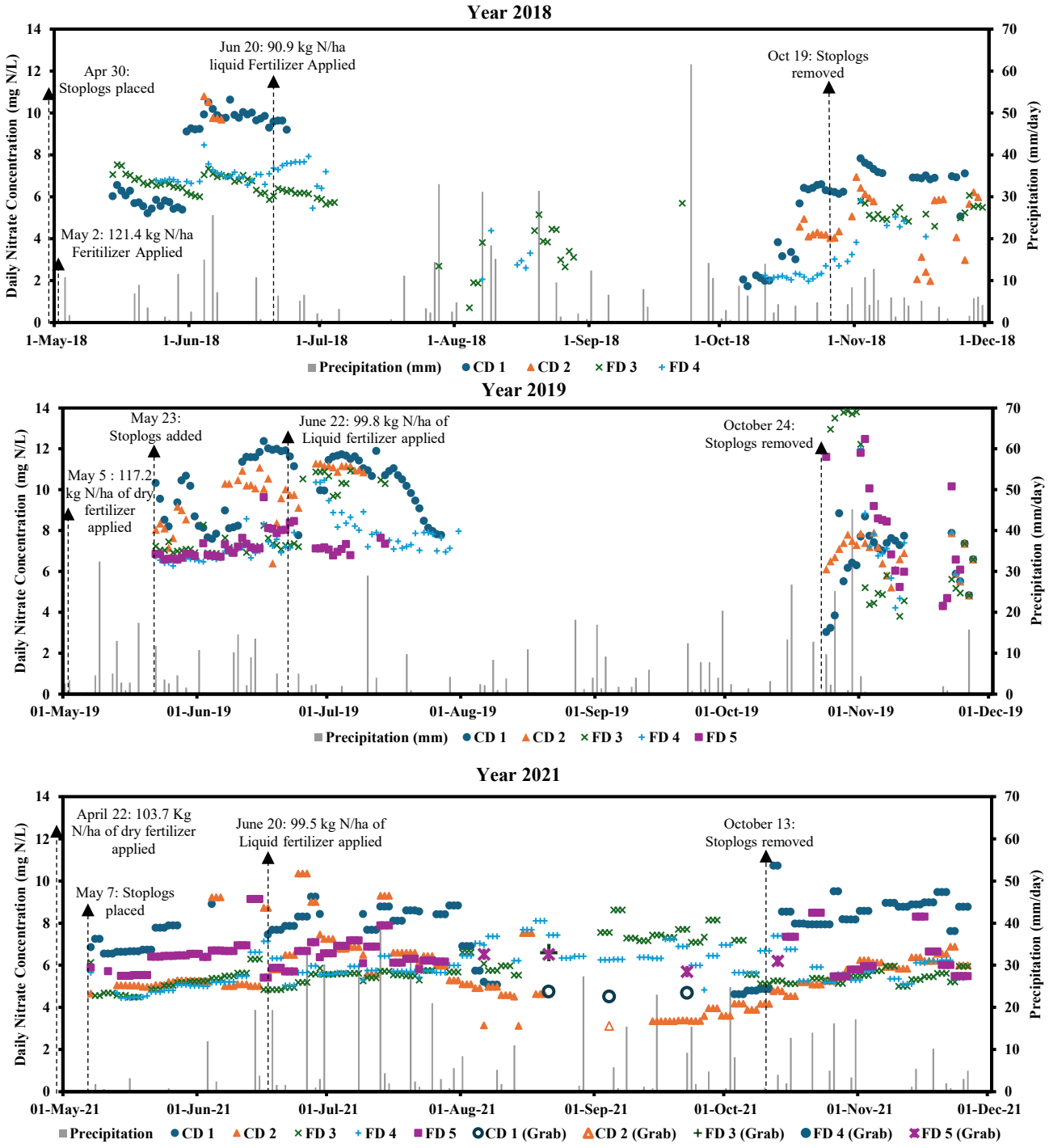

Figure 3-7. Daily trend of nitrate (mg N/L) concentration – across controlled (CD 1 and 2) and free (FD 3, 4 and 5) drainage structures during the 3-yr study with respect to daily precipitation trends (mm/day), the timing and quantity of fertilizer application and the timing of stoplog activities. In 2021, grabs samples were collected and denoted as Grab at each drainage structure. Note: Data collection was conducted only when there was flow.

The removal of stoplogs in October resulted in a sharp increase in NO_3^--N concentrations at

CD 1 for all three years (Figure 3-7). A similar trend was observed for CD 2 in 2018 and 2019 but was less prominent in 2021. The rapid increase in NO_3^--N concentrations with flow following the removal of stoplogs indicates that a gradient of NO_3^--N existed within the stored pore water and strongly suggests that denitrification was occurring at lower water depths behind the CDs during the GP. In the current study, in addition to observed concentration differences, denitrification was further corroborated by enumeration of the bacterial community at the CDs (discussed later in section 3.3.1.3). In PHP, draining freely, average CD NO_3^--N concentrations were significantly higher than FD in 2018 and 2021 (p-values = $6.9x10^{-5}$, $1.7x10^{-6}$, ANOVA), reverting to the concentration behavior seen in GP–Wet, under similar weather conditions and absence of crops, post-harvest. Concentration spikes were also observed in all drainage structures, indicating increased leaching during precipitation events.

3.3.3.2. Nitrogen – mass load

The mass load by period is shown in Figure 3-6 C (more detailed comparison can be found in Appendix G). In the three GPs 2018, CDs reduced cumulative NO_3^--N load by 82% in 2018, 32% in 2019 and 38% in 2021, compared to average FDs. CDs were expected to reduce the overall export of NO_3^--N in the GP as a function of flow and potentially concentration reduction via increased plant uptake and denitrification. Dividing GP into subperiods was beneficial as comparing the difference of concentration, cumulative flows and loads at CD vs. FD was used to understand and quantify the mechanisms at play. In GP-Wet lower cumulative load reductions were observed compared to cumulative flow reductions, indicating that an increase in NO_3^--N concentrations due to leaching at CD had a net impact on load. In other words, the mass difference between CD and FD compared to mass reduction solely attributed to flow indicated that leaching contributed 17%, 25% and 14% to loads, quantifying a negative effect of CD on load during wet conditions.

During 2018 and 2019 GP-Dry no net effect on load reductions from leaching, denitrification or plant uptake was observed as no significant differences in concentration were observed between CD and FD in 2018 and there was no flow in 2019. However, in 2021 GP-Dry significantly lower concentrations were recorded at CD compared to FD contributing to a small positive effect on load reduction of 0.3%. Assuming denitrification was the differentiating mechanism in 2021 compared to plant uptake, as precipitation was evenly distributed with only

short periods of potential plant stress, this small percentage could be attributed to denitrification. Regardless, the net positive effect of denitrification and plant uptake in GP-Dry on mass load reduction was insignificant when compared to the net effect of leaching in GP-Wet in the present study. Significant load discharges were observed when stoplogs were removed in all years for CDs peaking on the day stoplogs were taken out and subsequently declining as FP progressed. The mass load during FP represented 6% to 34% of the total NO_3^--N load at CDs. In the PHP, as expected, the drainage structures all flowing freely had statistically similar N loads (*p*-values ranging from 0.6 to 1.0, ANOVA).

The NO_3^--N mass reduction attributed to CD is well documented in the literature, ranging from 10% to 96%, with several studies reporting mass reduction being primarily due to flow abatement (Drury et al., 2001; Helmers et al., 2012; Jaynes, 2012; Smith et al., 2019; Verma & Cooke, 2012). However, other studies have reported a reduction in N loading as a combined result of reduced flow and NO_3^--N concentration reduction by denitrification or plant uptake (Adeuya et al., 2012; Sunohara et al., 2014). In the present study, CDs reduced export by 32% to 82% during the GP, falling within the range observed in the literature, and by 5% to 38% from planting to freeze-up which includes the flush and post-harvest periods. CD was shown to be most effective at CDs in 2018 when a period of precipitation at the beginning of GP was followed by a dry period, increasing NO_3^--N losses to plant uptake and denitrification.

3.3.3.3. Nitrogen – soil microbiome analysis at CD and FD plots

For each soil depth increment, soil samples were collected and the 16S rRNA gene was sequenced to determine the effect of CD implementation on the microbial community and, more specifically, the NO_3^--N reducing bacterial population, compared to free-draining soil, as a function of soil depth and soil total organic carbon (TOC) content. In terms of diversity, for the entire microbiome, an average of 971±114 and 983±78 OTUs were observed at CD 2 (representing the CD system) and FD 5 (representing the FD system), respectively, with the highest number of OTUs (1175 for CD and 1043 for FD) observed at the lowest depth of 76 cm from the surface for both systems. The Chao1 indices, which compares species richness at each location, were 1420±283 and 1500±121 at CD and FD, respectively, with no significant difference observed between the two systems (*p*-value = 0.54, ANOVA). Beta diversity analysis using Principal Coordinates Analysis (PCoA) visually showed diversity differences with respect to location and soil depth (Appendix

H). The microbiome community differed significantly at CD (p-value = 0.002, ANOSIM) compared to FD, but not within a system at different depths (p-value = 0.98, ANOSIM). The water level gradient within CD system may have provided conditions conducive to the growth of both aerobic and anoxic bacterial communities, in contrast to FD.

The relative abundance of OTUs present in soil samples at CD and FD were classified into 16 phyla. The top five phyla (with relative abundance >10% in most samples) were *Acidobacteria* (20.4% and 22%), *Actinobacteria* (24.1% and 14.4%), *Firmicutes* (16.5% and 7.8%), *Proteobacteria* (15.4% and 25.1%), and *Verrucomicrobiota* (2.2% and 10.6%) in CD and FD, respectively. These dominant phyla are typically observed in Canadian and US agricultural soils (Banerjee et al., 2016; Firth et al., 2023; Sheibani et al., 2013). Phyla are quite diverse, comprising bacteria that participate in versatile functions. The relative abundance of OTUs was then identified to the genus level and categorized based on their functions, as presented in Figure 3-8, comparing CD and FD at increasing soil depths. In total, 111 genera were identified.

The most abundant OTUs in the CD system at the genus level were Facultative bacteria, ranging from 23% to 28% among the six depths, with *Bacillus* (Saxena et al., 2020; Verbaendert et al., 2011), *Gaiella* (Liu et al., 2023), and *midas_44653* from the family Gemmatimonadaceae (Jia et al., 2019; Oshiki et al., 2022) as the top three dominant genera. Facultative bacteria are capable of switching electron acceptors based on favorable environmental conditions but utilizing NO_3^--N as one of the acceptors were identified and grouped together in the present study. On average, 53% higher relative abundance of Facultative bacteria (p-value = 0.002, paired t-test) were found in the CD system when compared to FD. Interestingly, at FD, carbohydrate- and protein-oxidizing genera, which strictly use oxygen as an electron acceptor, dominated with the average relative abundance of 29%, suggesting the presence of consistent oxygen at all depths, unlike CD. These differences in communities most abundant at CD and FD suggest the efficacy of CD in promoting the growth of NO_3^--N reducing over oxidising genera.

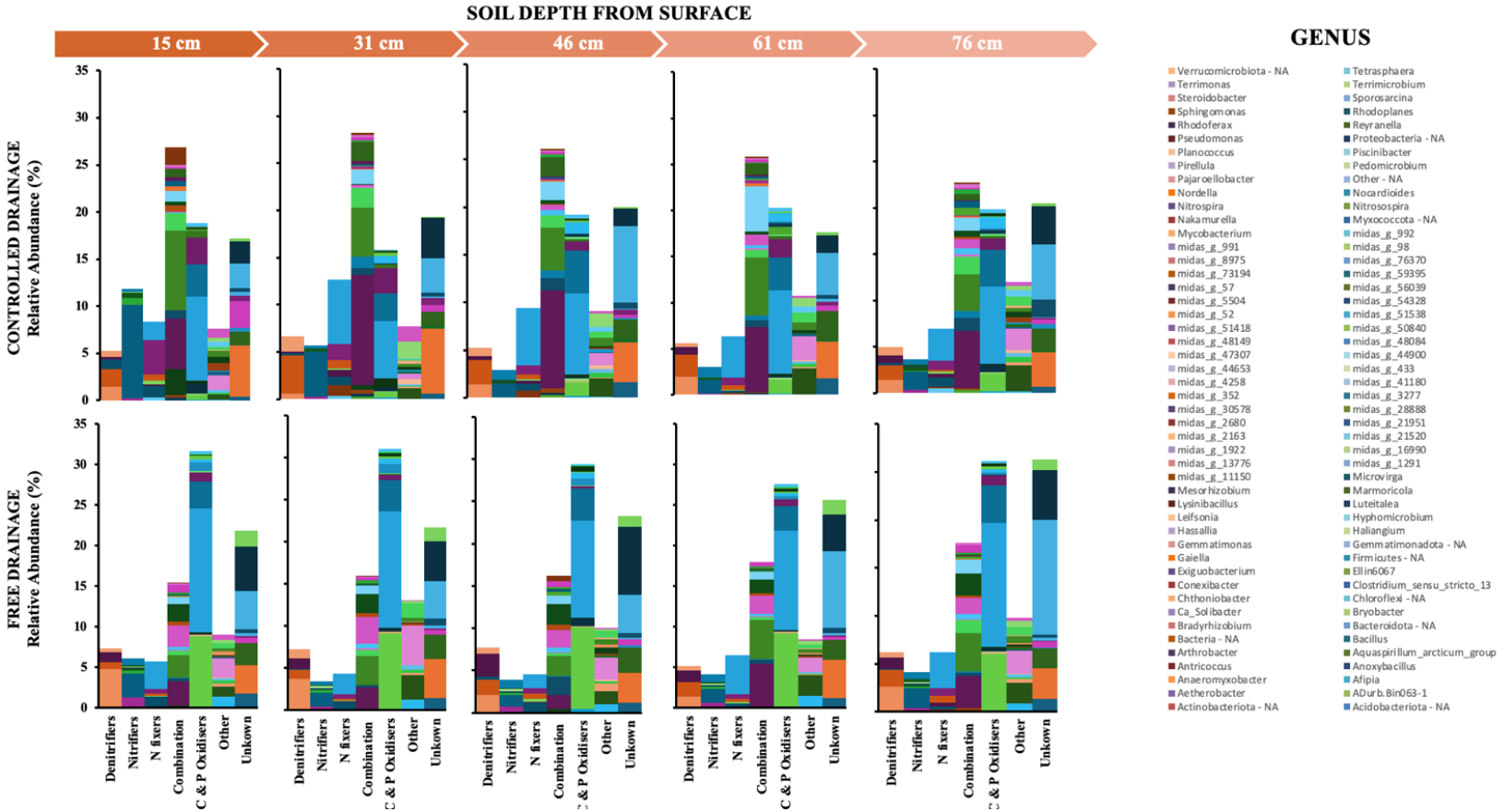

Figure 3-8. Average relative abundance of diverse types of bacteria at different soil depths across the controlled drainage (CD) and Free Drainage (FD) systems. Combination represents Facultative Bacteria, C & P Oxidisers include carbohydrate and protein oxidisers, other group include aerobic bacteria involved in pathways other than C&P oxidisation, Unknown group consists of bacteria identified only at Phylum level.

The observed genera characterised as denitrifiers were *Bradyrhizobium* (Franck et al., 2008; Shapleigh, 2006), *Conexibacter* (Monciardini et al., 2003), *Rhodoferax* (Dueholm et al., 2022; Kato & Ohkuma, 2021), *and Rhodoplanes* (Shapleigh, 2006; Zhang et al., 2022) and *Steroidobacter* (Dueholm et al., 2022). The average relative abundance of denitrifiers was 5.6±0.7% and 6.0±1.0% for CD and FD, respectively, and were statistically similar (*p*-value = 0.09, paired t-test). This observation suggests that CD potentially favoured the selection of Facultative bacteria over denitrifiers, as fluctuating shallower water tables likely favored facultative bacteria (limited by O_2 under water clogged conditions) over strictly anoxic bacteria. Within the systems, the NO_3^--N reducing community is represented by the sum of relative abundance of Facultative and denitrifying genera. Comparing CD to FD, statistical differences (*p*-value = 0.003, paired t-test) were observed for the NO_3^--N reducing communities, with a 35% greater relative abundance at CD than FD.

Genera differentiation based on the end-product of the NO_3^--N reduction reaction revealed a higher relative bacterial abundance at the CD for all end products when compared to FD. More information can be found in Appendix H. Notably, the relative abundance of N_2O greenhouse gas (GHG) releasing bacteria was small at 0.7% and 0.3% at CD and FD sites, respectively. Due to elevated soil water content, CD has a potential to increase N_2O and other GHG emissions (Dobbie & Smith, 2006; Ekwunife & Madramootoo, 2023). However, a few studies have reported positive reduction of N_2O emissions at CD (Abbasi et al., 2020; Elmi et al., 2005) while others observed no difference between CD and FD (Crézé & Madramootoo, 2019; Hagedorn et al., 2022; Nangia et al., 2013; Van Zandvoort et al., 2017).

TOC content was also measured in the soil samples where TOC at CD dropped with depth and remained consistently lower than FD (Appendix H), (*p*-value = 0.03, paired t-test). This could be due to TOC consumption by the larger NO_3^--N reducing bacterial community present in CDs (Schlüter et al., 2024). These observations in combination with lower GP-Dry NO_3^--N concentrations at CDs compared to FDs, validates denitrification as a definitive mechanism for removal of NO_3^--N under CD implementation, which has not, to the author's knowledge been conclusively identified in previous studies.

3.3.3.4. Phosphorus - concentration

The time series of SRP concentrations are presented in Figure 3-9 with CD 1 and CD 2 concentrations ranging between 0.004 – 0.21 mg P/L and 0.003 - 0.13 mg P/L, respectively, and FD concentrations ranging from 0.003 - 0.68 mg P/L. Granular P fertilizer was applied in late April to early May, at agronomic rates. In 2019, elevated one-day spikes in concentration were observed at all drainage structures except CD 2 following consecutive rainfall events in the first week of June (approximately a month after fertilizer application). No notable spike was observed in 2018 and 2021, although several precipitation events had occurred before sampling commenced. The overall mean SRP concentrations at CDs were comparable in all three years (Table 3-3 and detailed comparisons can be found in Appendix J) ranging from 0.01±0.02 to 0.02±0.01 mg P/L, while at FDs mean concentrations were in the range of 0.02±0.03 to 0.09±0.14 mg P/L. SRP was significantly lower in CDs (*p*-values ranging between 9.7×10^{-6} to 3.9×10^{-4}, ANOVA) when compared to FDs during the three-year study. This suggests a treatment effect.

Across all GPs in all years, the mean SRP concentrations were statistically lower in CDs when paired with FDs by 35-86% (*p*-values ranging between 6.1×10^{-5} to 1.1×10^{-4}, ANOVA). These lower concentrations (Table 3-3) observed during this period are hypothesized to be attributable to enhanced P sorption to the soil (due to increased retention time) and/or increased plant uptake. Notably, acrossthe three GPs, CDs experienced only one P leaching event (defined as any event with SRP threshold concentration > 0.2 mg/L) compared to 29 events at the FDs. Average soil extractable P levels were 47.6 kg P/ha in the CD plots and 71.2 kg P/ha in the FD plots. Higher soil P levels are positively correlated with P leaching losses (King et al., 2015); however, our difference was not statistically significant (*p*-value > 0.1, ANOVA), and the interpretation is further constrained by the limited number of composite samples (n = 4), which may not have fully captured site-scale spatial variability.

Following stoplog removal, CDs exhibited increased mean concentrations (0.03±0.00 to 0.07±0.06 mg P/L), compared to pre-removal conditions(0.01±0.01 to 0.03±0.02 mg P/L), before returning to background levels (0.01±0.00 to 0.02±0.01 mg P/L). This change was statistically significant(*p*-value = 2.6×10^{-5}, ANOVA in 2018), suggesting transient P desorption under stagnant water conditions behind stoplogs and subsequent mobilization during FP. In PHPs, mean concentrations at FDs were significantly higher than CDs in 2019 and 2021 (*p*-values = 0.004 and

0.03, ANOVA) suggesting an antecedent impact from CD during the GP on leaching during the PHP.

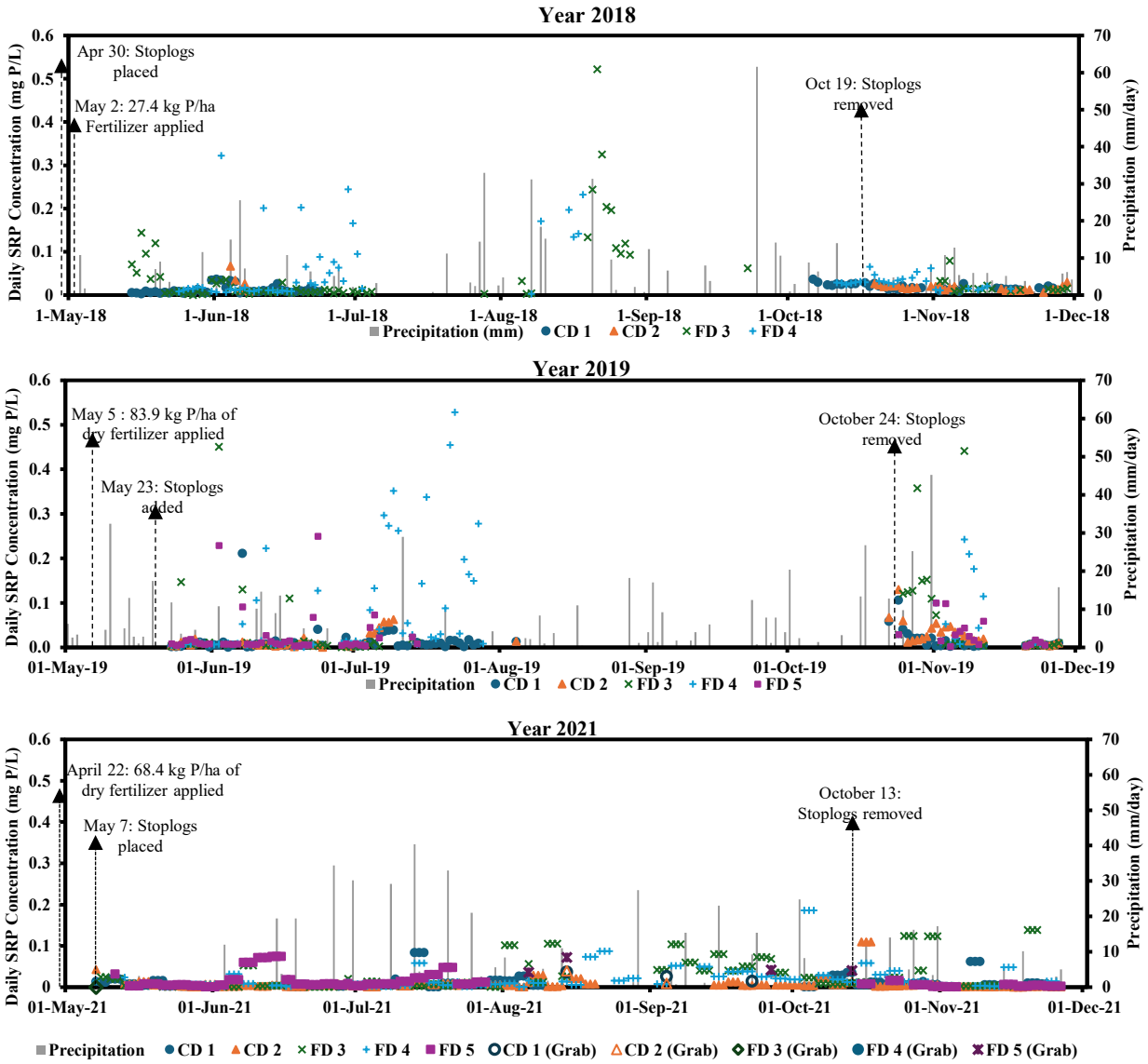

Figure 3-9. Trends of Soluble Reactive Phosphorus (SRP) (mg P/L) concentration - across drainage structures during the 3-yr study with respect to daily precipitation trends (mm/day), the timing and quantity of fertilizer application and the timing of stoplog activities. In 2021, grabs samples were collected and denoted as Grab at each drainage structure. Note: Data collection was conducted only when there was flow

Among the limited studies considering P, Sunohara et al. (2015) and Williams et al. (2015) reported no change in SRP concentrations at CD, whereas studies by Saadat et al. (2018b), Sanchez Valero et al. (2007), Satchithanantham et al. (2014) and Stampfli (2003) observed an increase in SRP concentrations at CD. These increases have been attributed in the literature to redox-driven processes, including the reductive dissolution of Fe (III) (hydr)oxides and potential mobilization

of associated P under saturated conditions, whereas Al-associated P is generally considered less sensitive to redox changes. Although these mechanisms were not directly measured in the present study, they may help explain variability among systems. The present study observed consistently lower SRP concentrations at CDs. This aligns with Nash et al. (2015), who reported significantly lower flow-weighted SRP concentration with CD (0.09 mg P/L) compared to that of FD (0.15 mg P/L), hypothesizing that during summer, CD conserved water, increased uptake of water and P by crops, thereby reducing amount of phosphorus available for loss through leaching. In the present study, the mean total corn (kernel + stalk) P uptake was 9% greater at CD sites than FD sites in 2018 (though not statistically significant) and approximately 47 times greater than the P mass lost through drainage. Increased plant uptake during GP could explain lower concentrations observed in both GP and PHP suggesting increased plant uptake could reduce leaching potential.

Table 3-3. Mean, standard deviation daily soluble reactive phosphorus (SRP) concentrations (mg P/L) at drainage structures over the entire study season and subdivided time periods.

	Complete Study Period [a]			**Growing Period [b]**			**Post-Harvest Period [c]**		
	2018	**2019**	**2021**	**2018**	**2019**	**2021**	**2018**	**2019**	**2021**
Plot	**Values across individual drainage structure (x10^{-2} mg P/L)**								
CD 1[d]	1.5±0.9	1.3±2.6	1.4±1.7	1.5±1.0	1.3±2.8	1.3±1.6	1.5±0.4	0.8±0.6	1.5±1.9
CD 2[d]	1.9±1.1	1.9±2.2	1.0±1.6	3.0±2.3	1.4±1.7	0.9±1.0	1.6±0.6	2.1±1.5	1.3±2.8
FD 3[e]	4.1±7.8[1]	4.2±9.1[1]	2.6±3.5[1,2]	4.8±8.7[1]	2.5±7.3	2.4±3.0[2]	1.9±1.6	6.8±11.9[1]	3.5±5.0
FD 4[e]	5.2±6.7[1,2]	8.6±14.4[1,2]	2.1±2.8[2]	5.9±7.6[1]	9.3±15.6[1,2]	2.1±3.0[2]	2.5±1.9[1,2]	6.4±8.1[1,2]	2.0±1.9
FD 5[e, f]	-	2.8±4.7[1]	1.7±2.0[2]	-	2.7±5.2	2.0±2.2[2]	-	3.0±3.1[1]	0.7±0.6
	Values across the systems (x10^{-2} mg P/L)								
Mean CD	1.6±0.9 [P]	1.5±1.9 [P]	1.1±1.5 [P]	1.6±1.1 [P]	1.2±1.7 [P]	1.0±1.0 [P]	1.6±0.5	1.5±0.8 [P]	1.4±2.4 [P]
Mean FD	5.4±7.6	8.6±13.8	2.4±2.8	6.4±8.6	9.1±15.4	2.5±2.5	2.2±1.9	7.0±8.9	2.3±3.6

[a] Refers as period between April 30 to November 30 (2018), May 22 to December 19 (2019) and May 7 to December 14 (2021).
[b] Refers to growing period – April 30 to October 18 (2018), May 22 to October 23 (2019) and May 7 to October 12 (2021).
[c] Refers to post-harvest period – October 28 to November 30 (2018), October 27 to December 19 (2019) and October 15 to December 14 (2021).
[d] Controlled drainage structures (CD 1 and CD 2) were controlled by placement of stoplogs in the drainage structures during the growing period. However, they drained freely in FP and PHP.
[e] Free drainage structures (FD 3, 4 and 5) were left to drain freely.
[f] In 2018, ISCO sampler at FD 5 was removed in the month of June. Partial concentration has not been used to compare concentrations.
[1] Significant difference observed (*p-value* < 0.05) when compared to CD 1 using ANOVA single factor.
[2] Significant difference observed (*p-value* < 0.05) when compared to CD 2 using ANOVA single factor.
[P] Significant difference observed (*p-value* < 0.05) when compared to average FD using ANOVA single factor.

3.3.3.5. Phosphorus – mass loads

The cumulative SRP mass load for the complete study period, subdivided by the three time periods (GP, FP, and PHP) for average CDs and FDs, is shown in Figure 3-6 D. During the GPs, CDs lost 0.001 to 0.009 kg P/ha to drainage, representing 11% to 30% of total cumulative load, while FDs lost 0.011 kg P/ha to 0.024 kg P/ha to drainage, representing draining 37% to 71% of the total cumulative load. As expected, a flush of mass SRP load was observed during FP. Load peaks were observed when the flow peaked and dropped to the background FD load at the end of the subperiod, releasing 11 % to 51% of the total cumulative load in 2 to 9 days.

Average CDs reduced cumulative load in GP by 96% in 2018, 78% in 2019 and 54% in 2021 when compared to average FD. The corresponding cumulative flow reductions at CDs were 83%, 64% and 57% in the respective three GPs, indicating a positive contribution of concentration reduction on load reduction in 2018 and 2019 and small negative contribution in 2021. However, when GP and FP are considered together, cumulative SRP load reductions were 78%, 38% and 37%, while the cumulative flow reductions at CDs were 55%, 58% and 46% while compared to average FDs during 2018, 2019 and 2021, respectively, indicating a positive contribution of concentration reduction in 2018 and a negative contribution in 2019 and 2021. In the PHP, cumulative mass loads at FD consistently exceeded those of CD 1 and 2 as higher concentrations at the FD governed the load variations with statistically similar cumulative flows across the drainage structures.

CDs were successful in reducing the net overall export (Figure 3-6 D). CDs retained SRP load by 65% in 2018, 57% in 2019 and 38% in 2021 when compared to FDs. By comparison, SRP loss in tile drainage was reduced by 66% with CD in a four-year study (Sunohara et al., 2016) and 44% in a clay loam soil in Southwestern Ontario (Zhang et al., 2015), due to reduction of flow. Nash et al. (2015) and Tan and Zhang (2011) reported 80% and 13.2% SRP reduction respectively, owing to flow and concentration reduction. The load reductions of the current study are within the range of previous studies. The study findings indicate P desorption in stagnant pore water behind CDs during dry periods while suggesting increased plant uptake with CD reduces P drainage concentrations during both GP and PHP.

3.3.3.6. Solids and particulate phosphorus

Tile drainage increases preferential flow through macropores, especially in high clay soils, leading to greater transport of solids and particulate phosphorus (King et al., 2015). CD has the potential to reduce solid migration during high precipitation events and perhaps reducing particulate releases and loads. This was tested in the present three-year study by analyzing composite samples that appeared turbid or contained solids for TSS and PP. Throughout the entire research study, a total of 33 samples at CDs and 106 samples at FDs were identified as cloudy. In the three GPs, the mean TSS concentrations were found to be 8±4 mg TSS/L and 15±9 mg TSS/L at CD and FD, respectively (p-value = 0.002, ANOVA), indicating that CD reduced TSS concentrations when stoplogs were in place, as depicted in Figure 3-10 A. However, high TSS concentrations were

observed at CDs during the three flush periods, ranging between 9 to 41 mg TSS/L, suggesting displacement of solids previously held behind by stoplogs during GP. In the PHP, as expected, no statistical differences were observed (p-value = 0.8, ANOVA) for TSS concentrations between CD and FD (Figure 3-10 B). Similarly, CDs successfully reduced PP concentrations during the three GPs when compared to FDs (p-value = 0.01, ANOVA) (Figure 3-10 C) while no statistical differences were observed in the PHP (p-value = 0.2, ANOVA) (Figure 3-10 D). The same trends were observed for TP (Appendix I). As expected, PP was found to correlate to TSS (R = 0.7).

The impact of CD on TSS and PP mass loads was distinctly observed in GP when compared to FD (Figure 3-10 E and 3-10 F). In all years, during GP, CDs reduced cumulative TSS exports significantly by 84% in 2018, 2% in 2019, and 93% in 2021 when compared to average FDs (p-value = 0.01, ANOVA). The minimal reduction seen in 2019 at CDs was a function of the higher cumulative flow (44% higher than FDs) on the days these samples were collected rather than concentration differences. TSS flux during FP was significant as any sedimented solids in the drainage lines were flushed out. However, the total TSS reductions during GP+FP at CDs were significantly lower (p-value = 0.04, ANOVA) when compared to those at average FDs, indicating the positive effect of CD on TSS load attenuation. Cumulative TSS loads during PHP were statistically similar between CD and FD, as hypothesized (p-value = 0.5, ANOVA).

PP exports during the three GPs were significantly reduced by 96% in 2018, 63% in 2019 and 97% in 2021 at CDs, compared to average FDs (p-value = 0.002, ANOVA) and are considerably higher than the observed reduction in flows. Therefore, the reduction in PP migration can be attributed to the physical damming effect of the CDs on the soil structure. Increased moisture retention at CD possibly reduced the formation of macropores and solids movement through macropore flow. During FP, higher exports of PP occurred due to higher flows and concentrations. Along with TSS, any settled solids in the drainage lines were likely flushed out during FP. PHP exports were similar between CDs and FDs in each year (p-value = 0.1, ANOVA). The total PP reductions during GP+FP at CDs were significantly lower (p-value =0.02, ANOVA) when compared to those at average FDs, indicating the positive effect of CD on PP load attenuation. Overall, CDs reduced the annual PP load by an average of 80% and annual TP loads (Appendix I) by 74%, 40% and 50% in 2018, 2019 and 2021, respectively.

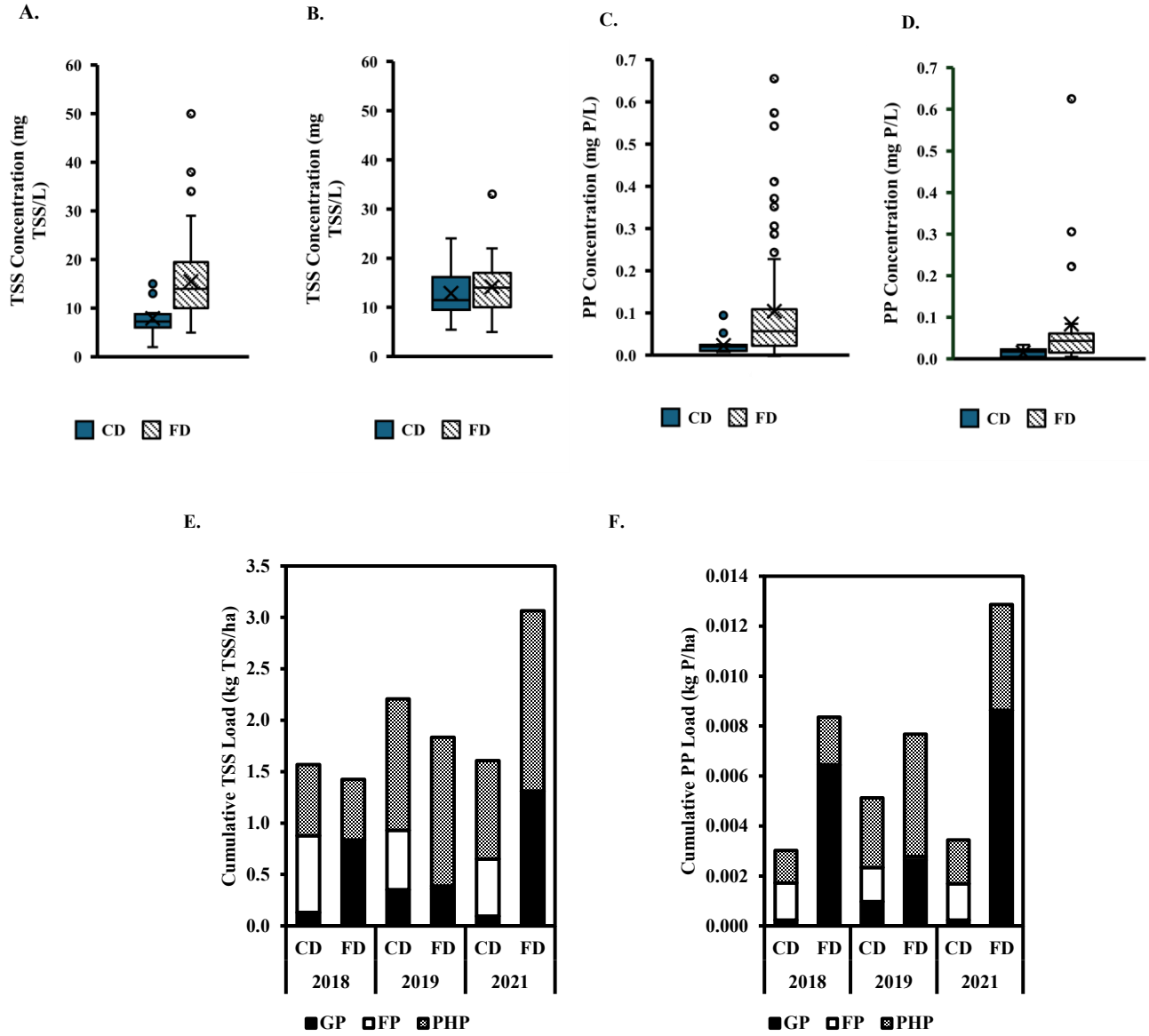

Figure 3-10. Concentration and load trends of total suspended solids (TSS) and particulate phosphorus (PP) - across average controlled drainage (CD) and free drainage (FD) structures during A) Growing Period (GP), B) Post-Harvest Period (PHP) for TSS (mg TSS/L) and C) GP, D) PHP for PP (mg P/L), E) Cumulative TSS load (kg TSS/ha) and F) Cumulative PP load (kg P/ha) over the 3-year study. Note: GP stands for Growing Period (period between stoplog installation after planting until removal before harvest), FP for Flush Period (period after stoplog removal until flows at CDs (now freely flowing) were similar to those of FD), and PHP for Post-Harvest Period (period between the end of FP until freeze-up of drainage structures).

Limited research has been conducted on the effects of CD on TSS, TP, and PP. Zhang et al. (2015) in a 4-year study in Southwestern Ontario reported a 50% reduction in TP load and a 33% reduction in PP load. The authors credited this reduction to flow, as minimal to no change in concentrations was observed. Similar reasoning and observations for TP reductions were made by

Tan and Zhang (2011). Frey et al. (2013), Sunohara et al. (2015) and Valero et al. (2007) reported significantly higher TP concentrations and but reduced TP loads at CD due to positive correlations to flow, which implies an effect on TSS as well. The present study shows CD has a statistically significant impact on reducing TSS and PP concentrations and load losses to drainage during GP+FP, which is likely attributed to the CD damming effect reducing macropore formation and flow. SRP accounted for 64% of TP load at CD and 76% of TP load at FD. This is consistent with literature where SRP loss as dissolved P has been found to be the dominant form of P in tile drainage, ranging from 66% to 86% (King et al., 2016; Zhang et al., 2015). These results reinforce the importance of considering PP load, which represents 36% of CD P load in this study, even as CD reduced PP load compared to FD.

3.4. Conclusions

This three-year research study highlights the impact of controlled drainage (CD) system on tile flow, nutrient concentrations, and loads, when compared to free drainage, with monitoring conducted from planting to freeze-up across three time periods - Growing Period (GP), Flush Period (FP) and Post-Harvest Period (PHP). Dividing the study into periods provided a unique opportunity to assess the aftermath of stoplog removal and to examine whether CD during GP had an antecedent effect on nutrient dynamics in the PHP until freeze-up. During GP, CD - maintained at shallower depths of 0.38 m and 0.44 m from the surface – reduced tile flow by 68%, nitrate loads by 51% and soluble reactive phosphorus (SRP) by 76%. Flow reductions were influenced by seasonal meteorological patterns, with the highest flow reductions observed during a year that transitioned from a period of surplus to deficit moisture conditions. Significantly reduced nitrate concentrations in dry periods of GP (33%), nitrate gradients observed in the dammed soil profile during FP and the 35% higher relative abundance of facultative denitrifying bacteria in the soil compared to FD, provides substantial evidence of denitrification mechanism under CD. Interestingly, SRP concentrations were significantly lower in GP and PHP, indicating increased crop uptake in GP may have reduced SRP availability for leaching in PHP – representing the only observed antecedent effect of CD in GP to PHP. Additionally, particulate phosphorous accounted for 36% of total phosphorus loads and its export was significantly reduced during GP+FP under CD, emphasizing the need to monitor both particulate and dissolved forms. Overall, CD implemented in GP effectively offset the hydrological and nutrient exports of FP and PHP -

reducing total flow (37%), nitrate (21%) and SRP (57%) loads from planting to freeze-up. This study clearly demonstrates that CD, as a tailored conservation practise, offers strong agro-environmental benefits and supports its broader adoption among grain farmers in similar climatic regions.

References

Abbasi, N. A., Madramootoo, C. A., Zhang, T., & Tan, C. S. (2020). Nitrous oxide emissions as affected by fertilizer and water table management under a corn-soybean rotation. *Geoderma*, *375*. https://doi.org/10.1016/j.geoderma.2020.114473

Adeuya, R., Utt, N., Frankenberger, J., Bowling, L., Kladivko, E., Brouder, S., & Carter, B. (2012). Impacts of drainage water management on subsurface drain flow, nitrate concentration, and nitrate loads in Indiana. *Journal of Soil and Water Conservation*, *67*(6), 474 LP – 484. https://doi.org/10.2489/jswc.67.6.474

Agricrop. (2023). *Monthly Rainfall Data*. https://www.agricorp.com/en-ca/Programs/ProductionInsurance/ForageRainfall/Pages/RainfallData.aspx

APHA. (2017). *Standard Methods for the Examination of Water and Wastewater* (23rd ed.). American Public Health Association.

Ball Coelho, B., Murray, R., Lapen, D., Topp, E., & Bruin, A. (2012). Phosphorus and sediment loading to surface waters from liquid swine manure application under different drainage and tillage practices. *Agricultural Water Management*, *104*, 51–61. https://doi.org/10.1016/j.agwat.2011.10.020

Banerjee, S., Baah-Acheamfour, M., Carlyle, C. N., Bissett, A., Richardson, A. E., Siddique, T., Bork, E. W., & Chang, S. X. (2016). Determinants of bacterial communities in Canadian agroforestry systems. *Environmental Microbiology*, *18*(6), 1805–1816. https://doi.org/10.1111/1462-2920.12986

Chun, J. A., & Cooke, R. A. (2008). Calibrating Agridrain Water Level Control Structures using generalised Weir and Orifice equations. *Applied Engineering in Agriculture*, *24*(5), 595–602.

Cordeiro, M. R. C., Ranjan, R. S., Ferguson, I. J., & Cicek, N. (2014). Nitrate, phosphorus, and salt export through subsurface drainage from corn fields in the canadian prairies. *Transactions of the ASABE*, *57*(1), 43–50. https://doi.org/10.13031/trans.56.10370

Crézé, C. M., & Madramootoo, C. A. (2019). Water table management and fertilizer application impacts on CO2, N2O and CH4 fluxes in a corn agro-ecosystem. *Scientific Reports 2019 9:1*, *9*(1), 1–13. https://doi.org/10.1038/s41598-019-39046-z

David, M., Drinkwater, L., & Mcisaac, G. (2010). Source of Nitrate Yields in the Mississippi River Basin. *Journal of Environmental Quality*, *39*, 1657–1667. https://doi.org/10.2134/jeq2010.0115

Dobbie, K. E., & Smith, K. A. (2006). The effect of water table depth on emissions of N2O from a grassland soil. *Soil Use and Management*, *22*(1), 22–28. https://doi.org/10.1111/J.1475-2743.2006.00002.X

Dring, C., Devlin, J. F., Boag, G., Sunohara, M. D., Fitzgibbon, J., Topp, E., & Lapen, D. R. (2016). Incentives and disincentives identified by producers and drainage contractors/experts on the adoption of controlled tile drainage in eastern Ontario, Canada. *Water Quality Research Journal of Canada*, *51*(1), 1–16. https://doi.org/10.2166/wqrjc.2015.047

Drury, C. F., Tan, C. S., Gaynor, J. D., Reynolds, W. D., Welacky, T. W., & Oloya, T. O. (2001). Tile Nitrate Loss in Continuous Corn and in a Soybean-Corn Rotation. *The Scientific World*, *1*, 163–169. https://doi.org/10.1100/tsw.2001.268

Drury, C. F., Tan, C. S., Reynolds, W. D., Welacky, T. W., Oloya, T. O., & Gaynor, J. D. (2009). Managing Tile Drainage, Subirrigation, and Nitrogen Fertilization to Enhance Crop Yields and Reduce Nitrate Loss. *Journal of Environmental Quality*, *38*(3), 1193–1204. https://doi.org/10.2134/jeq2008.0036

Drury, C. F., Tan, C. S., Welacky, T. W., Reynolds, W. D., Zhang, T. Q., Oloya, T. O., McLaughlin, N. B., & Gaynor, J. D. (2014). Reducing Nitrate Loss in Tile Drainage Water with Cover Crops and Water-Table Management Systems. *Journal of Environmental Quality*, *43*(2), 587–598. https://doi.org/10.2134/jeq2012.0495

Dueholm, M. K. D., Nierychlo, M., Andersen, K. S., Rudkjøbing, V., Knutsson, S., MiDAS Global Consortium, Albertsen, M., & Nielsen, P. H. (2022). MiDAS 4: A global catalogue of full-length 16S rRNA gene sequences and taxonomy for studies of bacterial communities in wastewater treatment plants. *Nature Communications 2022 13:1*, *13*(1), 1–15. https://doi.org/10.1038/s41467-022-29438-7

ECCC. (2018). *Canada-Ontario Lake Erie action plan - Partnering on Achieving Phosphorus Loading Reductions to Lake Erie from Canadian Sources* (Number February). https://www.canada.ca/en/environment-climate-change/services/great-lakes-protection/action-plan-reduce-phosphorus-lake-erie.html#toc0

ECCC. (2020). *Canadian Climate Normals 1981-2010 for Ottawa MacDonald-Cartier International Airport Station*. https://climate.weather.gc.ca/climate_normals/results_1981_2010_e.html?stnID=4337&autofwd=1

ECCC. (2023). *Daily Data Report - Climate - Environment and Climate Change Canada*. https://climate.weather.gc.ca/climate_data/daily_data_e.html?StationID=49568

Ekwunife, K. C., & Madramootoo, C. A. (2023). Influence of seasonal climate and water table management on corn yield and nitrous oxide emissions. *Agricultural Water Management*, *279*, 108207. https://doi.org/10.1016/J.AGWAT.2023.108207

Elmi, A., Burton, D., Gordon, R., & Madramootoo, C. (2005). Impacts of water table management on N2O and N2 from a sandy loam soil in Southwestern Quebec, Canada. *Nutrient Cycling in Agroecosystems*, *72*(3), 229–240. https://doi.org/10.1007/s10705-005-2920-9

Fausey, N. R. (2005). Drainage management for humid regions. *International Agricultural Engineering Journal*, *14*(4), 209–214. https://blancharddemofarms.org/wp-content/uploads/2021/06/DrainageWater-6.pdf

Firth, A. G., Brooks, J. P., Locke, M. A., Morin, D. J., Brown, A., & Baker, B. H. (2023). Soil bacterial community dynamics in plots managed with cover crops and no-till farming in the Lower Mississippi Alluvial Valley, USA. *Journal of Applied Microbiology*, *134*(2). https://doi.org/10.1093/jambio/lxac051

Franck, W. L., Chang, W. S., Qiu, J., Sugawara, M., Sadowsky, M. J., Smith, S. A., & Stacey, G. (2008). Whole-genome transcriptional profiling of Bradyrhizobium japonicum during chemoautotrophic growth. *Journal of Bacteriology*, *190*(20), 6697–6705. https://doi.org/10.1128/JB.00543-08

Frankenberger, J., Kladivko, E., Sands, G., Jaynes, D., Fausey, N., Helmers, M., Cooke, R., Strock, J., Nelson, K., & Brown, L. (2006). *Questions and answers about drainage water management for the Midwest*. https://www.extension.purdue.edu/extmedia/wq/wq-44.pdf

Frey, S. K., Topp, E., Ball, B. R., Edwards, M., Gottschall, N., Sunohara, M., Zoski, E., & Lapen, D. R. (2013). Tile Drainage Management Influences on Surface-Water and Groundwater Quality following Liquid Manure Application. *Journal of Environmental Quality*, *42*(3), 881–892. https://doi.org/10.2134/JEQ2012.0261

Hagedorn, J. G., Davidson, E. A., Fisher, T. R., Fox, R. J., Zhu, Q., Gustafson, A. B., Koontz, E., Castro, M. S., & Lewis, J. (2022). Effects of Drainage Water Management in a Corn–Soy Rotation on Soil N2O and CH4 Fluxes. *Nitrogen (Switzerland)*, *3*(1), 128–148. https://doi.org/10.3390/NITROGEN3010010/S1

Helmers, M., Christianson, R., Brenneman, G., Lockett, D., & Pederson, C. (2012). Water table, drainage, and yield response to drainage water management in southeast Iowa. *Journal of Soil and Water Conservation*, *67*(6), 495 LP – 501. https://doi.org/10.2489/jswc.67.6.495

Helmers, M. J., Abendroth, L., Reinhart, B., Chighladze, G., Pease, L., Bowling, L., Youssef, M., Ghane, E., Ahiablame, L., Brown, L., Fausey, N., Frankenberger, J., Jaynes, D., King, K., Kladivko, E., Nelson, K., & Strock, J. (2022). Impact of controlled drainage on subsurface drain flow and nitrate load: A synthesis of studies across the U.S. Midwest and Southeast. *Agricultural Water Management*, *259*, 107265. https://doi.org/10.1016/j.agwat.2021.107265

ICID. (2018). *World Drained Area -2018*. https://www.icid.org/world-drained-area.pdf

Jaynes, D. B. (2012). Changes in yield and nitrate losses from using drainage water management in central Iowa, United States. *Journal of Soil and Water Conservation*, *67*(6), 485 LP – 494. https://doi.org/10.2489/jswc.67.6.485

Jia, L., Jiang, B., Huang, F., & Hu, X. (2019). Nitrogen removal mechanism and microbial community changes of bioaugmentation subsurface wastewater infiltration system. *Bioresource Technology*, *294*, 122140. https://doi.org/10.1016/J.BIORTECH.2019.122140

Kato, S., & Ohkuma, M. (2021). A Single Bacterium Capable of Oxidation and Reduction of Iron at Circumneutral pH. *Microbiology Spectrum*, *9*(1). https://doi.org/10.1128/SPECTRUM.00161-21

King, K., Hanrahan, B., Stinner, J., & Shedekar, V. (2022). Field scale discharge and water quality response, to drainage water management. *Agricultural Water Management*, *264*(January), 107421. https://doi.org/10.1016/j.agwat.2021.107421

King, K., Williams, M., & Fausey, N. R. (2016). Effect of crop type and season on nutrient leaching to tile drainage under a corn-soybean rotation. *Journal of Soil and Water Conservation*, *71*, 56–68. https://doi.org/10.2489/jswc.71.1.56

King, K., Williams, W., Macrae, M. L., Fausey, N. R., Frankenberger, J., Smith, D. R., Kleinman, P. J. A., & Brown, L. C. (2015). Phosphorus Transport in Agricultural Subsurface Drainage: A Review. *Journal of Environmental Quality*, *44*(2), 467–485. https://doi.org/10.2134/jeq2014.04.0163

Kokulan, V. (2019). *Environmental and Economic Consequences of Tile Drainage Systems in Canada* (Number June). https://capi-icpa.ca/wp-content/uploads/2019/06/2019-06-14-CAPI-Vivekananthan-Kokulan-Paper-WEB.pdf

Kozich, J. J., Westcott, S. L., Baxter, N. T., Highlander, S. K., & Schloss, P. D. (2013). Development of a dual-index sequencing strategy and curation pipeline for analyzing amplicon sequence data on the miseq illumina sequencing platform. *Applied and Environmental Microbiology*, *79*(17), 5112–5120. https://doi.org/10.1128/AEM.01043-13

Labarge, G. (2022). *Developing Phosphorus and Potassium Recommendations for Field Crops*. Ohio State University Extension. https://ohioline.osu.edu/factsheet/agf-0515#

Licht, M. A., Archontoulis, S., & Hatfield, J. L. (2017). Corn water use and evapotranspiration. *Integrated Crop Management News. Iowa State University Extension and Outreach*, 1–6. https://crops.extension.iastate.edu/cropnews/2017/06/corn-water-use-and-evapotranspiration

Liu, X., Wang, H., Wang, W., Cheng, X., Wang, Y., Li, Q., Li, L., Ma, L., Lu, X., & Tuovinen, O. H. (2023). Nitrate determines the bacterial habitat specialization and impacts microbial functions in a subsurface karst cave. *Frontiers in Microbiology*, *14*, 1115449. https://doi.org/10.3389/FMICB.2023.1115449/BIBTEX

Liu, Y., Youssef, M. A., Chescheir, G. M., Appelboom, T. W., Poole, C. A., Arellano, C., & Skaggs, R. W. (2019). Effect of controlled drainage on nitrogen fate and transport for a subsurface drained grass field receiving liquid swine lagoon effluent. *Agricultural Water Management*, *217*, 440–451. https://doi.org/10.1016/J.AGWAT.2019.02.018

Madramootoo, C. A., Essien, M., & Ekwuknife, K. (2024). LONG-TERM BENEFITS OF CONTROLLED DRAINAGE. *Journal of the ASABE*, *67*(3), 565–571. https://doi.org/10.13031/ja.15542

Madramootoo, C. A., Helwig, T. G., & Dodds, G. T. (2001). Managing Water Tables to improve Drainage Water Quality in Quebec, Canada. *American Society of Agricultural Engineers*, *44*(6), 1511–1519.

Mathew, K. R. (2020). *A field-scale study of controlled tile drainage and a pond-wetland to attenuate nutrients from agricultural overland runoff and subsurface drainage on a farmer-operated seed farm in Saint-Isidore, ON* [University of Ottawa]. http://dx.doi.org/10.20381/ruor-26264

McDonald, I., & Janovicek, K. (2015, June 11). *2015 Ontario Soil N Survey*. Field Crop News, OMAFRA. https://fieldcropnews.com/2015/06/2015-ontario-soil-n-survey/

Mejia, M. N., Madramootoo, C. A., & Broughton, R. S. (2000). Influence of water table management on corn and soybean yields. *Agricultural Water Management*, *46*, 73–89.

Monciardini, P., Cavaletti, L., Schumann, P., Rohde, M., & Donadio, S. (2003). Conexibacter woesei gen. nov., sp. nov., a novel representative of a deep evolutionary line of descent within the class Actinobacteria. *International Journal of Systematic and Evolutionary Microbiology*, *53*(Pt 2), 569–576. https://doi.org/10.1099/IJS.0.02400-0

Nangia, V., Sunohara, M. D., Topp, E., Gregorich, E. G., Drury, C. F., Gottschall, N., & Lapen, D. R. (2013). Measuring and modeling the effects of drainage water management on soil greenhouse gas fluxes from corn and soybean fields. *Journal of Environmental Management*, *129*, 652–664. https://doi.org/10.1016/j.jenvman.2013.05.040

Nash, P. R., Nelson, K. A., Motavalli, P. P., Nathan, M., & Dudenhoeffer, C. (2015). Reducing Phosphorus Loss in Tile Water with Managed Drainage in a Claypan Soil. *Journal of Environmental Quality*, *44*(2), 585–593. https://doi.org/10.2134/jeq2014.04.0146

Ng, H. Y. F., Tan, C. S., Drury, C. F., & Gaynor, J. D. (2002). Controlled drainage and subirrigation influences tile nitrate loss and corn yields in a sandy loam soil in Southwestern Ontario. *Agriculture, Ecosystems & Environment*, *90*(1), 81–88. https://doi.org/https://doi.org/10.1016/S0167-8809(01)00172-4

OMAFRA. (1991). *Risk Of Alfalfa Winterkill*. http://www.omafra.gov.on.ca/english/crops/facts/91-072.htm#RISKO

OMAFRA Field Crop Team. (2017). Corn. In C. Brown (Ed.), *Agronomy Guide for Field Crops* (pp. 1–39). Ontario Ministry of Agriculture, Food and Rural Affairs. http://www.omafra.gov.on.ca/english/crops/pub811/pub811ch1.pdf

Onset Computer Cooperation. (2008). Barometric Compensation Assistant. In *White Paper Series*.

OSCIA. (2017). *Controlled Tile Drainage in Ontario* (Number March). https://www.ontariosoilcrop.org/wp-content/uploads/2023/02/CTD-Cost-Benefit-Analysis.pdf

Oshiki, M., Toyama, Y., Suenaga, T., Terada, A., Kasahara, Y., Yamaguchi, T., & Araki, N. (2022). N2O Reduction by Gemmatimonas aurantiaca and Potential Involvement of Gemmatimonadetes

Bacteria in N2O Reduction in Agricultural Soils. *Microbes and Environments*, *37*(2). https://doi.org/10.1264/JSME2.ME21090

Poole, C. A., Skaggs, R. W., Youssef, M. A., Chescheir, G. M., Crozier, C. R., & Schilfgaarde, V. (2018). Effect of Drainage Water Management on Nitrate Nitrogen Loss to Tile Drains in North Carolina. *Transactions of the ASABE*, *61*(3), 233–244. https://doi.org/10.13031/trans.12296

Que, Z., Seidou, O., Droste, R. L., Wilkes, G., Sunohara, M., Topp, E., & Lapen, D. R. (2015). Using AnnAGNPS to Predict the Effects of Tile Drainage Control on Nutrient and Sediment Loads for a River Basin. *Journal of Environmental Quality*, *44*(2), 629–641. https://doi.org/10.2134/JEQ2014.06.0246

Rabalais, N. N., Turner, R. E., & Wiseman, W. J. (2002). Gulf of Mexico Hypoxia, A.K.A. "The Dead Zone." *Annual Review of Ecology and Systematics*, *33*(1), 235–263. https://doi.org/10.1146/annurev.ecolsys.33.010802.150513

Riley, K. D., Helmers, M. J., Lawlor, P. A., & Singh, R. (2009). Water Balance Investigation of Drainage Water Management in Non-Weighing Lysimeters. *Applied Engineering in Agriculture*, *25*(4), 507–514. https://doi.org/10.13031/2013.27470

Saadat, S., Bowling, L., Frankenberger, J., & Kladivko, E. (2018a). Estimating drain flow from measured water table depth in layered soils under free and controlled drainage. *Journal of Hydrology*, *556*, 339–348. https://doi.org/10.1016/j.jhydrol.2017.11.001

Saadat, S., Bowling, L., Frankenberger, J., & Kladivko, E. (2018b). Nitrate and phosphorus transport through subsurface drains under free and controlled drainage. *Water Research*, *142*, 196–207. https://doi.org/10.1016/j.watres.2018.05.040

Sanchez Valero, C., Madramootoo, C. A., & Stämpfli, N. (2007). Water table management impacts on phosphorus loads in tile drainage. *Agricultural Water Management*, *89*(1–2), 71–80. https://doi.org/10.1016/j.agwat.2006.12.007

Satchithanantham, S., Sri Ranjan, R., & Bullock, P. (2014). Protecting water quality using controlled drainage as an agricultural bmp for potato production. *Transactions of the ASABE*, *57*(3), 815–826. https://doi.org/10.13031/trans.57.10385

Saxena, A. K., Kumar, M., Chakdar, H., Anuroopa, N., & Bagyaraj, D. J. (2020). Bacillus species in soil as a natural resource for plant health and nutrition. *Journal of Applied Microbiology*, *128*(6), 1583–1594. https://doi.org/10.1111/JAM.14506

Schlüter, S., Lucas, M., Grosz, B., Ippisch, O., Zawallich, J., He, H., Dechow, R., Kraus, D., Blagodatsky, S., Senbayram, M., Kravchenko, A., Vogel, H. J., & Well, R. (2024). The anaerobic soil volume as a controlling factor of denitrification: a review. *Biology and Fertility of Soils 2024 61:3*, *61*(3), 343–365. https://doi.org/10.1007/S00374-024-01819-8

Schott, L., Lagzdins, A., Daigh, A. L. M., Pederson, C., Brenneman, G., & Helmers, M. J. (2017). Drainage water management effect on corn planting date in southeast Iowa. *Journal of Soil and Water Conservation*, *72*(6), 564–574. https://doi.org/10.2489/jswc.72.6.564

Shapleigh, J. P. (2006). The Denitrifying Prokaryotes. In *The Prokaryotes* (pp. 769–792). Springer New York. https://doi.org/10.1007/0-387-30742-7_23

Shedekar, V. S., King, K. W., Fausey, N. R., Islam, K. R., Alfred, B., Soboyejo, O., Kalcic, M. M., & Brown, L. C. (2021). Exploring the effectiveness of drainage water management on water budgets and nitrate loss using three evaluation approaches. *Agricultural Water Management*, *243*(August 2020), 106501. https://doi.org/10.1016/j.agwat.2020.106501

Sheibani, S., Yanni, S. F., Wilhelm, R., Whalen, J. K., Whyte, L. G., Greer, C. W., & Madramootoo, C. A. (2013). Soil bacteria and archaea found in long-term corn (zea mays L.) agroecosystems in

Quebec, Canada. *Canadian Journal of Soil Science*, *93*(1), 45–57. https://doi.org/10.4141/CJSS2012-040

Skaggs, R. W., Fausey, N. R., & Evans, R. O. (2012). Drainage water management. *Journal of Soil and Water Conservation*, *67*(6), 167–172. https://doi.org/10.2489/jswc.67.6.167A

Smith, E. L., Vosman, A., Kellman, L., & Rodd, V. (2019). Impact of drainage type on simultaneous nitrogen losses in Atlantic Canada. *Canadian Journal of Soil Science*, *99*(1), 70–79. https://doi.org/10.1139/cjss-2018-0115

Soil Classification Working Group. (1998). *The Canadian System of Soil Classification* (Third). Agriculture and Agri-Food Canada. Publ.1646 (Revised).

Stampfli, N. (2003). *The effect of water table management on the migration of phosphorus and on grain corn yields* [McGill Univeristy]. https://escholarship.mcgill.ca/concern/theses/9p290c71c

Sunohara, M. D., Craiovan, E., Topp, E., Gottschall, N., Drury, C. F., & Lapen, D. R. (2014). Comprehensive Nitrogen Budgets for Controlled Tile Drainage Fields in Eastern Ontario, Canada. *Journal of Environmental Quality*, *43*(2), 617–630. https://doi.org/10.2134/jeq2013.04.0117

Sunohara, M. D., Gottschall, N., Craiovan, E., Wilkes, G., Topp, E., Frey, S. K., & Lapen, D. R. (2016). Controlling tile drainage during the growing season in Eastern Canada to reduce nitrogen, phosphorus, and bacteria loading to surface water. *Agricultural Water Management*, *178*(3), 159–170. https://doi.org/10.1016/j.agwat.2016.08.030

Sunohara, M. D., Gottschall, N., Wilkes, G., Craiovan, E., Topp, E., Que, Z., Seidou, O., Frey, S. K., & Lapen, D. R. (2015). Long-Term Observations of Nitrogen and Phosphorus Export in Paired-Agricultural Watersheds under Controlled and Conventional Tile Drainage. *Journal of Environmental Quality*, *44*(5), 1589–1604. https://doi.org/10.2134/jeq2015.01.0008

Tan, C. S., & Zhang, T. Q. (2011). Surface Runoff and Sub-surface Drainage Phosphorus Losses under Regular Free Drainage and Controlled Drainage with Sub-irrigation Systems in Southern Ontario. *Canadian Journal of Soil Science*, *91*(3), 349–359. https://doi.org/10.4141/CJSS09086

US EPA. (2007). *National Water Quality Inventory: Report to Congress, 2002 Reporting Cycle*. http://www.epa.gov/305b

US EPA. (2023). *Nonpoint Source: Agriculture*. https://www.epa.gov/nps/nonpoint-source-agriculture

USBR. (2001). *Water measurement manual: A Guide to Effective Water Measurement Practices for Better Water Management, 3rd ed.* https://www.usbr.gov/tsc/techreferences/mands/wmm/index.htm

Van Zandvoort, A., Lapen, D. R., Clark, I. D., Flemming, C., Craiovan, E., Sunohara, M. D., Boutz, R., & Gottschall, N. (2017). Soil CO2, CH4, and N2O fluxes over and between tile drains on corn, soybean, and forage fields under tile drainage management. *Nutrient Cycling in Agroecosystems*, *109*(2), 115–132. https://doi.org/10.1007/s10705-017-9868-4

Verbaendert, I., Boon, N., De Vos, P., & Heylen, K. (2011). Denitrification is a common feature among members of the genus Bacillus. *Systematic and Applied Microbiology*, *34*(5), 385–391. https://doi.org/10.1016/J.SYAPM.2011.02.003

Verma, S., & Cooke, R. (2012). Performance of drainage water management systems in Illinois, United States. *Journal of Soil and Water Conservation*, *67*, 453–464. https://doi.org/10.2489/jswc.67.6.453

Watson, S. B., Miller, C., Arhonditsis, G., Boyer, G. L., Carmichael, W., Charlton, M. N., Confesor, R., Depew, D. C., Höök, T. O., Ludsin, S. A., Matisoff, G., McElmurry, S. P., Murray, M. W., Peter Richards, R., Rao, Y. R., Steffen, M. M., & Wilhelm, S. W. (2016). The re-eutrophication of Lake Erie: Harmful algal blooms and hypoxia. *Harmful Algae*, *56*, 44–66. https://doi.org/10.1016/J.HAL.2016.04.010

Wesström, I., & Messing, I. (2007). Effects of controlled drainage on N and P losses and N dynamics in a loamy sand with spring crops. *Agricultural Water Management*, *87*(3), 229–240. https://doi.org/10.1016/j.agwat.2006.07.005

Williams, M. R., King, K. W., & Fausey, N. R. (2015a). Contribution of tile drains to basin discharge and nitrogen export in a headwater agricultural watershed. *Agricultural Water Management*, *158*(3), 42–50. https://doi.org/10.1016/j.agwat.2015.04.009

Williams, M. R., King, K. W., & Fausey, N. R. (2015b). Drainage water management effects on tile discharge and water quality. *Agricultural Water Management*, *148*, 43–51. https://doi.org/10.1016/j.agwat.2014.09.017

Zhang, H., Shi, Y., Dong, Y., Lapen, D. R., Liu, J., & Chen, W. (2022). Subsoiling and conversion to conservation tillage enriched nitrogen cycling bacterial communities in sandy soils under long-term maize monoculture. *Soil and Tillage Research*, *215*, 105197. https://doi.org/10.1016/J.STILL.2021.105197

Zhang, T., Tan, C. S., Zheng, Z. M., Welacky, T. W., & Reynolds, W. D. (2015). Impacts of Soil Conditioners and Water Table Management on Phosphorus Loss in Tile Drainage from a Clay Loam Soil. *Journal of Environmental Quality*, *44*(2), 572–584. https://doi.org/10.2134/jeq2014.04.0154

Chapter 4 - Constructed pond-wetland systems for treating cropping tile drainage in Eastern Canada: insights into solids and phosphorus retention

Abstract

Pond-wetland systems can be implemented as best management practices (BMPs) for phosphorus and total suspended solids (TSS) control, yet their performance under low phosphorus cropping system tile drainage conditions remains poorly characterized. This study evaluated TSS, particulate phosphorus (PP), and soluble reactive phosphorus (SRP) dynamics in an integrated pond-wetland system over five years (2016 - 2021) in a temperate, cold region. TSS removal was dominated by sedimentation, with deeper ponds (0.7 - 1.3 m) consistently achieving 46-80% reductions, while shallow ponds (0.08 - 0.3 m) acted as internal sources due to resuspension and biological productivity. PP retention followed similar patterns, driven by sedimentation, but moderated by depth-limited resuspension. Whereas SRP exhibited highly variable seasonal and annual behaviour, governed primarily by biological uptake, release, and sediment sorption rather than physical controls (depth, HRT). Cumulative mass balance indicated that sediment was the largest P sink (48% of retained P), followed by plant-available soil (27%), strongly-bound soil (15%), and plant uptake (7.2%), with the water column serving as a transient conduit. Overall, the system achieved modest net retention of P (TP: 18%, PP: 22%, SRP: 14% for concentrations, 17%, 24%, 15% for loads), reflecting significant internal cycling and seasonal reversals. Given the low influent P loads and limited SRP retention, pond-wetland systems alone are unlikely to provide meaningful P reduction under these conditions. Design modifications such as increased area or vegetation cover may improve PP retention but may not be justified from a management perceptive, indicating that alternative or complementary BMPs are required for effective P management.

4.1. Introduction

Over the past five decades, the Laurentian Great Lakes have experienced significant anthropogenic eutrophication, manifested in recurrent harmful algal blooms (HABs) and more than 20 hypoxic zones, including Lake Erie's extensive 1.2 million ha hypoxic region (Michalak et al., 2013; Tellier

et al., 2022). Agricultural intensification - driven by increased nutrient application, climate-driven shifts in precipitation and temperature, and expansion of tile-drainage infrastructure - has accelerated phosphorus (P) loading across the basin (FAOSTAT, 2025; Fortier, 2022; Mohamed et al., 2019; Statista, 2024; Watson et al., 2016). Approximately 75% of total phosphorus (TP) loading to Lake Erie originates from non-point sources (NPS), with agriculture as the dominant pathway (OMECP, 2024). The resulting ecological degradation is projected to cost Canadians up to CAD $5.3 billion (roughly US $4 billion) over the next three decades (GLSAB & GLWQB, 2023). Similar trends exist in Eastern Ontario's South Nation sub-watershed, where agriculture covers more than 40% of the landscape and median TP concentrations routinely exceed the provincial water quality objective of 0.03 mg/L, resulting 'poor' water quality classifications (SNCA, 2023).

In response, federal, provincial, and local initiatives have promoted beneficial management practises (BMPs) tailored to soil, topography, and farming practices to reduce agricultural nutrient export (ECCC & OMECP, 2018; OMAFA, 2002; OMAFA & OSCIA, 2019; OSCIA, 2023; SNCA, 2025a). Mitigation efforts have historically targeted TP, the primary limiting nutrient in freshwater (Schindler, 1977). However, bioavailable soluble reactive phosphorus (SRP) is increasingly recognized as contributing to HAB formation, prompting amendments to the Great Lakes Water Quality Agreement in 2012 (formally adopted in 2016) (ECCC & IJC, 2012). In the US Lake Erie watershed, increased tile drainage adoption has been linked to elevated SRP export and enhanced hydrological connectivity between fields and surface waters (Jarvie et al., 2017; Tedeschi et al., 2024). Although tile drains typically transport lower concentrations of total suspended solids (TSS) than overland flow (King et al., 2015), recent studies highlight TSS and solid-bound phosphorus migration even in subsurface drainage (Coelho et al., 2020; Jamieson et al., 2003; Que et al., 2015), underscoring the need for integrated BMPs capable of mitigating multiple water-quality parameters simultaneously.

Constructed pond-wetland systems combine the sedimentation capacity of treatment ponds with biogeochemical processing of free-surface constructed wetlands (FWS CWs) and represent a promising multifunctional BMP. Treatment ponds, widely used in stormwater management, consistently attenuate peak flows and remove >50% of TSS through sedimentation (Harper & Baker, 2007; Koch et al., 2014; Marques & Mandrak, 2024; Nietch et al., 2001; SC DHEC, 2005).

Agricultural ponds receiving overland runoff show comparable removal of solids and particulate phosphorous (PP) (48 to 89%) (Clary et al., 2020; Fiener et al., 2005; Robotham et al., 2021; Rushton & Bahk, 2001). Yet little is known about their effectiveness for SRP or for treating cropping-system tile drainage, as long-term monitoring is limited.

FWS CWs treating agricultural influent can remove 28 to 91% of TSS and act as P sinks through particulate settling, adsorption, and biomass uptake (Braskerud, 2002; Johannesson et al., 2011; Kynkäänniemi et al., 2013; Lavrnić, Nan, et al., 2020; Maynard et al., 2009; Tolomio et al., 2019). However, TSS and P can also be exported during high flow and event-driven conditions (Braskerud et al., 2005; Díaz et al., 2012; Kovacic et al., 2000; Tanner & Sukias, 2011). CW performance depends strongly on influent P load and form, hydraulic residence time (HRT), wetland design (geometry, wetland-to-catchment ratio, A_w:A_c), and exhibits significant seasonal and annual variability (Dunne et al., 2012; Land & Lu, 2016; Mendes et al., 2018; Reddy et al., 2023).

Most studies originate from warmer climate regions, such as Florida, California or parts of Midwestern US (Beutel et al., 2009; Díaz et al., 2012; Kovacic et al., 2006; Rabalais et al., 2002; SJRRP, 2006; U.S. DOI, 2015) in North America, creating uncertainty about effectiveness in more northern cold climates, where temperature-dependent P retention processes maybe be diminished (Arheimer & Pers, 2017; Wang et al., 2018). Scandinavian studies in temperate climates show highly variable or negligible TSS and P retention, with the highest removals occurring during summers (Blankenberg et al., 2015; Koskiaho et al., 2003; Krzeminska et al., 2023). Critically, few studies have evaluated FWS wetlands or hybrid pond-wetland systems receiving cropping tile drainage inflows in temperate cold climates with winter freeze-up. To fully assess sustainable P retention by these systems, it is essential to consider long-term mass balances, sediment accumulation over time, and the relative importance of key retention mechanisms (biomass uptake, sediment accretion, and soil adsorption), all of which remain poorly understood (Johannesson et al., 2011; VanZomeren et al., 2020).

Together, these gaps limit the ability to design and predict the performance of pond-wetland BMPs for northern cropping landscapes, where tile drainage is prevalent and climate conditions differ markedly from regions where most data originate. Against this backdrop, the

present 5-year (2016-2021) full-scale study in Eastern Ontario aimed to (i) evaluate the performance of a pond-wetland system in attenuating TSS, PP, and SRP from cropping tile drainage from spring-melt to system freeze-up; (ii) characterise seasonal variability; and (iii) quantify long-term mass balances and identify dominant retention mechanisms and storage in a cold-climate application. This work provides farm-scale evidence to support adoption and design of pond-wetland systems in Ontario and similar climatic regions facing nutrient-driven water quality challenges associated with cropping system tile drainage.

4.2. Methods and materials

4.2.1. Site description

The field study was conducted at Ferme Agriber, a cash crop operation located in St. Isidore, Ontario, Canada, which typically produces corn, soybean, and wheat, rotated annually. The study site is situated within the South Nation River sub-watershed (Figure 4-1 A), and the climate in this region is classified as temperate - humid continental (Kottek et al., 2006). The predominant soil types at the site are clay and clay-loam, with an average clay content of 30% and 25% sand. The topography of the farmland is relatively flat, with slopes of less than 1%.

A 240 m long (0.4 ha) free-water surface, pond-wetland system (45°23’55 N, 74°54’02 W) was designed and constructed by Ducks Unlimited Canada in Spring 2016, along the length of the natural ravine (approx. 700 m long x 3.2 m deep), occupying 0.93% of the total agricultural drainage area. The depth of the system varies from 0.08 m to 3.1 m, integrating the characteristics of treatment ponds and a free-water surface wetland system. This system intercepts tile drainage from 43 ha of farmland (Figure 4-1 B), which is naturally transported by a central drainage ditch without the use of pumps. The ravine slopes were planted with native trees and shrubs for slope stability and erosion control, while wildflower seed mixtures were planted to attract pollinators. A 6 m wide riprap spillway at the outlet of the system conveys system discharge into a downstream ditch that ultimately drains into the Scotch Creek R. within the St-Lawrence drainage basin.

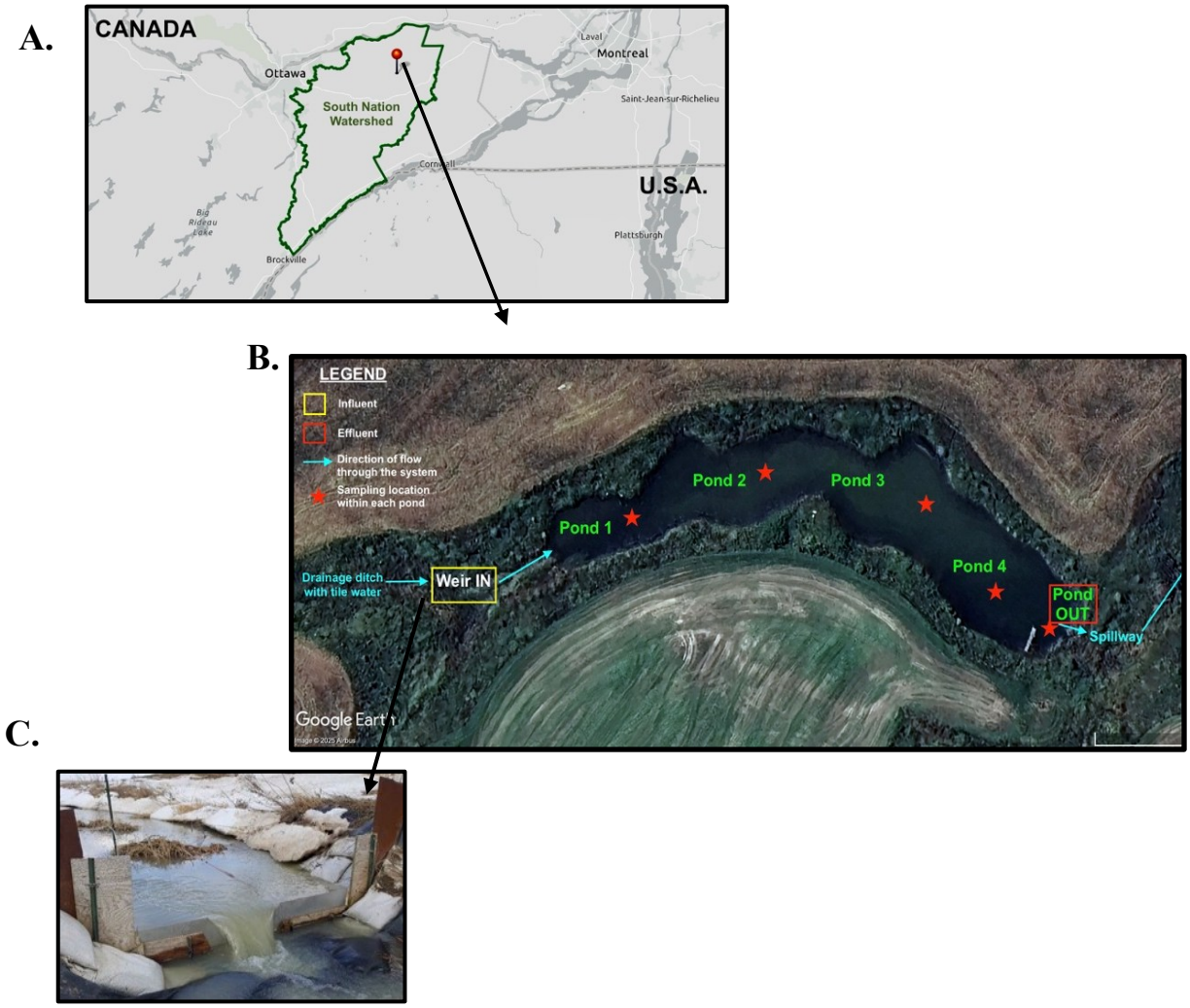

Figure 4-1. Location of field study – A. Geographic location of the study site within the South Nation watershed (SNCA, 2025b); B. Aerial image of the study site with locations of sampling spots and the direction of flow within the pond-wetland system. Google Earth Pro V 7.3.6.9796 imagery; C. Monitoring station at Weir-IN, the inlet to the system.

4.2.2. Monitoring of the system

The pond-wetland system was systematically monitored from its natural filling in October 2016 until freeze-up, and from spring thaw to freeze-up in 2017 to 2019 and in 2021[3] (April to November). The system was divided into five ponds, designated as Pond 1, 2, 3, 4 and OUT, following the direction of flow (Figure 4-1 B), to ensure consistent sampling and nutrient characterization, Their average depths of 0.08 m, 0.71 m, 0.62 m, 1.30 m, and 0.33 m, respectively, forming a sequence of very shallow – deep – deep – deepest – moderately shallow basins. Emergent macrophytes (*Typha latifolia* and *Juncus effusus*) established naturally in Pond 3 (12%

[3] The system was not monitored in 2020 due to COVID -19 lockdown restrictions.

coverage relative to pond area) and Pond OUT (42% of coverage relative to pond area), with a sparse population of *Juncus effusus* also observed at Pond 1. However, the total macrophyte coverage across the pond-wetland system remained <1% of the total surface area. Algal blooms were observed predominantly at Pond 1 in summers. An in-stream V-notch weir, referred to as Weir IN (Figure 4-1 C), was installed at the inlet to measure the inflows into the system.

The time series data for each field season was categorized according to the seasons of the Northern Hemisphere: Spring-melt (April), Late Spring (May 1 to June 20), Summer (June 21 to September 20) and Fall (September 21 to Freeze-up) (NRCC, 2024). This division into four distinct time periods facilitated the seasonal comparison of flow and nutrient responses within the pond-wetland system. From 2016 to 2018, daily precipitation and ambient air temperature data were collected using a HOBO weather station operated by the farm (Onset Computer Corp.). For the years of 2019 to 2021, weather data were obtained by combining information from the Moose Creek station, positioned within 20 km of the farm site (ECCC, 2023) and the St. Isidore Station, within 2 km of the farm (Agricrop, 2023).

4.2.3. Water quality sampling and analysis

ISCO 6712 full-size automatic portable samplers (Teledyne ISCO, Inc.) were used to collect composite water samples at two monitoring locations: upstream of Weir IN and at Pond OUT, via collection suction pipes attached to a permanent stake. Each sampler was powered by a battery, which was trickle charged via a solar panel. In 2019, the location of the collection pipe at Weir IN was relocated downstream positioned directly below the weir crest. This adjustment was made to mitigate the excessive collection of sediments and debris from the ditch. The daily composite samples from the monitoring locations comprised 3-4 aliquots per day, collected weekly from the farm. Grab samples were collected weekly at the weir and the five locations across the ponds, transported back to the laboratory in coolers with ice packs, and refrigerated until analysed. Details of 2016 and 2017 methodology can be found in Mathew, 2020. From 2018 to 2021, over 4400 samples were analyzed.

The unfiltered grab and composite samples were characterised for TSS using Dried TSS at 103°-105°C as per Standard Method 2540 D (APHA, 2017). TP was analyzed following a modified HACH Method 8190, wherein the unfiltered samples with reagents were transferred from the vial to a 50 mm cuvette (Mathew, 2020). This was conducted using the low range kit version

of Standard Methods 4500-P E. Ascorbic Acid Method, from 2016 to 2018, and subsequently by the Stannous Chloride method (Standard Methods 4500-P D) (APHA, 2017). The filtered samples were analysed for soluble reactive phosphorus as phosphate (PO_4^{3-}) using a modified HACH Method 8048 (Phosphorus, Reactive (Orthophosphate) - low range - a kit version of Standard Methods 4500-P E. Ascorbic Acid Method). In this methodology, the samples mixed with reagents were transferred from the vial to a 50 mm cuvette (Mathew, 2020) during 2016 to 2018, and the Stannous Chloride method (Standard Methods 4500-P D) (APHA, 2017) was employed in 2019 to 2021. In this study, TP and SRP concentrations are reported as elemental phosphorus (mg P/L) to ensure consistency with other field studies. Known standard solutions were measured every 20 samples with the standard error of $0.7 \pm 0.6\%$.

4.2.4. Determining water depths and flow rates

Water heights were computed using absolute pressure (kPa) and temperature of water (°C) recorded at 15 -minute interval by HOBO Water Level Data Logger-U20-001-04 (Onset Computer Corp.) set-up at the weir and Pond OUT. Subsequently, water flow rates at the weir were calculated. A similar data logger was installed at the top of the permanent stake at Weir IN to record barometric pressure[4] and temperature[5]. The data loggers were manually downloaded using HOBO Waterproof Shuttle during the weekly visits, transferred to a laptop computer, and processed using HOBOware Pro software (Version 3.7.21) to compute the sensor depth below the water surface (Onset Computer Cooperation, 2008). The equations used to calculate water height (h) are provided in Appendix C. The 'Zero' of the logger is approximately 20 mm from its bottom, and this was corrected for in the calculated water heights. A total of 23,500 data points were analysed for each monitoring location per year. During the weekly visits, manual measurements of water height were recorded using a measuring ruler at the weir crest and at Pond OUT, with error < 1 mm on the recorded height. These values were used to verify and calibrate the heights calculated from the depth loggers.

The instantaneous flow for each 15-minute interval was determined using the Kindsvater-Shen relationship for a V-notch, sharp crested weir at Weir IN (Chun & Cooke, 2008; Kulin & Compton, 1979; USBR, 2001) and was subsequently normalized by the drainage area. A pond-

[4]The barometric files from Weir IN from April 30th to June 16th, 2018, were corrupted and hence correlations were made with Weir OUT barometric files and used for this time period.
[5]In 2021, due to malfunctioning of logger, data from moose creek weather station were used to re-calibrate values obtained from the logger.

wetland water balance (Equation 4-1) was used to calculate the flow at the outlet (Pond OUT) -

$$Q_{in} + P.A - e.A = Q_{in} \text{ (Equation 4-1)}$$

where, Q_{in} is the influent flow at Weir IN in m^3/d, P is daily precipitation in m/d, A is the surface area of the pond-wetland system and e is the daily evaporation rate calculated using (m) the Hamon method for lake evaporation, which is given as-

$$e = 0.63 \times D^2 \times 10^{\frac{7.5T_a}{T_a+273}} \text{ (Equation 4-2)}$$

where e is the daily evaporation from a given lake (mm), T_a is the daily temperature (°C) and D is the ratio of maximum sunshine duration (hour) to 12 hours, and is determined using –

$$D = \frac{1}{90}\arccos\left\{-\tan(\varphi).\tan\left[23.45° \sin\left(\frac{J-80}{365} \times 260°\right)\right]\right\} \text{ (Equation 4-3)}$$

where φ is the latitude, J is the Julian day of date of interest. System volume changes recorded using depth logger at Pond OUT validated the selected ET model ($R^2 = 0.70$).

Seepage and infiltration losses from the pond-wetland system were assumed to be negligible. The bed of the system was compacted during construction, thereby limiting the potential for subsurface losses. In addition, the site is underlain by Bearbrook clay, which has low permeability and further reduces the likelihood of seepage. To assess this assumption, water level changes recorded by the HOBO data loggers during no-flow periods were compared with the difference between precipitation and ET. The resulting discrepancy was approximately 0.001 m in water height, corresponding to 2.9 m^3/d, which is insignificant relative to the overall system flow.

During winter (December-April), no flow was assumed to occur as the pond-wetland system was covered by a continuous thick ice layer. Tile drains remained completely frozen, with sustained snow cover across the study site. Any intermittent thaw or snowmelt would have been ponded on frozen soil surface and therefore assumed to have a negligible impact on the overall water balance.

4.2.5. Calculating hydrological variables

The water load (m^3) for each time interval was determined by multiplying the measured inflow rate (Q_i) or outflow rate (Q_o) (m^3/s) by the interval time (15 min). The daily water load (mm/day or $m^3/ha/d$) were computed by summing the 15-minute interval water load and dividing by the area of discharge (m^2 or ha).

$$\text{Daily Water Load}\left(\frac{\text{mm}}{\text{d}} \text{ or } \frac{\text{m}^3}{\text{ha}}\right) = \frac{\sum Q_i \times 15 \times 60}{\text{Area}} \quad \text{(Equation 4-4)}$$

Nutrient loads were calculated by multiplying the influent concentrations (C_i) or effluent concentrations (C_o) (mg TSS/L or mg P/L) by the daily discharged water load (m^3/d) and then dividing by area of discharge plot (ha) to obtain values in kg TSS or P/ha/d.

$$\text{Daily Mass Nutrient Load}\left(\frac{\text{kg nutrient}}{\text{ha d}}\right) = \frac{(\sum Q_i \times 15) \times C_i}{\text{Area}} \quad \text{(Equation 4-5)}$$

The percentage change was then calculated as follows -

$$\text{Change (\%)} = \frac{(C_i Q_i - C_o Q_o)}{C_i Q_i} \times 100 \quad \text{(Equation 4-6)}$$

The hydraulic retention time (HRT, day) across the system was determined using Equation 4-7 (Kadlec & Wallace, 2008)

$$\tau = \frac{V}{Q_{in}} = \frac{h\,A}{Q_{in}} \quad \text{(Equation 4-7)}$$

where V is volume of the system (m^3), h is the depth of the system (h) and A is the area (m^2). Porosity index (ε) = 0.95 for northern environment (Kadlec & Wallace, 2008) was applied to Pond 3 and Pond OUT only.

4.2.6. Sediment sampling and mapping

In 2021, a total of 30 sediment samples were collected from the five ponds (2 - 3 point transects per pond; spatial resolution shown in Figure 4-2 A), using a Sludge Judge™ (VWR International, LLC) with extended sections. Care was taken to minimize disturbance of the sediment bed during sampling from a rowboat; however, some variability may have been introduced. Sediment and water depths were recorded at each sampling location following collection, and spatial patterns in sediment depth are illustrated in Figure 4-2 B as a contour map across the pond-wetland system. Samples were analysed for total solids (TS) and volatile solids (VS) as per Method SM 2540 G (APHA, 2017), and for TP as P and SRP as P, using the methods described in Section 4.1.3., with the raw and unfiltered samples diluted as necessary. Measurement uncertainty associated with the Sludge Judge™ was approximately ±1 cm due to the plastic ball and connector assembly, with additional minor variability potentially introduced during sediment transfer to sample containers. While the sampling design provided representative coverage across the system, some spatial heterogeneity in sediment distribution may not have been fully captured.

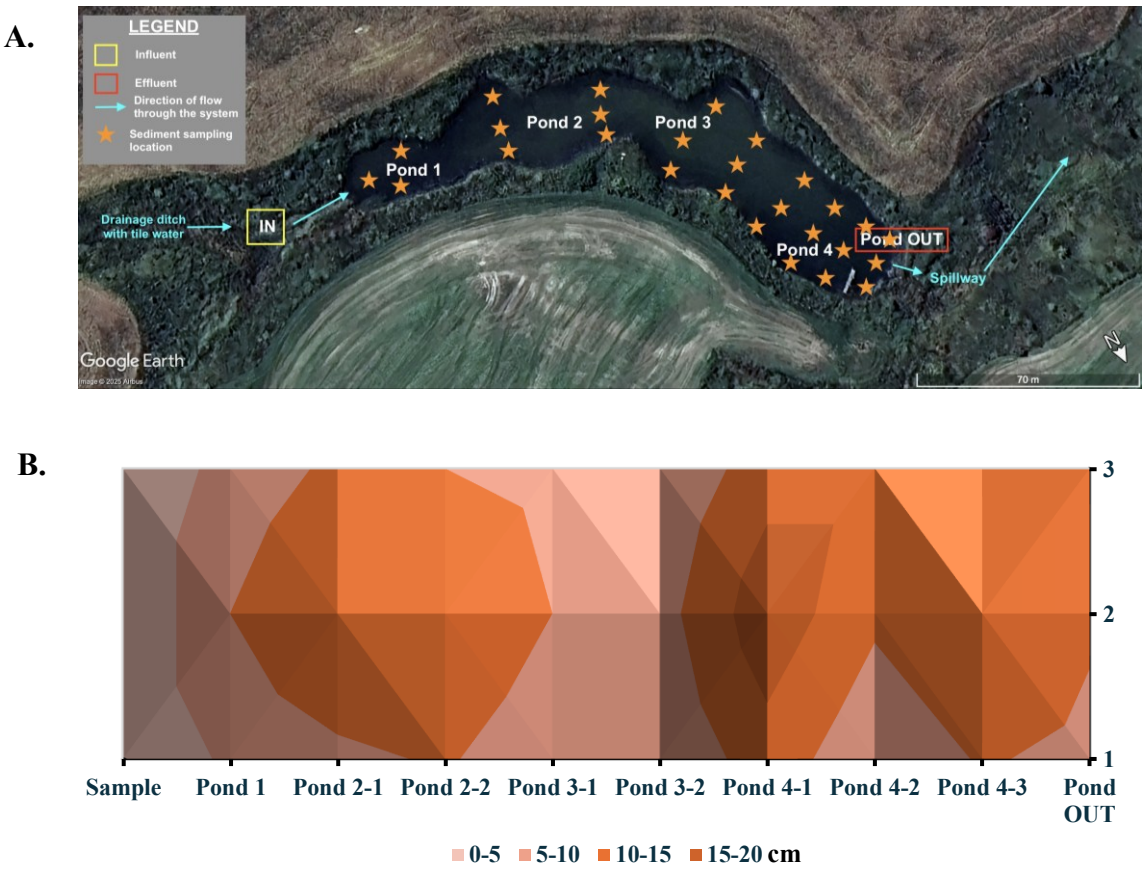

Figure 4-2. Sediment mapping - A. Location of sediment sampling spots across the pond-wetland system; B. Contour mapping of sediment depth across each pond within the system.

4.2.7. Macrophyte and soil sampling

The above-ground biomass of emergent macrophytes, including stem and leaves, as well as emergent vegetation, were collected during the summer and fall of 2021 from Pond 1, Pond 3, and Pond OUT. The density of the plant species was assessed by dividing the area into 1 m x 1 m quadrants at the ponds. The total area covered by these plants relative to the system was determined by comparing weekly photographs and aerial images from Google Earth. A macrophyte, representative in size of those within each quadrant, was harvested using heavy-duty pruning shears, and its height and stem diameter were recorded. All the collected samples were weighed and subsequently sent for plant tissue TP analyses to an external lab (Agriculture and Food Lab (AFL), Guelph, sodium bicarbonate method). A standard push soil core sampler was used to collect soil samples from each pond. Each sample was subdivided into five depths in increments of 5 cm, extending to a total depth of 25 cm. The samples were sent to an external lab (AFL, Guelph), where the samples were analyzed for P (sodium bicarbonate method extractable P method).

4.2.8. Statistical analysis

One-way Analysis of Variance (ANOVA) test was used to analyze mean daily concentrations to assess the impact of the pond-wetland system on nutrient concentration and mass attenuation in various time periods. Statistical significance was determined at a level (α) of 5% (p-value < 0.05) for water samples and 10% (p-value < 0.1) for soil and macrophyte samples. Multiple regression analysis was used to explore potential correlations between TSS, PP, and SRP concentrations (dependant variables) and the following explanatory (independent) variables: depth or 1/depth, outflow, concentration (Weir IN, effluent of the previous pond), HRT, precipitation (day of, 2-day, 3-day cumulative), temperature (day of, monthly, seasonal), overflow velocity, and windspeed. A stepwise mixed selection was conducted to identify the variables that significantly influenced the dependent variable. Furthermore, the datasets were partitioned to ascertain relationships within each pond and by season. Variance inflation factors (VIFs) were used to assess multicollinearity among the independent variables in the regression analysis. The statistical tests were performed in MS Excel and the confidence level was 95%.

4.3. Results and discussion

4.3.1. Meteorological conditions – precipitation, temperatures, and snow accumulated on ground.

Annual cumulative precipitation at the study site was below the 30-year normal (1991-2020) in 2016, 2018, 2019 and 2021, with totals ranging from 743 to 847 mm (ECCC, 2025). During the study period (April-November), precipitation in 2017 exceeded the 30-year average by 57%, whereas all the other years were 2 to 7% below normal. Accordingly, 2017 was the wettest year and 2019 the driest. Monthly precipitation timing and totals were also highly variable. For instance, May 2021 received 83% less precipitation than normal, whereas July 2017 exceeded normal levels by more than 182% (Figure 4-2).

Average monthly temperatures generally stayed within ± 1°C of the 30-year normal (ECCC, 2025). Seasonal average temperature varied among years, Spring-melt and Fall were 10 to 12% cooler than normal, whereas Late Spring and Summer remained relatively stable and close to their long 30-year averages. Average snow accumulation during the winters of 2018 and 2021 was 32% and 9% below the 30-yr normal, respectively. In contrast, 2017 and 2019 recorded snow depths 1.1 and 1.3 times greater than normal. These patterns align with the colder winter conditions

in those years and correspond to higher snowmelt volumes, in the order of 2019>2017>2021>2018. The water surface typically froze by mid-November, with a thick layer of ice persisting through winter and melting into early May as temperatures rose in spring.

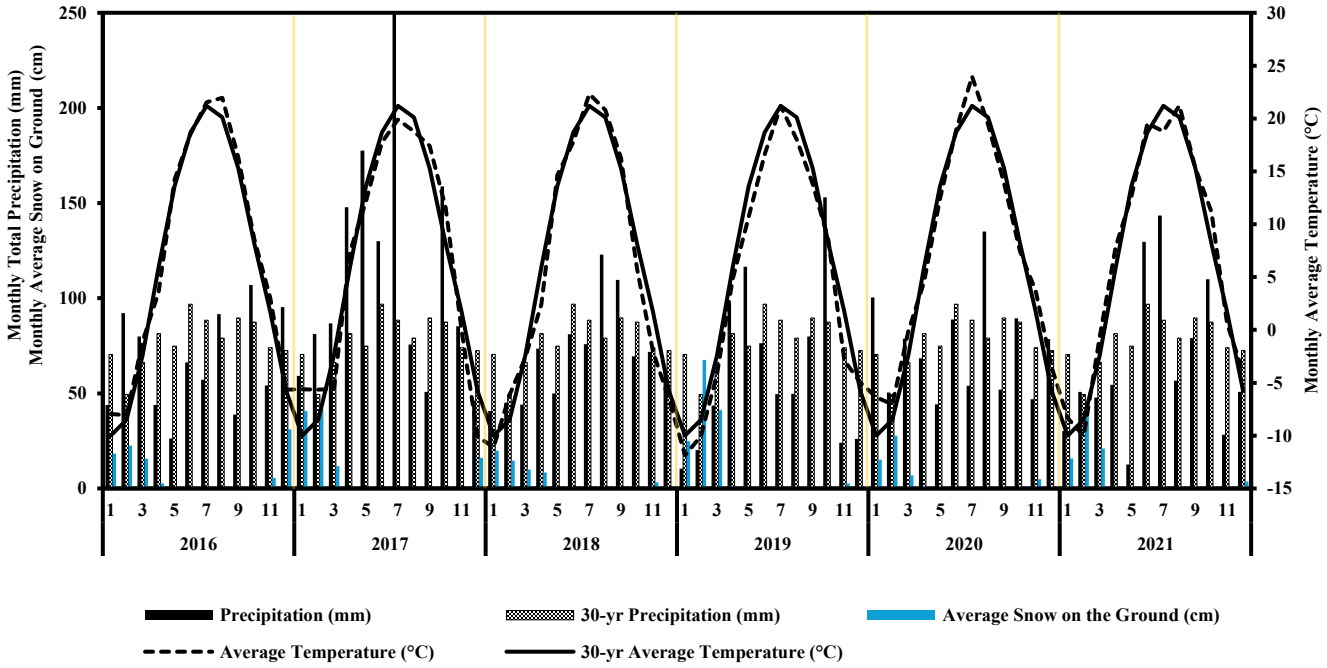

Figure 4-3. Monthly total precipitation (mm), accumulated snow on the ground (cm) and average monthly air temperature (°C) during the study period for Moose Creek Wells and St. Isidore Weather Stations, compared to 30-year Normal (1991-2020) at Ottawa International Airport (Agricrop, 2023; ECCC, 2024, 2025)

4.3.2. Hydrology – flows, hydraulic loads, and retention times

Over the 5-year study period, water flows through the pond-wetland system were governed by precipitation, evapotranspiration (ET), and accumulated snow. Figure 4-3 presents system daily outflow along with hydrological parameters. System outflow exhibited a clear seasonal pattern. Spring-melt (April) consistently produced the largest flows, controlled by antecedent snow depths. Using the 10:1 snow water equivalent (SWE) ratio (X. L. Wang et al., 2017), 2019 snowmelt volumes were 1.2 to 2.7 times greater than in 2017-2018 (Figure 4-2), corresponding to an average 21% higher cumulative spring-melt flow (88.5 mm/ha drained vs 64.9, 74.6 mm/ha drained). Outflows declined during Late Spring as ET increased, except in 2017, when precipitation was 137% above the 30-year normal (ECCC, 2025), resulting in Late Spring outflows 10% greater than spring-melt. Summer outflows were minimal in 2018 and 2019, with total flow of 16.9 mm/ha drained and 0.8 mm/ha drained respectively, whereas in 2017 they remained high owing to higher-than-normal precipitation (40 to 60% higher than summers of 2018, 2019). Fall outflows increased

in all years once precipitation exceeded ET, ranging from 33.5 to 80.5 mm/ha drained across years. Overall, cumulative flows followed a consistent hierarchy: Spring-melt > Fall > Late Spring > Summer. The system was hydraulically dormant during winters (December to March, highlighted by gray areas in Figure 4-3) due to frozen inlet ditch, thick ice cover, and snow accumulation.

The 2021 study year was abnormally dry with May precipitation 83% below than the 30-yr normal (ECCC, 2025), resulting in no inflow or outflow occurring during Late Spring and Summer, and stagnant water within the system. Inflow resumed only in late October, followed by a limited outflow before freeze-up, indicating system recharge after ET-driven water losses. This pattern aligns with observations from other constructed wetlands under prolonged no inflow conditions (Lavrnić, Alagna, et al., 2020; Mendes et al., 2018).

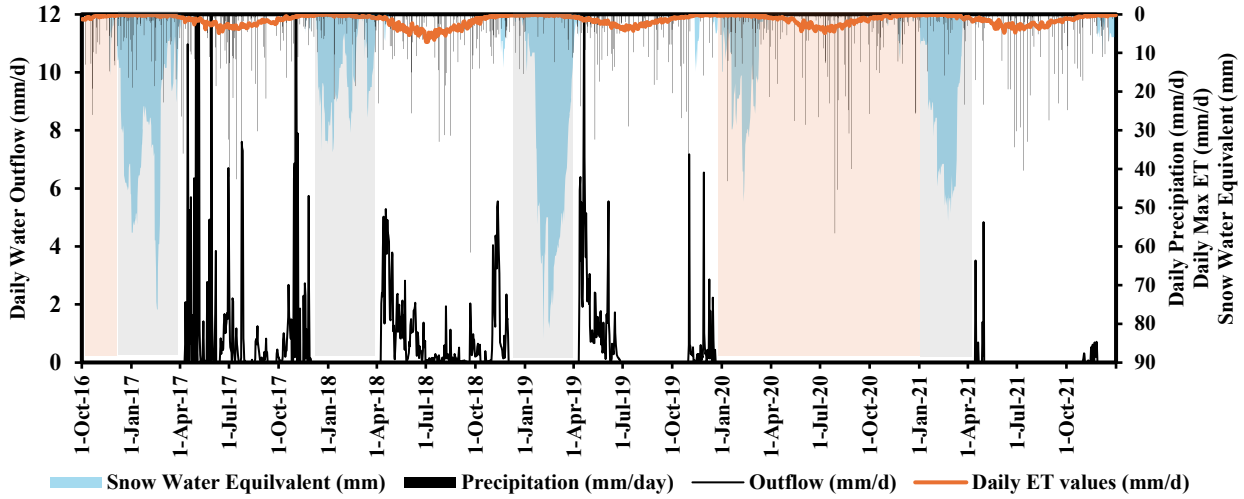

Figure 4-4. Daily trends of tile water outflow (mm/d/ha drained) leaving the Pond-Wetland System, precipitation (mm/d), evapotranspiration (ET) (mm/d) and snow water equivalent (SWE) (mm) are presented. The data gaps correspond to the following periods: 1. The winters of 2017- 2019 and 2021 (gray areas); 2. The fall of 2016 and the entirety of 2020, during which fieldwork was suspended due to COVID-19 lockdowns and restrictions; and 3. No inflow recorded during the Late Spring, Summer, and early Fall of 2021.

Across the study period, with a wetland-to-catchment area of 0.93%, the overall cumulative outflow of the system represented 92% of the cumulative inflow. This is consistent with other mid-west US and temperate constructed wetlands with similar ratios that report outflow was >80% of inflow (Kovacic et al., 2006; Kynkäänniemi et al., 2013), primarily due to ET, infiltration, and internal storage. Comparable retention has been reported in stormwater ponds (average 20%) (Harper & Baker, 2007; Lawrence et al., 1996; Nietch et al., 2001) and agricultural runoff systems (average 11%) (Oduor et al., 2023). Pond volumes varied from 45 m^3 to 2018 m^3 resulting in

seasonal HRTs varying from 0.1 to 3.6 days during Late Spring to 2.5 to 159.2 days during summer months with extended periods without flow, and 0.1 to 6.5 days in Fall. System-wide HRT for the full study was an average of 7.9 days. These results show that hydrologic seasonality makes annual HRT values poor predictors of system performance (Nilsson et al., 2023; Vymazal, 2017). The pronounced seasonal variability in flows and HRT has important implications for solids and nutrient retention processes within the system.

4.3.3. Total Suspended Solids (TSS)

4.3.3.1. Particle settling and TSS removal potential

TSS entering pond-wetland systems are primarily removed through sedimentation, filtration and vegetation interception, and flocculation (Beckingham et al., 2019; Harper & Baker, 2007; Kadlec & Wallace, 2008). Given that the present system is largely open water with less than 2% macrophyte coverage, we hypothesized that sedimentation (settling of TSS particles) would be the dominant TSS removal mechanism. Particle settling is governed by Stoke's law (Stokes, 1851), where particles settle when their settling velocity exceeds the water's overflow velocity. The standard stormwater surface-area sizing equation (Equation 4-8) incorporates Stoke's law to estimate the minimum surface area required to capture particles of different sizes (US EPA, 2009). While commonly applied to urban wet-retention ponds, this approach has also been applied to agricultural retention ponds in Quebec (Chrétien et al., 2016).

$$A_s = \frac{1.2\,Q}{V_S} \quad \text{(Equation 4-8)}$$

where A_s is the minimum pond surface area required to capture particles of given size, V_S is the particle settling velocity, and Q is the observed 90th or 95th percentile flow, including snowmelt and peak events. Soil at the study field, assessed at the beginning of the study, was mapped as Bearbrook clay, with varying distribution of sand, silt, and clay particles. Sand particles settle almost instantaneously, either in the drainage ditch or within the pond-wetland system. Using the Wentworth particle-size scale (USGS, 2006) - medium silt (30 μm), fine silt (10 μm) and clay (4 μm) - the minimum system surface areas required to capture 95th and 90th percentile flows were: 40 and 75 m^2 for 30 μm, 357 and 192 m^2 for 10 μm and 2230 and 1203 m^2 for 4 μm respectively. These calculations indicate that the present pond-wetland system is oversized for given range of particle sizes, supporting efficient sedimentation.

Applying Stoke's law to flow data from 2017 to 2019, the system captured 87 to 94% of 4 μm, and 100% of 10 μm and 30 μm. This confirms that settling effectively removes sand- and silt-sized particles, while a small fraction of clay-sized particles remains suspended. Similar trends were reported for agricultural wet ponds in Quebec (Chrétien et al., 2016) where sedimentation of silt and sand was the dominant treatment mechanism, while Maynard et al. (2009) observed that clay-based suspended solids were more susceptible to export than sand-based or silt-based solids, which typically settle more readily within wetland systems. These findings suggest that, when observed effluent TSS concentrations exceed influent values, particularly in upstream ponds, internal TSS generation and resuspension processes are likely dominating over settling-driven removal.

4.3.3.2. TSS - concentration

Mean influent TSS concentrations at Weir IN varied among the years, with the highest values observed during the first two monitoring seasons: 54 ± 56 mg TSS/L (median = 19 mg TSS/L) in late 2016 and 55 ± 81 mg TSS/L (median =16 mg/L) in 2017. These elevated concentrations likely reflect both system immaturity and exceptionally high precipitation in 2017 (57% above the 30-year normal) (ECCC, 2025). Influent TSS concentrations declined in 2018 (average = 33 ± 38 mg TSS/L, median = 19 mg/L) and reached the lowest levels in 2019 (average = 23 ± 16 mg TSS/L, median = 20 mg/L), the driest study year. Annual mean influent TSS followed cumulative flow patterns (2017 > 2018 > 2019), with an overall study mean of 42 ± 56 mg TSS/L. This value falls within the range (26 to 138 mg TSS/L) reported for *Dfb* temperate CWs but is lower than values reported for agricultural ponds and CW studies (> 150 mg TSS/L) (Table 4-1). Effluent TSS concentrations at Pond OUT were similar from 2017 to 2019, ranging between 13±9 mg/L to 16±14 mg TSS/L (p-value > 0.05, ANOVA). On a concentration basis, the system achieved a removal efficiency of 49% (p-value < 0.05, ANOVA), with the highest removal occurring during Summer and the lowest during Late Spring. Mean effluent concentrations were reduced to below the CCME freshwater guideline of 25 mg TSS/L (CCME, 1999) in all years with the exception of system startup during Fall 2016.

Monitoring at six locations along the flow path (Weir IN, Pond 1-4, and Pond OUT) provided insight into internal system processes (Figure 4-4). During Spring-melt (2017 - 2019), trends were captured only at Weir IN and Pond OUT, as the rest of the system remained under ice-

cover. Influent TSS concentrations during this period ranged from 9 to 30 mg TSS/L (study mean = 22 ± 21 mg TSS/L), with 37% removal observed at Pond OUT (p-value > 0.05, ANOVA). In this study, we hypothesize that lower spring concentrations are due to surface drainage of snow melt over frozen soil and is consistent with frozen-soil hydrology in tile-drained systems, where surface and subsurface flow paths are largely decoupled during snowmelt (Tedeschi et al., 2024). Seasonal influent TSS concentrations varied among the years, with Late Spring values ranging from 9 ± 4 to 18 ± 17 mg TSS/L, increasing during Summer (21 ± 4 to 72 ± 66 mg TSS/ L) and Fall (24 ± 21 to 154 ± 94 mg TSS/L). Elevated Summer and Fall concentrations were associated with high-rainfall events, particularly in Summer and Fall 2017 and Summer 2018.

Pond 1, the shallowest and non-vegetated pond of the system (mean depth = 0.08 m), consistently exhibited the highest mean TSS concentrations across all monitoring locations (65 ± 82 mg TSS/L) and regularly exceeded influent values at Weir IN. The greatest relative increases occurring during summers (82 to 210% above influent; Figure 4-4). The upstream placement and shallow depth of Pond 1 likely increased susceptibility to sediment resuspension driven by wind or flow-induced turbulence and bioturbation (Vymazal, 2010). In addition, consistently high algal biomass observed at Pond 1 suggests that internal biological production contributed to elevated summer TSS concentrations, supported by hypereutrophic TP concentrations (mean 0.27 mg P/L, OMECP (2014)) and concurrent seasonal increases in PP with reductions in SRP concentrations (discussed later in Section 4.4.4.1.), consistent with algal uptake and biomass accumulation. Higher mean TSS in Fall relative to Late Spring may reflect algal senescence coupled with increased Fall flows. Summer TSS concentrations during stagnant 2021 period were lower than during summers with flow. This decrease is consistent with reduced phosphorus inputs that would otherwise support algal growth (Brunet et al., 2021) as well as flow induced sediment resuspension.

For the study (2017 - 2019), Pond 2 (mean depth = 0.7 m) removed an average of 65% of the incoming TSS relative to Pond 1 (p-value < 0.05, ANOVA), although occasional seasonal exports occurred during Late Spring 2017 and Fall 2018 (~25%). Pond 3 (mean depth = 0.6 m), sparsely vegetated, provided limited additional reduction with periodic releases during Fall seasons. Pond 4, the deepest pond in this system (mean depth = 1.3 m), reduced mean TSS concentrations by 40% relative to Pond 3 (p-value < 0.05, ANOVA). However, Pond OUT, the

shallow (mean depth = 0.3 m) and moderately vegetated (~40% cover) outlet pond, showed an 11% increase in TSS, likely due to solids production from algal growth, biomass turnover and sediment resuspension, whereas the preceding Pond 4 consistently maintained low TSS concentration (13±11 mg TSS/L). It is likely that the vast majority of influent TSS is removed through sedimentation and that effluent TSS concentrations are governed primarily by internal production and sediment resuspension.

Table 4-1. Comparison of inflow and outflow total suspended solids (TSS) concentrations (mg TSS/L) and area-normalised cumulative mass loads (kg TSS/ha) for pond and constructed wetland systems receiving agricultural (runoff or drainage).

	Climatic Zone[1]	System type	Depth (m)	Mean concentration (mg TSS/L)			Cumulative mass load (kg TSS/ha)		
				IN	OUT	%	IN	OUT	%
This study	*Dfb*	PW^{T}	0.08 - 3.1	42	22	**49**	230.6	94.9	**59**
Rushton & Bahk (2001)	*Cfa*	TP^{R}	0.8	83	28	**66**	-	-	**98**
Koskiaho et al. (2003)	*Dfb*	SP + CW^{R}	2^{M}	26	-	**-**	-	-	**-5 to 41**
		CW^{T}	-	29	-	**-**	-	-	**8 to 16**
Fiener et al. (2005)	*Cfb*	TP^{R}	1.1 - 1.4	-	-	**-**	-	-	**54 to 85**
Díaz et al. (2012)	*Csa*	CW$^{T, R}$	0.5 - 1.5	238	103	**57**	-	-	**-**
		CW$^{T, R}$	0.5 - 1	242	20	**92**	-	-	**-**
		CW$^{T, R}$	0.5 - 1	242	15	**94**	-	-	**-**
		CW$^{T, R}$	0.5 - 1.3	583	38	**93**	-	-	**-**
Chrétien et al. (2016)	*Dfb*	TP^{R,E}	0.8	230	106	**54**	328	88	**73**
Lavrnić, Nan, et al. (2020)	*Cfa*	CW^{T}	0.4	162	78	**52**	286	88	**69**
Koskiaho & Puustinen (2019)	*Dfb*	CW^{R}	-	138^{F}	-	**-**	-	-	**7**
Ulén et al. (2019)	*Dfb*	SP + CW^{R}	0.03 - 1	-	-	**-**	-	-	**40**
Krzeminska et al. (2023)	*Dfb*	SP + CW^{R}	1.5 - 2.0 0.5	-	-	**-**	320	150	**53**

[1] Köppen–Geiger climate classification (Kottek et al., 2006)
PW = Pond-wetland, CW = Constructed wetland, SP = Sedimentation pond, TP = Treatment pond.
Dashes indicate values not reported in the original studies
[M]Max depth
[T]refers to tile drainage from cropping systems
[R]refers to runoff from cropping systems
[F] Flow-weighted mean concentrations
[E] Event-based study

Seasonal TSS concentrations are summarized in Figure 4-4 and Table K-1 in Appendix K. Late Spring (2017 - 2019) exhibited the lowest concentrations, with mean TSS at Pond 1 of 23±8

mg TSS/L, significantly higher than influent (p-value < 0.05, ANOVA). Concentrations decreased through Pond 2 - 4 before increasing at Pond OUT. Summer showed the highest TSS concentrations at Pond 1, subsequently captured by Pond 2 (77%, p-value < 0.05, ANOVA), with small reductions through Ponds 3 and 4, before increasing at Pond OUT by 24% relative to Pond 4. Fall had the highest influent TSS (86 ± 90 mg TSS/L), with reductions at Pond 1 (47%), further decline at Pond 2, non-significant increase at Pond 3, and additional removal at Pond 4 (p-value < 0.05, ANOVA). However, interannual comparisons revealed that the large apparent reduction at Pond 1 was influenced by high Fall 2017 influent (154±80 mg TSS/L); Fall 2018 and 2019 saw increases at Pond 1 (~ 30%) relative to their respective influents.

Comparison among ponds of differing depths indicates that deeper ponds provide more consistent TSS removal across seasons. During higher-flow periods in Late Spring and Fall (mean cumulative flow of 62.6 to 65.9 mm/ha drained), Pond 2 (0.7 m) removed only 28 to 36% of incoming TSS from Pond 1, whereas the deeper Pond 4 (1.3 m) removed a greater proportion of TSS exiting Pond 3 (39 to 57%). Under low-flow Summer conditions (mean cumulative flow = 30.8 mm/ ha drained), Pond 2 was effective, capturing 77% of incoming TSS from Pond 1, but this performance was not maintained during higher-flow periods. Across all seasons, Pond 4 consistently exhibited the lowest TSS concentrations and achieved cumulative removals of 46 to 80% relative to Weir IN (p-value < 0.05, ANOVA), the highest of any pond in the system. These observations suggest that increased pond depth is associated with more robust TSS removal performance across a range of hydrologic conditions, reducing resuspension, and thereby supporting its consideration in future system design.

Regression analysis corroborated these observed TSS patterns (Table 4-3). Across the full dataset, pond depth was the dominant control of TSS, with shallower areas associated with significantly higher TSS (β = +4.25; p–value < 0.001). This depth effect persisted seasonally, moderate in late spring and strongest in summer (β = +7.28; p–value < 0.001), closely aligning with field observations at Pond 1. At the individual pond scale, influent TSS (effluent from previous) significantly influenced effluent TSS in Ponds 2 through Pond OUT (β = +0.09 to +0.52), but not in Pond 1. Seasonal temperature exhibited pond-specific effects, with a positive association in Pond 1 (β = +4.28; p–value < 0.05) and negative associations in Ponds 2 and 3, suggesting contrasting roles of biological production and settling along the flow path. Hydrologic

variables (inflow and HRT) were not significant predictors of TSS, highlighting that internal biophysical processes outweighed flow-driven effects in this system. Precipitation (3-day cumulative) influenced TSS only in Late Spring, while windspeed showed no significant effect. Overall, regression results support that depth-mediated sedimentation, and resuspension/biomass turnover by temperature-driven biological activity, were the primary processes (drivers) of TSS variability within the system.

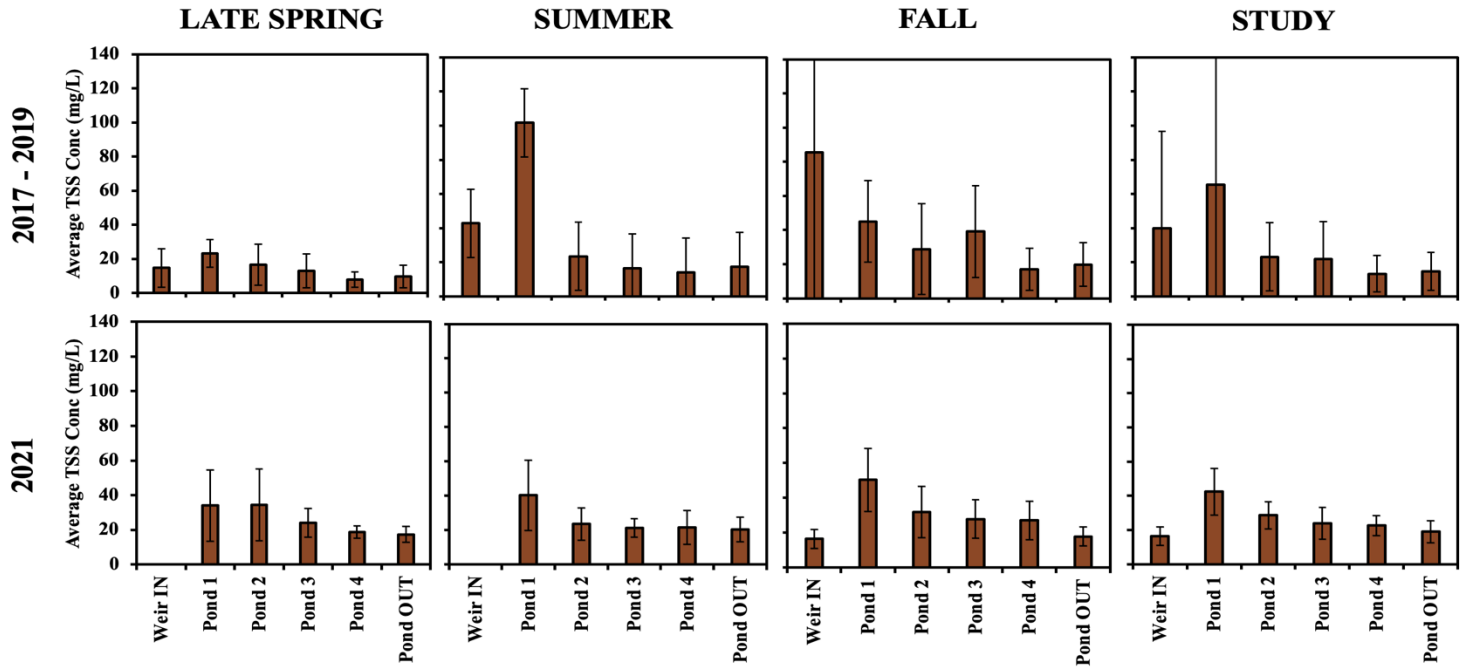

Figure 4-5. Average grab total suspended solids (TSS) in mg TSS/L across the Pond-Wetland System during the study at each monitoring location along the flow path, summarized by seasons and for the full study period (2017 to 2019, referred to as "Study"). Error bars denote 95% confidence intervals. Data for 2017-2019 and 2021 are presented separately, as 2021 represented a stagnant (no-flow) year, enabling comparison between flow and no-flow conditions.

Table 4-2. Seasonal cumulative loads of total suspended solids (TSS) in kg/ha at inlet and outlet of the pond-wetland system across the entire study, along with associated removal efficiencies.

	2016			2017			2018			2019			2021			Total		
	IN[a]	OUT[b]	%removal	IN[a]	OUT[b]	%removal	IN[a]	OUT[b]	%removal	IN[a]	OUT[b]	%removal	IN[a]	OUT[b]	%removal	IN[a]	OUT[b]	%removal
Spring-melt[c]	-	-	-	1.9	1.3	**35**	5.3	2.9	**46**	20.6	11.3	**45**	-	-	-	27.8	15.4	**45**
Late Spring[d]	-	-	-	10.9	8.8	**19**	8.7	4.7	**46**	9.7	3.2	**67**	-	-	-	29.3	16.7	**43**
Summer[e]	-	-	-	11.5	10.2	**12**	5.3	0.5	**91**	2.0	1.1	**46**	-	-	-	18.8	11.7	**38**
Fall[f]	6.4	4.6	**28**	112.0	25.2	**78**	31.1	19.1	**34**	4.6	1.7	**64**	0.6	0.7	**-31**	154.7	51.1	**67**
Total	6.4	4.6	**28**	136.3	45.2	**67**	50.4	27.2	**46**	36.9	17.2	**53**	0.6	0.7	**-31**	230.6	94.9	**59**

[a] Refers to Weir IN monitoring station, which acted as the inlet to the pond-wetland system
[b] Refers to Pond OUT, located at the end of the pond-wetland system
[c] Period between first measurement in early April to April 30, capturing the melt of accumulated snow on the ground
[d] Period between May 1 to June 20, referring to later spring season in northern hemisphere
[e] Period between June 21 to September 20, based on northern hemisphere season
[f] Period between September 21 to November 30, based on northern hemisphere season

Table 4-3. Multiple regression analysis of factors influencing total suspended solids (TSS) concentrations across the pond-wetland system, by pond and season.

Variables[a]	Combined Model[b]	Individual Ponds					Season		
		Pond 1	Pond 2	Pond 3	Pond 4	Pond OUT	Late Spring	Summer	Fall
1/depth	+4.25 (CI: 2.86, 5.64) ****	NA	NA	NA	NA	NA	+1.06 (CI: 0.52, 1.59)****	+7.28 (CI: 4.53, 10.23)****	NS
Influent concentration[c]	NS	NS	+0.09 (CI: -0.00, 0.17)**	+0.36 (CI: -0.01, 0.73)*	+0.18 (CI: -0.01, 0.36)*	+0.52 (CI: 0.26, 0.78)****	+0.25 (CI: 0.00, 0.49)**	NS	+0.24 (CI: 0.04, 0.44)**
Seasonal temperature	NS	+4.28 (CI: 0.11, 8.46) **	-0.89 (CI: -1.89, 0.12) *	-0.97 (CI: -1.90, -0.04)**	NS	NS	NA	NA	NA
Precipitation (-3 day cumulative)	NS	NS	NS	NS	NS	NS	+0.25 (CI: 0.02, 0.48)**	NS	NS
Inflow[d]	NS	NS	NS	NS	NS	NS	NS	NS	NS
HRT	NS	NS	NS	NS	NS	NS	NS	NS	NS
Windspeed	NS	NS	NS	NS	NS	NS	NS	NS	NS

[a] Reduced regression listed here with variables showing statistically significant effect on TSS concentration. Other variables tested, but not listed here include, precipitation (day of, -2 day), and temperature (daily and monthly averages).

[b] Refers to the complete study period grouped together across the system (n=193), $R^2 = 0.18$, Adjusted $R^2 = 0.15$. The regression equation is not shown, as the analysis was intended to evaluate variable effects on concentration, not for predictive modelling.

[c] Refers to effluent concentration from previous pond, which be influent of the pond in question.

[d] Refers to outflow from previous pond, which is the inflow of the pond in question.

CI refers to 95% confidence interval for beta coefficient.

Significance levels: * *p*-value <0.1, ** *p*-value < 0.05, *** *p*-value <0.01, **** *p*-value <0.001

NA indicates Not Applicable

NS indicates Not Significant (tested, *p*-value >0.1)

4.3.3.3. TSS – mass load

System Inlet and Outlet Loads

Cumulative TSS loads at Weir IN and Pond OUT (Table 4-2) showed positive load reductions in nearly all seasons and years. Load patterns closely followed both flow and concentration dynamics, however, change in concentration reduction primarily governed load retention trends ($R^2 = 0.82$). The system was constructed in spring 2016, with ponds filling over the summer and outflow commencing in Fall 2016, with initial seasonal removal efficiency of 28%. Removal efficiency increased markedly in 2017 (67% overall), driven largely by strong Fall retention, which accounted for 56% of the annual load retention despite large inflow loads (driven by 154 ± 94 mg TSS/L mean concentration). Performance in 2018 and 2019 were moderate, with pronounced seasonal variability: Summer removal was highest in 2018 (91%), while Late Spring and fall showed stronger retention in 2019 (67% and 64%). Spring-melt loads represented only 1.9% and 10% in 2017, 2018, but increased to 56% in the drier year 2019. Despite these differences, Spring-melt removals remained consistent (35 to 46% removal), likely due to low inflow TSS concentration associated with tile-driven snowmelt (Dumanski et al., 2015; Kokulan et al., 2019). The only seasonal export observed was a marginal 0.1 kg/ha during late-fall flow in 2021 following several months of no-flow conditions. Overall, the system removed 59% of TSS mass load during the study.

Internal Pond Loads

To evaluate internal dynamics, TSS loads were calculated at each pond (Figure 4-5 A), restricting inlet and outlet calculations to periods when all pond data were available (mid-May to mid-November 2017 to 2019). Cumulative TSS loads showed a consistent decline through each pond (except Pond 1), demonstrating strong sediment retention in the deeper ponds. A clear year-to-year hydrology impact on influent and internal load is seen, with 2017 producing the highest loads, followed by moderate loads in 2018 and very low loads in the dry year 2019. Between 2017 to 2019, a cumulative load of 153 kg/ha entered the system (Figure 4-5 A). Pond 1 exhibited increased TSS loads relative to Weir IN across all years by an average of 18%. This was due to sediment resuspension and internal algal production resulting from Pond 1's shallow depth (0.08 m). This indicates that a shallow inlet pond is a poor design choice for solids removal. A general progression of increased removal with distance was observed from Pond 2 to Pond 4. Pond 2 (0.7 m) was

effective at removing close to 50% of incoming solids, while Pond 3 (0.6 m) only removed an additional 6% of TSS load, and Pond 4 (1.3 m) removed a further 13% of TSS load. This indicates that one 0.7 m pond as 0.2% of drainage area is sufficient to achieve close to 50% removal and suggests that a 1.3 m pond is more effective than a 0.6 m pond at solids retention. The final shallow Pond OUT (0.3 m) exhibited a 22% increase in TSS load compared to Pond 4, suggesting a shallow moderately vegetated outlet pond is counterproductive for solids removal.

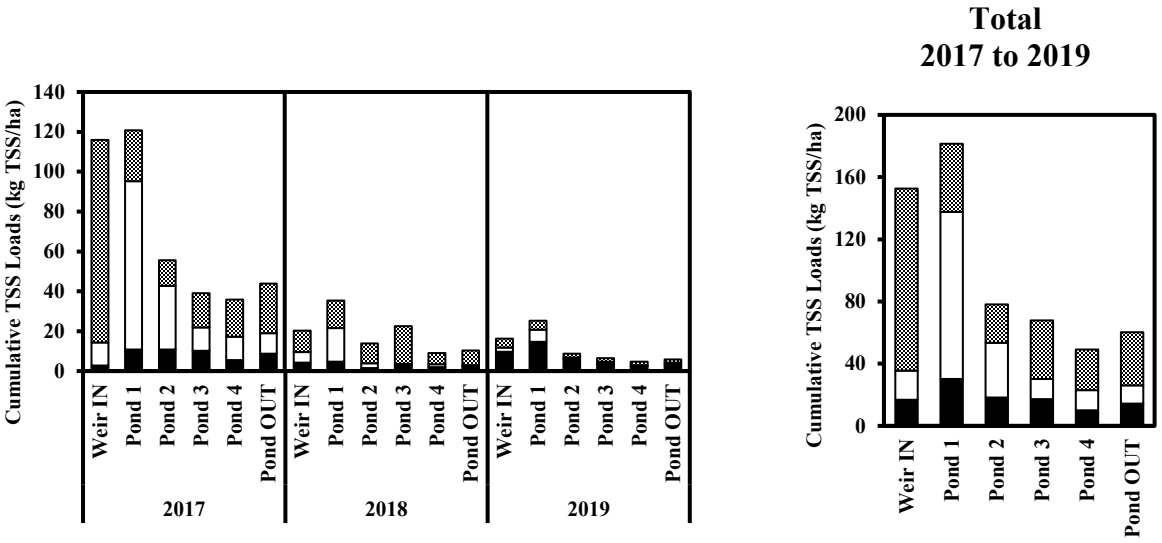

Figure 4-6. Cumulative total suspended solids (TSS) loads across the pond-wetland system during the study (May to November 2017 to 2019) on the left and total loads at the end of 2019 on the right. Note: Reported loads correspond to the non-frozen period, which is consistent across all sites. Accordingly, Weir IN and Pond OUT include only the intervals during which grab samples were collected at the pond monitoring locations. Year 2016 is excluded because pond samples were not collected, and Year 2021 is excluded due to limited number of samples collected in Fall.

4.3.3.4. Long-Term Mass Balance and design recommendations

From 2016 to 2021, a total of 12025 kg of TSS entered the system, of which 57% (6822 kg) was retained. TSS removed or trapped, along with internally generated materials, eventually accumulate as either new movable sediment or consolidated immovable new soil derived from the sediments (Kadlec & Wallace, 2008). Sediment mapping in 2021 indicated an average accumulation rate of 1.7 cm/yr, resulting in a mean sediment depth of 10.2 ± 3.2 cm at the end of the study. Based on standard dredging criterion - which recommend limiting volumetric capacity loss to 30% - sediment removal is recommended every 10 - 20 years (Miller et al., 2025; TRCA & CH2M, 2016). At the estimated accumulation rate, a 20-year interval between dredging events would require a sediment storage depth of 0.34 - 0.40 m. Sediment mapping also found a total solids mass (TS) of 7921 kg, closely matching calculated retention.

The observed 57% TSS retention by the system was within the reported TSS removal efficiencies (Table 4-2) in agricultural ponds (54 to 98%), higher than removals in CWs treating agricultural influent in *Dfb* climatic zones (-5 to 53%), and within the range for urban stormwater studies (50 to 94%) (Harper & Baker, 2007; Jones et al., 2012; Lawrence et al., 1996; SC DHEC, 2005; Schueler & Holland, 2000). Sedimentation was the dominant TSS removal mechanism, while internal processes, such as sediment resuspension, algal production and macrophyte senescence, contributed to additional TSS generation. Although effects of influent load, residence time, and vegetation (Braskerud et al., 2005; Krzeminska et al., 2023), were partly reflected in system's behavior, pond depth and internal biophysical processes were primary determinants of TSS behavior.

Shallow ponds inlet (Pond 1) and outlet (Pond OUT) consistently represented a disadvantage, exhibiting elevated internal TSS generation and exports. Although CWs typically promote TSS retention through sedimentation, and macrophytes can further enhance retention by reducing near-bed flow velocities and trapping within plant detritus (Brix, 1997), these benefits were not realized in the present system due to moderately vegetation coverage. In contrast, the deepest ponds demonstrated the highest and the most stable retention behavior. Pond 4 (1.3 m) dominated TSS removal during high- and moderate- flow years, while Pond 2 (0.7 m) performed better under low-flow conditions, highlighting that depth-controlled settling and reduced resuspension were more influential than the total number of ponds. Over 2017 - 2019, cumulative TSS removal relative to Weir IN was 68% for Pond 4 compared to 49% by Pond 2.

In Section 4.4.3.1., using the standard stormwater surface-area sizing equation (US EPA, 2009), the minimum pond surface area required to capture the smallest particle fraction (4 μm, clay) was estimated to be 2230 m^2 for 95th percentile flow and 1203 m^2 for 90th percentile flow. Considering both the particle capture requirements and the dredging constraint (limiting volumetric capacity loss to 30% over 20 years, and the estimated 0.34 to 0.40 m sediment storage depth), a deeper pond (1.3 m) is preferred to shallower alternative, 0.7 m. These observations suggest that a single pond with a mean depth of 1.3 m and a surface area of at least 2230 m^2 could achieve sediment retention comparable to the multi-pond system with varying depths.

Based on these dimensions, the corresponding storage volume would be 2899 m^3. With a

contributing catchment area of 43 ha, this single-pond configuration provides approximately 67.4 m^3/ ha of storage. This value is comparable to recommended urban wet pond designs (60 m^3/ ha) for catchments with less than 35% impervious cover, which aim to achieve 60% long-term TSS removal under Ontario's Environmental Design Criteria 3.0 for stormwater management (OMECP, 2017). However, it is lower than storage volumes reported in two agricultural pond studies (83 m^3/ ha and 264 m^3/ ha) that achieved comparable long-term TSS retention (~50%) (Chrétien et al., 2016; Fiener et al., 2005).

Taken together, the consistency between internal pond performance, normalized storage comparisons, and established design benchmarks provides a defensible basis for recommending a single, deeper pond configuration (mean depth = 1.3 m, surface area ≥ 2230 m^3, volume ≥ 2899 m^3) for the conditions evaluated in this study.

4.3.4. Phosphorus

4.3.4.1. Phosphorus - concentration

Annual concentrations (total, particulate and soluble reactive)

From 2016 to 2019, the pond-wetland system received influent TP concentrations ranging from 0.03 to as high as 1.10 mg P/L, with an overall mean of 0.16±0.18 mg P/L. SRP concentrations ranged from 0.01 to 0.28 mg P/L with a mean of 0.07±0.06 mg P/L. Average effluent concentrations were lower, with mean TP reduced by 18% (0.13 ± 0.09 mg P/L) and mean SRP by 14% (0.06 ± 0.05 mg P/L); however, these differences were not statistically significant (*p*-value > 0.1, ANOVA). Overall TP and SRP values in this study were mid-range of averages reported for agricultural treatment ponds receiving cropping drainage and comparable to constructed wetlands with similar A_w:A_c = 0.8 to 1.0% (Table 4-4). Comparing wetlands with similar A_w:A_c is previously shown as critical, as this metric strongly influences hydraulic loading and phosphorus treatment efficiency (Kill et al., 2022; Kovacic et al., 2000; Kynkäänniemi et al., 2013). Based on average concentrations, the system can be classified as hyper-eutrophic with TP > 0.1 mg P/L (CCME, 2004). However, effluent TP did not meet the Ontario's Provincial Water Quality Objective of < 0.02 mg P/L during the ice-free period (MOEE, 1994), although summer retention was occasionally high enough for this threshold to be reached.

Particulate phosphorus (PP), calculated by subtracting SRP from TP, comprised the majority of TP fraction (59%) in both influent and effluent and showed a moderate correlation

with TSS (R^2 = 0.57). This is atypical, as tile drainage is typically associated with SRP, not PP. Surface erosion of clayey soil with tile water movement (Johannesson et al., 2015; Kill et al., 2022; Ulén et al., 2019) in the drainage ditch upstream of Weir IN, could possibly explain this. The PP/TP and PP/SRP ratios varied seasonally and spatially along the system, indicating internal transformations and cycling. Therefore, the subsequent discussion focuses on PP and SRP dynamics as drivers of P behaviour.

Table 4-4. Comparison of inflow and outflow total phosphorus (TP), particulate phosphorus (PP), soluble reactive phosphorus (SRP) concentrations (mg P/L) and area-normalised cumulative mass loads (kg P/ha) for pond and constructed wetland systems receiving cropping (runoff or drainage).

	Climatic Zone[1]	System type	Area ratio[2] (%)	P species	Mean concentration (mg P/L)			Cumulative mass load (kg P/ha)		
					IN	OUT	%	IN	OUT	%
This study	*Dfb*	PW[T]	0.93	TP	0.16	0.13	**18**	1.0	0.8	**17**
				PP[C]	0.09	0.07	**22**	0.6	0.4	**24**
				SRP	0.07	0.06	**14**	0.4	0.3	**15**
Rushton & Bahk (2001)	*Cfa*	TP[R]	-	TP	1.40	0.59	**58**	-	-	**75**
				SRP	0.87	0.42	**51**	-	-	**67**
Kynkäänniemi et al. (2013)	*Dfb*	SP + CW[R]	0.60	TP[F]	0.30	0.18	**40**	193	-	**36**
				PP[F]	-	-	**-**	-	-	**46**
				DP[F]	0.10	0.06	**40**	-	-	**9**
Chrétien et al. (2016)	*Dfb*	TP[R]	0.50	TP[E]	0.43	0.22	**50**	1.1	0.5	**59**
Mendes et al. (2018)	*Cfb*	SP + CW[R]	1.10	TP[F,*]	0.18	0.09	**50**	-	-	**42**
			0.90	TP [F,*]	0.21	0.11	**48**	-	-	**51**
			1.10	TP [F,*]	0.22	0.18	**18**	-	-	**41**
Koskiaho & Puustinen (2019)	*Dfb*	CW[R]	1.30	TP[F]	0.22	-	**-**	-	-	**12**
				SRP[F]	0.02	-	**-**	-	-	**24**
Brunet et al. (2021)	*Dfa*	TP[R]	1.80	TP[F]	0.23	0.26	**-13**	2.3	2.1	**8**
				TDP[F]	0.15	0.14	**6**	-	-	**-**
Robotham et al. (2021)	*Cfb*	TP[R]	0.20	TP	0.08	0.09	**-34**	-	-	**-**
				PP	0.04	0.05	**-237**	-	-	**-**
				SRP	0.01	0.01	**29**	-	-	**-**

[1] Köppen−Geiger climate classification (Kottek et al., 2006)
[2] Area ratio reported as percent wetland or pond area relative to catchment area
PW = Pond-wetland, CW = Constructed wetland, SP = Sedimentation pond, TP = Treatment pond, DP = Dissolved P, TDP = Total DP
Dashes indicate values not reported in the original studies
[C]refers to PP concentrations calculated as TP minus SRP from weekly grab samples.
[T]refers to tile drainage from cropping systems
[R]refers to runoff from cropping systems
*median values
[F] Flow-weighted mean concentrations
[E] Event-based study

Internal Pond Concentrations and Seasonal Dynamics (PP and SRP)

To better understand the limited system-scale TP and SRP removal observed annually, internal system concentrations were examined seasonally, with a focus on PP and SRP dynamins along the flow path. During Spring-melt, PP and SRP concentrations at Weir IN followed TSS patterns, peaking in 2019 - the year of greatest snow accumulation (PP: 0.13 ± 0.07 mg P/L, SRP: 0.09 ± 0.03 mg P/L). However, unlike TSS, PP retention during this period was minimal (4 to 7% in 2018 - 2019), with net export observed in 2017 (PP 1.5x and SRP 4x influent). High PP retention was expected under ice, however, ice cover (December to April) likely promoted anoxic conditions in accumulated litter and sediments, favoring the release of iron-bound P (Reddy et al., 2023). This interpretation is supported by isolated under-ice samples collected in March 2017 and 2018, which showed elevated SRP (0.16 ± 0.08 mg P/L, n = 9).

Across flow years (2017-2019), seasonal influent PP and SRP concentrations were highest in Summer, followed by Fall and Late Spring (Figures 4-6, 4-7). Summer concentrations were episodic, reflecting summer (August) storm-driven flow events (> 40 mm/ha drained per event). Among ponds, average concentrations were highest in Fall and lowest in Late Spring, whereas during the stagnant year (2021), concentrations were uniformly lower and less variable.

During Late Spring, average PP and SRP declined by 20% and 19% respectively, at Pond 1 relative to influent. No significant changes were observed between Ponds 1-3 for either constituent, while slight non-significant increases occurred at Pond 4 and Pond OUT. These patterns suggest that short HRT (system = 5.9 days) likely constrained sedimentation and diffusion-regulated sorption processes (Reinhardt et al., 2005). During the stagnant year in 2021, PP (< 0.03 mg P/L) and SRP (< 0.02 mg P/L) remained consistently low across all ponds.

In summer, PP concentrations at shallow Pond 1 increased by 24% relative to Weir IN, coinciding with elevated TSS, while SRP concentrations declined by 44% (p - value < 0.05, ANOVA). This inverse relationship is consistent with algal and phytoplankton uptake of bioavailable P during peak growth and subsequent incorporation into biogenic PP (Reinhardt et al., 2005), offsetting modest Late Spring sedimentation through biological productivity and depth-related resuspension. Pond 2 (mean depth = 0.7 m) subsequently reduced PP by 49% and SRP by 40% (p-value < 0.05, ANOVA), indicating effective particulate sedimentation and sorption under

low-flow, high HRT summer conditions (pond average = 51.7 days) (Johannesson et al., 2011; Mendes et al., 2018). Beyond Pond 2, no significant changes in PP or SRP concentrations were observed, suggesting that upstream retention capacity was largely exhausted, with PP approaching background concentrations observed during stagnant Summer 2021 (Figures 4-6, 4-7).

During stagnant Summer 2021, SRP concentrations at Pond 1 remained similar to flow-period values, whereas Ponds 2 - OUT showed 20 - 54% lower concentrations than their respective flow-period values. The absence of inflow and outflow resulted in effectively infinite HRT, likely favoring diffusion-controlled sorption in the deeper downstream ponds. Although stagnant conditions can promote anoxic release of Fe-bound P (Dunne et al., 2005; Reddy et al., 1999), reduced sediment disturbance and lower organic matter likely allowed SRP concentrations to decrease toward apparent background levels (0.012 to 0.026 mg P/L).

In Fall, PP concentrations at Pond 1 increased by 2-3x relative to Summer, exceeding influent by > 100% in 2017-2019. SRP exhibited a similar increase, strongly indicating internal P release. Late-season algal senescence and subsequent mineralization can release dissolved inorganic P, which may be incorporated into particulate forms, elevating both SRP and PP concentrations (Díaz et al., 2012; Healy & Cawley, 2002). Pond 2 retained 65% of PP relative to Pond 1 (p-value < 0.05, ANOVA), whereas SRP showed no significant reductions between Ponds 1 - 3. Increased Fall flows, reduced HRT (system = 10.7 days), combined with upstream release, likely limited sorption efficiency, allowing SRP to propagate downstream. Pond 4 exerted a stabilizing effect, reducing PP concentrations by 37% (p-value < 0.1, ANOVA) and SRP by 24% (p-value > 0.1, ANOVA) relative to Pond 3.

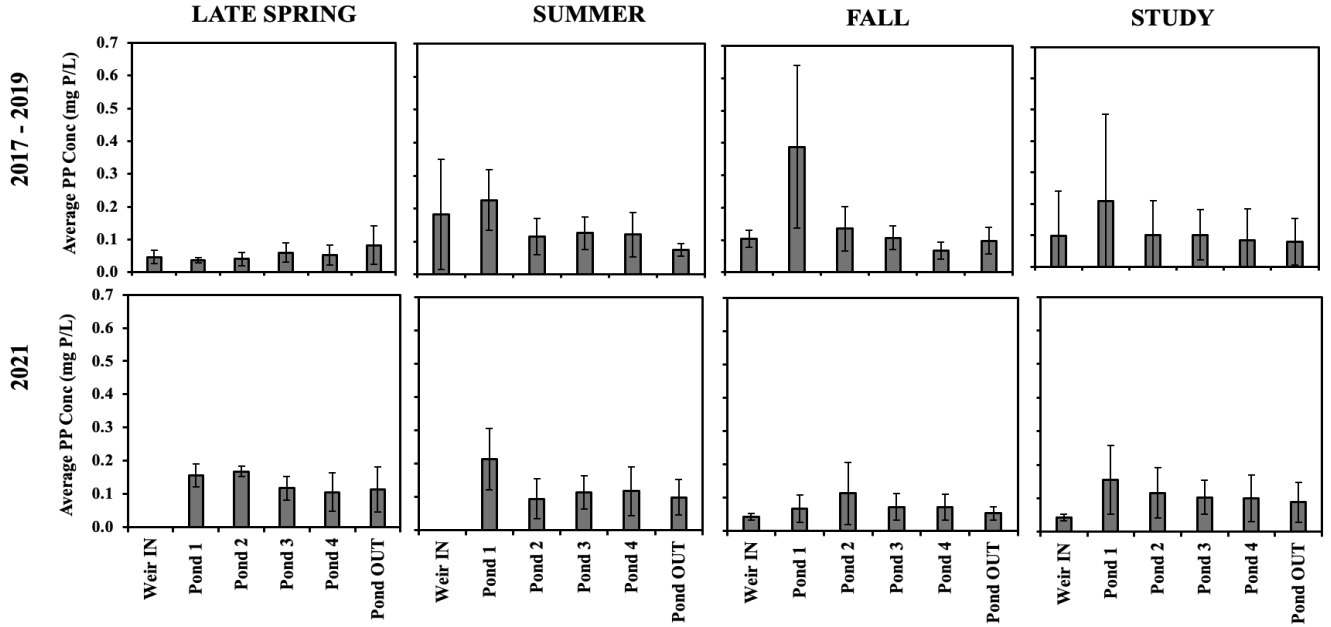

Figure 4-7. Average grab particulate phosphorus (PP) in mg P/L across the Pond-Wetland System during the study at each monitoring location along the flow path, summarized by season and for the full study period (2017 to 2019, referred to as "Study"). Error bars denote 95% confidence intervals. Data for 2017-2019 and 2021 are presented separately, as 2021 represented a stagnant (no-flow) year, enabling comparison between flow and no-flow conditions.

Table 4-5. Seasonal cumulative loads of particulate phosphorus (PP, x10^{-2} kg P/ha) at inlet and outlet of the pond-wetland system across the entire study, along with associated removal efficiencies.

	2016			2017			2018			2019			2021			Total		
	IN[a]	OUT[b]	%removal	IN[a]	OUT[b]	%removal	IN[a]	OUT[b]	%removal	IN[a]	OUT[b]	%removal	IN[a]	OUT[b]	%removal	IN[a]	OUT[b]	%removal
Spring-melt[c]	-	-	**-**	2.2	1.9	**11**	1.8	1.7	**4**	10.8	9.0	**16**	-	-	-	14.8	12.7	**14**
Late Spring[d]	-	-	**-**	9.0	9.7	**-9**	2.6	2.3	**13**	0.8	0.3	**66**	-	-	-	12.4	12.3	**1**
Summer[e]	-	-	**-**	11.0	6.5	**41**	1.0	0.4	**64**	0.2	0.0	**76**	-	-	-	12.2	6.9	**43**
Fall[f]	4.3	4.1	**5**	10.1	4.9	**52**	6.5	4.1	**36**	2.0	2.5	**-27**	0.1	0.1	**-19**	22.9	15.7	**32**
Total	4.3	4.1	**5**	32.2	23.0	**29**	11.9	8.5	**29**	13.8	11.5	**16**	0.1	0.1	**-19**	62.3	47.2	**24**

[a] Refers to Weir IN monitoring station, which acted as the inlet to the pond-wetland system

[b] Refers to Pond OUT, located at the end of the pond-wetland system

[c] Period between first measurement in early April to April 30, capturing the melt of accumulated snow on the ground

[d] Period between May 1 to June 20, referring to later spring season in northern hemisphere

[e] Period between June 21 to September 20, based on northern hemisphere season

[f] Period between September 21 to November 30, based on northern hemisphere season

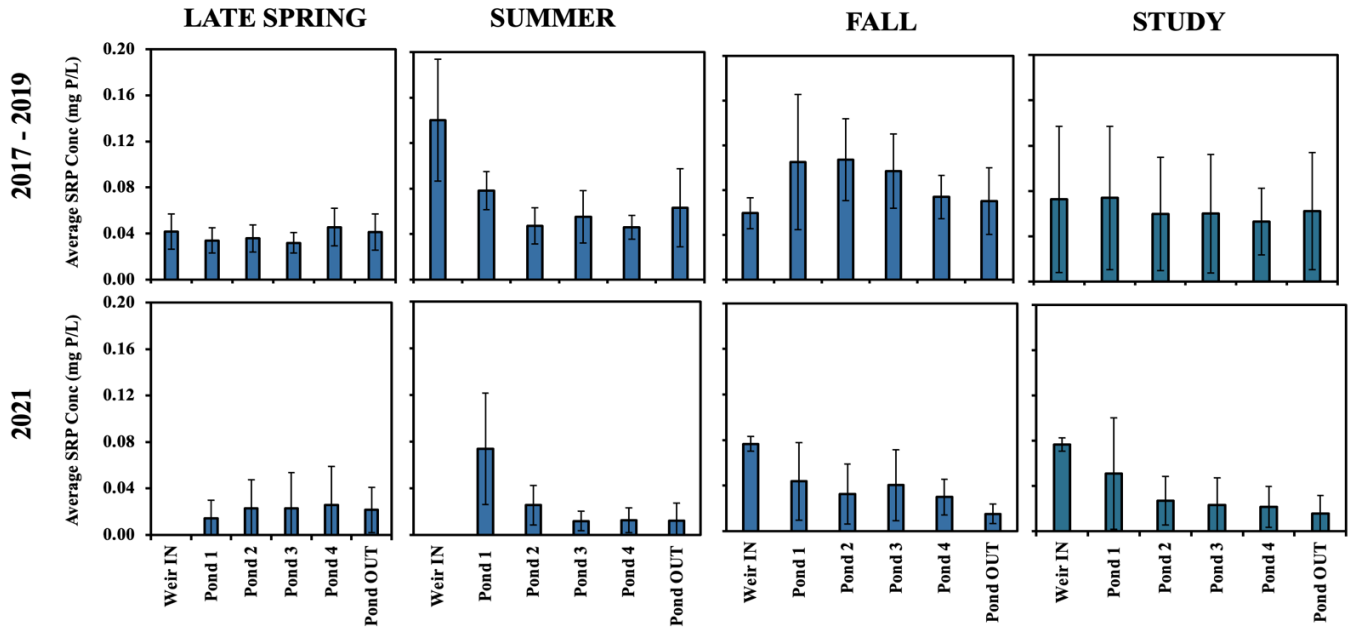

Figure 4-8. Average grab soluble reactive phosphorus (SRP) in mg P/L across the Pond-Wetland System during the study at each monitoring location along the flow path, summarized by season and for the full study period (2017 to 2019, referred to as "Study"). Error bars denote 95% confidence intervals. Data for 2017-2019 and 2021 are presented separately, as 2021 represented a stagnant (no-flow) year, enabling comparison between flow and no-flow conditions.

Table 4-6. Seasonal cumulative loads of soluble reactive phosphorus (SRP, $x10^{-2}$ kg P/ha) at inlet and outlet of the pond-wetland system across the entire study, along with associated removal efficiencies.

	2016			2017			2018			2019			2021			Total		
	IN[a]	OUT[b]	%removal	IN[a]	OUT[b]	%removal	IN[a]	OUT[b]	%removal	IN[a]	OUT[b]	%removal	IN[a]	OUT[b]	%removal	IN[a]	OUT[b]	%removal
Spring-melt[c]	-	-	-	2.3	7.6	**-228**	1.2	2.0	**-71**	8.1	6.2	**24**	-	-	-	11.6	15.8	**-37**
Late Spring[d]	-	-	-	4.0	2.0	**51**	4.1	1.6	**60**	1.5	1.7	**-12**	-	-	-	9.6	5.3	**45**
Summer[e]	-	-	-	7.5	4.8	**36**	0.6	0.2	**72**	0.1	0.0	**47**	-	-	-	8.1	4.9	**39**
Fall[f]	2.7	0.1	**95**	5.0	5.1	**-2**	3.4	3.5	**-4**	1.3	1.2	**5**	0.2	0.1	**67**	12.5	10.0	**20**
Total	2.7	0.1	**95**	18.7	19.4	**-4**	9.8	7.3	**25**	10.9	9.1	**17**	0.2	0.1	**67**	42.3	36.0	**15**

[a] Refers to Weir IN monitoring station, which acted as the inlet to the pond-wetland system

[b] Refers to Pond OUT, located at the end of the pond-wetland system

[c] Period between first measurement in early April to April 30, capturing the melt of accumulated snow on the ground

[d] Period between May 1 to June 20, referring to later spring season in northern hemisphere

[e] Period between June 21 to September 20, based on northern hemisphere season

[f] Period between September 21 to November 30, based on northern hemisphere season

Regression analysis supported these PP spatial and seasonal observations. TSS was the strongest and most consistent factor affecting PP across the system, being significant in 7 of the 9 regression runs (Table 4-7), confirming strong coupling between PP dynamics and particulate loading, settling, and resuspension (especially in shallower ponds). Pond depth also was also significant (p -value < 0.05) in the combined model (β: 5.8 x10^{-3}, p – value < 0.05), with elevated PP concentrations associated with shallower conditions, consistent with observations in Pond 1 and episodically at Pond 3 and Pond OUT. Seasonal temperature effects were significant in Pond 1 (p – value < 0.05), supporting biologically driven PP formation during Summer. Inflow was significant in both the combined and Pond 1 models, indicating storm-driven inflow pulses reduced settling efficiency upstream, while downstream ponds buffered these hydrologic effects. Despite several statistically significant predictors, the combined model explained a modest proportion of PP variability (R^2 = 0.2), consistent with previous treatment pond studies, where internal P cycling and legacy sediment effects contribute to PP variability (Brunet et al., 2021; Robotham et al., 2021). In contrast, regression analysis for SRP did not identify consistently significant predictors, highlighting complex, diffusion-controlled processes governing its downstream concentrations across seasons or ponds (Appendix M).

Collectively, results indicate that PP removal within the pond-wetland system was primarily driven by sedimentation, counteracted by depth-limited resuspension and biological productivity. Across the 2017-2019 study period, the overall study mean PP concentrations (Figure 4-6) at shallow Pond 1 (mean depth = 0.08 m) increased significantly by 110%, whereas the subsequent deeper Pond 2 (mean depth = 0.7 m) captured 52% of Pond 1's export (p-value < 0.05, ANOVA), returning concentrations close to Weir IN levels. Pond 3 (mean depth = 0.6, sparsely vegetated) saw no net change, suggesting that this depth and vegetation offered no additional retention. The deepest Pond 4 (mean depth = 1.3 m) further reduced PP by 15% relative to Pond 3 and 17% relative to Weir IN, achieving the study's lowest concentration = 0.08 ± 0.09 mg P/L.

SRP dynamics were governed by biological uptake during Summer and subsequent release in Fall, with sorption effective primarily under low-flow, high HRT conditions. Comparing overall mean SRP concentrations (Figure 4-7) relative to each pond's influent, shallow Pond 1 concentrations showed minimal SRP change, Pond 2 decreased by 18%, Pond 3 showed no effect and Pond 4 slightly decreased by 11%, before increasing again at Pond OUT (-17%). Despite small

insignificant differences between ponds, the greatest removal relative to Weir IN was observed at Pond 4 (27%, *p*-value<0.05, ANOVA), while Ponds 2 and 3 removed 17 to 18%, indicating only a modest depth effect.

The performance of moderately vegetated Pond OUT (~40% coverage area), contrasts with previous typical CWs or sedimentation basin + CW (Koskiaho & Puustinen, 2019; Mendes et al., 2018). In the present system, Pond 4 (1.3 m) functioned as sedimentation basin, followed by the shallow, moderately vegetated Pond OUT. However, the expected polishing effect was not consistently observed, as this pond exhibited seasonal increases in PP and/or SRP. These likely reflect episodic resuspension and seasonal turnover of accumulated organic material (Vymazal, 2013). The limited performance of Pond OUT likely reflects its shallow depth, relatively small area (and therefore reduced volume, HRT) and vegetation cover below commonly cited thresholds (> 50%) required to stabilize sediments and sustain macrophyte-mediated P processing (Kill et al., 2022; Koskiaho & Puustinen, 2019; Lavrnić, Nan, et al., 2020). Although the overall system falls within the recommended A_w:A_c of 0.5 to 2% for achieving sufficient HRT and stable flow velocities for P retention (Braskerud, 2002b; Wilcock et al., 2012), studies indicate that wetlands with low vegetated cover (<20%) remain sensitive to episodic flows and environmental fluctuations, particularly under low P loading conditions (Kill et al., 2022).

Consistent with this interpretation, Koskiaho & Puustinen (2019) reported that a wetland with an A_w:A_c of 1.3% and moderate vegetation observed large fluctuations in SRP and TP % retention ranging from -92 to 93%, primarily owing to lack of sufficient macrophyte coverage. Similar dynamics likely occurred in the present system, where shallow, moderately vegetated Pond OUT was more susceptible to sediment resuspension and algae growth. These findings suggest that establishing dense macrophyte cover early in shallow zones may be critical for improving P removal, as vegetation stabilises sediments, prevents resuspension, and suppresses algal growth (Mendes et al., 2018; Vymazal, 2013). Nevertheless, these results demonstrate that calculating system-scale removal solely between the inlet and outlet underestimates the extent of internal P processing in systems with varying depths.

Table 4-7. Multiple regression analysis of factors influencing Particulate Phosphorus (PP) concentrations across the pond-wetland system, by pond and season.

Variables[a]	Combined Model[b]	Individual Ponds					Season		
		Pond 1	Pond 2	Pond 3	Pond 4	Pond OUT	Late Spring	Summer	Fall
TSS	8.7×10^{-4} (CI: 8.7×10^{-5}, 1.3×10^{-3})****	8.4×10^{-4} (CI: 3.5×10^{-5}, 1.7×10^{-3})*	2.6×10^{-3}(CI: 7.3×10^{-4},4.4×10^{-3})**	2.2×10^{-3}(CI: 1.2×10^{-3},3.3×10^{-3})***	NS	NS	1.4×10^{-3}(CI: -2.9×10^{-4},3.8×10^{-3})*	8.4×10^{-4}(CI: -3.6×10^{-4},1.3×10^{-3})****	2.3×10^{-3}(CI: -2.5×10^{-4},4.4×10^{-3})**
1/depth	5.8×10^{-3} (CI: 8.27×10^{-4}, 0.01)**	NA	NA	NA	NA	NA	NS	NS	0.01 (CI: -1.4×10^{-4},0.02)*
Influent concentration[c]	NS	NS	NS	0.35 (CI: 0.14,0.56)**	NS	NS	0.77 (CI: 0.31, 1.23)**	NS	
Seasonal temperature	NS	8.5×10^{-3} (CI: 0.017, 8.2×10^{-4})*	NS	3.0×10^{-3}(CI: 4.7×10^{-4},5.6×10^{-3})*	NS	NS	3.2×10^{-3}(CI: -6.3×10^{-4}, 7.1×10^{-3})*	5.6×10^{-3}(CI: -0.01,6.2×10^{-4})*	NA
Inflow[d]	4.3×10^{5} (CI: 3.5×10^{-6}, 8.3×10^{-5})**	1.3×10^{-3}(CI: 4.1×10^{-5}, 0.2×10^{-4})**	NS	NS	NS	NS	NS	1.5×10^{-4}(CI: 9.4×10^{-5}, 2.1×10^{-4})*	NS
1/HRT	NS	-0.06 (CI: -0.02, -0.005)**	NS	NS	NS	NS	2.1×10^{-3}(CI: -3.4×10^{-4}, 4.3×10^{-3})*	-0.01(CI:-0.23, 3.1×10^{-5})**	NS

[a] Reduced regression listed here with variables showing statistically significant effect on PP concentration. Other variables tested, but not listed here include precipitation (day of, -1-day, -2 day), temperature (daily and monthly averages), hydraulic loading rate, soluble reactive phosphorus concentration, and windspeed.

[b] Refers to the complete study period grouped together across the system (n=237), $R^2 = 0.20$, Adjusted $R^2 = 0.17$. The regression equation is not shown, as the analysis was intended to evaluate variable effects on concentration, not for predictive modelling.

[c] Refers to effluent concentration from previous pond, which be influent of the pond in question.

[d] Refers to outflow from previous pond, which is the inflow of the pond in question.

CI refers to 95% confidence interval for beta coefficient.

Significance levels: * *p*-value <0.1, ** *p*-value < 0.05, *** *p*-value <0.01, **** *p*-value <0.001

NA indicates Not Applicable

NS indicates Not Significant (tested, *p*-value >0.1)

4.3.4.2. Phosphorus - mass load

System Inlet and Outlet Loads

Cumulative mass loads of PP and SRP at the system inlet and outlet revealed distinct seasonal and interannual patterns, reflecting the combined influence of hydrology, internal biogeochemistry, and physical settling processes (Table 4-5, 4-6). Overall, the pond-wetland system demonstrated moderate but consistent retention of PP across most years, whereas SRP was more variable, with periods of both high retention and pronounced export.

Annual PP retention ranged from 16 - 29%. Seasonal PP load changes ranged from net export (-27%) to strong retention (76%), though most periods exhibited positive retention. This indicates that sedimentation and particle-associated removal occurred under a wide range of hydrologic conditions. The strongest PP retention occurred during Summers, where PP removal (41 to 76%) increased progressively as cumulative flows decreased from 2017 to 2019 (72.0, 19.6 and 0.9 mm/ha drained, respectively). Corresponding HRTs ranged from 10 days to >550 days, favoring particle settling. In contrast, Spring-melt retention was low (< 16%), corresponding with periodic PP concentration export, reflecting high flows (69.1 to 94.9 mm/ha drained) and limited settling. The Spring-melt and Late Spring seasonality could be explained by the potential flushing of previously accumulated P under ice with high flows, while PP export in Falls of low discharge (2019 and 2021) likely suggests flush of previously settled fine sediments and seasonal turnover. In this study, PP patterns indicate that this system is capable of moderate settling but remains sensitive to internal disturbance. Notably, the 24% PP mass removal observed was much lower than the 57% TSS mass removal, suggesting phosphorus-rich fine particles are more easily suspended and transported downstream than bulk clay-based sediment (Maynard et al., 2009).

SRP loads were far more variable than PP. SRP export was observed during the Spring-melt periods of 2017 and 2018, indicating strong release from sediments combined with limited biological uptake in cold (mean temperature = 2.4 to 4.8 °C), low-light conditions (Paterson et al., 2017) and high flow. In contrast, SRP removal was generally strong in Late Spring and Summer, with retention of 36 - 72% in most years, reflecting elevated algal, microbial and macrophyte uptake and enhanced sorption capacity under warmer conditions with high HRTs. Key mechanisms for SRP retention include sorption to sediment/native soil or biological uptake (Brix, 1997; Johannesson et al., 2011; Koskiaho et al., 2003; Reddy et al., 2023). In this study, each of

these mechanisms played a role in different seasons. Annual relative SRP load retention ranged from -4 to 25% (2017 to 2019), highlighting the sensitivity of dissolved phosphorus to hydrological extremes: high flows promote SRP release and export, while stable summer conditions allow for efficient uptake and retention. Across the 2016 to 2021 (excluding 2020), approximately 15% of SRP loads were retained - lower than PP retention.

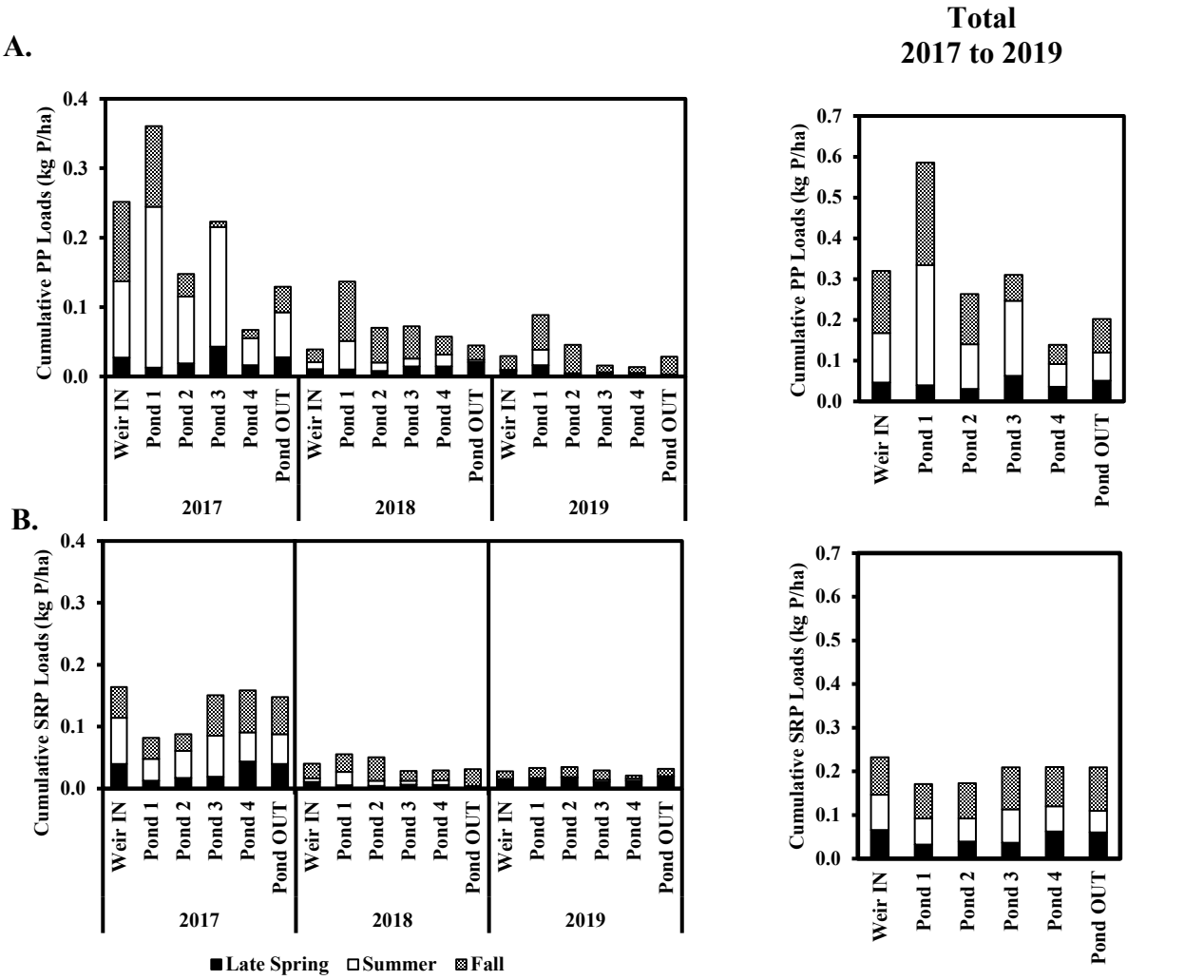

Figure 4-9. Cumulative loads across the pond-wetland system: A. Particulate phosphorus (PP) and B. Soluble reactive phosphorus (SRP) during the study (May to November 2017 to 2019) on the left and total loads at the end of 2019 on the right. Note: Reported loads correspond to the non-frozen period, which is consistent across all sites. Accordingly, Weir IN and Pond OUT include only the intervals during which grab samples were collected at the pond monitoring locations. Year 2016 is excluded because pond samples were not collected, and Year 2021 is excluded due to limited number of samples collected in Fall.

Owing to their depths, agricultural treatment ponds commonly achieve higher reductions in TP (average = 47%) (Table 4-4), largely driven by particulate sedimentation. In contrast, agricultural constructed wetlands with comparable A_w:A_c (0.8 to 1%) exhibit a wider range of

performance depending on P species, with average retentions of 30% for TP, 49% for PP, and 25% for SRP (Table 4-4). The present study, with an 18% TP load retention (PP: 24%, SRP: 15%), therefore performs comparably to the average reported in the cited studies

Internal Pond Loads

Consistent with the internal TSS load analysis, pond-specific PP and SRP loads were calculated for periods when internal pond samples were available (mid-May to mid-November). To ensure comparable time periods, Weir IN and Pond OUT loads were also calculated for this same interval, allowing consistent comparison of internal pond load variations. Figures 4-9 A and 4-9 B illustrate how retention and release processes vary along the system.

PP loads increased sharply at Pond 1 in all years, with evident increases in summer and fall, making it the dominant internal source of PP in the system due to resuspension and internal biological production. Downstream, PP loads declined progressively from Pond 2 (indicating onset of settling) through Pond 4, with largest reductions occurring at Pond 4. Increases in Pond OUT during 2017 and 2019 compared to Pond 4 suggest resuspension in the shallow partially vegetated outlet zone. Between 2017 and 2019, a cumulative load of 0.32 kg/ha entered the system at Weir IN. Pond 1 increased this load by 83% (to 0.58 kg/ha). Downstream, ponds reduced loads relative to the influent baseline by 18% at Pond 2, 12% at Pond 3 and 57% at Pond 4. However, resuspension at Pond OUT lowered the overall system retention to 37%.

SRP load reductions were more variable and year dependent. In 2017, Ponds 1 and 2 reduced SRP loads, whereas Ponds 3,4, and Pond OUT experienced increases, reflecting observed concentration patterns. In contrast, in 2018 and 2019, the pattern reversed, with increases in Ponds 1 and 2, reductions in Ponds 3 and 4 and slight increases in Pond OUT. These trends reflect the interplay of biological uptake, mineralization, and adsorption/desorption processes, influenced by seasonal hydrology. Overall, a cumulative load of 0.23 kg/ha entered the system. Relative to this baseline, Pond 1 and Pond 2 each reduced loads by 25%, while similar reductions of 9 to 10% were observed across Ponds 3 to OUT.

4.3.4.3. P mass balance across the system and design implications for P management

Treatment ponds and constructed wetland systems are typically considered net sinks for P, with long-term performance governed by the distribution of P among several storage compartments.

These include: (1) native hydric soil and deeply buried accreted sediment, which provide the most permanent storage through strongly-bound P (Dunne et al., 2006; Kadlec, 2005); (2) freshly accreted sediment, where inorganic- and organic-bound P accumulate through particulate settling and represent a moderately stable, long-term retention pathway (James et al., 2002; Uusitalo et al., 2003); (3) biological storage via uptake by macrophytes, algae and periphyton, which is generally small and transient – more characteristic of wetland zones than deeper ponds (Brix, 1997; Gottschall et al., 2007; Gu & Dreschel, 2008; Kill et al., 2022); and (4) water column, which serves as a temporary and highly labile P pool. The relative contribution of these compartments is critical for understanding long-term P retention in combined pond-wetland systems.

A conservative mass balance approach was applied to quantify net system retention (Braskerud, 2002b; Kadlec & Wallace, 2008). Between, 2016 and 2021, the pond-wetland system received about $P_{IN} = 51.4$ kg of cumulative TP mass loads via cropping system tile drainage, of which 18% ($P_{storage}$= 9.3 kg) was retained by the end of 2021 operating season (Figure 4-8). System-scale retention was defined as the difference between cumulative inflow and outflow loads:

$$P_{IN} - P_{OUT} = P_{storage} \quad \text{(Equation 4-9)}$$

The identified P storage compartments in the system include sediment, macrophytes, native soil, and the water column. Consequently, the above equation was expanded to Equation 4-10, with individual storages measured or estimated at the end of 2021 operating season. Using both equations, the unknown soil (strongly-bound P) compartment was determined.

$$P_{storage} = P_{sediment} + P_{macrophytes} + P_{soil\_plant\_available} + P_{soil\_strongly\_bound} + P_{water\ column}$$

(Equation 4-10)

Sediment mapping revealed spatial variability in accumulation across the system. Mean depths ranged from 6.0 to 10.0 cm (average 7.3 ± 2.9 cm) in Pond 1, increased at Pond 2 (11.6 ± 2.4 cm), and declined in Pond 3 (6.3 ± 1.9 cm). Interestingly, Pond 4 exhibited higher sediment accumulation (12.1 ± 3.4 cm), consistent with earlier observations that Pond 4 trapped more TSS than upstream Ponds 2 and 3. Sediment accumulation was also higher at Pond OUT (9.8 ± 1.1 cm), likely reflecting higher vegetation cover and associated plant litter. The average sediment accumulation rate was 1.7 cm/year since system was construction in 2016. Total P stored in

sediments was $P_{sediment}$ = 4.5 kg, representing 48% of retained P (storage) within the system. Thus, accumulated sediment represents the major sink for P in this low-P system. The water column represents the transient PP and SRP moving through the system, acting as a temporary conduit for P transfer to plants, sediment, and biota (Kadlec, 2005). This compartment represented only 7.2% of retained P, $P_{water\ column}$= 0.3 kg.

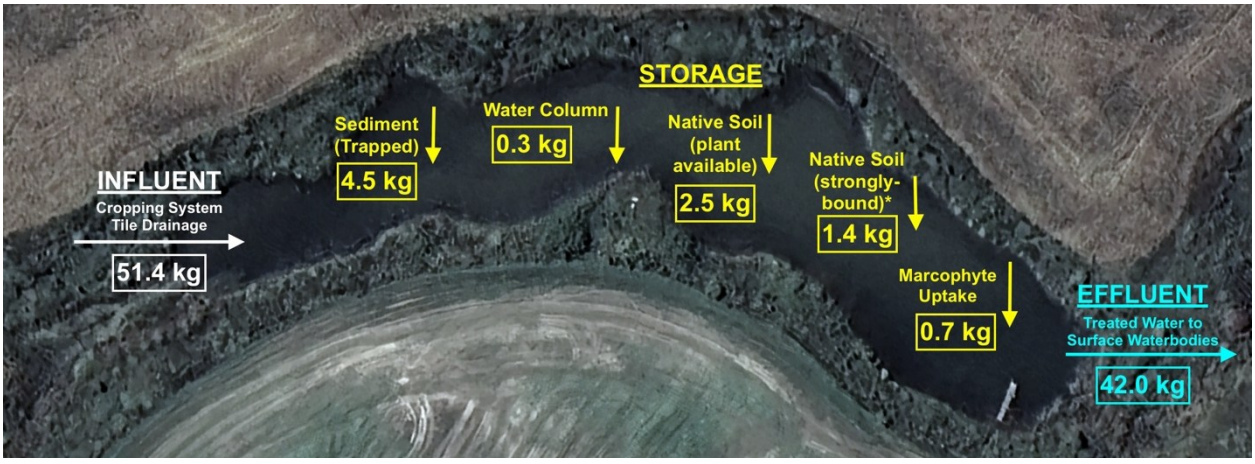

Figure 4-10. Total phosphorus mass balance across the pond-wetland system at the end of the study (2016 to 2021). Note: In 2020, field sampling was not carried out due to COVID-19 restrictions. TP values from year 2018 was used to calculate the total mass balance as weather conditions were similar in both the years and had the strongest correlation (R=0.9). *Native soil (strongly-bound) was estimated from the mass balance.

Wetland vegetation was allowed to establish naturally in this system, with *Typha latifolia* colonizing only at Pond 3 and Pond OUT, with densities of 29±2 and 31±3 plants/ m^2 and occupying about 2% and 40% of each pond area, respectively. *Juncus effusus,* was also present along the shoreline margins, occupying 10% and 4% of areas at Pond 3 and Pond OUT. These coverage values are considerably lower than > 50% typically reported in agricultural wetlands (Kill et al., 2022; Koskiaho & Puustinen, 2019; Lavrnić, Nan, et al., 2020) Above-ground P content (uptake) in *T.latifolia* ranged from 1.4 to 1.8 g/m^2 at Pond 3 and 2.7 to 4.0 g/m^2 at Pond OUT . *J. effusus* exhibited much lower P contents (0.2 to 0.4 g/m^2 at both ponds), suggesting *T.latifolia* at Pond OUT played a proportionally greater role in SRP uptake. These values were consistent with the reported ranges of 1.4 to 3.8 g/m^2 (Dunne et al., 2006; Gottschall et al., 2007; Lavrnić, Nan, et al., 2020). Total macrophyte uptake was 0.7 kg ($P_{macrophytes}$, 7.2%), which is considerably lower than values reported by Lavrnić, Nan, et al. (2020) and Vymazal et al. (2023) (14.1 to 21.9 kg), likely reflecting the low vegetation cover in this system.

The top 15-25 cm of the native soil was collected at the edges of each pond and partitioned

into 3 to 5 samples (in increments of 5 cm) to generate a soil P profile. A consistent declining trend of plant-available P with depth was observed in all ponds, suggesting that the upper soil layers provide more active sites for P sorption. The upper 0 -10 cm is reported to contain the highest total and liable P, resulting from active deposition, sorption, biological cycling, and redox processes (VanZomeren et al., 2020). Among the ponds, the highest P concentrations were observed at Pond OUT (12.9 to 9.7 mg/kg from top to bottom), followed by Pond 4 (11.3 mg/kg to 8.04 mg/kg), then Pond 1 (9.0 mg/kg to 7.6 mg/kg) while Pond 2 and Pond 3 exhibited similar profiles (5.1 mg/kg to 3.24 mg/kg). The observed values were below average of the range (0.1 to 30.5 mg/kg reported by VanZomeren et al. (2020), Lavrnić, Nan, et al. (2020) and Passoni et al. (2009) in CWs. In a comprehensive study in Ontario, Wang et al. (2015) reported an Olsen P and Qmax (parameters that measure soil's plant available P and maximum long-term P retention capacity) as of 42.4 mg/kg and 225 mg/kg, respectively for clay soils. Although the P storage capacity of wetland soils varies spatially and temporally as a function of clay content, organic matter, redox status, Al, Fe, Ca concentrations, soil pH, and land use history (Hansen et al., 2002; Reddy et al., 2023), the study by Wang et al. (2015) provides a cautious, but useful reference. Comparing to these values, plant-available P in this system was relatively low, suggesting that the soils are not close to P saturation. In this study, plant-available P in soil represented approximately 27% of total stored P ($P_{soil\_plant\_available} = 2.5$ kg).

Strongly-bound soil P ($P_{soil\_strongly\_bound}$) was estimated to be 1.4 kg, accounting for approximately 15% of total stored P. This fraction constitutes the third largest and represents the most stable long-term P pool within the pond-wetland system. The mass balance quantifies net P retention, however, seasonal reversals in PP and SRP loads and spatial redistribution among storage compartments, indicates that P undergoes considerable internal transfer among sediments, soil, biota, and the water column, rather than unidirectional accumulation.

The analysis of P concentration, mass load, and mass balance in this study clearly indicates that PP and SRP fractions are governed by distinct mechanism. PP retention was primarily governed by sedimentation, moderated by resuspension in shallow ponds and biological productivity. Shallow ponds (depths of 0.08 m and 0.3 m) with minimal to moderate vegetation, acted as internal sources of PP, and whereas deeper ponds (0.7 m and 1.3 m) consistently reduced PP concentrations and loads across hydrologic conditions. Because PP is solid-bound P, sediment

storage and dredging design criteria for TSS are applicable: a 20-year interval between dredging events would require a sediment storage depth of 0.34 - 0.40 m (Miller et al., 2025; TRCA & CH2M, 2016). Accordingly, a deeper pond (≥1.3 m) would be a defensible design approach for controlling particulate-associated P. This corresponds to Ontario's Environmental Design Criteria 3.0 for wet-ponds recommending mean depth varying between 1 to 2 m, to minimize re-suspension, prevent thermal stratification, reduce the risk of anoxic P release (OMECP, 2017).

SRP behavior, by contrast, was highly variable seasonally and annually. Regression analyses also did not identify consistent physical controls (depth, surface area, HRT), highlighting SRP dynamics are dominated by internal biological and geochemical processes, including biological uptake, release, and sediment sorption. Although the system meets typical CW and treatment pond design guidelines, such as A_w:A_c = 0.93% (recommended 0.5 to 2%), system HRT = 7.9 days (recommended at least of 7 days) (Reinhardt et al., 2005; Wilcock et al., 2012), SRP retention alternated with periods of export. The shallow, moderately vegetated Pond OUT, which functioned as a wetland cell, provided limited SRP benefit.

Compared to studies in Table 4-4, the inherently low influent P concentrations and loads from this system further constrain treatment performance. It is likely that the background SRP concentration (C*) within the pond-wetland system fell within the range of influent SRP concentration, thereby reducing the net adsorption of SRP (Wang et al., 2015). Additionally, under these conditions, relatively small internal fluxes - such as sediment resuspension, biological uptake/release, or sorption - can exceed net retention, generating complex spatial and seasonal variations in P concentrations and loads. Overall, the pond-wetland system achieved modest retentions (14 to 22% for concentrations, 15 to 24% for loads) indicating limited potential for meaningful P reduction, especially for SRP. Deeper pond designs are expected to improve PP retention, while SRP retention is largely considered as an areal-based process (Braskerud, 2002; Reddy et al., 2023). In principle, increasing the system surface area (A_w:A_c ~ 2) or vegetation density (> 50% of coverage) could offer incremental benefits, but under the low influent P conditions observed, may not be justified from a management perceptive. The findings of this study do not support recommending pond-wetland systems as a reliable BMP for P management, and alternative or complementary strategies should be considered. Deeper pond designs are expected to improve PP retention.

4.4. Conclusion

The study evaluated the efficacy of a pond-wetland system, with mean depths ranging from 0.08 to 1.3 m for treating tile drainage from a cropping system in a cold-climate region. Over five years, the system achieved significant total suspended solids (TSS) retention, reducing concentrations by 49%, and mass load by 59%, primarily through sedimentation. Deeper ponds (0.7 and 1.3 m) provided consistent TSS retention across hydrologic conditions. The consistency observed among internal pond performance, normalized sediment storage comparisons, and established design benchmarks suggests a single, deeper pond configuration (mean depth = 1.3 m, surface area-to-catchment ratio ≥ 0.5%, volume ≥ 67.4 m^3/ ha drained) would be sufficient to achieve effective TSS retention. In contrast, the shallow inlet pond (0.01 m, unvegetated), and shallow outlet wetland cell (0.3 m, moderately vegetated), frequently acted as internal sources of TSS and particulate phosphorus (PP) due to sediment resuspension and enhanced algae growth. Soluble reactive phosphorus (SRP) exhibited pronounced seasonal and interannual variability, largely governed by internal biological and geochemical processes, rather than physical design factors such as depth, surface area, or hydraulic retention time. Seasonal patterns were evident, with the highest TSS, PP concentrations occurring during Summer, while SRP concentrations peaked in Late Spring. Long-term mass balance analysis identified sediments as the dominant long-term P sink, accounting for nearly half of retained P, followed by plant-available soil, strongly-bound soil pools, and minimum storage in macrophytes. Overall, the pond-wetland system achieved modest net P retention (14-22% by concentrations, 15-24% by loads), indicating limited potential for meaningful P reduction, especially for SRP. Based on the relatively low P loading and the reductions observed, this study does not support recommending pond-wetland systems as a reliable BMP for P management, especially SRP, and alternative or complementary strategies should be considered.

References

Agricrop. (2023). *Monthly Rainfall Data*. https://www.agricorp.com/en-ca/Programs/ProductionInsurance/ForageRainfall/Pages/RainfallData.aspx

APHA. (2017). *Standard Methods for the Examination of Water and Wastewater* (23rd ed.). American Public Health Association.

Arheimer, B., & Pers, B. C. (2017). Lessons learned? Effects of nutrient reductions from constructing wetlands in 1996–2006 across Sweden. *Ecological Engineering*, *103*, 404–414. https://doi.org/10.1016/j.ecoleng.2016.01.088

Beckingham, B., Callahan, T., & Vulava, V. (2019). Stormwater Ponds in the Southeastern U.S. Coastal Plain: Hydrogeology, Contaminant Fate, and the Need for a Social-Ecological Framework. *Frontiers in Environmental Science*, *7*(July), 1–14. https://doi.org/10.3389/fenvs.2019.00117

Beutel, M. W., Newton, C. D., Brouillard, E. S., & Watts, R. J. (2009). Nitrate removal in surface-flow constructed wetlands treating dilute agricultural runoff in the lower Yakima Basin, Washington. *Ecological Engineering*, *35*(10), 1538–1546. https://doi.org/https://doi.org/10.1016/j.ecoleng.2009.07.005

Blankenberg, A. G. B., Haarstad Ketil, K., & Paruch, A. M. (2015). Agricultural Runoff in Norway: The Problem, the Regulations, and the Role of Wetlands. *The Role of Natural and Constructed Wetlands in Nutrient Cycling and Retention on the Landscape*, 137–147. https://doi.org/10.1007/978-3-319-08177-9_10

Braskerud, B. C. (2002). Factors affecting phosphorus retention in small constructed wetlands treating agricultural non-point source pollution. *Ecological Engineering*, *19*(1), 41–61. https://doi.org/10.1016/S0925-8574(02)00014-9

Braskerud, B. C., Tonderski, K. S., Wedding, B., Bakke, R., Blankenberg, A. -G. B., Ulén, B., & Koskiaho, J. (2005). Can constructed wetlands reduce the diffuse phosphorus loads to eutrophic water in cold temperate regions? *Journal of Environmental Quality*, *34*(6), 2145–2155. https://doi.org/10.2134/JEQ2004.0466

Brix, H. (1997). Do macrophytes play a role in constructed treatment wetlands? *Water Science and Technology*, *35*(5), 11–17. https://doi.org/10.1016/S0273-1223(97)00047-4

Brunet, C. E., Gemrich, E. R. C., Biedermann, S., Jacobson, P. J., Schilling, K. E., Jones, C. S., & Graham, A. M. (2021). Nutrient capture in an Iowa farm pond: Insights from high-frequency observations. *Journal of Environmental Management*, *299*. https://doi.org/10.1016/j.jenvman.2021.113647

CCME. (1999). *Canadian Environmental Quality Guidelines - Suspended sediments* (pp. 1–2). CCME.

CCME. (2004). Phosphorus: Canadian Guidance Framework for the Management of Freshwater Systems. In *Canadian Water Quality Guidelines for the Protection of Aquatic Life*.

Chrétien, F., Gagnon, P., Thériault, G., & Guillou, M. (2016). Performance Analysis of a Wet-Retention Pond in a Small Agricultural Catchment. *Journal of Environmental Engineering*, *142*(4), 04016005. https://doi.org/10.1061/(asce)ee.1943-7870.0001081

Chun, J. A., & Cooke, R. A. (2008). Calibrating Agridrain Water Level Control Structures using generalised Weir and Orifice equations. *Applied Engineering in Agriculture*, *24*(5), 595–602.

Clary, J., Leisenring, M., & Strecker, E. (2020). *International Stormwater BMP Database: 2020 Summary Statistics*. www.waterrf.org

Coelho, B. B., Bruin, A. J., Staton, S., & Hayman, D. (2020). Sediment and Nutrient Contributions from Subsurface Drains and Point Sources to an Agricultural Watershed. *Https://Doi.Org/10.1177/ASWR.S4471*, *3*(1). https://doi.org/10.1177/ASWR.S4471

Díaz, F. J., Ogeen, A. T., & Dahlgren, R. A. (2012). Agricultural pollutant removal by constructed wetlands: Implications for water management and design. *Agricultural Water Management*, *104*, 171–183. https://doi.org/10.1016/j.agwat.2011.12.012

Dumanski, S., Pomeroy, J. W., & Westbrook, C. J. (2015). Hydrological regime changes in a Canadian Prairie basin. *Hydrological Processes*, *29*(18), 3893–3904. https://doi.org/10.1002/HYP.10567;REQUESTEDJOURNAL:JOURNAL:10991085;WGROUP:STRING:PUBLICATION

Dunne, E. J., Coveney, M. F., Marzolf, E. R., Hoge, V. R., Conrow, R., Naleway, R., Lowe, E. F., & Battoe, L. E. (2012). Efficacy of a large-scale constructed wetland to remove phosphorus and

suspended solids from Lake Apopka, Florida. *Ecological Engineering*, *42*, 90–100. https://doi.org/10.1016/J.ECOLENG.2012.01.019

Dunne, E. J., Culleton, N., O'Donovan, G., Harrington, R., & Daly, K. (2005). Phosphorus retention and sorption by constructed wetland soils in Southeast Ireland. *Water Research*, *39*(18), 4355–4362. https://doi.org/https://doi.org/10.1016/j.watres.2005.09.007

Dunne, E. J., Reddy, R., Clark, & Mark W. (2006). Biogeochemical indices of phosphorus retention and release by wetland soils and adjacent stream sediments. *Wetlands*, *26*(4), 1026–1041. https://doi.org/10.1672/0277

ECCC. (2023). *Daily Data Report - Climate - Environment and Climate Change Canada*. https://climate.weather.gc.ca/climate_data/daily_data_e.html?StationID=49568

ECCC. (2024). *Daily Data Report for Moose Creek Wells Weather Station - Climate*. Environment and Climate Change Canada. https://climate.weather.gc.ca/historical_data/search_historic_data_e.html

ECCC. (2025). *Canadian Climate Normals 1991-2020 Data for Ottawa (Airport)*. Https://Climate.Weather.Gc.ca/Climate_normals/Index_e.Html.

ECCC, & IJC. (2012). *Great Lakes Water Quality Agreement*.

ECCC, & OMECP. (2018). *Canada-Ontario Lake Erie action plan : Partnering on achieving phosphorous loading reductions to Lake Erie from Canadian sources* (Number February).

FAOSTAT. (2025). *Cropland Nutrient Balance*. Food and Agriculture Organization of the United Nations (FAO). https://www.fao.org/faostat/en/#data/ESB/visualize

Fiener, P., Auerswald, K., & Weigand, S. (2005). Managing erosion and water quality in agricultural watersheds by small detention ponds. *Agriculture, Ecosystems and Environment*, *110*(3–4), 132–142. https://doi.org/10.1016/j.agee.2005.03.012

Fortier, R. (2022). *Seasonal trends in phosphorus export from three major Canadian Lake Erie tributaries* [McMaster Univeristy]. http://hdl.handle.net/11375/28275

GLSAB, & GLWQB. (2023). *Nutrients in Lake Erie and Lake Ontario: Synthesis of International Joint Commission Recommendations and Assessment of Domestic Action Plans*. https://www.ijc.org/sites/default/files/SAB_WQB_NutrientSynthesisReport_2023.pdf

Gottschall, N., Boutin, C., Crolla, A., Kinsley, C., & Champagne, P. (2007). The role of plants in the removal of nutrients at a constructed wetland treating agricultural (dairy) wastewater, Ontario, Canada. *Ecological Engineering*, *29*(2), 154–163. https://doi.org/10.1016/j.ecoleng.2006.06.004

Gu, B., & Dreschel, T. (2008). Effects of plant community and phosphorus loading rate on constructed wetland performance in Florida, USA. *Wetlands*, *28*(1), 81–91. https://doi.org/10.1672/07-24.1/METRICS

Hansen, N. C., Daniel, T. C., Sharpley, A. N., & Lemunyon, J. L. (2002). The fate and transport of phosphorus in agricultural systems. *Journal of Soil and Water Conservation*, *57*(6), 408–416. https://doi.org/10.1080/00224561.2002.12457473

Harper, H. H., & Baker, D. M. (2007). *Evaluation of Current Stormwater Design Criteria within the State of Florida: Final Report*.

Healy, M., & Cawley, A. M. (2002). Nutrient Processing Capacity of a Constructed Wetland in Western Ireland. *Journal of Environmental Quality*, *31*(5), 1739–1747. https://doi.org/10.2134/JEQ2002.1739;WGROUP:STRING:PUBLICATION

James, W. F., Barko, J. W., Eakin, H. L., Jamesa, W. F., Barkoaeb, J. W., & Eakina, H. L. (2002). Labile and refractory forms of phosphorus in runoff of the redwood river basin, minnesota. *Journal of Freshwater Ecology*, *17*(2), 297–304. https://doi.org/10.1080/02705060.2002.9663898

Jamieson, A., Madramootoo, C. A., & Enright, P. (2003). Phosphorus losses in surface and subsurface runoff from a snowmelt event on an agricultural field in Quebec. *Canadian Biosystems Engineering / Le Genie Des Biosystems Au Canada*, *45*.

Jarvie, H. P., Johnson, L. T., Sharpley, A. N., Smith, D. R., Baker, D. B., Bruulsema, T. W., & Confesor, R. (2017). Increased Soluble Phosphorus Loads to Lake Erie: Unintended Consequences of Conservation Practices? *Journal of Environmental Quality*, *46*(1), 123–132.

Johannesson, K. M., Andersson, J. L., & Tonderski, K. S. (2011). Efficiency of a constructed wetland for retention of sediment-associated phosphorus. *Hydrobiologia*, *674*(1), 179–190. https://doi.org/10.1007/s10750-011-0728-y

Johannesson, K. M., Kynkäänniemi, P., Ulén, B., Weisner, S. E. B., & Tonderski, K. S. (2015). Phosphorus and particle retention in constructed wetlands—A catchment comparison. *Ecological Engineering*, *80*, 20–31. https://doi.org/10.1016/J.ECOLENG.2014.08.014

Jones, J., Clary, J., Strecker, E., Quigley. M., & Moeller, J. (2012, March 1). *BMP Effectiveness for Nutrients, Bacteria, Solids, Metals, and Runoff Volume | Stormwater Solutions*. Stormwater Solutions. https://www.stormwater.com/bmps/article/13006936/bmp-effectiveness-for-nutrients-bacteria-solids-metals-and-runoff-volume

Kadlec, R. H. (2005). Phosphorus removal in emergent free surface wetlands. *Journal of Environmental Science and Health - Part A Toxic/Hazardous Substances and Environmental Engineering*, *40*(6–7), 1293–1306. https://doi.org/10.1081/ESE-200055832

Kadlec, R. H., & Wallace, S. D. (2008). *Treatment Wetlands* (Second). Taylor & Francis Group, LLC.

Kill, K., Grinberga, L., Koskiaho, J., Mander, Ü., Wahlroos, O., Lauva, D., Pärn, J., & Kasak, K. (2022). Phosphorus removal efficiency by in-stream constructed wetlands treating agricultural runoff: Influence of vegetation and design. *Ecological Engineering*, *180*. https://doi.org/10.1016/j.ecoleng.2022.106664

King, K., Williams, M., & Fausey, N. (2015). Contributions of Systematic Tile Drainage to Watershed-Scale Phosphorus Transport. *Journal of Environmental Quality*, *44*(2), 486–494. https://doi.org/10.2134/jeq2014.04.0149

Koch, B. J., Febria, C. M., Gevrey, M., Wainger, L. A., & Palmer, M. A. (2014). Nitrogen Removal by Stormwater Management Structures: A Data Synthesis. *JAWRA Journal of the American Water Resources Association*, *50*(6), 1594–1607. https://doi.org/10.1111/JAWR.12223

Kokulan, V., Macrae, M. L., Lobb, D. A., & Ali, G. A. (2019). Contribution of Overland and Tile Flow to Runoff and Nutrient Losses from Vertisols in Manitoba, Canada. *Journal of Environmental Quality*, *48*(4), 959–965. https://doi.org/https://doi.org/10.2134/jeq2019.03.0103

Koskiaho, J., Ekholm, P., Räty, M., Riihimäki, J., & Puustinen, M. (2003). Retaining agricultural nutrients in constructed wetlands—experiences under boreal conditions. *Ecological Engineering*, *20*(1), 89–103. https://doi.org/https://doi.org/10.1016/S0925-8574(03)00006-5

Koskiaho, J., & Puustinen, M. (2019). Suspended solids and nutrient retention in two constructed wetlands as determined from continuous data recorded with sensors. *Ecological Engineering*, *137*, 65–75. https://doi.org/10.1016/j.ecoleng.2019.04.006

Kottek, M., Grieser, J., Beck, C., Rudolf, B., & Rubel, F. (2006). World map of the Köppen-Geiger climate classification updated. *Meteorologische Zeitschrift*, *15*(3), 259–263. https://doi.org/10.1127/0941-2948/2006/0130

Kovacic, D. A., David, M. B., Gentry, L. E., Starks, K. M., & Cooke, R. A. (2000). Effectiveness of Constructed Wetlands in Reducing Nitrogen and Phosphorus Export from Agricultural Tile Drainage. *Journal of Environmental Quality*, *29*(4), 1262–1274. https://doi.org/10.2134/jeq2000.00472425002900040033x

Kovacic, D. A., Twait, R. M., Wallace, M. P., & Bowling, J. M. (2006). Use of created wetlands to improve water quality in the Midwest—Lake Bloomington case study. *Ecological Engineering*, *28*(3), 258–270. https://doi.org/https://doi.org/10.1016/j.ecoleng.2006.08.002

Krzeminska, D., Blankenberg, A.-G. B., Bechmann, M., & Deelstra, J. (2023). The effectiveness of sediment and phosphorus removal by a small constructed wetland in Norway: 18 years of monitoring and perspectives for the future. *Catena*, *223*, 106962. https://doi.org/10.1016/j.catena.2023.106962

Kulin, G., & Compton, P. R. (1979). A guide to methods and standards for the measurement of water flow. In *National Bureau of Standards, U.S. Department of Commerce* (Number 421). https://nvlpubs.nist.gov/nistpubs/Legacy/SP/nbsspecialpublication421.pdf

Kynkäänniemi, P., Ulén, B., Torstensson, G., & Tonderski, K. S. (2013). Phosphorus retention in a newly constructed wetland receiving agricultural tile drainage water. *Journal of Environmental Quality*, *42*(2), 596–605. https://doi.org/10.2134/jeq2012.0266

Land, M. R., & Lu, L. (2016). An Upper Bound on the Burning Number of Graphs. *Lecture Notes in Computer Science (Including Subseries Lecture Notes in Artificial Intelligence and Lecture Notes in Bioinformatics)*, *10088 LNCS*, 1–8. https://doi.org/10.1007/978-3-319-49787-7_1

Lavrnić, S., Alagna, V., Iovino, M., Anconelli, S., Solimando, D., & Toscano, A. (2020). Hydrological and hydraulic behaviour of a surface flow constructed wetland treating agricultural drainage water in northern Italy. *Science of the Total Environment*, *702*. https://doi.org/10.1016/j.scitotenv.2019.134795

Lavrnić, S., Nan, X., Blasioli, S., Braschi, I., Anconelli, S., & Toscano, A. (2020). Performance of a full scale constructed wetland as ecological practice for agricultural drainage water treatment in Northern Italy. *Ecological Engineering*, *154*. https://doi.org/10.1016/j.ecoleng.2020.105927

Lawrence, A. I., Marsalek, J., Ellis, J. B., & Urbonas, B. (1996). Stormwater detention & BMPs. *Journal of Hydraulic Research*, *34*(6), 799–813. https://doi.org/10.1080/00221689609498452

Marques, P., & Mandrak, N. E. (2024). Ecosystem Functions in Urban Stormwater Management Ponds: A Scoping Review. *Sustainability*, *16*(17), 7766. https://doi.org/10.3390/SU16177766/S1

Mathew, K. R. (2020). *A field-scale study of controlled tile drainage and a pond-wetland to attenuate nutrients from agricultural overland runoff and subsurface drainage on a farmer-operated seed farm in Saint-Isidore, ON* [University of Ottawa]. http://dx.doi.org/10.20381/ruor-26264

Maynard, J. J., O'Geen, A. T., & Dahlgren, R. A. (2009). Bioavailability and fate of phosphorus in constructed wetlands receiving agricultural runoff in the San Joaquin Valley, California. *Journal of Environmental Quality*, *38*(1), 360–372. https://doi.org/10.2134/JEQ2008.0088

Mendes, L. R. D., Tonderski, K., Iversen, B. V., & Kjaergaard, C. (2018). Phosphorus retention in surface-flow constructed wetlands targeting agricultural drainage water. *Ecological Engineering*, *120*, 94–103. https://doi.org/10.1016/j.ecoleng.2018.05.022

Michalak, A. M., Anderson, E. J., Beletsky, D., Boland, S., Bosch, N. S., Bridgeman, T. B., Chaffin, J. D., Cho, K., Confesor, R., Daloglu, I., DePinto, J. V., Evans, M. A., Fahnenstiel, G. L., He, L., Ho, J. C., Jenkins, L., Johengen, T. H., Kuo, K. C., LaPorte, E., … Zagorski, M. A. (2013). Record-setting algal bloom in Lake Erie caused by agricultural and meteorological trends consistent with expected future conditions. *Proceedings of the National Academy of Sciences of the United States of America*, *110*(16), 6448–6452. https://doi.org/10.1073/PNAS.1216006110/SUPPL_FILE/PNAS.201216006SI.PDF

Miller, B. K., Macgowan, B. J., & Reaves, R. P. (2025). *Are Constructed Wetlands a Viable Option for Your Waste Management System?* Department of Forestry and Natural Resources, Purdue University. https://extension.purdue.edu/extmedia/FNR/FNR-202.pdf

MOEE. (1994). *Water management: policies, guidelines, provincial water quality objectives | Ontario.ca*. https://www.ontario.ca/page/water-management-policies-guidelines-provincial-water-quality-objectives#section-13

Mohamed, M. N., Wellen, C., Parsons, C. T., Taylor, W. D., Arhonditsis, G., Chomicki, K. M., Boyd, D., Weidman, P., Mundle, S. O. C., Van Cappellen, P., Sharpley, A. N., & Haffner, D. G. (2019). Understanding and managing the re-eutrophication of Lake Erie: Knowledge gaps and research priorities. *Https://Doi.Org/10.1086/705915*, *38*(4), 675–691. https://doi.org/10.1086/705915

Nietch, C. T., Borst, M., & O'Shea, M. L. (2001). Stormwater treatment: Ponds vs. constructed wetlands. *Proceedings of the Engineering Foundation Conference*, *263*(Ms 104), 524–528. https://doi.org/10.1061/40602(263)39

Nilsson, J. E., Weisner, S. E. B., & Liess, A. (2023). Wetland nitrogen removal from agricultural runoff in a changing climate. *Science of the Total Environment*, *892*(2023). https://doi.org/10.1016/j.scitotenv.2023.164336

NRCC. (2024, November 21). *When do the seasons start?* Government of Canada. https://nrc.canada.ca/en/certifications-evaluations-standards/canadas-official-time/3-when-do-seasons-start

Oduor, B. O., Campo-Bescós, M. Á., Lana-Renault, N., Kyllmar, K., Mårtensson, K., & Casalí, J. (2023). Quantification of agricultural best management practices impacts on sediment and phosphorous export in a small catchment in southeastern Sweden. *Agricultural Water Management*, *290*, 108595. https://doi.org/10.1016/J.AGWAT.2023.108595

OMAFA. (2002). *Nutrient Management Act, 2002, S.O. 2002, c. 4 | ontario.ca*. OMAFA. OMAFA. https://www.ontario.ca/laws/statute/02n04

OMAFA, & OSCIA. (2019). *ONFARM applied research and monitoring*. OSCIA. https://www.ontariosoilcrop.org/onfarm/

OMECP. (2014, August 25). *Blue-green algae | ontario.ca*. Ontario Ministry of the Environment, Conservation and Parks. https://www.ontario.ca/page/blue-green-algae

OMECP. (2017). *Environmental design criteria | Stormwater Management Planning and Design Manual | ontario.ca*. https://www.ontario.ca/document/stormwater-management-planning-and-design-manual-0/environmental-design-criteria

OMECP. (2024). *Canada-Ontario Lake Erie Action Plan: 2024 Evaluation and Update Report*.

Onset Computer Cooperation. (2008). Barometric Compensation Assistant. In *White Paper Series*.

OSCIA. (2023). *Lake Erie Agriculture Demonstrating Sustainability* . OSCIA. https://www.ontariosoilcrop.org/lake-erie-agriculture-demonstrating-sustainability/

Passoni, M., Morari, F., Salvato, M., & Borin, M. (2009). Medium-term evolution of soil properties in a constructed surface flow wetland with fluctuating hydroperiod in North Eastern Italy. *Desalination*, *246*(1–3), 215–225. https://doi.org/10.1016/J.DESAL.2008.02.041

Paterson, A. M., Rühland, K. M., Anstey, C. V., & Smol, J. P. (2017). Climate as a driver of increasing algal production in Lake of the Woods, Ontario, Canada. *Lake and Reservoir Management*, *33*(4), 403–414. https://doi.org/10.1080/10402381.2017.1379574

Que, Z., Seidou, O., Droste, R. L., Wilkes, G., Sunohara, M., Topp, E., & Lapen, D. R. (2015). Using AnnAGNPS to Predict the Effects of Tile Drainage Control on Nutrient and Sediment Loads for a River Basin. *Journal of Environmental Quality*, *44*(2), 629–641. https://doi.org/10.2134/JEQ2014.06.0246

Rabalais, N. N., Turner, R. E., & Wiseman, W. J. (2002). Gulf of Mexico Hypoxia, A.K.A. "The Dead Zone." *Annual Review of Ecology and Systematics*, *33*(1), 235–263. https://doi.org/10.1146/annurev.ecolsys.33.010802.150513

Reddy, K. R., DeLaune, R. D., & Inglett, P. W. (2023). *Biogeochemistry of Wetlands* (2nd ed.). CRC Press.

Reddy, K. R., Kadlec, R. H., Flaig, E., & Gale, P. M. (1999). Streams and Wetlands: A Review. *Critical Reviews in Environmental Science and Technology*, *29*(1), 83–146.

Reinhardt, M., Gächter, R., Wehrli, B., & Müller, B. (2005). Phosphorus retention in small constructed wetlands treating agricultural drainage water. *Journal of Environmental Quality*, *34*(4), 1251–1259. https://doi.org/10.2134/jeq2004.0325

Robotham, J., Old, G., Rameshwaran, P., Sear, D., Gasca-Tucker, D., Bishop, J., Old, J., & McKnight, D. (2021). Sediment and Nutrient Retention in Ponds on an Agricultural Stream: Evaluating Effectiveness for Diffuse Pollution Mitigation. *Water 2021, Vol. 13, Page 1640*, *13*(12), 1640. https://doi.org/10.3390/W13121640

Rushton, B. T., & Bahk, B. M. (2001). Treatment of stormwater runoff from row crop farming in Ruskin, Florida. *Water Science and Technology*, *44*(11–12), 531–538. https://doi.org/10.2166/wst.2001.0876

SC DHEC. (2005). *South Carolina Storm Water Management BMP Handbook*. https://scdhec.gov/Environment/WaterQuality/Stormwater/BMPHandbook/

Schindler, D. W. (1977). Evolution of phosphorus limitation in lakes. *Science*, *195*(4275), 260–262. https://doi.org/10.1126/SCIENCE.195.4275.260/ASSET/CD9751DC-20A9-484E-85E8-F0881327FF27/ASSETS/SCIENCE.195.4275.260.FP.PNG

Schueler, T., & Holland, H. (2000). *Article 65: Irreducible Pollutant Concentrations Discharged From Stormwater Practices*. https://owl.cwp.org/mdocs-posts/elc_pwp65/

SJRRP. (2006). *San Joaquin River Restoration Program*. https://www.restoresjr.net/about/background-and-history/

SNCA. (2023). *State of the Nation - Watershed Report Card 2023*.

SNCA. (2025a). *Clean Water Program*. www.nation.on.ca/fr/programme-dassainissement-de-leau

SNCA. (2025b). *SNC Public Geoportal - Jurisdiction*. https://camaps.maps.arcgis.com/apps/webappviewer/index.html?id=7223f276b67c42e0959c1d0727f30a77

Statista. (2024, December 2). *Canada: fertilizer consumption by nutrient* . Statists Research Department. https://www.statista.com/statistics/1330033/canada-fertilizer-consumption-by-nutrient/

Stokes, G. G. (1851). On the effect of the internal friction of fluids on the motion of pendulums. *Transactions of the Cambridge Philosophical Society*, 8–106.

Tanner, C. C., & Sukias, J. P. S. (2011). Multiyear Nutrient Removal Performance of Three Constructed Wetlands Intercepting Tile Drain Flows from Grazed Pastures. *Journal of Environmental Quality*, *40*(2), 620–633. https://doi.org/10.2134/jeq2009.0470

Tedeschi, A. C., Fortier, R. A., & Chow-Fraser, P. (2024). Effects of increasing tile drainage and seasonal weather patterns on phosphorus loading from three major Canadian Lake Erie tributaries. *Journal of Great Lakes Research*, *50*(5), 102396. https://doi.org/10.1016/J.JGLR.2024.102396

Tellier, J. M., Kalejs, N. I., Leonhardt, B. S., Cannon, D., Höök, T. O., & Collingsworth, P. D. (2022). Widespread prevalence of hypoxia and the classification of hypoxic conditions in the Laurentian Great Lakes. *Journal of Great Lakes Research*, *48*(1), 13–23. https://doi.org/10.1016/J.JGLR.2021.11.004

Tolomio, M., Ferro, N. D., & Borin, M. (2019). Multi-year N and P removal of a 10-year-old surface flow constructed wetland treating agricultural drainage waters. *Agronomy*, *9*(4). https://doi.org/10.3390/agronomy9040170

TRCA, & CH2M. (2016). *Inspection and Maintenance Guide for Stormwater Management Ponds and Constructed Wetlands*. https://sustainabletechnologies.ca/app/uploads/2018/04/SWMFG2016_Guide_April-2018.pdf

Ulén, B., Geranmayeh, P., Blomberg, M., & Bieroza, M. (2019). Seasonal variation in nutrient retention in a free water surface constructed wetland monitored with flow-proportional sampling and optical sensors. *Ecological Engineering*, *139*. https://doi.org/10.1016/j.ecoleng.2019.105588

U.S. DOI. (2015). *Everglades Restoration Initiatives*. https://www.evergladesrestoration.gov/

US EPA. (2009). *Stormwater Wet Pond and Wetland Management Guidebook, February 2009*. www.stormwatercenter.net

USBR. (2001). *Water measurement manual: A Guide to Effective Water Measurement Practices for Better Water Management, 3rd ed.* https://www.usbr.gov/tsc/techreferences/mands/wmm/index.htm

USGS. (2006). *Wentworth grain size chart*. https://pubs.usgs.gov/of/2006/1195/htmldocs/images/chart.pdf

Uusitalo, R., Turtola, E., Puustinen, M., Paasonen-Kivekäs, M., & Uusi-Kämppä, J. (2003). Contribution of Particulate Phosphorus to Runoff Phosphorus Bioavailability. *Journal of Environmental Quality*, *32*(6), 2007–2016. https://doi.org/10.2134/JEQ2003.2007

VanZomeren, C. M., Berkowitz, J. F., Lemke, A. M., & Kirkham, K. G. (2020). Soil P Storage Capacity in Agricultural Treatment Wetlands: Can a System Designed for N Reduction Also Retain P? *Wetlands*, *40*(3), 503–514. https://doi.org/10.1007/s13157-019-01205-3

Vymazal, J. (2010). Constructed wetlands for wastewater treatment. *Water (Switzerland)*, *2*(3), 530–549. https://doi.org/10.3390/w2030530

Vymazal, J. (2013). Emergent plants used in free water surface constructed wetlands: A review. *Ecological Engineering*, *61*, 582–592. https://doi.org/10.1016/J.ECOLENG.2013.06.023

Vymazal, J. (2017). The Use of Constructed Wetlands for Nitrogen Removal from Agricultural Drainage: A Review. *Scientia Agriculturae Bohemica*, *48*(2), 82–91. https://doi.org/10.1515/sab-2017-0009

Vymazal, J., Láska, J., & Hnátková, T. (2023). The retention of nitrogen and phosphorus in aboveground biomass of plants growing in constructed wetlands treating agricultural drainage. *Ecological Engineering*, *194*, 107044. https://doi.org/10.1016/J.ECOLENG.2023.107044

Wang, M., Zhang, D., Dong, J., & Tan, S. K. (2018). Application of constructed wetlands for treating agricultural runoff and agro-industrial wastewater: a review. *Hydrobiologia*, *805*(1), 1–31. https://doi.org/10.1007/S10750-017-3315-Z/TABLES/5

Wang, X. L., Xu, H., Qian, B., Feng, Y., & Mekis, E. (2017). Adjusted Daily Rainfall and Snowfall Data for Canada. *Atmosphere - Ocean*, *55*, 155–168. https://doi.org/10.1080/07055900.2017.1342163

Wang, Y. T., O'Halloran, I. P., Zhang, T. Q., Hu, Q. C., & Tan, C. S. (2015). Phosphorus Sorption Parameters of Soils and Their Relationships with Soil Test Phosphorus. *Soil Science Society of America Journal*, *79*(2), 672–680. https://doi.org/10.2136/sssaj2014.07.0307

Watson, S. B., Miller, C., Arhonditsis, G., Boyer, G. L., Carmichael, W., Charlton, M. N., Confesor, R., Depew, D. C., Höök, T. O., Ludsin, S. A., Matisoff, G., McElmurry, S. P., Murray, M. W., Peter Richards, R., Rao, Y. R., Steffen, M. M., & Wilhelm, S. W. (2016). The re-eutrophication of Lake Erie: Harmful algal blooms and hypoxia. *Harmful Algae*, *56*, 44–66. https://doi.org/10.1016/J.HAL.2016.04.010

Wilcock, R. J., Müller, K., Van Assema, G. B., Bellingham, M. A., & Ovenden, R. (2012). Attenuation of nitrogen, phosphorus and E. coli inputs from pasture runoff to surface waters by a farm wetland:

The importance of wetland shape and residence time. *Water, Air, and Soil Pollution*, *223*(2), 499–509. https://doi.org/10.1007/S11270-011-0876-8/METRICS

Chapter 5 – Nitrogen dynamics and retention in a constructed pond-wetland treating tile drainage from a cold climate cropping system

Abstract

Integrated pond-wetland systems can mitigate nitrogen (N) export from cropping-system tile drainage, a major contributor to downstream nutrient accumulation and eutrophication. However, treatment performance in cold-climate regions remains constrained by seasonal hydrology, temperature, and carbon limitation. This study assessed N removal in a full-scale, pond-wetland system in Eastern Ontario, Canada, receiving tile drainage over five years (2016 - 2021), spanning Spring-melt (April) to system freeze-up (late November). Hydrologic, concentration, mass load, and denitrification-kinetic analyses quantified system-scale performance and internal nitrate (NO_3^--N) processing along the flow path. Inlet-outlet concentration monitoring indicated moderate retention of total nitrogen (27%) and NO_3^--N (30%), consistent with strong seasonal limitations. Internal monitoring revealed pronounced pond-to-pond gradients, with progressive NO_3^--N attenuation via denitrification and biological assimilation and maximum pond-scale removal upstream of the outlet (59%). In contrast, the terminal outlet wetland consistently produced NO_3^--N, likely due to shallow depth, limited storage capacity, and moderate vegetation cover that constrained hydraulic buffering during flow events and reduced macrophyte-mediated NO_3^--N processing. Seasonal patterns showed greatest NO_3^--N removal in Summer on both concentration and mass basis, intermittent removal in Late Spring and Fall and minimal in Spring-melt. Denitrification kinetics were best described by a cascading pond-to-pond areal-based first order P-k-C* model ($k = 0.14$ m/d; $\theta = 1.19$), indicating NO_3^--N removal scaled more strongly with benthic surface area than with water-column volume. Consistent with this, kinetic analyses showed ponds of ~0.6-0.7 m were sufficient for NO_3^--N removal, while deeper pond (1.3 m) provided no additional benefit. Overall, pond-wetland systems provided considerable N retention in cold climates, but accurate assessment and design optimization require internal-scale and seasonally resolved evaluations.

5.1. Introduction

Agricultural fertilizer application in Canada has increased substantially over the past decade, with Nitrogen (N)- based fertilizers accounting for most inputs (Statista, 2024). With N uptake efficiency averaging only 64% (FAOSTAT, 2025), a considerable fraction of applied N is readily transported primarily in the form of highly mobile nitrate (NO_3^--N) from agricultural fields through leaching, surface runoff, and subsurface tile drainage systems common in humid agricultural landscapes. Elevated NO_3^--N concentrations pose significant environmental risks, including eutrophication of surface waters, and contamination of groundwater used for potable supply. In Canada, high NO_3^--N concentrations in cropping-system tile drainage have been widely reported (Drury et al., 2009; Ng et al., 2002; Sunohara et al., 2014), frequently exceeding Canadian guidelines for the protection of aquatic life (3 mg NO_3^--N/L) (CCME, 2012) and the drinking water limit of 10 mg NO_3^--N/L (Health Canada, 2014). Although NO_3^--N pollution has traditionally been emphasized in coastal environments (Daigle, 2003), increasing concern has emerged regarding its mobility and accumulation in freshwater systems, including the Laurentian Great Lakes (Cooper, 2016), and specifically in the study area located in the St. Lawrence river basin (Working Group on the State of the St. Lawrence Monitoring, 2024).

To mitigate agricultural nutrient losses, various governmental action plans promote the implementation of Beneficial Management Practises (BMPs) that intercept and treat nutrient-rich drainage water. Among these, treatment ponds (retention ponds) are recommended under the St. Lawrence Action Plan (2021), while constructed wetlands (CWs), such as free-surface systems, are promoted by AAFC (2023) as mitigation BMPs. Strategically positioned along discharge pathways, these systems intercept tile drainage and overland flow without disrupting agricultural operations. Both BMPs maintain permanent pools of water but differ markedly in depth and vegetation, which influences N processing (AAFC, 2024).

N retention within treatment ponds and CWs occurs through interacting hydrological, physicochemical, and biological processes, with effectiveness varying spatially and seasonally (Beckingham et al., 2019; Kadlec & Wallace, 2008; Shilton, 2005). Physiochemical processes include sedimentation of particulate N, adsorption of ammonium, and ammonia volatilization, while biological pathways include N assimilation into plant and microbial biomass, and microbially mediated transformations such as ammonification, nitrification, denitrification, and

anaerobic ammonium oxidation (Lee et al., 2009; Vymazal, 2007). These processes contribute to both temporary N storage and permanent removal, primarily via denitrification to dinitrogen gas. In treatment ponds, N processing takes place within the permanent water column and associated sediments, rather than the littoral zone, where biological uptake is often limited (Gold et al., 2017; Harper & Herr, 1993; Nietch et al., 2001). In contrast, CWs operate as integrated sediment-plant-microbe systems in which dense vegetation and redox gradients promote multiple, sequential N retention and removal pathways (Mitsch & Gosselink, 2015; Reddy & DeLaune, 2008). Consequently, constructed pond-wetland systems that integrate treatment ponds with free-surface CWs represent a potentially multifunctional BMP by coupling physical sedimentation with enhanced biogeochemical N processing.

Reported N removal performance in ponds and wetlands is highly variable. Treatment ponds, widely used in stormwater management, have reported total nitrogen (TN) concentration reduction by an average 4 to 63% (Harper & Baker, 2007; SC DHEC, 2005) and NO_3^- by negative to 32% (Gold et al., 2017; Ivanovsky et al., 2018; Koch et al., 2014). Agricultural ponds receiving overland runoff have reported that TN reductions of 26% (Clary et al., 2020) and NO_3^- reductions ranging from 5 to 82% (Robotham et al., 2021; Rushton & Bahk, 2001). Whereas in colder-temperate agricultural CWs, TN reductions of -28 to 40% and NO_3^- reductions of -1 to 35% (Braskerud, 2002; Koskiaho et al., 2003; Nilsson et al., 2023; Pugliese et al., 2023; Steidl et al., 2019) have been observed. This variability reflects sensitivity to hydrologic loading, seasonal conditions, system scale, and geographic location. Notably, most of these performance assessments rely on inlet-outlet concentrations or load comparisons, rather than multiple, spatial sampling within the system for insights on internal system dynamics. This limitation is especially important in pond-wetland systems with varying depths where NO_3^- processing and transformation capacity may differ.

Denitrification is widely recognized as a dominant N transformation pathway in ponds and wetlands (Beutel et al., 2009; Brunet et al., 2021; Clary et al., 2020; Vymazal, 2007; Xue et al., 2009). However, this pathway is controlled by temperature-dependent microbial processes and declines sharply at low temperature conditions (Grebliunas & Perry, 2016; Sirivedhin & Gray, 2006). In cold-climate regions, extended periods of near-freezing temperatures and seasonal ice cover further suppress microbial activity within the water column and sediments (AAFC, 2024).

These constraints coincide with periods of high N loading during spring snowmelt and early growing-season precipitation, when plant uptake and biogeochemical processing capacity is minimal. Uusheimo et al. (2018) demonstrated that denitrification can be negligible in colder-temperate agricultural ponds and wetlands in winter and spring, highlighting the need for more full-scale, process-resolved studies in cold regions, particularly for systems treating low carbon, high NO_3^- cropping-system tile drainage.

The design and evaluation of treatment wetlands have traditionally relied on first-order degradation models, such as the P-k-C* model, developed largely from municipal wastewater treatment wetlands (Kadlec & Wallace, 2008). The applicability of these models to agricultural drainage remains uncertain due to differences in hydrologic regimes and influent water quality (Kadlec, 2000), and particularly for organic carbon deficient waters. These uncertainties are further amplified in pond-wetland systems composed of interconnected ponds arranged in series, where NO_3^- processing may occur sequentially along the flow path. Conventional first-order approaches assume uniform treatment within a single control volume; however, in pond-wetland systems, NO_3^- processing may be distributed among ponds with distinct depths, hydraulic residence time (HRT), and biogeochemical conditions (Shilton, 2005). Moreover, while denitrification in free-surface CWs is commonly conceptualised as an areal process governed by sediment-water interface area (Vymazal, 2007), treatment ponds concentrate activity within the permanent water column, where depth, volume and HRT exert stronger controls on NO_3^- transformations (Harper & Herr, 1993). The applicability of areal- versus volumetric-based kinetic models for describing NO_3^- removal in pond-wetland systems therefore remains unresolved, particularly in cold-climate environments.

This study addresses these knowledge gaps through a full-scale, multi-year evaluation of a cold-region pond-wetland system receiving high NO_3^--N, low carbon, tile drainage from a cropping-system. Specific objectives were to: 1. characterize hydrologic and seasonal controls on TN and NO_3^--N reduction from spring snowmelt to system freeze-up; 2. quantify internal, pond-scale N processing using spatially distributed concentration and mass-load analyses on an overall and seasonal basis; 3. evaluate denitrification kinetics within a cascading pond framework by comparing areal- and volumetric-based first-order models and implications for pond-wetland design (depth) in cold climates; and 4. conduct a system-scale TN mass balance to partition

removed N among temporary storage pools and permanent removal pathways. The practical objective was to provide full-scale field evidence to support the design and application of pond-wetland systems for treatment of cropping system tile drainage in Eastern Ontario and similar cold-climate regions.

5.2. Materials and Methods

5.2.1. Site Description

The full-scale study was conducted on a cash crop (corn-soybean-wheat) operation, Ferme Agriber, in St. Isidore, Eastern Ontario, Canada, which is situated within the Lower South Nation River sub-watershed (part of the larger Great Lakes - St. Lawrence River basin) (Figure 5-1 A). The climate in this area is categorised as temperate - humid continental (Kottek et al., 2006), characterized with four distinct seasons and precipitation occurring throughout the year. The farm is relatively flat (slope < 1%) with clay and clay-loam textures (Bearbrook Clay) dominating the soil profile. Cash crops were grown with minimum tillage, with fertilizer application carried out twice a year - dry N broadcast after planting followed by a mid-season liquid side-dress.

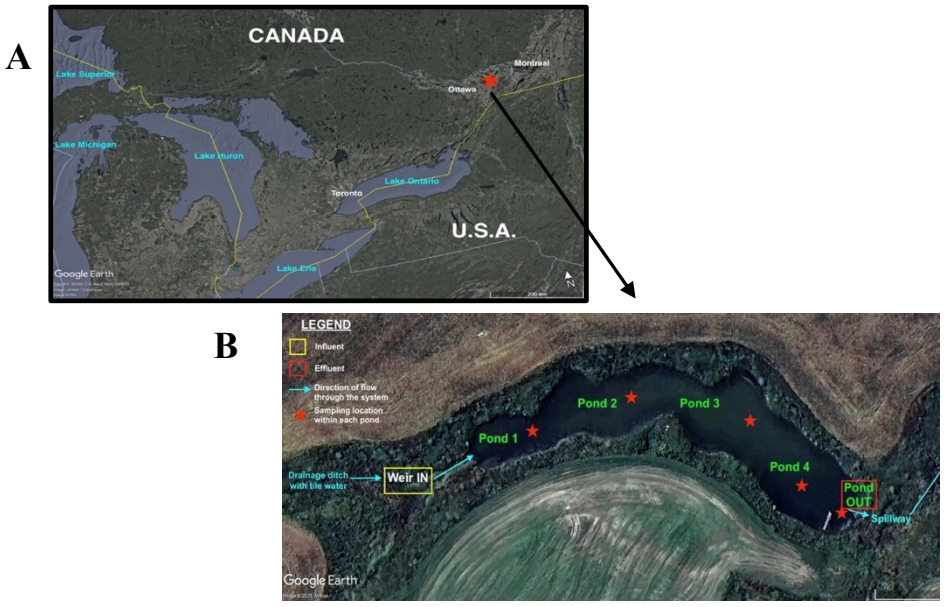

Figure 5 -1. Location of field study – A. Geographic location of the study site relative to the Great Lakes; B. Aerial image of the study site with locations of sampling locations and the direction of flow within the pond-wetland system. Google Earth Pro V 7.3.6.9796 imagery.

In 2016, A 240 m long (0.4 ha) free-water surface, pond-wetland system (45°23’55 N, 74°54’02 W) was constructed along the length of the natural ravine (approx. 700 m long x 3.2 m

deep), occupying 0.93% of the total agricultural drainage area. The system intercepts subsurface tile drainage water from 43 ha of farmland transported through gravity by a central drainage ditch. The depth of the system ranged from 0.08 m to 3.1 m (characteristic to treatment ponds and constructed wetlands) with emergent macrophytes (*Typha latifolia* and *Juncus effusus*) allowed to establish naturally. However, the total macrophyte coverage across the pond-wetland system remained <1% of the total surface area. During summer months, visible algal growth was observed predominantly in the shallow inlet zone of the system. The outlet of the pond-wetland consists of a 6 m wide riprap spillway which conveys wetland discharge into a downstream ditch that ultimately drains into the South Nation R. within the St-Lawrence drainage basin.

5.2.2. Monitoring of the system

The pond-wetland system was systematically monitored from its natural filling in October 2016 until freeze-up, and from spring thaw to freeze-up in 2017 to 2019 and in 2021[6] (April to November). To ensure consistent sampling and nutrient characterization, the system was divided into five ponds, designated as Pond 1, 2, 3, 4 and OUT, following the direction of flow (Figure 5-1 B). Their average depths of 0.08 m, 0.71 m, 0.62 m, 1.30 m, and 0.33 m, respectively, forming a sequence of very shallow – deep – moderately shallow – deepest – moderately shallow basins. An in-stream V notch weir served as the inlet to the system, marked as Weir - IN in Figure 5-1 B. To capture seasonal flow and nutrient variations across the system, each field season was subdivided based on northern hemisphere seasons: Spring-melt (April), Late Spring (May 1 to June 20), Summer (June 21 to September 20) and Fall (September 21 to Freeze-up) (NRCC, 2024). From 2016 to 2018, daily precipitation and ambient air temperature data were collected using a HOBO weather station operated by the farm (Onset Computer Corp.). From 2019 to 2021, weather data was obtained by combining information from the Moose Creek station, positioned within 20 km of the farm site (ECCC, 2023) and the St. Isidore Station, within 2 km of the farm (Agricrop, 2023).

5.2.3. Water quality sampling and analysis

Daily composite samples (consisting of three to four aliquots per day) were collected upstream of Weir IN and at the outlet of Pond OUT using ISCO 6712 full-size automatic portable samplers (Teledyne ISCO, Inc.). Sampler batteries were trickle-charged using solar panels. In 2019, the

[6] The system was not monitored in 2020 due to COVID -19 lockdown restrictions.

collection pipe at Weir IN was relocated downstream below the weir crest to reduce excessive collection of sediments and debris from the ditch bottom. Grab samples were also collected weekly at the weir, spillway, and at five locations across the ponds (shown in Figure 5-1 B). Following collection, samples were transported to the laboratory in coolers with ice packs and stored under refrigeration until analysis. Details of 2016 and 2017 methodology can be found in Mathew, 2020. From 2018 to 2021, over 4400 samples were analyzed.

Both grab and composite samples were characterised for NO_3^--N and NH_4^+-N, while grab samples were additionally characterised for TN and soluble chemical oxygen demand (sCOD). Only unfiltered grab samples were analysed for TN using HACH Method 10071 (low range, a test kit Persulfate Digestion method). Samples (100 mL) were then passed through 1.5 µm Whatman filters using a vacuum filtration apparatus connected to a Marathon Electric 110-115 ¼ HP vacuum pump (distributed by Thermo Fisher Scientific, Waltham, MA.). Filtered samples were analyzed for NO_3^--N using the ultraviolet (UV) spectrophotometric method (Standard Methods 4500- NO_3^- B) (APHA, 2017) and for total ammonia nitrogen (as NH_4^+-N) using the Nessler Method with Rochelle salt stabiliser (50%) and Nessler reagent (APHA, 1998). Filtered grab samples were also analysed for sCOD using HACH method 8000- low range, a test kit Dichromate Reagent Method (APHA, 2017). All analyses were conducted using a HACH DR6000 spectrophotometer. Quality control included analysis of standard samples with known concentrations every 20 samples with standard error of 0.7 $\pm$ 0.6%. Weekly *in situ* measurements of dissolved oxygen (DO), pH, and temperature were recorded at grab-sampling locations using a HACH-HQ40D multimeter. The pH varied between neutral to slightly alkaline (7.2 to 8.3) throughout the study period, while bulk water DO levels were strongly aerobic, ranging from 7.9 to 12.4 mg O_2/L, partially reflecting the diurnal effect of algal photosynthesis.

5.2.4. Determining water depths and flow rates

The weir and Pond OUT were equipped with HOBO Water Level Data Logger-U20-001-04 (Onset Computer Corp.), which recorded absolute pressure (kPa) and temperature of water (°C) at 15 -minute intervals. These data were used to compute water heights and subsequently, water flow rates at the weir. A similar data logger was installed at the top of a permanent stake at Weir IN to

record barometric pressure[7] and temperature[8]. The data loggers were manually downloaded using HOBO Waterproof Shuttle during the weekly visits and processed using HOBOware Pro software (Version 3.7.21) to compute the sensor depth below the water surface (Onset Computer Cooperation, 2008). The equations used to calculate water height (h) are provided in Appendix C. The 'Zero' of the logger is approximately 20 mm from its bottom, and this was corrected for in the calculated water heights. A total of 23,500 data points were analysed for each monitoring location per year. During the weekly visits, manual measurements of water height were also recorded using a measuring ruler/dowel at the weir crest and at Pond OUT, with error < 1 mm on the recorded height. These values were used to verify and calibrate the heights calculated from the depth loggers.

The instantaneous flow for each 15-minute interval was determined using the Kindsvater-Shen relationship for a V-notch, sharp crested weir at Weir IN (Chun & Cooke, 2008; Kulin & Compton, 1979; USBR, 2001) and was subsequently normalized by the drainage area. A pond-wetland water balance (Equation 5-1) was used to calculate the flow at the outlet (Pond OUT) -

$$Q_{in} + P.A - e.A = Q_{in} \quad \text{(Equation 5-1)}$$

where, Q_{in} is the influent flow in m^3/d, P is daily precipitation in m/d, A is the surface area of the pond-wetland system and e is the daily evaporation rate calculated using (m) the Hamon method for lake evaporation, which is given as-

$$e = 0.63 \times D^2 \times 10^{\frac{7.5T_a}{T_a+273}} \quad \text{(Equation 5-2)}$$

where e is the daily evaporation from a given lake (mm), T_a is the daily temperature (°C) and D is the ratio of maximum sunshine duration (hour) to 12 hours, and is determined using –

$$D = \frac{1}{90}\arccos\left\{-\tan(\varphi).\tan\left[23.45° \sin\left(\frac{J-80}{365} \times 260°\right)\right]\right\} \quad \text{(Equation 5-3)}$$

where φ is the latitude, J is the Julian day of date of interest.

Seepage and infiltration from the pond-wetland system were considered negligible. The system bed was compacted during construction, reducing the potential for subsurface water losses. Furthermore, the presence of Bearbrook clay at the site, characterised by low hydraulic

[7]The barometric files from Weir IN from April 30th to June 16th, 2018, were corrupted and hence correlations were made with Weir OUT barometric files and used for this time period.
[8]In 2021, due to malfunctioning of logger, data from moose creek weather station were used to re-calibrate values obtained from the logger.

conductivity, further limits seepage. This assumption was evaluated by comparing water level variations recorded by HOBO data loggers during no-flow conditions with the net difference between precipitation and ET. The observed discrepancy was approximately 0.001 m in water height, equivalent to 2.9 m^3/d, indicating that seepage losses were minimal relative to overall system flow.

During winter (December-April), no flow was assumed to occur as the pond-wetland system was covered by a continuous thick ice layer. Tile drains remained completely frozen, with sustained snow cover across the study site. Any intermittent thaw or snowmelt would have been ponded on frozen soil surface and therefore assumed to have a negligible impact on the overall water balance.

5.2.5. Calculating water and nutrient mass loads

Water load (m^3) for each time interval was calculated by multiplying the measured inflow (Q_i) or outflow rate (Q_o) (m^3/s) by the corresponding interval duration (15 min). Daily water load (mm/day or m^3/ha/d) were computed by summing the 15-minute interval water loads and dividing by the discharge area (m^2 or ha). NO_3^--N loads were determined by multiplying the influent concentrations (C_i) or effluent concentrations (C_o) (mg N/L) by the daily discharged water load (m^3/d) and then dividing by discharge area (ha) to obtain values in kg N/ha/d. Because the system was NO_3^--N dominated and TN concentrations were not available at daily resolution, the average Org N concentration derived from weekly grab samples (Section 5.3.3) was added to daily NO_3^--N concentrations to estimate daily TN concentrations. These estimated values were then used to calculate daily and cumulative TN mass loads for the system, based on the observed limited temporal variability in Org N concentrations relative to NO_3^--N. The N (concentration and load) removal percentage was calculated as the percent difference between influent and effluent values divided by the influent. Hydraulic retention time (HRT, days) across the system was determined using Equation 5-4 -

$$\tau = \frac{V}{Q_{in}} = \frac{\epsilon\, h\, A}{Q_{in}} \quad \text{(Equation 5-4)}$$

where V is volume of the system (m^3), h is the depth of the system (h) and A is the area (m^2). Porosity index (ε) = 0.95 for northern environment (Kadlec & Wallace, 2008) was applied to Pond 3 and Pond OUT only.

5.2.6. Sediment sampling and mapping

In 2021, a total of 30 sediment samples were collected from five ponds using 2-3 transets per pond (sampling layout shown in Figure 5-2 A) with a Sludge Judge^{TM} (VWR International, LLC) equipped with extended sections. Sampling was conducted from a rowboat, with efforts made to minimize disturbance of the sediment bed, although some variability may have been introduced. Sediment and water depths were recorded at each sampling location, and spatial variation in sediment depth across the pond-wetland system is presented as a contour map in Figure 5-2 B. Samples were analysed for total solids (TS) and volatile solids (VS) following Method SM 2540 G (APHA, 2017), TN, NH_4^+-N, and NO_3^--N using the methodologies mentioned in Section 5.3.3 by diluting the raw and filtered sample as required. Measurement uncertainty associated with the Sludge Judge^{TM} was approximately ±1 cm due to the plastic ball and connector assembly, with additional minor variability potentially introduced during sediment transfer to sample containers. While the sampling approach provided representative coverage of the system, some spatial heterogeneity in sediment distribution may not have neem fully captured.

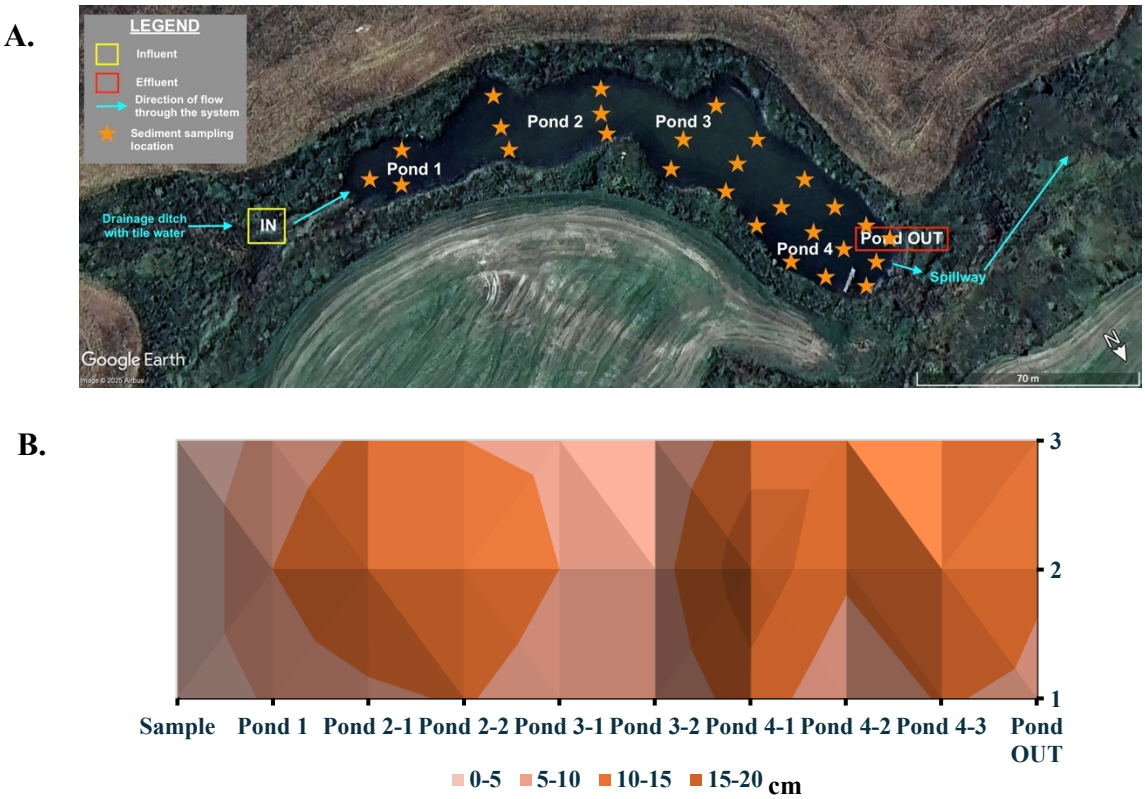

Figure 5-2. Sediment mapping - A. Location of sediment sampling spots across the pond-wetland system; B. Contour mapping of sediment depth across each pond within the system.

5.2.7. Macrophyte sampling and mapping

Above-ground biomass of emergent macrophyte (stem and leaves) and emergent vegetation were collected once in Summer and Fall 2021 from Pond 3 and Pond OUT. The density of the plant species was determined by dividing the area into 1 m x 1 m squares at the ponds. The total area covered by these plants relative to the system was determined by comparing weekly photos and aerial Google Earth images. A representative macrophyte was selected within each square and harvested using heavy duty pruning shears and its height and stem diameter measured. In the laboratory, the plant samples were weighed and sent for plant tissue TN analysis (combustion method) to an external lab (AFL, Guelph, ON).

5.2.8. Kinetic calculations for the pond-wetland system

Modified first-order rate constant k_A (areal, m/d) and k_v (volumetric, 1/d) were determined using the P-k-C* model (Equation 5-5) (Kadlec & Wallace, 2008) –

$$\left(\frac{C_e - C^*}{C_i - C^*}\right) = \frac{1}{\left(1+\frac{k_A}{(P\times HLR)}\right)^P} = \frac{1}{\left(1+\frac{k_v \times HRT}{P}\right)^P} \quad \text{Equation (5-5)}$$

where C_i is the mean inlet NO_3^--N concentration (mg N/L), C_e is mean outlet NO_3^--N concentration (mg N/L), C^* is the background NO_3^--N concentration (mg N/L), P is the apparent number of tanks in series (TIS) and HLR is the hydraulic loading rate (m/d). Temperature dependence of denitrification kinetics was incorporated using the Arrhenius temperature correction coefficient (θ) (Equation 5-6), and all rate constants are reported at reference temperature of 20°C:

$$k = k_T\, \theta^{(T-20)} \quad \text{Equation (5-6)}$$

Based on values reported in Kadlec & Wallace (2008), θ was evaluated within the recommended range (0.997 to 1.210) using multiple model runs conducted at a monthly temporal resolution. A single value of θ = 1.19 was selected as it provided the best overall model performance, as indicated by the coefficient of determination (R^2), across the full dataset. Once selected, this value of θ was held constant and applied uniformly across all monthly kinetic comparisons to ensure consistency and avoid overparameterization.

Both areal and volumetric equations of the P-k-C* model were applied to estimate first-order rate constant (k) values for NO_3^--N removal at system-scale and for individual ponds (Pond 1 through Pond OUT). The minimum NO_3^--N concentrations observed during periods of prolonged stagnation in 2021 were used to define the system-scale background concentration ($C^* = 0.2$), while

pond- and season- specific C^* values were used for internal comparisons. A value of P = 4 was selected for inlet-outlet system configuration and consistent with values reported for agricultural tile drainage wetland studies (Beutel et al., 2009; Karpuzcu & Stringfellow, 2012), whereas P =1 was used for the cascading model. Following the selection of θ, values of k_A and k_v were estimated using the Solver function in MS Excel by minimising the difference between observed and modelled outlet NO_3^--N concentrations. Model calibration was based on daily composite samples at inlet and outlet and grab samples for internal pond locations. Model performance was evaluated using the sum of squares (SS), root mean square of errors (RMSE), and coefficient of determination (R^2) as measures of goodness of fit.

To evaluate the influence of temporal aggregation on model performance, kinetic analyses were conducted at multiple temporal resolutions (daily, weekly, monthly, and seasonal). Monthly aggregation was ultimately selected for subsequent analyses, as it reduced short-term hydrologic variability and better approximated pseudo steady-state conditions required for application of P-k-C* model. The objective of this modelling exercise was to assess whether and at what temporal scale NO_3^--N dynamics in the pond-wetland system could be reasonably represented using the P-k-C* framework.

5.2.9. Statistical Analysis

Mean daily concentrations, water and nutrient loads were compared using ANOVA and paired t-test to determine effect of pond-wetland system on nutrient concentration and mass attenuation in various time periods. A *p*-value < 0.05 was used to identify statistical differences for water samples while *p*-value < 0.1 was used for soil and macrophyte data sets. The arithmetic mean, standard deviation, confidence interval at 95%, and count were calculated for drainage flow, nutrient concentrations, and loads from inlet to outlet of the system. Correlational analysis was applied when appropriate. The strength of correlation was defined such that a weak correlation was $0.1 < R < 0.3$, a moderate correlation was $0.3 \leq R < 0.7$ and a strong correlation was $R \geq 0.70$ (Schober et al., 2018).

5.3. Results and discussion

5.3.1. Meteorological conditions and hydrology

During this study, water flows through the pond-wetland system were driven primarily by precipitation, evapotranspiration (ET), and spring melt of accumulated snow. Cumulative April-November precipitation was 3 to 9% below the 30-year normal (1991-2020) in 2018, 2019, and 2021, while 2017 was exceptionally wet (61% above average) (ECCC, 2025). This produced the highest inflows (Table 5-1 A) and elevated Late Spring and Summer outflows that were 10 to 60% higher than in 2018-2019. Average seasonal flow patterns varied, with highest flows during Spring-melt, and the lowest during Summer, while Late Spring and Fall generated similar average flows. Complete hydraulic dormancy was observed each winter (December to March) due to frozen inlet ditch, snow accumulation, and thick ice cover.

Table 5-1. Hydrological Variables for the pond-wetland system (A) from April to November (2017 – 2019*), and (B) average hydraulic retention times across individual ponds and system (2017-2019*).

A.

Year	Inflow[a] (mm/ha drained)	Precipitation[a] (mm)	ET[a](mm)	Outflow[b] (mm/ha drained)
2017	298.9	1004.8	464.7	283.1
2018	234.7	654.8	476.6	217.1
2019	188.9	549.3	436.0	175.6

*In 2020, system was not monitored due to COVID-19 restrictions, and in 2021, the system was stagnant for most of the study period from late spring to late fall

[a]Represents cumulative values

[b]Calculated from water balance across the system.

B.

Time Period	Average Hydraulic Retention Time (d)					
	Pond 1	Pond 2	Pond 3	Pond 4	Pond OUT	System
Spring-Melt	0.0	0.4	0.4	1.3	0.0	**2.1**
Late Spring	0.1	1.0	1.2	3.6	0.1	**5.9**
Summer	3.6	51.7	59.0	159.2	2.5	**276.0**
Fall	0.1	1.9	2.1	6.5	0.1	**10.7**
Study	0.1	1.4	1.5	4.8	0.1	**7.9**

Winter snow accumulation was 32% and 9% below 30-year normal in 2018 and 2021, while 29 and 34% greater in 2017 and 2019 respectively, generating an average 21% higher cumulative Spring-melt flow (88.5 mm/ha drained vs 64.9, 74.6 mm/ha drained). The 2021 study year showed an atypical hydrologic response, with no Late Spring or Summer flow, resulting in stagnant water within the system, before discharging in late October. Across all years, the system discharged 92% of the cumulative inflow with losses due to ET and infiltration. The losses are consistent with agricultural runoff pond systems (average 89%) (Oduor et al., 2023) as well as

wetlands with similar wetland-to-catchment ratios (Kovacic et al., 2006; Kynkäänniemi et al., 2013).

Pond volumes ranged from 45 m^3 at Pond 1 to 2018 m^3 at Pond 4, affecting internal HRTs. Season had a strong effect on system HRT with much larger average Summer HRTs of 276 days (Table 5-1 B), driven by extended periods without flow, compared to Spring Melt, Late Spring and Fall periods, which ranged from 2.1 to 10.7 days. These large seasonal differences highlight the need to evaluate HRT at finer temporal scales than at annual study-scale (Nilsson et al., 2023; Vymazal, 2017), as they have important implications for nitrogen transformation processes within the system. Against this hydrologic context, the following sections examine how N concentrations responded at the system-scale and within individual ponds.

5.3.2. Concentrations – Nitrogen Speciation

5.3.2.1. Overall system – IN versus. OUT

Across the study period, NO_3^--N dominated TN concentrations (IN: 85%, OUT: 83%), followed by Org N (IN: 14%, OUT: 15%) and NH_4^+–N (IN: 1%, OUT: 3%), consistent with previous agricultural drainage studies (Brunet et al., 2021; Kovacic et al., 2000; Steidl et al., 2019; Thorén et al., 2004) and confirming that TN dynamics were primarily driven by NO_3^--N. Mean influent Org N concentrations were low (0.8 ± 0.8 mg N/L; median = 0.5 mg N/L), remained consistent across the system and unchanged at the outlet (0.9 ± 0.8 mg N/L; median = 0.5 mg N/L) (Figure 5-2, Table 5-3). Mean effluent NH_4^+- N concentrations (0.2 ± 0.3 mg N/L) were also statistically similar to influent (0.2 ± 0.3 mg N/L) (p-value > 0.1, ANOVA). Interpretation of Org N is subject to uncertainty because it was calculated by difference (TN less NO_3^--N and NH_4^+–N) and was based on a limited weekly-grab sample dataset; consequently, some observed fluctuations likely reflect inherent analytical error in addition to true variability. Overall, the low Org N and NH_4^+–N concentrations with minimal removal is consistent with systems receiving subsurface tile drainage, which typically exhibit low Org N and NH_4^+-N concentrations relative to surface runoff (Vymazal & Dvořáková Březinová, 2018), and exhibit low removal or export of reduced and Org N species (Groh et al., 2015; Koskiaho et al., 2003; Robotham et al., 2021; Steidl et al., 2019; Thorén et al., 2004).

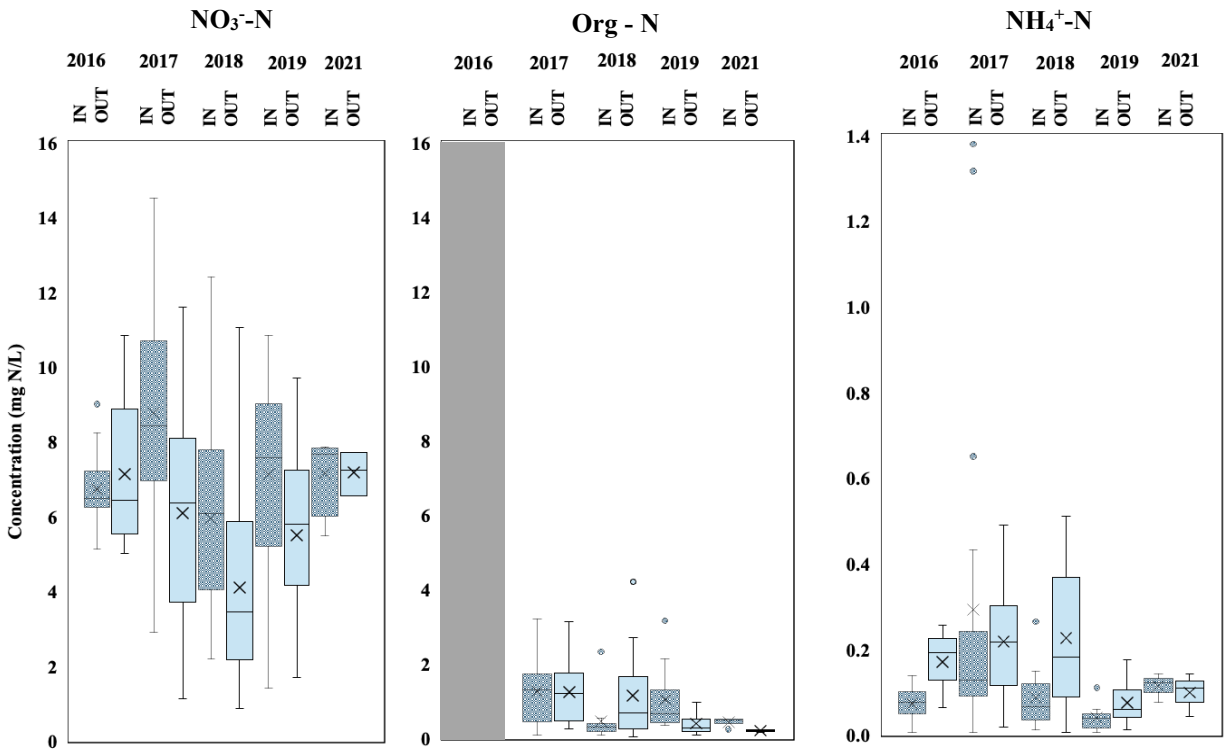

Figure 5-3. Box and whisker plots of nitrate (NO_3^--N), organic nitrogen (Org-N), and ammonia (NH_4^+–N) concentrations measured at the inlet (IN; Weir IN) and outlet (OUT; Pond OUT) of the pond-wetland system over the entire study (2016 to 2021). Note: 1. Composite samples were used for nitrate and ammonia and grab samples for Organic N; 2. Data from 2016 and 2021 represent late fall data only; 3. Organic N was calculated as the difference between TN, NO_3^--N, and NH_4^+–N concentrations; 4. TN was not measured in Year 2016 and is shown as gray areas in the Org-N graph; and 5. the y-axis scale for NH_4^+ –N was reduced for readability.

Composite samples collected at Weir IN and Pond OUT were used to evaluate system-scale NO_3^--N performance (IN vs OUT), including seasonal patterns, mass loads, and kinetic behaviour. Influent NO_3^--N ranged from 1.4 to 14.5 mg N/L with an overall mean of 7.4 ± 2.6 mg N/L (median = 7.5 mg N/L), consistent with influent concentrations reported for systems receiving cropping-system tile drainage (Table 5-2). Tile drainage from cropping systems is typically NO_3^--N dominated and low in dissolved organic carbon (DOC), which can constrain heterotrophic denitrification when electron donor availability limits microbial activity (Royer & David, 2005; Schipper et al., 2010; Vymazal & Dvořáková Březinová, 2018). Therefore, influent carbon availability was assessed using sCOD. sCOD is related to DOC as both represent organic matter in the aqueous phase, and COD is commonly approximated as ~2.7 times total organic carbon (TOC) or DOC based on oxidation stoichiometry and empirical observations (APHA, 2017; Metcalf & Eddy, 2014; Pinney et al., 2000). In this study, influent sCOD concentrations were low (mean = 16.0 ± 19.7 mg O_2/L, range = 2 to 54 mg O_2/L, Table 5-3), consistent with carbon-poor

influent conditions. Reported organic matter in comparable studies is often higher (COD: 24.3 - 53.4 mg O_2/L; TOC: 2.2 to 8.0 mg/L) (Kovacic et al., 2006; Lavrnić et al., 2020; Thorén et al., 2004), although direct comparison is limited because these studies report total COD rather than sCOD. Influent NO_3^--N differed among years (p-value < 0.05, ANOVA) (Table 5-3, Figure 5-2), with the highest concentrations observed in 2017, followed by 2019 and 2018. Overall, the system reduced 30% of the mean influent NO_3^--N concentrations (p-value < 0.05, ANOVA), placing performance above the mean reported removals across comparable temperate systems (Table 5-2). Although mean influent and effluent NO_3^--N concentrations exceeded the federal guideline for long-term exposure for aquatic life (3.0 mg NO_3^--N/L) (CCME, 2012), effluent concentrations consistently met the guideline during summer, indicating seasonally enhanced in-system processing.

Daily composite NO_3^--N concentrations at the inlet and outlet (Figure 5-3), shown relative to precipitation and outflow (2016-2019, 2021), exhibited distinct interannual variability and strong seasonal dependence on hydraulic patterns. Across most monitoring periods, IN concentrations exceeded OUT, indicating sustained NO_3^--N attenuation within the pond-wetland system. In 2017 (wettest year), persistent flow supported sustained IN and OUT concentrations. During Spring-melt, IN and OUT increased concurrently and were often comparable, suggesting limited net removal during peak-flow conditions. As flow transitioned into Late Spring and early Summer, OUT concentrations declined steadily during low-flow periods (seen as three distinct drops in Figure 5-3) despite elevated IN concentrations, suggesting enhanced system removal through denitrification and biological uptake under reduced hydraulic loading and warmer conditions. Storm events produced rapid IN increases, followed by delayed OUT increases (relative to previously dropped concentrations), indicating a lagged system response and short-term NO_3^--N transport. Late Summer concentrations were largely absent under minimal flow, while Fall flow resumption coincided with initially low concentrations that gradually increased with precipitation and discharge.

Table 5-2. Comparison of inflow and outflow total nitrogen (TN) and nitrate (NO_3^--N) concentrations (mg N/L) and area-normalised cumulative mass loads (kg N/ha) for pond and constructed wetland systems receiving cropping system runoff and drainage across temperate climatic zones.

	Climatic Zone[1]	System type	Area ratio[2] (%)	N species	Mean concentration (mg N/L)			Cumulative mass load (kg N/ha)		
					IN	OUT	%	IN	OUT	%
This study	*Dfb*	PW^T	0.93	TN^C	8.5	6.2	**27**	91.0	78.2	**14**
				NO_3^--N	7.4	5.2	**30**	78.9	66.0	**16**
Braskerud (2002)	*Dfc*	SP + CW^R	0.38	TN	5.1	4.4	**15**	29.5	25.2	**15**
				NO_3^--N	2.8	2.6	**7**	-	-	**-**
Thorén et al. (2004)	*Dfb*	PW^R	0.38	TN	6.4	4.3	**33**	6.4	5.5	**14**
				NO_3^--N	3.9	3.2	**18**	-	-	**-**
Kovacic et al. (2006)	*Dfa*	SP + CW^T	3.00	TN^F	18.4	12.8	**30**	-	-	**38**
				NO_3^--N^F	18.3	12.3	**33**	-	-	**37**
Groh et al. (2015)	*Dfa*	CW^T	3.00	TN	-	-	**-**	33.7	15.3	**55**
				NO_3^--N	-	-	**-**	33.0	14.7	**56**
Chrétien et al. (2016)	*Dfb*	TP^R	0.50	TN^E	1.8	1.0	**9**	3.5	1.7	**51**
Steidl et al. (2019)	*Cfb*	CW^T	0.45	TN*	7.2 to 14.2	5.5 to 14	**-**	42.4	41.1	**3**
				NO_3^--N*	7.3 to 12.3	0.3 to 10.6	**-**	-	-	**-**
Koskiaho & Puustinen (2019)	*Dfb*	CW^R	1.30	TN^F:	3.0	-	**-**	-	-	**9**
				NO_3^--N^F:	1.9	-	**-**	-	-	**6**
Lavrnić et al. (2020)	*Cfa*	CW^T	3.00	TN	12.6	12.3	**2.4**	34.2	16.3	**52**
				NO_3^--N	9.1	9.1	**0**	26.1	12.4	**52**
Brunet et al. (2021)	*Dfa*	TP^R	1.80	TN	5.6	3.0	**46**	10.2	6.5	**36**
				NO_3^--N	-	-	**-**	9.0	3.3	**64**
Robotham et al. (2021)	*Cfb*	TP^R	0.20	NO_3^--N	36.6	34.9	**5**	-	-	**-**

[1] Köppen−Geiger climate classification (Kottek et al., 2006)
[2] Area ratio reported as percent wetland or pond area relative to catchment area
PW = Pond-wetland, CW = Constructed wetland, SP = Sedimentation pond, TP = Treatment pond.
Dashes indicate values not reported in the original studies
[C]refers to refers to estimated daily TN concentrations calculated using daily NO_3^--N concentrations and average Org N concentrations derived from weekly grab samples.
[T]refers to tile drainage from cropping systems
[R]refers to runoff from cropping systems
*median values
[F] Flow-weighted mean concentrations
[E] Event-based study

In both 2018 and 2019, Spring-melt similarly produced concurrent IN and OUT increases, with occasional OUT exceeding IN, suggesting limited attenuation during peak hydrologic flushing and/or mobilization of internal NO_3^--N sources early in the season. As flow receded in

Late Spring, OUT concentrations declined markedly, consistent with enhanced removal under longer residence time. Short-term precipitation events such as 26 mm in early June 2018 and 34 mm in mid-May 2019, produced sharp OUT concentration peaks, consistent with episodic NO_3^--N export or release during high flow conditions. During prolonged low flow or stagnant Summer conditions, OUT concentrations remained consistently low indicating sustained NO_3^--N depletion within the system. Flow resumed in early fall, producing similar IN and OUT concentrations, consistent with a system reset under high-flow conditions and flushing of low NO_3^--N water and/or previously denitrified soils as observed in a parallel study on drainage water quality (Tanga et al., 2025), after which concentrations increased gradually through Fall.

In 2021, prolonged stagnant pond conditions corresponded to a progressive decline in NO_3^--N concentrations through Late Spring, consistent with continued NO_3^--N reduction via denitrification and/or biological assimilation under stagnant conditions. Once concentrations reached low / background levels, they remain suppressed throughout summer. Beginning in mid-October, concentrations increased gradually under cooler conditions and sustained rainfall, a seasonal pattern also evident in prior years during Fall, suggesting NO_3^--N production and/or release (potentially linked to biomass senescence, organic matter decay, or re-oxygenation effects). Concentrations declined during a short period in early mid-November with minimal precipitation and increased again following recharge and renewed flow. While inlet and outlet concentrations characterize overall system performance and seasonal responses, they provide limited insight into the internal processes governing NO_3^--N dynamics within the system.

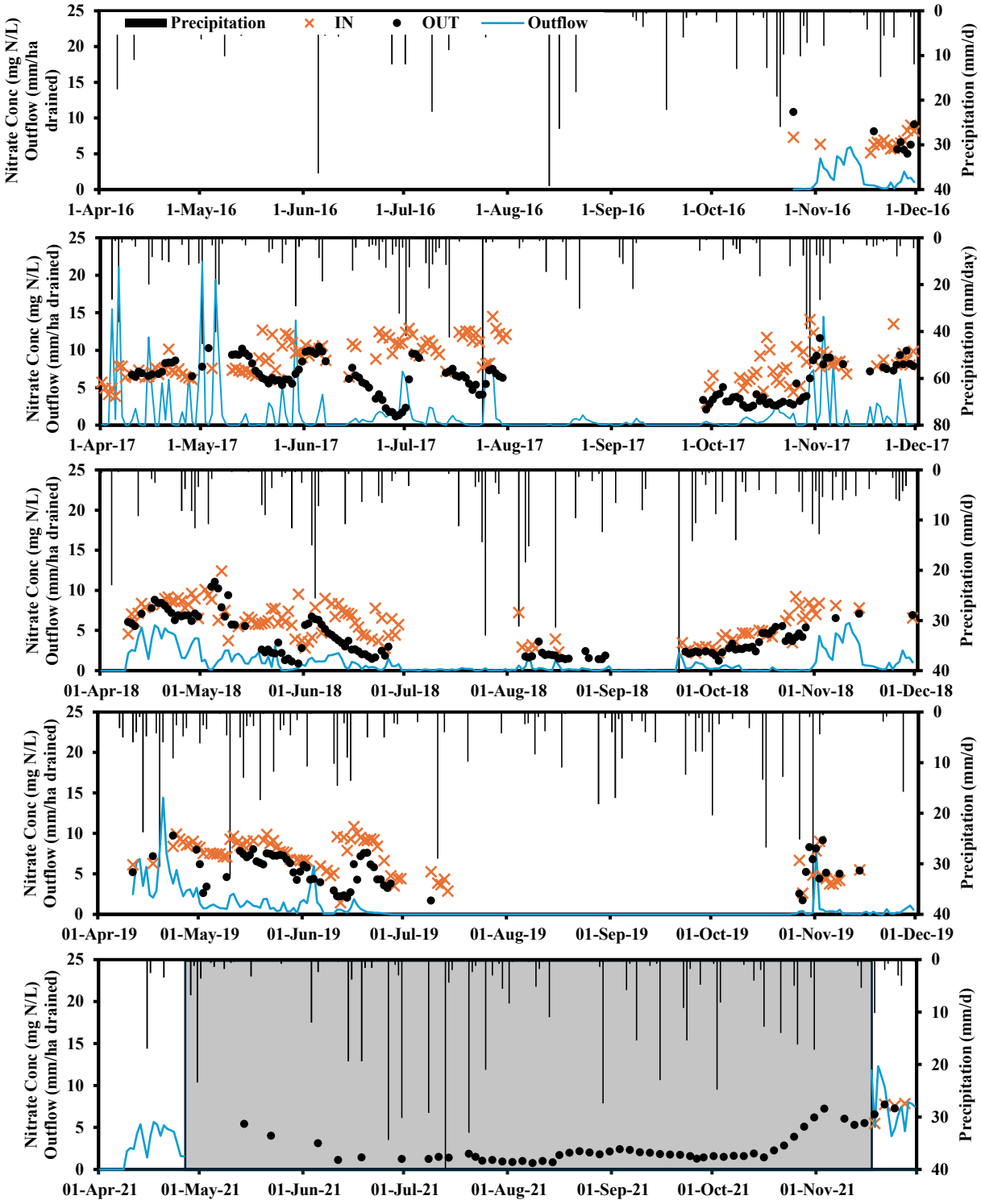

Figure 5-4. Trends of daily composite Nitrate (NO_3^--N) concentrations (mg N/L) at the inlet (IN; Weir IN) and outlet (OUT; Pond OUT) for the Pond-Wetland System. Samples were collected only during flow periods except during 2021, where the gray shaded area represents stagnant pond conditions.

5.3.2.2. Seasonality and internal pond dynamics

Monitoring at multiple locations along the flow path revealed pronounced internal NO_3^--N dynamics within the system (Table 5-3). Given that NO_3^--N comprised the dominant fraction of TN, this section focuses on the internal controls governing NO_3^--N behaviour. While denitrification requires organic carbon as an electron donor, water-column sCOD provides only an upper-bound indicator of dissolved organic carbon availability, as only a fraction of sCOD is readily biodegradable (labile) and effectively delivered to anoxic sediment and biofilm microsites where denitrification occurs (Reddy et al., 2023). In pond and wetland systems, effective denitrification typically requires higher sCOD:NO_3^--N ratios (≥5:1) due to limited carbon lability and competition with aerobic respiration (Bai et al., 2023; Baker, 1998; Li et al., 2017). Given the low influent average sCOD concentration (16.0 ± 19.7 mg O_2/L) and predominantly oxic water-column conditions, NO_3^--N removal was therefore likely supported primarily by internally produced carbon (e.g., decomposing macrophyte and algae detritus in sediment). Seasonal trends reflected a transition from hydrologically dominated conditions during Spring-melt to increasingly biogeochemically mediated processing during Late Spring and Summer.

During Spring-melt, sampling was limited to Weir IN and Pond OUT locations because intermediate ponds remained under ice cover. Across all three years, mean effluent NO_3^--N concentrations were similar to influent concentrations, with changes typically ≤ 0.9 mg N/L and removal ranging from -9 to 11% (study mean = 3%). This response is consistent with limited denitrification under cold temperatures (mean = 2.4 - 7.4°C), no plant uptake, short HRT (1.6 - 2.1 d), and predominantly oxic conditions (Reddy & DeLaune, 2008). Spring-melt sCOD concentrations were low (Weir IN = 8 ± 3 mg O_2/L; Pond OUT = 7 ± 3 mg O_2/L), consistent with carbon-poor influent conditions typical of tile drainage. Even the small, non-significant mean NO_3^--N decrease (0.2 mg N/L) would require ≥ 1 mg O_2/L of bioavailable sCOD (assuming a conservative 5:1 sCOD:NO_3^--N demand), indicating that denitrification during Spring-melt was additionally constrained by limited electron donor supply. Although Org N and NH_4^+-N concentrations remained low (≤ 1 mg N/L), export of both N species was observed. Elevated NO_3^--N and dissolved Org N export during Spring-melt has been attributed to freeze-thaw decomposition of plant detritus and enhanced solute mobilization under increased flow velocities (Groh et al., 2015; Thorén et al., 2004). Mechanistically, increased velocities may disrupt the

diffusive boundary layers around submerged macrophytes and sediments, increasing oxygen exchange, and favouring aerobic pathways including nitrification of NH_4^+ released from dissolved Org N, while simultaneously limiting denitrification (Reddy & Patrick, 1984).

Table 5-3. Seasonal and overall average ± standard deviation for Nitrate (NO_3^-- N), Organic N, and Ammonia (NH_4^+-N) concentrations from 2017 to 2019 study period.

Nitrate as N (mg N/L)							
	Weir IN[a]	**Pond 1[b]**	**Pond 2[b]**	**Pond 3[b]**	**Pond 4[b]**	**Pond OUT[a]**	**% removal***
Spring-melt[1]	7.4 ± 1.4	-	-	-	-	7.2 ± 1.0	3
Late Spring[2]	7.8 ± 2.1	6.9 ± 2.5	6.4 ± 2.3	5.4 ± 1.9	4.1 ± 1.0	5.8 ± 2.5 P	25
Summer[3]	8.3 ± 3.6	4.4 ± 2.8	2.8 ± 2.3 S	2.6 ± 1.9	2.3 ± 1.9	3.9 ± 2.4 P	53
Fall[4]	6.4 ± 2.6	4.8 ± 2.2	4.4 ± 2.1	4.1 ± 2.3	3.7 ± 2.4	4.6 ± 2.4 P	28
Study[5]	**7.4 ± 2.6**	**5.1 ± 2.8**	**4.1 ± 2.7**	**3.6 ± 2.3**	**3.0 ± 1.8**	**5.2 ± 2.5 P**	**30**
Organic N (mg N/L)							
	Weir IN [b]	**Pond 1[b]**	**Pond 2[b]**	**Pond 3[b]**	**Pond 4[b]**	**Pond OUT [b]**	**% removal***
Spring-melt[1]	1.0 ± 0.6	-	-	-	-	1.0 ± 0.6	-4
Late Spring[2]	1.1 ± 1.0	1.1 ± 1.1	1.6 ± 1.4	0.7 ± 0.8	1.1 ± 1.4	0.9 ± 0.8	19
Summer[3]	0.4 ± 0.4	1.2 ± 1.1	0.7 ± 0.8	0.8 ± 0.9	0.5 ± 0.6	1.2 ± 1.4	-180
Fall[4]	0.7 ± 0.5	0.2 ± 0.1	0.2 ± 0.1	0.2 ± 0.1	0.4 ± 0.7	0.7 ± 0.5	**-6**
Study[5]	**0.8 ± 0.8**	**1.0 ± 1.1**	**0.9 ± 1.1**	**0.6 ± 0.9**	**0.7 ± 0.9**	**1.0 ± 0.9**	**-8**
Ammonia (mg N/L)							
	Weir IN [b]	**Pond 1[b]**	**Pond 2[b]**	**Pond 3[b]**	**Pond 4[b]**	**Pond OUT [b]**	**% removal***
Spring-melt[1]	0.04 ± 0.03	-	-	-	-	0.12 ± 0.11	-170
Late Spring[2]	0.07 ± 0.05	0.17 ± 0.17S	0.17 ± 0.16	0.16 ± 0.12	0.15 ± 0.12	0.10 ± 0.10	-46
Summer[3]	0.34 ± 0.30	0.58 ± 0.53	0.24 ± 0.14S	0.27 ± 0.11	0.30 ± 0.20	0.28 ± 0.17	16
Fall[4]	0.16 ± 0.14	0.39 ± 0.44	0.20 ± 0.13	0.25 ± 0.15	0.26 ± 0.13	0.25 ± 0.10	-57
Study[5]	**0.16 ± 0.29**	**0.42 ± 0.46S**	**0.21 ± 0.14S**	**0.24 ± 0.13**	**0.26 ± 0.17**	**0.9 ± 0.15S**	**-19**
Soluble Chemical Oxygen Demand (mg O_2/L)							
	Weir IN [b]	**Pond 1[b]**	**Pond 2[b]**	**Pond 3[b]**	**Pond 4[b]**	**Pond OUT [b]**	**% removal***
Spring-melt[1]	8 ± 3	-	-	-	-	7 ± 3	6
Late Spring[2]	7 ± 3	13 ± 12	14 ± 9	10 ± 9	13 ± 9	10 ± 5P	-46
Summer[3]	39 ± 25	33 ± 29	24 ± 11	31 ± 14	28 ± 11	26 ± 9	34
Fall[4]	7 ± 2	15 ± 12	14 ± 9	17 ± 9	18 ± 9	12 ± 9	-75
Study[5]	**16 ± 20**	**23 ± 24**	**19 ± 11**	**23 ± 14**	**23 ± 12**	**15 ± 10**	**7**

[a] Refers to daily composite samples collected at the sampling locations
[b] Refers to weekly grab samples collected at the internal pond sampling locations
[1] Refers to period between beginning of April to April 30 each year.
[2] Refers to period between May 1 to June 20 each year
[3] Refers to period between June 21 to September 20 each year
[4] Refers to period between September 21 to November 30 each year.
[5] Refers to entire study (2016 to 2019). Year 2021 was not included as the system was stagnant.
P Significant difference observed (*p-value* < 0.05) when Weir IN is compared to Pond OUT using ANOVA single factor.

s Significant difference observed (*p-value* < 0.05) when compared to location's influent (in this case, previous pond effluent) using ANOVA single factor
* % removal (% retention) was calculated at Pond OUT compared to Weir IN.

In Late Spring, as flows decreased and temperatures increased (mean = 13.7 – 16.2°C), overall mean NO_3^--N declined by 25% between Weir IN and Pond OUT (*p*-value < 0.05, ANOVA). Removal increased with progressively lower seasonal flows each year, from 16% in 2017 to 30% in 2018, and 32% in 2019. Mean NO_3^--N concentrations declined gradually along the flow path, with reductions increasing from Pond 1 (11%) to Pond 4 (48%) relative to Weir IN (Table 5-3). This spatial pattern is consistent with increasing HRT downstream (0.1 to 3.6 d) and the development of stronger redox stratification in sediments as temperatures increased and flow decreased, increasing the persistence of anoxic microsites that support denitrification (Kadlec & Wallace, 2008). Mean sCOD increased across ponds relative to Weir IN (*p*-value < 0.05, ANOVA only with Pond 1), suggesting internally generated carbon sources (e.g., decaying vegetation in sediments) that likely supported NO_3^--N removal under otherwise carbon-limited influent conditions. In addition to denitrification, warming conditions and increasing biomass production may have supported seasonal NO_3^--N uptake via macrophyte and algal assimilation. No statistically significant differences were observed among individual ponds at $\alpha = 0.05$ (ANOVA), although concentrations in Pond 4 was significantly lower than in Pond 3 at $\alpha = 0.10$ (ANOVA).

Summer exhibited the highest mean overall NO_3^--N concentration reduction (53%), consistent with enhanced denitrification and biological assimilation under warmer temperatures (mean = 17.7 to 21.1°C) and prolonged HRT (2017 = 9.7 d, 2018 = 37.5 d, and 2019 = >500 d) (Bachand & Horne, 2005; Kadlec & Reddy, 2001; Lee et al., 2009). Summer also corresponded to the highest influent sCOD, which was significantly greater than other seasons (*p*-value < 0.05, ANOVA; Table 5-3), suggesting a larger seasonal pool of dissolved carbon to support microbial NO_3^--N processing. At Pond 1, NO_3^--N declined by a mean of 47%, and reductions in NO_3^--N (0.5 – 5.2 mg N/L) were concurrent with increases in Org N (0.2 – 0.9 mg N/L), and NH_4^+-N (up to 0.4 – 0.8 mg N/L). This suggests temporary assimilation of inorganic N into algal biomass followed by mineralization during turnover, occurring alongside net NO_3^--N removal (Kovacic et al., 2000; Mitsch & Gosselink, 2015). Downstream, the deeper Pond 2 (mean depth = 0.7 m) reduced NO_3^--N by 66% relative to concentrations exiting Pond 1 (*p*-value < 0.05, ANOVA). From Pond 2 to Pond 4, stable Org N and NH_4^+-N concentrations (Table 5-3), with progressive declines in NO_3^--

N and sCOD, indicate a transition away from short-term biomass recycling toward net NO_3^--N attenuation. The continued reduction in NO_3^--N from Pond 2 to Pond 4 without corresponding increases in Org N or NH_4^+-N is therefore most consistent with denitrification becoming the dominant pathway of NO_3^--N removal once the algal-mediated cycling diminished. Between Pond 2 to Pond 4, NO_3^--N concentrations decreased by 48%, before increasing at Pond OUT.

Fall conditions were broadly similar to Late Spring, with moderate but variable NO_3^--N removal (-10% to 35%; overall mean = 28%). Despite low influent sCOD (7 ± 2 mg O_2/L), outlet sCOD increased (*p*-value < 0.1, ANOVA), consistent with net release of soluble carbon from senescent vegetation and decomposition of accumulated organic matter (Table 5-3). This supports the interpretation of a carbon-limited system in which the major electron donor source is internally produced. However, declining temperatures (mean = 1.9 to 5.7°C), increased water-column oxygenation (10.1 to 12.4 mg O_2/L), and higher flows likely reduced persistence and accessibility to anoxic zones, constraining denitrification relative to summer conditions. Macrophyte uptake also likely declined in Fall due to senescence and N translocation to belowground biomass (Gottschall et al., 2007). During the brief late Fall flow in 2021, NO_3^--N concentrations increased sharply across the system (1.3 ± 0.5 - 5.7 ± 0.7 mg N/L to 6.7 ± 0.8 mg N/L) within all ponds, with influent averaging to 7.0 ± 0.8 mg N/L. This response suggests replacement of previously stagnant, reduced waters and rapid redistribution of NO_3^--N throughout the system (Figure 5-3).

Pond OUT, shallow (mean depth = 0.33 m) and most vegetated pond in the system (42% vegetation coverage), was expected to enhance NO_3^--N attenuation through macrophyte-mediated processes, including direct N assimilation (Bachand & Horne, 2005; Borin & Tocchetto, 2007; Gottschall et al., 2007), provision of redox-stratified habitat supporting denitrification (Soana et al., 2018, 2025), labile organic carbon supply via root exudates and decaying detritus (Bastviken et al., 2005; Sun et al., 2024), and coupled nitrification - denitrification at the root-soil-water interface (Mei et al., 2014; Sun et al., 2024), while concurrently reducing hydrodynamic disturbance and promoting sedimentation (Kadlec & Wallace, 2008; Vymazal, 2010). Contrary to these expectations, mean NO_3^--N increased substantially between Pond 4 and Pond OUT (study = +73%, *p*-value < 0.05, ANOVA, Table 5-3), indicating that Pond OUT did not consistently function as a polishing cell for NO_3^--N. Mean daily composite and weekly grab samples of NO_3^--N at Pond OUT were effectively the same at 5.2 ± 2.5 mg N/L and 5.1 ± 2.6 mg N/L, respectively,

alleviating a concern that differences in sampling frequency could explain the observed concentration increase at Pond OUT. The increase persisted across seasons and was most pronounced in summer (+70%), followed by Late Spring (+41%) and Fall (+24%), which contrasts with the expectation that vegetation-mediated nutrient removal in cold-climate ponds and CWs is strongest during the growing season (summer) (Brix, 2003).

During summer, outlet discharge occurred only during precipitation-induced flow events; consequently, summer NO_3^--N measurements at Pond OUT reflect episodic flushing conditions rather than quiescent (stagnant) pond conditions. Previous findings report that flow velocity regulates denitrification by controlling NO_3^- delivery and oxygen penetration into benthic biofilms. While moderate velocities can increase NO_3^- supply, elevated hydrodynamic conditions enhance oxygenation, shift microbial metabolism toward aerobic pathways, and suppress denitrification (Arnon et al., 2007; Sirivedhin & Gray, 2006; Soana et al., 2018). These hydrodynamic controls may have reduced the capacity for macrophyte-mediated NO_3^--N removal at Pond OUT while promoting NO_3^--N production. Late-Spring increases may reflect similar hydrodynamic controls in addition to release of assimilated N during tissue decay under winter ice-cover (Vymazal, 2007; White & Reddy, 2003). Increased NO_3^--N concentrations during Fall, when flows were higher and HRTs were reduced, may also reflect macrophyte phenology, as senescence can involve translocation of N belowground (Gottschall et al., 2007) along with release of labile N during decomposition.

This response contrasts with treatment-train recommendations in which a deeper sedimentation basin precedes a vegetated wetland polishing cell (Beutel et al., 2009; Kadlec, 2003; Kovacic et al., 2006). In the present system, this design sequence was broadly represented by the deeper Pond 4 (1.3 m) followed by the shallow, but moderately vegetated Pond OUT; however, the expected polishing effect was not consistently observed. This may reflect the shallow depth, relatively small area (and therefore reduced volume) and vegetation cover below commonly cited thresholds (> 50%) (Kill et al., 2022; Koskiaho & Puustinen, 2019; Lavrnić et al., 2020), limiting capacity to buffer high-flow events and sustain macrophyte-mediated NO_3^--N processing. Nevertheless, these results demonstrate that system-scale removal calculated solely between the inlet and outlet underestimated internal NO_3^--N processing. When evaluated relative to overall mean influent concentrations, NO_3^--N differed significantly among ponds (p-value < 0.05,

ANOVA), with relative removal on a concentration basis increasing progressively along the flow path and peaking at Pond 4 (NO_3^--N = 59%) before declining at Pond OUT (NO_3^--N = 30%).

5.3.3. Mass load retention

Evaluation of NO_3^--N mass loads provided additional insight into system performance by explicitly accounting for seasonal and interannual variability in flow conditions (discussed in section 5.4.1.). In contrast to concentration-based metrics, which reflect changes in water quality, mass load assessments directly quantify the system's effectiveness in reducing downstream NO_3^--N export under variable flow conditions. Cumulative seasonal and annual NO_3^--N loads at the inlet (Weir IN) and outlet (Pond OUT) varied strongly among years, highlighting the dominant role of hydrology in regulating NO_3^--N export from the system (Table 5-4).

Following system construction in Spring 2016, outflow occurred only during late Fall (October-November 2016), during which a seasonal NO_3^--N mass reduction of 48% was observed. Across the study period, annual influent NO_3^--N loads ranged from 6.9 to 26.2 kg N/ha, with the highest loads recorded in 2017, the wettest and highest-flow year (cumulative inflow = 299 mm/ha drained) and accounting for 42% of the total NO_3^--N loading delivered to the system over the study. Annual-system-scale NO_3^--N mass reduction was moderate overall and declined from 21% in 2017 to 16% in 2018 to 10% in 2019 (Table 5-4). These interannual differences was consistent with differences in total inflow and total mass input (2017 > 2018 > 2019).

Table 5-4. Seasonal cumulative loads of Nitrate (kg N/ha) at inlet and outlet of the pond-wetland system across the entire study, along with associated relative removal efficiencies.

	2016			2017			2018			2019			2021			Study
	IN[a]	OUT[b]	%	IN[a]	OUT[b]	%	IN[a]	OUT[b]	%	IN[a]	OUT[b]	%	IN[a]	OUT[b]	%	%
Cumulative mass load* (kg N/ha)																
Spring-melt[c]	-	-	-	3.0	3.3	**-12**	6.5	5.8	**12**	7.5	7.5	**-1**	6.5	5.8	**12**	**5**
Late Spring[d]	-	-	-	8.1	7.8	**4**	3.8	2.9	**25**	4.4	3.1	**30**	0.0	0.0	**0**	**16**
Summer[e]	-	-	-	7.5	3.6	**53**	0.5	0.2	**52**	0.1	0.0	**49**	0.0	0.0	**0**	**53**
Fall[f]	0.1	0.1	48[g]	7.6	6.0	**21**	5.2	4.7	**10**	1.5	1.4	**1**	0.4	0.2	**42**[g]	**16**
Total (Nitrate)	0.1	0.1	**48**	26.2	20.7	**21**	16.1	13.6	**16**	13.5	12.1	**10**	6.9	6.0	**13**	**17**
Total (TN)	0.1	0.1	**43**	29.8	23.7	**20**	18.8	15.8	**16**	15.6	13.9	**11**	7.9	8.8	**-12**	**14**

[a] Refers to Weir IN monitoring station, which acted as the inlet to the pond-wetland system
[b] Refers to Pond OUT, located at the end of the pond-wetland system
[c] Period between first measurement in early April to April 30, capturing the melt of accumulated snow on the ground
[d] Period between May 1 to June 20, referring to later spring season in northern hemisphere
[e] Period between June 21 to September 20, based on northern hemisphere season
[f] Period between September 21 to November 30, based on northern hemisphere season
[g] Represents period retention for when flow occurred or resumed (October-November)
* Daily NO_3^--N composite samples were used to calculate mass load at the two monitoring locations.

Seasonal loads indicate that NO_3^--N export was concentrated during Spring-melt, Late Spring and Fall. Although modest NO_3^--N mass reduction occurred during these periods (5 to 16%), high cumulative inflows, reduced HRTs, and relatively cold conditions limited the capacity for NO_3^--N removal via denitrification (Table 5-1 A, B, 5-4). Periods of weak or negative NO_3^--N mass reduction occurred during Spring-melt 2017 (HRT = 2.7 d), Late Spring 2017 (HRT = 4.1 d), Spring-melt 2019 (HRT = 1.6 d), and Fall 2019 (HRT = 18.7 d). These responses align with minimal concentration retention observed during the same periods, ranging from -12% to 4%, suggesting that hydrologic transport exceeded biogeochemical processing capacity, resulting in limited NO_3^--N export from net NO_3^--N production followed by flushing (e.g., Org N mineralization and nitrification, and senescence-associated N release in Fall).

In contrast, Summer consistently exhibited the highest percentage NO_3^--N mass reduction (49 to 53%), in agreement with concentration-based results and indicating enhanced in-system removal under warm temperatures and prolonged HRTs (9.7 to 781 d); conditions favourable for denitrification and sustained biological processing. However, Summer contributed relatively little to total annual NO_3^--N export in most years due to low or absent summer outflow, except in 2017, when sustained summer flow occurred. Notably, despite the highest summer cumulative outflow in 2017 (69.1 mm/ha drained) and relatively short HRT (9.7 d), the system reduced concentrations and mass export by 53%, highlighting the importance of warmer temperature-driven kinetics during this period. Nevertheless, the seasonal mismatch between NO_3^--N concentration and mass reduction demonstrates that high relative removal during low-flow periods does not necessarily translate into substantial reductions in annual NO_3^--N export.

To support system-scale TN export estimates, daily TN loads were estimated by combining daily composite NO_3^--N concentrations with average Org N contributions derived from weekly grab samples. Over the full monitoring period (2016 to 2021[9]), cumulative influent loads totalled 91.0 kg N/ha as TN and 78.2 kg N/ha as NO_3^--N, of which 14% TN and 17% NO_3^--N were removed at the system scale. These values fall within reported mass reduction ranges for temperate treatment ponds and constructed wetlands (TN: 3 to 55%; NO_3^--N: 6 to 64%; Table 5-2) and are comparable to or above average values reported for cold-climate (*Dfb*) temperate systems (6 to

[9] Year 2018 mass loads were used for year 2020 as May to November precipitation and temperature strongly correlated (R = 0.87, 0.98, respectively).

14%), where high seasonal NO_3^--N loads delivered during periods of short HRT frequently constrain denitrification.

Although inlet-outlet load reductions provide the net system response, internal monitoring demonstrated spatial variability in NO_3^--N processing along the flow path. When evaluated relative to influent loads during periods with internal pond sampling (2017-2019) (which does not include spring melt), NO_3^--N mass reduction increased progressively along the pond sequence, from 27% at Pond 1, to 31% at Pond 2 and 38% at Pond 3, reaching a maximum at Pond 4 (46%), before declining at Pond OUT (29%). This indicates that internal NO_3^--N removal occurred upstream, but net system performance was partially offset by downstream processes and/or hydrologic conditions influencing Pond OUT.

Taken together, these mass load analyses demonstrate that the pond-wetland system is capable of high NO_3^--N removal under favourable thermal and hydraulic conditions, but its overall effectiveness is constrained by seasonal timing of NO_3^--N delivery relative to denitrification and possibly plant uptake capacity. Because high-flow periods dominate annual NO_3^--N loading yet coincide with conditions that kinetically limit denitrification, inlet-outlet differences alone cannot isolate reaction-controlled removal. To address this limitation, denitrification kinetics were evaluated using a cascading pond-to-pond framework exploiting the series configuration of the system, as described in the following section.

5.3.4. Denitrification kinetic rates

Quantifying denitrification kinetics requires distinguishing reaction-driven NO_3^--N removal from hydrologically driven variability in NO_3^--N transport and export. In free-surface CW studies, denitrification rate constants (k) are commonly estimated using the areal-based P-k-C* model (Kadlec & Wallace, 2008), which derives apparent first-order kinetics from inlet-outlet concentration data and hydraulic loading rate. While effective for shallow wetlands with relatively uniform depth, the applicability of this approach to pond-wetland systems exhibiting pronounced spatial variability in depth and HRT is less certain.

To evaluate both model structure and spatial resolution, k values were estimated using (i) traditional inlet-outlet analyses (Kadlec & Wallace, 2008), and (ii) a cascading pond-to-pond framework, applying both areal- and volumetric-based P-k-C* equations. The cascading approach

exploits the series configuration of the pond system and reduces masking of internal processes inherent to inlet-outlet evaluations by resolving sequential NO_3^--N concentration gradients along the flow path. Cascading kinetic analyses were conducted at multiple temporal resolutions (daily, weekly, monthly, and seasonal) to assess the influence of temporal aggregation on model performance. Apparent k values derived at daily and weekly scales exhibited high variability due to short-term hydrologic fluctuations and concentration noise (R^2 = 0.02 – 0.19) and at seasonal scale, there were insufficient data points. Monthly aggregation reduced variability and produced stable concentration gradients for both inlet - outlet and cascading analyses and resulted in consistently high R^2 (0.74 - 0.83) for both areal- and volumetric-based equations. Monthly-scale analyses yielded the highest explanatory power following application of a consistent $\theta = 1.19$ and supports the assumption of pseudo steady-state conditions required for application of first-order P-k-C* model.

Across both spatial frameworks, cascading analyses improved model performance and interpretability relative to traditional inlet-outlet evaluations by explicitly resolving sequential NO_3^--N concentration gradients (Table 5-5). Within the cascading framework, the areal-based equation outperformed the volumetric (HRT-based) equation, yielding lower RMSE (1.23 vs 3.70) with slightly higher explanatory power (R^2 = 0.83 vs 0.81). These results indicate that, despite differences in depth and HRT among the ponds, apparent system-scale k values scaled more strongly with benthic surface area than with the water-column volume, consistent with sediment-dominated denitrification processes.

To further evaluate why the areal-based cascading model outperformed the volumetric model (i.e., whether performance scaled with benthic area rather than pond volume), k values were examined as a function of pond depth. k_A and k_V values for individual ponds were calculated by applying $\theta = 1.19$ and plotted against mean pond depth (Figure 5-4). Areal-based k values remained relatively consistent across ponds despite differences in depth, indicating minimal dependence on (green linear trendline). In contrast, volumetric-based k values exhibited a strong inverse relationship with depth, with disproportionately high values predicted for the shallow upstream pond as well as stronger correlation with depth between 0.6 and 1.3 m (black linear trendline) compared with the areal based kinetics. This demonstrates that an areal-based approach can be used to describe NO_3^- removal kinetics in pond cells with depths varying from 0.08 to 1.3

m.

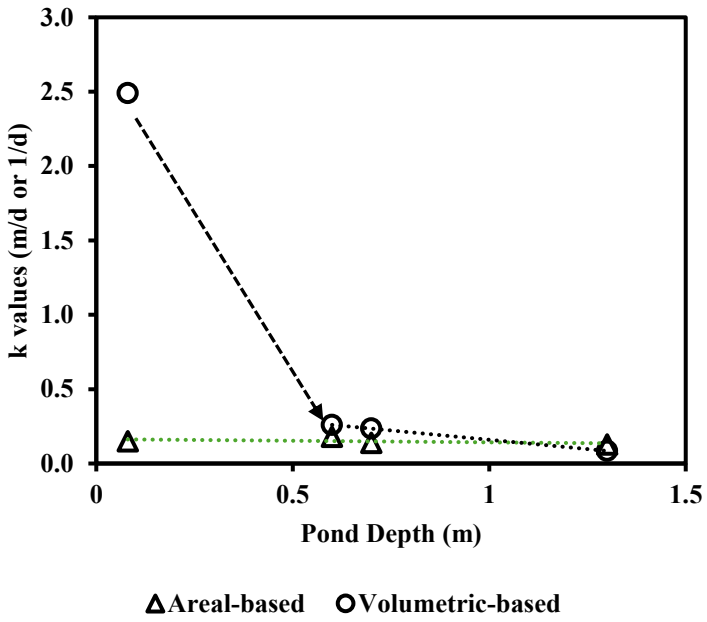

Figure 5-5. Comparison of denitrification rate constants (k) at individual ponds estimated using areal-based (m/d) and volumetric based (1/d) P-k-c* model plotted against mean pond depth. Note: Pond OUT was not included in this comparison as negative k values were calculated, consistent with export of NO_3^--N observed.

This also suggests a balance between increased direct contact with sediment in shallow ponds and higher redox gradients and longer HRTs in deeper ponds act to maintain consistent kinetics. In deeper ponds, the increased vertical distance between overlying water column and sediment denitrification zones constrains NO_3^--N delivery as water must traverse a longer diffusive pathway to reach denitrifying bacteria, reducing effective reaction rates (Uusheimo et al., 2018). Although deeper ponds provide increased volume and longer HRT, they also reduce effective contact between flowing water and reactive sediment and vegetative surfaces, thereby limiting NO_3^--N transformation efficiency (Koskiaho et al., 2003). In this study the deepest pond at 1.3 m exhibited an 18% lower areal k-value than the average of the three shallower ponds, suggesting depth may start to play a negative role in nitrate removal kinetics beyond 0.7 m.

Comparison with published values (Table 5-5) shows that cascading areal-based k values fall within the range reported for agricultural constructed wetlands and stormwater pond-wetland systems. Because system-scale estimates included Pond OUT, which exhibited increases in NO_3^--N relative to Pond 4 during several seasons, reported k values are likely conservative (i.e., underestimated). For the areal cascade model, if the system were defined to end at Pond 4, the resulting areal k value would increase to 0.16 m/d, with a higher R^2 (0.84) and lower RMSE (1.2).

Agreement with the broader literature supports the robustness of the estimated kinetics and reinforces the suitability of areal first-order equations for pond-wetland systems arranged in series. Overall, the cascading analysis demonstrates that denitrification kinetics in pond-wetland treatment systems are best described by areal scaling at a monthly temporal resolution in this region. The agreement between estimated k_A values and published ranges that P-k-C* framework can reasonably represent NO_3^--N removal dynamics in pond-wetland systems under cold-climate conditions.

Table 5-5. Comparison of areal (k_A) first-order nitrate removal rate constants reported for full-scale, pond-wetland, agricultural wetland, and stormwater treatment systems.

Studies	Region	Type of system	k_A (m/d)
This study[1] (inlet-outlet)*	Canada	Pond-wetland	0.10 (R^2 = 0.74)
This study[1] (cascading)*	Canada	Pond-wetland	**0.14 (R^2 = 0.83)**
Beutel et al. (2009)[2]	USA	Sedimentation Basin Constructed Wetland	0.31 0.53 – 0.54 (R^2 = 0.25)
Haverstock (2010)[2]	Canada	Constructed Wetland	0.002 – 0.07
Kadlec (2010)	USA	Constructed Wetland	0.241 - 0.35 (R^2 = 0.63 – 0.79)
Karpuzcu & Stringfellow (2012)[1]	USA	Constructed Wetland	0.04 0.79 0.12
Carleton et al. (2001)[2]	USA	Stormwater Wetland and Pond Database	-0.03 – 0.16
Merriman et al. (2017)[1]	Switzerland	Stormwater Wetland[3]	0.23 0.20

[1] Rate constants derived using P-k-C* model (Kadlec & Wallace, 2008)
[2] Rate constants derived using based on k-C* model (Kadlec & Knight, 1996)
[3] For wetlands with similar mean influent and effluent concentrations
*monthly temporal aggregation used in this study, for $\theta = 1.19$
-indicates not reported

5.3.5. Nitrogen mass balance

Nitrogen removal within treatment ponds and constructed wetland systems is governed by a combination of temporary storage and permanent transformation processes. A system-scale TN mass balance provides a useful framework for quantifying these pathways and evaluating their relative importance for long-term system performance. Major N attenuation and transformation pathways in pond-wetland systems include permanent removal via microbial denitrification; temporary accumulation in surface sediments and the water column; biological uptake and assimilation by macrophytes, algae, and periphyton; and longer-term storage in native hydric soils

and deeply buried accreted sediments (Bachand & Horne, 2005; Kadlec & Wallace, 2008; Vymazal, 2007; White & Reddy, 2009).

Over the monitoring period (2016 -2021), cumulative TN inputs to the pond-wetland system totaled 3,900 kg N, while cumulative TN export at the outlet was 3386 kg N, resulting in a net system-scale TN retention of 515 kg N (13% of the influent TN) (Figure 5-5). Annual TN load removal was strongly influenced by hydrologic variability. The temporary TN storage pool in the water column represented only 2.1% of the retained TN, indicating a relatively small but labile N pool dominated by dissolved inorganic species (NO_3^--N and NH_4^+-N) available for diffusion-driven transformation.

Sediment mapping conducted at the end of study (2021) indicated an average sediment thickness of 10.2 ± 3.2 cm across the system, corresponding to a mean accumulation rate of 1.7 cm/year since system construction in 2016. Sediment TN accumulation accounted for 10% (50.5 kg N) of the total retained TN. Areal sediment TN mass was fairly consistent among ponds, ranging from an average of 11.1 g N /m^2 at Pond 4 to 13.9 g N/m^2 at Pond 2. Compared to reported values in other systems (17.6 to 30.8 g N/m^2) (Steidl et al., 2019), the relatively low areal TN and limited sediment storage suggest that sediments functioned primarily as reactive zones facilitating N biogeochemical transformation rather than as long-term sequestration pools which is likely due to the young age of the system (Kadlec & Wallace, 2008; Reddy & DeLaune, 2008).

Vegetation was allowed to establish naturally, resulting in limited macrophyte coverage largely confined to Pond 3 and Pond OUT. *Typha latifolia* colonized at densities of 29±2 and 31±3 plants/m^2 at Pond 3 and Pond OUT, respectively, while *Juncus effusus* was restricted to shoreline margins, occupying approximately 10% and 4% of the surface areas at Pond 3 and Pond OUT, respectively. These coverage values are considerably lower than > 50% typically reported in agricultural wetlands (Kill et al., 2022; Koskiaho & Puustinen, 2019; Lavrnić et al., 2020). While studies some studies report dense vegetation development within three years of establishment, (Steidl et al., 2019), others have observed such development only after five years or more (Koskiaho & Puustinen, 2019; Mitsch et al., 2012).

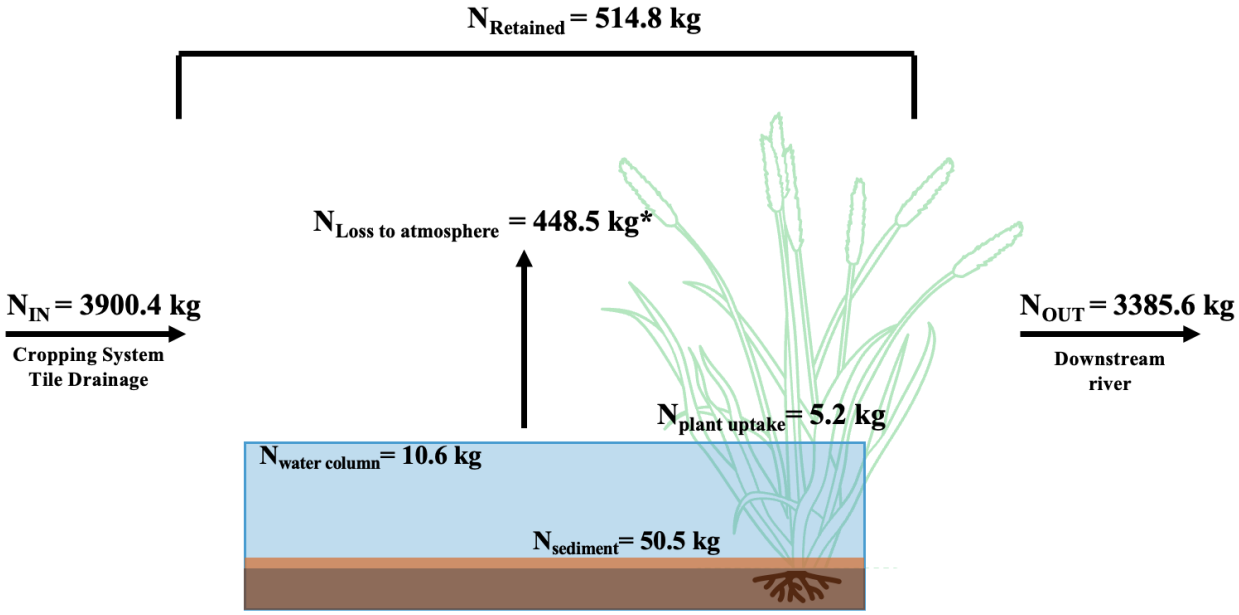

Figure 5-6. Long-term (2016 – 2021) total nitrogen (TN) mass balance for the pond-wetland system receiving cropping tile drainage. All values express as kg N. *Atmospheric nitrogen loss was inferred by difference and assumed to be dominated by denitrification, consistent with nitrate speciation and kinetic analyses. Note: 1. Field sampling was not conducted due to COVID-19 restrictions; TN values from year 2018 was used to estimate loads for that year.

Above-ground N content in *T.latifolia* ranged from 15.5 to 43.0 g/m^2, whereas *J. effusus* exhibited much lower values (1.6 to 2.5 g/m^2), indicating that *T.latifolia* at Pond OUT contributed to most of plant N uptake. These values fall within reported ranges for wetland vegetation (19.0 to 91.0 g/m^2) (Braskerud, 2002; Gottschall et al., 2007; Lavrnić et al., 2020; Vymazal & Dvořáková Březinová, 2018), although comparators will be affected by differences in vegetation density, system age, TN loading, and geographic context. Biological uptake by plants represented the smallest quantified N storage pool in the system, accounting for approximately 5.2 kg N, or 1.0% of the retained TN. Previous studies in temperate CW studies report vegetation N uptake in the range of 1 to 21% of annual N retention in denitrification-dominated systems (Braskerud, 2002; Gordon et al., 2021; Gottschall et al., 2007), suggesting that macrophyte – microbial removal interactions such as organic carbon supply, increased surface area for biofilm colonization, and rhizosphere oxygen regulation, are more important than direct plant N storage (Bachand & Horne, 2005; Nilsson et al., 2023; Soana et al., 2018, 2025; Sun et al., 2024). In this study, overall plant N storage remained limited and transient, reflecting restricted areal coverage and rapid biomass turnover.

After accounting for measured storage pools, the remaining 448.5 kg N (87% of retained

TN) was attributed to atmospheric N loss, inferred by difference from the system-scale mass balance and assumed to be dominated by microbial denitrification (Figure 5-5). This interpretation aligns with prior studies, which report denitrification as the primary N removal mechanism in similar systems. For example, Kovacic et al. (2000) attributed 90% of N removal to denitrification, with remainder attributed to plant uptake, while Braskerud (2002) reported a wider range, from 1.5 to 8.3% of N removal to denitrification and 1-21% through plant uptake, with remaining fraction likely due to sedimentation. Steidl et al. (2019) estimated that approximately 13% of N removal could be attributed to potential denitrification. The dominance of denitrification pathway in the present system relative to sediment and biotic storage indicates that the pond-wetland system functioned primarily as a transformation-driven N sink rather than a long-term N storage reservoir. Given the consistently NO_3^--N dominated N pool observed throughout the study, inferred gaseous N losses are most reasonably attributed to denitrification rather than to unquantified storage pathways. This interpretation is further supported by strong seasonal enhancement of NO_3^--N removal during warm, low-flow periods, and the superior performance of areal-based kinetic model fit, all of which point to denitrification as the principal mechanism of permanent N removal. The magnitude and persistence of this inferred gaseous loss over multiple years further suggest that denitrification capacity was maintained despite interannual variability in hydrology and N loading.

Importantly, the dominance of transformation-driven N removal was established within six years of system construction, indicating that effective sediment-associated denitrification can develop in cold-region pond-wetland systems, even prior to extensive vegetation establishment or long-term soil accretion. Together, these findings suggest that in cold-climates, hydrologic variability and flow-driven export primarily regulate the magnitude of system-scale TN retention, rather than altering the dominance of denitrification as the principal permanent N removal pathway.

5.4. Conclusion

This five-year study (2016 -2021) evaluated nitrogen (N) removal in a cold-region pond-wetland system receiving cropping system tile drainage from Spring-melt (April) to system freeze-up (late November), using integrated analyses of hydrology, concentration dynamics, mass loads, and denitrification kinetics. System-scale inlet-outlet concentrations indicated moderate removal of

total nitrogen (TN; 27%) and nitrate (NO_3^--N; 30%) reflecting strong seasonal and hydrologic constraints on treatment performance. Internal analyses showed NO_3^--N concentrations declined progressively along the treatment train (highest attenuation = 59%), consistent with denitrification and seasonal biological assimilation, before increasing at the terminal shallow, moderately vegetated outlet (Pond OUT) across seasons. This demonstrates that inlet and outlet metrics underestimated internal NO_3^--N processing and suggests that a shallow wetland cell may underperform unless designed with sufficient vegetation coverage and buffering capacity to sustain NO_3^--N attenuation during precipitation-driven events. Mass load analyses demonstrated that annual NO_3^--N export was governed primarily by seasonal timing of NO_3^--N delivery rather than by maximum in-system removal efficiency. Although summer exhibited the highest NO_3^--N load removal (53%), high-flow periods during other seasons dominated annual NO_3^--N export while coinciding with conditions that kinetically limited denitrification. A cascading pond-to-pond areal-based first order model best described system performance (rate constant, $k = 0.14$ m/d, $\theta = 1.19$, $R^2 = 0.83$), outperforming traditional inlet-outlet and volumetric (HRT-based) formulations. At pond scale, areal k exhibited minimal depth dependence compared to volumetric k, indicating that denitrification scaled more strongly with benthic surface area than with water-column volume. Areal k values were highest and comparable at 0.6-0.7 m and declined slightly at 1.3 m, suggesting a depth threshold beyond which increased water-column depth does not proportionally enhance NO_3^--N removal, and that moderate pond depths may maximize sediment-water contact and diffusive delivery of NO_3^--N. End-of-study system-scale TN mass balance results confirmed that temporary storage in sediments, vegetation, and the water column accounted for only a minor fraction of retained TN mass, while the majority of long-term retention was attributed to atmospheric loss dominated by microbial denitrification (87%). Overall, these full-scale results demonstrate that pond-wetland systems can provide considerable N removal in cold-climate regions and emphasize the importance of internal-scale and seasonally resolved assessments for accurately evaluating N removal performance in cold-treatment systems.

References

AAFC. (2023). *Constructed Wetlands*. Agriculture and Agri-Food Canada = Agriculture et agroalimentaire Canada.

AAFC. (2024). *Farm surface water management* . Agriculture and Agri-Food Canada (AAFC). https://agriculture.canada.ca/en/agricultural-production/water/ponds-and-dugouts/farm-surface-water-management

Agricrop. (2023). *Monthly Rainfall Data*. https://www.agricorp.com/en-ca/Programs/ProductionInsurance/ForageRainfall/Pages/RainfallData.aspx

APHA. (1998). Method 4500-NH4 B. In *Standard methods for the examination of water and wastewater* (20th ed.). APHA.

APHA. (2017). *Standard Methods for the Examination of Water and Wastewater* (23rd ed.). American Public Health Association.

Arnon, S., Gray, K. A., & Packman, A. I. (2007). Biophysicochemical process coupling controls nitrate use by benthic biofilms. *Limnology and Oceanography*, *52*(4), 1665–1671. https://doi.org/10.4319/LO.2007.52.4.1665;PAGE:STRING:ARTICLE/CHAPTER

Bachand, P. A. M., & Horne, A. J. (2005). Denitrification in Constructed free-water surface wetlands: II. Effects of vegetation and temperature. *Ecological Engineering*, *14*(1), 17–32. https://doi.org/10.1556/Pollack.10.2015.1.8

Bai, X., Li, J., & Chang, S. (2023). Effects of Different Carbon and Nitrogen Ratios on Nitrogen Removal Efficiency and Microbial Communities in Constructed Wetlands. *Water (Switzerland)*, *15*(24). https://doi.org/10.3390/W15244272

Baker, L. A. (1998). Design considerations and applications for wetland treatment of high-nitrate waters. *Water Science Technology*, (38), 389–395.

Bastviken, S. K., Eriksson, P. G., Premrov, A., & Tonderski, K. (2005). Potential denitrification in wetland sediments with different plant species detritus. *Ecological Engineering*, *25*(2), 183–190. https://doi.org/10.1016/J.ECOLENG.2005.04.013

Beckingham, B., Callahan, T., & Vulava, V. (2019). Stormwater Ponds in the Southeastern U.S. Coastal Plain: Hydrogeology, Contaminant Fate, and the Need for a Social-Ecological Framework. *Frontiers in Environmental Science*, *7*(July), 1–14. https://doi.org/10.3389/fenvs.2019.00117

Beutel, M. W., Newton, C. D., Brouillard, E. S., & Watts, R. J. (2009). Nitrate removal in surface-flow constructed wetlands treating dilute agricultural runoff in the lower Yakima Basin, Washington. *Ecological Engineering*, *35*(10), 1538–1546. https://doi.org/https://doi.org/10.1016/j.ecoleng.2009.07.005

Borin, M., & Tocchetto, D. (2007). Five year water and nitrogen balance for a constructed surface flow wetland treating agricultural drainage waters. *Science of The Total Environment*, *380*(1), 38–47. https://doi.org/https://doi.org/10.1016/j.scitotenv.2006.12.039

Braskerud, B. C. (2002). Factors affecting nitrogen retention in small constructed wetlands treating agricultural non-point source pollution. *Ecological Engineering*, *18*(3), 351–370. https://doi.org/10.1016/S0925-8574(01)00099-4

Brix, H. (2003). *Plants used in constructed wetlands and their functions*. https://www.researchgate.net/publication/230563384

Brunet, C. E., Gemrich, E. R. C., Biedermann, S., Jacobson, P. J., Schilling, K. E., Jones, C. S., & Graham, A. M. (2021). Nutrient capture in an Iowa farm pond: Insights from high-frequency observations. *Journal of Environmental Management*, *299*. https://doi.org/10.1016/j.jenvman.2021.113647

Carleton, J. N., Grizzard, T. J., Godrej, A. N., & Post, H. E. (2001). Factors affecting the performance of stormwater treatment wetlands. *Water Research*, *35*(6), 1552–1562. https://doi.org/10.1016/S0043-1354(00)00416-4

CCME. (2012). Canadian Water Quality Guidelines for the Protection of Aquatic Life NITRATE ION. In *CCME* (Number 3). https://ccme.ca/en/res/nitrate-ion-en-canadian-water-quality-guidelines-for-the-protection-of-aquatic-life.pdf

Chrétien, F., Gagnon, P., Thériault, G., & Guillou, M. (2016). Performance Analysis of a Wet-Retention Pond in a Small Agricultural Catchment. *Journal of Environmental Engineering*, *142*(4), 04016005. https://doi.org/10.1061/(asce)ee.1943-7870.0001081

Chun, J. A., & Cooke, R. A. (2008). Calibrating Agridrain Water Level Control Structures using generalised Weir and Orifice equations. *Applied Engineering in Agriculture*, *24*(5), 595–602.

Clary, J., Leisenring, M., & Strecker, E. (2020). *International Stormwater BMP Database: 2020 Summary Statistics*. www.waterrf.org

Cooper, M. J. (2016, March 1). Nitrogen limitation of algal biofilms in coastal wetlands of Lakes Michigan and Huron. *Great Lakes Connection, International Joint Commission*, *35*(1). https://doi.org/10.1086/684646

Daigle, D. (2003). Dead seas nutrient pollution in coastal waters. *Multinational Monitor*, *24*(9), 12–15. https://go.gale.com/ps/i.do?p=AONE&sw=w&issn=01974637&v=2.1&it=r&id=GALE%7CA109355430&sid=googleScholar&linkaccess=fulltext

Drury, C. F., Tan, C. S., Reynolds, W. D., Welacky, T. W., Oloya, T. O., & Gaynor, J. D. (2009). Managing Tile Drainage, Subirrigation, and Nitrogen Fertilization to Enhance Crop Yields and Reduce Nitrate Loss. *Journal of Environmental Quality*, *38*(3), 1193–1204. https://doi.org/10.2134/jeq2008.0036

ECCC. (2023). *Daily Data Report - Climate - Environment and Climate Change Canada*. https://climate.weather.gc.ca/climate_data/daily_data_e.html?StationID=49568

ECCC. (2025). *Canadian Climate Normals 1991-2020 Data for Ottawa (Airport)*. Https://Climate.Weather.Gc.ca/Climate_normals/Index_e.Html.

FAOSTAT. (2025). *Cropland Nutrient Balance*. Food and Agriculture Organization of the United Nations (FAO). https://www.fao.org/faostat/en/#data/ESB/visualize

Gold, A. C., Thompson, S. P., & Piehler, M. F. (2017). Water quality before and after watershed-scale implementation of stormwater wet ponds in the coastal plain. *Ecological Engineering*, *105*, 240–251. https://doi.org/10.1016/J.ECOLENG.2017.05.003

Gordon, B. A., Lenhart, C., Peterson, H., Gamble, J., Nieber, J., Current, D., & Brenke, A. (2021). Reduction of nutrient loads from agricultural subsurface drainage water in a small, edge-of-field constructed treatment wetland. *Ecological Engineering*, *160*. https://doi.org/10.1016/j.ecoleng.2020.106128

Gottschall, N., Boutin, C., Crolla, A., Kinsley, C., & Champagne, P. (2007). The role of plants in the removal of nutrients at a constructed wetland treating agricultural (dairy) wastewater, Ontario, Canada. *Ecological Engineering*, *29*(2), 154–163. https://doi.org/10.1016/j.ecoleng.2006.06.004

Grebliunas, B. D., & Perry, W. L. (2016). The role of C:N:P stoichiometry in affecting denitrification in sediments from agricultural surface and tile-water wetlands. *SpringerPlus*, *5*(1). https://doi.org/10.1186/s40064-016-1820-6

Groh, T. A., Gentry, L. E., & David, M. B. (2015). Nitrogen Removal and Greenhouse Gas Emissions from Constructed Wetlands Receiving Tile Drainage Water. *Journal of Environmental Quality*, *44*(3), 1001–1010. https://doi.org/10.2134/JEQ2014.10.0415

Harper, H. H., & Baker, D. M. (2007). *Evaluation of Current Stormwater Design Criteria within the State of Florida: Final Report*.

Harper, H. H., & Herr, J. L. (1993). *Treatment Efficiencies of Detention with Filtration Systems* (Number August).

Haverstock, M. J. (2010). *An Assessment of a Wetland-Reservoir Wastewater Treatment and Reuse System Receiving Agricultural Drainage Water in Nova Scotia*. Dalhousie University.

Health Canada. (2014). *Guidelines for Canadian Drinking Water Quality: Guideline Technical Document – Nitrate and Nitrite*. https://www.canada.ca/en/health-canada/services/publications/healthy-living/guidelines-canadian-drinking-water-quality-guideline-technical-document-nitrate-nitrite.html

Ivanovsky, A., Belles, A., Criquet, J., Dumoulin, D., Noble, P., Alary, C., & Billon, G. (2018). Assessment of the treatment efficiency of an urban stormwater pond and its impact on the natural downstream watercourse. *Journal of Environmental Management*, *226*, 120–130. https://doi.org/10.1016/J.JENVMAN.2018.08.015

Kadlec, R. H. (2000). The inadequacy of first-order treatment wetland models. *Ecological Engineering*, *15*, 105–119. https://ac.els-cdn.com/S0925857499000397/1-s2.0-S0925857499000397-main.pdf?_tid=a8ab7664-05ff-11e8-a39f-00000aacb35f&acdnat=1517345804_950c9c1e5b78c1e8cabd4035c84aceb1

Kadlec, R. H. (2003). Pond and wetland treatment. *Water Science and Technology*, *48*(5), 1–8. https://doi.org/10.2166/wst.2003.0266

Kadlec, R. H. (2010). Nitrate dynamics in event-driven wetlands. *Ecological Engineering*, *36*, 503–516. https://doi.org/10.1016/j.ecoleng.2009.11.020

Kadlec, R. H., & Knight, R. L. (1996). *Treatment Wetland*. Lewis Publishers Inc.

Kadlec, R. H., & Reddy, K. R. (2001). Temperature Effects in Treatment Wetlands. *Water Environment Research*, *73*(5), 543–557. https://doi.org/10.2175/106143001x139614

Kadlec, R. H., & Wallace, S. D. (2008). *Treatment Wetlands* (Second). Taylor & Francis Group, LLC.

Karpuzcu, M. E., & Stringfellow, W. T. (2012). Kinetics of nitrate removal in wetlands receiving agricultural drainage. *Ecological Engineering*, *42*, 295–303. https://doi.org/10.1016/j.ecoleng.2012.02.015

Kill, K., Grinberga, L., Koskiaho, J., Mander, Ü., Wahlroos, O., Lauva, D., Pärn, J., & Kasak, K. (2022). Phosphorus removal efficiency by in-stream constructed wetlands treating agricultural runoff: Influence of vegetation and design. *Ecological Engineering*, *180*. https://doi.org/10.1016/j.ecoleng.2022.106664

Koch, B. J., Febria, C. M., Gevrey, M., Wainger, L. A., & Palmer, M. A. (2014). Nitrogen Removal by Stormwater Management Structures: A Data Synthesis. *JAWRA Journal of the American Water Resources Association*, *50*(6), 1594–1607. https://doi.org/10.1111/JAWR.12223

Koskiaho, J., Ekholm, P., Räty, M., Riihimäki, J., & Puustinen, M. (2003). Retaining agricultural nutrients in constructed wetlands—experiences under boreal conditions. *Ecological Engineering*, *20*(1), 89–103. https://doi.org/https://doi.org/10.1016/S0925-8574(03)00006-5

Koskiaho, J., & Puustinen, M. (2019). Suspended solids and nutrient retention in two constructed wetlands as determined from continuous data recorded with sensors. *Ecological Engineering*, *137*, 65–75. https://doi.org/10.1016/j.ecoleng.2019.04.006

Kottek, M., Grieser, J., Beck, C., Rudolf, B., & Rubel, F. (2006). World map of the Köppen-Geiger climate classification updated. *Meteorologische Zeitschrift*, *15*(3), 259–263. https://doi.org/10.1127/0941-2948/2006/0130

Kovacic, D. A., David, M. B., Gentry, L. E., Starks, K. M., & Cooke, R. A. (2000). Effectiveness of Constructed Wetlands in Reducing Nitrogen and Phosphorus Export from Agricultural Tile Drainage. *Journal of Environmental Quality*, *29*(4), 1262–1274. https://doi.org/10.2134/jeq2000.00472425002900040033x

Kovacic, D. A., Twait, R. M., Wallace, M. P., & Bowling, J. M. (2006). Use of created wetlands to improve water quality in the Midwest—Lake Bloomington case study. *Ecological Engineering*, *28*(3), 258–270. https://doi.org/https://doi.org/10.1016/j.ecoleng.2006.08.002

Kulin, G., & Compton, P. R. (1979). A guide to methods and standards for the measurement of water flow. In *National Bureau of Standards, U.S. Department of Commerce* (Number 421). https://nvlpubs.nist.gov/nistpubs/Legacy/SP/nbsspecialpublication421.pdf

Kynkäänniemi, P., Ulén, B., Torstensson, G., & Tonderski, K. S. (2013). Phosphorus retention in a newly constructed wetland receiving agricultural tile drainage water. *Journal of Environmental Quality*, *42*(2), 596–605. https://doi.org/10.2134/jeq2012.0266

Lavrnić, S., Nan, X., Blasioli, S., Braschi, I., Anconelli, S., & Toscano, A. (2020). Performance of a full scale constructed wetland as ecological practice for agricultural drainage water treatment in Northern Italy. *Ecological Engineering*, *154*. https://doi.org/10.1016/j.ecoleng.2020.105927

Lee, C. G., Fletcher, T. D., & Sun, G. (2009). Nitrogen removal in constructed wetland systems. *Engineering in Life Sciences*, *9*(1), 11–22. https://doi.org/10.1002/ELSC.200800049;JOURNAL:JOURNAL:15213846;WGROUP:STRING:PUBLICATION

Li, J., Hao, H., Cheng, G., Liu, C., Ahmed, S., Shabbir, M. A. B., Hussain, H. I., Dai, M., & Yuan, Z. (2017). Enhancing nitrate removal from freshwater pond by regulating carbon/nitrogen ratio. *Frontiers in Microbiology*, *8*(SEP), 273572. https://doi.org/10.3389/FMICB.2017.01712/BIBTEX

Mathew, K. R. (2020). *A field-scale study of controlled tile drainage and a pond-wetland to attenuate nutrients from agricultural overland runoff and subsurface drainage on a farmer-operated seed farm in Saint-Isidore, ON* [University of Ottawa]. http://dx.doi.org/10.20381/ruor-26264

Mei, X. Q., Yang, Y., Tam, N. F. Y., Wang, Y. W., & Li, L. (2014). Roles of root porosity, radial oxygen loss, Fe plaque formation on nutrient removal and tolerance of wetland plants to domestic wastewater. *Water Research*, *50*, 147–159. https://doi.org/10.1016/J.WATRES.2013.12.004

Merriman, L. S., Hathaway, J. M., Burchell, M. R., & Hunt, W. F. (2017). Adapting the relaxed tanks-in-series model for stormwaterwetland water quality performance. *Water (Switzerland)*, *9*(9). https://doi.org/10.3390/w9090691

Metcalf, & Eddy. (2014). *Wastewater Engineering: Treatment and Resource Recovery* (5th ed.).

Mitsch, W., & Gosselink, J. (2015). Wetlands, 5th Edition. In *Wi Ley* (Vol. 91, Number 5). https://www.researchgate.net/publication/271643179_Wetlands_5th_edition

Mitsch, W. J., Zhang, L., Stefanik, K. C., Nahlik, A. M., Anderson, C. J., Bernal, B., Hernandez, M., & Song, K. (2012). Creating Wetlands: Primary Succession, Water Quality Changes, and Self-Design over 15 Years. *BioScience*, *62*(3), 237–250. https://doi.org/10.1525/bio.2012.62.3.5

Ng, H. Y. F., Tan, C. S., Drury, C. F., & Gaynor, J. D. (2002). Controlled drainage and subirrigation influences tile nitrate loss and corn yields in a sandy loam soil in Southwestern Ontario. *Agriculture, Ecosystems & Environment*, *90*(1), 81–88. https://doi.org/https://doi.org/10.1016/S0167-8809(01)00172-4

Nietch, C. T., Borst, M., & O'Shea, M. L. (2001). Stormwater treatment: Ponds vs. constructed wetlands. *Proceedings of the Engineering Foundation Conference*, *263*(Ms 104), 524–528. https://doi.org/10.1061/40602(263)39

Nilsson, J. E., Weisner, S. E. B., & Liess, A. (2023). Wetland nitrogen removal from agricultural runoff in a changing climate. *Science of the Total Environment*, *892*(2023). https://doi.org/10.1016/j.scitotenv.2023.164336

NRCC. (2024, November 21). *When do the seasons start?* Government of Canada. https://nrc.canada.ca/en/certifications-evaluations-standards/canadas-official-time/3-when-do-seasons-start

Oduor, B. O., Campo-Bescós, M. Á., Lana-Renault, N., Kyllmar, K., Mårtensson, K., & Casalí, J. (2023). Quantification of agricultural best management practices impacts on sediment and phosphorous export in a small catchment in southeastern Sweden. *Agricultural Water Management*, *290*, 108595. https://doi.org/10.1016/J.AGWAT.2023.108595

Onset Computer Cooperation. (2008). Barometric Compensation Assistant. In *White Paper Series*.

Pinney, M. L., Westerhoff, P. K., & Baker, L. (2000). Transformations in dissolved organic carbon through constructed wetlands. *Water Research*, *34*(6), 1897–1911. https://doi.org/10.1016/S0043-1354(99)00330-9

Pugliese, L., Heckrath, G. J., Iversen, B. V., & Straface, S. (2023). Treatment Systems for Agricultural Drainage Water and Farmyard Runoff in Denmark: Case Studies. In *Handbook of Environmental Chemistry* (Vol. 117). https://doi.org/10.1007/698_2021_784

Reddy, K. R., & DeLaune, R. D. (2008). Biogeochemistry of Wetlands : Science and Applications. *Biogeochemistry of Wetlands*. https://doi.org/10.1201/9780203491454

Reddy, K. R., DeLaune, R. D., & Inglett, P. W. (2023). *Biogeochemistry of Wetlands* (2nd ed.). CRC Press.

Reddy, K. R., & Patrick, W. H. (1984). Nitrogen transformations and loss in flooded soils and sediments. *Critical Reviews in Environmental Science and Technology*, *13*(4), 273–309. https://doi.org/10.1080/10643388409381709

Robotham, J., Old, G., Rameshwaran, P., Sear, D., Gasca-Tucker, D., Bishop, J., Old, J., & McKnight, D. (2021). Sediment and Nutrient Retention in Ponds on an Agricultural Stream: Evaluating Effectiveness for Diffuse Pollution Mitigation. *Water 2021, Vol. 13, Page 1640*, *13*(12), 1640. https://doi.org/10.3390/W13121640

Royer, T. V., & David, M. B. (2005). Export of dissolved organic carbon from agricultural streams in Illinois, USA. *Aquatic Sciences*, *67*(4), 465–471. https://doi.org/10.1007/S00027-005-0781-6/METRICS

Rushton, B. T., & Bahk, B. M. (2001). Treatment of stormwater runoff from row crop farming in Ruskin, Florida. *Water Science and Technology*, *44*(11–12), 531–538. https://doi.org/10.2166/wst.2001.0876

SC DHEC. (2005). *South Carolina Storm Water Management BMP Handbook*. https://scdhec.gov/Environment/WaterQuality/Stormwater/BMPHandbook/

Schipper, L. A., Robertson, W. D., Gold, A. J., Jaynes, D. B., & Cameron, S. C. (2010). Denitrifying bioreactors—An approach for reducing nitrate loads to receiving waters. *Ecological Engineering*, *36*(11), 1532–1543. https://doi.org/10.1016/J.ECOLENG.2010.04.008

Schober, P., Boer, C., & Schwarte, L. A. (2018). Correlation Coefficients: Appropriate Use and Interpretation. *Anesthesia & Analgesia*, *126*(5).

Shilton, A. N. (Andy N.). (2005). *Pond Treatment Technology*. IWA.

Sirivedhin, T., & Gray, K. A. (2006). Factors affecting denitrification rates in experimental wetlands: Field and laboratory studies. *Ecological Engineering*, *26*(2), 167–181. https://doi.org/https://doi.org/10.1016/j.ecoleng.2005.09.001

Soana, E., Gavioli, A., Tamburini, E., Fano, E. A., & Castaldelli, G. (2018). To mow or not to mow: reed biofilms as denitrification hotspots in drainage canals. *Ecological Engineering*, *113*, 1–10. https://doi.org/10.1016/j.ecoleng.2017.12.029

Soana, E., Vincenzi, F., Gavioli, A., & Castaldelli, G. (2025). Different Denitrification Capacity in Phragmites australis and Typha latifolia Sediments: Does the Availability of Surface Area for Biofilm Colonization Matter? *Water 2025, Vol. 17, Page 560*, *17*(4), 560. https://doi.org/10.3390/W17040560

St. Lawrence Action Plan. (2021). *Nonpoint source pollution - Projects 2021 -2026*. EECE. https://www.planstlaurent.qc.ca/en/developping-knowledge/water-quality/nonpoint-source-pollution

Statista. (2024, December 2). *Canada: fertilizer consumption by nutrient* . Statists Research Department. https://www.statista.com/statistics/1330033/canada-fertilizer-consumption-by-nutrient/

Steidl, J., Kalettka, T., & Bauwe, A. (2019). Nitrogen retention efficiency of a surface-flow constructed wetland receiving tile drainage water: A case study from north-eastern Germany. *Agriculture, Ecosystems and Environment*, *283*. https://doi.org/10.1016/j.agee.2019.106577

Sun, H., Zhou, Y., & Jiang, C. (2024). Regulating Denitrification in Constructed Wetlands: The Synergistic Role of Radial Oxygen Loss and Root Exudates. *Water 2024, Vol. 16, Page 3706*, *16*(24), 3706. https://doi.org/10.3390/W16243706

Sunohara, M. D., Craiovan, E., Topp, E., Gottschall, N., Drury, C. F., & Lapen, D. R. (2014). Comprehensive Nitrogen Budgets for Controlled Tile Drainage Fields in Eastern Ontario, Canada. *Journal of Environmental Quality*, *43*(2), 617–630. https://doi.org/10.2134/jeq2013.04.0117

Tanga, S., Lebeau, B., Crolla, A., Tsitouras, A., Garduño-Ibarra, I. R., & Kinsley, C. (2025). Controlled drainage – Effects on nutrient attenuation and water quality – A field study in Eastern Ontario, Canada. *Agricultural Water Management*, *319*, 109764. https://doi.org/10.1016/j.agwat.2025.109764

Thorén, A. K., Legrand, C., & Tonderski, K. S. (2004). Temporal export of nitrogen from a constructed wetland: Influence of hydrology and senescing submerged plants. *Ecological Engineering*, *23*(4–5), 233–249. https://doi.org/10.1016/j.ecoleng.2004.09.007

USBR. (2001). *Water measurement manual: A Guide to Effective Water Measurement Practices for Better Water Management, 3rd ed.* https://www.usbr.gov/tsc/techreferences/mands/wmm/index.htm

Uusheimo, S., Tulonen, T., Aalto, S. L., & Arvola, L. (2018). Mitigating agricultural nitrogen load with constructed ponds in northern latitudes: A field study on sedimental denitrification rates. *Agriculture, Ecosystems and Environment*, *261*, 71–79. https://doi.org/10.1016/j.agee.2018.04.002

Vymazal, J. (2007). Removal of nutrients in various types of constructed wetlands. *Science of The Total Environment*, *380*(1), 48–65. https://doi.org/https://doi.org/10.1016/j.scitotenv.2006.09.014

Vymazal, J. (2010). Constructed wetlands for wastewater treatment. *Water (Switzerland)*, *2*(3), 530–549. https://doi.org/10.3390/w2030530

Vymazal, J. (2017). The Use of Constructed Wetlands for Nitrogen Removal from Agricultural Drainage: A Review. *Scientia Agriculturae Bohemica*, *48*(2), 82–91. https://doi.org/10.1515/sab-2017-0009

Vymazal, J., & Dvořáková Březinová, T. (2018). Treatment of a small stream impacted by agricultural drainage in a semi-constructed wetland. *Science of The Total Environment*, *643*, 52–62. https://doi.org/10.1016/J.SCITOTENV.2018.06.148

White, J. R., & Reddy, K. R. (2003). Nitrification and Denitrification Rates of Everglades Wetland Soils along a Phosphorus-Impacted Gradient. *Journal of Environmental Quality*, *32*(6), 2436–2443. https://doi.org/https://doi.org/10.2134/jeq2003.2436

White, J. R., & Reddy, K. R. (2009). Biogeochemical Dynamics I: Nitrogen Cycling in Wetlands. In *The Wetlands Handbook* (pp. 213–227). https://doi.org/10.1002/9781444315813.ch9

Working Group on the State of the St. Lawrence Monitoring. (2024). *Overview of the State of the St. Lawrence 2024*.

Xue, Y., Kovacic, D., David, M., Gentry, L., Mulvaney, R., & Lindau, C. (2009). In Situ Measurements of Denitrification in Constructed Wetlands. *Journal of Environmental Quality - J ENVIRON QUAL*, *28*. https://doi.org/10.2134/jeq1999.00472425002800010032x

Chapter 6 – Relative impact of sediments versus stem-associated biofilms on nitrate removal in cold-climate pond-wetland system: Role of microbial potential and environmental constraints

Abstract

Pond-wetland systems can serve as effective beneficial management practices for intercepting nitrate (NO_3^--N) from tile drained cropping systems by integrating features of treatment ponds and constructed wetlands. However, the relative contributions of sediments and macrophyte-associated biofilms on NO_3^- removal, and the environmental controls governing denitrification efficiency in these combined systems, remain poorly understood. Here, field-based microbiome community analyses and batch-scale denitrification assays were used to assess relative NO_3^--N removal in a cold-climate pond-wetland system. Sediments supported higher microbial diversity and a 2.8-fold greater relative abundance of inferred denitrifying taxa than stem-associated biofilms, suggesting greater denitrification potential. Batch-scale incubations under controlled anoxic conditions exhibited zero-order kinetics under unamended condition (carbon-limited), shifting to first-order under carbon amended trials. The estimated rate constant normalised to surface area confirmed that sediments functioned as the dominant zone of NO_3^--N removal, 3 to 9 times more efficient than stem-associated biofilms, which contributed a secondary, condition-dependent role. The narrow range of Arrhenius temperature coefficient (θ = 1.05 to 1.13) revealed consistent temperature sensitivity of across habitats. Denitrification was strongly constrained by temperature at 4°C across all habitats, whereas organic carbon availability became the dominant limiting factor at 20°C. These results demonstrate that effective NO_3^--N removal in pond-wetland systems reflects the interaction of microbial potential with environmental constraints, providing process-based guidance for the design and management of treatment systems in cold-climate regions.

6.1. Introduction

Tile drainage is considered a major pathway of nitrate (NO_3^--N) export from intensively managed cropping systems to downstream surface waters by rapidly conveying NO_3^--N rich, low carbon water from fields to receiving waters, bypassing any riparian attenuation processes. This contributes to eutrophication, harmful algal blooms, and degradation of surface water quality

(Rabalais et al., 2002; Randall & Goss, 2008; Royer & David, 2005). These impacts are particularly relevant in cold-climate regions, such as Canada, where greater NO_3^--N loads are often delivered during periods of limited biological processing capacity (spring and fall), resulting in downstream accumulation and delayed ecological effects under warmer conditions (summer). Growing concern over NO_3^--N enrichment have been documented in regional freshwater systems including, the Laurentian Great Lakes (Cooper, 2016), and the St. Lawrence river basin (Working Group on the State of the St. Lawrence Monitoring, 2024).

In response, Beneficial Management Practices (BMPs) strategically positioned along discharge pathways are increasingly recommended as treatment approaches (ECCC, 2018; OMAFA & OSCIA, 2019; OSCIA, 2023). Pond-wetland systems represent a multifunctional BMP that integrates features of treatment ponds and free-water surface constructed wetlands into a single, nature-based system. These engineered systems incorporate deeper open-water zones (depth > 0.5 m) that increase hydraulic retention time and lower redox conditions with shallow (0.15 m to 0.3 m), vegetated areas that support macrophyte growth, collectively influencing NO_3^--N removal (Kadlec & Wallace, 2008). This hybrid configuration with varying water depths and volumes can potentially generate vertical and longitudinal gradients in redox conditions, organic carbon availability, and hydrodynamics, possibly making NO_3^--N removal within pond-wetland systems inherently spatially heterogeneous.

Denitrification is a dominant pathway for permanent NO_3^--N removal in treatment ponds and wetlands, mediated by facultative anaerobic bacteria that utilize NO_3^--N as an electron acceptor under low-oxygen (O_2) conditions (Beutel et al., 2009; Brunet et al., 2021; Clary et al., 2020; Vymazal, 2007; Xue et al., 2009). These taxonomically diverse bacteria, commonly referred to as denitrifiers, belong to various phyla including Proteobacteria, Bacteroidetes, Firmicutes, and Actinobacteria (Lee et al., 2009; Mellado & Vera, 2021; Wang et al., 2022). Within pond-wetland systems, sediments as well as biofilms attached to submerged macrophyte surfaces are widely recognized as hotspots of NO_3^- transformation, with denitrifiers preferentially residing in benthic microenvironments (Bastviken et al., 2005; Pang et al., 2016; Zhang et al., 2016). To a lesser extent, denitrification may occur via free-floating bacterial communities in the bulk water column under sufficiently reducing conditions (Bachand & Horne, 2005; Bastviken et al., 2004; Kadlec & Wallace, 2008). Sediments typically support sustained denitrification due to persistent anoxic

conditions and relatively stable access to organic carbon (Kjellin et al., 2007; Whitmire & Hamilton, 2005). In contrast, macrophyte-associated biofilms facilitate denitrification within localized, diffusion-limited microenvironments embedded within otherwise oxygenated water columns (Eriksson & Weisner, 1997; Toet et al., 2003). While biofilm-associated denitrification has been documented, its relative contribution to whole-system NO_3^--N removal, particularly in comparison with sediment-based processes across pond- and wetland- like sections, remains uncertain.

A major limitation in resolving habitat-specific NO_3^--N removal arises from a disconnect between studies that infer denitrification potential from microbial community composition and those that quantify bulk NO_3^--N removal rates. Microbiome analyses provide insight into the spatial distribution of taxa associated with N cycling (Pang et al., 2016; Zhang et al., 2016), but taxonomic affiliation alone does not directly quantify process rates. Conversely, bulk or system-scale rate measurements integrate across varied habitats, obscuring the mechanisms underlying spatial variability in removal efficiency (Gebremariam & Beutel, 2008; Grebliunas & Perry, 2016). Integrating microbial community analysis with process-based kinetic measurements may therefore improve understanding of how environmental conditions and habitat structure regulate denitrification in complex treatment systems.

Denitrification rates are governed by multiple interacting factors, including temperature, NO_3^--N availability, organic carbon bioavailability, and redox conditions (Bastviken et al., 2004; Poe et al., 2003; Sirivedhin & Gray, 2006). Temperature exerts a particularly strong influence by regulating enzymatic activity and diffusive transport across sediment-water and biofilm-water interfaces (Phipps & Crumpton, 1994; Stewart, 2003; Wang et al., 2022). In cold climate systems, temperature limitation may override spatial heterogeneity, masking depth- and carbon-related controls during much of the year, despite evidence that denitrification can persist at low temperatures (Richardson et al., 2011; Sirivedhin & Gray, 2006). In addition, tile drainage from cropping systems are typically characterised by high NO_3^--N and low dissolved organic carbon concentrations, further constraining denitrification under conditions where electron donor availability limits microbial activity (Royer & David, 2005; Schipper et al., 2010). Together, these considerations underscore the need for a process-based assessment of how temperature, carbon availability, and system depth interact to regulate NO_3^--N removal within pond-wetland systems.

The objective of this study was to evaluate spatial patterns and environmental controls on the theoretical microbial potential for NO_3^--N reduction in a pond-wetland system in Eastern Ontario, Canada receiving cropping system tile drainage. Recognizing that *in situ* denitrification occurs within complex redox environments containing both aerobic and anaerobic microsites, we integrated field-based microbial community analysis with controlled batch-scale denitrification assays conducted under anoxic conditions. These assays were used to quantify denitrification potential, expressed as NO_3^--N reduction rate constants independent of dissolved oxygen (DO) constraints. Specifically, we aimed to (i) assess variations in microbial community composition, particularly denitrifying taxa between stem-associated biofilm and sediment habitats across depth gradients; (ii) determine how temperature, stem depth of relative to surface water, organic carbon availability, and sediment depth regulate the magnitude of denitrification potential, and (iii) quantify and compare the relative impact of sediments and stem-associated biofilm habitats to denitrification potential based on habitat-specific surface area. By explicitly linking microbial potential with process-based kinetics, this study advances mechanistic understanding of NO_3^--N removal in pond-wetland systems and informs their design and management in cold-climate regions.

6.2. Methods and materials

6.2.1. Site description

In September 2021, sediment, macrophyte, bulk water samples were collected from a 5-year-old constructed pond-wetland system located on a cash-crop operation in St. Isidore, Eastern Ontario, Canada (45°23’55 N, 74°54’02 W) (Figure 6-1). The climate in this area is categorised as temperate - humid continental (Kottek et al., 2006), with clay and clay-loam textures dominating the soil profile. The system is 240 m in length, with a total surface area of 0.4 ha and combines the attributes of treatment ponds and free water surface constructed wetlands. The pond-wetland system intercepts subsurface tile drainage water from 43 ha of agricultural land, conveyed via gravity through a central drainage ditch.

To ensure consistent sampling and nutrient characterization, the system was divided into five ponds, designated as Pond 1, 2, 3, 4 and OUT, following the direction of flow (Figure 6-1). Water depth within the system ranged from 0.08 m to 3.1 m. Emergent macrophytes were allowed to establish naturally, resulting in *Typha latifolia* colonization primarily in Pond 3 and Pond OUT,

with densities of 29±2 and 31±3 plants/ m^2 and occupying about 2% and 40% of each pond area, respectively. *Juncus effusus,* was also present along the shoreline margins, respectively occupying 10% and 4% of areas at Pond 3 and Pond OUT. During summer months, visible algal growth was observed predominantly in the shallow inlet zone of the system. The outlet of the pond-wetland consists of a riprap spillway with a 6 m horizontal base conveying wetland discharge into a downstream ditch that ultimately drains into the South Nation R. within the St-Lawrence drainage basin.

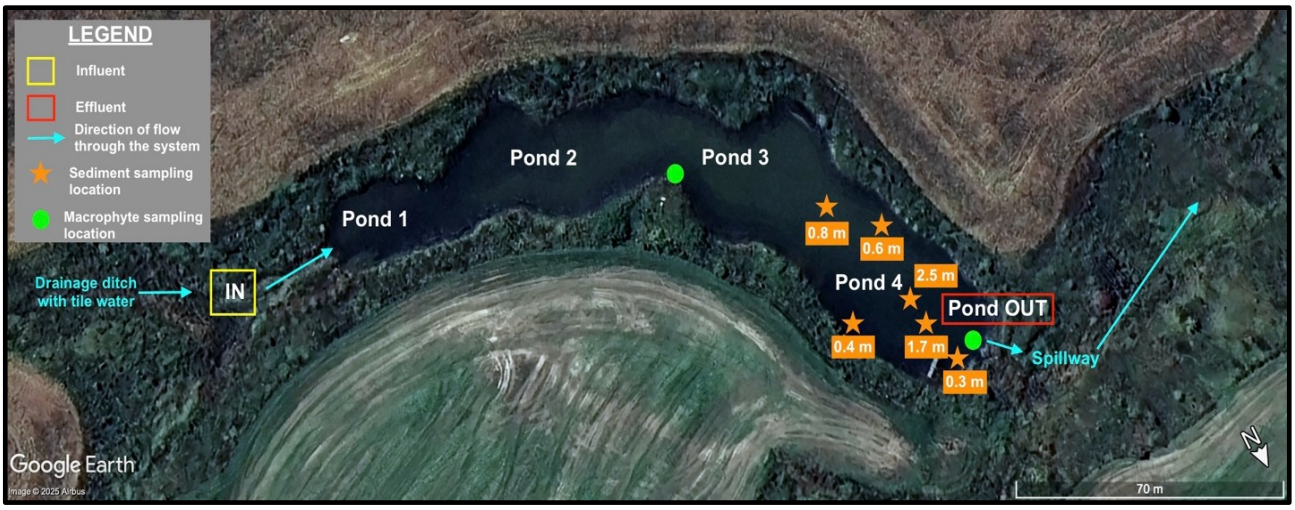

Figure 6-1. Location of field study – Aerial image of the study site with locations of sampling locations and the direction of flow within the pond-wetland system. Google Earth Pro V 7.3.6.9796 imagery.

6.2.2. Sediment and water quality sampling and analysis

Sediment samples were collected from Pond 4 and Pond OUT using Sludge Judge^{TM} sampler (VWR International, LLC) with extended sections. Samples were collected at representative depths of 0.3 m, 0.4 m, 0.6 m, 0.8 m, 1.7 m, and 2.5 m within the system (Figure 6-1). Sediment samples were manually homogenized prior to laboratory use. Bulk water samples were collected from Pond 4 using a peristaltic pump field sampler and were used for both water quality analysis and sediment incubation experiments. All samples were transported back to the laboratory on ice and stored at 4°C until analysis.

Unfiltered sediment samples were analysed for total solids (TS), volatile solids (VS) according to Standard Method SM 2540 G (APHA, 2017), total nitrogen (TN) using HACH Method 10071 (Persulfate Digestion, low range), total chemical oxygen demand (TCOD) using HACH method 8000 (Dichromate Reagent Method, high range), and total phosphorus (TP) using

Stannous Chloride method (Standard Methods 4500-P D) (APHA, 2017). Filtered sediment samples were analyzed for NO_3^--N using ultraviolet (UV) light (Standard Methods 4500-NO_3^- B) (APHA, 2017), soluble reactive phosphorus (SRP) using Stannous Chloride method (Standard Methods 4500-P D) (APHA, 2017), and total ammonia nitrogen (NH_4^+-N) using the Nessler Method which uses Rochelle Salt Stabiliser (50%) and Nessler Reagent (APHA, 1998).

Table 6-1. Characteristics of sediment collected at different depths representative of microbiome samples and of bulk water used for batch-scale denitrification experiments

Parameter	Pond Depth				Bulk water
	0.3 m	**0.8 m**	**1.7 m**	**2.5 m**	
TS (mg/L)	9420	14940	13610	17861	-
VS (mg/L)	1100	1340	1000	1510	-
TSS (mg/L)*	-	-	-	-	18
TCOD (mg/L)	1580	1738	1212	1150	-
TN (mg N/L)	134	116	112	100	5.8
TP (mg P/L)	7.0	9.5	10.9	13.3	0.05
NO_3^--N (mg N/L)	10.6	13.5	14.9	10.9	4.2
NH_4^+-N (mg N/L)	6.0	5.3	12.9	5.8	0.16
SRP (mg P/L)	0.20	0.23	0.25	0.17	0.02
sCOD (mg/L)*	-	-	-	-	16
Sediment Depth (m)	0.09	0.07	0.17	0.08	-

*tested only for bulk water sample
[C] used in carbon amendment (without, with) configurations

The unfiltered bulk water sample was analyzed for total suspended solids (TSS) using Standard Method 2540 D (103°-105°C) (APHA, 2017), as well as TP and TN. The filtered bulk water sample was analyzed for NO_3^--N, NH_4^+-N, SRP, and soluble chemical oxygen demand (sCOD) using HACH method 8000 (Dichromate Reagent Method, low range) (APHA, 2017). All analyses were conducted using HACH DR6000 spectrophotometer. Samples were diluted as necessary to fall within analytical detection ranges. Table 6-1 summarizes the characteristics of sediment collected at different depths representative of microbiome samples and the bulk water sample used in batch-scale denitrification experiments.

6.2.3. Macrophyte sampling

Macrophyte biomass (*Typha latifolia*) samples were collected from three individual plants from Pond 3 and Pond OUT (Figure 6-1). Above- and below- ground biomass was harvested; submerged plant stems were gently rinsed with site water and were sectioned under sterile conditions using disinfected pruning shears. Stems were divided into three equal sections (26.5 cm) based on

distance from sediment surface. The collected plant sections were immediately placed in containers filled with pond water from the corresponding sampling location to maintain local environmental conditions. Length and diameter of each section were measured using a ruler and calipers, with multiple measurements averaged for use in subsequent calculations.

6.2.4. Sediment and stem biofilm sample collection and PCR sequencing

The relative abundance of bacterial communities associated with sediments and macrophyte stem biofilms was evaluated by Polymerase Chain Reaction (PCR) sequencing of the 16S rRNA gene. In 2021, sediment samples were collected at depths of 0.3, 0.8 m, 1.7 m, and 2.7 m under sterile conditions. Biofilm samples were obtained by gently scraping the water-submerged portions of *Typha latifolia* stems collected from Pond 3 and Pond OUT at varying distances from the sediment surface. Samples were extracted by an external lab (Microbiome Insights, Richmond, BC), and the V4 region of the 16S gene was amplified according to a previously described protocol (Kozich et al., 2013). Raw FASTQ files were quality-filtered with minor trimming to remove low-quality sequences (median 63% of reads passed per sample). Taxonomy was assigned against the MiDAS 4.8.1 database, and amplicon sequence variants(ASVs) were placed within the MiDAS reference tree (Dueholm et al., 2022). Sequence data were analyzed using the phyloseq package in RStudio (v3.4.3), where rarefication was set to a sequencing depth of 3500 reads based on sequencing depth distributions. Reads were then transformed to relative abundances (%), and the operational taxonomic units (OTUs) were aggregated into taxonomic ranks for analysis and visualization. Genera were subsequently cross-referenced with established databases (e.g., MiDAS) and published literature to assign putative functional groupings. All functional interpretations presented in this study are therefore based on taxonomic affiliation and reported metabolic capabilities at genus level. Microbial alpha diversity was assessed using the Chao1 richness estimator and Shannon diversity index.

6.2.5. Batch-Scale Denitrification Experiments

Batch-scale denitrification assays were conducted using 300 mL glass biochemical oxygen demand (BOD) bottles. Prior to incubation, bulk water samples were analysed for background NO_3^--N (using methodology from section 6.3.2.). Experimental configurations are summarized in Table 6-2.

Each bottle received approximately 150 mL of homogenised sediment sample and 150 mL of bulk pond water, filling the bottle to the base of the neck to minimize headspace. For treatments

containing plant biomass, measured stem sections were added along with bulk water. The pond water added to the bottles was adjusted to 10 mg N/L using a sodium nitrate ($NaNO^-_3$) stock solution to reflect typical upper quartile concentrations observed in the system. Anaerobic conditions were established by purging bottles with compressed nitrogen (N_2) gas until DO in the bottles dropped to < 0.2 mg/L prior to incubation and sealing. Bottles were static and incubated in the dark at either constant 4°C or 20°C. A small volume of distilled water was added around the stopper to ensure an airtight seal, and bottle necks were wrapped in aluminium foil minimize evaporation.

Table 6-2. Summary of experimental configurations used in the batch-scale denitrification assays

Experiment	Configurations	Comparison Parameter	Comments
1	Stem + Pond water	Temperature (4°C vs 20°C) + Stem position relative to sediment surface; with/without supplemental carbon.	Results, triplicate trials
2	Sediment + Pond water	Temperature (4°C vs 20°C) + Pond depths within the system (0.3 m, 0.6 m, 0.8 m, and 1.7 m); with/without supplemental carbon.	

6.2.6. Batch-Scale – Experimental Design and Sampling

The experiments included sediment-only and plant-only treatments, with and without supplemental organic carbon. All treatments were conducted in triplicate. For carbon-amended treatments, MicroC® was used as a source of carbon and added at the start of incubation to achieve a C:N ratio of 10:1 (Grebliunas & Perry, 2016). Overlaying water samples (1 mL) were collected every 24 h using sterile syringes and filtered through a 0.45 µm membrane syringe filter. Following sampling, an equivalent volume of N_2 purged deionised water was added to prevent headspace formation. Experiments continued until NO_3^--N concentrations stabilized (approximately 7 days). Initial bottle concentrations varied based on nitrate in the sediment pore water and internal stem sections. As a certain degree of leaching was expected during the beginning of the trial (Gottschall et al., 2007; Vymazal, 2007; White & Reddy, 2003), sampling commenced after 24 hrs for stem configurations.

6.2.7. Data Analysis

First-order removal rate constants (k, 1/d) were calculated by linear regression of the natural logarithm of NO_3^--N concentration versus time, while zero-order rate constants (k_0, mg/L/d) were

calculated by linear regression of NO_3^--N concentration versus time, for all trials conducted at 4°C and 20°C. Because reaction kinetics varied over the course of some trials, an interval-based approach was used to identify distinct kinetics where appropriate. For each interval, both zero-order (linear) and first-order (exponential) models were fitted. The kinetic order for a given interval was determined by comparing the coefficients of determination (R^2) for each model: zero-order kinetics were assumed when linear regression yielded a higher R^2, and first-order kinetics were assumed when exponential model provided superior fit. The temperature dependence of reaction rates was evaluated using the Arrhenius temperature coefficient (θ), which describes the effect of temperature on enzymatic and biochemical reaction rates:

$$k_4 = k_{20}\,\theta^{(4-20)} \quad \text{Equation (6-1)}$$

Where k_4 and k_{20} represent first-order rate constants at 4 °C and 20 °C, respectively.
Statistical comparisons among treatments were conducted using one-way analysis of variance (ANOVA), with statistically significant difference defined with $\alpha = 0.05$. Alpha diversity analyses were conducted in R, and ANOVA was performed using standard functions in Microsoft Excel.

6.3. Results and discussion

6.3.1. Microbial Community Structure and Inferred Denitrification Potential

Stem-associated biofilms from submerged macrophytes and sediment were sampled from Pond 3 to OUT within the pond-wetland system. 16S rRNA gene sequencing was used to characterize the microbial community composition and infer the relative distribution of NO_3^--N reducing taxa. It is important to note that these data represent relative abundances rather than absolute abundance. Microbiome data are therefore interpreted as indicators of potential metabolic capacity, recognizing that taxonomic affiliation does not directly quantify process rates. Accordingly, microbial community composition is used to (i) characterise habitat-level differences in diversity and community structure between sediments and stem-associated biofilms, and (ii) identify the spatial distribution of taxa with known denitrification capacity. Only the latter is expected to directly inform denitrification kinetics discussed in Section 6.4.2., whereas broader diversity patterns provide ecological context.

Across the entire microbiome, sediment samples supported markedly higher microbial diversity than stem-associated biofilms. Sediments contained 1293 ± 141 OTUs, compared to 439 ± 134 OTUs, respectively. Estimated species richness (Chao1) was also consistently greater in

sediments (range = 1729 - 2842; mean = 2321 ± 391), than in stem biofilms (range = 450 - 956; average 656 ± 218). Similarly, Shannon diversity indices were higher in sediments (mean = 6.5 ± 0.2) than in biofilms (mean = 4.5 ± 0.5), indicating greater taxonomic richness and evenness in sediment-associated communities. These patterns reflect selective habitat filtering at plant surfaces, where physical structure, redox gradients, substrate availability (Flemming & Wuertz, 2019; Shirdashtzadeh et al., 2022) favour a narrower and more specialised set of microbial traits compared to the more heterogeneous sediment environment.

Consistent with these diversity patterns, stem-associated biofilm communities comprised OTUs from eight bacterial phyla, whereas sediment communities spanned fifteen phyla, indicating greater taxonomic breadth in sediments. Phylum Proteobacteria dominated both habitats (relative abundance of 30 - 49% in sediments and 33 - 61% in biofilms), consistent with their metabolic versatility and central role in nitrogen cycling in freshwater wetland systems (Fang et al., 2020; Mellado & Vera, 2021). In biofilm samples, other dominant phyla, with relative abundance >10% in most samples, included Cyanobacteria (27- 48%) and Bacteroidota (0.9 -16.0%), reflecting the importance of phototrophic and organic matter-associated taxa on plant surfaces. In sediment samples, additional dominant phyla included Firmicutes (6 - 26%), Cyanobacteria (10 - 24%), Desulfobactereota (9 - 20%), and Bacteroidota (7- 20%), groups widely reported in freshwater and constructed wetland studies (Rani et al., 2024; Shirdashtzadeh et al., 2022; Wang et al., 2022). While these phyla are not unique to this system, their contrasting distributions highlight differences in functional breadth and environmental stability between sediments and stem biofilms rather than differences in taxonomic novelty. At genus level, 74 biofilm-associated genera and 112 sediment-associated genera were detected grouped into seven functional categories based on published metabolic capabilities (Figure 6-2, 6-3).

Stem-associated biofilm communities exhibited clear vertical functional gradients (upper and lower stem) with the coexistence of aerobic and anoxic microenvironments within the biofilm matrix (Flemming & Wuertz, 2019) (Figure 6-2). Phototrophic taxa, primarily genera within the class Cyanobacteriia (such as *Planktothrix_NIVA-CYA_15*, *midas_g_59024*) dominated all stem biofilms (relative abundance of 20 - 35%), with consistently higher relative abundance in upper stem sections. This pattern reflects strong coupling between light availability and epiphytic growth in shallower waters.

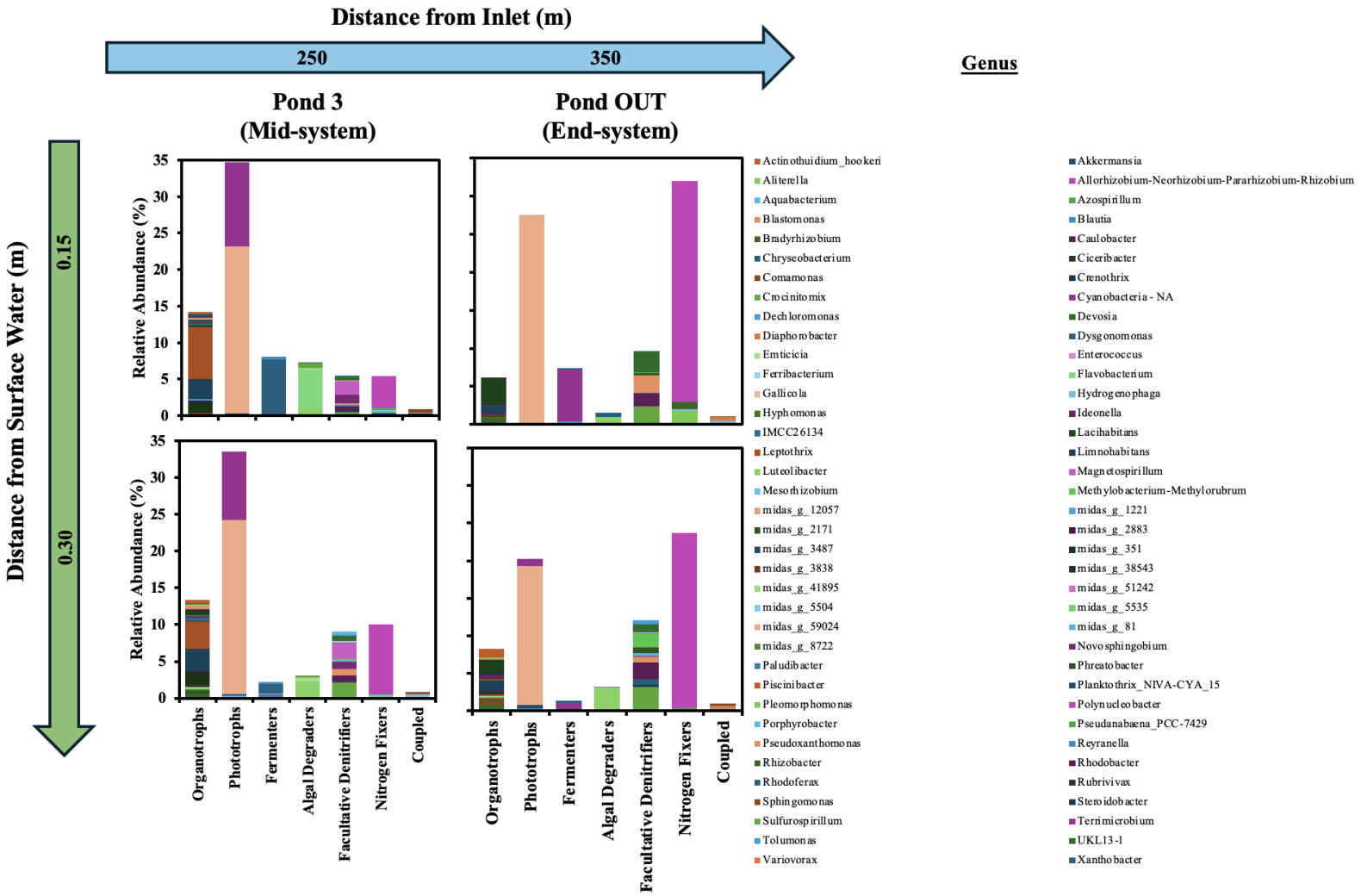

Figure 6-2. Relative abundance (%) of bacteria at the genus level in stem biofilm at Pond 3 (mid-system) and Pond OUT (end-system) - Relative abundance along gradients of distance from the surface water and from the inlet in the pond-wetland system, with bacteria grouped according to metabolic type. Note: Genera capable of heterotrophic ammonia oxidation and denitrification within the same bacteria were categorised under 'Coupled' group. The two locations differed in macrophyte coverage , with Pond 3 sparsely vegetated (~2% coverage) and Pond OUT moderately vegetated (~40% coverage).

In contrast, facultative denitrifying taxa, defined here as NO_3^--N reducing bacteria capable of growth under both oxic and anoxic conditions, increased toward lower stem sections, with relative abundance increasing by 19 to 46% along the vertical stem gradient. This vertical pattern likely reflects increasingly stable microhabitat conditions closer to the sediment-water interface, where reduced hydrodynamic disturbance, enhanced organic matter availability, and limited O_2 penetration promote redox stratification within stem-associated biofilms (Bastviken et al., 2005; Kjellin et al., 2007; Shirdashtzadeh et al., 2022).

Differences were also observed between locations: sparsely vegetated Pond 3 (2% macrophyte coverage by pond area; 29±2 plant/m^2) and moderately vegetated Pond OUT (40% coverage by pond area, 31±3 plants/m^2) Relative abundance of denitrifiers on upper stems were 55% higher and lower stems 32% higher at the end-system compared to the mid-system (Figure 6-4 A). This suggests that overall macrophyte rather than local stem density may exert a stronger control on near-stem hydrodynamics by reducing flow velocity and enhancing biofilm stability, which in turn promotes the development of presumably thicker, diffusion-limited microenvironments favourable to denitrifying taxa (Soana et al., 2018; Zhu et al., 2018). Key denitrifying genera identified with relative abundance exceeding 1% abundance include: *Sulfurospirillum, Devosia, Magnetospirillium, Pseudoxanthomonas, Rhodobacter and Methylobacterium-methylorubrum* (Dueholm et al., 2022; Goris & Diekert, 2016; Liu et al., 2025). Except for *Magnetospirillium*, these taxa exhibited a progressive increase in relative abundance from upper-stem sections in sparsely vegetated Pond 3 to lower stem sections in moderately vegetated Pond OUT (mean relative abundance increase from 0.5% to 1.8%; p - value < 0.1, paired t-test). Together, these results suggest that both vertical stem position relative to water surface and macrophyte coverage shape the distribution of denitrifying taxa in this pond-wetland system.

Classical autotrophic nitrifiers were not resolved or detected at appreciable relative abundance within stem biofilms. This likely reflects both ecological and methodological constraints, as nitrifying taxa often occur at low abundance within thin oxic micro-zones and may be underrepresented in 16S rRNA gene surveys targeting the V4 region (Wang et al., 2021; Zhou et al., 2024). Nevertheless, taxa capable of heterotrophic nitrification-denitrification, categorized in this study as Coupled (*Comamonas, Diaphorobacter, Hydrogenophaga, Rubrivivax,* and *Variovorax*), were consistently present at low relative abundance (<1%) (Dueholm et al., 2022;

Zhu et al., 2018). This distribution suggests that NO_3^--N reduction within stem biofilms is likely primarily supported by externally supplied NO_3^--N rather than by internally by coupled taxa, which is reasonable considering the relatively low NH_4^+-N in the water column.

Notably, the relative abundance of *Allorhizobium-Neorhizobium-Pararhizobium-Rhizobium* complex increased markedly from 4 -10% in mid-system samples to 23 - 29% in the end-system biofilms. Although this complex genus group are best known for N fixation, they exhibit considerable metabolic flexibility, including NO_3^--N assimilation and denitrification under low O_2 conditions (Dueholm et al., 2022). Bulk-water DO on the day of sampling ranged from 6.8 to 9.0 mg O_2/L; however, high bulk-water oxygenation does not preclude the development of hypoxic or anoxic micro-environments within biofilms under stagnant or low-flow conditions where O_2 transport is diffusion-limited (Bachand & Horne, 1999; Stewart, 2003). Reduced advective exchange in stem-dense or stagnant zones can further promote O_2 depletion in the interstitial water despite oxic overlying conditions (Sand-Jensen & Pedersen, 1999; Soana et al., 2018; Thorén et al., 2004). The enrichment of this group toward the end system under stagnant conditions, low-flow conditions is therefore consistent with adaption to O_2 limited biofilm micro-zones and flexible N metabolism rather than simple N limitation.

Sediment microbial communities exhibited pronounced depth-dependent structuring of inferred NO_3^--N reduction potential (Figure 6-3). The relative abundance of denitrifying taxa increased with depth, from an average 19 ± 0% at 0.3 m to 28 ± 1 % at 2.5 m (p – value < 0.1, paired t-test), consistent with increasingly reducing conditions. This shift coincided with a transition from sediment-surface-associated organotrophs (relative abundance of 29 ± 0%) and algal-associated communities (23 ± 0%) at 0.3 m toward deeper, redox-stratified sediments where NO_3^- respiration becomes more dominant. Unlike stem-associated biofilms, sediments exhibited depth-dependent patterns consistent with sustained anoxic conditions, supporting a more persistent and less spatially constrained denitrification potential.

A pronounced peak in relative abundance of fermentative taxa occurred at 0.8 m depth (30.1 ± 2.2%), driven largely by *Lactobacillus* (18.5%), indicating a redox transition zone where labile organic carbon supports fermentation under reducing conditions. Fermentative taxa were less abundant at shallow 0.3 m depth (relative abundance of 9%), consistent with more oxygenated

conditions, and declined again at greater depths (4 – 8%), likely due to competition with denitrifiers for labile carbon under stable anoxic conditions. These patterns suggest that sediments at 0.8 m depth represent a transient biogeochemical hotspot linking organic matter fermentation to depth-dependent NO_3^--N reduction.

The sediment NO_3^--N reducing community was dominated by heterotrophic denitrifiers (relative abundance of 11 – 18%), which increased consistently with increasing depth (Figure 6-4 B). Dominant genera (top 20% in relative abundance) included *Rhodoferax, Pseudonomas, midas_g_2171, Dechloromonas*, and *Rhodobacter* (Lee et al., 2009; Smriga et al., 2021), indicating organic carbon driven denitrification as the primary NO_3^--N reduction pathway. In contrast to the facultative and metabolically flexible taxa enriched in stem-associated biofilms, sediment denitrifiers were dominated by heterotrophic taxa typically associated with sustained anoxic conditions and organic carbon oxidation (Dueholm et al., 2022). The relative abundance of iron- and sulphur- associated taxa, such as *Ferribacterium* (4.1 – 5.8%), *Geobacter* (1.2 – 3.4%) *Sulfuritalea* (0.1 – 0.8%), and *Campylobacter* (0.3 – 1.1%) (Mellado & Vera, 2021; Wang et al., 2023), together with zones of elevated fermentation, suggests that conditions favourable for alternative NO_3^--N reduction pathways, including autotrophic denitrification or dissimilatory NO_3^--N reduction to NH_4^+-N (DNRA) may occur at specific depths (notably 0.8 m). However, confirmation of these pathways would require functional gene analysis (e.g., *nrfA*) or direct rate-based measurements (Dueholm et al., 2022).

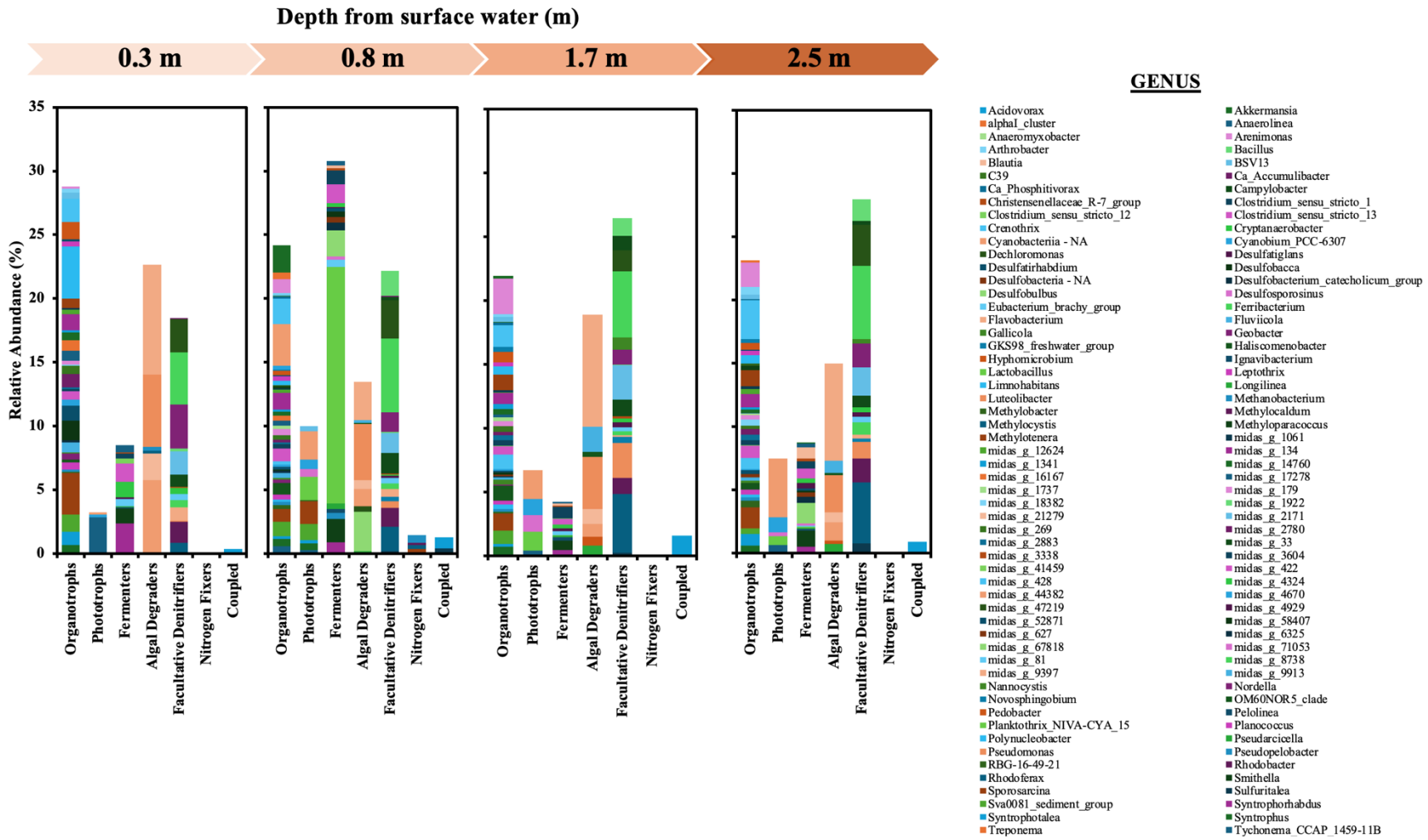

Figure 6-3. Relative abundance (%) of bacteria at the genus level in sediment - A. Relative abundance at different depths, relative to surface water, with bacteria grouped according to metabolic type. Note: Genera capable of heterotrophic ammonia oxidation and denitrification within the same bacteria were categorised under 'Coupled' group.

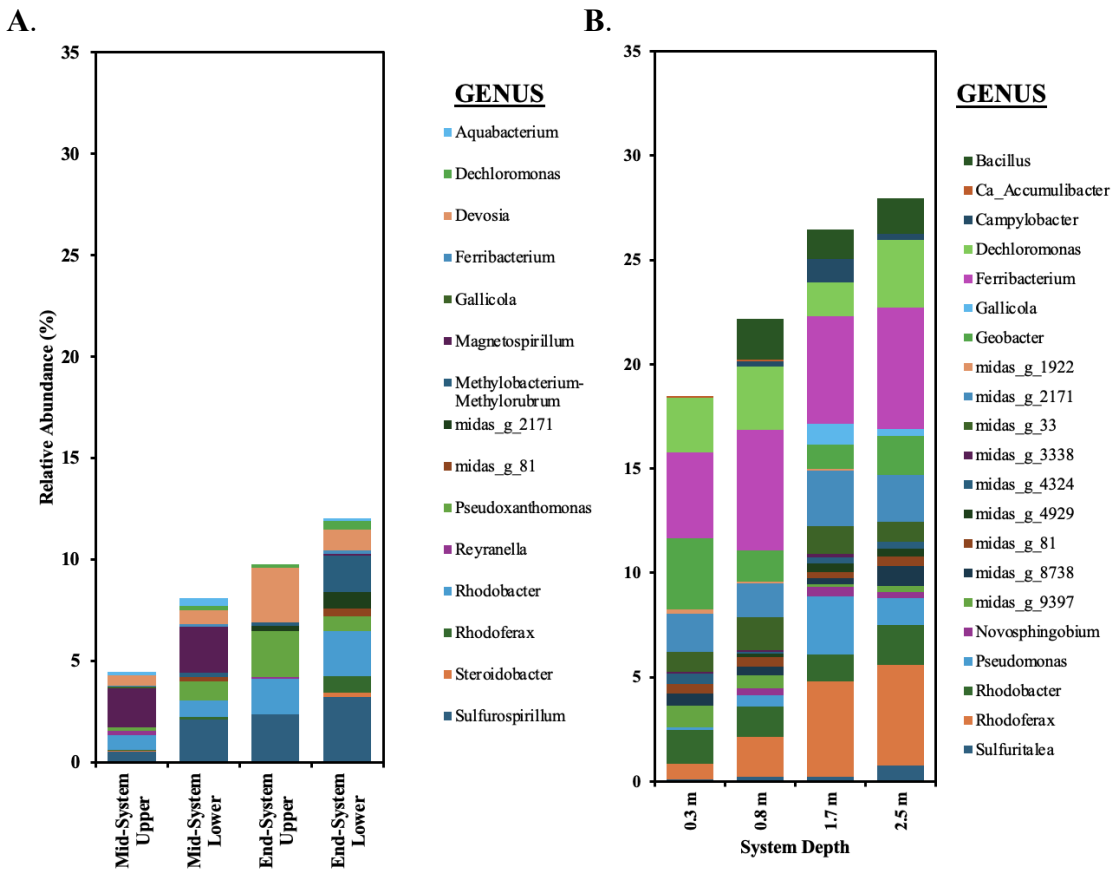

Figure 6-4. Distribution of denitrifying taxa within stem-associated biofilms at Upper (10-15cm) and Lower (15-30 cm) depths from water surface (A) and sediment with varying water column depths (B).

Overall, inferred denitrifying taxa were, on average 2.8 times more relatively abundant in sediments than in stem-associated biofilms (Figure 6-4 A, B), indicating distinct but complementary roles of these habitats in NO_3^--N reduction. This contrasts with Pang et al. (2016) who reported higher relative abundance of denitrifiers in the submerged macrophyte biofilms (7 to 19%) compared to sediment (2 to 4%). In the present system, denitrification potential in stem-associated biofilms was spatially constrained, increasing toward lower stem sections and areas of higher areal macrophyte coverage, whereas sediments exhibited stronger and more persistent denitrification potential with depth, consistent with stable anoxic conditions. The coexistence of deep sediment zones and shallow vegetated areas therefore promotes functional complementarity within the pond-wetland system, coupling reliable background denitrification in sediments with spatially and temporally dynamic NO_3^--N removal in stem-associated biofilms.

While these patterns reveal strong spatial organization of denitrification potential, the extent to which this potential is expressed as a measurable NO_3^- removal rate constant is governed

by multiple environmental constraints including O_2 availability, redox potential, temperature, pH, nitrate concentration, depth, and carbon availability (Lee et al., 2009; Vymazal, 2007). Denitrification is restricted to anoxic conditions; however, once anoxia is established, variation in measured rates may reflect inherent microbiome composition, including the relative abundance of denitrifying taxa, and their responses to environmental constraints.

6.3.2. Environmental Controls on Denitrification Kinetic Rates – Batch-Scale Study

Batch–scale kinetic experiments were conducted to quantify denitrification kinetics in sediment- and stem-associated biofilm compartments under idealized anoxic conditions and to evaluate whether spatial patterns in inferred denitrification potential identified through microbiome analysis are reflected in measured rate constants. Accordingly, higher NO_3^--N rate constants, either zero order (k_0) or first order (k_1), can be expected in sediments, particularly with increasing depth, and in biofilm sections with higher relative abundance of denitrifying taxa; deviations from this pattern would indicate the influence of dominant environmental constraints. Glass reactors (BOD bottles) containing pond water with either sediment from different pond depths or section of submerged plant stem (with attached biofilm) were incubated under anoxic conditions at two temperatures, with and without added carbon (Figure 6-5, 6-6, 6-7 and Table 6-3).

In bottles containing pond water only and maintained at DO below 0.2 mg/L, only 0.3 mg N/L reduction in NO_3^--N concentrations occurred over 7 days of incubation, indicating negligible denitrification activity in the bulk water column. This confirms that NO_3^--N reduction within the pond-wetland system is primarily associated with sediment and biofilm habitats rather than the bulk water column.

6.3.2.1. Temperature effect on denitrification

Trials were conducted at 4°C and 20°C as these temperatures correspond to fall/spring and summer conditions typical of temperate climatic zones, allowing assessment of how seasonal temperature regulates denitrification. Temperature exerted a strong and consistent effect on denitrification kinetics across both stem- and sediment-based experimental trials as NO_3^--N concentrations decreased more rapidly at 20°C than at 4°C in all configurations (Figure 6-5 to 6-7), demonstrating higher denitrification rates at elevated temperature. Rate constants (k_0 and k_1, Table 6-3 A) increased consistently from 4°C to 20°C (p – value < 0.05, paired t-test), consistent with temperature-dependent enhancement of enzymatic activity (Wang et al., 2022) and increased

diffusive transport of NO_3^- to microbial communities (Phipps & Crumpton, 1994). Similar results have been reported in other wetland studies: Sirivedhin & Gray (2006) observed a two-order-of-magnitude increase in wetland sediment denitrification rates as temperature rose from 4°C to 25°C, while Ng & Gunaratne (2011) reported that rates doubled with each 10°C increase in temperature.

Calculated temperature coefficients (θ = 1.05 to 1.13; Table 6-3 B) fell within the range previously reported for constructed wetland systems (1.05 to 1.21) (Bachand & Horne, 2005; Beutel et al., 2009). The narrow θ range indicates consistent temperature sensitivity of across compartments, suggesting system-wide temperature effects rather than preferential enhancement within a single compartment (Kadlec & Reddy, 2001). Despite differences in relative abundance of denitrifying taxa, θ values were comparable in sediments, indicating that temperature sensitivity appears independent of microbial richness. Elevated θ values were observed under carbon-amended conditions (1.13 for both stem and sediment trials; *p*-value < 0.05, ANOVA) compared the rest (1.06 to 1.09), likely reflecting the removal of substrate limitation at 20°C.

Sediment microbial communities maintained higher denitrification activity at low temperature compared to stems, consistent with more stable anoxic conditions and greater labile carbon availability (Kjellin et al., 2007; Whitmire & Hamilton, 2005). Although denitrification is often considered negligible below 5°C (Yan & Xu, 2013), measurable activity has been reported at 4°C or lower, albeit at lower rates (Richardson et al., 2011). Studies documenting sustained denitrification in macrophyte-associated biofilms at temperatures of 8 to 10 °C (Schaller et al., 2004; Soana et al., 2018; Toet et al., 2003) further illustrate that temperature responses are strongly context-dependent and mediated by habitat structure, redox conditions, macrophyte type, and associated organic carbon availability.

Table 6-3. Denitrification rate constants (k) at 4°C and 20°C (A.) and temperature coefficients (θ) (B.) measured in batch experiments for sediment and stem components relative to pond depth, carbon, and stem-section relative to water surface.

A.

	Temperature	Condition	Phase	Days	Model	k_0 value (mg/L/d)	k_1 value (1/d)
Stem	4°C	Upper	1	1-7	Zero	0.32 ± 0.19	
		Lower	1	1-7	Zero	0.38 ± 0.05	
		Without C	1	1-7	Zero	0.38 ± 0.05	
		With C	1	1-7	Zero	0.54 ± 0.15	
	20°C	Upper	1	1-7	Zero	1.58 ± 0.50	

		Lower	1	1-4	Zero	0.83 ± 0.15	
			2	4-7	Zero	1.62 ± 0.19	
		Without C	1	1-5	Zero	0.90 ± 0.15	
			2	5-7	Zero	1.95 ± 0.19	
		With C	1	1-6	First		0.45 ± 0.15
Sediment	4°C	0.3 m	1	0-4	Zero	0.62 ± 0.11	
			2	4-7	-	0.00 ± 0.00	
		0.6 m	1	0-7	Zero	0.81 ± 0.10	
		0.8 m	1	0-4	-	0.00 ± 0.00	
			2	4-7	Zero	0.95 ± 0.43	
		1.7 m	1	0-4	Zero	0.66 ± 0.15	
			2	4-6	Zero	1.38 ± 0.20	
		Without C	1	0-6	Zero	0.90 ± 0.14	
		With C	1	0-6	Zero	0.97 ± 0.07	
	20°C	0.3 m	1	0-7	First	1.72 ± 0.39*	0.10 ± 0.04
		0.6 m	1	0-2	Zero	2.67 ± 0.04	
		0.8 m	1	0-2	Zero	2.56 ± 0.16	
		1.7 m	1	0-2	Zero	2.78 ± 0.15	
		Without C	1	0-2	Zero	2.67 ± 0.19	
		With C	1	0-1	First		1.96 ± 0.16

k_0 : zero-order rate constant
k_1 : first-order rate constant
* represents zero-order rate constant determined for Day 0 - 3 (chosen to be comparable with the 4°C experiment)
- (dash) in the Model column indicates no change in nitrate concentration observed; no kinetic rate constant was determined.

B.

	Stem				**Sediment**					
	Upper Stem[a]	**Lower Stem[a]**	**Without Carbon[a]**	**With Carbon[b]**	**0.3 m[a]**	**0.6 m[a]**	**0.8 m[a]**	**1.7 m[a]**	**Without Carbon[a]**	**With Carbon[b]**
θ	1.10	1.09	1.09	1.13	1.07	1.08	1.06	1.05	1.07	1.13*

[a]Calculated using zero order rate constants at 4°C and 20°C.
[b]Calculated using first order rate constants at 4°C and 20°C
Note:
1. For configurations with multiple k values, the faster (Phase 2) value at a given temperature was used.
2. For With Carbon trials where the 4°C rate constant was zero-order but the 20°C constant was first-order, zero-order was converted to first-order for consistent comparison of θ. The corresponding R^2 variation was < 0.3.

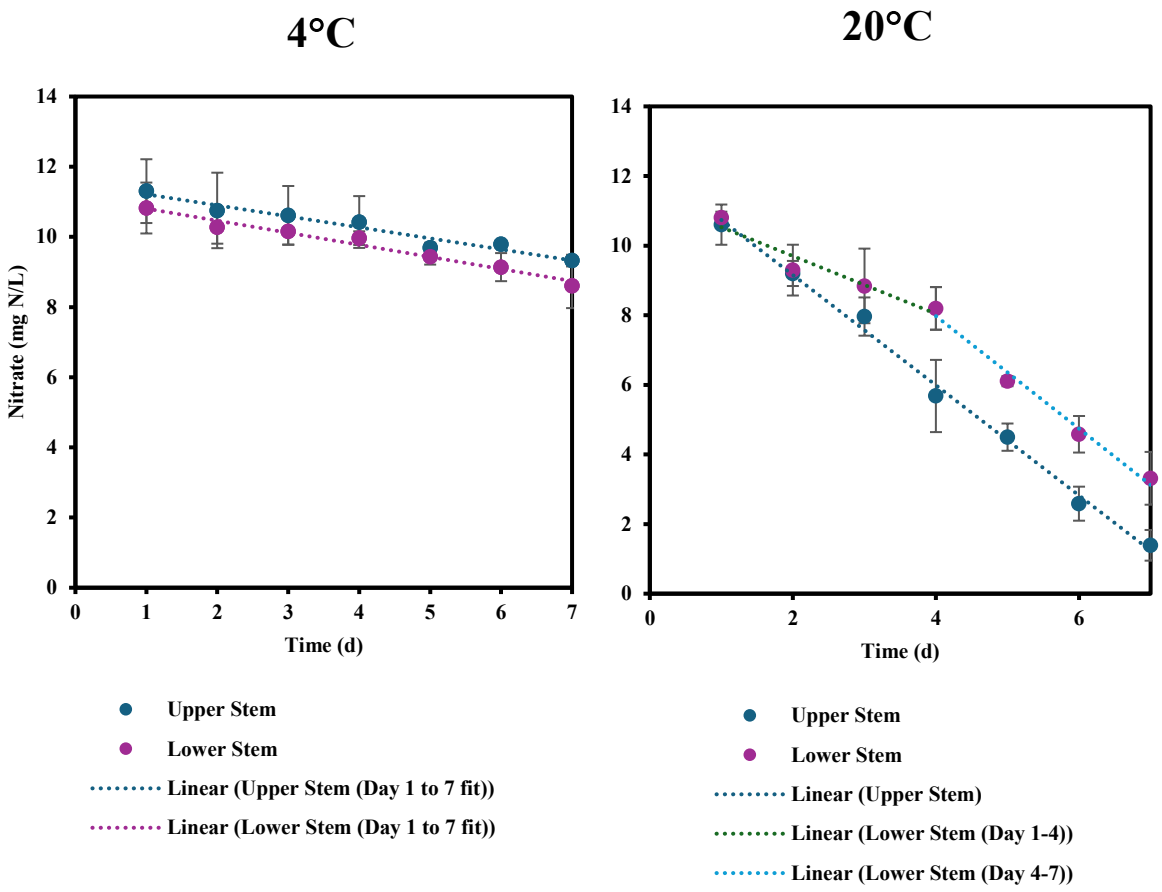

Figure 6-5. Nitrate (NO_3^--N) concentration profiles over time during batch-scale experiments (stem + pond water configuration), showing the effects of stem depth (upper stem - 0 - 30 cm from water surface vs. lower stem – 30 - 60 cm from water surface) at 4°C and 20°C. Points represent measured NO_3^--N concentrations (mean of triplicate measurements ± standard deviation), and dotted lines represent linear fits used to determine zero order kinetic rate constant. R^2 for these fits varied from 0.95 to 1.00.

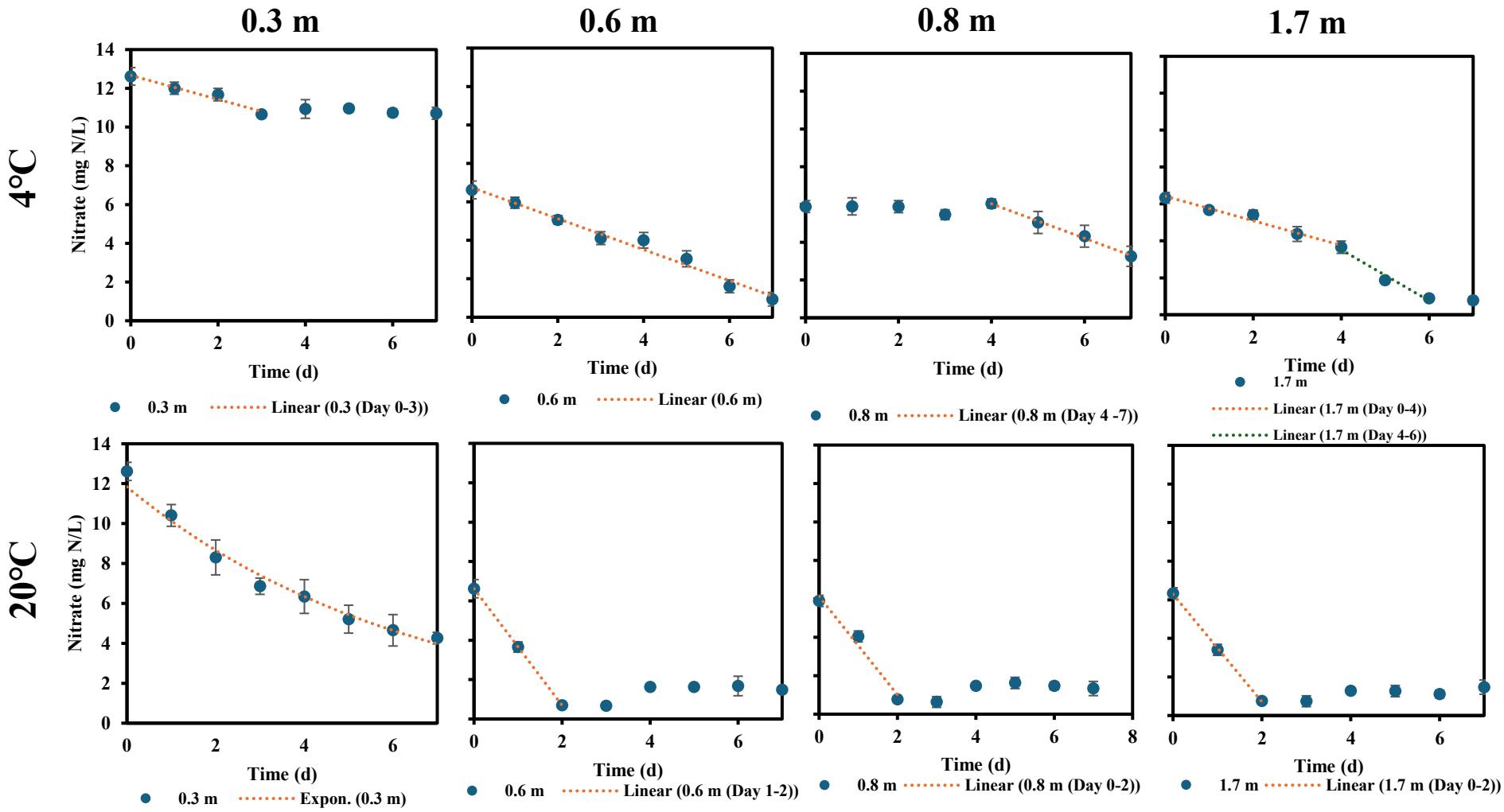

Figure 6-6. Nitrate (NO_3^--N) concentration profiles over time during batch-scale experiments (sediment + pond water configuration), showing the effects of pond depth at which sediment was collected (0.3 m, 0.6 m, 0.8 m, and 1.7 m) at 4°C and 20°C. Note: 1. Points represent measured NO_3^--N concentrations (mean ± standard deviation of triplicates); 2. dotted lines represent linear and exponential fits used to determine kinetic rate constants, with R^2 varied between 0.97 to 1.00; and 3. Day zero NO_3^--N concentration for each configuration was calculated from equal volumes of sediment and pond water.

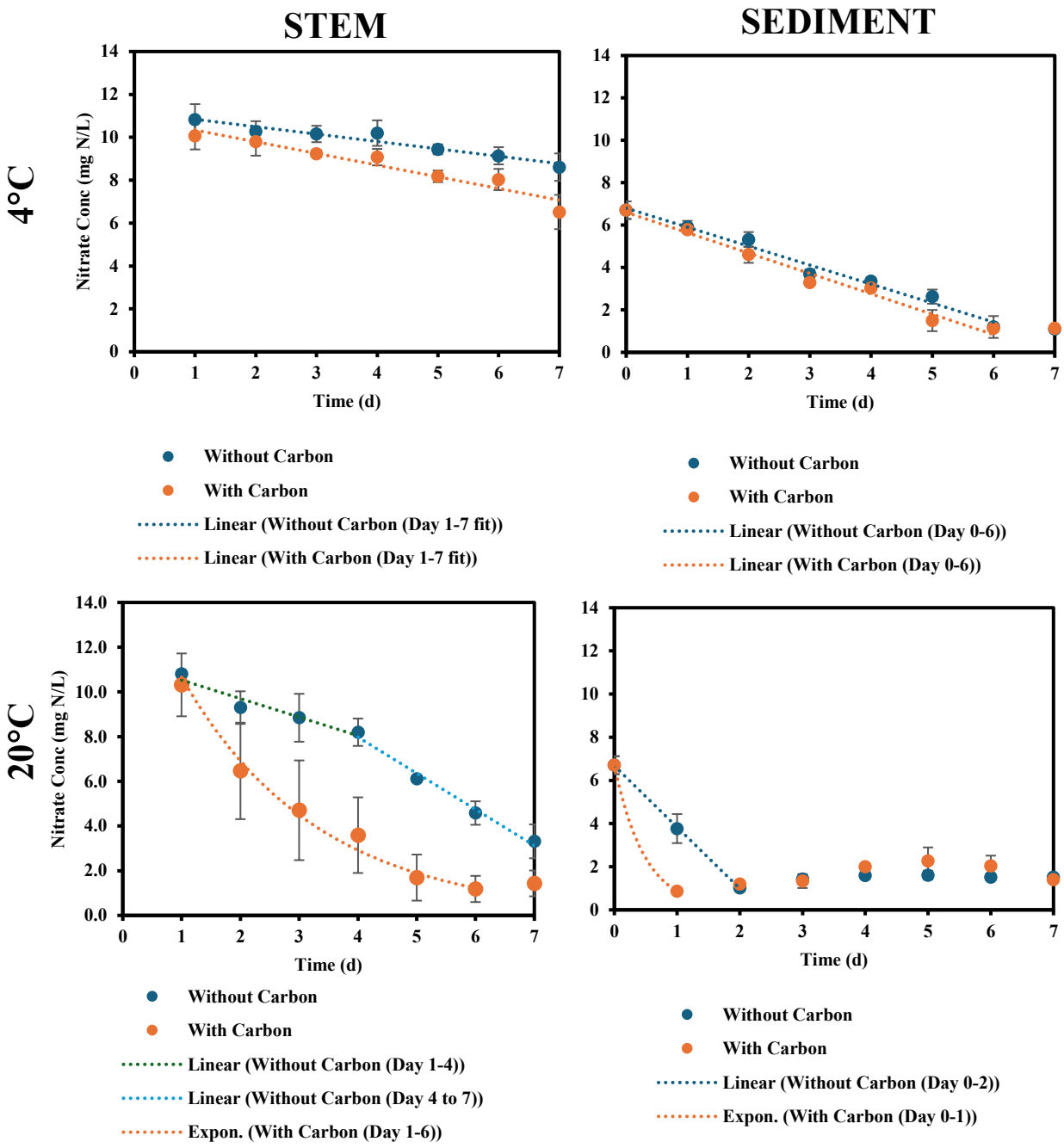

Figure 6-7. Nitrate (NO_3^--N) concentration profiles over time during batch-scale experiments (stem + pond water and sediment + pond water configurations), showing the effects of carbon amendment (with vs. without carbon) at 4°C and 20°C. Points represent measured NO_3^--N concentrations (mean of triplicate measurements ± standard deviation), and dotted lines represent linear and exponential fits used to determine kinetic rate constant. Note: In figure for sediment configuration at 20°C, Day 0 was estimated using the fit equation of without C trend in order to calculate representative kinetic rate constant.

6.3.2.2. Stem section effects

In stem trials containing stem section and pond water, we hypothesized that (i) lower stem sections (15-30 cm relative to water surface) would exhibit higher denitrification rate, and (ii) NO_3^--N reduction would decline and potentially cease over time due to carbon limitation. The only external source of carbon in these trials was sCOD of 16 mg O_2/L present in the bulk pond water. While denitrification requires organic carbon as an electron donor, sCOD represents only an upper-bound estimate of dissolved organic carbon availability, as only a fraction is readily biodegradable and accessible to anoxic biofilm microsites where denitrification occurs (Reddy et al., 2023). Although stoichiometric requirements for heterotrophic denitrification suggest relatively low sCOD:NO_3^--N ratios (~2.47 g sCOD per g NO_3^--N) (Metcalf & Eddy, 2014), effective denitrification in pond-wetland systems typically requires higher ratios (≥5:1), due to limited carbon lability and diffusion constraints within biofilms (Bai et al., 2023; Baker, 1998; Li et al., 2017). NO_3^--N concentrations initially increased by 0.2 to 2.2 mg N/L on Day 1 relative to the initial concentration (10 mg N/L), indicating a short-term release of NO_3^--N from stem tissues prior to subsequent decline. This response is consistent with internal stored NO_3^--N release during stem senescence reported in pond-wetland systems (Gottschall et al., 2007; Vymazal, 2007; White & Reddy, 2003) and highlights that this process can generate short-term NO_3^--N pulses. To avoid confounding effects from these initial NO_3^--N pulses, kinetic rate constants were calculated from Day 1 onward.

Denitrification in stem-based trials followed zero-order kinetics, with linear declines in NO_3^--N concentrations over time (Figure 6-5). At 4°C, a single k_0 described kinetics for upper and lower stem sections. At 20°C, only the lower stem trial exhibited two distinct phases: an initial slower phase (Days 1- 4 for lower; k_0 = 0.83 mg/L/d) followed by a faster second phase with higher k_0 values (1.6 mg/L/d). The initial phase likely reflects microbial acclimation to the trial environment, and/or potential diffusion limitations within biofilms (Kumakura et al., 2023; Stewart, 2003). Accordingly, Phase 2 k_0 values were used for comparative analysis. This two-phase behavior was not observed at 4°C, likely because low temperature constrained microbial metabolism and enzyme activity and masked any detectable acclimation effects.

k_0 values were slightly higher in lower stem sections than in upper sections at both temperatures (Table 6-3 A); however, these differences were not statistically significant (*p*–value > 0.1, paired-test), indicating that the microbial communities on stems 0-15 and 15-30 cm from

the water surface had the same capacity to support denitrification under anoxic conditions. This contrasts with hypothesis (i), which predicted higher activity in lower sections due to closer proximity to sediments and the rhizosphere, where greater access to labile organic carbon, NO_3^--N from coupled nitrification-denitrification, and more stable hydrodynamic conditions are typically expected (Bastviken et al., 2005; Kjellin et al., 2007; Shirdashtzadeh et al., 2022). Although microbiome analysis showed a 19% higher relative abundance of denitrifiers in upper stem sections (end-system upper vs. lower; Figure 6-5), this difference did not translate into higher denitrification activity, highlighting that microbial relative abundance alone does not necessarily determine activity in stem-associated biofilms. This observation is consistent with the broader temperature analysis (θ = 1.09 - 1.10 for stems; Table 6-3 B), which indicated uniform intrinsic temperature sensitivity along the plant axis. The consistent zero-order kinetics observed across stem sections and temperature indicate that denitrification rates were constrained by microbial capacity and carbon accessibility rather by NO_3^--N concentration.

Continued NO_3^--N reduction occurred from Day 1 through 7 in all stem trials (Figure 6-5), contrary to hypothesis (ii). At 20°C, net NO_3^--N removal in upper and lower stem trials ranged from 7.5 ± 1.0 to 9.2 ± 0.9 mg N/L, corresponding to a minimum sCOD demand of 18.5 ± 2.5 to 22.8 ± 2.3 mg O_2/L based on a ratio of 2.47:1 sCOD:NO_3^--N or a more likely ratio of 37.5 ± 5.1 to 46.1 ± 4.6 mg O_2/L. The sustained decline in NO_3^--N concentrations suggests that denitrifying taxa in stem-associated biofilms accessed internally available carbon sources. Several mechanisms may account for this observation. First, extracellular polymeric substances (EPS) produced by the biofilm, which can constitute 50 to 90% of biofilm organic carbon, can serve as an internal carbon reservoir under anoxic conditions (Bishop et al., 1995; Flemming & Wingender, 2010). Second, fermentative taxa within the biofilm community (2.2 - 8.1% relative abundance; Figure 6-2) may generate labile carbon intermediates through the anaerobic breakdown of organic matter or EPS, thereby supporting denitrification via cross-feeding (Petersen et al., 2025; Wu et al., 2021). Third, preparation of stem sections for incubations may have facilitated the release of internal stored carbon or gradual leaching of endogenous plant-derived carbon from stem tissues (sugars and amino acids) (Brix, 1997; Ding et al., 2023).

Carbon-limitation was further evaluated using carbon-amended trials (sCOD:NO_3^--N = 10:1) with lower stem sections and compared to unamended treatments at both temperatures

(Figure 6-7). This ratio exceeded theoretical stoichiometric requirements by approximately four-fold and allowed isolation of temperature and carbon effects on denitrifying taxa independent of stem position. At 4°C, carbon addition produced a modest, non-significant increase in denitrification rates (k_0 increased from 0.38 to 0.54 mg/L/d; *p*-value > 0.1, ANOVA), with kinetics remaining zero-order. In the unamended trials at this temperature, total NO_3^--N concentration decline ranged from 2.0 ± 0.7 to 2.3 ± 0.6 mg N/L; indicating the sCOD available could have been adequate. This trend along with the insignificant increase in k_0 even with carbon addition suggests that while labile carbon influenced denitrification at low temperature, overall microbial activity remained constrained by reduced metabolic and enzymatic activity.

In contrast, at 20°C, carbon amendment produced a pronounced acceleration of NO_3^--N removal and a shift from zero-order to first-order kinetics, relative to 4°C (*p*-value < 0.05, paired t-test, Table 6-3 A.), indicating a transition from carbon-limited conditions to NO_3^--N dependent denitrification. In unamended 20°C trials, NO_3^--N concentrations declined to 5.1 mg N/L by Day 7, whereas carbon-amended trials reached similar levels by Day 2-3 and continued to 1.2 mg N/L by Day 7 (Figure 6-7). These results demonstrate the temperature dependent kinetic rates of the existing stem-associated biofilms under anoxic conditions with excess carbon.

6.3.2.3. Sediment and system depth effects

Sediment-based trials were conducted under controlled anoxic conditions to remove DO constraints and promote NO_3^--N reduction as the dominant electron-accepting process. The sediment layer occupied approximately 0.08 m of the reactor height, which falls within the range of sediment thickness observed *in situ* (0.07 to 0.17 m). This depth encompasses the sediment-water interface and underlying material, thereby including the zone where denitrification is expected to be most active. Across most sediment trials, NO_3^--N removal was best described by zero-order kinetics (Figure 6-6) indicating limitation of labile organic carbon rather than NO_3^--N concentrations, as commonly reported in systems receiving low carbon, high NO_3^--N cropping tile drainage (Royer & David, 2005; Schipper et al., 2010). k_0 constants at 20°C were significantly higher than at 4°C (*p*-value < 0.05, paired t-test, Table 6-3 A), reflecting enhanced microbial metabolism, enzymatic activity under warmer conditions (Phipps & Crumpton, 1994; Reddy et al., 2023; Wang et al., 2022). At 4°C, k_0 increased with depth, consistent with an increasing relative abundance of denitrifying taxa from 19% at 0.3 m, to 22 % at 0.8 m, and the highest relative

abundance at 1.7 m (27%) (Figure 6-4 B). This depth-dependent enhancement in k_0 aligns with progressively more reducing conditions at depth. In contrast, at 20°C, although, k_0 at 0.3 m (Day 0-3, 1.72 ± 0.39 mg/L/d) remained lower at greater depths, k_0 values among the 0.6 - 1.7 m sediments were comparatively similar (2.56 ± 0.16 to 2.78 ± 0.15 mg/L/d). These temperature-dependent patterns indicate that, under warmer conditions, denitrifying taxa were sufficiently metabolically active that denitrification rates became primarily constrained by carbon availability rather than microbial relative abundance. By contrast, at 4°C, both reduced microbial activity and limited electron donor availability jointly constrained denitrification.

Shallow sediments (0.3 m) exhibited minimal NO_3^--N reduction at 4°C, with measurable zero-order removal occurring only during the initial four days of incubation; thereafter, concentrations remained largely unchanged (Figure 6-6). At 20°C, kinetics shifted to first-order behaviour, characteristic by a sustained, gradual decline in NO_3^--N, suggesting reduced carbon limitation and a shift toward NO_3^--N controlled kinetics. These sediments were collected from a macrophyte-dense area of Pond OUT (Figure 6-1), Previous studies have shown that macrophyte-colonized sediments can enhance NO_3^--N removal by supplying labile carbon through root exudates and decaying litter, while also regulating NO_3^--N availability via assimilation and release, relative to unvegetated sediments (Bastviken et al., 2005; Eriksson & Weisner, 1997; Soana et al., 2018; Toet et al., 2003). The likely presence of background organic carbon in this zone may have supported first-order removal at 20°C. However, the relatively low abundance of denitrifying bacteria in these shallow sediments (19 ± 0%) suggests that denitrification at 4°C was constrained by limited microbial potential and low temperature, resulting in only short-lived NO_3^--N reduction.

Intermediate-depth sediments (0.6 m and 0.8 m) exhibited sustained zero-order NO_3^--N removal at 4°C, although temporal patterns differed between the depths (Figure 6.6). At 0.6 m, NO_3^--N concentrations declined linearly over 7-day incubation, whereas 0.8 m sediments displayed an initial lag phase followed by linear decline beginning Day 4, suggesting microbial acclimatation prior to the onset of active denitrification (Kumakura et al., 2023). Despite this delay, k_0 values at 0.8 m were higher than those at 0.6 m, although differences were not statistically significant. At 20°C, NO_3^--N declined rapidly at both depths, reaching 0.7 ± 0.1 mg N/L at 0.6 m

and 0.8 ± 0.0 mg N/L at 0.8 m within two days.

Deepest sediments (1.7 m) exhibited a two-phase zero-order kinetic pattern at 4°C, with a slower initial phase followed by accelerated NO_3^--N decline commencing on Day 4, culminating at 1.0 ± 0.4 mg N/L by Day 7. This pattern suggests microbial acclimation under continued carbon limitation, similar to patterns observed in 0.8 m sediment at 4°C and non-amended stem trials at 20°C. At 20°C, these sediments showed the fastest NO_3^--N removal among non-carbon-amended sediment trials, with concentrations decreasing to 0.2 ± 0.1 mg N/L within 2 days (p-value < 0.05, ANOVA, Table 6-3 A, Figure 6.6). This depth also harboured the highest relative abundance of denitrifying bacteria when compared to 0.3 to 0.8 m depths (Figure 6-4 B), supporting a high microbial potential for rapid NO_3^--N reduction under favourable temperature conditions.

For intermediate and deep sediments at 20°C, a minor increase in NO_3^--N (0.8 to 1.1 mg N/L) was observed on Day 4 and persisted through the end of incubation, despite bulk DO maintained below 0.2 mg O_2/L. Microbiome data indicated the presence of metabolically flexible "Coupled" taxa (heterotrophic nitrification-denitrification) at relative abundances of 1.0 to 1.6% in 0.6 to 1.7 m sediments, compared to 0.3% in 0.3 sediment (Figure 6-3). These microorganisms can oxidize NH_4^+-N during brief O_2 exposure and persist under predominantly anoxic conditions (Erler et al., 2011; Zhu et al., 2018). Transient O_2 may have been introduced at the sediment-water interface during daily sampling and water replacement, providing a short window for nitrification of NH_4^+-N present in the sediment to NO_3^--N. Accordingly, the observed NO_3^--N accumulation on Day 4 likely suggests transient NO_3^--N production via nitrification combined with carbon limitation following the initial denitrification phase, rather than passive leaching.

The consistent zero-order kinetics observed across most sediments at both temperatures (except 0.3 m at 20°C) indicate that the background sCOD concentration in bulk water (16 mg O_2/L), together with any inherent organic carbon in the sediment was insufficient to fully relieve electron donor limitation. When a 10:1 sCOD:NO_3^--N amendment was applied to sediments in a separate trial, the response to carbon amendment varied with temperature. At 4°C, both unamended and carbon-amended treatments exhibited zero-order kinetics, with carbon addition producing only minor and statistically insignificant increases in rate constants (p-value > 0.1, paired t-test, Table 6-3 A), indicating that microbial activity was primarily constrained by temperature rather

than electron donor availability (Figure 6-7). In contrast, at 20°C, carbon-amended trials shifted to first-order kinetics and exhibited the highest rate constants observed in the study (k_1 = 1.96 ± 0.16 1/d), whereas unamended trial remained zero-order. NO_3^--N declined rapidly to 0.9 mg N/L within one day, reflecting high denitrification capacity when both temperature and bioavailable carbon were favorable with same microbial potential as the unamended trials.

Overall, the sediment NO_3^--N removal reflects the interplay between microbial denitrification potential, temperature, and labile carbon availability. Shallow sediments are predominantly constrained by limited microbial relative abundance, whereas intermediate/deep sediments are primarily limited by the carbon availability at both temperatures. Warmer conditions accelerate enzymatic rates and microbial activity, enabling rapid NO_3^--N removal, particularly in sediments with high relative abundance of denitrifiers.

6.3.3. Relative roles of sediments and stem-associated biofilms in nitrate removal

Taken together, the experimental results demonstrate a clear functional partitioning between sediments and stem-associated biofilms in regulating NO_3^--N removal within the pond-wetland system. This partitioning was evaluated by integrating field-based microbiome analyses (Section 6.4.1) with batch-scale kinetic trials (Section 6.4.2). In relative abundance terms, inferred denitrifying taxa were, on average, 2.8 times more abundant in sediments than in stem-associated biofilms, indicating greater denitrification potential in sediments, consistent with their more stable and sustained anoxic conditions.

With microbial potential established, the relative impact of sediments and stem-associated biofilms to denitrification was quantified using batch trials under fully anoxic conditions, thereby isolating maximum potential denitrification capacity. Because NO_3^--N removal in pond and wetland systems is widely regarded as an areal based process rather than depth-controlled (Vymazal, 2007), rate constants normalised to surface area occupied by sediment or stem-biofilm would allow for a direct areal-based assessment of their relative contributions.

Within the trials, stem-associated biofilms provided a surface area of 0.00840 m^2, whereas sediments contributed 0.00375 m^2, corresponding to approximately 2.24 times greater surface area associated with stems. Despite this, sediments consistently exhibited higher denitrification efficiency per unit area. Under unamended carbon trials at 20°C, the ratio of rate constant to surface

area revealed a 3.1-fold greater denitrification capacity in sediments relative to stem-associated biofilms. Under carbon-amended conditions at 20°C (ideal conditions), this contrast amplified considerably to a 9.7- fold difference.

To place these findings in a field-scale context, denitrification efficiencies were scaled to a representative 1 m^2 vegetated plot at Pond OUT with an average water depth of 0.3 m. Observed macrophyte densities (31±3 plants/ m^2) were within the lower range reported in the literature (28 to 50 plants/ m^2) (Gebremariam & Beutel, 2008; Heinz, 2012; Soana et al., 2025; Wu, 2014). Based on this density and the stem dimensions (mean diameter = 1.8 ± 1.3 cm, submerged stem height = 0.3 m), the total stem-associated biofilm surface area was estimated to be 0.52 m^2 per m^2 of pond surface, while the sediment-water interface would effectively occupy the full horizontal footprint (1 m^2). Assuming fully anoxic conditions throughout the water column, sediment-associated denitrification would exceed stem-associated biofilm activity by 6-fold under unamended carbon conditions and 19-fold with carbon addition, reflecting both greater intrinsic denitrification efficiency and larger effective surface area.

Conceptually, these results indicate that under ideal denitrifying conditions, defined by sustained anoxia, warm temperature, and sufficient labile carbon, sediments represent the dominant zone of NO_3^--N removal within the pond-wetland system. This dominance arises from a combination of higher denitrifying bacteria relative abundance, greater intrinsic denitrification efficiency per unit area, and a larger effective surface area at the system scale. However, stem-associated biofilms are not inconsequential. Despite lower denitrification efficiency relative to sediments, macrophyte stems provide higher reactive surface area and support measurable NO_3^--N removal. Contrary to previous studies emphasizing macrophyte dominated denitrification over sediment (Eriksson & Weisner, 1997; Pang et al., 2016; Toet et al., 2003), our findings indicate stem-associated biofilms likely function as a complementary, condition-dependent NO_3^--N sink that augments sediment-driven denitrification, rather than as primary control on system-scale NO_3^--N removal.

6.4. Conclusion

This study demonstrates that denitrification in a pond-wetland system receiving tile drainage from cropping systems is primarily governed by the interaction of microbial potential, temperature, and

organic carbon availability. By integrating microbiome analysis with batch-scale kinetic measurements, sediments consistently supported sustained denitrification across depths and temperatures, exhibiting higher zero-order rate constants at 20°C (1.72 ± 0.39 to 2.78 ± 0.15 mg/L/d) and increasing relative abundance of denitrifying taxa with depth (from 19% at 0.3 m to 27% at 1.7 m), more favourable redox conditions. Denitrification in both sediments and stem-associated biofilms followed zero-order kinetics at both 4 and 20°C, indicating a strong carbon limitation rather than nitrate (NO_3^--N) limitation under baseline conditions. In contrast, stem-associated biofilms played a secondary and more conditional role in NO_3^--N removal, with no corresponding increase in rate constants despite differences in microbial abundance Carbon amendment(chemical oxygen demand: NO_3^--N=10:1) shifted denitrification to first-order kinetics and increased rate constants in both stems (0.45 ± 0.15 1/d) and sediments (1.96 ± 0.16 1/d) at 20 °C. When normalized to sediment and stem surface area of macrophyte covered part of the pond, sediment-associated denitrification exceeded stem-associated denitrification by 6 times under carbon-limited conditions and 19 times under carbon-enriched conditions. These findings highlight the importance of sediment versus macrophyte stem-associated biofilms in denitrification in pond-wetland systems treating tile drainage, particularly in cold-climate regions with limited labile carbon inputs. While batch-scale experiments provide mechanistic insight under controlled conditions, the derived rate parameters and design implications are not directly transferable to field conditions, where flowrate, oxygen dynamics, and seasonal variability regulate *in situ* denitrification.

References

APHA. (1998). Method 4500-NH4 B. In *Standard methods for the examination of water and wastewater* (20th ed.). APHA.

APHA. (2017). *Standard Methods for the Examination of Water and Wastewater* (23rd ed.). American Public Health Association.

Bachand, P. A. M., & Horne, A. J. (1999). Denitrification in constructed free-water surface wetlands: II. Effects of vegetation and temperature. *Ecological Engineering*, *14*(1–2), 17–32. https://doi.org/10.1016/S0925-8574(99)00017-8

Bachand, P. A. M., & Horne, A. J. (2005). Denitrification in Constructed free-water surface wetlands: II. Effects of vegetation and temperature. *Ecological Engineering*, *14*(1), 17–32. https://doi.org/10.1556/Pollack.10.2015.1.8

Bai, X., Li, J., & Chang, S. (2023). Effects of Different Carbon and Nitrogen Ratios on Nitrogen Removal Efficiency and Microbial Communities in Constructed Wetlands. *Water (Switzerland)*, *15*(24). https://doi.org/10.3390/W15244272

Baker, L. A. (1998). Design considerations and applications for wetland treatment of high-nitrate waters. *Water Science Technology*, (38), 389–395.

Bastviken, S. K., Eriksson, P. G., Martins, I., Neto, J. M., Leonardson, L., & Tonderski, K. (2004). Potential Nitrification and Denitrification on Different Surfaces in a Constructed Treatment Wetland. *Journal of Environmental Quality*, *33*(1), 411–411. https://doi.org/10.2134/jeq2004.4110

Bastviken, S. K., Eriksson, P. G., Premrov, A., & Tonderski, K. (2005). Potential denitrification in wetland sediments with different plant species detritus. *Ecological Engineering*, *25*(2), 183–190. https://doi.org/10.1016/J.ECOLENG.2005.04.013

Beutel, M. W., Newton, C. D., Brouillard, E. S., & Watts, R. J. (2009). Nitrate removal in surface-flow constructed wetlands treating dilute agricultural runoff in the lower Yakima Basin, Washington. *Ecological Engineering*, *35*(10), 1538–1546. https://doi.org/https://doi.org/10.1016/j.ecoleng.2009.07.005

Bishop, P. L., Zhang, T. C., & Fu, Y. C. (1995). Effects of biofilm structure, microbial distributions and mass transport on biodegradation processes. *Water Science and Technology*, *31*(1), 143–152. https://doi.org/10.1016/0273-1223(95)00162-G

Brix, H. (1997). Do macrophytes play a role in constructed treatment wetlands? *Water Science and Technology*, *35*(5), 11–17. https://doi.org/10.1016/S0273-1223(97)00047-4

Brunet, C. E., Gemrich, E. R. C., Biedermann, S., Jacobson, P. J., Schilling, K. E., Jones, C. S., & Graham, A. M. (2021). Nutrient capture in an Iowa farm pond: Insights from high-frequency observations. *Journal of Environmental Management*, *299*. https://doi.org/10.1016/j.jenvman.2021.113647

Clary, J., Leisenring, M., & Strecker, E. (2020). *International Stormwater BMP Database: 2020 Summary Statistics*. www.waterrf.org

Cooper, M. J. (2016, March 1). Nitrogen limitation of algal biofilms in coastal wetlands of Lakes Michigan and Huron. *Great Lakes Connection, International Joint Commission*, *35*(1). https://doi.org/10.1086/684646

Ding, Y., Wang, D., Zhao, G., Chen, S., Sun, T., Sun, H., Wu, C., Li, Y., Yu, Z., Li, Y., & Chen, Z. (2023). The contribution of wetland plant litter to soil carbon pool: Decomposition rates and priming effects. *Environmental Research*, *224*. https://doi.org/10.1016/J.ENVRES.2023.115575

Dueholm, M. K. D., Nierychlo, M., Andersen, K. S., Rudkjøbing, V., Knutsson, S., MiDAS Global Consortium, Albertsen, M., & Nielsen, P. H. (2022). MiDAS 4: A global catalogue of full-length 16S rRNA gene sequences and taxonomy for studies of bacterial communities in wastewater treatment plants. *Nature Communications 2022 13:1*, *13*(1), 1–15. https://doi.org/10.1038/s41467-022-29438-7

ECCC. (2018). Great Lakes Freshwater Ecosystem Initiative. In *ECCC*. https://www.canada.ca/en/canada-water-agency/freshwater-ecosystem-initiatives/great-lakes/great-lakes-protection.html

Eriksson, P. G., & Weisner, S. E. B. (1997). Nitrogen Removal in a Wastewater Reservoir: The Importance of Denitrification by Epiphytic Biofilms on Submersed Vegetation. *Journal of Environmental Quality*, *26*(3), 905–910. https://doi.org/10.2134/JEQ1997.00472425002600030043X;PAGE:STRING:ARTICLE/CHAPTER

Erler, D. V., Tait, D., Eyre, B. D., & Bingham, M. (2011). Observations of nitrogen and phosphorus biogeochemistry in a surface flow constructed wetland. *Science of The Total Environment*, *409*(24), 5359–5367. https://doi.org/10.1016/J.SCITOTENV.2011.08.052

Fang, J., Yang, R., Cao, Q., Dong, J., Li, C., Quan, Q., Huang, M., & Liu, J. (2020). Differences of the microbial community structures and predicted metabolic potentials in the lake, river, and wetland sediments in Dongping Lake Basin. *Environmental Science and Pollution Research International*, *27*(16), 19661–19677. https://doi.org/10.1007/S11356-020-08446-4

Flemming, H. C., & Wingender, J. (2010). The biofilm matrix. *Nature Reviews Microbiology 2010 8:9*, *8*(9), 623–633. https://doi.org/10.1038/nrmicro2415

Flemming, H. C., & Wuertz, S. (2019). Bacteria and archaea on Earth and their abundance in biofilms. *Nature Reviews Microbiology 2019 17:4*, *17*(4), 247–260. https://doi.org/10.1038/s41579-019-0158-9

Gebremariam, S. Y., & Beutel, M. W. (2008). Nitrate removal and DO levels in batch wetland mesocosms: Cattail (Typha spp.) versus bulrush (Scirpus spp.). *Ecological Engineering*, *34*(1), 1–6. https://doi.org/10.1016/J.ECOLENG.2008.06.005

Goris, T., & Diekert, G. (2016). The Genus Sulfurospirillum. *Organohalide-Respiring Bacteria*, 209–234. https://doi.org/10.1007/978-3-662-49875-0_10

Gottschall, N., Boutin, C., Crolla, A., Kinsley, C., & Champagne, P. (2007). The role of plants in the removal of nutrients at a constructed wetland treating agricultural (dairy) wastewater, Ontario, Canada. *Ecological Engineering*, *29*(2), 154–163. https://doi.org/10.1016/j.ecoleng.2006.06.004

Grebliunas, B. D., & Perry, W. L. (2016). The role of C:N:P stoichiometry in affecting denitrification in sediments from agricultural surface and tile-water wetlands. *SpringerPlus*, *5*(1). https://doi.org/10.1186/s40064-016-1820-6

Heinz, S. I. (2012). *Population biology of Typha latifolia L. and Typha angustifolia L.: establishment, growth and reproduction in a constructed wetland*. Technical Univeristy of Munich.

Kadlec, R. H., & Reddy, K. R. (2001). Temperature Effects in Treatment Wetlands. *Water Environment Research*, *73*(5), 543–557. https://doi.org/10.2175/106143001x139614

Kadlec, R. H., & Wallace, S. D. (2008). *Treatment Wetlands* (Second). Taylor & Francis Group, LLC.

Kjellin, J., Hallin, S., & Wörman, A. (2007). Spatial variations in denitrification activity in wetland sediments explained by hydrology and denitrifying community structure. *Water Research*, *41*(20), 4710–4720. https://doi.org/10.1016/j.watres.2007.06.053

Kottek, M., Grieser, J., Beck, C., Rudolf, B., & Rubel, F. (2006). World map of the Köppen-Geiger climate classification updated. *Meteorologische Zeitschrift*, *15*(3), 259–263. https://doi.org/10.1127/0941-2948/2006/0130

Kozich, J. J., Westcott, S. L., Baxter, N. T., Highlander, S. K., & Schloss, P. D. (2013). Development of a dual-index sequencing strategy and curation pipeline for analyzing amplicon sequence data on the miseq illumina sequencing platform. *Applied and Environmental Microbiology*, *79*(17), 5112–5120. https://doi.org/10.1128/AEM.01043-13

Kumakura, D., Yamaguchi, R., Hara, A., & Nakaoka, S. (2023). Disentangling the growth curve of microbial culture. *Journal of Theoretical Biology*, *573*, 111597. https://doi.org/10.1016/J.JTBI.2023.111597

Lee, C. G., Fletcher, T. D., & Sun, G. (2009). Nitrogen removal in constructed wetland systems. In *Engineering in Life Sciences* (Vol. 9, Number 1, pp. 11–22). https://doi.org/10.1002/elsc.200800049

Li, J., Hao, H., Cheng, G., Liu, C., Ahmed, S., Shabbir, M. A. B., Hussain, H. I., Dai, M., & Yuan, Z. (2017). Enhancing nitrate removal from freshwater pond by regulating carbon/nitrogen ratio. *Frontiers in Microbiology*, *8*(SEP), 273572. https://doi.org/10.3389/FMICB.2017.01712/BIBTEX

Liu, Y., Gao, H., Wang, Z., Xue, P., Chen, X., Wang, B., & Wen, G. (2025). Nitrogen cycling blocked in constructed wetlands: Mechanisms, developments, and challenges—A review. *Water Research X*, *29*, 100401. https://doi.org/10.1016/J.WROA.2025.100401

Mellado, M., & Vera, J. (2021). Microorganisms that participate in biochemical cycles in wetlands. In *Canadian Journal of Microbiology* (Vol. 67, Number 11, pp. 771–788). Canadian Science Publishing. https://doi.org/10.1139/cjm-2020-0336

Metcalf, & Eddy. (2014). *Wastewater Engineering: Treatment and Resource Recovery* (5th ed.).

Ng, W. J., & Gunaratne, G. (2011). Design of tropical constructed wetlands. *Wetlands for Tropical Applications: Wastewater Treatment by Constructed Wetlands*, 69–93. https://doi.org/10.1142/9781848162983_0005

OMAFA, & OSCIA. (2019). *ONFARM applied research and monitoring*. OSCIA. https://www.ontariosoilcrop.org/onfarm/

OSCIA. (2023). *Lake Erie Agriculture Demonstrating Sustainability* . OSCIA. https://www.ontariosoilcrop.org/lake-erie-agriculture-demonstrating-sustainability/

Pang, S., Zhang, S., Lv, X. Y., Han, B., Liu, K., Qiu, C., Wang, C., Wang, P., Toland, H., & He, Z. (2016). Characterization of bacterial community in biofilm and sediments of wetlands dominated by aquatic macrophytes. *Ecological Engineering*, *97*, 242–250. https://doi.org/10.1016/J.ECOLENG.2016.10.011

Petersen, J. F., Valk, L. C., Verhoeven, M. D., Nierychlo, M. A., Singleton, C. M., Dueholm, M. K. D., & Nielsen, P. H. (2025). Diversity and physiology of abundant Rhodoferax species in global wastewater treatment systems. *Systematic and Applied Microbiology*, *48*(1), 126574. https://doi.org/10.1016/J.SYAPM.2024.126574

Phipps, R. G., & Crumpton, W. G. (1994). Factors affecting nitrogen loss in experimental wetlands with different hydrologic loads. *Ecological Engineering*, *3*(4), 399–408. https://doi.org/https://doi.org/10.1016/0925-8574(94)00009-3

Poe, A. C., Piehler, M. F., Thompson, S. P., & Paerl, H. W. (2003). Denitrification in a constructed wetland receiving agricultural runoff. *Wetlands*, *23*(4), 817–826. https://doi.org/10.1672/0277-5212(2003)023[0817:DIACWR]2.0.CO;2

Rabalais, N. N., Turner, R. E., & Wiseman, W. J. (2002). Gulf of Mexico Hypoxia, A.K.A. "The Dead Zone." *Annual Review of Ecology and Systematics*, *33*(1), 235–263. https://doi.org/10.1146/annurev.ecolsys.33.010802.150513

Randall, G. W., & Goss, M. J. (2008). Nitrate Losses to Surface Water Through Subsurface, Tile Drainage. In J. L. Hatfield & R. F. Follett (Eds.), *Nitrogen in the Environment: Sources, Problems, and Management* (2nd ed., pp. 145–175). Elsevier Science & Technology.

Rani, A., Chauhan, M., Kumar Sharma, P., Kumari, M., Mitra, D., & Joshi, S. (2024). Microbiological dimensions and functions in constructed wetlands: A review. In *Current Research in Microbial Sciences* (Vol. 7). Elsevier Ltd. https://doi.org/10.1016/j.crmicr.2024.100311

Reddy, K. R., DeLaune, R. D., & Inglett, P. W. (2023). *Biogeochemistry of Wetlands* (2nd ed.). CRC Press.

Richardson, W. B., Strauss, E. A., Bartsch, L. A., Monroe, E. M., Cavanaugh, J. C., Vingum, L., & Soballe, D. M. (2011). Denitrification in the Upper Mississippi River: rates, controls, and contribution to nitrate flux. *Https://Doi.Org/10.1139/F04-062*, *61*(7), 1102–1112. https://doi.org/10.1139/F04-062

Royer, T. V., & David, M. B. (2005). Export of dissolved organic carbon from agricultural streams in Illinois, USA. *Aquatic Sciences*, *67*(4), 465–471. https://doi.org/10.1007/S00027-005-0781-6/METRICS

Sand-Jensen, K., & Pedersen, O. (1999). Velocity gradients and turbulence around macrophyte stands in streams. *Freshwater Biology*, *42*(2), 315–328. https://doi.org/10.1046/J.1365-2427.1999.444495.X

Schaller, J. L., Royer, T. V, David, M. B., & Tank, J. L. (2004). Denitrification associated with plants and sediments in an agricultural stream. In *Am. Benthol. Soc* (Vol. 23, Number 4).

Schipper, L. A., Robertson, W. D., Gold, A. J., Jaynes, D. B., & Cameron, S. C. (2010). Denitrifying bioreactors—An approach for reducing nitrate loads to receiving waters. *Ecological Engineering*, *36*(11), 1532–1543. https://doi.org/10.1016/J.ECOLENG.2010.04.008

Shirdashtzadeh, M., Chua, L. H. C., & Brau, L. (2022). Microbial Communities and Nitrogen Transformation in Constructed Wetlands Treating Stormwater Runoff. In *Frontiers in Water* (Vol. 3). Frontiers Media S.A. https://doi.org/10.3389/frwa.2021.751830

Sirivedhin, T., & Gray, K. A. (2006). Factors affecting denitrification rates in experimental wetlands: Field and laboratory studies. *Ecological Engineering*, *26*(2), 167–181. https://doi.org/https://doi.org/10.1016/j.ecoleng.2005.09.001

Smriga, S., Ciccarese, D., & Babbin, A. R. (2021). Denitrifying bacteria respond to and shape microscale gradients within particulate matrices. *Communications Biology 2021 4:1*, *4*(1), 570-. https://doi.org/10.1038/s42003-021-02102-4

Soana, E., Gavioli, A., Tamburini, E., Fano, E. A., & Castaldelli, G. (2018). To mow or not to mow: reed biofilms as denitrification hotspots in drainage canals. *Ecological Engineering*, *113*, 1–10. https://doi.org/10.1016/j.ecoleng.2017.12.029

Soana, E., Vincenzi, F., Gavioli, A., & Castaldelli, G. (2025). Different Denitrification Capacity in Phragmites australis and Typha latifolia Sediments: Does the Availability of Surface Area for Biofilm Colonization Matter? *Water 2025, Vol. 17, Page 560*, *17*(4), 560. https://doi.org/10.3390/W17040560

Stewart, P. S. (2003). Diffusion in biofilms. *Journal of Bacteriology*, *185*(5), 1485–1491. https://doi.org/10.1128/JB.185.5.1485-1491.2003;WEBSITE:WEBSITE:ASMJ;REQUESTEDJOURNAL:JOURNAL:JB;JOURNAL:JOURNAL:JB;ISSUE:ISSUE:DOI

Thorén, A. K., Legrand, C., & Tonderski, K. S. (2004). Temporal export of nitrogen from a constructed wetland: Influence of hydrology and senescing submerged plants. *Ecological Engineering*, *23*(4–5), 233–249. https://doi.org/10.1016/j.ecoleng.2004.09.007

Toet, S., Huibers, L. H. F. A., Van Logtestijn, R. S. P., & Verhoeven, J. T. A. (2003). Denitrification in the periphyton associated with plant shoots and in the sediment of a wetland system supplied with sewage treatment plant effluent. *Hydrobiologia*, *501*(1), 29–44. https://doi.org/10.1023/A:1026299017464/METRICS

Vymazal, J. (2007). Removal of nutrients in various types of constructed wetlands. *Science of The Total Environment*, *380*(1), 48–65. https://doi.org/https://doi.org/10.1016/j.scitotenv.2006.09.014

Wang, H., Bagnoud, A., Ponce-Toledo, R. I., Kerou, M., Weil, M., Schleper, C., & Urich, T. (2021). Linking 16S rRNA Gene Classification to amoA Gene Taxonomy Reveals Environmental Distribution of Ammonia-Oxidizing Archaeal Clades in Peatland Soils . *MSystems*, *6*(4). https://doi.org/10.1128/MSYSTEMS.00546-21;WGROUP:STRING:PUBLICATION

Wang, J., Long, Y., Yu, G., Wang, G., Zhou, Z., Li, P., Zhang, Y., Yang, K., & Wang, S. (2022). A Review on Microorganisms in Constructed Wetlands for Typical Pollutant Removal: Species, Function, and Diversity. In *Frontiers in Microbiology* (Vol. 13). Frontiers Media S.A. https://doi.org/10.3389/fmicb.2022.845725

Wang, R., Cui, L., Li, J., Li, W., Zhu, Y., Hao, T., Liu, Z., Lei, Y., Zhai, X., & Zhao, X. (2022). Response of nir-type rhizosphere denitrifier communities to cold stress in constructed wetlands with different water levels. *Journal of Cleaner Production*, *362*, 132377. https://doi.org/10.1016/J.JCLEPRO.2022.132377

Wang, S., Wang, R., Vyzmal, J., Hu, Y., Li, W., Wang, J., Lei, Y., Zhai, X., Zhao, X., Li, J., & Cui, L. (2023). Shifts of active microbial community structure and functions in constructed wetlands responded to continuous decreasing temperature in winter. *Chemosphere*, *335*, 139080. https://doi.org/10.1016/J.CHEMOSPHERE.2023.139080

White, J. R., & Reddy, K. R. (2003). Nitrification and Denitrification Rates of Everglades Wetland Soils along a Phosphorus-Impacted Gradient. *Journal of Environmental Quality*, *32*(6), 2436–2443. https://doi.org/https://doi.org/10.2134/jeq2003.2436

Whitmire, S. L., & Hamilton, S. K. (2005). Rapid Removal of Nitrate and Sulfate in Freshwater Wetland Sediments. *Journal of Environmental Quality*, *34*(6), 2062–2071. https://doi.org/10.2134/JEQ2004.0483;PAGE:STRING:ARTICLE/CHAPTER

Working Group on the State of the St. Lawrence Monitoring. (2024). *Overview of the State of the St. Lawrence 2024*.

Wu, L., Wei, W., Xu, J., Chen, X., Liu, Y., Peng, L., Wang, D., & Ni, B. J. (2021). Denitrifying biofilm processes for wastewater treatment: Developments and perspectives. *Environmental Science: Water Research and Technology*, *7*(1), 40–67. https://doi.org/10.1039/D0EW00576B

Wu, M. (2014). Potential of Typha as Plant Candidates for Sludge Treatment Wetlands. *GSTF Journal of BioSciences (JBio) 2014 3:1*, *3*(1), 1-. https://doi.org/10.7603/S40835-014-0001-Z

Xue, Y., Kovacic, D., David, M., Gentry, L., Mulvaney, R., & Lindau, C. (2009). In Situ Measurements of Denitrification in Constructed Wetlands. *Journal of Environmental Quality - J ENVIRON QUAL*, *28*. https://doi.org/10.2134/jeq1999.00472425002800010032x

Yan, Y., & Xu, J. (2013). Improving Winter Performance of Constructed Wetlands for Wastewater Treatment in Northern China: A Review. *Wetlands 2013 34:2*, *34*(2), 243–253. https://doi.org/10.1007/S13157-013-0444-7

Zhang, S., Pang, S., Wang, P., Wang, C., Guo, C., Addo, F. G., & Li, Y. (2016). Responses of bacterial community structure and denitrifying bacteria in biofilm to submerged macrophytes and nitrate. *Scientific Reports*, *6*. https://doi.org/10.1038/srep36178

Zhou, X., Liu, X., Liu, M., Liu, W., Xu, J., & Li, Y. (2024). Comparative evaluation of 16S rRNA primer pairs in identifying nitrifying guilds in soils under long-term organic fertilization and water management. *Frontiers in Microbiology*, *15*. https://doi.org/10.3389/fmicb.2024.1424795

Zhu, W., Wang, C., Hill, J., He, Y., Tao, B., Mao, Z., & Wu, W. (2018). A missing link in the estuarine nitrogen cycle?: Coupled nitrification-denitrification mediated by suspended particulate matter. *Scientific Reports 2018 8:1*, *8*(1), 2282-. https://doi.org/10.1038/s41598-018-20688-4

Chapter 7 - Conclusions

This thesis dissertation presents a multi-year, full-scale evaluation of two recommended agricultural beneficial management practises (BMPs) - Controlled Drainage (CD) and a Pond-Wetland system for treating low carbon, low phosphorus, and high nitrate (NO_3^--N) cropping system tile drainage during non-frozen periods (April to November) in a cold-climate region. By addressing technology-specific knowledge gaps related to performance and removal mechanisms, this work aims to support the adoption and optimization of these BMPs among grain producers in similar climatic conditions.

7.1. Controlled Drainage (*Chapter 3*)

This three-year study provides a comprehensive evaluation of the impacts of CD on tile flow and nutrient concentrations and loads relative to free (conventional) tile drainage. Monitoring from planting to freeze-up across the Growing Period (GP), Flush Period (FP) and Post-Harvest Period (PHP) captured temporal dynamics in flow and nutrient exports.

As expected, CD markedly reduced tile flow (68%), NO_3^--N by 51%, and soluble reactive phosphorus (SRP) by 76% compared to free drainage in GP. As hypothesized, flow and nutrient losses increased significantly during FP, draining up to 14% of study cumulative flow, 20% of total NO_3^--N load, and 32% of total SRP load in short span of 2 to 9 days following stoplog removal. No clear antecedent effect of CD deployed during GP were observed in PHP, except for lower SRP concentrations. Denitrification was determined as a significant NO_3^--N removal mechanism under CD, supported by 35% higher relative abundance of facultative denitrifying bacteria in CD soil compared to FD, significantly reduced NO_3^--N concentrations in dry periods of GP (33%), and NO_3^--N gradients observed in the dammed soil profile during FP. In addition to dissolved nutrients, CD significantly reduced total suspended solids (TSS) and solid-bound P, which accounted for 36% of total P, highlighting the importance of monitoring both particulate and dissolved nutrient form. Overall, despite increased export in FP, CD implemented during GP resulted in cumulative reductions of 37% in the tile flow, 21% in NO_3^--N, and 57% in SRP loads by from planting to freeze-up.

7.2. Pond-Wetland System (*Chapters 4, 5 and 6*)

This five-year study evaluated the performance of a 0.4 ha integrated pond-wetland system

receiving NO_3^--N rich, low-carbon, and low SRP tile drainage from a cropping system in a cold-region. The system comprised of multiple ponds with mean depths ranging from 0.1 to 1.3 m, enabling assessment of internal, depth-related nutrient processing. Collectively, the findings provide insights into treatment effectiveness, dominant removal mechanisms, and design considerations for cold-region pond-wetland systems.

Overall system performance and dominant removal mechanisms:

- The system provided effective retention of TSS, with reductions of 49% by concentration and 59% by mass, primarily through sedimentation.
- Moderate NO_3^--N removal was achieved (30% by concentration; 16% by mass), largely via microbial denitrification under favourable seasonal conditions.
- Among the phosphorus species, PP exhibited moderate removal (24% by concentration; 22% by mass) driven by sedimentation, whereas SRP dynamics showed modest net removal (14% by concentration; 15% by mass), driven by internal biological uptake, release, and sediment sorption.

Seasonal and spatial variability:

- Treatment performance exhibited strong seasonal variability, ranging from intermittent or negative removal during colder, high-flow periods (Spring-melt, Late Spring, and Fall) to consistently higher removal efficiencies during warmer, low-flow Summer conditions.
- Internal pond-scale analyses revealed considerable spatial heterogeneity, demonstrating that inlet-outlet metrics alone underestimated internal nutrient processing and masked key mechanisms governing system performance.

N removal kinetics and microbial controls:

- A cascading pond-to-pond areal-based first order model best described NO_3^--N removal (rate constant, $k = 0.14$ m/d, $\theta = 1.19$, $R^2 = 0.83$), outperforming traditional inlet-outlet and volumetric (hydraulic retention time-based) constructed wetland models.
- NO_3^--N removal scaled more strongly with benthic surface area than with water-column volume, with pond-scale comparisons indicating that moderate depths (~0.6-0.7 m) would be sufficient for NO_3^--N removal, while deeper pond (1.3 m) provided no additional benefit.
- Field-based microbiome community analyses and controlled, anoxic, batch-scale denitrification trials identified sediments as the dominant habitat of NO_3^--N removal,

exhibiting 2.8-fold higher relative abundance of denitrifying taxa and 3- to 9-fold higher area-normalized rate constants compared to stem-associated biofilms.

- Batch-scale trails demonstrated zero-order denitrification kinetics under unamended condition (carbon-limited), shifting to first-order kinetics with carbon addition, while temperature strongly constrained denitrification at 4°C across all habitats, and organic carbon availability became the dominant limiting factor at 20°C.

Practical design implications and recommendations

Primary:

- For TSS and PP - A single deeper pond configuration with a mean depth = 1.3 m surface area-to-catchment area ≥ 0.52% would be sufficient.
- Denitrification controls the sizing, use design parameters (k = 0.14 m/d, θ = 1.19) to determine the total surface area. Then, subtract the area of 1.3 m deep pond as calculated above, and split the remaining area equally between a 0.6 m pond and a 0.3 m, vegetated wetland cell.
- Do not design a pond-wetland system for low SRP influent concentration loading (0.1 mg P/L).

Secondary

- Persistent sediment resuspension and elevated algal productivity in the shallow, unvegetated inlet pond (0.08 m) indicate that shallow ponds are unsuitable as inlet cells; a deeper initial pond would reduce resuspension.
- Similarly, the shallow outlet wetland cell (0.3 m) underperformed possibly due to insufficient vegetation coverage (< 50%) and insufficient area, therefore larger area and active planting is recommended.

Overall, while the pond-wetland system demonstrated clear effectiveness for NO_3^--N and TSS removal, the relatively low P loading and modest P reductions observed, particularly for SRP, do not support recommending this system as a primary BMP for P management under similar conditions.

7.3. Synthesis - comparison between the two agricultural BMPs

Overall, the findings of this dissertation show a clear trade-off between efficiency and scale when comparing CD and the pond-wetland system. Importantly, the systems receive different inputs: the

pond-wetland system captures tile drainage and surface runoff, whereas CD treats tile drainage alone, so direct comparisons should be made with caution. On a concentration basis, CD consistently achieved greater reductions in nutrients and solids, and it also showed higher percentage mass removal for NO_3^--N, SRP, and PP. However, when evaluated on an absolute mass removal basis and cost-effectiveness ($/kg reduced), the pond-wetland system generally performed better (Table 7-1). This distinction is important because mass removal and cost are often more relevant for watershed-scale management decisions. Looking at individual parameters, NO_3^--N, the primary concern in cropping tile-drained systems, showed comparable performance between the two BMPs, with CD achieving slightly higher (21%) mass removal but the pond-wetland system removing more total mass overall (12.9 kg/ha drained vs 4.4 kg/ha drained by CD). For P, particularly under low influent concentrations, CD demonstrated higher % mass reductions for SRP and PP; however, the cost per kg removed was extremely high for both systems (Table 7-1), suggesting that neither approach is especially cost-effective for P mitigation under these conditions. In contrast, the pond-wetland system substantially outperformed CD in removing TSS, achieving much greater mass removal and doing so at much lower cost - approximately 27 times cheaper per kilogram removed.

Table 7-1 Comparison of nutrient and sediment removal efficiency and cost-effectiveness ($ per kg nutrient reduced) between controlled drainage (2018-2019, 2021) and a pond-wetland system (2016 -2021), expressed as mass removal, percent reduction, and cost per kilogram reduced

	Controlled Drainage (2018, 2019, & 2021)					**Pond-wetland system (2016 to 2021)**				
Parameter	**Mass FD (kg/ha drained)**	**Mass CD (kg/ha drained)**	**Mass removal (kg/ha drained)**	**%mass removal**	**$/kg reduced**	**Mass IN (kg/ha drained)**	**Mass OUT (kg/ha drained)**	**Mass removal (kg/ha drained)**	**%mass removal**	**$/kg reduced**
Nitrate	20.4	16.0	4.4	**21**	**6**	78.9	66.0	12.9	**16**	**7**
Particulate phosphorus	0.03	0.01	0.02	**60**	**1225**	0.6	0.4	0.2	**24**	**478**
Soluble reactive phosphorus	0.09	0.04	0.05	**57**	**490**	0.4	0.3	0.1	**15**	**955**
Total suspended solids	6.3	5.4	0.9	**15**	**27**	230.6	94.9	135.7	**59**	**1**

Taken together, these findings underscore that, beyond treatment performance, economic feasibility and implementation constraints are key factors in determining the suitability of these systems. From an economic and implementation perspective, CD represents a low-cost (Table 7-2) and minimally land-intensive management practice with only 0.0009% of the drained area

occupied by control structures. The total upfront capital cost for installing five control structures was estimated at $7,214 (approximately $275/ha drained), which falls below the range ($308/ha to $480/ha) reported in previous studies (Christianson et al., 2013; Crabbé et al., 2012; Frankenberger et al., 2024; Nistor & Lowenberg-DeBoer, 2007). Annualized costs were also modest, estimated at $278 ($10.6/ha/yr), primarily due to depreciation, with negligible maintenance requirements. The system is operationally simple, with anticipated lifespan of approximately 20 years, and only biannual manual adjustments required in this region and similar climatic zones. Beyond environmental benefits, CD demonstrated potential agro-economic benefits, including a 21% increase in crop yield in one year when water retention likely alleviated soil moisture stress.

In comparison, the pond–wetland system (0.4 ha; 0.93% of drained area) required substantially higher capital investment (Table 7-3). Total upfront costs were estimated at $43,463 ($1,011/ha), increasing to $58,263 ($1,355/ha) when land acquisition was included. Although routine annual costs are expected to be minimal (Kovacic et al., 2006), long-term maintenance requirements include periodic vegetation management and sediment dredging. Based on observed accumulation rates (1.7 cm/yr), dredging would be required approximately every 15 years, with an estimated dredging cost at $3,341 per event, approximately $77.7/ha, or $5.2/ha/yr when annualized. Design guidance suggests dredging when sediment accumulation exceeds 25 cm or 30% of volumetric capacity (Miller et al., 2025; TRCA & CH2M, 2016), both of which align with projected timelines for this system. The pond-wetland system also requires permanent land conversion, reducing productive agricultural area, and typically involves a longer establishment period before optimal treatment performance is achieved. However, it offers additional co-benefits, including potential irrigation water storage during drought conditions, beneficial reuse of dredged sediments (land application as a soil amendment) under a Non-Agricultural Source Material (NASM) plan, regulated under O.Reg. 267/03 of the Nutrient Management Act in Ontario (OMAFA, 2002, 2023), and ecosystem services such as habitat provision, biodiversity enhancement, and aesthetic or recreational value.

Table 7-2 Detailed cost analysis for installation and operation of controlled drainage structures, including capital investment and annual operating expenses

Item	Cost per structure	Total cost
CAPITAL COSTS (UPFRONT)		

Cost of control structure (AgriDrain Corp.)	$870	5 x $870 = $4,350
Cost of stoplogs (5" or 7") + Metal lid + stoplog handle (2') (AgriDrain Corp.)	($25 x 7) + $121 + $30	5 x $326= $1,630
Cost of V-notch Weir + Stoplog retainer + Grease + Stoplog assist (AgriDrain Corp.)	$71 + $21 +$22 + $82 = $196	(5 x ($71+$21)) +$22 + $82 = $564
Backhoe rental per day (1-ton mini excavator) (local company quote)		$220
Personnel required, minimum 3 (including 1 drainage specialist)		6 hr x $75 = $450
		$7,214 or $275/ha
ANNUAL COSTS		
Depreciation (Crabbé et al., 2012)	5% x $870 = $43.5	5 x $43.5 = $218 or $8.3/ha/yr
Maintenance (lubrication)	Assumed negligible	$0
Operating cost	2 visits x 1 hr x $30	$60 or $2.3/ha/yr
		$278 or $10.6/ha/yr

Table 7-3 Detailed cost analysis associated with design, construction, and maintenance of a pond-wetland system, including capital investment and dredging expenses

Item	Total cost
CAPITAL COSTS (UPFRONT)	
Engineering design and permits	$8,948
Construction, excavation, soil movement	$34,515
	$43,463 or $1,011/ha
Land purchase (if required) for this region = $37,000/ha	$14,800
	$58,263 or $1,355/ha
DREDGING COSTS	
Hydraulic (suction-based) dredger rental per day (local company quote)	**$2,056**
Labor cost	$165 per hr or 5 x $165 = $825
12-ton manure spreader rental per day (Premier Equipment rentals)	$460
	$3,341 or $77.7/ha or $5.2/ha/yr

Overall, neither system is universally superior, as effectiveness depends on management objectives and site constraints. If the primary goal is to reduce nutrient and solids concentrations at the field scale, especially where land is limited and low-cost implementation is prioritized, CD is likely the more suitable option due it its efficiency and simplicity. In contrast, if the objective is to maximise total mass removal and cost-effectiveness at larger scales, particularly for solids and particulate-associated pollutants, the pond-wetland system may be preferable. Ultimately, these BMPs are best viewed as complementary, with selection guided by site-specific condition, target pollutants, and economic and land-use considerations.

7.4. Future Research

This dissertation introduced a novel approach to determining the role of denitrification in CD

through microbiome analysis of soil. Building on these findings, future research could include repeated soil sampling over the course of stoplog deployment to capture temporal trends in the relative abundance of denitrifying bacteria, providing a more detailed understanding of microbial dynamics and NO_3^--N removal process. Previous, limited studies (Elmi et al., 2002; Liu et al., 2018; Sunohara et al., 2016; Tournebize et al., 2017) have evaluated the removal of contaminants such as herbicides (including but not limited to atrazine and glyphosate), per- and polyfluoroalkyl substances (PFAS), microplastics, and if manure is applied, pathogens such as E.coli, *Campylobacter spp*. and *Arcobacter butzleri*. Applying these analyses in the context of this study would provide additional insight into the broader treatment potential of these BMPs in cold-climate regions. Although a few studies have evaluated greenhouse gas (GHG) emissions from CD and constructed wetland systems (Ekwunife & Madramootoo, 2023; Groh et al., 2015; Nangia et al., 2013), future research could build on this work by integrating GHG emissions with microbial analyses, thereby linking microbiome functional potential to actual GHG fluxes. While batch denitrification trials provided estimates of the theoretical maximum denitrification potential in sediments and stem-associated biofilms, future studies could build on this work by incorporating additional factors that influence denitrification such as carbon availability in sediments, pH, stem biofilm thickness, co-limiting nutrients (such as P) that may indirectly limit microbial activity suggested by previous studies (Grebliunas & Perry, 2016; Soana et al., 2025).

Reference

Christianson, L., Tyndall, J., & Helmers, M. (2013). Financial comparison of seven nitrate reduction strategies for Midwestern agricultural drainage. *Water Resources and Economics*, *2–3*, 30–56. https://doi.org/10.1016/J.WRE.2013.09.001

Crabbé, P., Lapen, D. R., Clark, H., Sunohara, M., & Liu, Y. (2012). Economic benefits of controlled tile drainage: Watershed Evaluation of Beneficial Management Practices, South Nation River basin, Ontario. *Water Quality Research Journal of Canada*, *47*(1), 30–41. https://doi.org/10.2166/wqrjc.2012.007

Ekwunife, K. C., & Madramootoo, C. A. (2023). Influence of seasonal climate and water table management on corn yield and nitrous oxide emissions. *Agricultural Water Management*, *279*, 108207. https://doi.org/10.1016/J.AGWAT.2023.108207

Elmi, A. A., Madramootoo, C., Egeh, M., Liu, A., & Hamel, C. (2002). Environmental and agronomic implications of water table and nitrogen fertilization management. *Journal of Environmental Quality*, *31*(6), 1858–1867. https://doi.org/10.2134/jeq2002.1858

Frankenberger, J., McMillan, S. K. W., Williams, M. R., Mazer, K., Ross, J., & Sohngen, B. (2024). Drainage Water Management: A review of nutrient load reductions and cost effectiveness. *Journal of the ASABE*, *67*(4), 1077–1092. https://doi.org/10.13031/ja.15549

Grebliunas, B. D., & Perry, W. L. (2016). The role of C:N:P stoichiometry in affecting denitrification in sediments from agricultural surface and tile-water wetlands. *SpringerPlus*, *5*(1). https://doi.org/10.1186/s40064-016-1820-6

Groh, T. A., Gentry, L. E., & David, M. B. (2015). Nitrogen Removal and Greenhouse Gas Emissions from Constructed Wetlands Receiving Tile Drainage Water. *Journal of Environmental Quality*, *44*(3), 1001–1010. https://doi.org/10.2134/JEQ2014.10.0415

Kovacic, D. A., Twait, R. M., Wallace, M. P., & Bowling, J. M. (2006). Use of created wetlands to improve water quality in the Midwest—Lake Bloomington case study. *Ecological Engineering*, *28*(3), 258–270. https://doi.org/https://doi.org/10.1016/j.ecoleng.2006.08.002

Liu, L., Cloutier, M., Craiovan, E., Edwards, M., Frey, S. K., Gottschall, N., Lapen, D. R., Sunohara, M., Topp, E., & Khan, I. U. H. (2018). Quantitative real-time PCR-based assessment of tile drainage management influences on bacterial pathogens in tile drainage and groundwater. *Science of the Total Environment*, *624*, 1586–1597. https://doi.org/10.1016/j.scitotenv.2017.10.200

Miller, B. K., Macgowan, B. J., & Reaves, R. P. (2025). *Are Constructed Wetlands a Viable Option for Your Waste Management System?* Department of Forestry and Natural Resources, Purdue University. https://extension.purdue.edu/extmedia/FNR/FNR-202.pdf

Nangia, V., Sunohara, M. D., Topp, E., Gregorich, E. G., Drury, C. F., Gottschall, N., & Lapen, D. R. (2013). Measuring and modeling the effects of drainage water management on soil greenhouse gas fluxes from corn and soybean fields. *Journal of Environmental Management*, *129*, 652–664. https://doi.org/10.1016/j.jenvman.2013.05.040

Nistor, A. P., & Lowenberg-DeBoer, J. (2007). Drainage water management impact on farm profitability. *Journal of Soil and Water Conservation*, *62*(6), 443–447. https://go-gale-com.proxy.bib.uottawa.ca/ps/i.do?p=AONE&sw=w&issn=00224561&v=2.1&it=r&id=GALE%7CA172427309&sid=googleScholar&linkaccess=fulltext

OMAFA. (2002). *Nutrient Management Act, 2002, S.O. 2002, c. 4 | ontario.ca*. OMAFA. OMAFA. https://www.ontario.ca/laws/statute/02n04

OMAFA. (2023, March). *Non-agricultural source materials (NASM)*. Https://Www.Ontario.ca/Page/Non-Agricultural-Source-Materials-Nasm#section-1.

Soana, E., Vincenzi, F., Gavioli, A., & Castaldelli, G. (2025). Different Denitrification Capacity in Phragmites australis and Typha latifolia Sediments: Does the Availability of Surface Area for Biofilm Colonization Matter? *Water 2025, Vol. 17, Page 560*, *17*(4), 560. https://doi.org/10.3390/W17040560

Sunohara, M. D., Gottschall, N., Craiovan, E., Wilkes, G., Topp, E., Frey, S. K., & Lapen, D. R. (2016). Controlling tile drainage during the growing season in Eastern Canada to reduce nitrogen, phosphorus, and bacteria loading to surface water. *Agricultural Water Management*, *178*(3), 159–170. https://doi.org/10.1016/j.agwat.2016.08.030

Tournebize, J., Chaumont, C., & Mander, Ü. (2017). Implications for constructed wetlands to mitigate nitrate and pesticide pollution in agricultural drained watersheds. *Ecological Engineering*, *103*, 415–425. https://doi.org/10.1016/J.ECOLENG.2016.02.014

TRCA, & CH2M. (2016). *Inspection and Maintenance Guide for Stormwater Management Ponds and Constructed-Wetlands*. https://sustainabletechnologies.ca/app/uploads/2018/04/SWMFG2016_Guide_April-2018.pdf

Appendix

A. Construction Maps and Photos of Controlled Drainage System (Courtesy of OMAFA, SNCA and Kinsley et al. (2019))

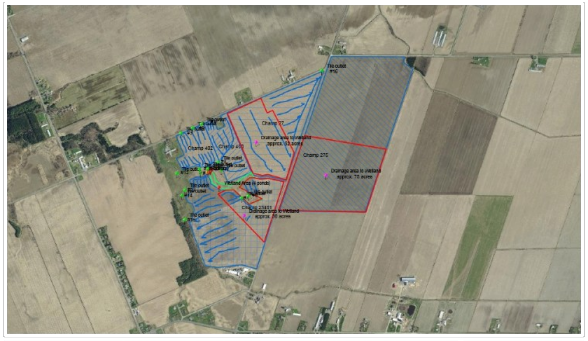

B. Construction Maps and Photos of Pond-Wetland System (Courtesy of Ducks Limited and Kinsley et al. (2019))

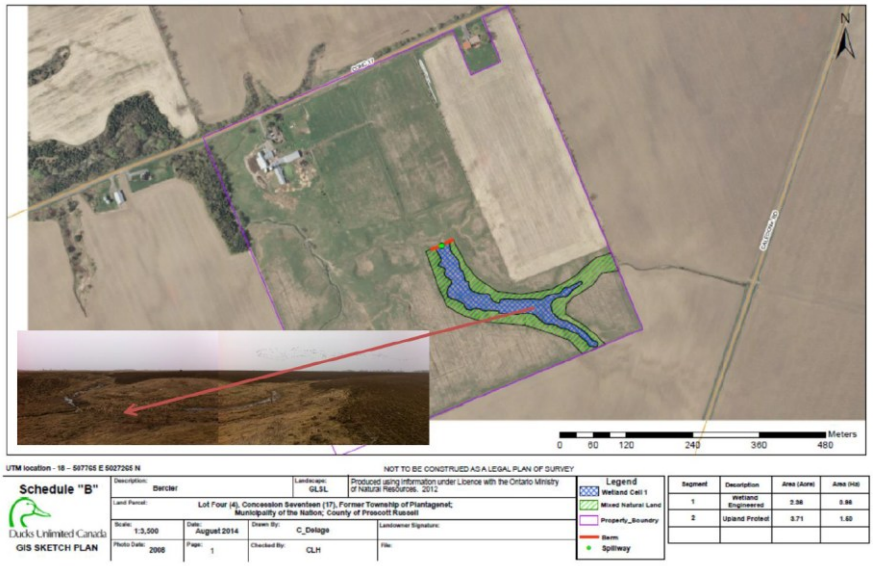

Shrubs:
Red-Osier Dogwood
Sandbar Willow
Nannyberry
Black Elderberry
Beaked Hazelnut
Serviceberry
Black Chokeberry

Trees:
White Spruce
Bur Oak
Red Maple
Black Walnut
Black Willow
Mountain Ash

Habitat Structures:
Swallow Boxes
Hen Houses
Basking Platforms
Dead Woody Debris

Trenching to Key In Dyke

Dyke Construction Begins

Opening of the Spillway

Lining Spillway with Geotextile & Blast Rock

View Upstream of Spillway

View Downstream to Spillway

View (DS) Pond 2 to Spillway

View (US) Pond 3 to Headwater

C. Calculation of water height (h) and water flow rate (Q)

1. Fluid density, ρ (Kg/m^3) was computed from the water temperature (T in °C) recorded for each point, via:

$$\rho = \{999.83952 + (16.945176\ T) - (7.9870401e-03\ T^2) - (46.170461e-06\ T^3) + (105.56302e-09\ T^4) - (280.54253e-12\ T^5)\}/(1 + 16.879850e-03\ T) \quad \text{(Equation 1)}$$

where, T is the temperature of water recorded by depth logger in °C

2. Fluid density, ρ was converted to lb/ft^3 via:

$$\rho = 0.0624279606\ \rho \quad \text{(Equation 2)}$$

3. Hydraulic Pressure, P_{hyd} (kPa) was calculated at each time, using:

$$P_{hyd} = P_{real} - P_{baro} \quad \text{(Equation 3)}$$

where, P_{real} is measured absolute down-well pressure (kPa) and P_{baro} is measured barometric pressure values (kPa).

4. Hydraulic Pressure (kPa) was converted to sensor depth, D_{real} (m) using the following equation:

$$D_{real} = FEET\_TO\_METERS \times (KPA\_TO\_PSI \times PSI\_TO\_PSF \times P_{hyd})/\rho \quad \text{(Equation A.4)}$$

where, FEET_TO_METERS = 0.3048, KPA_TO_PSI = 0.1450377 and PSI_TO_PSF = 144.0

D_{real} (ft), annotated as D_R was calculated by modifying equation 4 as:

$$D_R = (KPA\_TO\_PSI \times PSI\_TO\_PSF \times P_{hyd})/\rho \text{ (Equation 4)}$$

5. Effective height of the water, h_e(m) was calculated via:

$$h = D_{real} + k_h \quad \text{(Equation 5)}$$

$$k_h = 0.001[\theta(1.395\theta - 4.296) + 4.135] \text{ (Equation 6)}$$

Where, k_h is head correction factor for V notch weir in meters and θ is angle of V notch Weir in radians.

Background on equations, constants, and Coefficients for CD, FD and Weir IN

The values of C_e and K_h can be calculated using Equation 7 and 8, respectively; and also estimated empirically using the figure below.

$$C_e = \theta(0.02286\theta - 0.05734) + 0.6115 \quad \text{(Equation 7)}$$

$$k_h = 0.001[\theta(1.395\theta - 4.296) + 4.135] \text{ (Equation 8)}$$

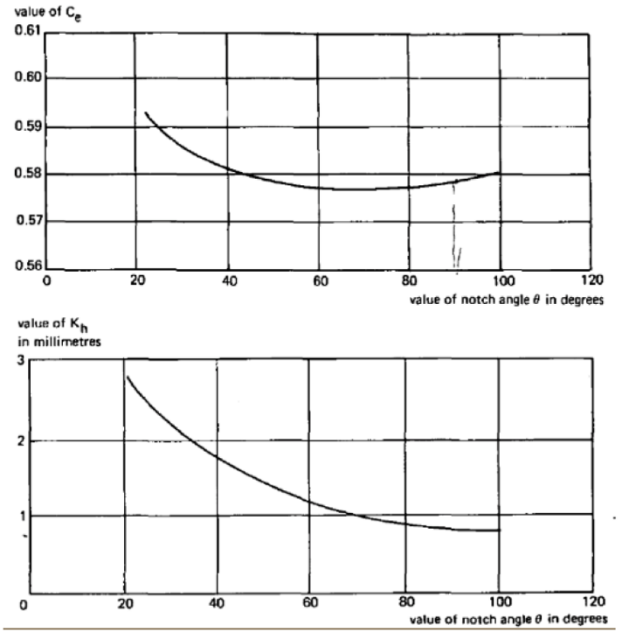

Figure C-1. Empirical Determination of constants C_e and K_h in V - Notch Weir Equation (USBR, 2001)

Using Figure C-1 for CDS, the weir angle is 22.5 degrees and as such, the constant Ce can be approximated at 0.59 and K_h at 2.6 mm or 0.0266 m. Similarly, for weir IN, the weir angle is 90 degrees, Ce was found to be 0.57 and K_h at 0.0008m. The calculated values as per the equations are below in Table.

Table C-1. Calculated Components of V-notch Weir Equation for CDS and FDS

Parameter	General Equation	Constants for CDS and FDS	Constants for Weir IN
C_e (dimensionless)	$\theta(0.02286\theta - 0.05734) + 0.6115$	0.5925	0.5778
K_h (m)	$0.001[\theta(1.395\theta - 4.296) + 4.135]$	0.00266	0.000829
θ (radians)		0.3926	1.5709

The discharge characteristics are based on The Kindsvater-Carter method, which defines an equation for a rectangular, sharp-crested weir as:

$$Q_e = C_e L_e H_e^{\frac{3}{2}} \quad \text{(Equation 9)}$$
$$L_e = L + k_b \text{ (Equation 10)}$$
$$H_e = H + k_h \text{ (Equation 11)}$$

Where, Q is the flow over the weir in ft^3/s, C_e is the effective coefficient of discharge, L is the length of the weir crest in ft, k_b is the correction factor to obtain effective weir length, B is the average width of the approach channel in ft, H is the head measured above the weir crest in ft and k_h is a correction factor having a value of 0.003 ft.

k_b, is dependent on the ratio of L/B, the length of the weir crest in ft/ average width of the approach channel in ft and is defined by the following graph:

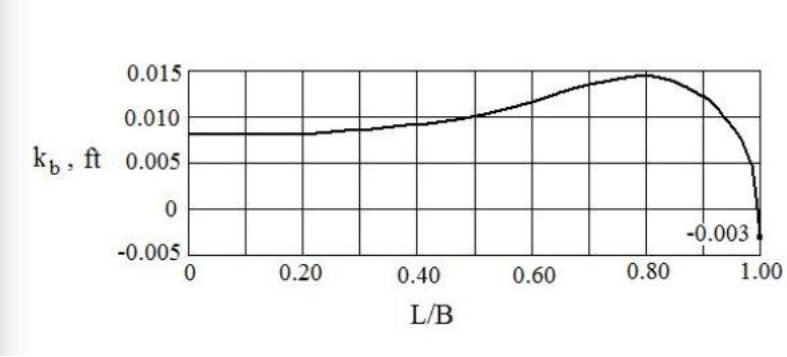

Figure C-2. Determination of k_b to calculate flow over a Rectangular Weir (USBR, 2001)

In a suppressed weir, L = B (see figure below) and therefore, L/B = 1 and k_b = -0.003 as per the graph above. Similarly, Ce can be calculated in relation to H/P where L/B=0. Using the table below, where L/B = 1, C_1 = 0.4 and C_2 = 3.220.

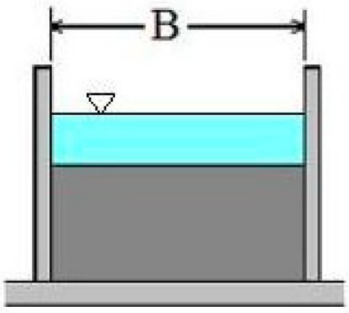

L/B	C_1	C_2
0.2	-0.0087	3.152
0.4	0.0317	3.164
0.5	0.0612	3.173
0.6	0.0995	3.178
0.7	0.1602	3.182
0.8	0.2376	3.189
0.9	0.3447	3.205
1.0	0.4000	3.220

Figure C-3. Left - Schematic of a Suppressed Sharp Crested Rectangular Weir (USBR, 2001); Right - Determination of C_1 and C_2 for the Calculation of Flow over a Rectangular Weir (USBR, 2001).

$$C_e = C_1\left(\frac{H}{P}\right) + C_2 \text{ (Equation 12)}$$
$$C_e = 0.400\left(\frac{H}{P}\right) + 3.220 \text{ (Equation 13)}$$

Therefore,

$$Q = \left(0.4\left(\frac{H_e}{P}\right) + 3.220\right)(L - 0.003)(H_e + 0.003)^{\frac{3}{2}} \text{ (Equation 14)}$$

The values of B, or the average width of the approach channel are standardised for the CDS 1 (0.314 m) and CDS 2 (0.162 m).

Modifications of flow equations for this research study

The following equations were used to calculate the water flows for the various heights of each drainage structure).

1. When the water height was less than the height up to bottom of V-notch

$$Q = 0 \quad \text{(Equation 15)}$$

2. When the water height was greater than the bottom of the V-notch but less than or equal to the top of the V-notch, the V-notch, Sharp Crested weir equation was used.

$$Q = \frac{8}{15} C_e \sqrt{2g} \tan\left(\frac{\theta}{2}\right) h_e^{\frac{5}{2}} \quad \text{(Equation 16)}$$

Where, Q is Discharge (flow rate) over weir in m^3/s, C_e is Effective discharge co-efficient, h_e is Effective height of water (m) = h – height of the stoplogs (m), θ is angle of V notch Weir in Radians, g is acceleration due to gravity (m^2/s).

3. When the water height was greater than the height up to the top of the V-notch, the weir was assumed to act as a suppressed sharp-crested rectangular weir. The assumption was that the sides of the flow channel acted as the ends of a rectangular weir, with no side contraction and no contraction of the nappe from the width of the channel (USBR, 2001). Hence, the total water flow in this case was calculated as the sum of the water flow using the suppressed rectangular weir equation and the maximum flow of water through the V-notch.

If H/P > 0.33, the Kindsvater – Carter equation for suppressed rectangular weir was used–

$$Q = \left(0.4\left(\frac{H_e}{P}\right) + 3.220\right)(L - 0.003)(H_e + 0.003)^{\frac{3}{2}} + Q_{max} \text{ (Equation 17)}$$

If H/P < 0.33,

$$Q = 3.33\ B\ H^{3/2} \text{ (Equation 18)}$$

where, Q is Discharge (flow rate) over weir in ft^3/s, H_e is Effective height of water (ft) = D_R – height of the stoplogs (ft), P is the vertical distance to the weir crest from the approach pool invert (ft) and Q_{max} is the maximum flowrate through the v-notch in ft^3/s.

The flow rate, Q, calculated using Equations 15 and 16 was converted to m^3/s and combined with Q calculated using Equations 17 and 18 to obtain a continuous time series. The calculated flow was normalized to the drainage area per sampling location.

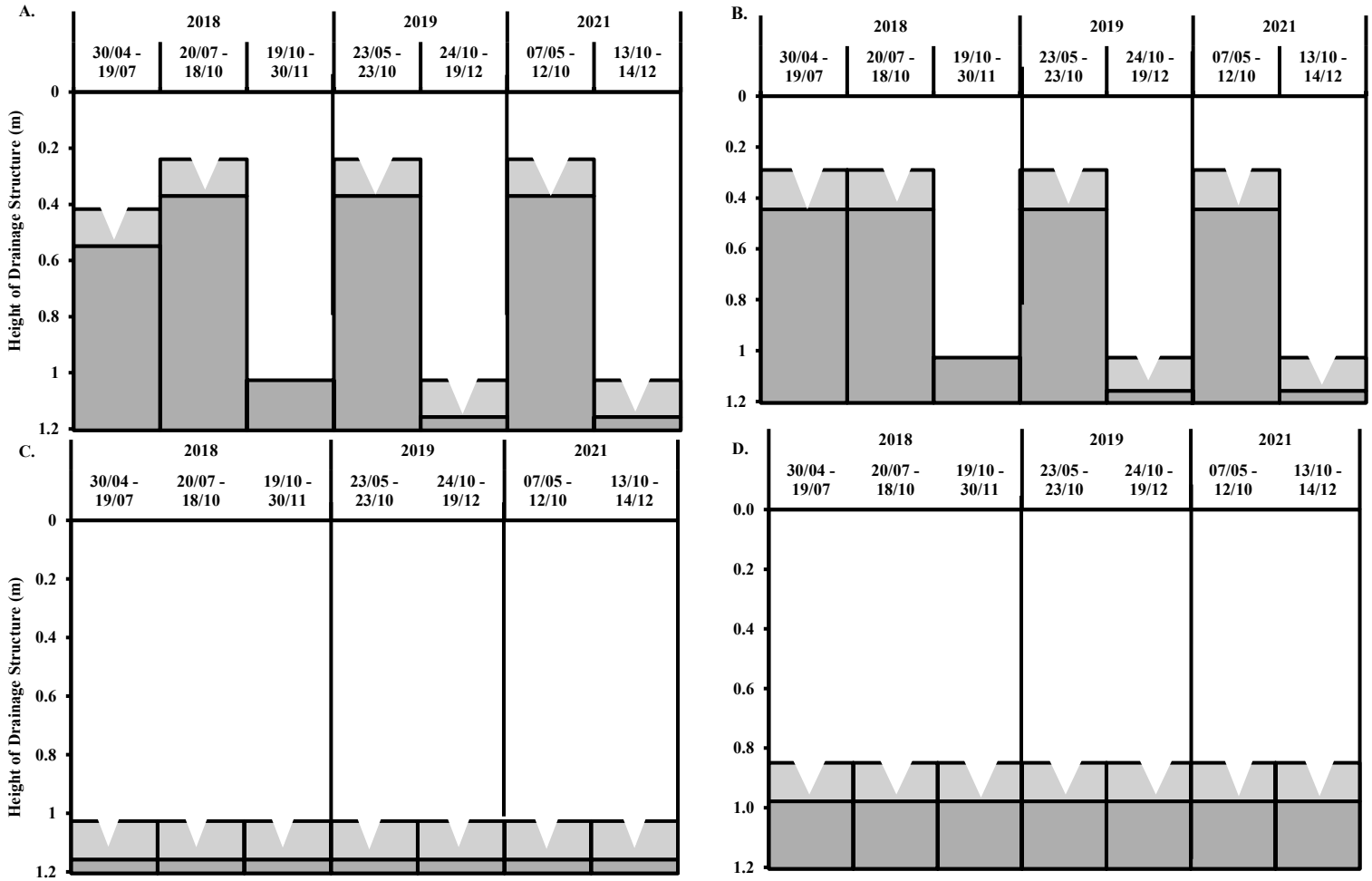

Figure C-5. Trend of Outlet Depths maintained - CD 1 (A), CD 2 (B), FD 3 & 5 (C) and FD 4 (D) using stoplogs during study years. As seen in A. additional stoplog was added at CD 1 in 2018 and in 2019, 2021, a V-notch weir log at the bottom of the CD to structurally mimic FDs.

D. Meteorological Conditions – Correlation Results

Comparison of Ferme Agriber Weather Station Data to Ottawa International Airport Data

The weather data recorded from April 30 to November 30 were, 2018 at Ferme Agriber were compared against weather data available from the Ottawa International Airport weather station obtained from Environment and Climate Change Canada online website and were plotted below.

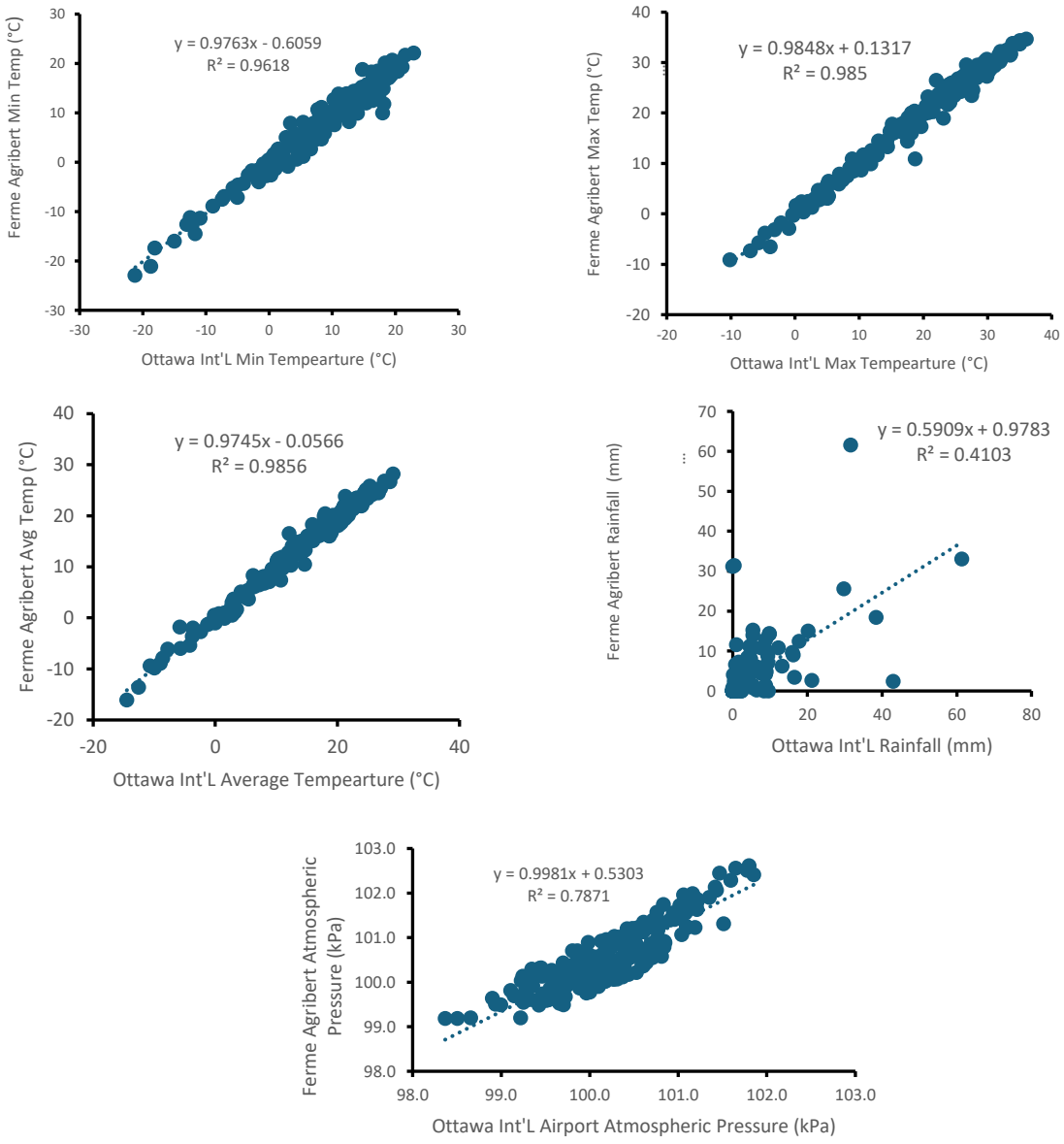

Figure D-1. Comparison of Ferme Agriber Weather Conditions and Temperature to Ottawa International Airport. Hourly and Daily weather data were used from the Environment Canada Historical Weather Data (Environment and Climate Change Canada, 2023)

Comparison of Moose Creek Weather Station Data to Agricrop Data

Precipitation data for growing season (May 1st, 2019, to August 31st, 2019) was obtained from Agricrop Ltd online website, an agency of government of Ontario. This data deemed to be most accurate was then compared with stations closest to St. Isidore such as, Moose Creek and St. Albert obtained from Environment and Climate Change Canada online website. Based on comparison graph below, Moose Creek data was chosen for the missing dates. The same logic was used for 2021 data as well (not shown here).

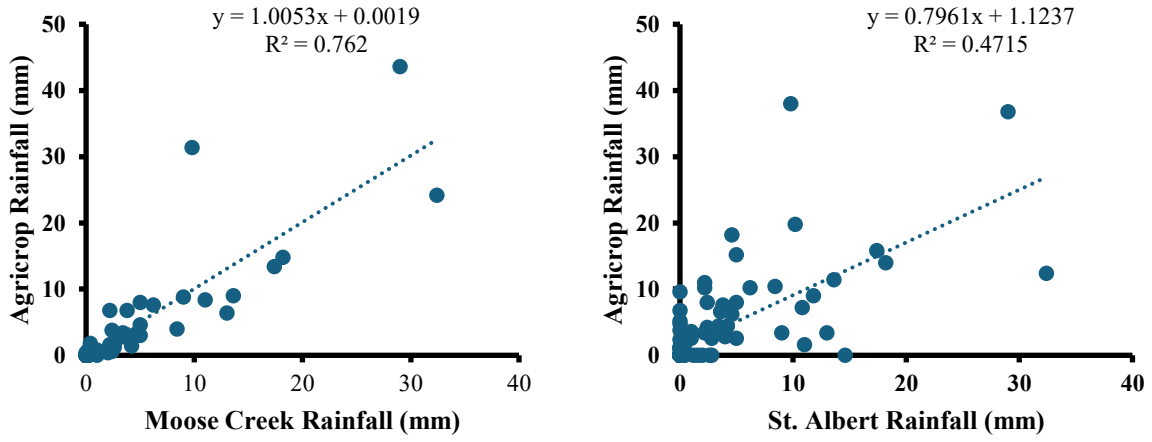

Figure D-2. Comparison of Agricrop Rainfall Data to data from Moose Creek and St. Albert Stations. Daily weather data were used from the Agricrop and Environment Canada Historical Weather Data (Agricrop, 2023; Environment and Climate Change Canada, 2023)

Reference

Agricrop, 2023. Monthly Rainfall Data [WWW Document]. URL https://www.agricorp.com/en-ca/Programs/ProductionInsurance/ForageRainfall/Pages/RainfallData.aspx (accessed 2.27.23).

Environment and Climate Change Canada, 2023. Daily Data Report - Climate - Environment and Climate Change Canada [WWW Document]. URL https://climate.weather.gc.ca/climate_data/daily_data_e.html?StationID=49568 (accessed 2.23.23).

E. Estimating Soil Water Balance, Root Stress and Crop Yield

The Soil-Water Balance Method (OMAFRA, 2008)

This method was used to determine the crop available water and periods of water stress during the growing season. Soil water balance is a function of crop factor, evapotranspiration (ET)for a given region, precipitation, and available soil moisture at the start of the growing season. The crop factors

for various stages of corn growth were obtained from (Al-Kaisi, 2000).

The following assumptions were made: 1) the crop root zone is considered as a reservoir of available water; 2) the reservoir was full when field capacity was reached; 3) crop water use (ET) removed water from the reservoir; 4) rainfall and irrigation added water to the reservoir. The following essential information was required about the operation to calculate evapotranspiration rates. Note: The water retained in the soil following a saturating rainfall and draining the excess water is termed as the reservoir.

Table E-1. Information required to Calculate Root Stress for Corn Rooting Depth 600 mm (24 inches) (OMAFRA, 2008)

Parameter	Details
Weather Station	St. Isidore, on-farm
Soil texture	Clay loam
Available water capacity of soil texture (mm of water/mm of soil)	0.15 - 0.18, average 0.17
Rooting depth (mm)	600
Estimate of maximum amount of crop-available soil water in the root zone (field capacity) Available water capacity of the soil texture x crop rooting depth	= 0.17 x 600 = 102 mm
Allowable soil water depleting in the root zone (irrigation point, i.e., plant root is in stress) 50% maximum amount of crop-available soil water in the root zone	= 102 mm x 0.5 = 51 mm

Crop Water Use/Need

The water balance method (OMAFRA, 2008) was applied to corn crops grown on Ferme Agriber in all study years. Plant water stress is defined as soil moisture conditions of less than 50% of the field capacity. In such situations, CDS can maintain a soil moisture reservoir and reduce plant water stress during the crop growing season.

Corn was planted on May 8, 2018, May 7, 2019, and April 24, 2021, and harvested on November 8, 2018, October 29, 2019, and October 25, 2021. Figure 4 shows the total crop-available soil water in the root zone at field capacity (in this case = 102 mm) for this study, with stress threshold at 51 mm. In 2018, the corn crop experienced water stress over 18 days, from July 7-24, and again for a short period from July 31 to Aug. 3, as seen in Figure 4. In 2019, the corn

crop was in stress for almost 50% of the days from planting to harvest, with a total of 86 uninterrupted days (July 25 to Oct. 16). In 2021, the stress periods were scattered, unlike in previous years, with three periods of six days each in June, August, and September.

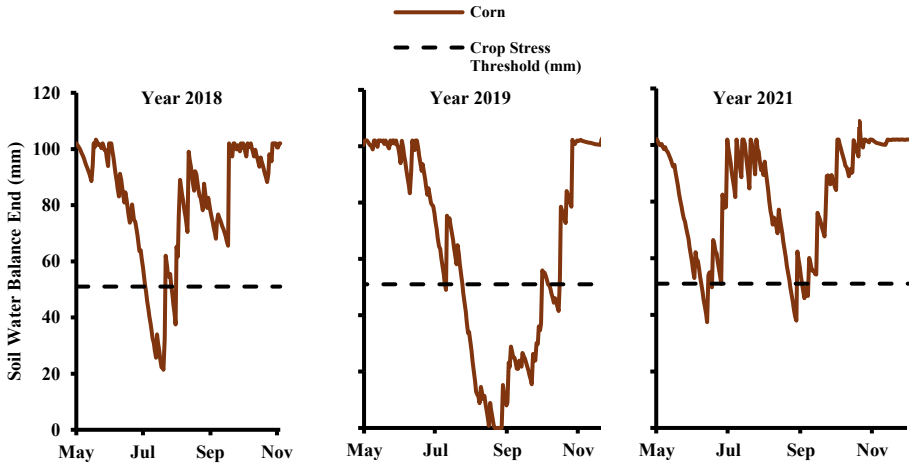

Figure E-1. Soil Water Balance for corn - Demonstrating that corn was under water stress during three-year study.

During these periods of crop stress, except from end of August to October 2019 and end of August to September 2021, corn was in V12, VT, and R1 – Silking (OMAFRA Field Crop Team, 2017)**.** These developmental stages occur around 42, 66 and 68 days after planting, respectively. During these critical vegetative growth and reproductive stages, corn is highly susceptible to heat or drought, which negatively affects ear size, number of potential kernels, pollen viability, and pollen transfer (Lapen et al., 2004; OMAFRA Field Crop Team, 2017). Any stress during these stages can cause greater yield loss than any other stage of corn crop development. As explained by Neilsen (2020), any drought stress at the V12 stage could decrease the yield by 3–4 percent per day, at the VT stage by 8 percent per day, and during the R1 stage, drought stress would decrease the yield by 6 percent per day. As such, these stress periods provided the highest risk to corn yield in 2019, followed by 2018 and 2021. During these periods, the use of a controlled tile drainage system could retain water in the field and mitigate drought conditions.

Crop Yield

In the present study, CD was expected to increase yield under the theoretical assumption that by elevating the water table, plant roots would have increased access to water, consequently supporting crop growth during periods of water stress. The soil water balance revealed that the corn crop was under stress for 22, 86, and 18 d in 2018, 2019, and 2021, respectively. In addition,

GP in 2018 and 2019 received lower precipitation than the 30 - year normal, whereas 2021 had higher precipitation.

The average corn yield at Ferme Agriber was 213 bu/ac, 192 bu/ac and 206 bu/ac, respectively across all fields during the three study years. Notably, the lowest yield was observed in 2019, which experienced the most substantial crop stress of all years. The study average yields were higher by 28%, 27% and 23% than regional (Prescott and Russell) average corn yields of 151 bu/ac, 144 bu/ac and 163 bu/ac, in 2018, 2019 and 2021, respectively (OMAFRA, 2023). This would be due to a variety of factors including agronomic practices, seed selection, soil, water table in addition to the proportion of the fields under CD.

In 2018[10], the average corn yield for CD fields was 233±25 bu/ac compared to 193±2 bu/ac for FD fields. The 21% difference in yield ($p < 0.05$, ANOVA) can be attributed to CD maintaining moisture in the soil during a GP where precipitation was followed by a dry period with corn experiencing stress at a critical time. The effect of CD on corn yield has been demonstrated to vary in previous studies, with a substantial increase of 64% in corn yield (Ng et al., 2002; Tan et al., 1999), a mere 3-4% increase (Cicek et al., 2010; Ghane et al., 2012), no significant increase (Fausey, 2005; Verma and Cooke, 2012; Youssef et al., 2023), and a negative effect on yield (Helmers et al., 2012). Any positive effect on crop yield due to the implementation of a CD can be an important incentive among crop cultivators to implement the practise.

Reference

Al-Kaisi, M., 2000. Crop water use or evapotranspiration | Integrated Crop Management [WWW Document]. Iowa State Univeristy. URL https://crops.extension.iastate.edu/encyclopedia/crop-water-use-or-evapotranspiration (accessed 3.11.21).

Cicek, H., Sunohara, M., Wilkes, G., McNairn, H., Pick, F., Topp, E., Lapen, D.R., 2010. Using vegetation indices from satellite remote sensing to assess corn and soybean response to controlled tile drainage. Agric Water Manag 98, 261–270. https://doi.org/https://doi.org/10.1016/j.agwat.2010.08.019

Fausey, N.R., 2005. Drainage management for humid regions. International Agricultural Engineering Journal 14, 209–214.

Ghane, E., Fausey, N.R., Shedekar, V.S., Piepho, H.P., Shang, Y., Brown, L.C., 2012. Crop yield evaluation under controlled drainage in Ohio, United States. J Soil Water Conserv 67, 465–473. https://doi.org/10.2489/jswc.67.6.465

Helmers, M., Christianson, R., Brenneman, G., Lockett, D., Pederson, C., 2012. Water table, drainage, and yield response to drainage water management in southeast Iowa. J Soil Water Conserv 67, 495 LP – 501. https://doi.org/10.2489/jswc.67.6.495

Lapen, D.R., Topp, G.C., Gregorich, E.G., Curnoe, W.E., 2004. Least limiting water range indicators of soil quality and corn production, eastern Ontario, Canada. Soil Tillage Res 78, 151–170. https://doi.org/https://doi.org/10.1016/j.still.2004.02.004

[10] In 2019 and 2021, due to data loss by the farmer at the study site, individual plot yield comparisons could not be carried out in these two years.

Neilsen, R.L., 2020. Drought and Heat Stress Effects on Corn Pollination [WWW Document]. The Corn Growers Guidebook. URL https://www.agry.purdue.edu/ext/corn/pubs/corn-07.htm (accessed 3.20.21).

Ng, H.Y.F., Tan, C.S., Drury, C.F., Gaynor, J.D., 2002. Controlled drainage and subirrigation influences tile nitrate loss and corn yields in a sandy loam soil in Southwestern Ontario. Agric Ecosyst Environ 90, 81–88. https://doi.org/https://doi.org/10.1016/S0167-8809(01)00172-4

OMAFRA, 2023. Ontario field crop area and production estimates by county - Grain Corn [WWW Document]. OMAFRA. URL https://data.ontario.ca/dataset/ontario-field-crop-area-and-production-estimates-by-county (accessed 1.21.25).

OMAFRA, 2008. Irrigation Scheduling Using Evapotranspiration Data: The Water Balance Method. Guelph.

OMAFRA Field Crop Team, 2017. Corn, in: Brown, C. (Ed.), Agronomy Guide for Field Crops. Ontario Ministry of Agriculture, Food and Rural Affairs, pp. 1–39.

Tan, C.S., Drury, C.F., Ng, H.Y.F., Gaynor, J.D., 1999. Effect of controlled drainage and subirrigation on subsurface tile drainage nitrate loss and crop yield at the farm scale. Canadian Water Resources Journal 24, 177–186. https://doi.org/10.4296/cwrj2403177

Verma, S., Cooke, R., 2012. Performance of drainage water management systems in Illinois, United States. J Soil Water Conserv 67, 453–464. https://doi.org/10.2489/jswc.67.6.453

Youssef, M.A., Strock, J., Bagheri, E., Reinhart, B.D., Abendroth, L.J., Chighladze, G., Ghane, E., Shedekar, V., Norman, N.R., Frankenberger, J.R., Helmers, M.J., Dan, D.B., Kladivko, E., Negm, L., Nelson, K., Pease, L., 2023. Impact of controlled drainage on corn yield under varying precipitation patterns: A synthesis of studies across the U.S. Midwest and Southeast. Agric Water Manag 275, 107993. https://doi.org/10.1016/J.AGWAT.2022.107993

F. Flow Variations: Paired Field Assessment at CD and FD systems

Table F-1. Mean, Standard Deviation Normalised Daily Flow and p value from paired t-test at paired drainage structures for the entire study period.

Site Pair	CD			FD			Change (%)		
	2018	2019	2021	2018	2019	2021	2018	2019	2021
CD 1 vs FD 3	0.4±1.3	0.7±1.9P	0.7±1.3	0.6±1.3	1.0±2.6	0.7±1.1	20	28	9
CD 1 vs FD 4	0.4±1.3	0.7±1.9P	0.7±1.3	0.5±1.1	0.9±2.1	1.0±2.3	14	20	34
CD 1 vs FD 5	0.4±1.3	0.7±1.9P	0.7±1.3	0.5±1.1	1.0±2.4	0.7±2.2	16	24	4
CD 2 vs FD 3	0.3±0.9P	0.7±1.5P	0.6±1.2	0.6±1.3	1.0±2.6	0.7±1.1	50	30	18
CD 2 vs FD 4	0.3±0.9P	0.7±1.5P	0.6±1.2	0.5±1.1	0.9±2.1	1.0±2.3	46	23	20
CD 2 vs FD 5	0.3±0.9P	0.7±1.5P	0.6±1.2	0.5±1.1	1.0±2.4	0.7±2.2	47	27	42

P Statistically significant difference, $p<0.05$ observed between a CDS and FDS pair, using Paired t-test.

Table F-2. Mean and Standard Deviation Normalised Daily Flows and p-value from paired t-test test for Growing Period

Site Pair	CD			FD			Change (%)		
	2018	2019	2021	2018	2019	2021	2018	2019	2021
CD 1 vs FD 3	0.2±0.8P	0.2±0.7P	0.2±0.8P	0.5±1.3	0.7±2.2	0.4±0.9	52	68	39
CD 1 vs FD 4	0.2±0.8	0.2±0.7P	0.2±0.8P	0.3±0.8	0.4±1.3	0.6±2.0	29	45	61
CD 1 vs FD 5	0.2±0.8P	0.2±0.7P	0.2±0.8P	0.5±1.2	0.7±2.3	0.4±0.7	52	67	38
CD 2 vs FD 3	0.1±0.4P	0.2±0.6P	0.2±0.6P	0.5±1.3	0.7±2.2	0.4±0.9	85	70	59
CD 2 vs FD 4	0.1±0.4P	0.2±0.6P	0.2±0.6P	0.3±0.8	0.4±1.3	0.6±2.0	78	48	74
CD 2 vs FD 5	0.1±0.4P	0.2±0.6P	0.2±0.6P	0.5±1.2	0.7±2.3	0.4±0.7	85	69	58

P Statistically significant difference, $p<0.05$ observed between a CDS and FDS pair, using Paired t-test.

Table F-3. Mean and Standard Deviation Normalised Daily Flows and p-value from paired t-test test for Flush Period

Site Pair	CD			FD			Change (%)		
	2018	2019	2021	2018	2019	2021	2018	2019	2021
CD 1 vs FD 3	2.7±4.6	1.1±2.0	5.1±6.0	0.0±0.0	0.3±0.6	0.1±0.1	-11417	-236	-10026
CD 1 vs FD 4	2.7±4.6	1.1±2.0	5.1±6.0	0.0±0.1	0.1±0.2	0.1±0.1	-14416	-792	-7548
CD 1 vs FD 5	2.7±4.6	1.1±2.0	5.1±6.0	0.2±0.1	0.6±0.7	0.1±0.1	-1597	-101	-5149
CD 2 vs FD 3	1.7±1.3P	2.6±3.7	2.7±3.7	0.0±0.0	0.3±0.6	0.1±0.1	-7234	-648	-5346
CD 2 vs FD 4	1.7±1.3P	2.6±3.7	2.7±3.7	0.0±0.1	0.1±0.2	0.1±0.1	-9144	-1886	-4013
CD 2 vs FD 5	1.7±1.3P	2.6±3.7	2.7±3.7	0.2±0.1	0.6±0.7	0.1±0.1	-981	-346	-2723

Note: Significance test was not carried for this period.

Table F-4. Mean and Standard Deviation Normalised Daily Flows and p-value from paired t-test test for Post-Harvest Period

Site Pair	CD			FD			Change (%)		
	2018	2019	2021	2018	2019	2021	2018	2019	2021
CD 1 vs FD 3	1.0±1.2	1.2±3.0	1.6±1.4	1.2±1.0	1.2±3.7	1.7±1.0	17	1	1
CD 1 vs FD 4	1.0±1.2P	1.2±3.0P	1.6±1.4	1.7±1.8	1.7±3.2	2.1±2.8	42	29	20
CD 1 vs FD 5	1.0±1.2	1.2±3.0	1.6±1.4	1.0±0.7	1.0±2.5	1.5±4.0	-2	-17	-7
CD 2 vs FD 3	1.0±1.5	1.0±1.6	1.6±1.5	1.2±1.0	1.2±3.7	1.7±1.0	20	15	1
CD 2 vs FD 4	1.0±1.5P	1.0±1.6P	1.6±1.5	1.7±1.8	1.7±3.2	2.1±2.8	44	39	21
CD 2 vs FD 5	1.0±1.5	1.0±1.6	1.6±1.5	1.0±0.7	1.0±2.5	1.5±4.0	2	-1	-7

P Statistically significant difference, $p<0.05$ observed between a CDS and FDS pair, using Paired t-test.

Table F-5 High Precipitation Criteria for single day and cluster events during the 3-year study period

Study Period	Average (μ) ± Standard Deviation (σ)	μ+1 σ P (mm/d)			μ+2 σ P (mm/d)			μ+3 σ P (mm/d)		
3 years	7.5±9.0	16.5			25.5			34.5		
		Number of events (count)								
		2018	2019	2021	2018	2019	2021	2018	2019	2021
		10	9	18	7	5	8	3	1	3

A cluster event was defined as consecutive precipitation events that were greater than μ+1 σ and were treated as one event for simplicity. Some cluster events may also include a single day high precipitation and such circumstances, the cluster event was considered.

High Precipitation Events - Impact of CD on peak and total event flow

A high precipitation event was defined as a single-day precipitation or multi-day cluster event greater than μ+1 σ (mm/day). Many high events were observed over the study period, with 18 events in 2021, 10 events in 2018 and 9 events in 2019 (Table F-5). It was hypothesised that CD attenuates peak and total event flow through initial storage in soil macropores as well as through potentially reduced water movement due to the damming effect.

In this study, the flow response to these events varied largely depending on the timing of the events rather than the precipitation intensity. The events that occurred in June and early July saw an immediate response by all DS on the same day (t) or t+1, with peaks observed between t and t+3. As the growing season progressed, between late July and late September, little to no response was seen in the CD structures and a delayed first response from FD structures (t+1 to t+2), with a peak observed between t+1 and t+3. For example, the highest precipitation event during the study, with a magnitude of 61.6 mm occurred on September 21, 2018, where no flow was observed at CD 1 and CD 2, while at the FDs flows were a mere 0.1 to 0.9 mm. In fact, around midsummer, CD flows were absent in all years, producing 100% reduction of peak and total event flow when compared with FD flows.

Comparing all 37 high events, CD reduced total drainage volume by 11% ($p < 0.05$, paired t-test for 3/3 pairs) and peak flows by 14% ($p < 0.05$, paired t-test for 4/6 pairs) compared to average FD. In a 2-year study with 22 storm events, Bou Lahdou et al. (2019) observed CD decreased event drainage volume by 22%±12% and peak flows by 29%±16% ($p < 0.01$, rank sum test) when compared to FD, owing to increased soil moisture at CD. To check the effectiveness of a full water reservoir (i.e., when water level was at the overflow level) at CD during high precipitation, events that generated peaks and total flows greater than 4 mm/day at least in one of the DS locations and had any existing flow before the high event flow were selected. Using this criterion, the number of events was narrowed down to six peak and total flow events (when stoplogs were in) (Table E-6). For total event flows, no statistical differences ($p > 0.1$, paired t-test), except for CD 2 vs. FD 4, were observed. Peak flows at 15 min, 1-hour and 1-day intervals were also statistically similar ($p > 0.1$, ANOVA) and the length of the flow events did not vary considerably between the CD and FD in all years. Thus, the beneficial effect of CD is that any sort of storage led to total volume

and peak attenuation. However, there was no effect of CD on water movement through the soil when the reservoir is full.

Table F-6. Statistical Analysis of Flow variation (mm/d) during high precipitation events using Paired t-test at 15 min, 1 hour and 24-hour time intervals during growing season.

Site Pair	CDS	FDS	P value
Peak at 15 min interval (mm/d)			
CD 1 vs FD 3	0.08±0.06	0.1±0.1	0.65
CD 1 vs FD 4	0.08±0.06	0.4±0.5	0.19
CD 1 vs FD 5	0.08±0.06	0.1±0.1	0.80
CD 2 vs FD 3	0.07±0.08	0.1±0.1	0.55
CD 2 vs FD 4	0.07±0.08	0.4±0.5	0.19
CD 2 vs FD 5	0.07±0.08	0.1±0.1	0.69
Peak at 1 hour interval (mm/d)			
CD 1 vs FD 3	0.29±0.22	0.34±0.31	0.74
CD 1 vs FD 4	0.29±0.22	1.11±2.12	0.29
CD 1 vs FD 5	0.29±0.22	0.32±0.37	0.89
CD 2 vs FD 3	0.26±0.26	0.34±0.31	0.59
CD 2 vs FD 4	0.26±0.26	1.11±2.12	0.29
CD 2 vs FD 5	0.26±0.26	0.32±0.37	0.74
Peak at 24-hour interval (mm/d)			
CD 1 vs FD 3	3.53±2.23	3.32±2.49	0.80
CD 1 vs FD 4	3.53±2.23	6.25±6.21	0.17
CD 1 vs FD 5	3.53±2.23	2.61±1.92	0.33
CD 2 vs FD 3	2.92±1.74	3.32±2.49	0.66
CD 2 vs FD 4	2.92±1.74	6.25±6.21	0.12
CD 2 vs FD 5	2.92±1.74	2.61±1.92	0.71
Total Event at 24-hour interval (mm/d)			
CD 1 vs FD 3	7.28	6.48	0.65
CD 1 vs FD 4	7.28	11.38	0.18
CD 1 vs FD 5	7.28	4.72	0.21
CD 2 vs FD 3	5.13	6.48	0.45
CD 2 vs FD 4	5.13	11.38	**0.06**
CD 2 vs FD 5	5.13	4.72	0.79
Significant difference considered when P<0.1 using paired t-test			

G. Nitrate as N Concentration and Load Variations: Paired Field Assessment at CD and FD systems

Table G-1. Mean, Standard Deviation Normalised Daily concentration, Load, and p value from Paired t-test test at paired drainage structures for the entire study period.

Site Pair	CD			FD			Change (%)		
	2018	2019	2021	2018	2019	2021	2018	2019	2021
Mean Daily Nitrate Concentration (mg NO_3-N/L)									
CD 1 vs FD 3	6.9±2.3	9.0±2.3	7.8±1.5 P	5.7±1.4	8.1±2.7	5.7±0.9	-21	-11	-36
CD 1 vs FD 4	6.9±2.3	9.0±2.3	7.8±1.5 P	5.2±2.2	7.4±1.3	5.9±0.8	-32	-22	-31
CD 1 vs FD 5	6.9±2.3	9.0±2.3	7.8±1.5 P	-	7.5±1.5	6.4±0.8	-	-21	-21
CD 2 vs FD 3	5.5±2.3	8.5±2.0	5.6±1.5	5.7±1.4	8.1±2.7	5.7±0.9	3	-5	2
CD 2 vs FD 4	5.5±2.3	8.5±2.0	5.6±1.5	5.2±2.2	7.4±1.3	5.9±0.8	-6	-15	6
CD 2 vs FD 5	5.5±2.3	8.5±2.0	5.6±1.5	-	7.5±1.5	6.4±0.8	-	-14	13
Mean Daily Nitrate Mass Load[a] (x 10^{-2} kg NO_3-N/ha day)									
CD 1 vs FD 3	2.9±9.6	3.2±12.4	4.4±9.6 P	3.2±8.7	3.7±17.6	3.4±6.1	9	12	-30
CD 1 vs FD 4	2.9±9.6	3.2±12.4	4.4±9.6	1.9±6.2	3.6±15.6	4.9±12.5	-50	11	10
CD 1 vs FD 5	2.9±9.6	3.2±12.4	4.4±9.6	1.8±5.4	3.9±18.7	3.6±13.9	-65	17	-21
CD 2 vs FD 3	1.3±5.2	2.7±8.1	3.1±7.1	3.2±8.7	3.7±17.6	3.4±6.1	60	26	8
CD 2 vs FD 4	1.3±5.2	2.7±8.1	3.1±7.1 P	1.9±6.2	3.6±15.6	4.9±12.5	34	25	36
CD 2 vs FD 5	1.3±5.2	2.7±8.1	3.1±7.1	1.8±5.4	3.9±18.7	3.6±13.9	27	30	14

P Statistically significant difference, $p<0.05$ observed between a CDS and FDS pair, using Paired t-test.

Table G-2. Mean and Standard Deviation Normalised Daily concentration, Load, and p-value from paired t-test test for Growing Period

Site Pair	CD			FD			Change (%)		
	2018	2019	2021	2018	2019	2021	2018	2019	2021
Mean Daily Nitrate Concentration (mg NO_3-N/L)									
CD 1 vs FD 3	6.9±2.8	10.2±1.5	7.2±1.4 P	5.9±1.4	8.1±1.5	5.8±1.0	-18	-25	-23
CD 1 vs FD 4	6.9±2.8	10.2±1.5	7.2±1.4 P	5.8±2.1	7.5±1.0	5.9±0.9	-19	-35	-20
CD 1 vs FD 5	6.9±2.8	10.2±1.5	7.2±1.4 P	-	7.2±0.6	6.4±0.7	-	-40	-11
CD 2 vs FD 3	10.1±0.5	9.9±1.3	5.5±1.7	5.9±1.4	8.1±1.5	5.8±1.0	-72	-22	7
CD 2 vs FD 4	10.1±0.5	9.9±1.3	5.5±1.7	5.8±2.1	7.5±1.0	5.9±0.9	-74	-32	8
CD 2 vs FD 5	10.1±0.5	9.9±1.3	5.5±1.7	-	7.2±0.6	6.4±0.7	-	-37	15
Mean Daily Nitrate Mass Load[a] (x 10^{-2} kg NO_3-N/ha day)									
CD 1 vs FD 3	2.0±7.7	2.4±7.9	1.8±6.9	2.9±9.3	3.3±15.9	2.0±5.2	30	27	12
CD 1 vs FD 4	2.0±7.7	2.4±7.9	1.8±6.9 P	1.9±6.1	2.8±9.3	3.5±12.3	-9	13	49
CD 1 vs FD 5	2.0±7.7	2.4±7.9	1.8±6.9	1.3±5.5	2.8±14.0	1.9±5.0	-51	14	9
CD 2 vs FD 3	0.4±3.1 P	1.6±5.7	1.3±5.5 P	2.9±9.3	3.3±15.9	2.0±5.2	87	52	35
CD 2 vs FD 4	0.4±3.1 P	1.6±5.7	1.3±5.5 P	1.9±6.1	2.8±9.3	3.5±12.3	80	43	62
CD 2 vs FD 5	0.4±3.1 P	1.6±5.7	1.3±5.5 P	1.3±5.5	2.8±14.0	1.9±5.0	72	43	32

P Statistically significant difference, $p<0.05$ observed between a CDS and FDS pair, using Paired t-test.

Table G-3. Mean and Standard Deviation Normalised Daily concentration and Load for Flush Period

Site Pair	CD			FD			Change (%)		
	2018	2019	2021	2018	2019	2021	2018	2019	2021
Mean Daily Nitrate Concentration (mg NO_3-N/L)									
CD 1 vs FD 3	6.3±0.3	3.4±0.4	9.5±1.7	-	12.1±1.0	5.3±0.0	-	73	-81
CD 1 vs FD 4	6.3±0.3	3.4±0.4	9.5±1.7	2.4±0.3	11.6±0.0	7.4±0.0	-168	71	-29
CD 1 vs FD 5	6.3±0.3	3.4±0.4	9.5±1.7	-	11.6±0.0	6.2±0.0	-	71	-53
CD 2 vs FD 3	4.3±0.3	6.4±0.3	4.8±0.1	-	12.1±1.0	5.3±0.0	-	49	-13
CD 2 vs FD 4	4.3±0.3	6.4±0.3	4.8±0.1	2.4±0.3	11.6±0.0	7.4±0.0	-82	45	-4
CD 2 vs FD 5	4.3±0.3	6.4±0.3	4.8±0.1	-	11.6±0.0	6.2±0.0	-	45	8
Mean Daily Nitrate Mass Load[a] (x 10^{-2} kg NO_3-N/ha day)									
CD 1 vs FD 3	15.9±25.9	3.5±6.0	30.1±32.7	0.0±0.0	4.0±6.7	0.3±0.4	-	13	-11292
CD 1 vs FD 4	15.9±25.9	3.5±6.0	30.1±32.7	0.0±0.1	1.5±2.6	0.5±0.7	-37887	-133	-6012
CD 1 vs FD 5	15.9±25.9	3.5±6.0	30.1±32.7	0.3±0.2	5.2±9.1	0.5±0.7	-5062	34	-6198
CD 2 vs FD 3	7.4±5.9	15.7±22	13.2±17.9	0.0±0.0	4.0±6.7	0.3±0.4	-4258	-296	-4917
CD 2 vs FD 4	7.4±5.9	15.7±22	13.2±17.9	0.0±0.1	1.5±2.6	0.5±0.7	-17600	-955	-2592
CD 2 vs FD 5	7.4±5.9	15.7±22	13.2±17.9	0.3±0.2	5.2±9.1	0.5±0.7	-2305	-199	-2673

Note: Significance test was not carried for this period.

Table G-4. Mean and Standard Deviation Normalised Daily concentration, Load and p-value from Paired t-test for Post-Harvest Period

Site Pair	CD			FD			Change (%)		
	2018	2019	2021	2018	2019	2021	2018	2019	2021
Mean Daily Nitrate Concentration (mg NO_3-N/L)									
CD 1 vs FD 3	6.9±0.6	6.8±1.2	8.7±0.7 **P**	5.3±0.4	7.4±3.9	5.3±0.3	-21	8	-64
CD 1 vs FD 4	6.9±0.6	6.8±1.2	8.7±0.7 **P**	4.2±1.0	6.7±2.0	5.8±0.5	-32	-2	-50
CD 1 vs FD 5	6.9±0.6	6.8±1.2	8.7±0.7 **P**	-	7.8±2.5	6.5±1.0	-	13	-33
CD 2 vs FD 3	4.9±1.6	6.6±1.1	6.0±0.7	5.3±0.4	7.4±3.9	5.3±0.3	3	11	-13
CD 2 vs FD 4	4.9±1.6	6.6±1.1	6.0±0.7	4.2±1.0	6.7±2.0	5.8±0.5	-6	1	-4
CD 2 vs FD 5	4.9±1.6	6.6±1.1	6.0±0.7	-	7.8±2.5	6.5±1.0		15	8
Mean Daily Nitrate Mass Load[a] (x 10^{-2} kg NO_3-N/ha day)									
CD 1 vs FD 3	3.8±8.4	7.1±24.6	10.3±11 **P**	5.4±6.3	5.5±25.3	7.0±6.8	29	-31	-47
CD 1 vs FD 4	3.8±8.4	7.1±24.6	10.3±11	2.8±7.4	7.9±32.2	8.7±12.4	-39	10	-19
CD 1 vs FD 5	3.8±8.4	7.1±24.6	10.3±11	4.2±4.4	9.1±33.5	8.1±24.8	9	22	-28
CD 2 vs FD 3	4.2±9.6	7.0±12.6	7.5±8.2	5.4±6.3	5.5±25.3	7.0±6.8	21	-27	-6
CD 2 vs FD 4	4.2±9.6	7.0±12.6	7.5±8.2	2.8±7.4	7.9±32.2	8.7±12.4	-53	12	14
CD 2 vs FD 5	4.2±9.6	7.0±12.6	7.5±8.2	4.2±4.4	9.1±33.5	8.1±24.8	0	24	7

P Statistically significant difference, $p<0.05$ observed between a CDS and FDS pair, using Paired t-test.

H. Soil Microbiome Analysis – CD versus FD system

Table H-1. Average and 95% confidence interval of the Alpha diversity of the microbiome communities.

Parameters	CD	FD
Observed (OTU)	970.7±114.4	983.0±77.5
Chao1 Estimator	1420.0±282.6	1499.6±120.9
Simpson Diversity	0.9964±0.0008	0.9963±0.0006

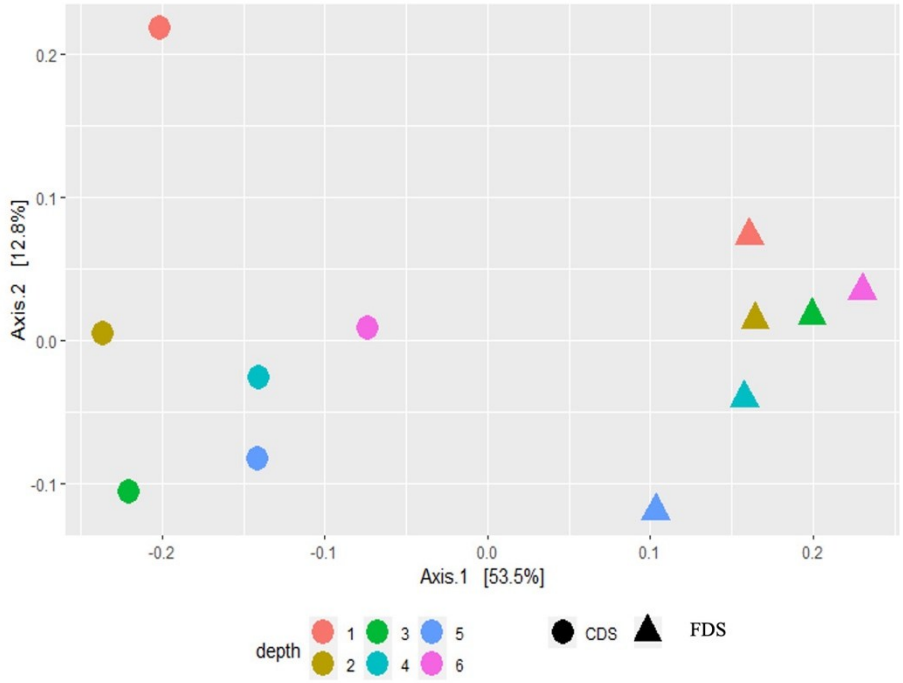

Figure H-1. PCoA of microbiome populations at CD and FD as a function of depth with weighted-unifrac distances

<u>Denitrification End-Products -</u>

Nitrogen gas (N_2) is typically the most common end-product of denitrification. However, nitrite (NO_2^-), nitrous oxide (N_2O), ammonium (NH_4^+), and nitric oxide (NO) can also be produced based on genes in bacteria or environmental conditions (Giles et al., 2012; Kraft et al., 2014). In this study, the genes are the primary factor responsible for the different end products observed among 24 of the 26 identified NO_3^- reducing genera. Twelve genera were identified as N_2 producing bacteria, four as NO_2^- producing, three as NH_4^+ producing, two as N_2O and three as NO by-product.

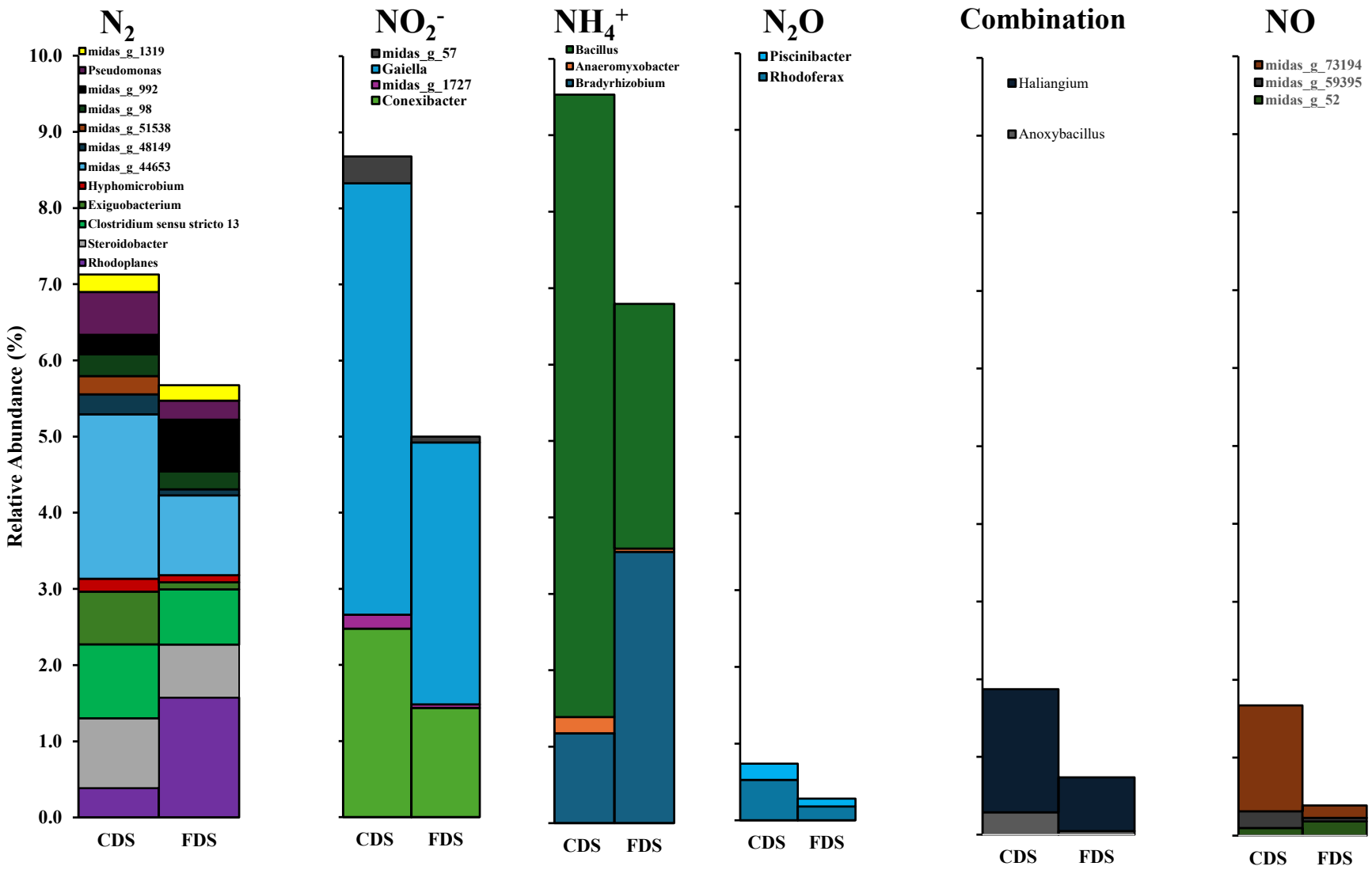

Figure H-2. Distribution of Nitrate Reducing Bacteria by Genus across CD and FD based on product of reduction reaction.

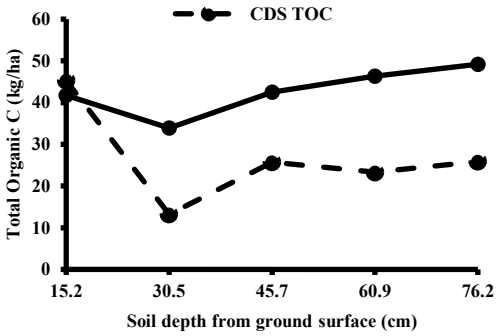

Figure H.3. Trend of TOC content in soil – At CD and FD shown as a function of depth from the field surface.

I. Total Phosphorous as P – Concentration and Load – CD versus FD

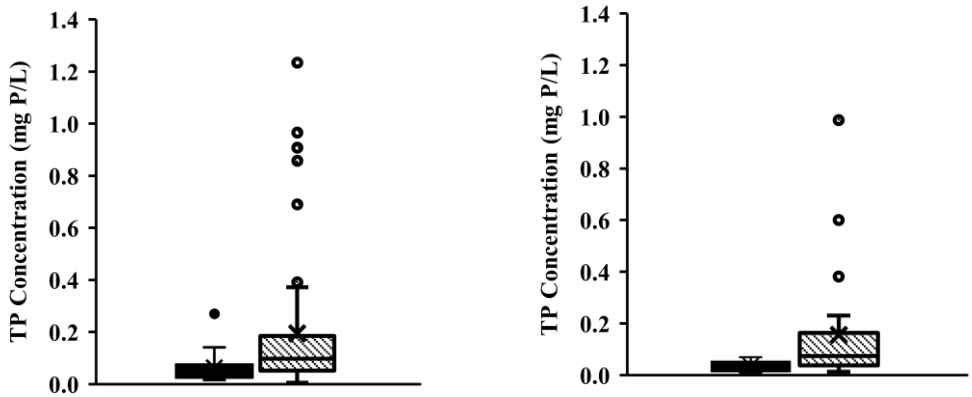

Figure I.1. Box Plots of Total Phosphorus Concentrations - across CD and FD structures during GP (Left) and PHP (Right) for TP (mg TP/L) over the 3-year study.

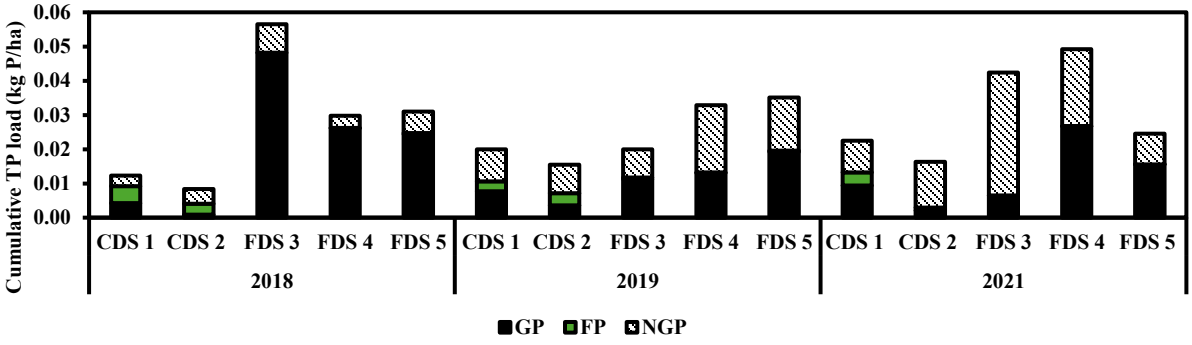

Figure I.2. Trends of Cumulative Loads - as Total Phosphorus (TP as P) at Controlled Drainage Structures (CD) and Free Drainage Structures (FD) during the 3-year study (2018, 2019 and 2021).

J. SRP as P Concentration and Load Variations: Paired Field Assessment at CD and FD systems.

Table J-1. Mean, Standard Deviation Normalised Daily concentration, load, and p value from Paired t-test at paired drainage structures for the entire study period.

Site Pair	CD			FD			Change (%)		
	2018	2019	2021	2018	2019	2021	2018	2019	2021
Mean Daily SRP Concentration (mg PO_4-P/L)									
CD 1 vs FD 3	0.02±0.01 P	0.01±0.03 P	0.01±0.02	0.04±0.08	0.04±0.09	0.03±0.03	63	68	47
CD 1 vs FD 4	0.02±0.01 P	0.01±0.03 P	0.01±0.02	0.05±0.07	0.09±0.14	0.02±0.03	71	85	31
CD 1 vs FD 5	0.02±0.01	0.01±0.03 P	0.01±0.02	-	0.03±0.05	0.02±0.02	-	53	18
CD 2 vs FD 3	0.02±0.01	0.02±0.02 P	0.01±0.02 P	0.04±0.08	0.04±0.09	0.03±0.03	54	55	63
CD 2 vs FD 4	0.02±0.01	0.02±0.02 P	0.01±0.02 P	0.05±0.07	0.09±0.14	0.02±0.03	63	78	52
CD 2 vs FD 5	0.02±0.01	0.02±0.02 P	0.01±0.02 P	-	0.03±0.05	0.02±0.02	-	33	42
Mean Daily SRP Mass Load[a] (x 10^{-5} kg PO_4-P/ha day)									
CD 1 vs FD 3	0.6±2.9 P	0.4±2.7	1.0±4.7	2.2±8.3	0.9±6.5	1.5±6.0	75	54	35
CD 1 vs FD 4	0.6±2.9	0.4±2.7	1.0±4.7 P	1.0±4.9	1.5±11.2	1.8±8.6	44	71	47
CD 1 vs FD 5	0.6±2.9	0.4±2.7	1.0±4.7	0.8±2.3	1.9±13.8	0.7±3.6	31	77	-31
CD 2 vs FD 3	0.4±1.6 P	1.2±7.3	0.7±4.0	2.2±8.3	0.9±6.5	1.5±6.0	82	-23	54
CD 2 vs FD 4	0.4±1.6	1.2±7.3	0.7±4.0 P	1.0±4.9	1.5±11.2	1.8±8.6	60	21	62
CD 2 vs FD 5	0.4±1.6 P	1.2±7.3	0.7±4.0	0.8±2.3	1.9±13.8	0.7±3.6	51	39	6

P Statistically significant difference, $p<0.05$ observed between a CDS and FDS pair, using Paired t-test.

Table J-2. Mean and Standard Deviation Normalised Daily concentration, load, and p-value from Paired t-test for Growing Period

Site Pair	CD			FD			Change (%)		
	2018	2019	2021	2018	2019	2021	2018	2019	2021
Mean Daily SRP Concentration (mg PO_4-P/L)									
CD 1 vs FD 3	0.01±0.01 P	0.01±0.03	0.01±0.02	0.05±0.09	0.02±0.07	0.02±0.03	69	48	46
CD 1 vs FD 4	0.01±0.01 P	0.01±0.03 P	0.01±0.02	0.06±0.08	0.09±0.16	0.02±0.03	75	86	37
CD 1 vs FD 5	0.01±0.01	0.01±0.03	0.01±0.02	-	0.03±0.05	0.02±0.02	-	53	35
CD 2 vs FD 3	0.03±0.02	0.01±0.02	0.01±0.01 P	0.05±0.09	0.02±0.07	0.02±0.03	38	46	64
CD 2 vs FD 4	0.03±0.02	0.01±0.02 P	0.01±0.01 P	0.06±0.08	0.09±0.16	0.02±0.03	50	85	59
CD 2 vs FD 5	0.03±0.02	0.01±0.02 P	0.01±0.01 P	-	0.03±0.05	0.02±0.02	-	51	57
Mean Daily SRP Mass Load[a] (x 10^{-5} kg PO_4-P/ha day)									
CD 1 vs FD 3	0.2±0.8 P	0.2±0.7	0.6±4.6	2.4±9.2	0.5±2.1	0.3±0.6	90	57	-78
CD 1 vs FD 4	0.2±0.8 P	0.2±0.7 P	0.6±4.6	1.0±4.9	0.6±2.5	1.5±9.6	78	68	62
CD 1 vs FD 5	0.2±0.8 P	0.2±0.7	0.6±4.6	0.8±2.3	1.0±8.1	0.5±1.6	64	81	-25
CD 2 vs FD 3	0.1±0.4 P	0.1±0.5 P	0.1±0.6 P	2.4±9.2	0.5±2.1	0.3±0.6	98	73	62
CD 2 vs FD 4	0.1±0.4 P	0.1±0.5 P	0.1±0.6 P	1.0±4.9	0.6±2.5	1.5±9.6	95	80	92
CD 2 vs FD 5	0.1±0.4 P	0.1±0.5	0.1±0.6 P	0.8±2.3	1.0±8.1	0.5±1.6	92	88	73

P Statistically significant difference, $p<0.05$ observed between a CDS and FDS pair, using Paired t-test.

Table J-3. Mean and Standard Deviation Normalised Daily concentration and load for Flush Period

Site Pair	CD			FD			Change (%)		
	2018	2019	2021	2018	2019	2021	2018	2019	2021
Mean Daily SRP Concentration (mg PO_4-P/L)									
CD 1 vs FD 3	0.02±0.00	0.06±0.04	0.04±0.0	-	0.09±0.05	0.01±0.0	-	36	-266
CD 1 vs FD 4	0.02±0.00	0.06±0.04	0.04±0.0	0.03±0.01	0.03±0.0	0.01±0.0	48	-103	-198
CD 1 vs FD 5	0.02±0.00	0.06±0.04	0.04±0.0	-	0.03±0.0	0.04±0.0	-	-103	12
CD 2 vs FD 3	0.02±0.00	0.07±0.06	0.01±0.0	-	0.09±0.05	0.01±0.0	-	26	-37
CD 2 vs FD 4	0.02±0.00	0.07±0.06	0.01±0.0	0.03±0.01	0.03±0.0	0.01±0.0	42	-133	-12
CD 2 vs FD 5	0.02±0.00	0.07±0.06	0.01±0.0	-	0.03±0.0	0.04±0.0	-	-133	67
Mean Daily SRP Mass Load[a] (x 10^{-5} kg PO_4-P/ha day)									
CD 1 vs FD 3	6.2±12.9	12.1±21.0	16.7±23.0	0.0±0.0	1.0±1.6	0.0±0.1	-	-1065	-34490
CD 1 vs FD 4	6.2±12.9	12.1±21.0	16.7±23.0	0.1±0.2	0.4±0.6	0.1±0.1	-7229	-3171	-21161
CD 1 vs FD 5	6.2±12.9	12.1±21.0	16.7±23.0	0.4±0.2	1.3±2.3	0.3±0.4	-1295	-829	-5328
CD 2 vs FD 3	3.7±3.6	30.5±50.1	3.6±4.9	0.0±0.0	1.0±1.6	0.0±0.1	-	-2833	-7361
CD 2 vs FD 4	3.7±3.6	30.5±50.1	3.6±4.9	0.1±0.2	0.4±0.6	0.1±0.1	-4254	-8134	-4486
CD 2 vs FD 5	3.7±3.6	30.5±50.1	3.6±4.9	0.4±0.2	1.3±2.3	0.3±0.4	-729	-2237	-1071

Note: Significance test was not carried for this period.

Table J-4. Mean and Standard Deviation Normalised Daily concentration, load and p-value from paired t-test for Post-Harvest Period

Site Pair	CD			FD			Change (%)		
	2018	2019	2021	2018	2019	2021	2018	2019	2021
Mean Daily SRP Concentration (mg PO_4-P/L)									
CD 1 vs FD 3	0.01±0.00	0.01±0.01	0.01±0.02	0.02±0.02	0.07±0.12 P	0.04±0.05	23	88	59
CD 1 vs FD 4	0.01±0.00	0.01±0.01	0.01±0.02	0.03±0.02	0.06±0.08 P	0.02±0.02	42	87	27
CD 1 vs FD 5	0.01±0.00	0.01±0.01	0.01±0.02	-	0.03±0.03 P	0.01±0.01	-	71	-
CD 2 vs FD 3	0.02±0.01	0.02±0.02	0.01±0.03	0.02±0.02	0.07±0.12	0.04±0.05	18	69	63
CD 2 vs FD 4	0.02±0.01	0.02±0.02	0.01±0.03	0.03±0.02	0.06±0.08	0.02±0.02	38	67	35
CD 2 vs FD 5	0.02±0.01	0.02±0.02	0.01±0.03	-	0.03±0.03	0.01±0.01	-	28	-
Mean Daily SRP Mass Load[a] (x 10^{-5} kg PO_4-P/ha day)									
CD 1 vs FD 3	0.7±1.3	0.5±1.1	1.5±2.7	1.9±2.8 P	3.3±15.0	4.6±10.8 P	64	85	68
CD 1 vs FD 4	0.7±1.3	0.5±1.1	1.5±2.7	0.8±1.8	5.7±26.6	2.7±5.5	16	91	46
CD 1 vs FD 5	0.7±1.3	0.5±1.1	1.5±2.7	1.6±2.3 P	6.3±28.5	1.5±6.4	57	92	0
CD 2 vs FD 3	1.3±3.0	3.5±8.4	2.1±7.4	1.9±2.8	3.3±15.0	4.6±10.8	34	-5	55
CD 2 vs FD 4	1.3±3.0	3.5±8.4	2.1±7.4	0.8±1.8	5.7±26.6	2.7±5.5	-55	40	24
CD 2 vs FD 5	1.3±3.0	3.5±8.4	2.1±7.4	1.6±2.3	6.3±28.5	1.5±6.4	21	45	-41

P Statistically significant difference, $p<0.05$ observed between a CDS and FDS pair, using Paired t-test.

K. Total suspended solids concentration (mg/L) trend across the pond-wetland system subdivided by years and seasons

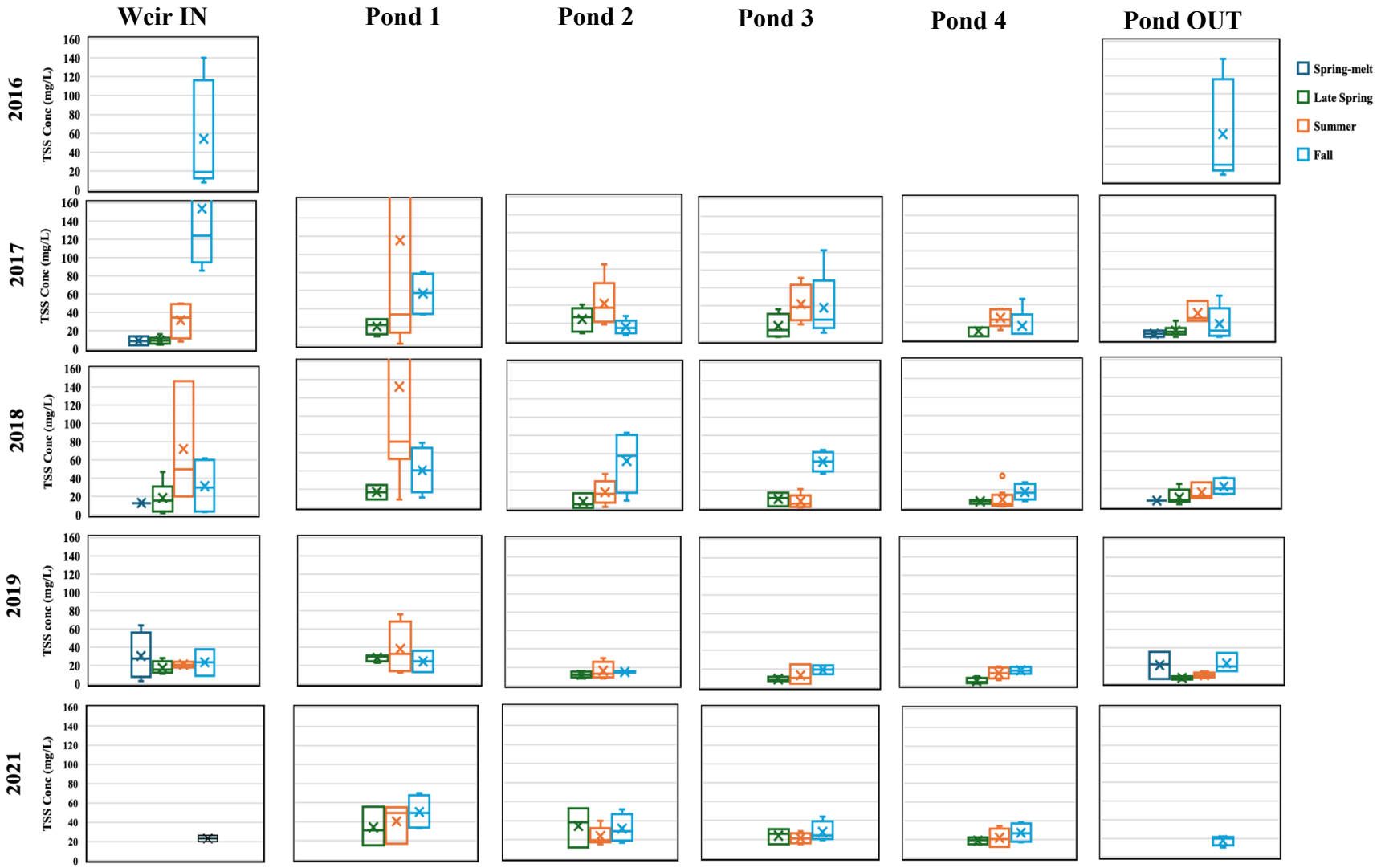

Figure K-1. Boxplots of total suspended solids concentration trends across the pond-wetland system subdivided by years of study and seasons.

Table K-1. Seasonal and overall average ± standard deviation for 2017 to 2019 study period.

	Weir IN	Pond 1	Pond 2	Pond 3	Pond 4	Pond OUT	% removal*
Spring-melt[a]	22 ± 21	-	-	-	-	14 ± 12	37
Late Spring[b]	15 ±11	23 ± 8 P	17 ± 12	13 ± 8	8 ± 5	10 ± 7	34
Summer[c]	43 ± 42	102 ± 109 P	23 ± 19 P	16 ± 18	14 ± 11	17 ± 13	59
Fall[d]	86 ± 90	45 ± 24	29 ± 27	39 ± 27	17 ± 12 P	20 ± 13	77
Study[e]	**40 ± 57**	**65 ± 82**	**23 ± 20** P	**22 ± 22**	**13 ± 11** P	**15 ± 11**	**63**

[a] Refers to period between beginning of April to April 30 each year.
[b] Refers to period between May 1 to June 20 each year
[c] Refers to period between June 21 to September 20 each year
[d] Refers to period between September 21 to November 30 each year.
[e] Refers to entire study (2017 to 2019). Year 2021 was not included as the system was stagnant.
P Significant difference observed (*p-value* < 0.05) when compared to location's influent (in this case, previous pond effluent) using ANOVA single factor.
* % removal (% retention) was calculated at Pond OUT compared to Weir IN.

L. Particulate Phosphorous concentration (mg P/L) trend across the pond-wetland system subdivided by years and seasons

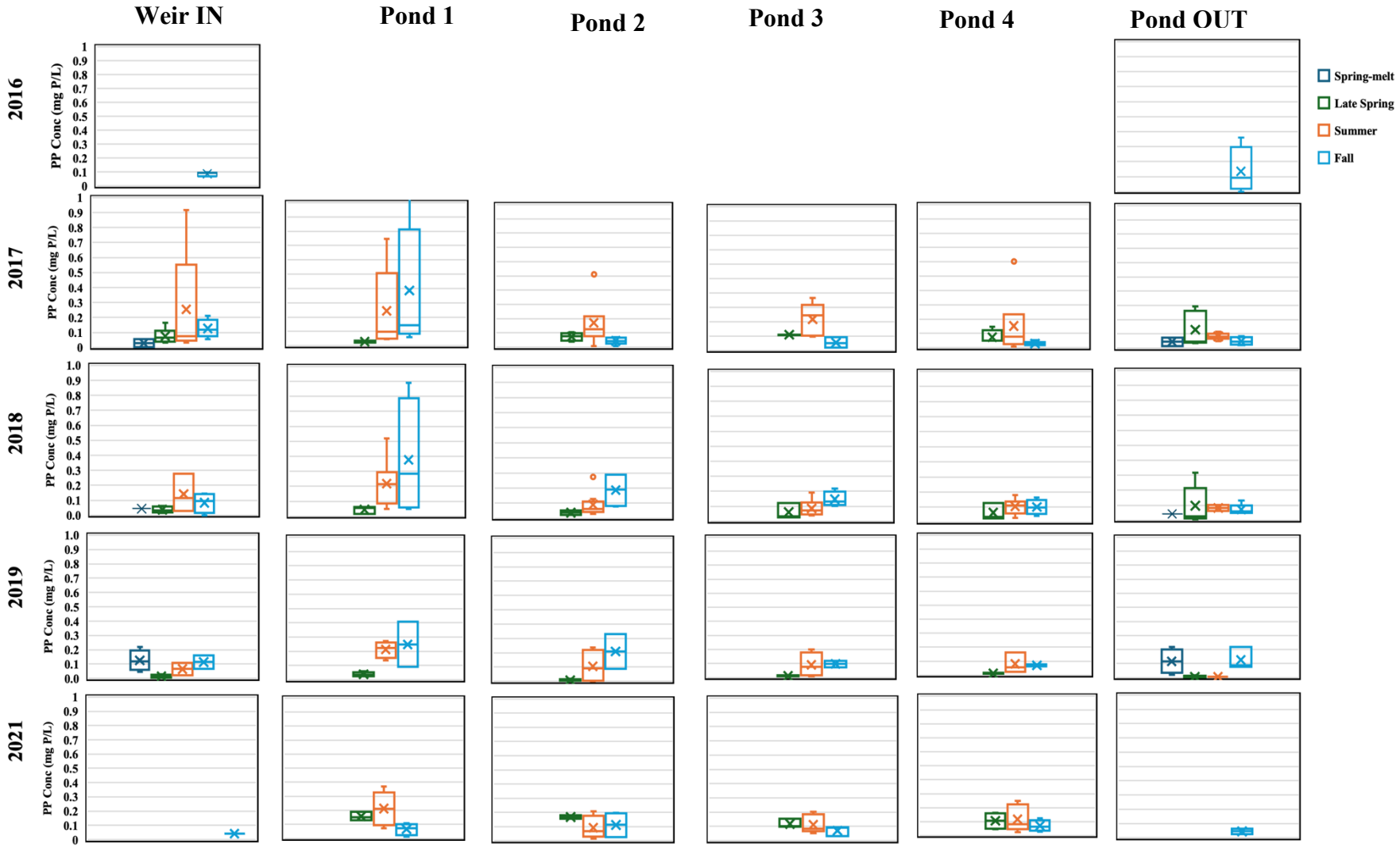

Figure L-1. Boxplots of particulate phosphorus concentration trends across the pond-wetland system subdivided by years of study and seasons.

M. Soluble reactive phosphorous concentration (mg P/L) trend across the pond-wetland system subdivided by years and seasons

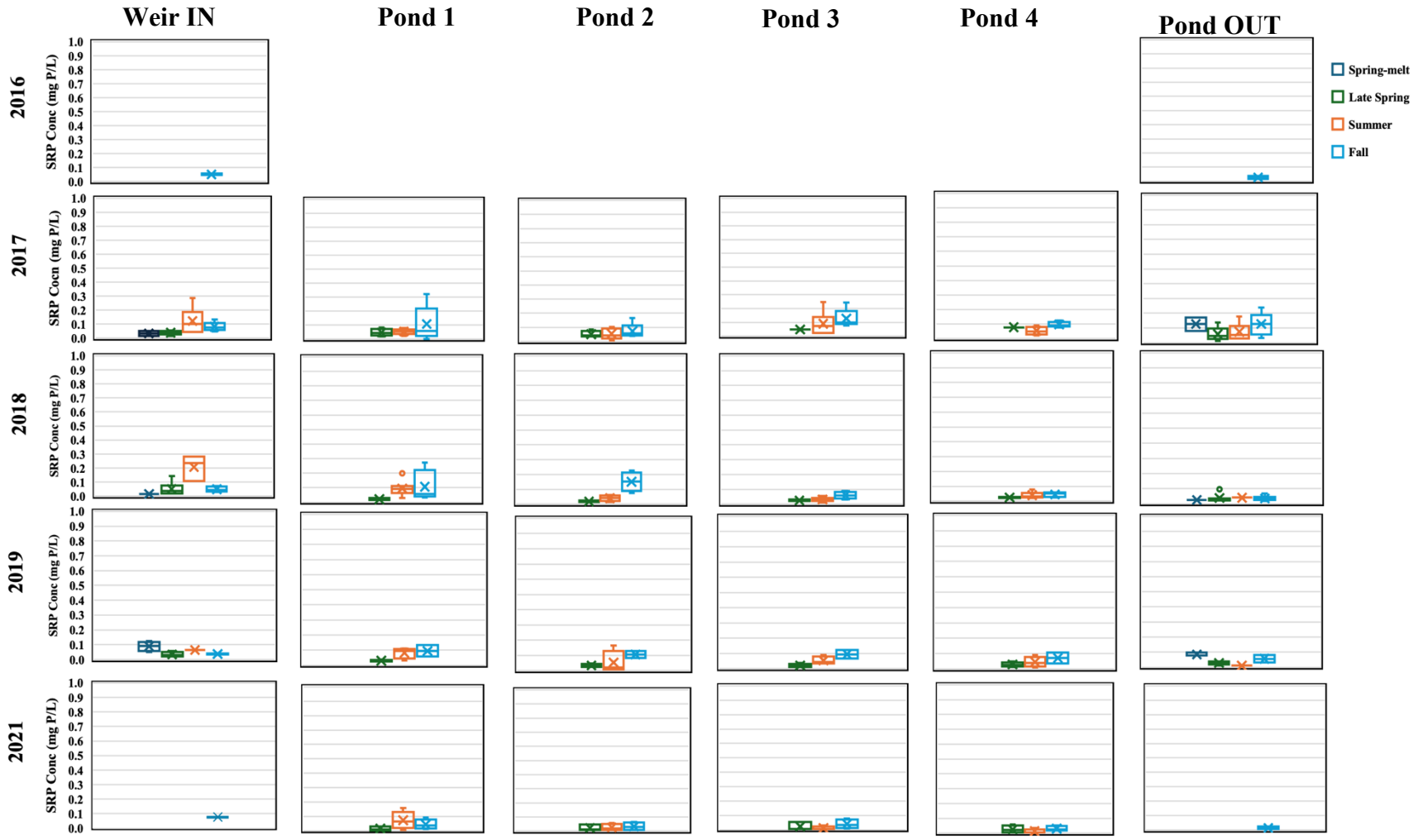

Figure M-1. Boxplots of soluble reactive phosphorus concentration trends across the pond-wetland system subdivided by years of study and seasons.
Note: The y-axis has been set to match particulate phosphorus trends from L-1.

Table M-1. Multiple regression analysis of factors influencing soluble reactive phosphorus (SRP) concentrations across the pond-wetland system, by pond and season.

Variables[a]	Combined Model[b]	Individual Ponds					Season		
		Pond 1	Pond 2	Pond 3	Pond 4	Pond OUT	Late Spring	Summer	Fall
Influent concentration[c]	-0.13 (CI: -0.27, 0.01)*	NS	NS	NS	NS	NS	NS	NS	NS
Inflow[d]	NS	NS	NS	NS	NS	NS	NS	$3.7x10^{-5}$(CI: $2.5x10^{-6}$, $7.8x10^{-5}$)*	NS
1/depth	NS	NA	NA	NA	NA	NA	NS	NS	NS
Precipitation (3-day cumulative)	NS	NS	NS	NS	NS	NS	NS	$-1.9x10^{-3}$(CI: $3.5x10^{-3}$, $4.2x10^{-4}$)**	NS
1/HRT	NS	NS	NS	NS	NS	NS	NS	NS	NS
Seasonal temperature	NS	NS	NS	NS	NS	NS	NS	$4.4x10^{-3}$(CI: $1.1x10^{-3}$,$7.7x10^{-3}$)***	NS

[a] Reduced regression listed here with variables showing statistically significant effect on SRP concentration. Other variables tested, but not listed here include precipitation (day of, -1-day), temperature (daily and monthly averages), hydraulic loading rate, %plant coverage, and area of the pond.

[b] Refers to the complete study period grouped together across the system (n=207), $R^2 = 0.04$, Adjusted $R^2 = 0.012$

[c] Refers to effluent concentration from previous pond, which be influent of the pond in questions

[d] Refers to outflow from previous pond, which is the inflow of the pond in question.

CI refers to 95% confidence interval for beta coefficient.

Significance levels: * *p*-value <0.1, ** *p*-value < 0.05, *** *p*-value <0.01, **** *p*-value <0.001

NA indicates Not Applicable

NS indicates Not Significant (tested, *p*-value >0.1)